UNIVERSITAT DE BARCELONA

Rhodolith beds in the Menorca Channel.
Taxonomic diversity, structural complexity, and monitoring strategies for conservation

Andrea Cabrito Rubau

Aquesta tesi doctoral està subjecta a la llicència ***Reconeixement- NoComercial – CompartirIgual 4.0. Espanya de Creative Commons***.

Esta tesis doctoral está sujeta a la licencia ***Reconocimiento - NoComercial – CompartirIgual 4.0. España de Creative*** **Commons**.

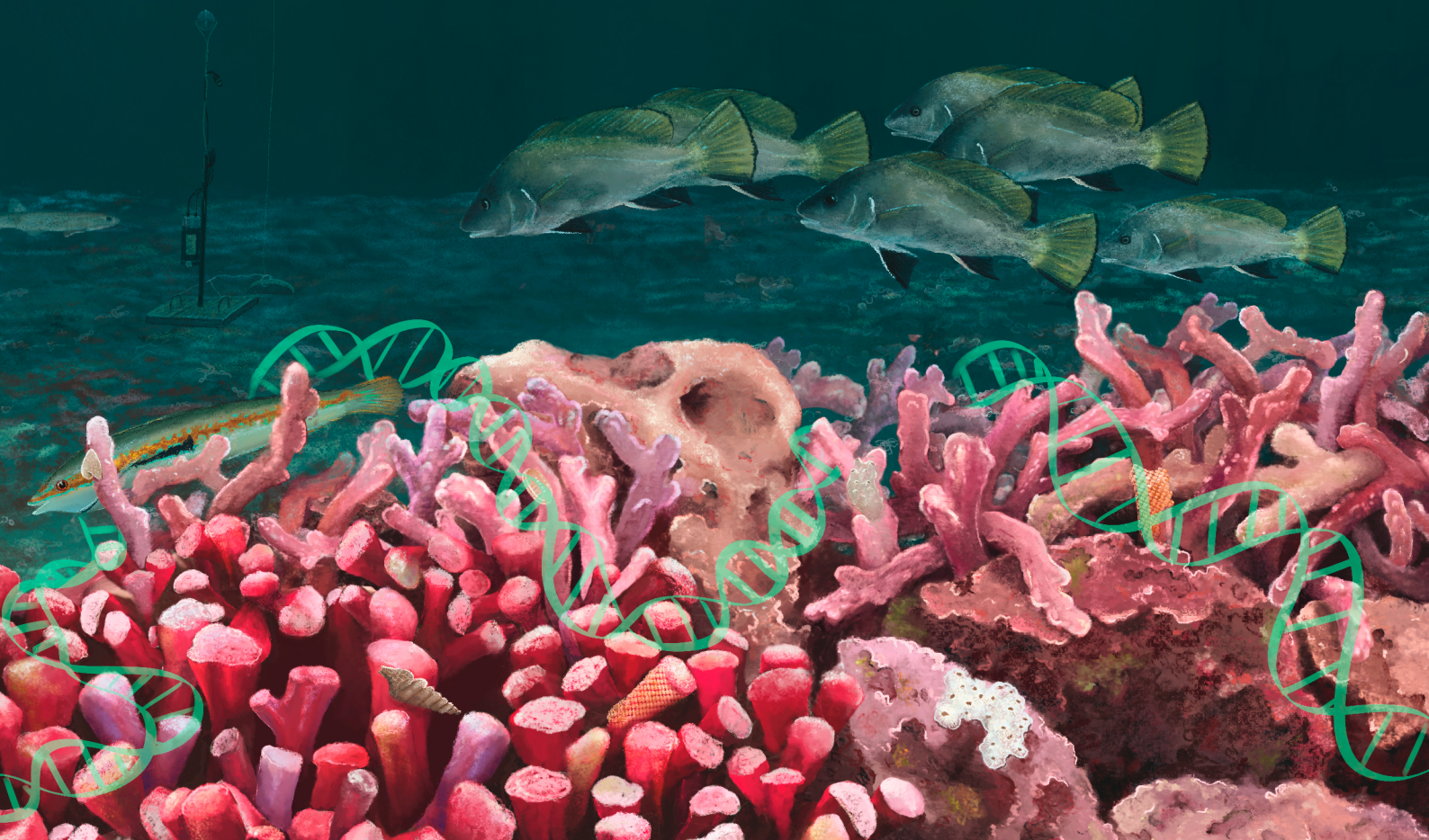
This doctoral thesis is licensed under the ***Creative Commons Attribution-NonCommercial-ShareAlike 4.0. Spain License***.

Rhodolith beds in the Menorca Channel

Taxonomic diversity, structural complexity, and monitoring strategies for conservation

Andrea Cabrito Rubau

Ph.D. Thesis 2025



UNIVERSITAT DE BARCELONA
Facultat de Ciències de la Terra

Fons de rodòlits del Canal de Menorca: Diversitat taxonòmica, complexitat estructural i estratègies de seguiment per a la conservació

Andrea Cabrito Rubau

2025

Rhodolith beds in the Menorca Channel: taxonomic diversity, structural complexity, and monitoring strategies for conservation

Andrea Cabrito Rubau

Thesis presented to obtain the Doctoral degree by the University of Barcelona (UB), Ph.D. Program in Marine Sciences

Ph.D. Advisors:

Dr. Francesc Maynou Hernández
(Institut de Ciències del Mar, CSIC)

Dra. Silvia de Juan Mohan
(Instituto Mediterráneo de Estudios Avanzados, CSIC)

Academic tutor:

Dra. Creu Palacín Cabañas
(Universitat de Barcelona, UB)

2025

The present thesis was conducted in the Institut de Ciències del Mar (ICM-CSIC, Barcelona, Spain) associated to the project MaCoBioS (Marine Coastal Ecosystem Biodiversity and Services in a Changing World. EU H2020 contract nº 869710). This thesis acknowledges the 'Severo Ochoa Centre of Excellence' accreditation (CEX2019-000928-S) to the ICM-CSIC and the 'Maria de Maetzu' accredited to the IMEDEA-CSIC (CEX2021-001198).

Recommended citation:

Cabrito, A. (2025). Rhodolith beds in the Menorca Channel: taxonomic diversity, structural complexity, and monitoring strategies for conservation. Ph.D. Thesis, University of Barcelona.

Design of the main and back covers: Joan Mir Arguimbau

Credit illustrations in covers from Chapter 2.1 to 2.4 and Anex I and II: Joan Mir Arguimbau

“ The cure for anything is salt water:
sweat, tears or the sea.”

Karen Blixen.

Acknowledgments – Agradecimientos – Agraïments

No sé si mai em vaig parar a prendre consciència del que representava fer una tesis doctoral ni si era el camí que volia seguir. El que si que tinc clar és que la curiositat que sempre he dut dins és el que ha fet que la ciència em mogui amb passió i em faci qüestionar-me i avaluar-me constantment. Si he arribat fins aquí i he acabat fent la tesis ha estat gràcies a les dues persones que van apostar per mi tot i no tenir una beca pre-doctoral i em van empènyer en aquesta aventura, els qui m'han dirigit la tesis. **Silvia**, encara recordo la primera "entrevista" que vaig fer amb tu, on ja em vas deixar caure la possibilitat de fer una tesis i el que et vaig respondre. Doncs no només vas aconseguir que em sentís com a casa sinó que estava aprenent tant de tu i de forma tan ràpida, que no et va ser massa difícil fer-me agafar ganes de tirar endavant la meva pròpia tesis. Sempre t'estaré molt agraïda per tota la confiança dipositada en mi i per la oportunitat que em vas brindar. Ha estat un plaer ser una de les teves primeres doctorands! **Francesc**, gràcies per no tallar-me mai les ales, per donar-me la llibertat que m'has donat sempre de preguntar-me, tenir idees boges i buscar la forma de dur-les a terme. Gràcies per tot el suport que m'has donat constantment. No només has fet d'aquest camí una autèntica aventura i m'has ajudat i ensenyat un munt, sinó que no has parat de nodrir les meves ganes d'aprendre i conèixer empenyent-me a viatjar, fer congressos, cursos i fins i tot unes opos! Realment el meu creixement durant aquests anys ha estat increïble i això es gràcies a haver tingut uns directors com vosaltres. Gràcies de tot cor als dos!

No ha estat un camí fàcil però se'ns dubte molt enriquidor i, en part, es gràcies a totes les persones amb qui he col·laborat i amb qui he compartit, durant aquest temps. **Montse**, llàstima que no vaig ser a temps d'embarcar-me amb tu a la aventura de la campanya de CriMa on segur que hagués après encara més del que ja vaig aprendre treballant prop teu. Gràcies per la teva constància i per ser allà sempre que se't necessita. Només nosaltres sabem el que va representar ser "los ojos del ROV". També m'agradaria agrair el suport que em van donar tant la **Sara** com la **Ruth** durant aquells mesos, així com tot el temps dedicat al SEM d'en **José Manuel**. Moltíssimes gràcies a tots, va ser un paler i tenim un llibre! Menció especial a la millor "partner in crime" des de CriMa, fins ara. **Laia**, tu ets d'aquelles persones que haurien de ser a cada paràgraf: companya de "fenya", de tesis, de campanyes, de congressos i de vida, doncs també t'has convertit en una amiga indispensable! Crec que si he pogut arribar fins aquí, en part, ha estat perquè t'he tingut "a prop". Tinc moltíssima sort d'haver coincidit amb tu i et trobo molt a faltar (veu nostre). I recorda: no tenim paraula, cap de les dues anava a fer la tesis i aquí ens tens! Jejeje! T'estimo molt!

Darrere d'una tesis on hi ha hagut mostrejos i campanyes, s'hi amaga la col·laboració i ajuda de moltíssima gent. M'agradaria començar agraint al projecte MaCoBioS per la contractació d'aquests anys i perquè començar en un projecte europeu m'ha donat la oportunitat de conèixer i col·laborar amb grans persones. **Remy** and **David**, thank you very much for your support and help. It has been a real pleasure to work with you! **Cindy** and **Ewan**, you guys are great, you have been the soul of MaCoBioS

project! Thank you for the support in the fieldwork in the Menorca Channel, for the interest shown at all times in my research and for encouraging me to participate at UNESCO, despite my stage fright. **Raphael** and **Loïc** I don't forget you, thank you very much for the days of sampling in Mallorca, for the little moments on the beach and the excursions in the mountains, I had a great time with you during these days! And to you, my dear **Géraldine**, who helped me sort the rhodoliths for hours and hours, I couldn't be more grateful, it was a real pleasure to meet you! Las campañas en el Canal de Menorca, los nudos marineros, el mal tiempo, nuestra seguridad, la de las muestras y los aparatos no podrían haber estado en mejores manos que en las tuyas, patrón. **Guillermo**, sin ti y la Rodman no hubiese sido posible y por ello quiero darte las gracias. Per últim, en recordar les campanyes, no puc deixar d'agrair a l'Hotel Amorós i, particularment a tu **Marga**, que no només ens vas fer sentir com a casa sinó que ens vas donar tot de facilitats i has seguit mantenint l'interès per la nostra recerca i el contacte, ets la millor!

Voldria agrair també a la resta de persones que han col·laborat amb mi durant aquesta tesis i que m'han ajudat d'alguna manera a tirar la feina endavant o a enriquir-me aprenent noves tècniques que aplicar en un futur. A la part del grup de l'IMEDEA, **Maria del Mar** i **Chema**, moltes gràcies per l'ajuda ja sigui obrint i mostrejant cores, a la Rodman o preparant boles de pasta de sardina, heu fet que les meves estades a Mallorca fossin molt més divertides! Quiero agradeceros también a vosotros, **Hilmar** y **Andrés**, ya que ambos me habéis prestado atención, ayuda y habéis sido una mano amiga con la que tener debates científicos interesantes. A ti **Viviana**, por aceptarme de visita en Coruña, enseñarme todo lo que llegas a saber en taxonomía de rodolitos, por las conversaciones, los ánimos, los consejos y las oportunidades, pero, en especial, por tu tiempo. I would also like to thank **Sara Kaleb** and **Annalisa Falace** who, without knowing me, decided to include me in their work on *Sporolithon* and gave me the opportunity to do my first taxonomic work neotyping a species. I am really grateful, it was a real honour. Als meus dos solets del CEAB, **Jesús** i **Elena**, gràcies per la paciència explicant-me les coses i per deixar-me fer amb vosaltres les primeres llibreries de metabarcoding, he après molt de vosaltres i tinc ganes de seguir aprenent. Soc conscient que us dec encara moltes birres jejej! A l'**Owen** i en **Xavi Turón**, milions de gràcies per deixar-me venir a aprendre amb vosaltres, per obrir-me les portes i per posar-ho tot tant fàcil. I a tu **Marc**, gràcies per la paciència (prometo que no trigo en treure't els Cores del congelador) i, sobretot, gràcies per aquell cafè on va sorgir la idea de fer els vibrocores, una bona aventura tot plegat!

Han estat tres anys i mig intensos com doctoranda però he tingut la sort de ser en un centre on m'han fet sentir que som una gran família i m'han recolzat i animat en tot moment, començant pel moment en el que vaig decidir fer les oposicions. Es per això que vull agrair a tots els **companys que ens vam presentar junts a les opos**, gràcies per el recolzament, per el traspàs d'apunts, la confiança i el bon rotllo que va haver en tots i cadascun dels viatges a Madrid i dels exàmens. Si us plau, hem de celebrar-ho d'una vegada! **Joan Mir**, a tu també vull agrair-te les estones junts, els congressos, el suport i els

consells però, sobretot, que m'hagis fet els dissenys de portades preciosos que m'has fet per aquesta tesis, ets un crack! A la **Silvia Joly** per ser la millor al laboratori i tenir sempre una resposta o un consell que donar-me en els moments de drames on les PCRs decideixen no funcionar. A la **Mercedes** que m'ha aguantat al despatx del davant fent la boja, amb la música a tope i que m'ha deixat reactius i puntes de pipeta o el que fes falta sempre que ho he necessitat. A mi compi de despacho **Cristina** que, aunque a veces hable sola (jejeje), tiene un corazón enorme y no ha parado de ayudarme y aconsejarme en todo. Al **Pere Puig** amb qui vaig començar una relació de mentor-mentee que a mi m'ha ajudat moltíssim, fent-me agafar perspectiva i donant-me consells. A tots ells, i en general a tot el departament de recursos: moltes gràcies!

Evidentment, tinc unes paraules especials per al meu grupet de "científicos fiesteros" i pel meu "consejo de sabios" i aniré un per un però no sense deixar abans per escrit el Aquelarre que aquells que vam pujar a Andorra vam crear, i que diu així (no li busqueu sentit): "*La perra del arcobaleno mecía un cazzo de mucha gente traumatizada por un equipo internacional, médico-forense, español, y después, fue PVC mientras comía almendras con sal marina, debajo de su marido muerto stecchito por violencia doméstica entre su molle andorrana, aragonesa, imbécil de Tarragona centro, durante un discurso católico medieval televisado y, M.R estaba abierto de piernas, completamente mojado*". Ahora sí, empiezo por mis niñas bonitas. **Silvia**, no sé qué hubiese sido de mí, estos años, sin ti tan cerca. Siempre estuviste ahí, en el lab, en las cenas, en las cervezas, en las duras y en las maduras. No tengo palabras para decirte cuanto te agradezco todo el soporte moral que me has dado. Siempre seremos el "dream-team" de organizar eventos. ¡Gracias por existir! A la **Tosca**, per ser la tia més tot-terreny que conec, per acompanyar-me en la meva bogeria i apuntar-se a tots els plans sense pensar, perquè amb tu he rigut i he ballat el que no està escrit, perquè per a mi no ets una més i vull que sàpigues que aquí tens casa teva. Gràcies per ensenyar-me l'autèntic significat de "gezellig"! A **Noelia**, quien, entre cafés y horas infinitas de conversaciones, ha ejercido de «mami» en la ciencia, mostrándome el camino, secándome las lágrimas, no soltándome nunca la mano y demostrándome lo que es la ciencia más honesta que existe. ¡Gracias por todo tu soporte, has sido indispensable! A la mia sorella italiana, **Elena**, sei stata senza dubio la cosa migliore di MaCoBioS. Grazie per tutti i momento passati insieme a Barcellona, Venezia, Andorra o Parigi. Trovarti è stato un dono prezioso perché non sapevo di poter capire qualcuno così bene in così poco tempo. Grazie per continuare nella mia vita! A todas vosotras: ¡os quiero mucho! Quiero agradecer también a mis niños favoritos que han aguantado a estas locas y han sido parte de mi soporte diario. **Rodrigo**, aún recuerdo cuando llegaste y pensé que alguien tan serio como tu iba a durar dos días en un grupito como el nuestro. ¡Que equivocada estaba! Gracias por todos los momentos que has estado ahí para soportar mis quejas, por todos los consejos y, sobre todo, gracias por prepararme el café por la mañana y por darme bogavantes ¡jejej! A **Giulio**, mi ricitos de oro, gracias por aparecer de golpe para darme la frescura y alegría que me diste. Echo mucho de menos entendernos con una sola mirada porque rey, creo que tú y yo somos los maestros de la picardía y de la bromita maliziosa. Grazie

per essere nella mia vita, ma ricorda: è un mondo difficile. Al nostre "sugar-baby" del grup, **Diego**, no sé ni quan et vam adoptar però has estat una peça indispensable del meu dia a dia. No se com agrair-te tants cafès, birres i pitis junts, tant parlar de tot, de les nits d'insomni i del que ens preocupa a la vida. Gràcies per ser "si a tot sempre". A mi queridísimo **FAFA**, contigo no me bastan 4 líneas para agradecerte todo, pero a estas alturas poco puedo decir que no sepas ya. Gracias por aparecer en mi vida y por dejarme conocerte, por todo lo que me has enseñado, ayudado y corregido y, sobre todo, gracias por seguir ahí. Magari seguir coincidiendo en el futuro. ¡Que Spiderman y Neptuno estén contigo siempre que les necesites! A todos vosotros chicos: ¡os quiero mucho! No me olvido de mencionar a nuestros proveedores de gasolina en formato de fermentado de cebada o de cafeína con hielo, ¡gracias a la Yammi, la Guingueta, el Monchos y la Terraza de Marina por hidratarnos siempre!

No puc no tenir en compte a aquelles persones que han esdevingut essencials durant aquests anys aportant-me un suport moral i logístic indispensable, doncs part d'aquesta tesis també és gràcies al vostre ajut. **Tanit** gràcies per tot el suport i tota l'ajuda que m'has ofert. Tenir-te a Barcelona i a Mallorca aquests anys ha contribuït a que no em sentís ni trobés sola. Gràcies també a la **Irene** per totes les xerrades juntes i a tota la família **Planells-Inglada** a qui ja sento com família adoptiva mallorquina. En especial a tu, **Helena**, que no només m'has ofert allotjament, sinó que m'has deixat el cotxe, m'has cuinat, m'has vingut a recollir i el millor de tot, t'has interessat per la meva ciència. Sou les millors! Gracis de tot cor.

Si molts dies he aconseguit no ofuscar-me i seguir endavant, ha estat gràcies a poder-me evadir al mar. Bussejar m'ha curat sempre qualsevol mal estar, però fer-ho acompanyada dels millors tritons que una sirena podria tenir encara ha estat millor. Gràcies **Toni** per totes les vegades que m'has proposat bussejar per veure'ns i fer-me saber que estava desconnectada, sempre seràs el "sexy-instructor" més guay del món! Gracias **Nacho** por cada uno de los momentos y buceos contigo. Sin duda, volvería a elegirte para perderme a 40 m de profundidad. Gràcies **Ivan** per ser un "motivat" de la vida i motivar-me a mi en pensar la següent escapada. Gràcies també al **Miquel Pontes** i a tot el grup **ViMar** per ser casa, per mantenir la família unida i per seguir endavant amb els mostrejos. Sortir amb vosaltres m'ha carregat les piles i m'ha donat forces a continuar. No em puc deixar als "cracks" de BCN diving club, **Òscar Cobo** i **Bernat Saumell,** gràcies per confiar en mi des del primer dia i per inclourem en aquesta aventura. No teniu ni idea de com m'han enriquit, motivat i ajudat a seguir cadascuna de les reunions amb vosaltres. També al **C.P.V.B.** i als companys de rem tant de l'**ICM** com dels **sèniors** i a la **Teresa**, les sortides de rem amb vosaltres m'han anat genial per desconnectar i agafar forces els últims mesos.

Parlant d'esbarjo i coses que m'han ajudat a desconnectar, m'agradaria agrair també al grup **Zetak** a qui he vist actuar 6 vegades durant la tesis. Eskerrik asko abesti batekin transmititzen duzun guztiagatik. Aaztiyen da zalantzarik gabe nire diskorik gogokoena. Eskerrik asko zure sustraiei, lurrari eta zure hizkuntzari kantatzeagatik. Behar nuen energia guztia eman didazu!

Recordo perfectament quan vaig tenir clar que estudiaria biologia i va ser durant la ESO quan vaig tenir la sort de ser alumne del **Jordi Galbany** i l'**Alícia**, és per això que vull agrair-vos la passió que em vau transmetre per la ciència. Gràcies! Els anys d'universitat van ser intensos però no haguessin estat el mateix sense aquelles persones que van fer d'aquell camí un camí únic. **Karen** y **Anabel**, todo empezó con vosotras decidiendo si bata o bota, gracias por ser las mejores compañeras que podía tener, por cada uno de los momentos y lecciones aprendidas, pero, sobre todo, gracias por seguir estando ahí. ¡Os quiero mucho! En especial a ti Capri (y a tus Bubbies), gracias por tu incondicionalidad, por tu forma de querer y cuidar y por ser irremplazable. Al meu Gru **Carles**, que em va acollir com minion ja fa molts anys i no m'ha deixat mai sola i a l'**Alba** per tota l'ajuda i coneixement que m'heu transmès al llarg d'aquests anys. Serà un plaer veure créixer a la **Cora** i em feia il·lusió que aquesta sigui la primera tesis en la que apareix el seu nom (jejeje!). A mi trío de personas favoritas del máster, **Júlia**, **Anna** y **Natxo**, nada hubiese sido lo mismo sin vosotros, gracias por aparecer en mi vida para hacerla mucho más interesante, ¡tenemos que vernos más! Tota aquesta aventura i passió per la taxonomia va començar amb tu **Manuel Ballesteros**, però amb nudibranquis. Gràcies per haver-me seguit la pista tots aquests anys posteriors al TFG, estic desitjant reprendre tots aquells treballs que tenim a mitges, t'ho prometo! A la **Creu Palacín**, milions de gràcies per absolutament tot: per posar-me en contacte amb la Silvia, per fer-me de tutora UB durant la tesis, per respondre sempre tant ràpid i estar sempre tant disposada a ajudar, ets la millor! A la **Cristina Linares**, gràcies per tot el que vaig aprendre amb tu durant el TFM i per haver seguit allà al cap dels anys per escoltar-me i aconsellar-me sempre. Evidentment, no podies faltar tu, company de mar, de Turies i de converses llargues i profundes. **Sergi**, vas començar sent professor, m'has fet de mentor durant totes les etapes i t'has convertit en amic i en família. Gràcies per absolutament tot, sobretot, per no deixar que em fes "trampes al solitari". Tinc ganes de pujar les veles de nou amb tu!

Sempre he dit que per saber on anem a vegades cal mirar d'on venim. Res de tot això hagués estat possible sense el suport constant «de casa», el de família i amics. Aquesta tesis també ha estat gràcies a tots vosaltres que no m'heu deixat caure mai. A la meva germana de sempre i per sempre, **Natàlia**, moltíssimes gràcies per ser-hi incondicionalment des de fa 30 anys. Sense el teu suport i les infinites hores que t'he "plorat" i m'has recolzat, estic segura que hagués volgut llençar la tovallola molts cops. Gràcies per demostrar-me que res ens separarà! I a tu **Miki**, gràcies per mostrar tot l'interès que mostres cada cop que explico alguna cosa del mar, per recolzar-me i per recordar-me "que soc una crack" quan més m'ha calgut sentir-ho. Gràcies de tot cor als dos per ser casa i ser la família que una tria, us estimo molt! A la **iaia Dolors** i al **Pepe** voldria agrair-los l'admiració amb la que sempre han escoltat les meves historietes i la paciència quan he vingut menys sovint per feina i a tu padrí, tota la passió que m'has transmès pel mar. A tu **iaia Pepi**, m'agradaria agrair-te la tossudesa, la franquesa i les ganes de viure, doncs son qualitats que he agafat de tu i que m'han dut a ser on soc. Gràcies per seguir-me cuidant des d'allà, iaiona. Al meu **tiet Ramón**, gràcies per sentir cada petita victòria amb la mateixa il·lusió o més

que nosaltres mateixos, per ser-hi sempre per donar un consell a temps i per voler brindar cada fita. A tota la meva família política que no s'han estalviat unes bones turres de part meva durant tots aquests anys, **Susana**, **Jose**, **Hèctor**, **Sara** i **Joel**, gràcies de tot cor per la paciència i per escoltar-me i animar-me sempre a seguir endavant, sou els millors! A tu **Miqui**, que tens la capacitat de fer-me riure com ningú ho fa i ets de les persones que més vegades m'ha dit "estic molt orgullós de tu". Vull que sàpigues que jo també estic molt orgullosa de tu, tete. Ets i sempre seràs el nen dels meus ulls! A tu, **mama** que sempre has cregut que arribaria lluny i cada cosa nova que he fet l'has seguit amb il·lusió i entusiasme. Per ensenyar-me a apreciar la bellesa en les petites coses i a ser tant delicada i detallista com ho ets tu. Gràcies per dur-me al món i animar-me a que me'l mengi com una guerrera! A tu **papa**, perquè si alguna persona m'ha agafat de la mà quan tenia por, m'ha assecat les llàgrimes quan no podia més i m'ha arrancat un somriure a temps, aquest has estat tu. Gràcies per ser el millor confident, per seguir tant de prop tot el procés i per no deixar-me mai sola. Sense tu, ni seria qui soc ni seria on soc. Gràcies de tot cor (i moltes gràcies pels tuppers setmanals!). Us estimo moltíssim, família! Ah! No m'oblido de vosaltres **Pipa** i **Chía**, les meves rates preferides, gràcies per acompanyar-me aquest últim any i omplir-me la casa d'amor i les nits de soroll, sou fantàstiques.

Finalment, però no menys important, m'agradaria mostrar el meu més sincer agraïment al meu company de vida. **Dani**, t'ha tocat la pitjor part, el dia a dia, veurem angoixada, eufòrica, patint, ansiosa, un alt i baix constant amb la tesis, amb la vida en general, amb el futur, amb tot. No només has estat a l'altura sinó que t'has passat el nivell. No puc imaginar-me millor persona amb qui decidir (com diem sempre), "complicar-me la vida". Gràcies per ser, per davant de tot el meu amic, gràcies per estimar-me de la manera més genuïna, per acompanyar-me, recolzar-me i animar-me en tot. Gràcies per seguir creixent i descobrint junts, per equivocar-nos, per parlar, per respectar, per compartir i, sobretot, per ser un equip. Gràcies per fer de la vida una autèntica aventura i per seguir-nos escollint a diari. Gràcies, de tot cor. T'estimo molt nudiset!

Ara si, per acabar amb la turra m'agradaria agrair-te a tu, **Andrea Cabrito.** Per seguir aquí, per no haver desistit tot i haver-t'ho plantejat molts cops. Per lluitar, per estar, per ser i per sentir com ho fas. Perquè t'agraeixes poc i hauries de fer-ho més i avui, toca. Gràcies per ser qui ets i per la perseverança, estic enormement orgullosa de tu i t'estimo molt.

Barcelona, c/ Besalú en silenci durant les nits.

Abril del 2025

Table of Contents

Abstract **1**

Resumen **2**

Resum **3**

SECTION I - GENERAL INTRODUCTION, OBJECTIVES AND METHODOLOGY. **5**

1.1. General Introduction 7

1.1.1. Rhodolith beds 7

1.1.2. Rhodolith- forming species identification 17

1.1.3. Mediterranean rhodolith beds 24

1.1.4. Traditional sampling methods in mesophotic benthic habitats. 27

1.1.5. Knowledge gaps. 28

1.2. Objectives and Hypothesis 30

1.3. General Methodology 32

1.3.1. Menorca Channel as study area 32

1.3.2. Sampling and fieldwork – MaCoBioS project. 34

1.3.3. Data analysis 40

References Section I 54

SECTION II - RESULTS **73**

2.1. **CHAPTER I:** Morphological insights into the three-dimensional complexity of rhodolith beds 75

Abstract 77

2.1.1. Introduction 78

2.1.2. Methodology 79

2.1.3. Results 85

2.1.4. Discussion 92

Acknowledgments 95

References 95

Supplementary Material 103

2.2. CHAPTER II: Taxonomic complexity and conservation implications of Mediterranean mesophotic rhodoliths beds. 109

Abstract 111

2.2.1. Introduction 112

2.2.2. Methodology 115

2.2.3. Results 118

2.2.4. Discussion 128

Acknowledgments 130

References 130

Supplementary Material 141
2.3. **CHAPTER III**: Neotypification of the *Sporolithon mediterraneum* Heydrich (Sporolithales, Corallinophycidae, Rhodophyta) and the status of *Sporolithon* in the Mediterranean Sea. 159
Abstract 161
2.3.1. Introduction 162
2.3.2. Methodology 163
2.3.3. Results 164
2.3.4. Discussion 168
Acknowledgments 172
References 172
Supplementary Material 177
2.4. **CHAPTER IV**: Non-extractive fish diversity assessment in Mediterranean rhodolith beds.. 185
Abstract 187
2.4.1. Introduction 188
2.4.2. Methodology 190
2.4.3. Results 197
2.4.4. Discussion 204
Acknowledgments 207
References 208
Supplementary Material 216
2.5. Summary of the results 231
SECTION III - SUMMARY OF DISCUSSIONS 237
SECTION IV - SUMMARY OF CONCLUSIONS 253
SECTION V - SUMMARY OF CONTRIBUTIONS 259
APPENDIX I – ORIGINAL PUBLISHED PAPERS AND DRAFTS BELONGING TO THIS THESIS……...267
APPENDIX II – ORIGINAL PUBLISHED PAPERS AND DRAFTS THAT DO NOT FORM PART OF THIS THESIS BUT ARE LINKED……...309

Abstract

Rhodolith beds, formed by free-living calcareous red algae, represent ecologically valuable and structurally complex habitats that contribute significantly to benthic biodiversity and ecosystem functioning. Their intricate three-dimensional architecture provides refugia for other organisms, positioning them among the most important biogenic habitats in the marine realm. However, in the Mediterranean Sea, these habitats remain insufficiently characterized, both in terms of their structural complexity and species composition, which hampers the development of effective conservation and management strategies. This thesis investigates the ecological, taxonomic, and functional dimensions of rhodolith beds in the Menorca Channel (western Mediterranean), integrating morphological, molecular, and ecological approaches across four complementary studies.

First, I assessed rhodolith morphological diversity using three-dimensional analyses and comparing core zones of the bed (high rhodolith density) to adjacent areas with lower density. The results revealed that rhodoliths in core areas exhibited more complex morphologies, larger size, and higher interstitial space—key indicators of habitat complexity that are often underestimated by traditional two-dimensional methods. Second, I addressed the knowledge gap in species composition by combining classical taxonomy with molecular techniques, revealing a cryptic diversity of at least 15 rhodolith-forming species. These findings contrast with current Habitats Directive, which focus on just two species predominant in the Atlantic, and underscore the need to revise conservation policies to reflect the true diversity of rhodoliths in the Mediterranean. Third, I clarified the taxonomic status of the poorly known species *Sporolithon mediterraneum*, for which I designated a neotype based on a specimen from mesophotic depths of the Tyrrhenian Sea. Morphological and molecular analyses confirmed the distinctiveness of this species from other *Sporolithon* taxa and established a robust framework for future identifications. Finally, I explored the application of three non-intrusive monitoring tools—environmental DNA, underwater video, and passive bioacoustics—to characterize fish assemblages associated with rhodolith beds. Their combined use revealed high species richness, including endangered and cryptic species, while also capturing variability related to habitat heterogeneity and trawling exposure.

Altogether, this thesis highlights the underestimated structural and taxonomic complexity of rhodolith beds in the western Mediterranean and emphasizes the value of integrating multidisciplinary tools to understand and monitor these vulnerable habitats. The results contribute to the refinement of habitat assessments, species inventories, and conservation frameworks, with direct implications for regional marine biodiversity management and the development of non-destructive monitoring strategies.

Key Words: Coralline algae, rhodoliths, maërl, biodiversity, morphometrics, molecular approach, taxonomy, monitoring techniques.

Resumen

Los lechos de rodolitos, formados por algas rojas calcáreas de vida libre, representan hábitats ecológicamente valiosos y estructuralmente complejos que contribuyen de manera significativa a la biodiversidad bentónica y al funcionamiento de los ecosistemas. Su arquitectura tridimensional proporciona refugio a otros organismos, situándolos entre los hábitats biogénicos más importantes del medio marino. En el mar Mediterráneo, su complejidad estructural y su composición específica siguen estando poco caracterizadas, dificultando el desarrollo de estrategias efectivas de conservación y gestión. Esta tesis investiga la dimensión ecológica, taxonómica y funcional de los fondos de rodolitos en el Canal de Menorca (Mediterráneo occidental), integrando enfoques morfológicos, moleculares y ecológicos a través de cuatro estudios complementarios.

Primero, evalúo la diversidad morfológica de los rodolitos mediante análisis tridimensionales comparando las zonas centrales del lecho (alta densidad de rodolitos) con las áreas adyacentes de menor densidad. Los resultados revelan que los rodolitos en las zonas centrales presentan morfologías más complejas, de mayor tamaño y espacio intersticial —indicadores clave de la complejidad del hábitat que se subestiman con los métodos tradicionales bidimensionales. Además, contribuí al conocimiento sobre la composición específica combinando taxonomía clásica con técnicas moleculares, revelando una diversidad críptica de al menos 15 especies formadoras de rodolitos. Estos hallazgos contrastan con la Directiva Habitats, que se centra únicamente en dos especies predominantes en el Atlántico, y subrayan la necesidad de revisar las políticas de conservación para reflejar la verdadera diversidad de rodolitos del Mediterráneo. Además, clarifiqué el estatus taxonómico de *Sporolithon mediterraneum*, y designé el neotipo basado en un ejemplar de profundidades mesofóticas del mar Tirreno. Los análisis morfológicos y moleculares confirmaron la singularidad de esta especie con respecto a otros taxones del género *Sporolithon* y establecieron un marco sólido para futuras identificaciones. Por último, exploré la aplicación de tres herramientas de monitoreo no intrusivas —ADN ambiental, vídeo submarino y bioacústica— para caracterizar la comunidad de peces asociada a los lechos de rodolitos. Su uso combinado reveló una alta riqueza específica, incluyendo especies amenazadas y crípticas y captó variabilidad relacionada con la heterogeneidad del hábitat y la exposición a la pesca de arrastre.

Esta tesis resalta la complejidad estructural y taxonómica de los lechos de rodolitos, a menudo subestimada, del Mediterráneo occidental y destaca el valor de integrar herramientas multidisciplinares para comprender y monitorear estos hábitats. Los resultados contribuyen a mejorar las evaluaciones de hábitat, los inventarios de especies y los marcos de conservación, con implicaciones directas para la gestión de la biodiversidad marina regional y el desarrollo de estrategias de monitoreo no destructivas.

Palabras clave: Algas coralinas, rodolitos, maërl, biodiversidad, morfometría, enfoque molecular, taxonomía, técnicas de seguimiento.

Resum

Els llits de rodòlits (o grapissar), formats per algues vermelles calcàries de vida lliure, representen hàbitats ecològicament valuosos i estructuralment complexos que contribueixen de manera significativa a la biodiversitat bentònica i al funcionament dels ecosistemes. La seva arquitectura tridimensional proporciona refugi a altres organismes, situant-los entre els hàbitats biogènics més importants del medi marí. En la mar Mediterrània, la seva complexitat estructural i composició específica continuen estant poc caracteritzades, dificultant el desenvolupament d'estratègies efectives de conservació i gestió. Aquesta tesi investiga la dimensió ecològica, taxonòmica i funcional dels fons de rodòlits en el Canal de Menorca (Mediterrani occidental), integrant enfocaments morfològics, moleculars i ecològics a través de quatre estudis complementaris.

Primer, avaluo la diversitat morfològica dels rodòlits mitjançant anàlisis tridimensionals comparant les zones centrals del llit (amb alta densitat de rodòlits) amb les àrees adjacents de menor densitat. Els resultats van revelar que els rodòlits en les zones centrals presentaven morfologies més complexes, més grandària i més espai intersticial —indicadors clau de la complexitat de l'hàbitat que se subestimen amb els mètodes tradicionals bidimensionals. En segon lloc, contribueixo al coneixement sobre la composició específica combinant la taxonomia clàssica amb tècniques moleculars, revelant una diversitat críptica d'almenys 15 espècies formadores de rodòlits. Aquestes troballes contrasten amb la Directiva Hàbitats, que es centra únicament en dues espècies predominants a l'Atlàntic, i subratllen la necessitat de revisar les polítiques de conservació per a reflectir la veritable diversitat dels rodòlits del Mediterrani. A més, aclareixo l'estatus taxonòmic de *Sporolithon mediterraneum*, i designo el neotip basat en un exemplar de fondària mesofòtica de la mar Tirrena. Les anàlisis morfològiques i moleculars van permetre confirmar la singularitat d'aquesta espècie respecte a altres tàxons del gènere *Sporolithon* i establir un marc sòlid per a futures identificacions. Finalment, exploro l'aplicació de tres eines de seguiment no intrusives —ADN ambiental, vídeo submarí i bioacústica— per a caracteritzar la comunitat de peixos associada als llits de rodòlits. El seu ús combinat va revelar una alta riquesa específica, incloent-hi espècies amenaçades i críptiques i va captar variabilitat relacionada amb l'heterogeneïtat de l'hàbitat i l'exposició a la pesca d'arrossegament.

Aquesta tesi ressalta la complexitat estructural i taxonòmica dels llits de rodòlits, sovint subestimada, del Mediterrani occidental i destaca el valor d'integrar eines multidisciplinàries per a comprendre i fer el seguiment d'aquests hàbitats. Els resultats contribueixen a perfeccionar les avaluacions d'hàbitat, els inventaris d'espècies i els marcs de conservació, amb implicacions directes per a la gestió de la biodiversitat marina regional i el desenvolupament d'estratègies de seguiment no destructives.

Paraules clau: Algues coral·lines, rodòlits, maërl, biodiversitat, morfometria, enfoc molecular, taxonomia, tècniques de seguiment.

SECTION I

GENERAL INTRODUCTION, OBJECTIVES AND METHODOLOGY.

1.1. General Introduction

1.1.1. Rhodolith beds

Coralline algae are a highly diverse and globally distributed group of red macroalgae (Rhodophyta, Corallinophycidae) characterized by calcified cell walls. They inhabit both marine and freshwater environments (Jardim et al., 2022) and represent a benthic group with an extensive bathymetric range, reaching the limits of the photic zone (Littler et al., 1985; Irvine & Chamberlain, 1994; Riosmena-Rodríguez, 2017). Moreover, they exhibit remarkable adaptability, thriving under a wide range of environmental conditions, including variations in light, temperature, and hydrodynamics (Lugilde Yáñez et al., 2022; McCoy & Kamenos, 2015). This group comprises five orders within the subclass Corallinophycidae: Corallinales, Corallinapetrales, Hapalidiales, Rhodogorgonales, and Sporolithales. According to Lugilde Yáñez et al., (2022), these orders included approximately 35 genera and 775 species. Nowadays, these numbers are slightly higher due to the description of new genera such as *Thalassolithon* Trentin, Moschin & Moro, 2023, and *Boreolithothamnion* P.W. Gabrielson, Maneveldt, Hughey & V. Peña, 2023, as well as new species including some *Porolithon* species (Jeong et al., 2023), *Boreolithothamnion* species (Gabrielson et al., 2023a), *Phymatolithon* species (Liu & Lin, 2023), *Roseolithon* species (Gabrielson et al., 2023a), *Thalassolithon* species (Trentin et al., 2023) and *Sporolithon* species (Gabrielson et al., 2023b). In recent decades, coralline algae have received increasing attention in the scientific literature (**Fig.1.1.1**). This is due to their global importance in coastal ecosystem function and their high sensitivity to projected environmental changes (McCoy & Kamenos, 2015; Jardim et al., 2025).

Coralline algae have calcified thalli with low growth rates of approximately 0.01 – 5 mm yr^{-1} depending on the species and environment (Adey & McKibbin, 1970; Blake & Maggs, 2003; Steller et al., 2007). The process by which these algae calcify has not yet been studied in depth, although Littler (1976) suggested several hypotheses for the calcification process related to hydrodynamics, herbivory pressure, abrasion resistance and/or protection against epiphytic species and light intensity. In addition, Schubert et al. (2021) showed the importance of morphology in the calcification process by observing differences between morphotypes, as well as between different branch or protrusion characteristics.

Traditionally, and based on their external morphology, coralline algae are separated in two groups: (i) geniculate or jointed algae (erect fronds with uncalcified segments known as genicula) and (ii) non-geniculate or non-jointed algae (thalli lacking uncalcified segments) (Johansen, 1981; Irvine & Chamberlain, 1994; Lugilde Yáñez et al., 2022). This morphological distinction does not align with the phylogeny of coralline algae. The order Corallinales includes both geniculate and non-geniculate taxa, suggesting evolutionary reversals in some taxa to the ancestral non-geniculate form (Hind et al., 2018). Non-geniculate coralline algae can exhibit either a free-living or encrusting morphology, with the latter

appearing as flat structures or featuring branch-like projections (Irvine & Chamberlain, 1994). While some species are exclusively encrusting, others can adopt both free-living and encrusting forms (Hernandez-Kantun et al., 2015). This morphological variability has led to the proliferation of terms used to describe coralline algae. This is especially noticed in the lack of cohesion on free-living non-geniculate coralline algae terminology. As Jardim et al. (2025) reported, the European Red List of Habitats differentiates between the terms "maërl beds" for the Atlantic and "rhodolith beds" for the Mediterranean, even though both are defined as “sedimentary bottoms characterized by any morphology and species of unattached non-geniculate calcareous red algae” (European Commission et al., 2016). Interestingly, *Lithothamnion corallioides* (P.Crouan & H.Crouan) P.Crouan & H.Crouan, 1867 and *Phymatolithon calcareum* (Pallas) W.H.Adey & D.L.McKibbin ex Woelkerling & L.M.Irvine 1986, species commonly linked to the term "maërl" in the Atlantic, are explicitly identified in the European Red List as the primary species present in "Mediterranean rhodolith beds." Meanwhile, the latest OSPAR Benthic Habitats Commission report acknowledges maërl beds as habitats under threat and/or in decline but does not include rhodolith beds in its assessment (OSPAR, 2023).

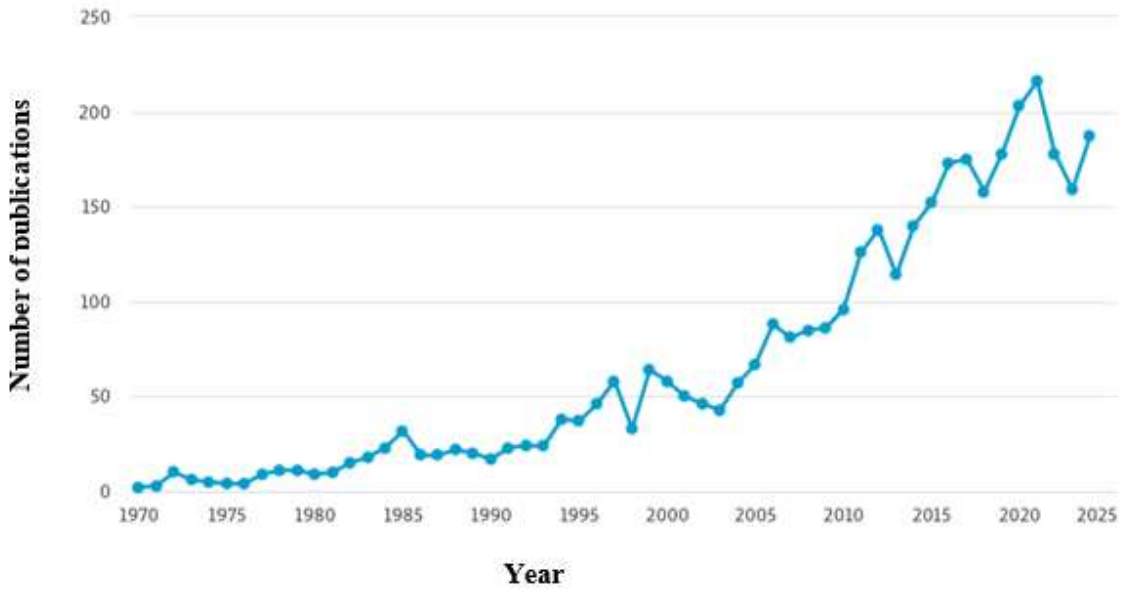


Fig.1.1.1. SCOPUS search for coralline algal publications during the period of 1970–2024. Search terms: TITLE-ABS-KEY (("coralline alga") OR ("coralline red alga") OR ("coralligene") OR ("coralligenous") OR ("maërl") OR ("maërl") OR ("rhodolite") OR ("rhodolith") OR ("rhodolithe")). Total number of publications = 3670.

To standardize the nomenclature, Jardim et al. (2025) proposed a morpho-functional organismic typology for coralline algae, as illustrated in **Fig.1.1.2**. According to this framework, the term rhodolith sensu stricto refers exclusively to nucleated nodules, while maërl sensu stricto encompasses only non-nucleated forms. In contrast, rhodolith sensu lato includes all nodular forms, and maërl sensu lato also incorporates non-nodular fragments.

In the Mediterranean, and specifically in the study area of this thesis—the Menorca Channel—, nodular, non-geniculate coralline algal forms are present, coexisting with other non-coralline calcifying red algal species and also covered by crustose coralline algae (CCA). These assemblages align closely with the description of rhodolith beds provided by Jardim et al. (2025) within the M1-Marine ecosystems classification, specifically M1.10 - Coralline algal beds. According to Jardim et al. (2025), rhodolith beds are defined as habitats composed of *"free-living nodules of non-geniculate coralline algae and non-coralline calcifying red algae"*.

Therefore, throughout this thesis, we will refer to the case study habitats as Rhodolith Beds (RBs).

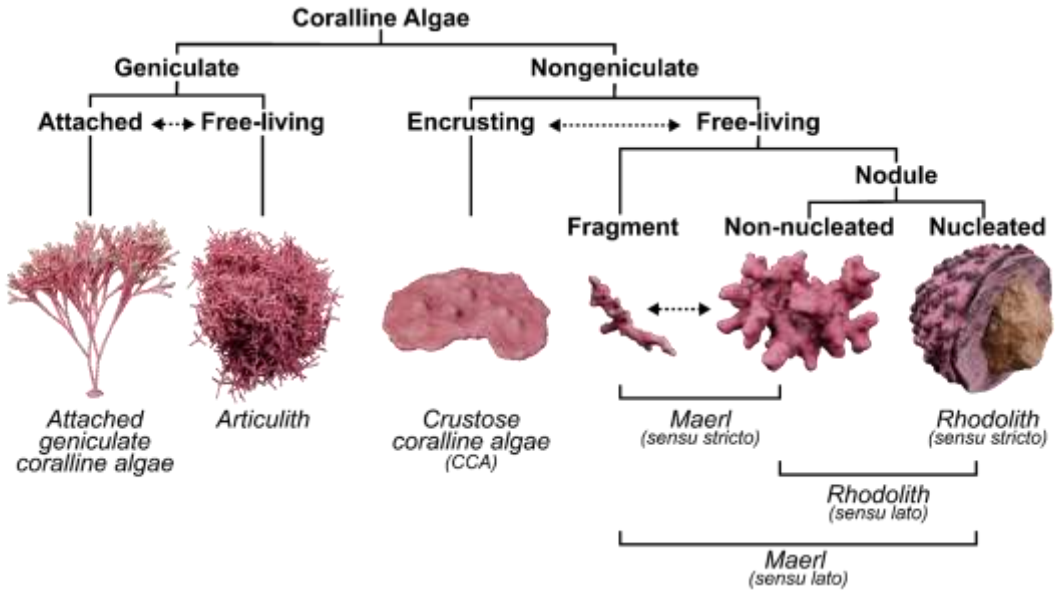


Fig.1.1.2. Proposed morpho-functional organismal typology for coralline algae. The morphologies are examples of the variety in growth forms. Arrows represent reproductive strategies that enable shifts between different types. Source: Jardim et al. (2025).

1.1.1.1. Distribution

RBs are among the most widespread marine habitats (Riosmena-Rodríguez, 2017; Rendina et al., 2022; Tuya et al., 2023). They are known to occur from the Arctic (Teichert, 2014) to Antarctica (Schwarz et al., 2005), and are particularly common in tropical regions, where they can cover large portions of the continental shelf (Brasileiro et al., 2016). In the Atlantic Ocean, they have been described along the coasts of Europe, including the British Isles, Brittany, and the Iberian Peninsula (Grall & Hall-Spencer, 2003), as well as on the Brazilian shelf, where they form extensive carbonate platforms (Amado-Filho & Pereira-Filho, 2012). In the Pacific, they have been described in the Gulf of California and along the coasts of Japan, where their development is closely linked to oceanographic conditions and nutrient availability (Steller et al., 2003).

RBs are distributed globally, occurring in a wide range of marine environments from shallow waters to mesophotic depths exceeding 100 m, depending on light penetration and water transparency (Foster, 2001). Their distribution is influenced by environmental factors such as light availability, hydrodynamic conditions, and sedimentation rates (Foster, 2001; Steller et al., 2003). They are particularly abundant in regions with stable substrates and adequate light penetration, where they contribute significantly to marine biodiversity and the carbon cycle (Schubert et al., 2024). It is known that RBs are mostly located around islands and capes, on top of submarine plateau, marine terraces, interisland or island-mainland channels and banks (Basso et al., 2017).

In the Mediterranean Sea, rhodoliths are common in sublittoral zones with oligotrophic waters and low sedimentation rates (Basso et al., 2016). The Menorca Channel is a notable hotspot, hosting diverse assemblages of coralline algae and associated fauna (Barberá et al., 2012a), where one of the most extensive RBs in the Mediterranean is found. However, knowledge of rhodoliths distribution in the Mediterranean remains limited, despite the ideal environmental conditions in the region for RBs beds development (Martin et al., 2014).

Understanding the spatial distribution, and its environmental drivers of RBs is critical for their conservation. These habitats not only support marine biodiversity but also provide essential ecosystem services, such as carbon sequestration and habitat provision (Tuya et al., 2023). Future research should focus on mapping their extent, refining predictive models, and addressing their vulnerability under changing environmental conditions.

1.1.1.2. Ecological importance

Coralline algae contribute to local biodiversity by shaping or transforming habitats, earning them the designation of ecosystem engineers (Foster, 2001; Pezzolesi et al., 2017). Like other species that create foundational habitats - such as forests, coral reefs, seagrasses, oyster reefs, mussel beds, saltmarshes, and seaweed communities- rhodoliths are considered foundation species (Altieri et al., 2007; Silliman et al., 2011). Foundation species are defined by their dominance in ecosystem biomass and their position at or near the base of networks of mutualistic or non-trophic interactions (Bulleri et al., 2024; Ellison, 2019). They are capable of defining ecosystems, controlling biological diversity and modulating critical ecosystem processes (Ellison, 2019; Pereira & da Gama Bahia, 2021). As highlighted by Bulleri et al. (2024), these species create physical structures that facilitate the establishment and persistence of other species through three primary mechanisms: (i) reducing environmental stress, (ii) alleviating predation or competitive pressure, and (iii) enhancing resource availability.

As ecosystem engineers, RBs beds significantly influence biodiversity by providing habitats that support a higher diversity of invertebrates than adjacent soft sediments, and a high diversity of fish (Moura et al., 2021; Anderson et al., 2023; Bulleri et al., 2024). Largely, this is due to the morphological

structure of the rhodoliths themselves as their hollow structures offer protected sites for fish egg and larvae and refuge for numerous invertebrates (Gagnon et al., 2012; Teichert, 2014). In this way, they become crucial habitats for the life cycles of various commercially important species, particularly during their early developmental stages, such as the Atlantic cod (*Gadus morhua*) and scallops (*Pecten maximus*) (Steller et al., 2003; Kamenos et al., 2004; Hall-Spencer et al., 2006; Costa et al., 2020; Moura et al., 2021). RBs do not only increase the abundance and richness of epifaunal organisms (Riosmena-Rodríguez, 2017; Otero-Ferrer et al., 2020), but also of some epiphytic filamentous and fleshy macroalgae that, like the rhodoliths themselves, also provide shelter and are a resource for various marine organisms (Chaves et al., 2013; Fulton et al., 2020; Bulleri et al., 2024), thus increasing the ecosystem value of RB.

The ecological role of RBs extends beyond supporting biodiversity: RBs also contribute to ecosystem connectivity. By linking habitats, such as seagrass beds, mangroves, and coral reefs, they ensure the survival of juvenile fish, create migratory corridors for reef fish heading to spawning grounds, and increase reef species abundance (Costa et al., 2020; Moura et al., 2021; Carneiro et al., 2022). RBs beds have been shown to act as the most connected structuring habitat in detritic continental shelves by sharing species with surrounding habitats (de Juan et al., 2023).

RBs also play a critical role in regulating ecosystem processes, particularly in the global carbon cycle. As calcifying organisms, they act as natural solutions for mitigating anthropogenic CO_2 emissions (Tuya et al., 2023). These habitats are characterized by high carbonate production rates and substantial carbonate stock accumulation (Teed et al., 2020; Tuya et al., 2023). Moreover, non-living carbonate deposits dissolve slowly due to microbial respiration, a process that increases alkalinity and sequesters CO_2 (Burdett et al., 2018; Tuya et al., 2023). However, the role of RBs as carbon sinks or sources remains a topic of active research. The carbon fluxes of RBs are influenced by community composition; higher algal biomass associated with rhodoliths enhances net primary production, while greater faunal abundance may increase carbon release through respiration (Schubert et al., 2024). Additionally, rhodolith species composition plays a significant role in determining net productivity and associated carbon dynamics (Qui-Minet et al., 2021; Schubert et al., 2022).

The ecosystem services provided by RBs extend to provisioning services that benefit various industries. These include agricultural applications (e.g., fertilizers, soil pH regulation, and limestone production), cosmeceuticals (e.g., toothpaste and bath salts), food (e.g., dietary supplements), and biomedicine (e.g., bone implants and antimicrobial agents) (Blunden et al., 1975; Amado-Filho & Pereira-Filho, 2012; Dias, 2000). For instance, extracts from the rhodolith-forming species *Lithothamnion calcareum* have demonstrated efficacy in suppressing the proliferation of human colon cancer cell lines, suggesting potential for use as a dietary chemopreventive agent against colon polyp formation (Aslam et al., 2009; 2010). Ecosystem services provided by RBs, include the cultural identity of coastal areas, as seen in the

"Popcorn Beaches" of the Canary Islands, where these unique formations form striking beach deposits (A. Harvey et al., 2018; Rebelo et al., 2022).

In summary, RBs provide vital ecosystem functions and services across ecological, regulatory, and economic domains. From enhancing biodiversity and supporting ecosystem connectivity to contributing to carbon cycling and offering valuable resources for industrial and biomedical applications, these habitats are integral to the ecological value of subtidal habitats and sustainability of marine ecosystems. They are currently the target of conservation effort, particularly due to their vulnerability of anthropogenic stressors (Barbera et al., 2003; Pezzolesi et al., 2017). However, it remains unknown whether all RBs and rhodolith-forming species contribute equally to these ecosystem functions.

1.1.1.3. Anthropogenic impacts and climate change effects

For centuries, rhodoliths were extensively harvested across Western Europe, particularly during the 18th to 20th centuries, for use in agriculture and horticulture as a soil conditioner. Annual extraction reached approximately 300,000 tons, with large-scale operations employing dredges and industrial processing methods (Blunden et al., 1975). However, while direct extraction once posed the greatest threat to RBs, their primary challenges today stem from the combined effects of climate change and human-induced local stressors, like fishing and pollution. Ocean warming, acidification, and bottom trawling have become the dominant pressures in the Mediterranean RBs, leading to habitat degradation, reduced calcification, and physical destruction of these critical ecosystems (Trégarot et al., 2024). Furthermore, it is still unknown whether all species respond similarly to human impacts, or whether different impacts have varying effects on rhodolith-forming species and morphologies. Addressing the species-specific response to these contemporary threats is essential to safeguard the ecological and cultural value of RBs for future generations.

1.1.1.3.1. Ocean Warming

By the end of this century, global average surface temperatures could rise by up to 4.3 °C if current emission trends remain unchecked (IPCC, 2019). This level of warming is expected to trigger widespread ripple effects across the climate system, ecosystems, and the services they provide (Koerich et al., 2024). In response, species will need to adapt, tolerate the changes, spread in the most optimal distribution areas, or face extinction, depending on their physiological, ecological, and evolutionary capacities (Berg et al., 2010).

Rhodoliths may be sensitive to temperature fluctuations because their metabolic processes—such as growth (including carbon uptake and calcification), photosynthesis, and respiration—are highly temperature-dependent (Steller et al., 2007). Research indicates that when temperatures rise approximately 5 °C above ambient levels, coralline algae often experience reduced calcification (Cornwall et al., 2019). However, the extent of these effects varies among species (Koerich et al., 2024;

Trégarot et al., 2024). Additionally, other critical processes, such as reproduction, may also be disrupted, even if calcification remains unaffected (Cornwall et al., 2019; Schubert et al., 2019).

The response of rhodoliths to ocean warming depends largely on their thermal tolerance (which, as explained, remains poorly understood for most rhodolith-forming species), geographic distribution, and habitat depth. Temperate species generally exhibit greater resilience to temperature fluctuations compared to their tropical counterparts, while intertidal species are more tolerant of thermal variability than those in deeper waters (Martin & Hall-Spencer, 2017). In the North-East Atlantic, higher latitudes may act as refuges for some species due to cooler conditions under climate change scenarios (Simon-Nutbrown et al., 2020), while at lower latitudes, changes in depth range may partially safeguard habitat suitability (Fragkopoulou et al., 2021). However, in the Mediterranean, warming poses a significant threat. The fragmented distribution of RBs and their limited dispersal capacity heighten their vulnerability, although empirical studies on these effects are still lacking (Kružić, 2014).

While minor temperature increases may enhance or have neutral effects on growth, photosynthesis, or calcification, surpassing critical thermal thresholds leads to detrimental outcomes, including bleaching and substantial declines in these processes (Koerich et al., 2024). The impacts of ocean warming on rhodoliths will therefore vary depending on the species involved (Qui-Minet et al., 2019; Koerich et al., 2024) and their interaction with additional stressors. These include ocean acidification (Scherner et al., 2016; Trégarot et al., 2024), fishing pressures (Fragkopoulou et al., 2021; Trégarot et al., 2024), pollution (Schubert et al., 2019), and the specific characteristics of their habitats and associated communities (Harvey et al., 2013; Rich et al., 2018).

1.1.1.3.2. Ocean Acidification

Human activities have significantly accelerated their impact on the oceans since the Industrial Revolution. Atmospheric CO_2 concentrations have reached 400 ppm (NOAA, 2019), the highest level recorded in the past 800,000 years (Lüthi et al., 2008; Koerich et al., 2024). This anthropogenic alteration affects not only the global climate but also biogeochemical cycles and vital marine ecosystems.

The ocean plays a critical role in mitigating atmospheric CO_2 levels, absorbing approximately 30% of anthropogenic carbon emissions (IPCC, 2019). However, this uptake comes at a cost: the increased absorption of CO_2 is driving ocean acidification, reducing calcium carbonate ($CaCO_3$) saturation in surface waters. The ocean's carbonate system is governed by a series of chemical reactions:

$$CO_{2(atm)} \leftrightarrow CO_{2(aq)} + H_2O \leftrightarrow H_2CO_3 \leftrightarrow H^+ + HCO_3^- \leftrightarrow 2H^+ + CO_3^{2-}$$

where CO_2 reacts with water to form carbonic acid (H_2CO_3). This acid dissociates, releasing hydrogen ions (H^+) that lower the pH and reduce carbonate ion (CO_3^{2-}) availability, crucial for the formation of calcium carbonate.

The dissolution of $CaCO_3$ depends on the concentrations of CO_3^{2-} and calcium ions (Ca^{2+}). Calcium carbonate is primarily produced biologically, forming the shells and skeletons of marine organisms, including the structures of coralline red algae (Koerich et al., 2024). Of the six polymorphic forms of $CaCO_3$, aragonite and calcite are the most common in marine organisms. Coralline red algae deposit $CaCO_3$ as high-magnesium calcite (Mg-calcite or dolomite), a form significantly more soluble than aragonite or calcite (Koerich et al., 2024). This high solubility makes coralline red algae particularly vulnerable to changes in seawater saturation states (Ragazzola et al., 2013).

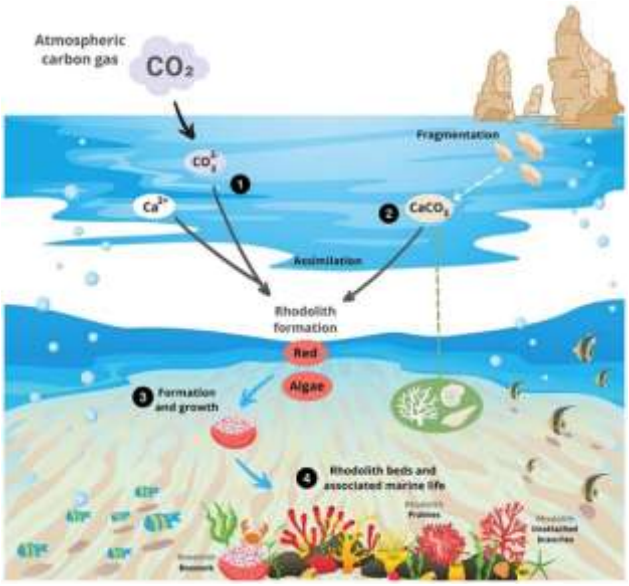


Fig.1.1.3. Diagram of red calcareous algae calcification. **Source:** de Araújo Costa et al. (2023).

Given their susceptibility to ocean acidification (OA), research on coralline algae has increased substantially. A Scopus review by Trégarot et al. (2024) revealed that 82% of studies on RBs identified OA as a critical stressor. However, the effects of decreasing pH on coralline algae are varied. Some studies report negative impacts on photosynthesis, calcification, and structural integrity (Büdenbender et al., 2011; Kato et al., 2014; Ragazzola et al., 2021), while others find no significant changes or even positive responses (Noisette et al., 2013a; Noisette et al., 2013b; Sordo et al., 2016). These discrepancies depend on species-specific traits, such as the proportion of dolomite in their skeletons, and the duration of exposure (Koerich et al., 2024). In addition, Schubert et al. (2021) found significant differences between species but also between morphologies in terms of pH dynamics at the algal thallus surface, suggesting not only species-specific responses to OA, but possible differences in phenotypic plasticity that may result in different susceptibilities to long-term exposure to OA. Furthermore, Kamenos et al. (2013) demonstrated that, when the shift to low pH occurs at a rapid rate, weaknesses in the calcite

skeleton are detected. Therefore, despite evolutionary adaptation, the ability of coralline algae to cope with OA may be determined primarily by the rate of OA, rather than its magnitude (Kamenos et al., 2013).

1.1.1.3.3. Interaction of local stressors with climate change

The combined effects of ocean warming and acidification (OA), significantly increase the vulnerability of RBs. Under all Representative Concentration Pathways (RCPs), a marked decline in suitable habitats is projected, with reductions ranging from 38% by 2050 to 83.7% by 2100 under RCP 8.5 scenarios (Simon-Nutbrown et al., 2020). In addition to these combined effects of climate change, the effect of local stressors such as sedimentation, nutrient enrichment, trawling or the presence of invasive species must be considered to understand the scenario faced by RBs.

Sedimentation further threatens rhodoliths by increasing turbidity and reducing light availability, negatively affecting rhodolith survival (Aguirre et al., 2012). In the Bay of Brest (Brittany), *Lithothamnion* sp. rhodoliths die after 41 days of burial (Ehrhold et al., 2021). However, sedimentation effects vary with climate; during colder periods, rhodolith accumulation rates appear positively correlated with sedimentation (Ehrhold et al., 2021).

Bottom trawling physically damages rhodoliths, causing high mortality while also increasing turbidity and light limitation (de Juan et al., 2013; Fragkopoulou et al., 2021; Illa-López et al., 2023).

Nutrient enrichment has complex effects. While Qui-Minet et al. (2019) report no significant impact on primary production and calcification in *Lithothamnion corallioides* during summer, they found that moderate nutrient enrichment during winter could benefit rhodoliths by preventing dissolution but opportunistic species may thrive under nutrient availability competing with rhodoliths and reducing their survival (Qui-Minet et al., 2019). Despite limited studies (primarily on a single species), findings compiled in Trégarot et al. (2024) review suggested that nutrient enrichment and warming may have a neutral net effect on rhodoliths (**Fig.1.1.4**).

In shallow areas, invasive algae (*Womersleyella setacea, Caulerpa racemosa* var. *cylindracea*, and *Caulerpa taxifolia*) threaten RBs by outcompeting them for light and resources (Kružić, 2014). Future changes in OA and temperature may further promote non-calcifying and epiphytic algae, reducing rhodolith calcification rates through shading. Simultaneously, OA and warming could impair grazers, such as gastropods and sea urchins, decreasing their control over epiphyte growth and exacerbating rhodoliths decline (Legrand et al., 2017).

In conclusion, the combined effects of climate change effects with local stressors pose significant threats to the persistence of RBs. Their ecological importance and vulnerability underscore the urgent need for targeted research and conservation measures to protect these critical habitats.



Fig.1.1.4. Cumulative overall effects of local stressors combined with climate change drivers for RBs in the North-East Atlantic. **Source:** Trégarot et al., 2024.

1.1.1.4. Protection regulations

Rhodolith and maërl beds are considered non-renewable resources due to their slow growth rates and vulnerability to anthropogenic impacts. At the European level, the Natura 2000 network was established to protect critical habitats, including RBs, under the EU Habitats Directive (92/43/EEC). This directive specifically lists key rhodolith-forming species such as *Lithothamnion corallioides* and *Phymatolithon calcareum* in Annex V, emphasizing sustainable exploitation compatible with their favorable conservation status. Additionally, the Mediterranean Fisheries Regulation (EC no. 1967/2006) prohibits destructive practices like trawling and dredging over rhodolith grounds, reinforcing habitat protection. Internationally, initiatives such as the "Action Plan for the Conservation of Coralligenous and Other Mediterranean Bioconstructions" (UNEP-MAP, 2008) and the EU Marine Strategy Framework Directive (2008/56/EC) aim to achieve "Good Environmental Status" for marine ecosystems. These protection initiatives are bolstered by research highlighting the detrimental effects of bottom trawling on rhodolith habitats (e.g., Bordehore et al., 2003; Barberá et al., 2017). Protection measures represent a comprehensive framework for safeguarding RBs, which are critical for biodiversity and ecosystem functioning in the Mediterranean Sea, but, as mentioned above, the lack of definition of the specific composition of these habitats in the Mediterranean makes it difficult to take effective protection measures for each RB.

In conclusion, understanding the species composition of RBs is crucial to address existing knowledge gaps, as responses to climate change and local stressors may vary depending on the species involved and their interactions with each other. Furthermore, the structural complexity of the habitat they create is highly dependent on the species involved. Different rhodolith-forming species may show different

levels of resistance or vulnerability to environmental pressures, which influences the overall stability and persistence of these ecosystems. In addition, species interactions within RBs can generate synergistic effects that shape habitat complexity and ecosystem function. However, current legislation only considers the two most widely distributed species, overlooking the diversity of rhodolith assemblages and their potential ecological functions. To effectively protect and understand the intricate dynamics of these ecosystems, it is essential to identify and study the full range of species and their morphologies that contribute to the formation of RBs, ensuring a holistic approach to their conservation and management.

1.1.2. Rhodolith- forming species identification

RBs are typically associated with the coastal detrital biocenosis, where Pérès (1967) identified three distinct facies: pralines, nullipores (commonly referred to as maërl), and unattached Peyssonneliales. These facies reflect differences in rhodoliths morphology, from spherical forms resembling confectionery to branched and twisted structures. A fourth facies, corresponding to small concretionary blocks or boxwork rhodoliths, was later added by Meinesz et al. (1983). Basso (1998) further refined the terminology and classification of these facies, providing a clearer framework for their study. Despite their ecological importance, RBs remain underexplored, with limited information available on their distribution, species composition, and conservation status (Pergent & Pergent-Martini, 2015; Tuya et al., 2023).

Identifying rhodoliths species is often challenging. For centuries, phycologists have worked to define the morpho-anatomical traits that distinguish different species. However, their high phenotypic plasticity, shaped by environmental factors, further complicates species identification (Bosence, 1976, 1983; Steller & Foster, 1995; Foster, 2001; Carro et al., 2014; Lugilde Yáñez et al., 2022). When the external morphology is insufficient, internal vegetative and reproductive traits must be examined, though these characteristics can be difficult to observe and may be shared among species, sometimes even across genera.

Woelkerling (1988) seminal work on coralline algae established a set of morphological traits traditionally used for species identification. However, advances in molecular techniques have led to significant revisions in the classification of families and subfamilies (Le Gall & Saunders, 2007; Le Gall et al., 2010; Nelson et al., 2015; Rösler et al., 2016; Peña et al., 2020; Jeong et al., 2021).

Faced with these challenges, the most reliable approach combines morpho-anatomical and molecular analyses to ensure correct species identification. The external and internal vegetative characters as well as reproductive characters used for taxonomic identification of rhodoliths species are explained below.

1.1.2.1. Vegetative characters of rhodoliths: external morphology

The most common morphological characteristics used to describe coralline algae include growth form, color, texture, as well as the extent, size, and thickness of the encrusting thallus, and the type of margin in non-geniculate species. Coralline algae exhibit significant morphological variability (Woelkerling, 1983). A single species can display a wide range of growth forms, which are often shared with other species, making reliable identification challenging (Harvey & Woelkerling, 2007; Lugilde Yáñez et al., 2022).

The extent, dimensions, and thickness of the encrusting thallus are generally variable, although occasionally useful. In contrast, the margin of the encrusting thallus is often considered a reliable trait for distinguishing certain species of the genus *Phymatolithon*, which may exhibit a whitish, thickened margin (Lugilde Yáñez et al., 2022).

Color is not generally regarded as a diagnostic trait, but rather as an indicative one. Studies have shown substantial color variation within species, such as *Lithophyllum byssoides*, *L. hibernicum*, and *Phymatolithon* sp. (Irvine & Chamberlain, 1994; Hernández-Kantún et al., 2015; Pezzolesi et al., 2017). However, in some cases, color can aid identification. For instance, Irvine & Chamberlain (1994) noted that pink is the most common color for maërl-forming species, while *P. lusitanicum* is grayish-pink (Peña et al., 2015a). Similarly, *L. nitorum* typically exhibits an orange hue. Cabioch & Mendoza (2003) highlighted the shiny texture of *Mesophyllum lichenoides*, also observed in *M. expansum* (Peña et al., 2015b). Conversely, some *Phymatolithon* species often display a matte texture (Irvine & Chamberlain, 1994).

1.1.2.2. Vegetative characters of rhodoliths: internal morphology

Internal vegetative morphology is extensively used to identify and differentiate coralline algal species. Key traits include thallus organization, epithallial and subepithallial initial cells, types of cell connections, germination discs, and trichocytes, some of which are considered essential for taxonomic identification (Lugilde Yáñez et al., 2022).

The coralline algal thallus consists of filaments formed by cells derived from a meristematic cell, which may vary in elongation depending on the genus (Giraud & Cabioch, 1977). Based on the position of these meristematic cells, two types are distinguished: terminal initials at the margins, responsible for lateral growth, and subepithallial or subterminal initials, responsible for vertical growth. Thalli are generally dorsiventral in organization and can be monomerous or dimerous (Woelkerling, 1988) (**Fig.1.1.5**).

Some genera, such as *Lithophyllum*, include species with both types of thalli (Lugilde Yáñez et al., 2022). In a monomerous encrusting thallus (**Fig.1.1.5A**), basal filaments develop parallel to the substrate, forming the medulla, while cortical filaments curve toward the surface (Irvine &

Chamberlain, 1994; Woelkerling, 1988). This type of thallus is typical of genera such *as Lithothamnion, Phymatolithon,* and *Mesophyllum* (Irvine & Chamberlain, 1994). Medullary filaments in *Mesophyllum* form concentric arcs of cells, a coaxial organization (Lemoine, 1928). When absent, the arrangement is referred to as non-coaxial or plumose (Woelkerling, 1988).

Dimerous thalli (**Fig.1.1.5B**) develop a unistratified basal filament of medullary cells and multistratified erect filaments forming the cortex, arising from extended meristematic initials within a pseudoparenchyma (Irvine & Chamberlain, 1994). Genera exhibiting dimerous thalli include *Lithophyllum*, *Titanoderma*, *Hydrolithon*, *Pneophyllum*, and *Melobesia* (Irvine & Chamberlain, 1994).

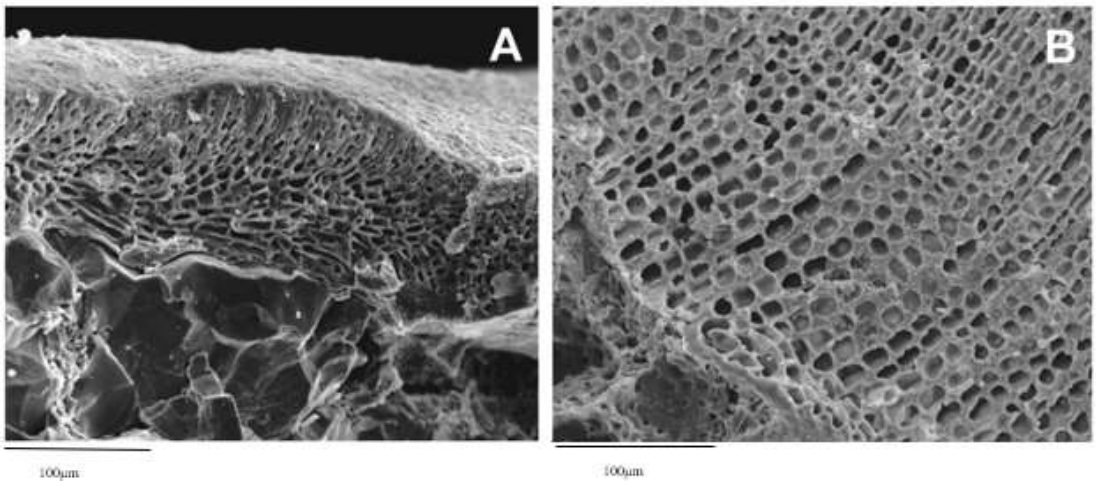


Fig.1.1.5. Internal morphology of the thallus, scanning electron microscope (SEM). **A.** *Phymatolithon* sp. thallus monomer. **B.** Thallus dimer of *Lithophyllum* sp. **Source:** Lugilde Yáñez et al. (2022).

The thallus surface is another valuable characteristic for distinguishing between genera, as it typically follows one of three distinct patterns: (i) the *Phymatolithon* type (**Fig.1.1.6A, B**), characterized by polygonal cells, a flat margin, and wide intercellular spaces; (ii) the *Pneophyllum* type (**Fig.1.1.6C**), distinguished by rounded cells and reduced intercellular spaces and (iii) the *Leptophytum* type (**Fig.1.1.6D**), which features a thickened margin and wide intercellular spaces. However, as with many morphological traits, some genera, such as *Lithophyllum*, may display two or more surface types, adding complexity to their identification (Lugilde Yáñez et al., 2022).

Primary pit connections (synapses) between cortical cells of the same filament are present in all groups of coralline algae (Giraud & Cabioch, 1977). In contrast, secondary pit connections, which are those that occur between cortical cells of contiguous filaments, are a character almost exclusive to the subfamily Lithophylloideae (Harvey et al., 2005) (**Fig.1.1.7A, B**). Cell fusions are larger connections present in all calcified orders of Corallinophycidae (Peña et al., 2020; Jeong et al., 2021; Lugilde Yáñez et al., 2022) (**Fig.1.1.7C, D**). In some genera of the subfamily Hydrolithoidae, fusions are very abundant and occur in almost all cell walls (Irvine & Chamberlain, 1994; Kato et al., 2011; Peña et al., 2019).

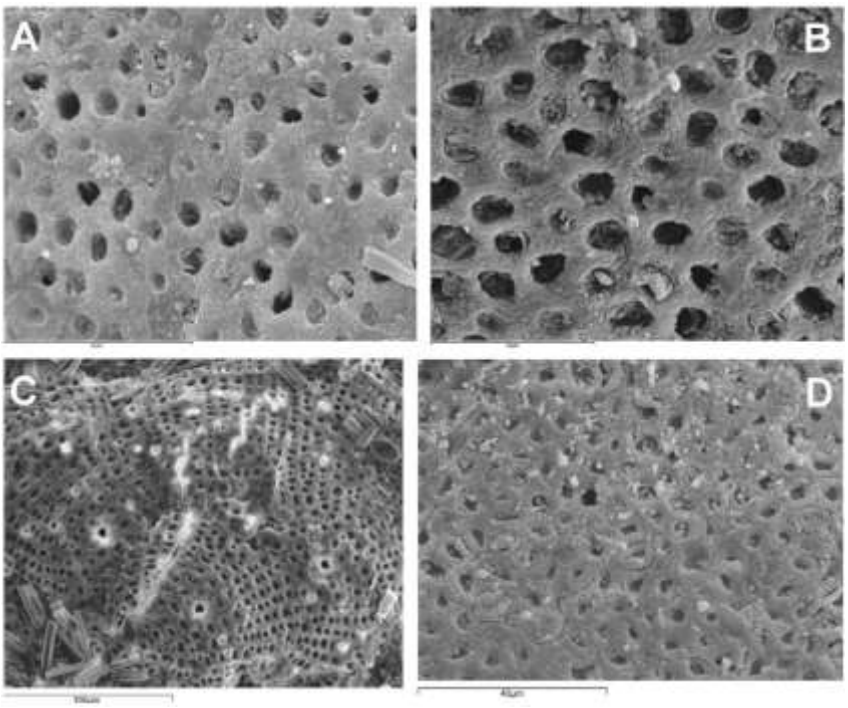


Fig.1.1.6. Cells in surface view (SEM). **A**. *Phymatolithon* type from a *Mesophyllum* sp. **B**. *Phymatolithon* type from a *Phymatolithon* sp. **C**. *Pneophyllum* type. **D**. *Leptophytum* type from a *Phymatolithon* sp. **Source**: extracted from Lugilde Yáñez et al. (2022).

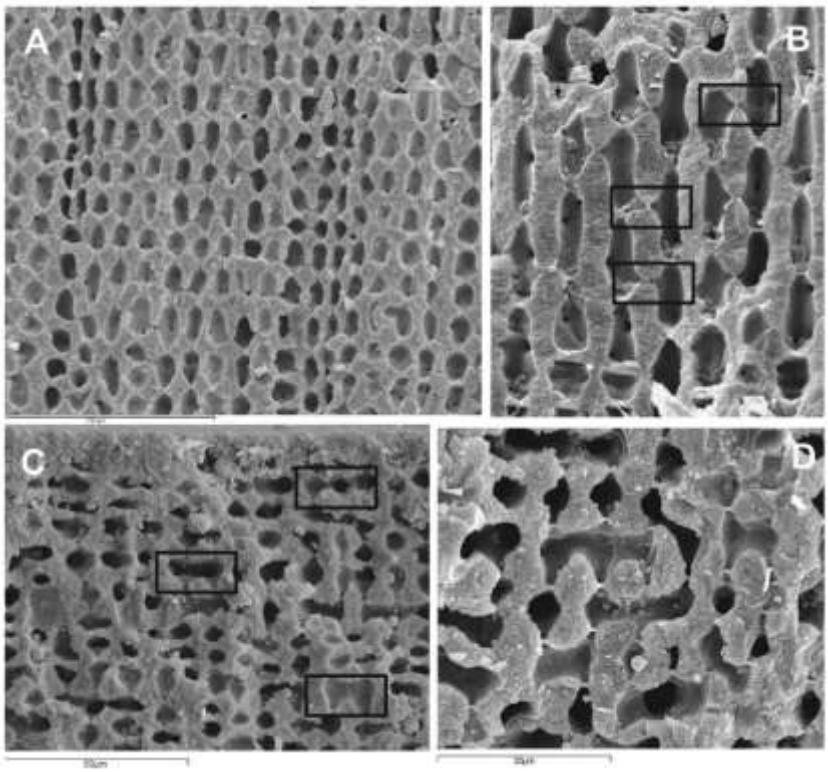


Fig.1.1.7. A-B. Primary synapses or pit connections (same filament) and secondary pit connections (adjacent filaments) in *Lithophyllum* sp. **C-D.** Contiguous filament cells connected by cell fusions in *Phymatolithon* sp. **Source:** Lugilde Yáñez et al. (2022).

Another character considered diagnostic in several species are the epithallial cells, both for their shape, dimensions and layered organization (Giraud & Cabioch, 1977; Irvine & Chamberlain, 1994; Hernández-Kantún et al., 2015). Some authors distinguish epithallial cells in three different morphologies: domed as in *Phymatolithon,* cup-shaped as in *Lithothamnion* or rounded as in *Mesophyllum* (Irvine & Chamberlain, 1994) (**Fig.1.1.8**). The initial subepithelial cells are those that come immediately after the epithallial cells that have meristematic activity (Woelkerling & Irvine, 1986) and show differences in size in some genera, for example, in *Phymatolithon* the initial subepithelial cells are usually similar in size or shorter than the underlying cortical cells, whereas for *Lithothamnion* and *Mesophyllum,* they are usually equal to or longer than the cortical cells (Irvine & Chamberlain, 1994) (**Fig.1.1.8**).

Some cortical cells have the capacity to develop into trichocytes (**Fig.1.1.9**), which are cells that carry a specialized structure (a filament), the function of which is not yet clear (Lugilde Yáñez et al., 2022) and which acquire a larger size than the adjacent vegetative cells. Trichocytes have been described in non-geniculate thin-stemmed coralline algae such as *Fosliella* and in geniculate coralline algae such as *Jania* or *Corallina*. They have also been described in non-geniculate algae such as *Neogoniolithon* (Mateo-Cid, 2006) or *Spongites* (Caragnano et al., 2018), where unusually large cells known as megacells were sometimes seen to be generated (Lugilde Yáñez et al., 2022). Trichocytes rarely occur in Hapalidiales and *Sporolithon* (Walker, 1984; Townsend et al., 1995; Athanasiadis & Ballantine, 2014; Lugilde Yáñez et al., 2022).

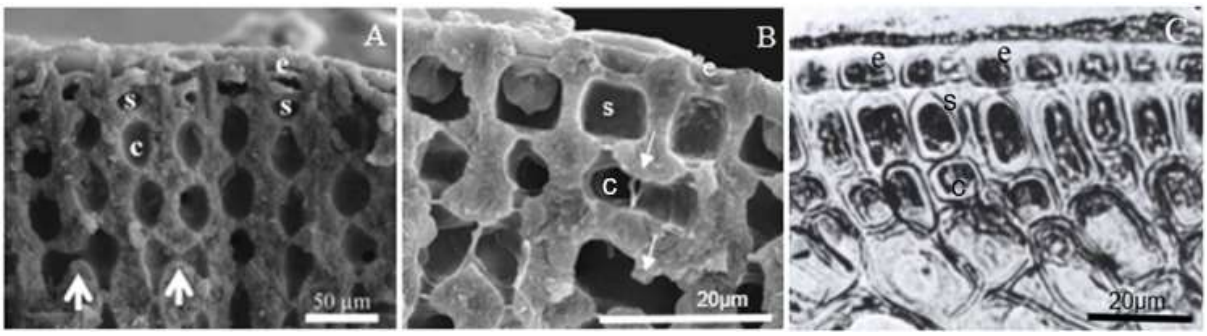


Fig.1.1.8. A. Domed epithallial cells (e), subepithallial cells (s) as short as or shorter than cortical cells (c). Cortical cells joined by cell fusions (arrows) in *Phymatolithon lusitanicum* (image extracted from Peña et al., 2015a). **B.** Epithalial cells in cup-shape (e) and initial subepithaline cells (s) larger than underlying cortical cells (c) joined by cell fusions (arrows) in *Lithothamnion* sp. (image modifyied from Lugilde Yáñez et al., 2022). **C.** Rounded epithallial cells (e) and initial subepithallial cells (s) larger than underlying cortical cells (c) of *Mesophyllum lichenoides* (image modified from Woelkerling and Irvine, 1986).

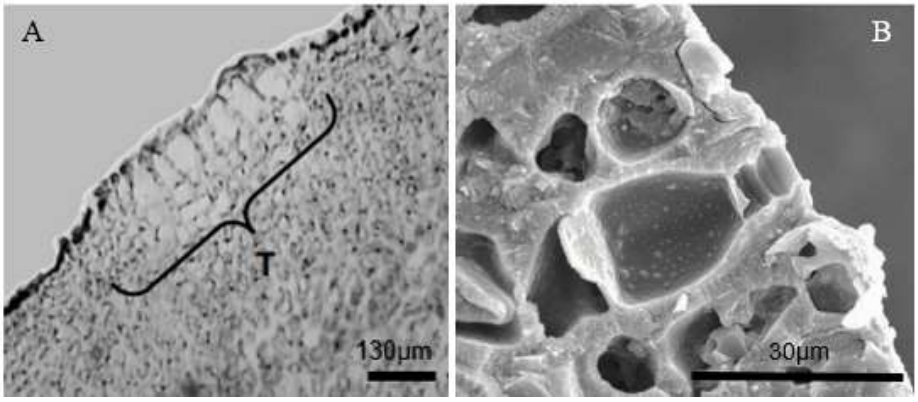


Fig.1.1.9. A. Detail of trichocytes (T) in horizontal rows in *Neogoniolithon fosliei* (image extracted from Mateo – Cid, 2006). **B.** (SEM) Transversal section of a trichocyte and megacel in *Spongites* sp. (image extracted from Lugilde Yáñez et al., 2022).

1.1.2.3. Reproductive characteristics of coralline algae

Coralline algae have both sexual and asexual reproduction (**Fig.1.1.10**). Their life cycle, mostly isomorphic, includes three phases: haploid gametophytic (produces gametes), diploid carposporophytic (generates carpospores) and diploid sporophytic (produces haploid tetraspores) (Woelkerling, 1988; Irvine & Chamberlain, 1994). Both sexual and asexual reproduction involves conceptacles (Johansen, 1981). The sexual and carposporocyst conceptacles are uniporate (Lugilde Yáñez et al., 2022). Spermatocytes are captured by the carpogonia, and after fertilisation, a diploid carposporophyte is formed inside the female uniporate conceptacle (Irvine & Chamberlain, 1994) (**Fig.1.1.10**).

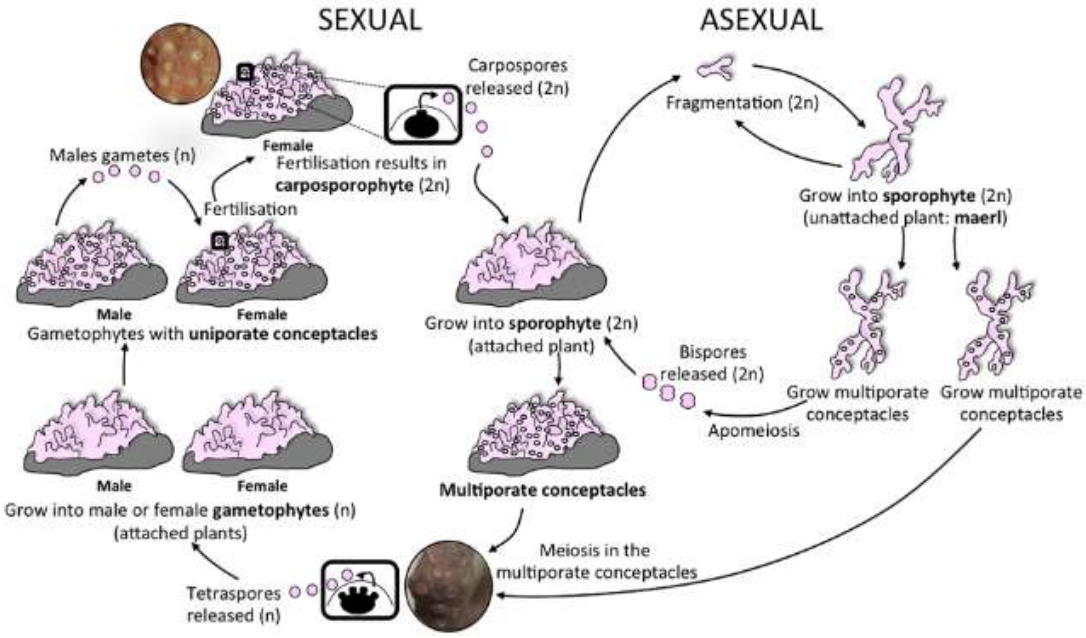


Fig.1.1.10. Life cycle of the coralline alga *Phymatolithon calcareum* (Pardo et al., 2019). Sexual reproduction involves alternation between diploid sporophytes and haploid gametophytes. **Source:** Pardo et al., 2019.

The specific reproductive structures such as the different types of tetrasporocyst-forming structures that can be observed on the sporophyte, as well as the type of tetrasporangia, vary among the five orders of the Corallinophycidae (**Fig.1.1.11**) (Jeong et al., 2021).

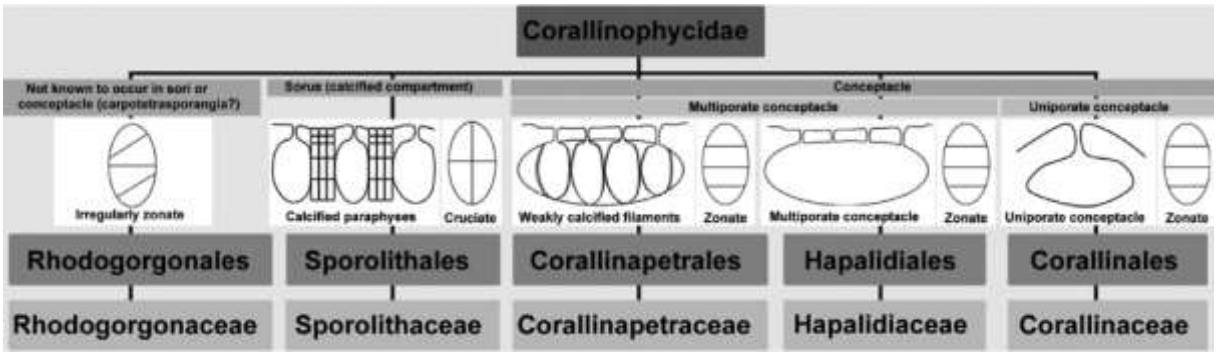


Fig.1.1.11. Specific reproductive structures of the five orders of Corallinophycidae. Extracted from Jeong et al. (2021).

In the order Rhodogorgonales it has not been observed whether the sporangia occur in conceptacles or sori but the tetrasporangia are known to be irregularly zoned in morphology (Jeong et al., 2021). Within the orders with conceptacles, the order Corallinales have uniporate conceptacles that may have a calcified structure called columella (**Fig.1.1.12A, B**). The orders Hapalidiales and Corallinapetrales have multiporate conceptacles. While Hapalidiales have a single chamber with several pores (**Fig.1.1.12C, D**), Corallinapetrales have individual compartments separated by weakly calcified filaments grouped in a chamber (**Fig.1.1.12E, F**). Finally, the Sporolithales present superficially single sori with rosette cells around them. They have individual calcified compartments for each tetrasporocyst with triangular stalk cells in the base (**Fig.1.1.12G, H**). The tetrasporangia of Corallinales, Hapalidiales and Corallinapetrales are zonate while those of Sporolithales are cruciate (**Fig.1.1.11**).

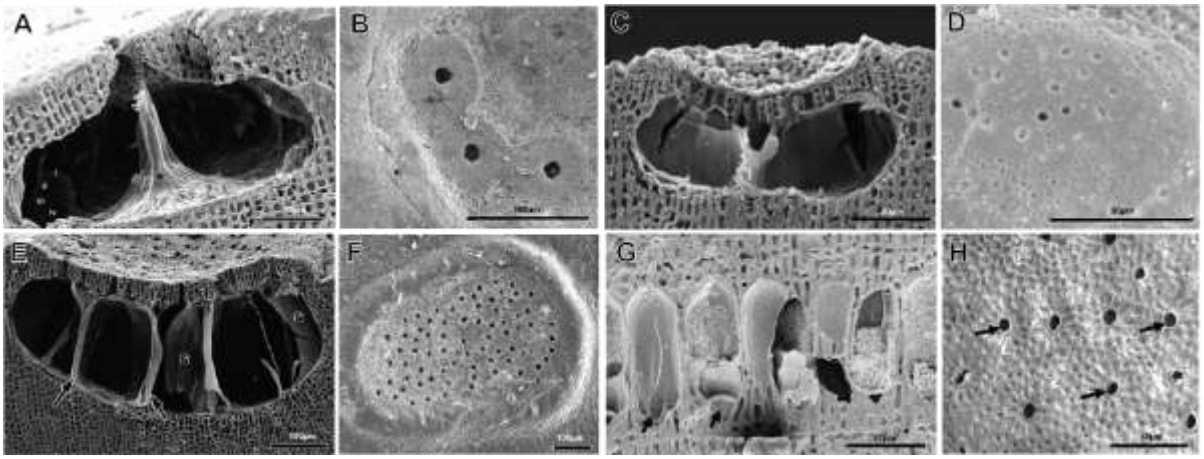


Fig.1.1.12. Examples of conceptacles and sori (SEM). **A.** Transverse fracture of thallus showing tetrasporangia (count in Roman numbers) inside the uniporate conceptacle with calcified columella (asterisk) from a

Lithophyllum neocongestum (Extracted from Hernandez-Kantun et al., 2016). **B.** Surface view of uniporate conceptacles in *Lithophyllum. Hibernicum* (Extracted from Lugilde Yáñez et al., 2022). **C.** Vertical section showing multiporate sporangial conceptacles and clearly laminated from *Phymatolithon lusitanicum* (Extracted from Peña et al., 2015a). **D.** Surface view of a multiporate conceptacle in *Phymatolithon lamii* (Extracted from Lugilde Yáñez et al., 2022). **E.** Vertical fracture through sporangial conceptacle showing elliptical-shaped chamber and sporangia (s) separated by weakly calcified remnant sterile filaments (arrows) from *Corallinapetra gabrielii* (Extracted from Jeong et al., 2021). **F.** Magnified surface view of tetrasporangial conceptacle pore plate from *Corallinapetra gabrielii* (Extracted from Jeong et al., 2021). **G.** Detail of single tetrasporangial compartments with stalk cells (arrows) in *Sporolithon amadoi* (Extracted from Richards et al., 2019). **H.** Surface view of tetrasporangial sorus with tetrasporangial pores (arrows) and rosette cells in *Sporolithon amadoi* (Extracted from Richards et al., 2019).

In asexual reproduction, the mechanisms that stand out are the formation of bisporocysts, common in cold waters and in certain genera, and fragmentation, predominant in maërl-forming species such as *Phymatolithon calcareum.* This method allows clonal propagation, especially in environments with low genotypic diversity. Propagule formation is also observed in some species, highlighting the adaptive diversity of these algae (Lugilde Yáñez et al., 2022).

There are other characteristics that can serve as diagnostics to distinguish between genera or specific species of coralline algae. For example, as listed in Lugilde Yáñez et al. (2022) the filaments of cells surrounding the pore channel are an indicative of the species according to their arrangement and orientation, their more or less elongated shape and their projection within the pore. Other examples are: whether the pore channel is tubular or triangular and conical in shape, the presence of specialised intercalary cells, the number of cell layers from the base of the sporocyst conceptacles to the surface, the dimensions of the conceptacles or the surface morphology of the cells surrounding the pores (Lugilde Yáñez et al., 2022).

1.1.3. Mediterranean rhodolith beds

RBs have existed in oceans precursor to the current Mediterranean for approximately 140 million years (Chatalov et al., 2015; Kittle et al., 2022). Scientific interest in these habitats dates back to the late 19th century, culminating in a comprehensive review by Jacquotte (1962). Since then, research has progressively advanced, with numerous studies conducted throughout the 20th and 21st centuries (Basso et al., 2017; Ingrassia et al., 2023, and references therein).

Mediterranean RBs are generally found at depths ranging from 30 to 100 meters, although their distribution can extend from 9 to 150 meters depending on environmental conditions (Aguilar et al., 2009; Basso et al., 2016). Light availability, influenced by water transparency, is a critical factor determining their depth distribution, as these habitats are typically located in mesophotic zones (Cerrano et al., 2019; Deidun et al., 2022). As we observed in Illa-López et al. (2023) and Demestre et al. (2024),

the fragmented distribution of RBs across the Mediterranean is shaped by substrate type, bottom currents and anthropogenic impacts, including fishing activities (Basso et al., 2017). The study of distribution and mapping of RBs in the Mediterranean is complex, largely due to their depth, which results in limited available information. Martin et al. (2014) compiled the existing data and projected distribution models for this habitat, showing that many areas in the Mediterranean have optimal conditions for the presence of RBs (**Fig.1.1.13**).

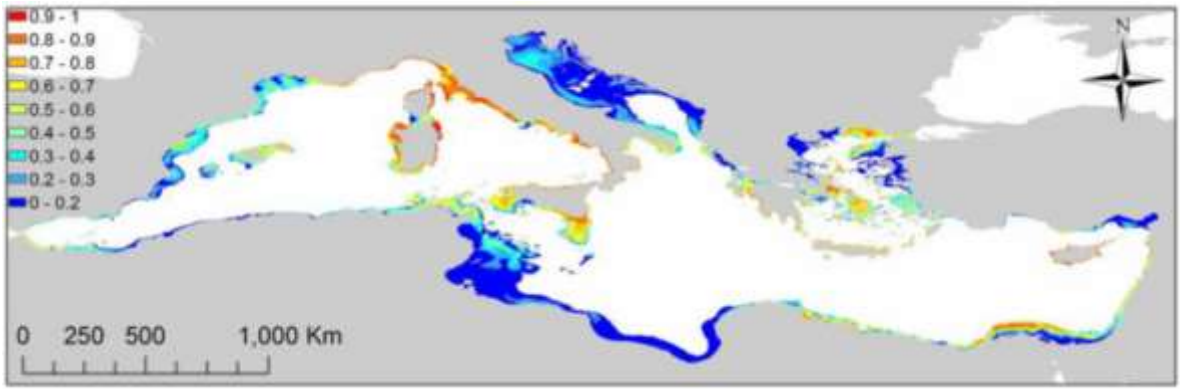


Fig.1.1.13. Spatial distribution showing occurrence probabilities for maërl or RBs across the Mediterranean Sea, as predicted by Martin et al. (2014) using distribution modelling. Extracted from Martin et al. (2014).

The extent of RBs varies widely. The Menorca Channel hosts the largest known bed in the Mediterranean, covering 918 km^2 and, followed by a 200 km^2 bed in the southeast of Malta (Barberá et al., 2012a; Tabone et al., 2024). In contrast, smaller beds are common, such as those in Tabarca (Spain), Campania (Italy), and Apulia (Italy), which cover less than 10 km^2 (Bordehore et al., 2003; Chimienti et al., 2020). Surface cover of rhodoliths in RBs is also variable, typically ranging between 43% and 74%, with some areas, like Lampedusa, exceeding 87% (Maggio et al., 2022; Tabone et al., 2024), although there are many areas with scattered rhodoliths with covers below 40% (Demestre et al., 2024; Illa-López et al., 2023).

The morphology and density of rhodolith accumulations are also influenced by environmental factors, including type of sediment and hydrodynamic conditions (Foster et al., 2013). For example, RBs on the east coast of Spain occur at depths of 40-65 meters on coarse substrates and within a temperature range of 14.5 – 15.5 ºC. These parameters, along with bottom currents and sediment dynamics, are crucial in shaping rhodoliths distribution (Illa-López et al., 2023). However, factors such as nutrient inputs, invasive species, and limited ecological connectivity may also play significant roles.

The ecological significance of Mediterranean rhodoliths bed has been recognized under the Marine Strategy Framework Directive (MSFD 2008/56/EC), which prioritizes achieving "Good Environmental Status" (GES) of marine waters (Basso et al., 2016). As a consequence of this recognition, recent knowledge has expanded in terms of distribution, extent, species composition and impacts (Piazzi et al., 2024). However, some knowledge gaps persist, particularly regarding their small-scale

heterogeneity and long-term temporal changes. Wide-scale mapping and monitoring efforts are essential for their effective conservation (Basso et al., 2017; Illa-López et al., 2023).

In conclusion, Mediterranean RBs are invaluable ecological components of marine ecosystems. However, their conservation and management require a deeper understanding of their distribution and composition by species and morphological types. As well as effective monitoring programs of biodiversity associated with these habitats.

1.1.3.1. Mediterranean species composition

Compared to Atlantic RBs, Mediterranean beds are unique due to their multitaxonomic composition and higher coralline biodiversity (Basso et al., 2017). They serve as critical habitats for numerous species, yet comprehensive comparisons of species associated with different rhodoliths facies are still lacking (Bianchi & Morri, 2025). Additionally, most of the knowledge about eastern Mediterranean rhodoliths comes from fossil records, with limited understanding of their modern distribution and structure (Baarli et al., 2012; Dulin et al., 2020).

The Mediterranean RBs composition vary significantly depending on location and depth. The two most common, well-studied, widely documented and globally distributed species, *Lithothamnion corallioides* and *Phymatolithon calcareum*, are present in most cases and are expected to be most abundant. However, Mediterranean endemic species such as *Lithothamnion valens* and *Lithothamnion minervae*, which are exclusively distributed in the Mediterranean, are also frequently found (Rendina et al., 2020; Del Río et al., 2022; Ingrassia et al., 2023; Demestre et al., 2024). The multispecific Mediterranean RBs exhibit different proportions of species and morphologies depending on the location and depth, although monospecific beds also exist in the Mediterranean, such as the one in the Piccolo Sea (Italy) composed solely of *Neogoniolithon brassica-florida* (Pierri et al., 2024).

The morphological complexity of these habitat-forming species and the difficulty of distinguishing between species within the same genus – or even between genera – without detailed microscopy and molecular analyses have led many studies to focus on morphotypes rather than species composition (Deidun et al., 2022; Maggio et al., 2022; Tabone et al., 2024). For instance, studies by Deidun et al. (2022) and Maggio et al. (2022) classified rhodoliths into the three main growth forms originally described by Basso et al. (2016): pralines, branched and boxwork forms. However, correlating these morphotypes with species is challenging, as most rhodolith-forming species in the Mediterranean can adopt multiple morphologies. Ingrassia et al. (2023) reported that *L. corallioides, P. calcareum, L. minervae, Lithophyllum racemus* and *Lithophyllum stictiforme* were found across all three growth forms. In addition, to add further complexity, these species may grow together overlying the calcareous skeleton of other dead rhodolith species and rhodoliths formed by more than one species may be found (Basso et al., 1998).

Beyond these widespread species, studies have documented additional taxa contributing to the complexity of Mediterranean RBs. Rindi et al. (2019) listed different rhodolith-forming species reported in the Mediterranean by different authors, such as *Sporolithon ptychoides, Lithophylum dentatum, Lithophyllum incrustans, L. racemus, N. brassica-florida, Spongites fruticulosus, L. corallioides, L. minervae, L. valens, Mesophyllum philippii, Mesophyllum sphaericum, P. calcareum* and the recently described *Phymatolithon lusitanicum* (Peña et al., 2015a). Similarly, Piazzi et al. (2024) reported other species in the Mediterranean such as *Roseolithon crispatum* among the most abundant species in the Gorgona RBs. Rendina et al. (2020) identifies 13 calcified algal taxa in the deep RBs of Campania coast (SW Italy) including, among others here mentioned, the *Neogoniolithon mamillosum* (synonym of *Neogoniolithon hauckii*) and Bracchi et al. (2019) also included *Phymatolithon lenormandii* and *Lithophyllum stictiforme* as a rhodolith-forming species in the Mediterranean. Finally, recent studies have also described new species in the Mediterranean, such as *Lithophyllum pseudoracemus* (Caragnano et al., 2020), further expanding the known biodiversity of RBs.

In the Mallorca Channel (near our study area), some species of calcified algal were visually detected but not confirmed: *L.* cf. *stictiforme, Lithophyllum* spp., *Lithothamnion* spp., *L.* cf. *valens, Phymatolithon* spp., *Mesophyllum* cf. *alternans, M.* cf. *lichenoides, S. fruticulosus* and *Spongites* spp (Massutí et al., 2022). In the Menorca Channel (our case study), Farriols et al. (2022) visually identified only three representative species (*L. valens, S. fruticulosus* and *P. calcareum*) among the multiple species present in these multispecific RBs. In addition to rhodolith-forming species and *Peyssonnelia* species (especially *Peyssonnelia rosa-marina*), it is common to found other algae whose composition and coverage depends on the particular conditions of each seabed: *Osmundaria volubilis, Phyllophora crispa* or *Kallymeniales* (Moranta et al., 2014). Finally, associated with these RBs, in some areas of the Menorca Channel there are also facies of *Laminaria rodriguezii* (Ordines & Massutí, 2009).

These findings underscore the ecological importance of Mediterranean RBs, which provide complex, biogenic habitats formed by a combination of dominant and secondary species adapted to diverse environmental conditions and morphologies.

Nevertheless, despite there is a wide range of rhodolith-forming species detected in the Mediterranean, many of them have been visually identified but not confirmed, as for example in the case study of the Menorca channel, the target of this thesis.

1.1.4. Traditional sampling methods in mesophotic benthic habitats.

In the Mediterranean, RBs remain relatively understudied compared to their Atlantic counterparts. Many studies have been anecdotal, often reporting rhodoliths as bycatch in fisheries impact assessments rather than as the primary focus of research (e.g. de Juan et al., 2013). Expanding knowledge of species diversity and their distribution is essential to enhance their protection, but studying them presents

significant challenges, as Mediterranean RBs are typically found at great depths. Furthermore, traditional sampling techniques are extractive and can cause damage to these fragile ecosystems.

Traditional sampling methods in mesophotic benthic habitats have historically relied on techniques such as dredging, trawling, and grab sampling to collect biological and sedimentary material from the seafloor (Gray & Elliott, 2009). These methods, while effective for obtaining broad-scale data, often lack the precision needed to capture the fine-scale heterogeneity of these habitats and can be destructive to sensitive ecosystems like RBs and coralligenous assemblages (Bordehore et al., 2003; Basso et al., 2017).

Advances in scuba diving techniques, including technical diving with mixed gases, have expanded access to mesophotic zones, allowing for in situ observations and non-invasive sampling down to depths of 150 meters (Cerrano et al., 2019; Pyle, 2000). However, the limited bottom time and logistical constraints of diving have spurred the development of remote technologies such as remotely operated vehicles (ROVs) and drop cameras, which complement traditional methods by enabling detailed visual surveys and targeted sampling in deeper areas (Gambi et al., 2009; Deidun et al., 2022). In parallel, technological advancements have led to the development of novel, less invasive methods for biodiversity assessment. Techniques such as environmental DNA (eDNA) metabarcoding allow for the detection of species diversity within a habitat by analyzing trace DNA present in the environment, while bioacoustics enables the study of habitat activity through the sounds emitted by various species. These emerging methodologies continue to advance and holds great potential for biodiversity monitoring in deep-sea habitats without causing damage to the seafloor. Because they offer a more environmentally friendly approach and can be cost-effective and time-efficient, there is a need to explore their effectiveness in the study of mesophotic and deep-sea ecosystems. Nowadays, despite these advancements, traditional sampling remains a valuable tool for collecting specimens and sediment samples, especially when combined with modern, less invasive approaches to minimize environmental impact (Basso et al., 2016; Ingrassia et al., 2023).

1.1.5. Knowledge gaps.

This thesis aims to address and complement some of the current gaps in knowledge regarding RBs, focusing on the largest Mediterranean RB, located in the Menorca Channel, Balearic Islands, Spain.

- Although several studies report the presence of rhodolith-forming species in different Mediterranean RBs, there is still a lack of research on their specific diversity. This gap hinders the generation of detailed distribution maps and a comprehensive understanding of the species diversity coexisting within the same RB. **Chapters II** and **III** of this thesis aim to expand knowledge on the diversity of rhodolith-forming coralline algae in the Menorca Channel, employing an approach that integrates molecular identification with morpho-anatomical

characterization. This integrated approach is essential for understanding the complexity of the habitat, as well as for providing essential information for future studies on the functional diversity of rhodoliths species and their response to stress. A precise understanding of the species composition of RBs can be particularly valuable in physiological studies at the community level. This is because a single species will exhibit a specific response to variable parameters related to climate change. The overall community response will vary based on the combined species-specific responses. In addition, increasing knowledge on species diversity can contribute to improving conservation regulations for these habitats in the Mediterranean, improving biodiversity inventories, and facilitating studies on the spatial distribution of species across the region.

- One of the key ecological characteristics that make RBs particularly relevant is their structural complexity. While some studies have examined the relationship between structural complexity, environmental variables, and fishing impacts – showing that higher structural complexity can be associated with better environmental status - there is still a significant knowledge gap regarding the link between the specific species composition of RBs and their morphological complexity. This gap is largely due to the high phenotypic plasticity of many of these species. **Chapter I** of this thesis explores the three-dimensional structure of rhodoliths morphotypes to better understand their ecological importance and environmental status, emphasizing the need to consider their three-dimensionality as an indicator of their role as ecologically important habitat.
- Despite many studies highlight the ecological importance of RBs as habitat providers and nursery areas for commercially important fish species, there is still a lack of research aimed to routinely and effectively monitoring the diversity of fish species that rely on these habitats. However, one of the main challenges in studying Mediterranean RBs is their depth and their vulnerability, which complicates sampling logistics and demands non-invasive biodiversity monitoring. In **Chapter IV** of this thesis, a novel sampling system is employed for first time, combining three distinct techniques: bioacoustics, environmental DNA (eDNA) and video imaging, applied to a well-preserved RB. This study evaluates the capability, feasibility, and cost-effectiveness of these methods. By doing so, it enhances our understanding of the fish species associated with Mediterranean RBs, while providing insights into how different techniques can be integrated to obtain a more comprehensive representation of species diversity, habitat composition, and biological activity within ecologically significant environments. Furthermore, this study aims to lay the groundwork for establishing effective monitoring systems that do not rely on environmentally destructive techniques, particularly in areas with well-documented biodiversity inventories.

1.2. Objectives and Hypothesis

The primary objective of this thesis is to enhance our understanding of Mediterranean RBs, focusing on their species composition, their morphological and three-dimensional structural complexity and their role as a habitat provider by assessing associated fish diversity. These habitats, composed by free living nodules of (typically branched) red coralline algae that accumulated over the seabed, create intricate three-dimensional structures. Such structural complexity supports remarkable biodiversity and serves as critical nursery grounds for numerous species, including those of commercial or of ecological importance. RBs are highly sensitive to human-induced impacts and environmental changes. Their conservation requires non-invasive and innovative approaches to study their biodiversity and morphological structure.

This thesis is structured in four sections and two appendices. In the first section, (**Section I**), the general introduction has been presented and now the objectives of this thesis will be explained. Furthermore, following this section, you will find the methods used and the main knowledge gaps. Then, **Section II** includes the research results of this thesis. These results are divided in four chapters (**I** – **IV**), each one is guided by specific initial hypotheses:

- The first chapter explores the structural complexity of rhodoliths, focusing on their role as bioengineers. The hypothesis driving this chapter is that the core area of the RB has the highest morphological complexity, which decreases with distance as rhodolith density gradually declines over the sandy/detritic bottom. Using morphometric analyses, this chapter proposes methods to quantify the bi- and three-dimensional spaces that shape biodiversity and small-scale habitat heterogeneity in well-preserved RBs along a gradient from the core habitat to peripheral zones.
- The second chapter investigates the species composition of rhodolith-forming algae, combining morphological and molecular analyses. The driving hypothesis is that, underlying the observed diversity of morphotypes, the bed is composed by multiple species belonging to different genera of Hapalidiales, Corallinales and Sporolithales; therefore, current species lists are underestimating the species composition of Mediterranean RBs. This chapter seeks to identify and characterize these species, providing a comprehensive understanding of their contributions to these multi-specific habitats. Such findings are essential for effective conservation, as current regulations often focus on widely distributed European species.
- The third chapter focuses on the neotypification and taxonomic re-description of a species in the genus *Sporolithon.* Although *Sporolithon ptychoides* has previously been reported in the Mediterranean, our hypothesis is that the species observed in this study represents *Sporolithon mediterraneum*. By providing molecular data and a refined taxonomic framework, this chapter

addresses a critical gap in the representation of Sporolithales within the Mediterranean RBs, further enriching our understanding of their biodiversity.

- The fourth chapter evaluates three low-impact survey methods for studying and monitoring the fish diversity associated with RBs in the Menorca Channel. Our hypothesis is that employing multiple non-invasive monitoring techniques will provide a more integrated and accurate understanding of the fish diversity within these habitats, while minimizing survey impacts. The chapter aims to assess the strengths and complementarities of three different survey techniques, offering valuable insights for long-term biodiversity monitoring.

Following the presentation of the chapters, this thesis includes **Section III**, which summarizes the discussions; **Section IV**, which presents the main conclusions; and **Section V**, which summarizes the contributions presented. **Appendix I** includes the original versions of the published works that form this thesis and **Appendix II** includes related publications from parallel collaborations that significantly contributed to shaping the thesis narrative.

Overall, this thesis integrates ecological, morphological and molecular perspectives to unravel the RBs' structural complexity and its associated biodiversity. Guided by the hypotheses, it aims to provide essential knowledge for the conservation and management of these vulnerable habitats, aligning with international directives and fostering a deeper appreciation of their ecological value.

1.3. General Methodology

1.3.1. Menorca Channel as study area

The study area is located in the Menorca Channel, in the Western Mediterranean between the islands of Mallorca and Menorca. This channel spans 3353.4 km^2, reaching a maximum depth of 100 meters (Moranta et al., 2014). The high transparency of its waters allows photosynthesis to occur up to its maximum depth, fostering the development of a diverse algal community. In particular, it is a place where rhodoliths can be found with a coverage of <50% with two large RBs of high densities (>50% of coverage). These RBs act as substrate for other non-calcifying red algae such as *Peyssonnelia* and *Osmundaria*, growing on top of some rhodoliths. Additionally, the LIFE+INDEMARES project (Moranta et al., 2014) identified patches of the endemic brown alga *Laminaria rodriguezii* distributed on the RBs, that attach to the hard substrate provided by rhodoliths (**Fig.1.3.1**).

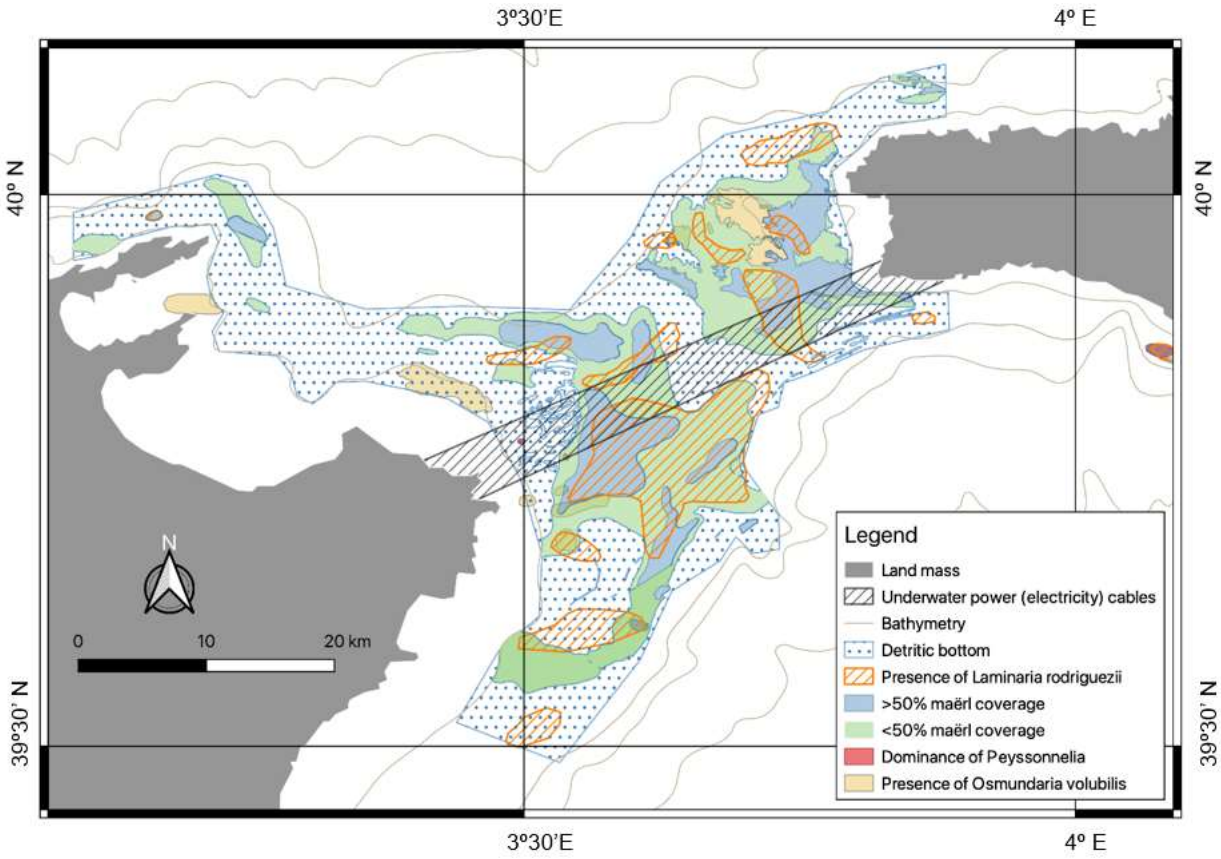


Fig.1.3.1. Principal habitats of the Menorca Channel. Extracted from de Juan et al. (2023).

In 2016, the Menorca Channel was designated a European Site of Community Importance (SCI ESZZ16002), and a trawling ban was enacted for most of the channel, based on extensive research by the INDEMARES project. Additionally, since the 1970s, the presence of underwater electricity cables between Mallorca and Menorca islands has established an exclusion zone crossing the channel where trawling is prohibited, providing over five decades of protection for the sea bed.

The combination of a gently sloping continental shelf, and the prevalence of moderate bottom currents creates optimal conditions for the accumulation of rhodoliths. As a result, this study area hosts the largest identified RB in the Western Mediterranean, covering an area of 304 km². The density of rhodoliths decreases with distance from the center of this bed, which we defined as the "Core Habitat" toward peripheral areas (**Fig.1.3.2**). This density variation is influenced by both topography, with depth increasing southeastward and decreasing toward the coast to the west, and environmental factors, such as the sandy platform of the Bay of Alcudia affecting the northwestern area.

The favorable conservation status of the Menorca Channel is also due to relatively low trawl fishing pressure in the Balearic Islands compared to other Mediterranean areas. Although trammel net fishing is routinely practiced in the channel, trawl fishing has historically been low (Barbera et al., 2003) (**Fig.1.3.2**). Trawling restrictions are in place for coastal waters shallower than 50 m, and since 2016, a trawling ban was extended throughout the central part of the channel (Order AAA/1479/2016 of September 7) (**Fig.1.3.2**). In addition, historically many trawlers avoided the highly dense RBs as the nets could be entangled and damaged (fishers personal communication).

This study area was selected based on previous research identifying a well-developed and preserved RB, alternating with detritic bottoms and biogenic assemblages formed by other algal species (de Juan et al., 2023; Moranta et al., 2014). It was chosen as a study area to investigate and expand our knowledge on rhodoliths because of its good state of conservation. Understanding the structure and composition of this habitat, starting from the best-preserved ecological baseline available, can help us to appreciate the value of these shelf Mediterranean habitats. This baseline allows us to comparatively analyse other RBs and assess their ecological status.

Twelve random survey stations were established between 48 to 75 m depth, covering a gradient of rhodoliths density within the largest patch of rhodoliths in the Menorca channel (**Fig.1.3.2**). This sampling plan was designed by combining original dredge and video studies (see section 1.3.2) and results and knowledge extracted from the literature (such as Barberá et al., 2012; Moranta et al., 2014; de Juan et al., 2023). These stations, while being in an area of low trawl impact, have varying degrees of historical exposure to trawling. For this purpose, we defined those stations close to the limit of the 2016 extension of the reserve, and which were therefore exposed before 2016, as 'exposed', and those stations within the reserve area or shallower than 50 m where trawling is not allowed as 'not exposed'. In addition, rhodolith abundance was not assumed to be the same throughout the area, as we observe locations with patches above or below the 50% cover. Those stations on the margin of the rhodoliths bed have rhodoliths scattered in the sand without forming a well-constructed bed, being another type of habitat. Finally, some of these stations are located in the 'core habitat' where the best conditions for rhodoliths and the higher coverage and abundance of rhodoliths is expected while the rest are in the 'adjacent area' (**Fig.1.3.2**).

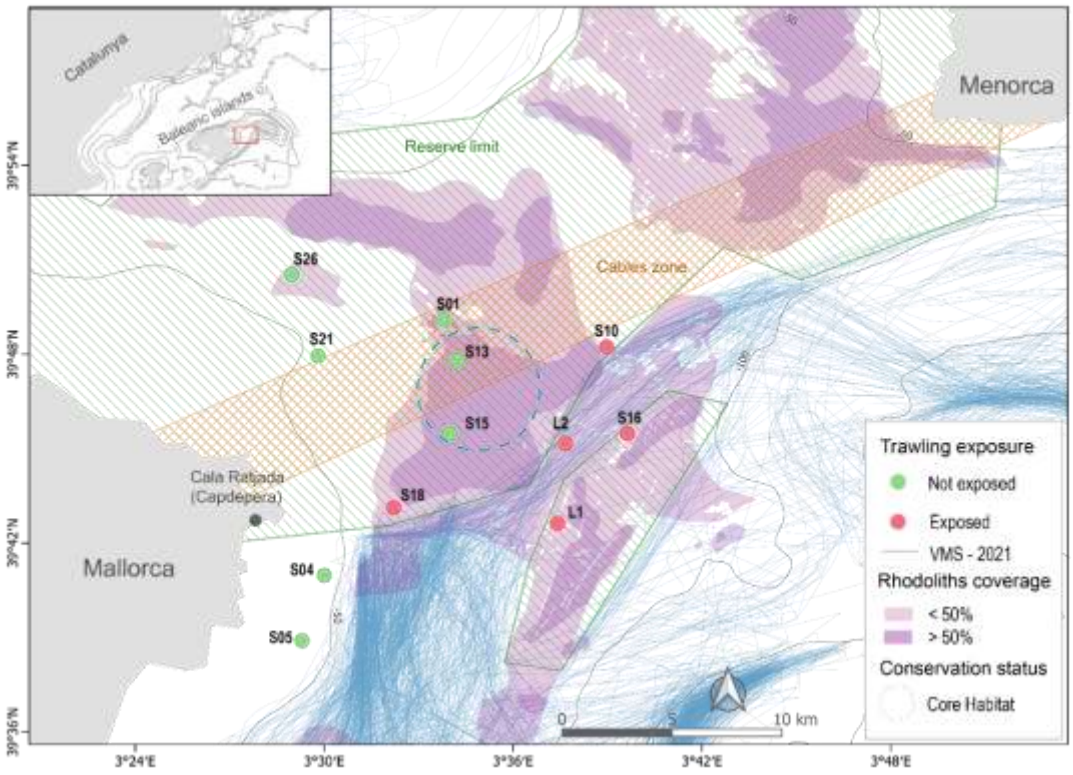


Fig.1.3.2. Representation of the twelve selected stations along the Menorca Channel. In red the 'Exposed' areas, those considered disturbed by the effects of trawling (sediment resuspension and physical damage) before 2016 and relatively impacted after 2016 because they are at the limits of the protection boundaries. In green those that are 'Not exposed' to the effects of trawling either because they are at shallow depths or because they were fully protected before and after the 2016 protection measures. The blue circle is the area we define as 'Core habitat', i.e. the area where the physical and environmental conditions are best for rhodolith growth. The blue lines are the VMS footprints of 2021. Rhodolith densities are shown in pink and purple.

1.3.2. Sampling and fieldwork – MaCoBioS project.

During the summers of 2021 and 2022, and within the framework of the H2020 European project MaCoBioS (https://macobios.eu/), sea sampling missions were carried out to monitor the biodiversity and environmental status of the area and to take samples of rhodoliths. These field trips were carried out aboard a small 12 m motor boat based in Cala Ratjada. Due to the different objectives of the study, but also due to technical failures, the adverse weather conditions that we could encounter (as the Menorca Channel is a complicated area for navigation when there is wind and waves), and the depth of the different stations, it was not possible to sample all the stations with the same methods.

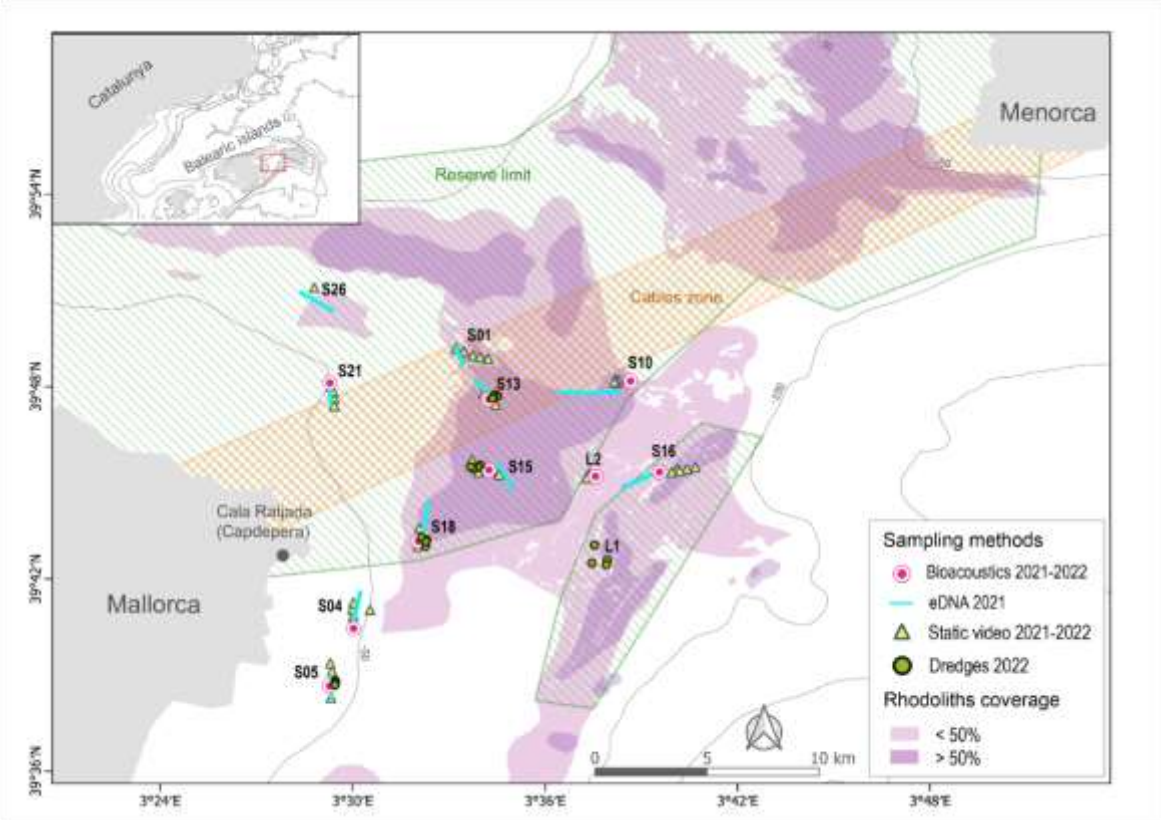


Fig.1.3.3. Representation of the type of sampling carried out at each of the twelve stations of the study. The home port in Mallorca, Cala Ratjada and the zones that delimit the protected area and the submarine cable zone are marked.

Thus, eleven of the twelve stations were sampled during the summers of 2021 and 2022 with at least two of the three non-intrusive techniques (video, eDNA or bioacoustics), collecting as much information as time and weather allowed. Finally, during the summer of 2022, physical samples of rhodoliths were collected with a naturalistic dredge at five of the twelve stations (**Fig.1.3.3** and **Table 1.3.1**).

The three first chapters of this thesis are based on dredge sampling to characterize the morphology of rhodoliths and the rhodolith-forming species diversity of this area. The last chapter is based on the sampling of demersal fish by the three non-intrusive techniques to assess the ecological importance of RBs as habitat provider. Therefore, in order to avoid repeating information, this section explains the particularities of each sampling technique in the order in which they occurred.

Table 1.3.1. Sampling methods used in each station.

Station	Video	eDNA	Bioacoustics	Dredges
S26	X	X		
S21	X	X	X	
S01	X	X		

S13	X	X	X	X
S10	X	X	X	
S15	X	X	X	X
S18	X	X	X	X
L1				X
L2	X		X	
S16	X	X	X	
S04	X	X	X	
S05	X	X	X	X

1.3.2.1. Video (static cameras) sampling

In order to provide a small-scale characterization of the type of habitat over which the stations are located, five stable tripods were set up with two watertight, circular housings in which two GoPro 7 video cameras (1920 x 1440 HD resolution) recorded simultaneously (**Fig.1.3.4**). To ensure the stability of the tripod when it lays over the bottom, four 1kg pieces of ballast were attached with flanges to the four ends of the tripod base. The recordings were also inspected to investigate the usefulness of video cameras for detecting the presence of fish to meet the objectives of **Section II – Chapter IV**.

The cameras were set to record while still at the sea surface before deployment. They were then deployed with the tripods secured to a line with intermediate buoys, preventing excess line from passing in front of the camera. The line was also tied to a buoy, which was left floating on the surface. After fixing the exact coordinates of the launch, we proceeded to the next launch, maintaining an average separation of about 350 m. The tripods were recovered after ca. 40’ of recording.

Details of video analysis are explained in **Section II - Chapter IV**.



Fig.1.3.4. Tripod system with two waterproof housings for GoPro (left). Tripod system during launching (right).

1.3.2.2. eDNA sampling

In order to explore alternative techniques to identify fish diversity and thus to meet the objectives from **Section II – Chapter IV**, environmental DNA samplings were carried out at several sites on RB and on surrounding detrital sands. The eDNA samples were taken during MaCoBioS fieldwork campaigns. Due to the depth of the stations, the use of scuba divers (**Fig.1.3.5** -right) was not feasible so we adapted the technique by towing the water pump from the vessel (**Fig.1.3.5**-left), approximately 5 m above the seabed. Each transect lasted 45 minutes, during which 45 L of seawater were filtered.

The water pump was equipped with a 0.2 µm polyethersulfone filter to retain small DNA fragments released by organisms in their immediate environment (Miya, 2022). The part where the water enters is covered to avoid contamination and is uncovered just before launching.

Two replicates were collected at each station. Onboard the vessel, a buffer solution was added to the filters in order to preserve the DNA. Finally, they were stored at room temperature and subsequently shipped to the SpyGen laboratories (https://www.spygen.com/fr/). Gloves were worn at all times when handling and changing filters between stations.

Details of DNA extraction and amplification and further analysis are explained in detail in **Section II - Chapter IV**.



Fig.1.3.5. Modified system of the water pump (left). Traditional eDNA sampling through scuba divers (right).

1.3.2.3. Bioacoustics sampling

In order to explore alternative techniques to identify fish diversity and thus to achieve the objectives of **Section II - Chapter IV**, a bioacoustic sampling was carried out. A system equipped with an HTI-92-WB hydrophone (High Tech Inc., USA) with a sensitivity of 155 ±3 dB re 1 V/µPa and a flat frequency response of 5 Hz to 50 kHz, connected to a compact SDA14 stand-alone recorder (RTSys®, France), was deposited on the seabed. Another hydrophone was connected to this recorder to acquire sounds continuously at a sampling frequency of 78 kHz and a resolution of 24 bits. To keep the structure stable

and one meter above the seabed, the recorder was attached to a metal rod fixed to a concrete base with sufficient weight so that the whole system would not tip over. The first hydrophone was attached to the upper end of this metal rod (one meter above the base) and, connected to it and secured with a line, was the second hydrophone separated one meter from the first one. In order to keep one hydrophone one meter away from the other one that was fixed to the structure, an intermediate buoy was added (**Fig.1.3.6**). The whole structure was secured with another line connected to a surface buoy to keep the device located.

The recorder was always deployed in the evening and recovered the following day. Recordings were made at night because most temperate water fish vocalize predominantly at night (Bolgan et al., 2019; Picciulin et al., 2012), and interference with anthropogenic noise is greatly reduced.

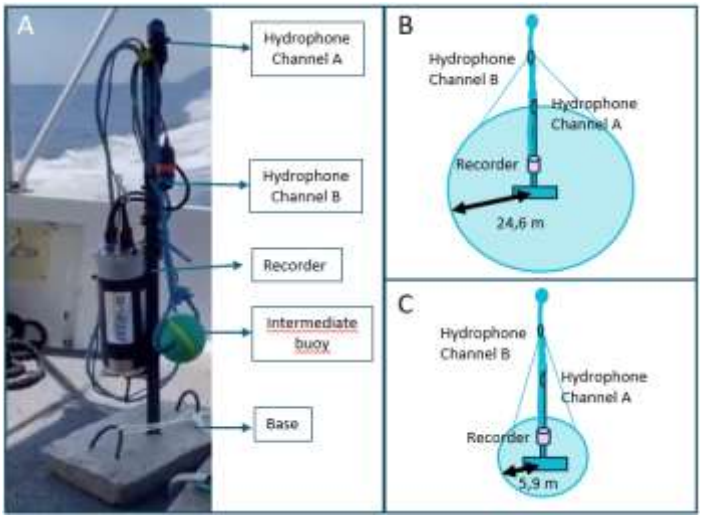


Fig.1.3.6. Two-hydrophone system deployed during the study (**A**). Setting for benthic sound detection at a radius of 24.6 m (**B**) and 5.9 m (**C**).

This two-hydrophone system (**Fig.1.3.6**-A) was used to obtain benthic sounds produced by both fish and invertebrates at different amplitude radii (**Fig.1.3.6**-B, C). The audio recordings obtained were processed by the company Chorus (https://chorusacoustics.com/). In this study, only sounds from fish have been used. Those from invertebrates are still being analysed. For the fish sounds, only the records from microphone A were used, which gives an accuracy of between 50 and 300 m radius of the device.

Details of sound processing are explained in **Section II - Chapter IV**.

1.3.2.4. Rhodolith sampling

In order to study the morphological and species composition of the Menorca Channel and fulfil the objectives defined in **Chapters I** to **III**, it was strictly necessary to obtain rhodoliths specimens from the study area. To make rhodolith sampling as unobtrusive as possible, a naturalist dredge of 45 cm x 18.5 cm opening with a 1 mm mesh size (**Fig.1.3.7**, left) was used. For this, five stations were selected,

two inside the 'core habitat' and three in the 'adjacent area' (see **Fig.1.3.2** and **Fig.1.3.3**). Five dredge hauls were made at each dredging station, although not all five samples were successful.

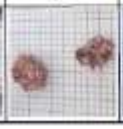
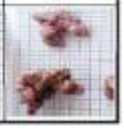


Fig.1.3.7. Naturalist dredge used during the sampling (left). Rhodoliths being air-dried and photographed during the navigation time between stations (right).

For each dredge, a volume of approximately 7L of the content was systematically extracted, distributed in a tray and photographed. The proportion of live and dead rhodoliths was visually estimated on board for each tray. The rhodoliths were classified into nine morphotypes (A to I), described based on the six used in Barberá et al. (2012b) with some modifications that further divided heterogeneous groups (**Table 1.3.2**). These nine morphotypes belong to the three main rhodolith categories or growth forms according to Basso et al. (2016): "Branched" (Br), "Praline" (PR) and "Boxwork" (Bo). The rhodoliths were grouped by morphotypes, photographed on a graduated white board (**Fig.1.3.7**, right) and air-dried during three days. Finally, they were stored in zip bags with silica gel. A total of 3877 rhodoliths were obtained and dry stored. The rhodoliths obtained here were used in **Section II – Chapter I** but also in **Section II – Chapters II** and **III.**

In addition, a sample of approx. 100 g of sediment extracted from each dredge was stored for granulometry analysis and determination of carbonate contents, while the remaining content of the dredges was returned to the sea. Finally, pieces of rhodoliths as well as small extra sediment samples were kept frozen at -20ºC for future metabarcoding and barcoding studies.

Table 1.3.2. Rhodolith growth forms and description of morphotypes defined in the finer classification (A to I).

	BRANCHED				PRALINES			BOXWORK	
MORPHOTYPES	Large size with wide branching	Small size, less and short branching	Small size with slender branches	Many short branches. Spherical	Rough, bumpy and quite irregular	Rounded with small protusions or short branches	Rounded with many thick and smooth protusions	Rounded and incrusted in other substratum	Irregular form, incrusted in other substratum
	A	B	C	D	E	F	G	H	I
									

1.3.3. Data analysis

1.3.3.1. Habitat characterization

The video cameras deployed during the campaign were not only used as a non-destructive technique to assess fish diversity in **Chapter IV** but also to confirm the habitat characterization expected from INDEMARES maps. This approach ensured a clear understanding of the habitat composition studied across the different chapters.

Video imaging is used to characterize abiotic (e.g., substrate type, rugosity, slope) and biotic components of the habitat (e.g., rhodolith coverage, presence of macroalgae, and signs of biotic activity) (de Juan et al., 2015; Illa-López et al., 2023; Kuhnz et al., 2022; Loh et al., 2019), providing a semi-quantitative estimation of small-scale biophysical heterogeneity. One of the main limitations of working with video footage is the quality of the images obtained, which can be influenced by several factors, including the resolution and specifications of the cameras used, water transparency, lighting conditions, and even the angle at which the cameras settle on the seafloor after deployment. Poor visibility or inadequate positioning can hinder the ability to accurately assess habitat characteristics and species presence.

Despite these challenges, video cameras remain an invaluable tool, particularly when working in well-documented and previously studied areas where the general characteristics of the habitat and substrate are already known. In such cases, video imaging provides a reliable method for habitat characterization at small-scales, detecting structural changes over time, and monitoring biological activity. Additionally, compared to more invasive or labor-intensive sampling techniques, video surveys offer a fast, cost-effective, and minimally intrusive approach to long-term habitat monitoring, making them an essential method for ecological assessments and conservation planning.

As we could observe in Illa-López et al. (2023) and Demestre et al. (2024), it is relatively difficult to quantify the rhodoliths coverage of the bottom relying on information extracted from the ROV video images; however, these images are useful to identify heterogeneity at small scales. Static cameras were used for this thesis and, with the experience gained from the two previous studies mentioned above, the habitats were classified based on rhodolith coverage into three types: (i) RBs with more than 50% coverage, (ii) detritic biogenic habitats with less than 50% rhodolith cover, and (iii) detritic biogenic habitats with less than 10% rhodolith cover. Additionally, a more detailed description of habitat components was included, considering the presence of additional algal species contributing to biogenic complexity, indicators of bioturbation, and spatial heterogeneity in habitat continuity. By integrating this information with existing maps generated with empirical data, we can identify small-scale habitat variability, identify possible fragmentation and other biophysical attributes. This provides a valuable framework for interpreting the ecological patterns explored throughout this thesis.

While rhodolith coverage characterization has been considered throughout all chapters of this thesis, more detailed information regarding the description of the different video sampling stations can be found in **Section II – Chapter IV**.

1.3.3.2. Rhodolith composition

1.3.3.2.1. Morphometrics

To achieve the objectives of **Section II - Chapter I**, and to explore the complexity generated by morphologies with their three-dimensional structure in RBs, a morphometric study was carried out. First, with a general exploration of the morphometric measurements through images in two dimensions. Then, by focusing on the morphotype that has larger size and a branching growth-form. Finally, we focused on extracting the same metrics in three dimensions to explore the correlation between 2D and 3D approaches, and to analyse how much information we lose by working with 2D in the complex morphologies exhibited by rhodoliths.

1.3.3.2.2. Treatment of rhodoliths for 2D measurements.

All rhodoliths were photographed live on graduated cardboard before being air-dried and stored in silica gel. These images were then used to count how many total rhodoliths had been sampled and to get the proportions of each morphotype as explained in **Section II - Chapter I**.

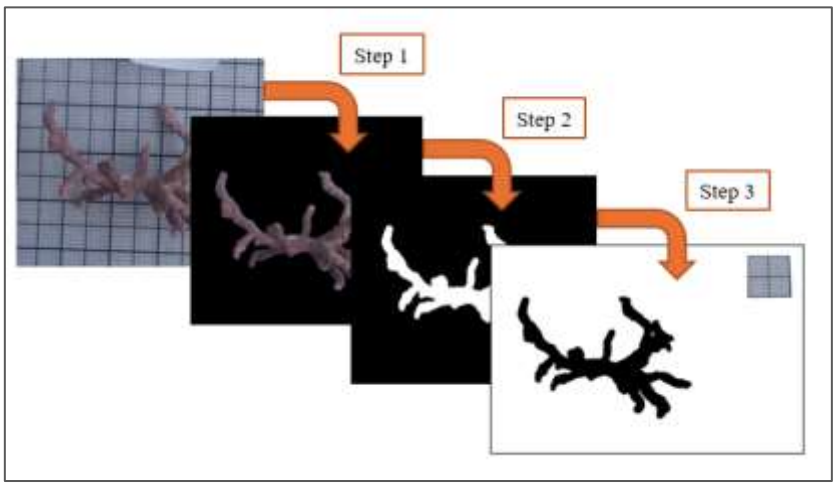


Fig.1.3.8. Transformation of the images in three steps using photoshop to get the shape of the rhodoliths in black and white.

Then, to obtain the morphometric measurements in two dimensions, the images were transformed with the help of Photoshop in 3 steps (**Fig.1.3.8**): in the first step, the background of the grid was removed; then, in the second step, the shape of the rhodolith was converted to white; finally, in the third step, the image was inverted getting the shape of the rhodolith in black and a square of the grid was recalled to be able to calibrate the distances and, therefore, to obtain the measurements. The metrics were obtained

using ImageJ 1.52a software (Schneider et al., 2012). For each image, the distance was calibrated considering that the squares left in the images measured 1cm and creating the conversion to pixels. Then, using the default version of the program, measurements were extracted for: the maximum and minimum axis of the fitted ellipse, the surface of the projected area, the shape perimeter, the angle, the Feret length and the Feret's angle. In addition, measures of the relationships between the latter, such as the circularity, the roundness and aspect ratio, were obtained.

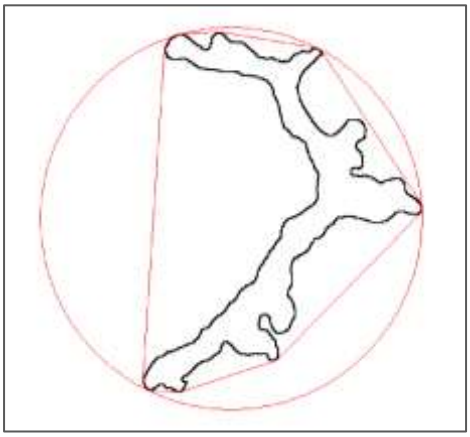


Fig.1.3.9. ConvexHull (internal) and bounding circle (external) example created by ImageJ.

Then, the Convex Hull was created using the plugin "Hull and Circle" v.2.1b contributed by A. Karperien (https://imagej.net/ij/plugins/hull-circle.html). This is like replacing the freehand selection polygon with its convex hull determined by the gift-wrapping algorithm. The convex hull can be thought of as a rubber band wrapped around the points defining the selection. The algorithm also generates the bounding circle around it, which is determined by the largest amplitude across the hull, and if that circle does not include all the points, the triangle that forms the smallest circle containing all the points of the hull is used. (**Fig.1.3.9**). With this plugin, the area of the convex hull and its relation to the area of the rhodolith as a measure of Solidity were calculated automatically. Subsequently, the interstitial space was calculated with the difference between the area of the convex hull and the area of the rhodolith, understanding the interstitial space as all the free space generated by the shape of the rhodolith due to its ramifications and its complex form, which we assume is a proxy for settlement space or refuge for infauna. Finally, after being air-dried and preserved in silica gel, the dry weights of the rhodoliths were taken.

The concrete specifications of each measure, their formulas and representations are detailed in **Section II - Chapter I**.

1.3.3.2.3. Treatment of rhodoliths for 3D measurements.

For the three-dimensional measurements of morphotype A defined in this work (see **Table 1.3.2**), a selection of 30 rhodoliths of this morphology was taken after air-drying, weighing and two-dimensional measurements. Using a high-precision blue light 3D scanner (Revopoint MINI) with an accuracy down to 0.02 mm, the entire shape of the rhodoliths was scanned and by processing the scans obtained with the help of Revoscan and Revostudio software (http://www.revopoint3d.com) the rhodoliths were digitally recreated. We call these recreations "digital twins".

Once the digital twins were obtained, we created an ad hoc script in R to obtain measurements for the surface area, the maximum length from the center of mass, the volume and the convex hull volume in a three-dimensional form. Before applying the script, we verified multiple times, with the Rhinoceros software (https://www.rhino3d.com/) (**Fig.1.3.10**), that the measurements obtained with both methods were consistent, thus validating our script. With these measurements, the three-dimensional interstitial space was calculated as the difference between the volume and the convex hull volume. Understanding in this case that it is all the free space in three dimensions left by the rhodolith due to its complexity of shape. Finally, to obtain the measures for the Feret diameter and the roundness in three dimensions, the Slicer program v. 5.2.2 (Fedorov et al., 2012) was used.

The R libraries used to create the script of this part, an example of a digital twin as well as further clarification of the measurements used, are specified in **Section II - Chapter I**.

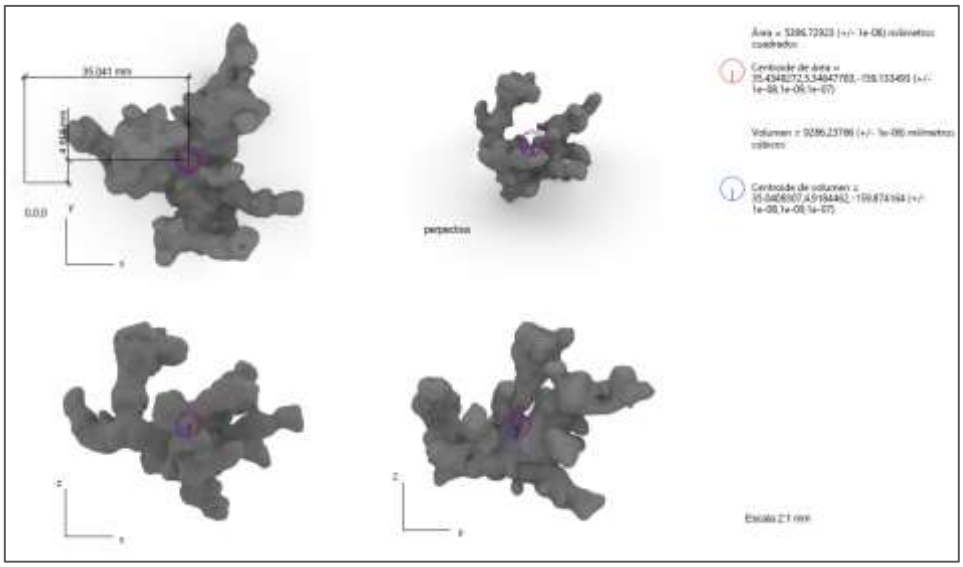


Fig.1.3.10. Example of measures obtained with Rhinoceros software. Credits: Guillem Larred (naval engineer).

1.3.3.2.4. Microscopy methods

For the study of the morphological characters of the rhodolith species, to assess the aims for **Section II - Chapters II** and **III**, it was necessary to prepare the rhodoliths for different microscopy techniques.

Initially, the rhodoliths were superficially examined under a binocular microscope to identify features such as the type and arrangement of sori, which might indicate the group or family to which the rhodolith belonged. We also looked for evidence of overlapping growths, suggesting the presence of more than one species on the same rhodolith (Foster, 2001). During this process, we took the opportunity to document and photograph the associated fauna and flora visible on the rhodolith's surface or occupying its interstitial spaces. These notes and photographs were collected with the aim of

taxonomically identifying the macrofauna associated with the rhodoliths and studying their relationship with the different rhodolith morphologies in greater detail, an objective to be addressed in the future.

Subsequently, transverse and longitudinal sections of the branches and protrusions were prepared to observe the shape and distribution of the cells. Small pieces of the surface epithelium were also removed to analyze the epithallial cells and conceptacles in greater detail. When conceptacles were present, efforts were made to section them as precisely as possible for further examination. Due to the extremely hard and calcareous structure of these algae, obtaining the desired sections was often challenging. A wooden block, a pickaxe, and a hammer were used to deliver sharp blows and section the rhodoliths at the points of interest.

The analysis of these structures using light microscopy is highly challenging due to the calcium carbonate composition of the rhodoliths and the thickness of the fragments obtained. Consequently, this technique was employed only when strictly necessary (e.g., in **Chapter III** of **Section II**). To observe the structures under the light microscope, the rhodoliths must first be decalcified using 10% nitric acid, followed by the preparation of cryostat sections with a cryomicrotome (Leica CM3050 S).

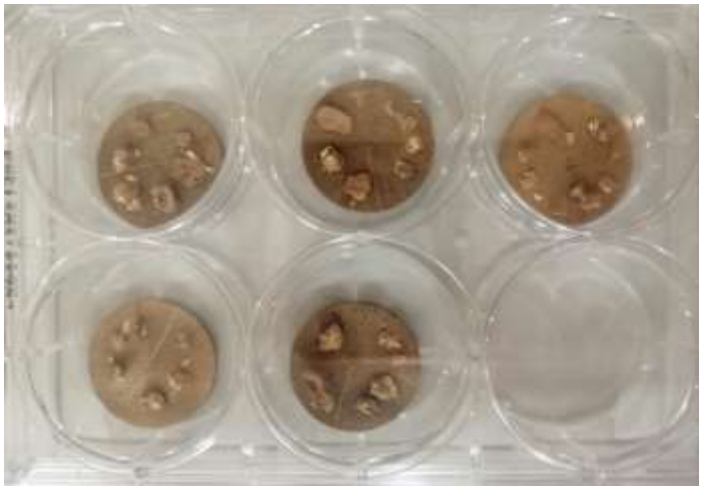


Fig.1.3.11. Preparations for SEM of fragments on aluminum carbon holders coated with gold.

Scanning electron microscopy (SEM) was performed with JSM 6400 (Jeol, Japan) and Hitachi S-3500N (Hitachi High-Technologies Co., Japan) microscopes at a DW of 14 mm. Rhodolith fragments were mounted on carbon and aluminum holders using carbon adhesive tape and coated with a 15 nm gold layer using the Quorum Q150R S sputter coater (Quorum Technologies Ltd.) (**Fig.1.3.11**). When it was necessary to measure cells of the different vegetative cell types or reproductive characteristics, SEM tools were used to make the relevant measurements while photographing.

The identification of rhodolith-forming species in **Section II - Chapters II** and **III** required the examination of key taxonomic characteristics described in the literature. These analyses were conducted

by using a combination of optical and scanning microscopy. Specific features studied included the type of thallus and the organization of the medulla and cortex (monomeric/dimeric thallus, coaxial/non-coaxial medulla), as well as the morphology and size of the cells forming the filaments—particularly the initial epithallial and subepithallial cells. Additionally, the type of connections between adjacent filament cells (secondary pit connections or cell fusions) and the structure of reproductive features (conceptacles) were also investigated. This approach ensured accurate identification and confirmation of the rhodolith-forming species.

The deposition of some of the specimens in official herbaria is indicated in each chapter.

1.3.3.2.5. Molecular protocols

From the selected and air-dried rhodoliths, a total of 120 specimens (**Table 1.3.3**) were cleaned from epiphytes under a stereomicroscope and selected surfaces were filed with the use of a rotary hand tool (Dremel®) to obtain powder from the epithelial cell layer for DNA extraction (**Fig.1.3.12**). Then, genomic DNA was extracted using a NucleoSpin® Tissue kit (Macherey-Nagel, GmbH and Co, KG, Germany), following the manufacturer's protocol. The final product of the extractions contained in a 1.5 mL Eppendorf was stored in a -20°C freezer.

Once DNA extractions were obtained, their concentration was measured using a Nanodrop spectrophotometer, and their quality was assessed by observing the A260/A280 and A260/A230 ratios (**Table 1.3.4**). Since the DNA concentrations and quality were generally low, a common issue reported in the literature and by experts for calcareous organisms, the protocol was continued for all extractions with Nanodrop readings above 1 ng/µL.



Fig.1.3.12. Extraction of powder from the surface tissue using the Dremel (left). Powder obtained (right).

Table 1.3.3. Summary of the 120 specimens selected for DNA extraction. Successful amplification of the three molecular markers *psb*A, COI and *rbc*L indicated.

DD/MM/YY	Original CODE	SITE	DREDGE	MORPHOLOGY	SUBJECT	DRY MATERIAL	FREEZE MATERIAL	IMAGE	MORPHOTYPE	NEW CODE	DNA extracted	PCR-psbA	PCR-COI	PCR-rbCL
27-07-22	L1D1M3.4	L1	D1	M3	4	X	X	X	A	L1A4	x	contamination		
27-07-22	L1D1M2.2	L1	D1	M2	2	X	no	X	B	L1B1	x	contamination		
28-07-22	L1D3M8.1	L1	D3	M8	1	X	X	X	H	L1H12	x	contamination		
29-07-22	S15D3M2.3	S15	D3	M2	3	X	X	X	B	S15B9	x	contamination		
29-07-22	S15D4M5.3	S15	D4	M5	3	X	X	X	G	S15G7	x	contamination		
01-08-22	S18D3M2.2	S18	D3	M2	2	X	X	X	B	S18B7	x	contamination		
01-08-22	S18D1M2.1	S18	D1	M2	1	X	X	X	E	S18E1	x	contamination		
01-08-22	S18D2M5.2	S18	D2	M5	2	X	X	X	E	S18E10	x	contamination		
01-08-22	S18D1M4.2	S18	D1	M4	2	X	X	X	F	S18F2	x	contamination		
02-08-22	S5D2M1.1	S5	D2	M1	1	X	X	X	H	S5H1	x	contamination		
02-08-22	S5D1M6.1	S5	D1	M6	1	X	X	X	I	S5I1	x	contamination		
02-08-22	S5D1M8.1	S5	D1	M8	1	X	X	X	F	S5F5	x	contamination		
02-08-22	S5D1M7.2	S5	D1	M7	2	X	X	X	I	S5I3	x	low		
02-08-22	S5D1M1.2	S5	D1	M1	2	X	X	X	F	S5F1	x	poor quality		
03-08-22	S13D1M5.1	S13	D1	M5	1	X	X	X	E	S13E3	x	yes	contamination	contamination
03-08-22	S13D1M6.3	S13	D1	M6	3	X	X	X	H	S13H2	x	yes	contamination	contamination
02-08-22	S5D2M2.1	S5	D2	M2	1	X	X	X	G	S5G1	x	yes	poor quality	contamination
01-08-22	S18D1M5.4	S18	D1	M5	4	X	X	X	E	S18E7	x	yes		contamination
03-08-22	S13D3M5.2	S13	D3	M5	2	X	X	X	H	S13H9	x	yes	contamination	yes
03-08-22	S13D4M6.1	S13	D4	M6	1	X	X	X	I	S13I13	x	yes	contamination	yes
01-08-22	S18D2M2.1	S18	D2	M2	1	X	X	X	A	S18A2	x	yes	contamination	yes
01-08-22	S18D2M1.1	S18	D2	M1	1	X	X	X	C	S18C4	x	yes	contamination	yes
01-08-22	S18D4M4.2	S18	D4	M4	2	X	X	X	D	S18D7	x	yes	contamination	yes
02-08-22	S5D1M2.2	S5	D1	M2	2	X	X	X	C	S5C1	x	yes	contamination	yes
03-08-22	S13D2M6.1	S13	D2	M6	1	X	X	X	C	S13C1	x	yes	contamination	yes
29-07-22	S15D1M1.4	S15	D1	M1	4	X	X	X	D	S15D1	x	yes	contamination	yes
01-08-22	S18D3M1.3	S18	D3	M1	3	X	X	X	C	S18C8	x	yes	contamination	yes
01-08-22	S18D4M5.3	S18	D4	M5	3	X	X	X	H	S18H10	x	yes	contamination	yes
02-08-22	S5D1M3.2	S5	D1	M3	2	X	X	X	D	S5D7	x	yes	contamination	yes
02-08-22	S5D3M7.3	S5	D3	M7	3	X	X	X	X	S5X3	x	yes	contamination	yes
29-07-22	S15D1M2.3	S15	D1	M2	3	X	X	general	A	S15A3	x	yes	poor quality	yes
28-07-22	L1D4M5.3	L1	D4	M5	3	X	X	X	C	L1C17	x	yes	poor quality	yes
03-08-22	S13D2M6.3	S13	D2	M6	3	X	X	X	B	S13B9	x	yes	poor quality	yes
03-08-22	S13D3M2.4	S13	D3	M2	4	X	X	X	E	S13E14	x	yes	poor quality	yes
03-08-22	S13D4M7.3	S13	D4	M7	3	X	X	X	F	S13F1	x	yes	poor quality	yes
03-08-22	S13D3M1.4	S13	D3	M1	4	X	X	X	G	S13G11	x	yes	yes	yes
29-07-22	S15D1M2.2	S15	D1	M2	2	X	X	general	A	S15A2	x	yes	yes	yes
28-07-22	L1D2M6.2	L1	D2	M6	2	X	X	X	C	L1C9	x	yes	yes	yes
27-07-22	L1D1M7.3	L1	D1	M7	3	X	X	X	I	L1I10	x	yes	yes	yes
29-07-22	S15D2M1.4	S15	D2	M1	4	X	X	X	C	S15C8	x	yes	yes	yes
29-07-22	S15D2M1.1	S15	D2	M1	1	X	X	X	D	S15D2	x	yes	yes	yes
29-07-22	S15D4M6.4	S15	D4	M6	4	X	X	X	I	S15I11	x	yes	yes	yes
29-07-22	S15D3M4.4	S15	D3	M4	4	X	X	X	E	S15E28	x	yes		yes
29-07-22	S15D2M2.1	S15	D2	M2	1	X	X	X	G	S15G1	x	yes		yes
29-07-22	S15D3M7.4	S15	D3	M7	4	X	X	X	H	S15H7	x	yes		yes
01-08-22	S18D1M1.1	S18	D1	M1	1	X	X	X	D	S18D1	x	yes		yes
01-08-22	S18D3M4.2	S18	D3	M4	2	X	X	X	G	S18G8	x	yes		yes
01-08-22	S18D1M6.1	S18	D1	M6	1	X	X	X	I	S18I1	x	yes		yes
02-08-22	S5D3M5.2	S5	D3	M5	2	X	X	X	D	S5D25	x	yes		yes
28-07-22	L1D2M4.2	L1	D2	M4	2	X	X	X	E	L1E2	x	yes	contamination	
28-07-22	L1D3M1.3	L1	D3	M1	3	X	check	X	G	L1G2	x	yes	contamination	
03-08-22	S13D3M4.3	S13	D3	M4	3	X	X	X	C	S13C5	x	yes	contamination	

29-07-22	**S15D3M1.2**	S15	D3	M1	2	X	X	X	C	**S15C10**	x	yes	contamination
02-08-22	**S5D1M2.4**	S5	D1	M2	4	X	X	X	C	**S5C2**	x	yes	contamination
03-08-22	S13D1M1.2	S13	D1	M1	2	broken	X	X	A	**S13A2**	x	yes	contamination
03-08-22	S13D4M1.3	S13	D4	M1	3	X	Note label 1.2	X	A	**S13A23**	x	yes	contamination
02-08-22	**S5D3M2.1**	S5	D3	M2	1	X	X	X	F	**S5F8**	x	yes	contamination
29-07-22	**S15D1M4.1**	S15	D1	M4	1	X	X	X	E	**S15E1**	x	yes	yes
28-07-22	**L1D3M5.4**	L1	D3	M5	4	X	X	X	F	**L1F6**	x	yes	yes
02-08-22	**S5D3M4.2**	S5	D3	M4	2	X	X	X	D	**S5D21**	x	yes	
02-08-22	**S5D1M4.3**	S5	D1	M4	3	X	X	X	F	**S5F4**	x	yes	
27-07-22	L1D1M3.3	L1	D1	M3	3	X	X	X	A	**L1A3**	x	yes	
27-07-22	**L1D1M4.2**	L1	D1	M4	2	X	X	X	B	**L1B3**	x	yes	
28-07-22	**L1D3M1.1**	L1	D3	M1	1	X	X	X	E	**L1E4**	x	yes	
28-07-22	**L1D3M7.1**	L1	D3	M7	1	X	X	X	I	**L1I15**	x	yes	
03-08-22	**S13D1M3.1**	S13	D1	M3	1	X	X	X	B	**S13B1**	x	yes	
03-08-22	**S13D2M6.4**	S13	D2	M6	4	X	X	X	D	**S13D1**	x	yes	
29-07-22	S15D4M3.3	S15	D4	M3	3	X	X	X	A	S15A12	x	yes	
29-07-22	S15D1M3.1	S15	D1	M3	1	X	X	X	A	**S15A5**	x	yes	
29-07-22	**S15D2M8.2**	S15	D2	M8	2	X	X	X	E	**S15E18**	x	yes	
29-07-22	**S15D1M4.3**	S15	D1	M4	3	X	X	X	E	**S15E3**	x	yes	
29-07-22	**S15D4M1.1**	S15	D4	M1	1	X	X	X	F	**S15F2**	x	yes	
29-07-22	**S15D4M1.3**	S15	D4	M1	3	X	X	X	F	**S15F4**	x	yes	
29-07-22	**S15D4M5.2**	S15	D4	M5	2	X	X	X	G	**S15G6**	x	yes	
01-08-22	**S18D2M3.1**	S18	D2	M3	1	X	X	X	B	**S18B2**	x	yes	
01-08-22	**S18D2M4.4**	S18	D2	M4	4	X	X	X	E	**S18E9**	x	yes	
01-08-22	**S18D3M4.3**	S18	D3	M4	3	X	X	X	G	**S18G9**	x	yes	
02-08-22	**S5D3M1.1**	S5	D3	M1	1	X	X	X	A	**S5A1**	x	yes	
02-08-22	**S5D1M5.1**	S5	D1	M5	1	X	X	X	D	**S5D10**	x	yes	
02-08-22	**S5D2M3.4**	S5	D2	M3	4	X	X	X	D	**S5D15**	x	yes	
02-08-22	**S5D1M4.2**	S5	D1	M4	2	X	X	X	F	**S5F3**	x	yes	
02-08-22	**S5D1M7.1**	S5	D1	M7	1	X	X	X	I	**S5I2**	x	yes	
03-08-22	**S13D1M4.1**	S13	D1	M4	1	X	X	X	E	**S13E1**	x	yes	
03-08-22	**S13D1M7.3**	S13	D1	M7	3	X	X	X	I	**S13I3**	x	yes	
28-07-22	**L1D4M3.1**	L1	D4	M3	1	X	X	X	H	**L1H16**	x	yes	
27-07-22	**L1D1M8.2**	L1	D1	M8	2	X	X	X	H	**L1H3**	x	yes	
28-07-22	L1D2M5.1	L1	D2	M5	1	X	X	X	A	**L1A5**	x		
28-07-22	**L1D3M6.4**	L1	D3	M6	4	X	X	X	G	**L1G4**	x		
28-07-22	**L1D2M2.3**	L1	D2	M2	3	X	X	X	I	**L1I13**	x		
28-07-22	**L1D4M2.1**	L1	D4	M2	1	X	X	X	I	**L1I19**	x		
27-07-22	**L1D1M5.3**	L1	D1	M5	3	X	X	X	I	**L1I2**	x		
03-08-22	S13D2M2.3	S13	D2	M2	3	X	X	X	A	**S13A15**	x		
03-08-22	**S13D2M5.2**	S13	D2	M5	2	X	X	X	B	**S13B6**	x		
03-08-22	**S13D3M4.1**	S13	D3	M4	1	broken	X	X	C	**S13C3**	x		
03-08-22	**S13D2M3.2**	S13	D2	M3	2	X	X	X	G	**S13G4**	x		
03-08-22	**S13D2M8.4**	S13	D2	M8	4	X	X	X	I	**S13I7**	x		
29-07-22	S15D4M3.2	S15	D4	M3	2	X	X	X	A	**S15A11**	x		
29-07-22	**S15D1M5.4**	S15	D1	M5	4	X	X	X	B	**S15B2**	x		
29-07-22	**S15D4M7.4**	S15	D4	M7	4	X	X	X	E	**S15E36**	x		
29-07-22	**S15D4M1.2**	S15	D4	M1	2	X	X	X	F	**S15F3**	x		
29-07-22	**S15D4M6.3**	S15	D4	M6	3	X	X	X	I	**S15I10**	x		
29-07-22	**S15D2M7.3**	S15	D2	M7	3	X	X	general	I	**S15I7**	x		
01-08-22	S18D1M3.2	S18	D1	M3	2	X	X	X	A	**S18A1**	x		
01-08-22	**S18D3M2.4**	S18	D3	M2	4	X	X	X	B	**S18B9**	x		
01-08-22	**S18D1M4.1**	S18	D1	M4	1	X	X	X	F	**S18F1**	x		
01-08-22	**S18D2M4.1**	S18	D2	M4	1	X	X	X	G	**S18G2**	x		
01-08-22	**S18D3M6.3**	S18	D3	M6	3	X	X	X	I	**S18I7**	x		
01-08-22	**S18D4M5.1**	S18	D4	M5	1	X	X	X	I	**S18I9**	x		
02-08-22	S5D1M2.3	S5	D1	M2	3	X	X	X	D	S5D5	x		
02-08-22	**S5D3M7.2**	S5	D3	M7	2	X	X	X	X	**S5X2**	x		

Table 1.3.4. Example of DNA concentrations (ng/µL), absorbances in A260, A230 and A280 and its ratios.

Sample Name	Nucleic Acid (ng/µL)	A260/A280	A260/A230	A260	A280	Nucleic Acid Factor	Baseline Correction (nm)	Baseline Absorbance
S5A1	0.515	9.276	2.471	0.01	0.001	50	340	0.01
S13A2	1.274	2.167	0.235	0.025	0.012	50	340	0.004
S13A23	2.546	1.823	1.578	0.051	0.028	50	340	0.014
S15A5	4.366	1.506	0.82	0.087	0.058	50	340	0.07
S15A11	1.506	1.811	0.913	0.03	0.017	50	340	0.005
S18A1	0.389	0.684	0.743	0.008	0.011	50	340	0.025
S18A2	0.449	0.934	-3.113	0.009	0.01	50	340	0.006
L1A5	0.956	0.842	0.328	0.019	0.023	50	340	0.006
L1A3	2.592	1.406	0.701	0.052	0.037	50	340	0.031
S15A2	1.262	1.214	1.09	0.025	0.021	50	340	-0.013

Three molecular markers were selected for sequencing: *psb*A (encoding the Photosystem II reaction center protein D1), *rbc*L (encoding the large subunit of the enzyme ribulose-1,5-bisphosphate carboxylase/oxygenase), and COI (encoding cytochrome c oxidase subunit I). Priority was given to *psb*A and *rbc*L. Polymerase chain reaction (PCR) was used to amplify these regions. To perform the PCR, a reaction mix was prepared as outlined in **Table 1.3.5**, following Peña et al. (2015b) protocol. Subsequently, 2 µL of the DNA extraction product was added to the mix, resulting in a total reaction volume of 25 µL per sample.

Table 1.3.5. PCR mix reaction following Peña et al. (2015b) protocol.

Reagen	Stock Concentration	Final Concentration	Reaction 1 X (volume)
H_2O mili Q	-	-	16.66 µL
Buffer	10 x	1x	2.5 µL
$MgCl_2$	25 mM	2.5 mM	2.5 µL
dNTPs	8mM	0.192 mM	0.6 µL
Primer F	10 µM	0.1µM	0.25 µL
Primer R	10 µM	0.1 µM	0.25 µL
Taq polim.	5 Uds/µL	1.2 Uds)	0.24 µL
Subtotal			**23 µL**
DNA			2 µL
TOTAL			**25 µL**

The *psb*A locus was PCR-amplified for all specimens using the primer pair *psb*A-F1/*psb*A-R1 (Yoon et al., 2002), following the thermal profile for PCR reactions described by Bittner (2009). The *rbc*L locus was PCR-amplified using two overlapping primer combinations: F57-R1150 and F753-RrbcL-Start (Freshwater & Rueness, 1994; Gabrielson, et al., 2023b), following the thermal profile for PCR reactions outlined by Hernandez-Kantun et al. (2016). In some cases, such as when amplifying type materials, the primer combination F1150Cor–RbcStart was used, yielding a trimmed fragment of 293

bp (1172–1464), and following the thermal profile described by Saunders & Moore (2013). For COI, the primer pair GazF/GazR was used to amplify the long fragment (Saunders, 2005) following the thermal profile described in Peña et al. (2015b). When this combination failed, the primer pair GazF/GCorR3 was used to amplify a shorter fragment (Peña et al., 2015b), following the thermal profile described by Saunders & McDevit (2012). All primers used are specified in **Table 1.3.6** and each corresponding chapter mentions which ones have been used. All thermal cycles used are detailed in **Fig.1.3.13**.

Table 1.3.6. Primers used in this thesis.

PRIMER	
psbA -F1 (*psb*A)	5’ – ATG ACT GCT ACT TTA GAA AGA CG – 3’
psbA-R1 (*psb*A)	5’ – GCT AAA TCT ARW GGG AAG TTG TG – 3’
F57 (*rbc*L)	5’ – GTA ATT CCA TAT GCT AAA ATG GG – 3’
R1150 (*rbc*L)	5’ – GCA TTT GTC CGC AGT GAA TAC C – 3’
F753 (*rbc*L)	5’ GGA AGA TAT GTA TGA AAG AGC – 3’
RrbcS-start (*rbc*L)	5’ – GTT CTT GTG TTA ATC TCA A – 3’
F1150Cor (*rbc*L)	5’ – GGT ATA CAT TGT GGA CAA ATG C – 3’
Gaz-F1 (COI)	5’ – TCA ACA AAT CAT AAA GAT ATT GG – 3’
Gaz-R1 (COI)	5’ – ACT TCT GGA TGT CCA AAA AAY CA – 3’
GCcor3 (COI)	5’ – TGA TTY TTY GGA CAT CCT GA – 3’

After repeated attempts, and due to the fact that the DNA concentrations obtained were always very low (< 5 ng/µL), following the advice of the Molecular Biology Service of Universidade da Coruña, the PCR recipe was modified using a ready-to-use MasterMix with an enzyme capable of working with very low DNA concentrations. The MasterMix is from NZYTECH (https://www.nzytech.com/en/mb359-supreme-nzytaq-ii-2x-colourless-master-mix/) and already includes the dNTPs, reaction buffer and additives at optimal concentrations for the efficient amplification of a wide range of DNA templates. Thus, only MiliQ water and DNA extraction product need to be added, greatly simplifying the process. A total PCR volume of 20 µL is used as indicated in

Table 1.3.7. PCRs were prepared in 8-well strips containing 6 samples, a positive control and a negative control.

Table 1.3.7. New PCR mix reaction using the enriched MasterMix.

Reagen	**Stock Concentration**	**Final Concentration**	**Reaction 1 X (volume)**
H_2O mili Q	-	-	7.2 µL
MasterMix	0.2 Uds/µL	2 Uds	10 µL
Primer F	10 µM	0.1µM	0.4 µL
Primer R	10 µM	0.1 µM	0.4 µL
Subtotal			**18 µL**
DNA			2 µL
TOTAL			**20 µL**

To examine whether the PCRs had worked well, 2x agarose gels for electrophoresis were prepared with TBE and using 'SaveView' as an intercalant to allow observation of the DNA in the bands. In the gel, the wells were loaded with 1 µL of PCR product from each sample and 5 µL of H2O miliQ and 2 µL of 100 bp ladder was loaded in the first well to see the size and position of the bands. It was left to run in the electrophoresis cuvette at 80 V for 30 min. Once the electrophoresis gel was run, only those samples where a clear band was visible on the gel were sent for purification and sequencing (**Fig.1.3.14**). If a band appeared on the electrophoresis gel in the negative control and/or no band appeared in the positive control, the PCR was considered failed and the process was repeated, thus reducing false negatives and contaminations that could occur during the process.

The PCR products were kept at 4ºC and 10 µL per sample plus 1 µL of each primer used were sent to GenoScreen (https://www.genoscreen.fr/en/) for purification and sequencing using the Sanger method.

psbA Bittner (2009)	**COI** Peña et al. (2015b)	**COI** Saunders & McDevit (2012)
95°C – 4 min 95°C – 30 seg 52°C – 40 seg 72°C – 50 seg } x 45 72°C – 5 min 10°C – inf.	95°C – 2 min 94°C – 30 seg 50°C – 40 seg 72°C – 40 seg } x 40 72°C – 5 min 12°C – inf.	95°C – 2 min 95°C – 30 seg 45°C – 30 seg 72°C – 1 min } x 5 95°C – 30 seg 46.5°C – 30 seg 72 °C – 1 min } x 35 72°C – 5 min 12°C – inf.

rbcL Hernandez-Kantún et al. (2016)	***rbcL*** Saunders & Moore (2013)
94°C – 1 min 30 segs 94°C – 25 seg 48°C – 30 seg 72°C – 60 seg } x 40 72°C – 5 min 12°C – inf.	95°C – 2 min 93°C – 1 min 47°C – 1 min 72°C – 2 min } x 35 72°C – 2 min 12°C – inf.

Fig.1.3.13. PCR cycles used to amplify the different molecular markers.

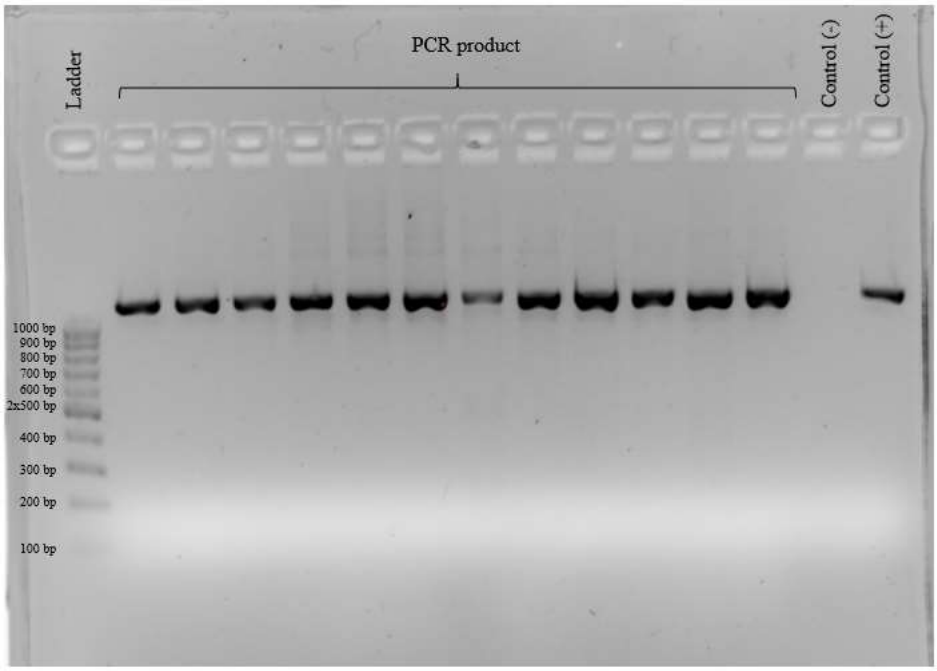


Fig.1.3.14. Example of an electrophoresis gel with the PCR product for *rbc*L marker.

1.3.3.3. Fish diversity

Fish species richness is a widely used descriptor of aquatic biodiversity and serves as an essential indicator of the ecological condition of aquatic ecosystems (Pompeu et al., 2021). It is frequently used to evaluate biological responses to environmental changes (Xenopoulos & Lodge, 2006) and to assess the health of marine ecosystems (Karr, 1981; Pont et al., 2009; Whittier et al., 2007). However, species richness is highly dependent on sampling effort, which can underestimate the true number of species present in an area, and potentially lead to misrepresentations of ecological conditions and trends (Pompeu et al., 2021). This challenge is particularly critical when sampling resources are limited, requiring careful balancing of site-specific versus regional sampling needs to ensure adequate biodiversity assessments (Hughes et al., 2021; Hughes & Peck, 2008).

Invertebrate communities associated with rhodolith habitats have been extensively studied (Amado-Filho et al., 2007; Foster et al., 2013) including Mediterranean RBs (Barberá et al., 2012; de Juan et al., 2013; 2023), and, due to their cryptic nature, traditionally imply invasive sampling such as dredges and grabs. Demersal fish play a critical role in the connection between benthic habitats and pelagic food webs. They rely on benthic prey and habitat structures, which are often conceptualized as 'essential fish habitat' (Hewitt et al., 2015; Peterson et al., 2000). Despite their importance, fish species inhabiting these areas remain largely unexplored from an ecological perspective (Otero-Ferrer et al., 2020; Pereira-Filho et al., 2015). This strong link between benthic macrofauna, flora, and demersal fish underscores the potential for these species to act as surrogate indicators for benthic macrofaunal and floral diversity, particularly for epibenthic communities (Colloca et al., 2003; Hewitt et al., 2015). However, growing concerns about biodiversity loss highlight the importance of understanding these associations, as declines in species richness and increasing homogenization are recognized as key indicators of ecosystem degradation (Pompeu et al., 2021; Rahel, 2000). Addressing these trends requires not only efficient sampling strategies, but also targeted conservation efforts that protect essential habitats and underexplored environments like RBs, which are vital to maintaining fish diversity.

In this study, to achieve the objectives of **Section II – Chapter IV**, given the challenges of sampling and the focus on fish diversity in a well-preserved area, we opted to work primarily with species presence/absence data. This decision was driven by the high mobility of fish, making species richness the most suitable diversity index for analyses involving video, eDNA, and acoustic methods.

Innovative techniques have their pros and cons. Some of them are at an early stage of development due to the lack of reference libraries, such as the bioacoustics libraries for fish. Moreover, current technological advances will significantly improve these techniques in the future (e.g., video, both in terms of image quality and artificial intelligence (AI) – based detection). Considering all the limitations, Richness of fish was assessed with the three techniques. To obtain Richness data from the video images,

the videos were analyzed and the presence of the species was identified at the lowest possible taxonomic level. With the limitations of visibility and movement of some fish, as well as the distance to the camera, it was rarely possible to get to species level so the different taxa identified were noted. As for the sampling carried out with eDNA, the MOTUs obtained during the study were taxonomically assigned; however, because some MOTUs do not correspond to the presence of a particular species but may correspond to the presence of a particular family or several species that are not well resolved, the Richness of MOTUs was considered. Finally, for the data obtained with bioacoustics, and due to the few libraries for fish that are currently developed, (at the moment of the study only 5 categories of sounds corresponding to 5 large groups of fish could be identified), the richness of sounds was considered as a measure of the acoustic diversity produced by fish. In addition, the abundance of sounds was also considered in this case.

Details in how Richness of fish was calculated for all the techniques are specified in **Section II – Chapter IV**.

References Section I

Adey, W.H., & McKibbin, D.L. (1970). Studies on the Maërl Species Phymatolithon calcareum (Pallas) nov. Comb. And Lithothamnium coralloides Crouan in the Ria de Vigo. *Botanica Marina, 13*(2), 100–106. https://doi.org/10.1515/botm.1970.13.2.100

Aguilar, R., Pastor, X., de la Torriente, A. & García, S. (2009). Deep-sea coralligenous beds observed with ROV on four seamounts in the Western Mediterranean. *UNEP-MAP-RAC/SPA, Proceedings of the 1st Mediterranean Symposium on the Conservation of the Coralligenous and Others Calcareous Bio-Concretions. Tabarka, Tunis: CAR/ASP Publishing*, 147–149.

Aguirre, J., Braga, J.C., Martín, J.M. & Betzler, C. (2012). Palaeoenvironmental and stratigraphic significance of Pliocene rhodolith beds and coralline algal bioconstructions from the Carboneras Basin (SE Spain). *Geodiversitas*, *34*(1), 115–136. https://doi.org/10.5252/g2012n1a7

Altieri, A.H., Silliman, B.R. & Bertness, M.D. (2007). Hierarchical organization via a facilitation cascade in intertidal cordgrass bed communities. *The American Naturalist*, *169*(2), 195–206.

Amado-Filho, G.M., Maneveldt, G., Manso, R.C.C., Marins-Rosa, B.V., Pacheco, M.R., & Guimarães, S. (2007). Structure of rhodolith beds from 4 to 55 meters deep along the southern coast of Espírito Santo State, Brazil. *Ciencias Marinas*, *33*(4), Article 4. https://doi.org/10.7773/cm.v33i4.1148

Amado-Filho, G. & Pereira-Filho, G. (2012). Rhodolith beds in Brazil: A new potential habitat for marine bioprospection. *Brazilian Journal of Pharmacognosy*, *22*. https://doi.org/10.1590/S0102-695X2012005000066

Anderson, A., Pinheiro, H.T., Batista, M., Francini-Filho, R.B., Gomes, L., Bernardino, A., Horta, P. & Joyeux, J.C. (2023). Biogeographic patterns of marine fishes associated with rhodolith beds in the Southwestern Atlantic reveal an ecotone of biodiversity. *Biodiversity and Conservation*, *32*(2), 821–837.

Aslam, M., Kreider, J., Paruchuri, T., Bhagavathula, N., DaSilva, M., Zernicke, R., Goldstein, S. & Varani, J. (2010). A Mineral-Rich Extract from the Red Marine Algae Lithothamnion calcareum Preserves Bone Structure and Function in Female Mice on a Western-Style Diet. *Calcified Tissue International*, *86*, 313–324. https://doi.org/10.1007/s00223-010-9340-9

Aslam, M.N., Bhagavathula, N., Paruchuri, T., Hu, X., Chakrabarty, S. & Varani, J. (2009). Growth-inhibitory effects of a mineralized extract from the red marine algae, Lithothamnion calcareum, on Ca^{2+}-sensitive and Ca^{2+}-resistant human colon carcinoma cells. *Cancer Letters*, *283*(2), 186–192.

Athanasiadis, A. & Ballantine, D.L. (2014). The genera Melyvonnea gen. Nov. And Mesophyllum ss (Melobesioideae, Corallinales, Rhodophyta) particularly from the central Atlantic Ocean. *Nordic Journal of Botany*, *32*(4), 385–436.

Baarli, B.G., Santos, A., da Silva, C.M., Ledesma-Vázquez, J., Mayoral, E., Cachao, M. & Johnson, M.E. (2012). Diverse macroids and rhodoliths from the upper Pleistocene of Baja California Sur, Mexico. *Journal of Coastal Research*, *28*(1), 296–305.

Barbera, C., Bordehore, C., Borg, J. A., Glémarec, M., Grall, J., Hall-Spencer, J.M., de la Huz, Ch., Lanfranco, E., Lastra, M., Moore, P.G., Mora, J., Pita, M.E., Ramos-Esplá, A.A., Rizzo, M., Sánchez-Mata, A., Seva, A., Schembri, P.J. & Valle, C. (2003). Conservation and management of northeast Atlantic and Mediterranean maërl beds. *Aquatic Conservation: Marine and Freshwater Ecosystems*, *13*(S1), S65–S76. https://doi.org/10.1002/aqc.569

Barberá, C., Comalada, N., Joher, S., Valls-Mir, M., Díaz-Valdés, M. & Moranta, J. (2012b). Analysis of morphological characteristics of rhodoliths as indicator of habitat complexity and fishing effects. *Centro Oceanográfico de Baleares*.

Barberá, C., Mallol, S., Vergés, A., Cabanellas-Reboredo, M., Díaz, D. & Goñi, R. (2017). Maërl beds inside and outside a 25-year-old no-take area. *Marine Ecology Progress Series*, *572*, 77–90. https://doi.org/10.3354/meps12110

Barberá, C., Moranta, J., Ordines, F., Ramón, M., de Mesa, A., Díaz-Valdés, M., Grau, A.M. & Massutí, E. (2012a). Biodiversity and habitat mapping of Menorca Channel (western Mediterranean): Implications for conservation. *Biodiversity and Conservation*, *21*(3), 701–728. https://doi.org/10.1007/s10531-011-0210-1

Basso, D. (1998). Deep rhodolith distribution in the Pontian Islands, Italy: A model for the paleoecology of a temperate sea. *Palaeogeography, Palaeoclimatology, Palaeoecology*, *137*(1), 173–187. https://doi.org/10.1016/S0031-0182(97)00099-0

Basso, D., Babbini, L., Kaleb, S., Bracchi, V.A. & Falace, A. (2016). Monitoring deep Mediterranean rhodolith beds. *Aquatic Conservation: Marine and Freshwater Ecosystems*, *26*(3), 549–561. https://doi.org/10.1002/aqc.2586

Basso, D., Babbini, L., Ramos-Esplá, A.A. & Salomidi, M. (2017). Mediterranean Rhodolith Beds. In R. Riosmena-Rodríguez, W. Nelson, & J. Aguirre (Eds.), *Rhodolith/Maërl Beds: A Global Perspective* (pp. 281–298). Springer International Publishing. https://doi.org/10.1007/978-3-319-29315-8_11

Berg, M.P., Kiers, E.T., Driessen, G., Van Der Heijden, M., Kooi, B. W., Kuenen, F., Liefting, M., Verhoef, H.A. & Ellers, J. (2010). Adapt or disperse: Understanding species persistence in a changing world. *Global Change Biology*, *16*(2), 587–598.

Bianchi, C.N. & Morri, C. (2025). Different rhodolith assemblages host distinct associated species but similar ecological groups: A case study in NW Mediterranean Sea. *Aquatic Botany*, *196*. Scopus. https://doi.org/10.1016/j.aquabot.2024.103826

Bittner, L. (2009). *Phylogénie des Corallinales (Rhodophyta) et analyse de leur diversité génétique dans le Pacifique Sud* [PhD Thesis]. Paris, Muséum national d'histoire naturelle.

Blake, C. & Maggs, C.A. (2003). Comparative growth rates and internal banding periodicity of maërl species (Corallinales, Rhodophyta) from northern Europe. *Phycologia*, *42*(6), 606–612. https://doi.org/10.2216/i0031-8884-42-6-606.1

Blunden, G., Binns, W.W. & Perks, F. (1975). Commercial Collection and Utilisation of Maërl. *Economic Botany*, *29*(2), 140–145.

Bolgan, M., Soulard, J., Di Iorio, L., Gervaise, C., Lejeune, P., Gobert, S. & Parmentier, E. (2019). The sea chordophones make the mysterious /Kwa/: Emitter identification of the dominating fish sound in Mediterranean seagrass meadows. *Journal of Experimental Biology*, jeb.196931. https://doi.org/10.1242/jeb.196931

Bordehore, C., Ramos-Esplá, A.A. & Riosmena-Rodríguez, R. (2003). Comparative study of two maërl beds with different otter trawling history, southeast Iberian Peninsula. *Aquatic Conservation: Marine and Freshwater Ecosystems*, *13*(S1), S43–S54. https://doi.org/10.1002/aqc.567

Bosence, D. W. J. (1976). Ecological studies on two unattached coralline algae from western Ireland. *Palaeontology*, 19(2), 365-395.

Bosence, D. W. J. (1983). Description and Classification of Rhodoliths (Rhodoids, Rhodolites). In T. M. Peryt (Ed.), *Coated Grains* (pp. 217–224). Springer. https://doi.org/10.1007/978-3-642-68869-0_19

Brasileiro, P.S., Pereira-Filho, G. H., Bahia, R. G., Abrantes, D. P., Guimarães, S.M.P.B., Moura, R.L., Francini-Filho, R.B., Bastos, A.C. & Amado-Filho, G.M. (2016). Macroalgal composition and community structure of the largest rhodolith beds in the world. *Marine Biodiversity*, *46*(2), 407–420. https://doi.org/10.1007/s12526-015-0378-9

Büdenbender, J., Riebesell, U. & Form, A. (2011). Calcification of the Arctic coralline red algae Lithothamnion glaciale in response to elevated CO2. *Marine Ecology Progress Series*, *441*, 79–87. https://doi.org/10.3354/meps09405

Bulleri, F., Schubert, N., Hall-Spencer, J.M., Basso, D., Burdett, H.L., Francini-Filho, R.B., Grall, J., Horta, P.A., Kamenos, N.A., Martin, S., Nannini, M., Neves, P., Olivé, I., Peña, V., Ragazzola, F., Ribeiro, C., Rinde, E., Sissini, M., Tuya, F. & Silva, J. (2024). Positive species interactions structure rhodolith bed communities at a global scale. *Biological Reviews*, brv.13148. https://doi.org/10.1111/brv.13148

Burdett, H., Perna, G., McKay, L., Broomhead, G. & Kamenos, N. (2018). Community-level sensitivity of a calcifying ecosystem to acute in situ CO2 enrichment. *Marine Ecology Progress Series*, *587*, 73–80. https://doi.org/10.3354/meps12421

Cabioch, J. & Mendoza, M.L. (2003). Mesophyllum expansum (Philippi) comb. Nov.(Corallinales, Rhodophytes), et mise au point sur les Mesophyllum des mers d'Europe. *Cahiers de Biologie Marine*, *44*(3), 257–274.

Caragnano, A., Foetisch, A., Maneveldt, G. W., Millet, L., Liu, L.-C., Lin, S.-M., Rodondi, G. & Payri, C. E. (2018). Revision of Corallinaceae (Corallinales, Rhodophyta): Recognizing Dawsoniolithon gen. nov., Parvicellularium gen. nov. and Chamberlainoideae subfam. nov. containing Chamberlainium gen. nov. and Pneophyllum. *Journal of Phycology*, *54*(3), 391–409. https://doi.org/10.1111/jpy.12644

Caragnano, A., Rodondi, G., Basso, D., Peña, V., le Gall, L. & Rindi, F. (2020). Circumscription of *Lithophyllum racemus* (Corallinales, Rhodophyta) from the western Mediterranean Sea reveals the species *Lithophyllum pseudoracemus sp. Nov*. *Phycologia*, *59*(6), 584–597. https://doi.org/10.1080/00318884.2020.1829348

Carneiro, P. B., Ximenes Neto, A. R., Jucá-Queiroz, B., Teixeira, C. E., Feitosa, C. V., Barroso, C. X., Matthews-Cascon, H., de Morais, J. O., Freitas, J. E., Santander-Neto, J., de Araújo, J.t., Monteiro, L.H.U., Pinheiro, L.S., Braga, M.D.A., Cordeiro, R.T.S., Rossi, S., Bejarano, S., Salani, S., Garcia, T.M., Lotufo, T.M.C., Smith, T.B., Faria, V.V. & Soares, M.O. (2022). Interconnected marine habitats form a single continental-scale reef system in South America. *Scientific Reports*, *12*(1), 17359.

Carro, B., Lopez, L., Peña, V., Bárbara, I. & Barreiro, R. (2014). DNA barcoding allows the accurate assessment of European maërl diversity: A Proof-of-Concept study. *Phytotaxa*, *190*(1), 176. https://doi.org/10.11646/phytotaxa.190.1.12

Cerrano, C., Bastari, A., Calcinai, B., Di Camillo, C., Pica, D., Puce, S., Valisano, L. & Torsani, F. (2019). Temperate mesophotic ecosystems: Gaps and perspectives of an emerging conservation challenge for the Mediterranean Sea. *The European Zoological Journal*, *86*(1), 370–388. https://doi.org/10.1080/24750263.2019.1677790

Chamberlain, Y. (1990). The genus Leptophytum (Rhodophyta, Corallinaceae) in the British Isles with descriptions of Leptophytum bornetii, L. elatum sp. Nov. And L. laeve. *British Phycological Journal*, *25*(2), 179–199.

Chatalov, A., Bonev, N. & Ivanova, D. (2015). Depositional characteristics and constraints on the mid-Valanginian demise of a carbonate platform in the intra-Tethyan domain, Circum-Rhodope Belt, northern Greece. *Cretaceous Research*, *55*, 84–115.

Chaves, L., Pereira, P. & Feitosa, J. (2013). Coral reef fish association with macroalgal beds on a tropical reef system in North-eastern Brazil. *Marine and Freshwater Research*, *64*(12), 1101–1111.

Chimienti, G., Rizzo, L., Kaleb, S., Falace, A., Fraschetti, S., Giosa, F.D., Tursi, A., Barbone, E., Ungaro, N. & Mastrototaro, F. (2020). Rhodolith Beds Heterogeneity along the Apulian Continental Shelf (Mediterranean Sea). *Journal of Marine Science and Engineering*, *8*(10), 813. https://doi.org/10.3390/jmse8100813

Colloca, F., Cardinale, M., Belluscio, A. & Ardizzone, G. (2003). Pattern of distribution and diversity of demersal assemblages in the central Mediterranean Sea. *Estuarine, Coastal and Shelf Science*, *56*(3–4), 469–480.

Commission, E., Environment, D.G. for, Rodwell, J., García Criado, M., Gubbay, S., Borg, J., Otero, M., Janssen, J., Haynes, T., Beal, S., Nieto, A., Calix, M., Sanders, N., Saunders, G., Micu, D. & Kennedy, M. (2016). *European red list of habitats. Part 1, Marine habitats*. Publications Office. https://doi.org/doi/10.2779/032638

Cornwall, C.E., Diaz-Pulido, G. & Comeau, S. (2019). Impacts of Ocean Warming on Coralline Algal Calcification: Meta-Analysis, Knowledge Gaps, and Key Recommendations for Future Research. *Frontiers in Marine Science*, *6*, 186. https://doi.org/10.3389/fmars.2019.00186

Costa, A.C.P., Garcia, T.M., Paiva, B.P., Ximenes Neto, A.R. & Soares, M. de O. (2020). Seagrass and rhodolith beds are important seascapes for the development of fish eggs and larvae in tropical coastal areas. *Marine Environmental Research*, *161*, 105064. https://doi.org/10.1016/j.marenvres.2020.105064

Crouan, P.L. & Crouan, H.M. (Hippolyte Marie). (1867). *Florule du Finistère. Contenant les descriptions de 360 espèces nouvelles de sporagames, de nombreuses observations et une synonymie des plantes cellulaires et vasculaires qui croissent spontanément dans ce département; accompagnées de trente-deux planches où est représentée l'organographie, faite sur l'état vif, des fruits et des tissus de 198 genres d'algues avec la plante grandeur naturelle ou réduite plus une planche supplémentiare ou sont figurés 24 champignons nouveaux*. Paris, F. Klincksieck; [etc. etc.], 1867. https://www.biodiversitylibrary.org/item/43942

de Araújo Costa, D., Massei, K., Moura, A., Christoersen, M. L. & Dolbeth, M. (2023). RHODOLITHS: OUR "ROCK-AND-ROLLING" UNDERWATER FRIENDS. *The Ocean, Volume 2*, 132.

de Juan, S., Hewitt, J., Thrush, S. & Freeman, D. (2015). Standardising the assessment of Functional Integrity in benthic ecosystems. *Journal of Sea Research*, *98*, 33–41. https://doi.org/10.1016/j.seares.2014.06.001

de Juan, S., Lo Iacono, C. & Demestre, M. (2013). Benthic habitat characterisation of soft-bottom continental shelves: Integration of acoustic surveys, benthic samples and trawling disturbance intensity. *Estuarine, Coastal and Shelf Science*, *117*, 199–209. https://doi.org/10.1016/j.ecss.2012.11.012

de Juan, S., Ospina-Alvarez, A., Hinz, H., Moranta, J. & Barberá, C. (2023). The continental shelf seascape: A network of species and habitats. *Biodiversity and Conservation*, *32*, 1271-1290. https://doi.org/10.1007/s10531-023-02552-8.

Deidun, A., Marrone, A., Gauci, A., Galdies, J., Lorenti, M., Mangano, M., Cutajar, K., Mirto, S. & Sarà, G. (2022). Structure and biodiversity of a Maltese maërl bed: New insight into the associated assemblage 24 years after the first investigation. *Regional Studies in Marine Science*, *52*, 102262.

Del Río, J., Ramos, D.A., Sánchez-Tocino, L., Peñas, J. & Braga, J. C. (2022). The Punta de la Mona Rhodolith Bed: Shallow-Water Mediterranean Rhodoliths (Almuñecar, Granada, Southern Spain). *Frontiers in Earth Science*, *10*, 884685. https://doi.org/10.3389/feart.2022.884685

Demestre, M., Soto, S., Durán, R., del Arco, J. A. G., Cabrito, A., Illa-López, L., Maynou, F., Sánchez, P., García-de-Vinuesa, A. & Emelianov, M. (2024). Reconstruction of the Maërl habitat to better understand its ecological integrity. *Science of The Total Environment*, *912*, 168752. https://doi.org/10.1016/j.scitotenv.2023.168752

Dias, G. (2000). Marine bioclasts: Calcareous algae. *Revista Brasileira de Geofísica*, *18*, 307–318.

Dulin, T., Avnaim-Katav, S., Sisma-Ventura, G., Bialik, O.M., & Angel, D.L. (2020). Rhodolith beds along the southeastern Mediterranean inner shelf: Implications for past depositional environments. *Journal of Marine Systems*, *201*, 103241. https://doi.org/10.1016/j.jmarsys.2019.103241

Ehrhold, A., Jouet, G., Le Roy, P., Jorry, S.J., Grall, J., Reixach, T., Lambert, C., Gregoire, G., Goslin, J., Roubi, A., Penaud, A., Vidal, M. & Siano, R. (2021). Fossil maërl beds as coastal indicators of late Holocene palaeo-environmental evolution in the Bay of Brest (Western France). *Palaeogeography, Palaeoclimatology, Palaeoecology*, *577*, 110525. https://doi.org/10.1016/j.palaeo.2021.110525

Ellison, A. M. (2019). Foundation species, non-trophic interactions, and the value of being common. *Iscience*, *13*, 254–268.

Farriols, M. T., Irlinger, C., Ordines, F., Palomino, D., Marco-Herrero, E., Soto-Navarro, J., Jordà, G., Mallol, S., Díaz, D., Martínez-Carreño, N., Díaz, J. A., Fernandez-Arcaya, U., Joher, S., Ramírez-Amaro, S., de la Ballina, N.R., Vázquez, J.T. & Massutí, E. (2022). Recovery Signals of Rhodoliths Beds since Bottom Trawling Ban in the SCI Menorca Channel (Western Mediterranean). *Diversity*, *14*(1), Article 1. https://doi.org/10.3390/d14010020

Fedorov, A., Beichel, R., Kalpathy-Cramer, J., Finet, J., Fillion-Robin, J.C., Pujol, S., Bauer, C., Jennings, D., Fennessy, F., Sonka, M., Buatti, J., Aylward, S., Miller, J.V., Pieper, S. & Kikins, R. (2012). 3D Slicer as an image computing platform for the Quantitative Imaging Network. *Magnetic Resonance Imaging*, *30*(9), 1323–1341.

Foster, M.S. (2001). Rhodoliths: Between Rocks and Soft Places. *Journal of Phycology*, *37*(5), 659–667. https://doi.org/10.1046/j.1529-8817.2001.00195.x

Foster, M.S., Filho, G.M. A., Kamenos, N.A., Riosmena-Rodriguez, R. & Steller, D.L. (2013). *Rhodoliths and rhodolith beds* (M. A. Lang, R. L. Marinelli, S. J. Roberts, & P. R. Taylor, Eds.; 39; Issue 39, pp. 143–155). Smithsonian Institution Scholarly Press. http://opensi.si.edu/index.php/smithsonian/catalog/book/48

Fragkopoulou, E., Serrão, E.A., Horta, P.A., Koerich, G. & Assis, J. (2021). Bottom Trawling Threatens Future Climate Refugia of Rhodoliths Globally. *Frontiers in Marine Science*, *7*, 594537. https://doi.org/10.3389/fmars.2020.594537

Freshwater, D.W. & Rueness, J. (1994). Phylogenetic relationships of some European Gelidium (Gelidiales, Rhodophyta) species, based on rbcL nucleotide sequence analysis. *Phycologia*, *33*(3), 187–194.

Fulton, C.J., Berkström, C., Wilson, S.K., Abesamis, R.A., Bradley, M., Åkerlund, C., Barrett, L.T., Bucol, A.A., Chacin, D.H., Chong-Seng, K.M., Coker, D.J., Depczynski, M., Eggertsen, L., Eggertsen, M., Ellis, D., Evans, R.D., Graham, N.A.J., Hoey, A.S., Holmes, T.H., Kulbicki, M., Leung, P.T.Y., Lam, P.K.S., van Lier, J., Matis, P.A., Noble, M.M., Pérez-Matus, A., Piggott, C., Radford, B.T., Tano, S. & Tinkler, P. (2020). Macroalgal meadow habitats support fish and fisheries in diverse tropical seascapes. *Fish and Fisheries*, *21*(4), 700–717.

Gabrielson, P. W., Hughey, J. R., Peña, V., Richards, J.L., Saunders, G.W., Twist, B., Farr, T. & Nelson, W.A. (2023b). Asia Pacific *Sporolithon* (Corallinophycidae, Rhodophyta) species revised based on DNA sequencing of type specimens and including *S. crypticum sp. Nov.*, *S. immotum sp. Nov*. And *S. nodosum sp. Nov. Phycologia*, *62*(6), 593–607. https://doi.org/10.1080/00318884.2023.2225309

Gabrielson, P.W., Maneveldt, G.W., Hughey, J.R. & Peña, V. (2023a). Taxonomic contributions to Hapalidiales (Corallinophycidae, Rhodophyta): Boreolithothamnion gen. nov., Lithothamnion redefined and with three new species and Roseolithon with new combinations. *Journal of Phycology*, *59*(4), 751–774. https://doi.org/10.1111/jpy.13353

Gagnon, P., Matheson, K. & Stapleton, M. (2012). *Variation in rhodolith morphology and biogenic potential of newly discovered rhodolith beds in Newfoundland and Labrador (Canada)*. *55*(1), 85–99. https://doi.org/10.1515/bot-2011-0064

Gambi, M.C., Buia, M.C., Massa-Gallucci, A., Cigliano, M., Lattanzi, L. & Patti, F.P. (2009). The "pink mile": Benthic assemblages of rhodolith and mäerl beds (Corallinales) off the Island of Ischia (Tyrrhenian Sea). *Proceedings of the 1st Mediterranean Symposium on the Conservation of the Coralligenous and Others Calcareous Bio-Concretions (Tabarka, 15-16 January 2009). RAC/SPA Publ., Tunis*, 197–200.

Giraud, G. & Cabioch, J. (1977). *Caractères généraux de l'ultrastructure des Corallinacées (Rhodophycées).*

Grall, J. & Hall-Spencer, J. (2003). Problems facing maërl conservation in Brittany. *Aquatic Conservation: Marine and Freshwater Ecosystems*, *13*, S55.

Gray, J.S. & Elliott, M. (2009). *Ecology of Marine Sediments: From Science to Management*. Oxford University Press. https://doi.org/10.1093/oso/9780198569015.001.0001

Hall-Spencer, J., White, N., Gillespie, E., Gillham, K. & Foggo, A. (2006). Impact of fish farms on maërl beds in strongly tidal areas. *Marine Ecology Progress Series*, *326*, 1–9. https://doi.org/10.3354/meps326001

Harvey, A., Johnson, M.E. & Harvey, R. (2018). Heterozoan carbonate-enriched beach sand and coastal dunes—With particular reference to rhodoliths, Dirk Hartog Island, Shark Bay, Western Australia. *Facies*, *64*, 1–18.

Harvey, A. & Woelkerling, W. (2007). A guide to nongeniculate coralline red algal (Corallinales, Rhodophyta) rhodolith identification. *Ciencias Marinas*, *33*(4), 411–426.

Harvey, B.P., Gwynn-Jones, D. & Moore, P.J. (2013). Meta-analysis reveals complex marine biological responses to the interactive effects of ocean acidification and warming. *Ecology and Evolution*, *3*(4), 1016–1030.

Harvey, S.A., Woelkerling, J.W., Farr, T., Neill, K. & Nelson, W. (2005). Coralline algae of central New Zealand: An identification guide to common'crustose'species. *NIWA Information Series*, *57*, 1–145.

Hernández-Kantun, J.J., Gabrielson, P., Hughey, J.R., Pezzolesi, L., Rindi, F., Robinson, N.M., Peña, V., Riosmena-Rodriguez, R., Gall, L.L. & Adey, W. (2016). Reassessment of branched Lithophyllum spp. (Corallinales, Rhodophyta) in the Caribbean Sea with global implications. *Phycologia*, *55*(6), 619–639. https://doi.org/10.2216/16-7.1

Hernández-Kantun, J.J., Rindi, F., Adey, W.H., Heesch, S., Peña, V., Le Gall, L. & Gabrielson, P.W. (2015). Sequencing type material resolves the identity and distribution of the generitype *Lithophyllum incrustans* , and related European species *L. hibernicum* and *L. bathyporum* (Corallinales, Rhodophyta). *Journal of Phycology*, *51*(4), 791–807. https://doi.org/10.1111/jpy.12319

Hernández-Kantún, J.J., Riosmena-Rodriguez, R., Hall-Spencer, J.M., Peña, V., Maggs, C.A. & Rindi, F. (2015). Phylogenetic analysis of rhodolith formation in the Corallinales (Rhodophyta). *European Journal of Phycology*, *50*(1), 46–61. https://doi.org/10.1080/09670262.2014.984347

Hewitt, J.E., Wang, D., Francis, M., Lundquist, C. & Duffy, C. (2015). Evaluating demersal fish richness as a surrogate for epibenthic richness in management and conservation. *Diversity and Distributions*, *21*(8), 901–912. https://doi.org/10.1111/ddi.12336

Hind, K.R., Gabrielson, P.W., Jensen, C. & Martone, P.T. (2018). Evolutionary reversals in Bossiella (Corallinales, Rhodophyta): First report of a coralline genus with both geniculate and nongeniculate species. *Journal of Phycology*, *54*(6), 788–798. https://doi.org/10.1111/jpy.12788

Hughes, R.M., Herlihy, A.T. & Peck, D.V. (2021). Sampling efforts for estimating fish species richness in western USA river sites. *Limnologica*, *87*, 125859.

Hughes, R.M. & Peck, D.V. (2008). Acquiring data for large aquatic resource surveys: The art of compromise among science, logistics, and reality. *Journal of the North American Benthological Society*, *27*(4), 837–859.

Illa-López, L., Cabrito, A., de Juan, S., Maynou, F. & Demestre, M. (2023). Distribution of rhodolith beds and their functional biodiversity characterisation using ROV images in the western

Mediterranean Sea. *Science of The Total Environment*, *905*, 167270. https://doi.org/10.1016/j.scitotenv.2023.167270

Ingrassia, M., Pierdomenico, M., Casalbore, D., Falese, F. G. & Chiocci, F. L. (2023). A Review of Rhodolith/Maërl Beds of the Italian Seas. *Diversity*, *15*(7). Scopus. https://doi.org/10.3390/d15070859

IPCC. (2019). Special report: The ocean and cryosphere in a changing climate.

Irvine, L.M. & Chamberlain, Y.M. (1994). *Seaweeds of the British Isles.: Vol. 1 Rhodophyta*. https://www.cambridge.org/core/journals/journal-of-the-marine-biological-association-of-the-united-kingdom/article/abs/lm-irvine-ym-chamberlain-seaweeds-of-the-british-isles-volume-1-rhodophyta-part-2b-corallinales-hildenbrandiales-vii-276p-london-hmso-1994-a-collaborative-project-of-the-british-phycological-society-and-the-natural-history-museum-price-3000/06E5241E06B42A6933C8334594BC0412

Jacquotte, R. (1962). Etude des fonds de maërl de Méditerranée. *Recueil des Travaux de la Station Marine d'Endoume*, *26*(41), 141–216.

Jardim, V.L., Gauthier, O., Toumi, C. & Grall, J. (2022). Quantifying maërl (rhodolith) habitat complexity along an environmental gradient at regional scale in the Northeast Atlantic. *Marine Environmental Research*, *181*, 105768. https://doi.org/10.1016/j.marenvres.2022.105768

Jardim, V.L., Grall, J., Barros-Barreto, M.B., Bizien, A., Benoit, T., Braga, J.C., Brodie, J., Burel, T., Cabrito, A., Diaz-Pulido, G., Gagnon, P., Hall-Spencer, J.M., Helias, M., Horta, P.A., Joshi, S., Kamenos, N.A., Kolzenburg, R., Krieger, E.C., Legrand, E., Page, T.M., Peña, V., Ragazzola, F., Rasmusson, L.M., Rendina, F., Schubert, N., Silva, J., Tâmega, F.T.S., Tauran, A. & Burdett, H.L. (2025). A Common Terminology to Unify Research and Conservation of Coralline Algae and the Habitats They Create. *Aquatic Conservation: Marine and Freshwater Ecosystems, 35(3), e70121*. https://doi.org/10.1002/aqc.70121

Jeong, S.Y., Gabrielson, P.W., Hughey, J.R., Hoey, A.S., Cho, T.O., Abdul Wahab, M.A. & Diaz-Pulido, G. (2023). New branched Porolithon species (Corallinales, Rhodophyta) from the Great Barrier Reef, Coral Sea, and Lord Howe Island. *Journal of Phycology*, *59*(6), 1179–1201. https://doi.org/10.1111/jpy.13387

Jeong, S.Y., Nelson, W.A., Sutherland, J.E., Peña, V., Le Gall, L., Diaz-Pulido, G., Won, B.Y. & Cho, T.O. (2021). Corallinapetrales and Corallinapetraceae: A new order and family of coralline red algae including Corallinapetra gabrielii comb. nov. *Journal of Phycology*, *57*(3), 849–862. https://doi.org/10.1111/jpy.13115

Johansen, H.W. (1981). *Coralline algae, a first synthesis*. CRC Press.

Kamenos, N.A., Moore, P.G. & Hall-Spencer, J.M. (2004). Nursery-area function of maërl grounds for juvenile queen scallops Aequipecten opercularis and other invertebrates. *Marine Ecology Progress Series*, *274*, 183–189

Kamenos, N.A., Burdett, H.L., Aloisio, E., Findlay, H.S., Martin, S., Longbone, C., Dunn, J., Widdicombe, S. & Calosi, P. (2013). Coralline algal structure is more sensitive to rate, rather than the magnitude, of ocean acidification. *Global Change Biology*, *19*(12), 3621–3628. https://doi.org/10.1111/gcb.12351

Karr, J.R. (1981). Assessment of biotic integrity using fish communities. *Fisheries*, *6*(6), 21–27.

Kato, A., Baba, M. & Suda, S. (2011). REVISION OF THE MASTOPHOROIDEAE (CORALLINALES, RHODOPHYTA) AND POLYPHYLY IN NONGENICULATE SPECIES WIDELY DISTRIBUTED ON PACIFIC CORAL REEFS 1. *Journal of Phycology*, *47*(3), 662–672.

Kato, A., Hikami, M., Kumagai, N.H., Suzuki, A., Nojiri, Y. & Sakai, K. (2014). Negative effects of ocean acidification on two crustose coralline species using genetically homogeneous samples. *Marine Environmental Research*, *94*, 1–6.

Kittle, R., Richards, J., Sauvage, T., Gabriel, D., Schmidt, W. & Fredericq, S. (2022). A new species of Phymatolithon Foslie, P. abuqirensis (Hapalidiaceae, Hapalidiales), from Mediterranean Egypt. *Frontiers in Marine Science*, *9*. https://doi.org/10.3389/fmars.2022.922389

Koerich, G., Sissini, M.N. & Horta, P.A. (2024). Major Threats to Rhodolith Beds: Ocean Acidification, Global Warming, and Local Stressors. In P. A. Horta & M. N. Sissini (Eds.), *Brazilian Rhodolith Beds: Oasis of Marine Biodiversity to be protected* (pp. 163–184). Springer Nature Switzerland. https://doi.org/10.1007/978-3-031-61449-1_8

Kružić, P. (2014). Bioconstructions in the Mediterranean: Present and Future. In S. Goffredo & Z. Dubinsky (Eds.), *The Mediterranean Sea: Its history and present challenges* (pp. 435–447). Springer Netherlands. https://doi.org/10.1007/978-94-007-6704-1_25

Kuhnz, L.A., Gilbane, L., Cochrane, G.R. & Paull, C.K. (2022). Multi-factor biotopes as a method for detailed site characterization in diverse benthic megafaunal communities and habitats in deep-water off Morro Bay, California. *Deep Sea Research Part I: Oceanographic Research Papers*, *190*, 103872. https://doi.org/10.1016/j.dsr.2022.103872

Le Gall, L., Payri, C.E., Bittner, L. & Saunders, G.W. (2010). Multigene phylogenetic analyses support recognition of the Sporolithales ord. Nov. *Molecular Phylogenetics and Evolution*, *54*(1), 302–305.

Le Gall, L. & Saunders, G.W. (2007). A nuclear phylogeny of the Florideophyceae (Rhodophyta) inferred from combined EF2, small subunit and large subunit ribosomal DNA: establishing the new red algal subclass Corallinophycidae. *Molecular Phylogenetics and Evolution*, *43*(3), 1118–1130.

Legrand, E., Riera, P., Lutier, M., Coudret, J., Grall, J. & Martin, S. (2017). Species interactions can shift the response of a maërl bed community to ocean acidification and warming. *Biogeosciences*, *14*(23), 5359–5376. https://doi.org/10.5194/bg-14-5359-2017

Lemoine, P. (1928). Un nouveau genre de Mélobésiées: Mesophyllum. *Bulletin de La Société Botanique de France*, *75*(2), 251–254.

Littler, M.M. (1976). Calcification and its role among the macroalgae. *Micronesica*.

Littler, M.M., Littler, D.S., Blair, S.M. & Norris, J.N. (1985). Deepest known plant life discovered on an uncharted seamount. *Science (New York, N.Y.)*, *227*(4682), 57–59. https://doi.org/10.1126/science.227.4682.57

Liu, L.C. & Lin, S.M. (2023). Systematic revision of the non-geniculate coralline genus *Phymatolithon* (Hapalidiales, Rhodophyta) from Taiwan, including three new species. *Phycologia*, *62*(6), 561–573. https://doi.org/10.1080/00318884.2023.2202533

Loh, T., Archer, S.K. & Dunham, A. (2019). Monitoring program design for data-limited marine biogenic habitats: A structured approach. *Ecology and Evolution*, *9*(12), 7346–7359. https://doi.org/10.1002/ece3.5261

Lugilde Yáñez, J., Bárbara, I. & Peña, V. (2022). *Algas coralinas (Corallinophycidae, Rhodophyta) de Galicia y norte de Portugal* (2022nd ed.). Servizo de Publicacións da UDC. https://doi.org/10.17979/spudc.000004

Lüthi, D., Le Floch, M., Bereiter, B., Blunier, T., Barnola, J.M., Siegenthaler, U., Raynaud, D., Jouzel, J., Fischer, H., Kawamura, K. & Stocker, T.F. (2008). High-resolution carbon dioxide concentration record 650,000–800,000 years before present. *Nature*, *453*(7193), 379–382.

Maggio, T., Perzia, P., Pazzini, A., Campagnuolo, S., Falautano, M., Mannino, A.M., Allegra, A. & Castriota, L. (2022). Sneaking into a Hotspot of Biodiversity: Coverage and Integrity of a Rhodolith Bed in the Strait of Sicily (Central Mediterranean Sea). *Journal of Marine Science and Engineering*, *10*(12), Article 12. https://doi.org/10.3390/jmse10121808

Massutí, E., Sánchez-Guillamón, O., Farriols, M.T., Palomino, D., Frank, A., Bárcenas, P., Rincón, B., Martínez-Carreño, N., Keller, S., López-Rodríguez, C., Díaz, J.A., López-González, N., Marco-Herrero, E., Fernandez-Arcaya, U., Valls, M., Ramírez-Amaro, S., Ferragut, F., Joher, S., Ordinas, F. & Vázquez, J.T. (2022). Improving Scientific Knowledge of Mallorca Channel Seamounts (Western Mediterranean) within the Framework of Natura 2000 Network. *Diversity*, *14*(1). Scopus. https://doi.org/10.3390/d14010004

Martin, C.S., Giannoulaki, M., De Leo, F., Scardi, M., Salomidi, M., Knittweis, L., Pace, M.L., Garofalo, G., Gristina, M., Ballesteros, E., Bavestrello, G., Belluscio, A., Cebrian, E., Gerakaris, V., Pergent, G., Pergent-Martini, C., Schembri, P.J., Terribile, K., Rizzo, L., Souissi, J.B., Bonacorsi, M., Guarnieri, G., Krzelj, M., Macic, V., Punzo, E., Valavanis, V. & Fraschetti, S. (2014). Coralligenous and maërl habitats: Predictive modelling to identify their spatial distributions across the Mediterranean Sea. *Scientific Reports*, *4*(1), 5073. https://doi.org/10.1038/srep05073

Martin, S. & Hall-Spencer, J.M. (2017). Effects of Ocean Warming and Acidification on Rhodolith/Maërl Beds. In R. Riosmena-Rodríguez, W. Nelson, & J. Aguirre (Eds.),

Rhodolith/Maërl Beds: A Global Perspective (pp. 55–85). Springer International Publishing. https://doi.org/10.1007/978-3-319-29315-8_3

Mateo-Cid, L.E. (2006). *Estudio taxonómico de los géneros Neogoniolithon, Spongites y Pneophyllum (Corallinales, Rhodophyta) en la costa del Atlántico de México* [PhD Thesis]. Universidad Autónoma Metropolitana.

McCoy, S.J. & Kamenos, N.A. (2015). Coralline algae (Rhodophyta) in a changing world: Integrating ecological, physiological, and geochemical responses to global change. *Journal of Phycology*, *51*(1), 6–24. https://doi.org/10.1111/jpy.12262

Meinesz, A., Boudouresque, C.F., Falconetti, C., Astier, J.M., Bay, D.L., Blanc, J.J., Bourcier, M., Cinelli, F., Cirik, S., Cristiani, G., Geronimo, I.D., Giaccone, G., Harmelin, J.G., Laubier, L., Lovrić, A.Ž., Molinier, R., Soyer, J. & Vamvakas, C. (1983). *Normalisation des symboles pour la représentation et la cartographie des biocénoses benthiques littorales de Méditerranée*. https://api.semanticscholar.org/CorpusID:132627455

Miya, M. (2022). Environmental DNA Metabarcoding: A Novel Method for Biodiversity Monitoring of Marine Fish Communities. *Annual Review of Marine Science*, *14*(1), 161–185. https://doi.org/10.1146/annurev-marine-041421-082251

Moranta, J., Barberá, C., Druet Vélez, M., Díaz-Valdés, M., Zaragoza, N., Tello-Antón, M.O., López-Jurado, J.L., Balbín, R., Flexas, M. del M., Fernández, M., Hidalgo, M., Domínguez, M., Quetglas, A., Goñi, R., Mallol, S., Sánchez-Delgado, F., Ambroso, S. & Comalada, N. (2014). *Caracterización ecológica de la plataforma continental (50-100 m) del canal de Menorca*. https://digital.csic.es/handle/10261/318214

Moura, R.L., Abieri, M.L., Castro, G.M., Carlos-Júnior, L.A., Chiroque-Solano, P.M., Fernandes, N.C., Teixeira, C.D., Ribeiro, F.V., Salomon, P.S., Freitas, M.O., Gonçalves, J.T., Neves, L.M., Hackradt, C.W., Felix-Hackradt, F., Rolim, F.A., Motta, F.S., Gadig, O.B.F., Pereira-Filho, G.H. & Bastos, A.C. (2021). Tropical rhodolith beds are a major and belittled reef fish habitat. *Scientific Reports*, *11*(1), 794. https://doi.org/10.1038/s41598-020-80574-w

Nelson, W.A., Sutherland, J.E., Farr, T.J., Hart, D.R., Neill, K.F., Kim, H.J. & Yoon, H.S. (2015). Multi-gene phylogenetic analyses of New Zealand coralline algae: Corallinapetra Novaezelandiae gen. Et sp. Nov. And recognition of the Hapalidiales ord. Nov. *Journal of Phycology*, *51*(3), 454–468.

Noisette, F., Duong, G., Six, C., Davoult, D. & Martin, S. (2013a). Effects of elevated pCO2 on the metabolism of a temperate rhodolith Lithothamnion corallioides grown under different temperatures. *Journal of Phycology*, *49*(4), 746–757. https://doi.org/10.1111/jpy.12085

Noisette, F., Egilsdottir, H., Davoult, D. & Martin, S. (2013b). Physiological responses of three temperate coralline algae from contrasting habitats to near-future ocean acidification. *Journal of Experimental Marine Biology and Ecology*, *Complete*(448), 179–187. https://doi.org/10.1016/j.jembe.2013.07.006

Ordines, F. & Massutí, E. (2009). Relationships between macro-epibenthic communities and fish on the shelf grounds of the western Mediterranean. *Aquatic Conservation: Marine and Freshwater Ecosystems*, *19*(4), 370–383. https://doi.org/10.1002/aqc.969

OSPAR, 2023. Benthic Habitats Thematic Assessment, in: OSPAR, 2023: Quality Status Report 2023. OSPAR Commision, London.

Otero-Ferrer, F., Tuya, F., Bosch Guerra, N., Herrero-Barrencua, A., Abreu, A. & Haroun, R. (2020). Composition, structure and diversity of fish assemblages across seascape types at Príncipe, an understudied tropical island in the Gulf of Guinea (eastern Atlantic Ocean). *African Journal of Marine Science*, *42*(4), 381–391. https://doi.org/10.2989/1814232X.2020.1826358

Pardo, C., Guillemin, M.L., Peña, V., Bárbara, I., Valero, M. & Barreiro, R. (2019). Local Coastal Configuration Rather Than Latitudinal Gradient Shape Clonal Diversity and Genetic Structure of Phymatolithon calcareum Maërl Beds in North European Atlantic. *Frontiers in Marine Science*, *6*, 149. https://doi.org/10.3389/fmars.2019.00149

Peña, V., De Clerck, O., Afonso-Carrillo, J., Ballesteros, E., Bárbara, I., Barreiro, R. & Le Gall, L. (2015b). An integrative systematic approach to species diversity and distribution in the genus *Mesophyllum* (Corallinales, Rhodophyta) in Atlantic and Mediterranean Europe. *European Journal of Phycology*, *50*(1), 20–36. https://doi.org/10.1080/09670262.2014.981294

Peña, V., Le Gall, L., Rösler, A., Payri, C.E. & Braga, J.C. (2019). Adeylithon bosencei gen. Et sp. Nov.(Corallinales, Rhodophyta): A new reef-building genus with anatomical affinities with the fossil Aethesolithon. *Journal of Phycology*, *55*(1), 134–145.

Peña, V., Pardo, C., López, L., Carro, B., Hernandez-Kantun, J., Adey, W.H., Bárbara, I., Barreiro, R., & Gall, L.L. (2015a). Phymatolithon lusitanicum sp. nov. (Hapalidiales, Rhodophyta): The Third Most Abundant Maërl-Forming Species in the Atlantic Iberian Peninsula. *Cryptogamie, Algologie*, *36*(4), 429–459. https://doi.org/10.7872/crya/v36.iss4.2015.429

Peña, V., Vieira, C., Braga, J.C., Aguirre, J., Rösler, A., Baele, G., De Clerck, O. & Le Gall, L. (2020). Radiation of the coralline red algae (Corallinophycidae, Rhodophyta) crown group as inferred from a multilocus time-calibrated phylogeny. *Molecular Phylogenetics and Evolution*, *150*, 106845.

Pereira, R.C. & da Gama Bahia, R. (2021). Rhodoliths: Can Its Importance on a Large Scale Be Promoted by a Microscale and Invisible Phenomenon? *Frontiers in Marine Science*, *8*. https://doi.org/10.3389/fmars.2021.630517

Pereira-Filho, G.H., de Cerqueira Veras, P., Francini-Filho, R.B., de Moura, R.L., Pinheiro, H.T., Gibran, F.Z., Matheus, Z., Neves, L.M. & Amado-Filho, G.M. (2015). Effects of the sand tilefish Malacanthus plumieri on the structure and dynamics of a rhodolith bed in the Fernando de Noronha Archipelago, tropical West Atlantic. *Marine Ecology Progress Series*, *541*, 65–73.

Pérès, J.M. (1967). The mediterranean benthos. *Oceanography and Marine Biology: An Annual Review*.

Pergent, G., & Pergent-Martini, C. (2015). Cartography of main coastal ecosystems (corallignenous and rhodolith beds) along the corsican coasts. *Proceedings of 2nd mediterranean symposium on the conservation of coralligenous and other calcareous bio-concretions*, 37.

Peterson, C.H., Summerson, H.C., Thomson, E., Lenihan, H.S., Grabowski, J., Manning, L., Micheli, F. & Johnson, G. (2000). Synthesis of linkages between benthic and fish communities as a key to protecting essential fish habitat. *Bulletin of Marine Science*, *66*(3), 759–774.

Pezzolesi, L., Falace, A., Kaleb, S., Hernandez-Kantun, J.J., Cerrano, C. & Rindi, F. (2017). Genetic and morphological variation in an ecosystem engineer, *Lithophyllum byssoides* (Corallinales, Rhodophyta). *Journal of Phycology*, *53*(1), 146–160. https://doi.org/10.1111/jpy.12488

Piazzi, L., Basso, D., Falace, A., Kaleb, S., Ria, M. & Cecchi, E. (2024). Macroalgal assemblages associated to Mediterranean rhodolith beds. *Aquatic Botany*, *194*. Scopus. https://doi.org/10.1016/j.aquabot.2024.103785

Picciulin, M., Sebastianutto, L., Codarin, A., Calcagno, G. & Ferrero, E.A. (2012). Brown meagre vocalization rate increases during repetitive boat noise exposures: A possible case of vocal compensation. *The Journal of the Acoustical Society of America*, *132*(5), 3118–3124. https://doi.org/10.1121/1.4756928

Pierri, C., Longo, C., Falace, A., Gravina, M.F., Gristina, M., Kaleb, S., Lazic, T., Lisco, S., Moretti, M., Putignano, M., Ravisato, M., Trani, R., Dadamo, M. & Albano, P.G. (2024). Invertebrate diversity associated with a shallow rhodolith bed in the Mediterranean Sea (Mar Piccolo of Taranto, south-east Italy). *Aquatic Conservation: Marine and Freshwater Ecosystems*, *34*(1), e4054. https://doi.org/10.1002/aqc.4054

Pompeu, P.S., de Carvalho, D.R., Leal, C.G., Leitão, R.P., Alves, C.B.M., Braga, D.F., Castro, M.A., Junqueira, N.T. & Hughes, R.M. (2021). Sampling efforts for determining fish species richness in megadiverse tropical regions. *Environmental Biology of Fishes*, *104*(11), 1487–1499. https://doi.org/10.1007/s10641-021-01184-7

Pont, D., Hughes, R.M., Whittier, T.R. & Schmutz, S. (2009). A predictive index of biotic integrity model for aquatic-vertebrate assemblages of western US streams. *Transactions of the American Fisheries Society*, *138*(2), 292–305.

Pyle, R.L. (2000). Assessing undiscovered fish biodiversity on deep coral reefs using advanced self-contained diving technology. *Marine Technology Society Journal*, *34*(4), 82–91.

Qui-Minet, Z.N., Coudret, J., Davoult, D., Grall, J., Mendez-Sandin, M., Cariou, T. & Martin, S. (2019). Combined effects of global climate change and nutrient enrichment on the physiology of three temperate maërl species. *Ecology and Evolution*, *9*(24), 13787–13807. https://doi.org/10.1002/ece3.5802

Qui-Minet, Z.N., Davoult, D., Grall, J., Delaunay, C., Six, C., Cariou, T. & Martin, S. (2021). Physiology of maërl algae: Comparison of inter- and intraspecies variations. *Journal of Phycology*, *57*(3), 831–848. https://doi.org/10.1111/jpy.13119

Ragazzola, F., Foster, L.C., Form, A. U., Büscher, J., Hansteen, T. H. & Fietzke, J. (2013). Phenotypic plasticity of coralline algae in a high CO 2 world. *Ecology and Evolution*, *3*(10), 3436–3446.

Ragazzola, F., Marchini, A., Adani, M., Bordone, A., Castelli, A., Cerrati, G., Kolzenburg, R., Langeneck, J., Di Marzo, C., Nannini, M. Raiteri, G., Romanelli, E., Santos, M., Vasapollo, C., Pipitone, C. & Lombardi, C. (2021). An intertidal life: Combined effects of acidification and winter heatwaves on a coralline alga (Ellisolandia elongata) and its associated invertebrate community. *Marine Environmental Research*, *169*, 105342.

Rahel, F.J. (2000). Homogenization of fish faunas across the United States. *Science*, *288*(5467), 854–856.

Rebelo, A.C., Martín-González, E., Melo, C.S., Johnson, M.E., González-Rodríguez, A., Galindo, I., Quartau, R., Baptista, L., Avila, S.P. & Rasser, M.W. (2022). Rhodolith beds and their onshore transport in Fuerteventura Island (Canary Archipelago, Spain). *Frontiers in Marine Science*, *9*, 917883.

Rendina, F., Buonocore, E., di Montanara, A.C. & Russo, G. F. (2022). The scientific research on rhodolith beds: A review through bibliometric network analysis. *Ecological Informatics*, *70*, 101738. https://doi.org/10.1016/j.ecoinf.2022.101738

Rendina, F., Kaleb, S., Caragnano, A., Ferrigno, F., Appolloni, L., Donnarumma, L., Russo, G.F., Sandulli, R., Roviello, V. & Falace, A. (2020). Distribution and Characterization of Deep Rhodolith Beds off the Campania coast (SW Italy, Mediterranean Sea). *Plants*, *9*(8), Article 8. https://doi.org/10.3390/plants9080985

Rich, W.A., Schubert, N., Schläpfer, N., Carvalho, V.F., Horta, A.C. & Horta, P.A. (2018). Physiological and biochemical responses of a coralline alga and a sea urchin to climate change: Implications for herbivory. *Marine Environmental Research*, *142*, 100–107.

Richards, J.L., Bahia, R.G., Jesionek, M.B. & Fredericq, S. (2019). Sporolithon amadoi sp. Nov. (Sporolithales, Rhodophyta), a new rhodolith-forming non-geniculate coralline alga from offshore the northwestern Gulf of Mexico and Brazil. *Phytotaxa*, *423*(2), 49–67. https://doi.org/10.11646/phytotaxa.423.2.1

Rindi, F., Braga, J.C., Martin, S., Peña, V., Le Gall, L., Caragnano, A. & Aguirre, J. (2019). Coralline Algae in a Changing Mediterranean Sea: How Can We Predict Their Future, if We Do Not Know Their Present? *Frontiers in Marine Science*, *6*, 723. https://doi.org/10.3389/fmars.2019.00723

Riosmena-Rodríguez, R. (2017). Natural History of Rhodolith/Maërl Beds: Their Role in Near-Shore Biodiversity and Management. In R. Riosmena-Rodríguez, W. Nelson, & J. Aguirre (Eds.), *Rhodolith/Maërl Beds: A Global Perspective* (pp. 3–26). Springer International Publishing. https://doi.org/10.1007/978-3-319-29315-8_1

Rösler, A., Perfectti, F., Peña, V. & Braga, J. C. (2016). Phylogenetic relationships of corallinaceae (Corallinales, Rhodophyta): Taxonomic implications for reef-building corallines. *Journal of Phycology*, *52*(3), 412–431. https://doi.org/10.1111/jpy.12404

Saunders, G.W. (2005). Applying DNA barcoding to red macroalgae: A preliminary appraisal holds promise for future applications. *Philosophical Transactions of the Royal Society B: Biological Sciences*, *360*(1462), 1879–1888.

Saunders, G.W. & McDevit, D.C. (2012). Methods for DNA barcoding photosynthetic protists emphasizing the macroalgae and diatoms. In *DNA barcodes: Methods and protocols* (pp. 207–222). Springer.

Saunders, G.W. & Moore, T.E. (2013). *Refinements for the amplification and sequencing of red algal DNA barcode and RedToL phylogenetic markers: A summary of current primers, profiles and strategies*. *28*(1), 31–43. https://doi.org/10.4490/algae.2013.28.1.031

Scherner, F., Pereira, C.M., Duarte, G., Horta, P.A., e Castro, C.B., Barufi, J.B. & Pereira, S.M.B. (2016). Effects of ocean acidification and temperature increases on the photosynthesis of tropical reef calcified macroalgae. *PloS One*, *11*(5), e0154844.

Schneider, C.A., Rasband, W.S. & Eliceiri, K.W. (2012). NIH Image to ImageJ: 25 years of image analysis. *Nature Methods*, *9*(7), 671–675.

Schubert, N., Hofmann, L.C., Almeida Saá, A.C., Moreira, A.C., Arenhart, R.G., Fernandes, C.P., de Beer, D., Horta, P.A. & Silva, J. (2021). Calcification in free-living coralline algae is strongly influenced by morphology: Implications for susceptibility to ocean acidification. *Scientific Reports*, *11*(1), Article 1. https://doi.org/10.1038/s41598-021-90632-6

Schubert, N., Peña, V., Salazar, V.W., Horta, P.A., Neves, P., Ribeiro, C., Otero-Ferrer, F., Tuya, F., Espino, F., Schoenrock, K., Hofmann, L.C., Le Gall, L., Santos, R. & Silva, J. (2022). Rhodolith physiology across the Atlantic: Towards a better mechanistic understanding of intra-and interspecific differences. *Frontiers in Marine Science*, *9*, 921639.

Schubert, N., Salazar, V., Rich, W., Bercovich, M.V., Saá, A.A., Fadigas, S., Silva, J. & Horta, P. (2019). Rhodolith primary and carbonate production in a changing ocean: The interplay of warming and nutrients. *Science of the Total Environment*, *676*, 455–468.

Schubert, N., Tuya, F., Peña, V., Horta, P.A., Salazar, V.W., Neves, P., Ribeiro, C., Otero-Ferrer, F., Espino, F., Schoenrock, K., Ragazzola, F., Olivé, I., Giaccone, T., Nannini, M., Mangano, M. C., Sará, G., Mancuso, F.P., Tantillo, M.F., Bosch-Belmar, M., Martin, S., Le Gall, L., Santos, R. & Silva, J. (2024). "Pink power"—The importance of coralline algal beds in the oceanic carbon cycle. *Nature Communications*, *15*(1), 8282. https://doi.org/10.1038/s41467-024-52697-5

Schwarz, A.M., Hawes, I., Andrew, N., Mercer, S., Cummings, V. & Thrush, S. (2005). Primary production potential of non-geniculate coralline algae at Cape Evans, Ross Sea, Antarctica. *Marine Ecology Progress Series*, *294*, 131–140.

Selig, E.R. & Bruno, J.F. (2010). A global analysis of the effectiveness of marine protected areas in preventing coral loss. *PLos One*, *5*(2), e9278.

Silliman, B.R., Bertness, M.D., Altieri, A.H., Griffin, J.N., Bazterrica, M.C., Hidalgo, F.J., Crain, C.M. & Reyna, M.V. (2011). Whole-community facilitation regulates biodiversity on Patagonian rocky shores. *PLoS One*, *6*(10), e24502.

Simon-Nutbrown, C., Hollingsworth, P.M., Fernandes, T.F., Kamphausen, L., Baxter, J.M. & Burdett, H.L. (2020). Species Distribution Modeling Predicts Significant Declines in Coralline Algae Populations Under Projected Climate Change With Implications for Conservation Policy. *Frontiers in Marine Science*, *7*, 575825. https://doi.org/10.3389/fmars.2020.575825

Sordo, L., Santos, R., Barrote, I. & Silva, J. (2018). High CO 2 decreases the long-term resilience of the free-living coralline algae Phymatolithon lusitanicum. *Ecology and Evolution*, *8*(10), 4781–4792.

Sordo, L., Santos, R., Reis, J., Shulika, A. & Silva, J. (2016). A direct CO2 control system for ocean acidification experiments: Testing effects on the coralline red algae Phymatolithon lusitanicum. *PeerJ*, *4*, e2503.

Steller, D.L. & Foster, M.S. (1995). Environmental factors influencing distribution and morphology of rhodoliths in Bahía Concepción, B.C.S., México. *Journal of Experimental Marine Biology and Ecology*, *194*(2), 201–212. https://doi.org/10.1016/0022-0981(95)00086-0

Steller, D.L., Hernandez-Ayón, J.M., Riosmena-Rodríguez, R. & Cabello-Pasini, A. (2007). Effect of temperature on photosynthesis, growth and calcification rates of the free-living coralline alga Lithophyllum margaritae. *Ciencias Marinas*, *33*(4), Article 4. https://doi.org/10.7773/cm.v33i4.1255

Steller, D.L., Riosmena-Rodríguez, R., Foster, M.S. & Roberts, C.A. (2003). Rhodolith bed diversity in the Gulf of California: The importance of rhodolith structure and consequences of disturbance. *Aquatic Conservation: Marine and Freshwater Ecosystems*, *13*(S1), S5–S20. https://doi.org/10.1002/aqc.564

Tabone, L., Knittweis, L., Aguilar, R., Alvarez, H., Borg, J.A., Garcia, S., Schembri, P.J. & Evans, J. (2024). Habitat characterization, anthropogenic impacts and conservation of rhodolith beds off southeastern Malta. *Aquatic Conservation: Marine and Freshwater Ecosystems*, *34*(4). Scopus. https://doi.org/10.1002/aqc.4148

Teed, L., Bélanger, D., Gagnon, P. & Edinger, E. (2020). Calcium carbonate (CaCO3) production of a subpolar rhodolith bed: Methods of estimation, effect of bioturbators, and global comparisons. *Estuarine Coastal and Shelf Science*, *242*, 106822. https://doi.org/10.1016/j.ecss.2020.106822

Teichert, S. (2014). Hollow rhodoliths increase Svalbard's shelf biodiversity. *Scientific Reports*, *4*(1), Article 1. https://doi.org/10.1038/srep06972

Townsend, R.A., Woelkerling, W.J., Harvey, A.S. & Borowitzka, M. (1995). An account of the red algal genus Sporolithon (Sporolithaceae, Corallinales) in southern Australia. *Australian Systematic Botany*, *8*(1), 85–121.

Trégarot, E., D'Olivo, J.P., Botelho, A. Z., Cabrito, A., Cardoso, G.O., Casal, G., Cornet, C.C., Cragg, S.M., Degia, A.K., Fredriksen, S., Furlan, E., Heiss, G., Kersting, D.K., Maréchal, J.P., Meesters, E., O'Leary, B.C., Pérez, G., Seijo-Núñez, C., Simide, R., van der Geest, M. & de Juan, S. (2024). Effects of climate change on marine coastal ecosystems – A review to guide research and management. *Biological Conservation*, *289*, 110394. https://doi.org/10.1016/j.biocon.2023.110394

Trentin, R., Moschin, E., Grapputo, A., Rindi, F., Schiaparelli, S. & Moro, I. (2023). Multi-gene phylogeny reveals a new genus and species of Hapalidiales (Rhodophyta) from Antarctica: *Thalassolithon adeliense gen . & sp. nov. Phycologia*, *62*(1), 83–98. https://doi.org/10.1080/00318884.2022.2147745

Tuya, F., Schubert, N., Aguirre, J., Basso, D., Bastos, E.O., Berchez, F., Bernardino, A.F., Bosch, N.E., Burdett, H.L., Espino, F., Fernández-Gárcia, C., Francini-Filho, R.B., Gagnon, P., Hall-Spencer, J.M., Haroun, R., Hofmann, L.C., Horta, P.A., Kamenos, N.A., Le Gall, L., Magris, R.A., Martin, S., Nelson, W.A., Neves, P., Olivé, I., Otero-Ferrer, F., Peña, V., Pereira-Filho, G.H., Ragazzola, F., Rebelo, A.C., Ribeiro, C., Rinde, E., Schoenrock, K., Silva, J., Sissini, M.N. & Tâmega, F.T.S. (2023). Levelling-up rhodolith-bed science to address global-scale conservation challenges. *Science of The Total Environment*, *892*, 164818. https://doi.org/10.1016/j.scitotenv.2023.164818

Walker, R. (1984). *Trichocytes and megacells in cultured crusts of three British species of Lithothamnium and Phymatolithon (Corallinaceae, Rhodophyta)*.

Whittier, T.R., Hughes, R.M., Stoddard, J.L., Lomnicky, G.A., Peck, D.V. & Herlihy, A.T. (2007). A structured approach for developing indices of biotic integrity: Three examples from streams and rivers in the western USA. *Transactions of the American Fisheries Society*, *136*(3), 718–735.

Woelkerling, W.J. (1983). A taxonomic reassessment of Lithophyllum (Corallinaceae, Rhodophyta) based on studies of RA Philippi's original collections. *British Phycological Journal*, *18*(3), 299–327.

Woelkerling, W.J. (1988). The coralline red algae: An analysis of the genera and subfamilies of nongeniculate Corallinaceae. *(No Title)*.

Woelkerling, W.J. & Irvine, L. M. (1986). The typification and status of Phymatolithon (Corallinaceae, Rhodophyta). *British Phycological Journal*, *21*(1), 55–80.

Xenopoulos, M.A. & Lodge, D.M. (2006). Going with the flow: Using species–discharge relationships to forecast losses in fish biodiversity. *Ecology*, *87*(8), 1907–1914.

Yoon, H.S., Hackett, J.D. & Bhattacharya, D. (2002). A single origin of the peridinin- and fucoxanthin-containing plastids in dinoflagellates through tertiary endosymbiosis. *Proceedings of the National Academy of Sciences of the United States of America*, *99*(18), 11724–11729. https://doi.org/10.1073/pnas.172234799

SECTION II

RESULTS

2.1. **CHAPTER I:** Morphological insights into the three-dimensional complexity of rhodolith beds

Andrea Cabrito, Silvia de Juan, Hilmar Hinz, Francesc Maynou

Cabrito, A., de Juan, S., Hinz, H., & Maynou, F. (2024). Morphological insights into the three-dimensional complexity of rhodolith beds. Marine Biology, 171(6), 127. https://doi.org/10.1007/s00227-024-04437-y



Abstract

The ecological importance of rhodolith beds stems from their role as structurally complex three-dimensional habitat formed by free-living red calcareous algae. Their structural singularity is due to the great variety of complex and branching morphologies exhibited by rhodoliths that create interstitial spaces and increase their surface area. This increases the ecological niches for cryptofauna and provide refuge for a high number of organisms, which is why rhodolith beds are considered biodiversity hotspots. In this work, we studied a rhodolith bed located in the Menorca Channel, formed by several species of red calcareous algae that exhibit a great variety of morphologies that form an extensive and heterogeneous habitat. This study explored the morphological diversity of the rhodolith bed, comparing the 'Core Habitat' (within the center of the bed with highest densities of rhodoliths) with the boundaries or 'Adjacent Habitat' where rhodolith density was lower. Our results show that all rhodolith growth forms (branched, pralines and boxwork) in the Core Habitat had higher interstitial space and were larger than the ones from adjacent zones. Moreover, we explored three-dimensional techniques to study morphological characteristics that have historically been studied in two dimensions. This study contributes to the knowledge of morphological diversity in well-preserved rhodolith beds from continental shelves in the western Mediterranean Sea and reinforces the use of three-dimensional measurements, specifically the interstitial space of branched rhodoliths, to provide more accurate data on habitat complexity.

Key words: coralline algae, red calcareous algae, biodiversity, morphometrics, Mediterranean Sea.

Correspondence:

Andrea Cabrito (ORCID:0000-0002-3429-5201). Institut de Ciències del Mar (ICM-CSIC), Barcelona 08003, Spain. Email: cabrito@icm.csic.es

2.1.1. Introduction

Rhodoliths are free living, long-lived and slow-growing non-geniculate calcareous algae (Rhodophyta: Corallinaceae, also known as maërl). They accumulate as rhodolith beds in subtidal areas characterized by coarse, detritic sediments consisting of gravels and clean sands (Illa-López et al. 2023). They are distributed globally (Riosmena-Rodríguez et al. 2017) in environments where bottom currents prevent their burial by finer sediment, and where irradiance is low but still adequate for photosynthesis (Peña et al. 2014; Carvalho et al. 2020). In consequence, the depth limit of rhodolith beds is determined by the optical properties of the water body (transparency, turbidity, sediment load), affecting quality and intensity of light reaching the seabed (Basso et al. 2017). In Mediterranean islands, rhodoliths thrive at great depths, reaching 100 m in the Mediterranean western basin (Ballesteros 1988; Barberá et al. 2012a), and reported at a maximum depth of 137 m for the Mallorca channel in the Balearic Islands (Massutí et al. 2022).

Rhodolith beds build hard, three-dimensional complex structures that provide substrate for other algae and invertebrates (Bordehore et al. 2003; Teichert et al. 2014). These organisms are often referred to as ecosystem engineers (Nelson 2009). Rhodoliths can acquire various complex morphologies, from highly branched to massive round thalli (Bosence 1983). Therefore, they provide a greater array of microhabitats at different scales, from the interstitial spaces between branches (Bernard et al. 2019; Fredericq et al. 2019; Boyé et al. 2019) to the seascape level by increasing habitat heterogeneity (Amado Filho et al. 2017). In consequence, the accumulation of rhodoliths over sandy sediments contributes to increase the local and regional biodiversity (Bernard et al. 2019; de Juan et al. 2023).

Previous studies identified a relationship between rhodolith morphological complexity and the associated biodiversity. In particular, the diversity of cryptofauna is related to thallus size, growth form and structural complexity (Kamenos et al. 2004; Steller et al. 2003; Figueiredo et al. 2007), with higher diversity associated with highly branched forms (Steller et al. 2003; Foster et al. 2007; Meihoub-Berlandi et al. 2012; Méndez-Trejo et al. 2021). High-density of rhodoliths also favours higher benthic fauna richness (Veras et al. 2020), while larger sizes of rhodoliths seem to facilitate reproduction and feeding in fishes and invertebrates (Steller et al. 2003; Gagnon et al. 2012).

Physical processes such as sedimentation or turbulence can affect rhodolith morphology and, therefore, their associated communities (Pérez-Peris et al. 2023). Trawl or dredge fishing contribute to increased sedimentation rates (Puig et al. 2015), and to physical damage of the rhodolith (e.g., breaking or chipping) (Cabanellas-Reboredo et al. 2017; Gabara et al. 2018). Rhodolith beds have a high conservation value; they are included in the European “Habitats Directive” (Council Directive 92/43/EEC). However, in the Mediterranean, they continue to face threats from trawling activities (de Juan et al. 2013) and current protection measures are often inadequate. Due to their slow growth (of the

order of 1 mm yr^{-1}, Blake et al. 2007) rhodoliths exhibit exceptionally low renewal rates, which can result in slow recovery trajectories (Tauran et al. 2020).

This study focuses on rhodoliths from a well preserved rhodolith bed in the Menorca Channel (Balearic Islands, Western Mediterranean, 3º45' E, 39º75' N) (Barberá et al. 2012a). The main objective of the study is to describe and measure the morphology of rhodoliths, as a proxy for habitat structural complexity. By analyzing samples from the well-preserved rhodolith bed, this study (i) analyses the diversity of rhodolith morphologies; (ii) determines the allometric growth curve for each of the major morphologies; (iii) produces a discriminant rule to classify rhodoliths based on few morphometric measurements; (iv) compares 2D with 3D measurements of branched rhodoliths to examine whether simple, relatively easy to measure 2-D metrics would be sufficient to describe the morphometry of a naturally 3-D object. This is relevant because, given the intricate three-dimensional growth pattern of rhodoliths, 2D metrics may lack the precision and accuracy needed to effectively describe their shape or interstitial space. This estimation is important as it is directly linked to the ecological functions facilitated by rhodoliths, which inherently exist in three dimensions.

The understanding of the structural complexity of rhodolith beds, achieved by exploring objectives i to iv, is essential for deducing their functional importance (Stelzer et al. 2021) and to improve their protection and preservation status globally (del Río et al. 2022).

2.1.2. Methodology

Study area

The study area is located in the Menorca Channel between 45 and 80 m depth (**Fig.1.3.1**), and was selected based on previous studies (Moranta et al. 2014) that identified a well-developed and preserved rhodolith bed that alternates with detritic bottoms and biogenic assemblages formed by other species of algae (de Juan et al. 2023). The Menorca Channel was declared a European Site of Community Importance (LIC ESZZ16002) in 2016, including a trawling ban for most of the channel. Moreover, the presence of underwater communication cables crossing the channel delimits an exclusion area that has been protected from trawling for more than 5 decades.

The presence of the cables' exclusion zone, a gently sloping continental shelf (reaching a maximum depth of 100 meters) and the prevalence of strong bottom currents creates optimal conditions for the development of rhodolith beds. As a consequence, the study area includes the largest identified rhodolith bed in the region, which has an extension of 304 Km^2 (**Fig.2.1.1**). As the distance from this bed increases, the depth increases towards the south-east and decreases towards the coast (west), with the north-west area being influenced by the sandy platform of the bay of Alcudia (**Fig.2.1.1**). In addition to the variation of these environmental factors, the density of rhodoliths decreases as the distance from the center of the rhodolith bed increases, hereafter referred to as Core Habitat (**Fig.2.1.1**).

We assessed the variation of rhodolith morphology in relation to the distance to the Core Habitat. Five sampling stations were deployed from the center to the periphery of the rhodolith bed (or Core Habitat). Sampling stations were thus classified into: (i) "Core Habitat", including samples within the cable zone at 69 m depth (S13) and in the trawl exclusion area close to the cable zone at 58.8 m depth (S15), where rhodolith cover is typically > 50%; (ii) "Adjacent Habitat", including samples far from the cables zone at 56 and 74 m depth (S18 and L1, respectively), where rhodolith cover is less than 50%, and "outside the reserve area" at 48.5 m depth (S5), where rhodoliths are scarce (**Fig.2.1.1**). The percentage cover of rhodoliths at each station was extracted from Moranta et al. (2014), where a spatially-structured survey was conducted to estimate the habitats distribution in the channel. To verify the rhodolith coverage at a small-scale (1 to 10 m), additional video images were obtained using still cameras (see Supplementary Material – **Fig.2.1.S1**).

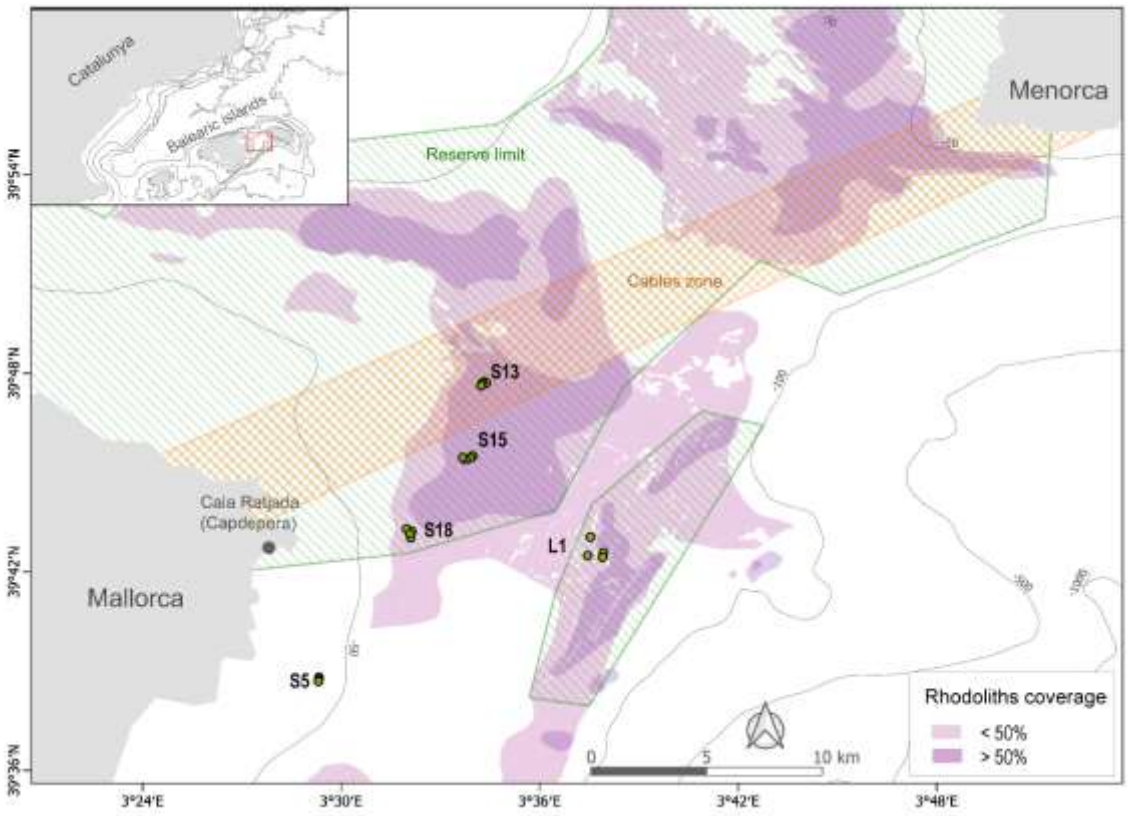


Fig.2.1.1. Map of the study area in the Menorca Channel, showing the positions of the dredges (green dots). Area limited by the cables zone ("Cables zone" in the figure, established in 1971) and the "Trawl Exclusion Reserve" (declared 2016, green cross-hatch). Source: INDEMARES (Moranta et al. 2014).

Data acquisition

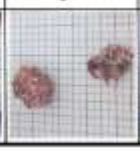
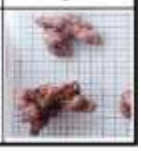
We collected four samples per station using a "Naturalist" Dredge (frame 45 x 18.5 cm, fitted to a 1 mm mesh bag) in summer 2022. Nineteen valid samples were recovered, as only three dredges could be collected in S5 (example in Supplementary Material – **Fig.2.1.S2**). For each sample, a volume of

approximately 7,000 cm^3 of the content was systematically extracted, distributed in a tray and photographed. The proportion of live and dead rhodoliths was visually estimated on board for each tray.

The rhodoliths were classified into nine morphotypes (A to I), described based on the six used in Barberá et al. (2012b) with some modifications that further divided heterogeneous groups (**Table 2.1.1**). These nine morphotypes belong to the three main rhodolith categories or growth forms according to Basso et al. (2016): "Branched" (Br), "Praline" (PR) and "Boxwork" (Bo). The rhodoliths were grouped by morphotypes, photographed on a graduated white board, and dry-stored. A total of 3877 rhodoliths were counted in the photographs (see Supplementary Material **Table 2.1.S1**). The number and frequency of the morphotypes (A to I) and growth forms in each sample were estimated from the photographs.

A sample of 100 g of sediment extracted from each dredge was stored for granulometry analysis, while the remaining content of the dredges was returned to the sea. A subsample of 20 g of sediment was used for the analysis of grain size. The granulometry was analysed using a laser diffraction particle size analyser (HORIBA LA-950V2) after disaggregation and removal of the biogenic fraction (10% H_2O_2 solution) and dispersion in ultrasonic bath.

Table 2.1.1. Rhodolith growth forms (top) and description of morphotypes defined in the finer classification (A to I)

	BRANCHED				PRALINES			BOXWORK	
MORPHOTYPES	Large size with wide branching	Small size, less and short branching	Small size with slender branches	Many short branches. Spherical	Rough, bumpy and quite irregular	Rounded with small protusions or short branches	Rounded with many thick and smooth protusions	Rounded and incrusted in other subtratum	Irregular form, incrusted in other subtratum
	A	B	C	D	E	F	G	H	I
									

2.1.2.1. 2D - Measurements

From the rhodolith samples (i.e. 3877 rhodoliths photographed on board), five individuals for each morphotype per station (when possible) were selected and set aside. This selection resulted in a total of 189 rhodoliths belonging to the nine morphotypes (Supplementary Material **Table 2.1.S2**). These 189 rhodoliths were photographed individually to obtain 2D morphological metrics. A total of 15 metrics was obtained for each rhodolith. The *maximum* and *minimum axis of the fitted ellipse* (Amax and Amin, mm), the *surface of the projected area* (A, mm^2), *Convex Hull area* (CHA, mm^2), *shape perimeter* (P, mm), the *angle* (a, º), the *Feret length* (Lmax, mm) and *Feret's angle* (Fa, º) were obtained measuring the rhodolith shape and estimating the convex hull of the shape. These metrics were obtained using the default measurement routines in ImageJ 1.52a software (Schneider et al. 2012), except for CHA which

was obtained with the plugin "Hull and Circle" v.2.1b contributed by A. Karperien (http://imagej.net/ij/plugins/hull-circle.html).

In addition, the dimensionless metrics *circularity* (C), *roundness* (R), *aspect ratio* (AR) and *solidity* (S) were automatically determined by ImageJ program according to the following formulas:

$$C = 4\pi \frac{A}{P^2}$$

$$R = 4\frac{A}{\pi A_{max}^2}$$

$$AR = \frac{A_{max}}{A_{min}}$$

$$S = \frac{A}{CHA}$$

Finally, three additional metrics were obtained:

(i) the *interstitial space* (IS, mm^2) as the missing space (area) between the convex hull area and the rhodolith surface area

$$IS = CHA - A$$

(ii) the individual dry weight (W, g) and

(iii) the *shape coefficient* (D, Kooijman 2010) extracted from:

$$D = \sqrt[3]{\frac{W}{2.71 Lmax^3}}$$

being d = 2.71 g/cm^3 the density of calcite.

2.1.2.2. 2D/3D Measurements in branched morphotype A

Given that the difference between 2D and 3D metrics is likely to be more noticeable in the branched growth form, this analysis focuses only on morphotype A. We sub-sampled a new set of 30 rhodoliths (from the stored dry sample) classified as branched (morphotype A) and collected in the stations S13 and S15 (Supplementary Material **Fig.2.1.S3)**. The 30 rhodoliths were photographed and dry weighed individually. Then, the images were processed through ImageJ as described in the previous section. To compare the 2D and 3D information extracted, the measurements assessed are subscripted "2D": the *maximum ellipse axis* ($Amax_{2D}$), the *Maximum Feret diameter* ($Lmax_{2D}$), the *perimeter* (P_{2D}), the *surface area* (A_{2D}), *the convex hull area* (CHA_{2D}), the *roundness* (R_{2D}), the *solidity* (S_{2D}) and the *interstitial space* (IS_{2D}).

For 3D measurements, digital twins of selected rhodoliths were created using high-precision blue light 3D scanner (Revopoint MINI) with a precision of up to 0.02 mm and the associated programs Revoscan and Revostudio (www.revopoint3d.com). For each 3D model twin, the *surface area* (A_{3D}, mm^2), the *maximum length from the center of mass* (L_{3D}, mm), the *volume* (V_{3D}, mm^3) and the *convex hull volume* (CHV_{3D}, mm^3) were calculated using an *ad-hoc* R script based on libraries Rvcg, geometry and MeshesTools, while *the maximum Feret diameter* ($Lmax_{3D}$) and the *roundness* (R_{3D}) were obtained using Slicer program v. 5.2.2 (Fedorov et al. 2012). With these measurements the 3D *interstitial space* (IS_{3D}, mm^3) was calculated as the difference between the volume of the convex hull and the volume of the rhodolith:

$$IS_{3D} = CHV_{3D} - V_{3D}$$

The solidity in 3D (S_{3D}) was calculated with the relation between the 3D rhodolith volume and the 3D convex hull volume:

$$S_{3D} = \frac{V_{3D}}{CHV_{3D}}$$

Finally, we obtained a matrix of 17 metrics (8 from 2D, 8 from 3D and the weight) measured for the 30 rhodolith samples (see Supplementary Material - **Fig.2.1.S5**).

2.1.2.3. Statistical Analysis

Morphological rhodolith composition of the study area

Differences in the proportion of growth forms (Br, Pr and Bo) between Core Habitat and Adjacent Habitat stations were analysed with PERMANOVA, with a model design including "Station" nested within Habitat factor with two levels (Core and Adjacent Habitat). Both factors were treated as fixed factors. The proportions were arcsin transformed for this analysis. The routine adonis2 of R package *vegan* was used (Oksanen et al. 2022).

2D - General Measurements analysis

After removing nine outliers (determined through exploratory data analysis with the aid of boxplots), 180 measured rhodoliths were used to fit several models. Firstly, a regression model was performed to assess the W/L relation, with L corresponding to the Feret's diameter, by linearizing the allometric growth equation:

$$W = aL_{max}{}^{b}$$

This was done for the pool of 180 rhodoliths and for each category or growth form (Br, Bo, Pr) separately. Then, to evaluate the significance of the difference in the values of the *a* and *b* parameter of this relation between the three growth forms, we performed a generalized linear model (GLM) from

package *stats* (R Corer Team, 2022) fitted with a Gaussian distribution with logarithm link. To examine the possibility of overdispersion in the data, we performed a dispersion test from the package *AER* (Kleiber, C., 2022).

2D - Multivariate analyses

A PCA was performed on the full 2D metrics data set to reduce the number of variables while preserving the maximum variance possible of the original data set. This reduction in dimensionality facilitates visualization and data interpretation. Function prcomp from the R *stats* package was used. To accomplish that, we standardized all 15 morphometric variables measured from the 180 rhodoliths (**Table 2.1.2**).

To examine how these variables, perform as morphology classifiers, we selected the less correlated variables based on the Pearson correlation test from package *corrplot* (Wei and Simko, 2021) to perform a Linear Discriminant Analysis (LDA) from package *MASS* (Venables and Ripley, 2002). The numeric variables used in the model were: *Maximum Feret diameter* (L_{max}), *Roundness* (R) and *Solidity* (S) and the classification factor was the Growth form (Br, Pr and Bo). To fit the model, the variable Lmax was log-transformed, and Solidity and Roundness were arcsin-transformed. With these transformations, the assumptions for LDA of multivariate normality and homoscedasticity between groups were met. Multivariate normality of the metrics by morphology was not rejected according to the Royston's multivariate normality test (p-value = 0.05 for Branched; p-value = 0.40 for Pralines and p-value = 0.88 for Boxwork), using *MVN* package (Korkmaz et al. 2014). The hypothesis of homocedasticity could not be rejected based on Box's M-test for homogeneity of covariances matrices (X^2 = 18.562, df = 12, p-value = 0.0996) of the *biotools* package (da Silva, 2021). The matrix of 180 individuals was randomly re-sampled to split the data into a training data matrix (70%) to train the model, and a test data matrix (30%) to test the model. To achieve better prediction accuracy, this process was repeated a total of 100 times.

Table 2.1.2. Graphical representation of the 15 morphometric variables measured

Area (A)	**Perimeter (P)**	**ConvexHull Area (CHA)**	**Interstitial Space (IS)**	**Solidity (S)**
				
Maximum axis (Amax)	**Minimum axis (Amin)**	**Angle (a)**	**Aspect Ratio (AR)**	**Weight**



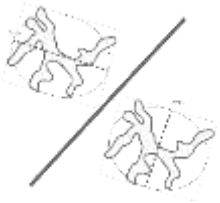
Feret diameter (Lmax)



Feret angle (Fa)



Circularity (C)

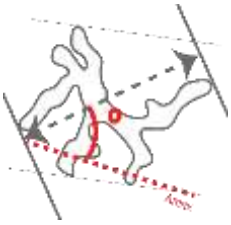


Roundness (R)



Shape coefficient (D)











2D/3D-Morphotype A measurements analysis

With the matrix of 17 morphological variables (8 in 2D, 8 in 3D and the weight) a Pearson correlation test was performed from package *corrplot* (Wei and Simko, 2021) to assess correlation between the two measurements. Furthermore, considering the total available surface area and the volume as key morphological measurements of high biological interest for metabolic or growth studies, linear models from package `stats` were fitted between the surface area measured in 2D (A_{2D}) and in 3D (A_{3D}) and between the surface area measured in 2D (A_{2D}) and the total volume measured in 3D (V_{3D}).

All statistical analyses were computed in R (R Development Core Team 2022) under version 4.2.1.

2.1.3. Results

2.1.3.1. Morphological rhodolith composition of the study area

The proportion of dead (bleached) rhodoliths was predominantly low (< 20%), with exceptions found in three samples from station L1, two samples from stations S5 and S13, that had no dead rhodoliths, while three samples from S18 had higher percentages, one reaching 50% coverage by dead rhodoliths (Supplementary Material **Fig.2.1.S4**).

All stations exhibited similar sediment compositions, primarily gravel (85% or higher), with minimal silt and clay (never exceeding 15%). Branched forms predominated in 50-90% of the samples, with lower proportions of pralines (5-40%) and boxwork (0-30%). However, variations in rhodolith morphologies were observed within samples colected at the same station, suggesting high small-scale heterogeneity. The Adjacent Habitat station L1 was very heterogeneous, and boxwork forms were more prevalent in several samples (**Fig.2.1.2**).

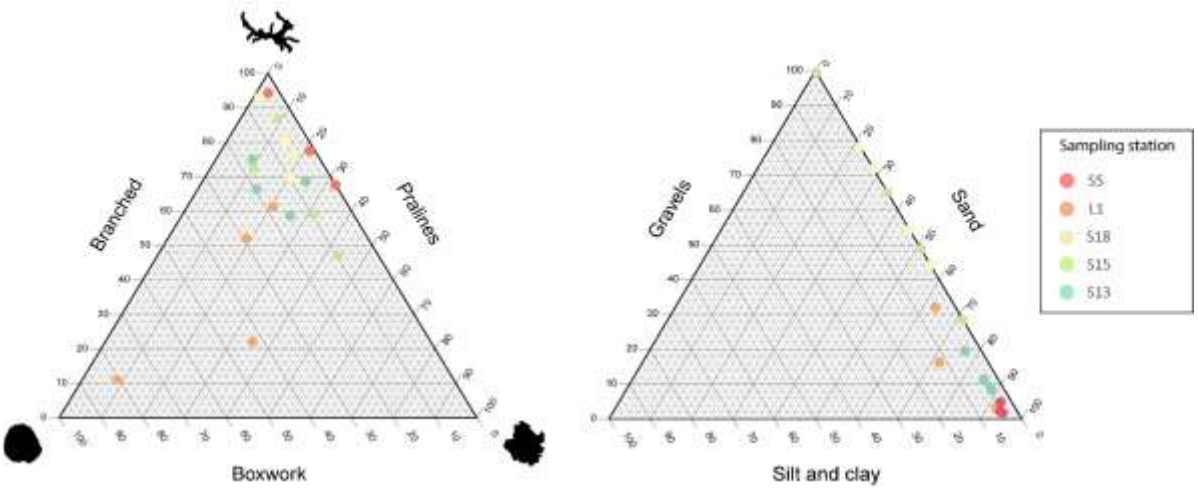


Fig.2.1.2. Ternary plot of sediment composition showing the proportion of gravels, sand, silt and clay (right) and ternary plot of rhodolith growth forms composition showing the proportion of branched, pralines and boxwork rhodoliths (left). Each dredge represented and color-coded following the stations sampled

Of the 3877 rhodoliths photographed, 69.2% were branched, 19.1% pralines and 11.8% boxwork (**Fig.2.1.3**, left panel). From these, the most abundant morphotypes were the Branched types C (37.53%), B (14.70%) and A (10.14%), and the Praline E (14.24%) (see **Table 2.1.1** for reference to the morphotypes). The proportions and representation of rhodlith morphotypes remained consistent across the two habitats (PERMANOVA p(F) = 0.211); however, the PERMANOVA test identified significant effects of the factor Station within habitat (PERMANOVA p(F) = 0.003).

At S5, the dominant morphotypes were branched (D) and praline (F), which were scarce at other stations. These differences likely stem from the habitat, as S5 is characterized by sand with scattered rhodoliths, and it is considered outside the rhodolith bed. Consequently, S5 was excluded from the statistical analyses conducted in this section and the subsequent one.

The stations within the Core Habitat exhibited more consistent proportions of morphologies compared to those in the Adjacent Habitat. Specifically, the dominant branched morphotype A decreased in abundance from station S13 to S15 and further to L1, where it was absent, while the branched Morphotype C remained consistently abundant across all stations, with the highest representation observed at adjacent station S18. The non-branched morphotypes were never dominant but appeared relatively frequently in station L1. The praline morphotype E was represented equally in all stations. The praline morphotype G occurred mostly in the stations from Core Habitat. The boxwork growth forms (morphotypes H and I) were proportionally represented in all core and adjacent stations except in S15 where mophotype H was predominant.

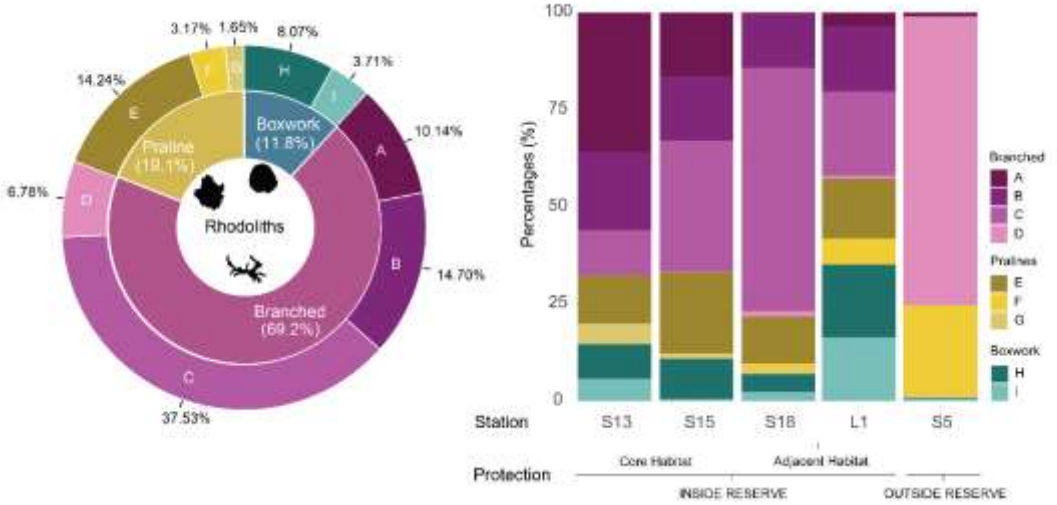


Fig.2.1.3. Total proportions of each growth form (Br, Pr and Bo) considering all stations together (left). Percentage of morphotypes (A to I) coverage in each station (right)

2.1.3.2. 2D- Morphological measurements

The PCA revealed the main morphometric variables describing the 2D rhodolith shape. These results showed that 46.7% of the variance could be explained by the first dimension while the second dimension explained 25.2% of the variance. **Fig.2.1.4** shows that the most differentiated group is the one formed by the branched forms. Praline and boxwork overlapped in the biplot.

The variables *Maximum Feret diameter* (Lmax), *area* (A) and *convex hull area* (CHA), *weight* (W) and the *maximum* and *minimum ellipse axis* (Amax and Amin) were highly correlated and their variability is represented by the first dimension (PCA X-axis). *Shape coefficient* (D), *Circularity* (C), *Solidity* (S) and *Roundness* (R) were also correlated and defined by the second dimension (PCA Y-axis). *Aspect Ratio* (AR) and *Roundness* (R) were negatively correlated, indicating that branched forms have lower roundness (and higher aspect ratio) than pralines and boxwork rhodoliths.

Because of the high correlation between several shape measurements, only a representative subset (Lmax, IS, W, A, D and P) was used to examine differences between samples recovered from the Core Habitat and the Adjacent Habitat (**Fig.2.1.5**). Boxwork growth forms tended to be bigger, longer and heavier than praline and these than branched forms (**Fig.2.1.5**). Moreover, there was a clear effect of the Core Habitat in terms of interstitial space, maximum Feret diameter and area. These metrics had greater values in all growth forms in the stations within the Core Habitat compared to the stations from the Adjacent Habitat.

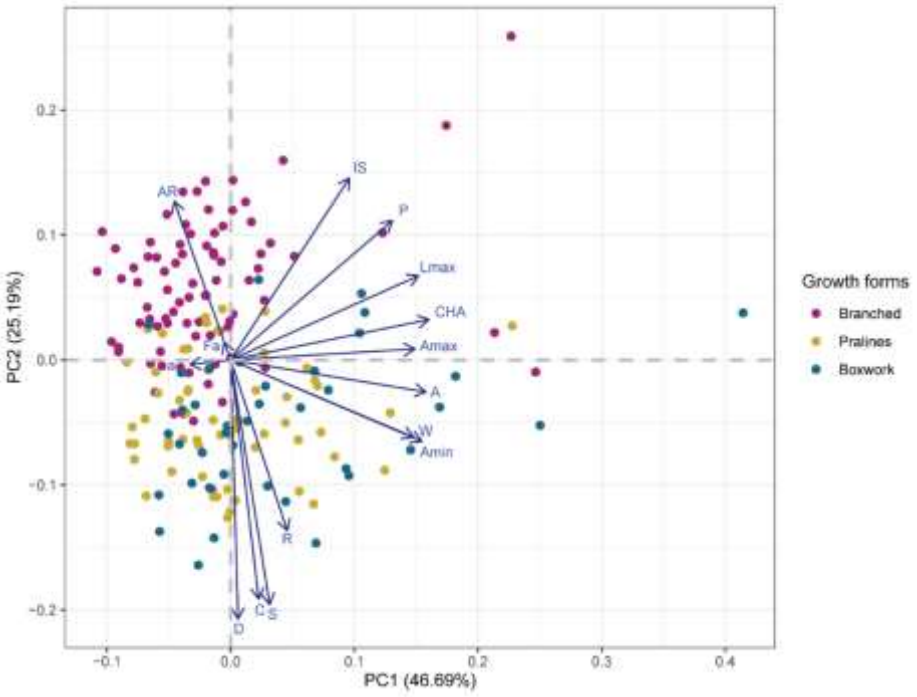


Fig.2.1.4. Principal components analysis (PCA) of individual rhodolith metrics from the Menorca Channel. A: area; a: angle; Amax: Maximum Ellipse Axis; Amin: Minimum Ellipse Axis; AR: Aspect Ratio; C: Circularity; CHA: Convex Hull Area; D: Shape coefficient; Fa: Feret angle; IS: Interstitial Space; Lmax: Maximum Feret diameter; P: Perimeter; R: Roundness; S: Solidity; W: Weight

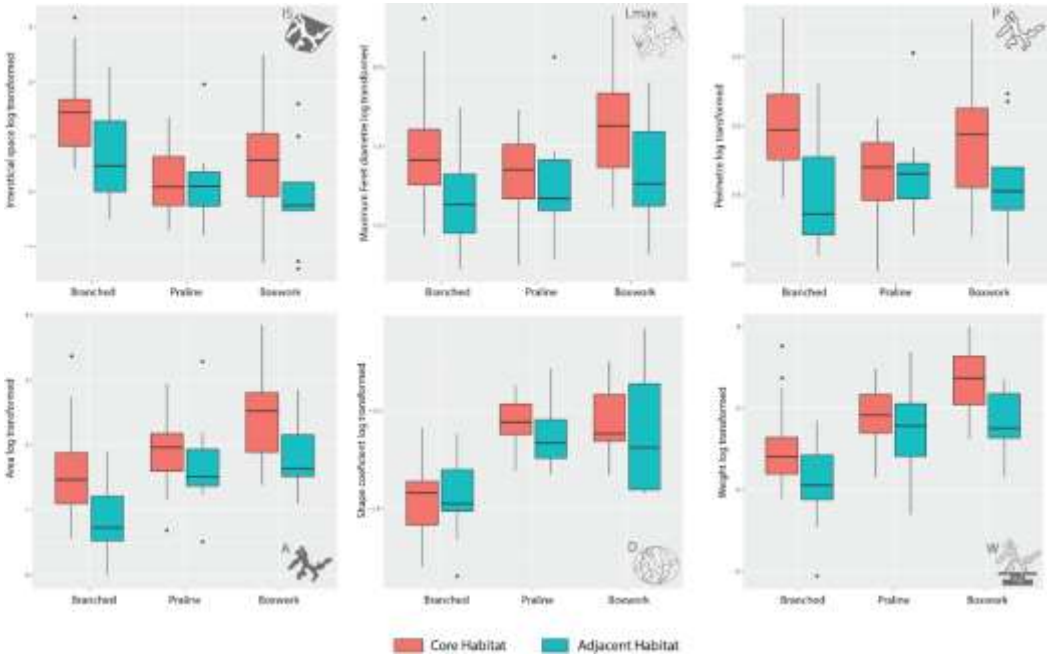


Fig.2.1.5. Boxplots for a subset of six morphological variables both in Core Habitat and in Adjacent Habitat for the three growth forms of rhodoliths. From left to right at the top: Interstitial space (IS), Maximum Feret diameter (Lmax) and Perimeter (P). From left to right at the bottom: Area (A), Shape coefficient (D) and Weight (W). All variables were log transformed

The allometric growth curves ($W = a\ L^b$) were estimated for each rhodolith growth form based on the linear models fitted for the relationship between weight and the Lmax (**Fig.2.1.6**). The parameter *a* was significantly different between Boxwork and Branched curves (p value < 0.001), but not between Praline and Branched curves (p value = 0.097). The parameter *b* showed no significant differences between growth forms. Therefore, the three groups showed a similar allometric growth rate, despite the groups having significantly different weights for the same length. The test for overdispersion was significant (p-value < 0.001), but with a low value of dispersion 1.80.

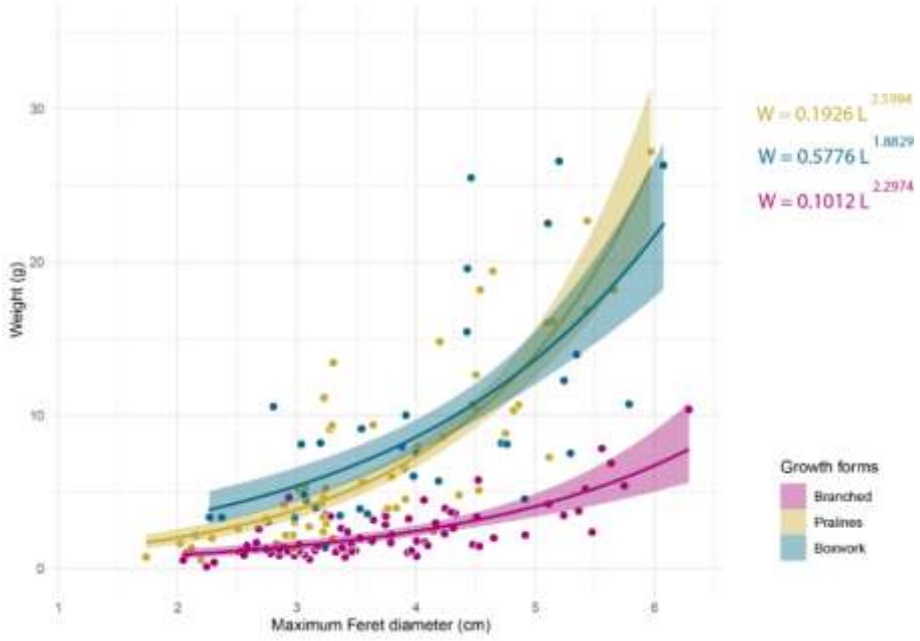


Fig.2.1.6. Rhodolith allometric growth curves, representing the relation between Lmax and W for each morphotype or growth form

2.1.3.3. Discriminant analysis

A linear discriminant analysis was used to build a classifier to predict growth forms from a set of relatively easy to measure variables. The results of the LDA showed that, although the three groups had a large degree of overlap, they can be statistically distinguished. The variables with the greatest weight in defining the first dimension of the LDA were the *Roundness* (R) and the *Solidity* (S) while the *Maximum Feret diameter* (Lmax) had the greatest weight in the second dimension. The first LDA axis explained 96.6% of the variance. This first direction separates the rhodoliths with greatest solidity (less branching), roundness and relatively large Lmax in the positive axis, from the rhodoliths with less S (more branching) and less R in the negative axis. The second LDA dimension explained the rest of the variance (3.37%), driven by Lmax, with longer rhodoliths in the positive axis and shorter in the negative one. Thus, the first dimension separates the largest, most rounded and solid rhodoliths (both Pralines and Boxwork growth forms) from the Branched forms. (**Fig.2.1.7**). The classification equations based on *Maximum Feret diameter*, *Roundness* and *Solidity* are:

LDA1: 1.996 [Lmax] **+ 0.252 [R] +0.274[S]**

LDA2: **21.232 [Lmax]** + 0.123 [R] + 0.147 [S]

Applying the estimation model to the data test, we found that the classification rate was correct in 63.15% of the cases. After reproducing the analysis 100 times and running the predictive model, the classification rate for a new rhodolith was 69.5%, being the percentages of success for each growth form different (**Table 2.1.3**). The best classified form was always Branched with 88.13% of success. The more common misclassification was obtained when classifying a Boxwork as a Praline (40.87% of times) or a Praline as a Boxwork (30.73% of times).

Table 2.1.3. Table of predictions when classifying rhodoliths according to the variables considered in the LDA

	Predicted Class		
Real Class	Branched	Praline	Boxwork
Branched	0.8813	0.096	0.0225
Praline	0.1364	0.5563	0.3073
Boxwork	0.0608	0.4087	0.5304

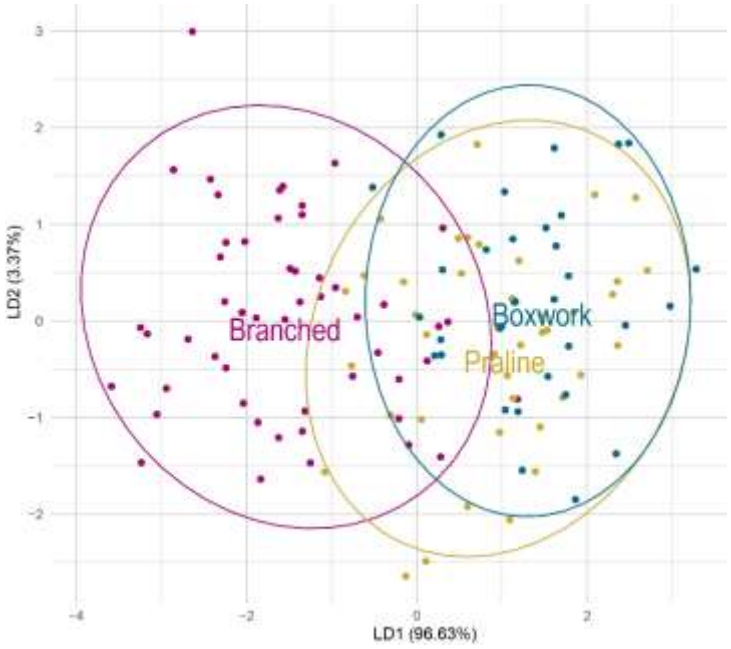


Fig.2.1.7. Representation of the Linear Discriminant Analysis (LDA)

2.1.3.4. 3D –Morphological measurements in a subset of morphotype A

A 3D model twin of the complete rhodolith shape (**Fig.2.1.8**) and its corresponding measurements were obtained for 30 rhodoliths. The correlation test showed that both sets of metrics (2D vs. 3D) are highly

correlated (Supplementary Material **Fig.2.1.S5**) especially a metric on two different dimensions (e.g., Area 2D and Area 3D), but also between metrics in the same dimension (e.g. Perimeter 2D with Area 2D).

The linear models (with intercept at 0) fitted between 2D and 3D area and between 2D area and the volume, showed that both sets were highly correlated (R=0.99 and R=0.98, respectively) (**Fig.2.1.9**). The 3D area resulted in 4.27 times the 2D area (**Fig.2.1.9**a), while the volume was 6.45 times the 2D area (**Fig.2.1.9**b). These equations can be useful in estimating the ecologically meaningful quantities (area, volume) in 3D from their equivalent quantities in 2D, which are much easier to measure.

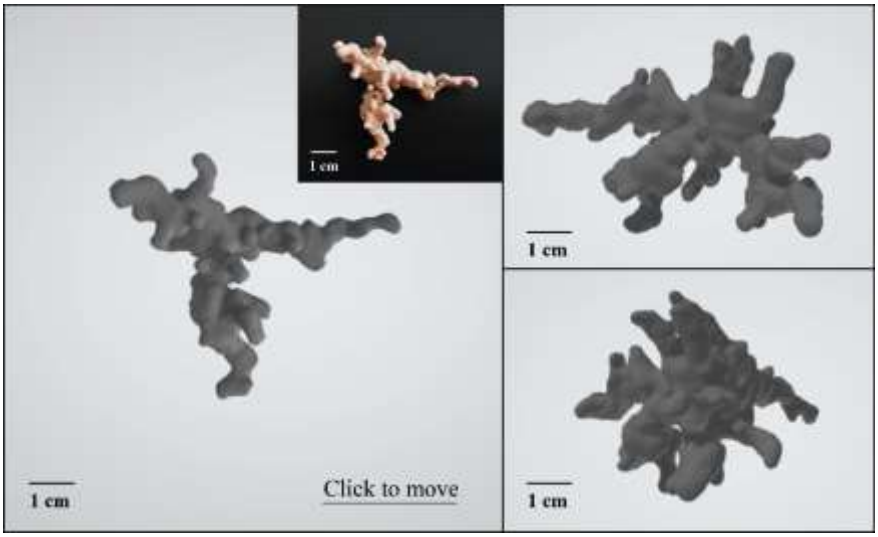


Fig.2.1.8. Example of 3D model twin from a morphotype A rhodolith

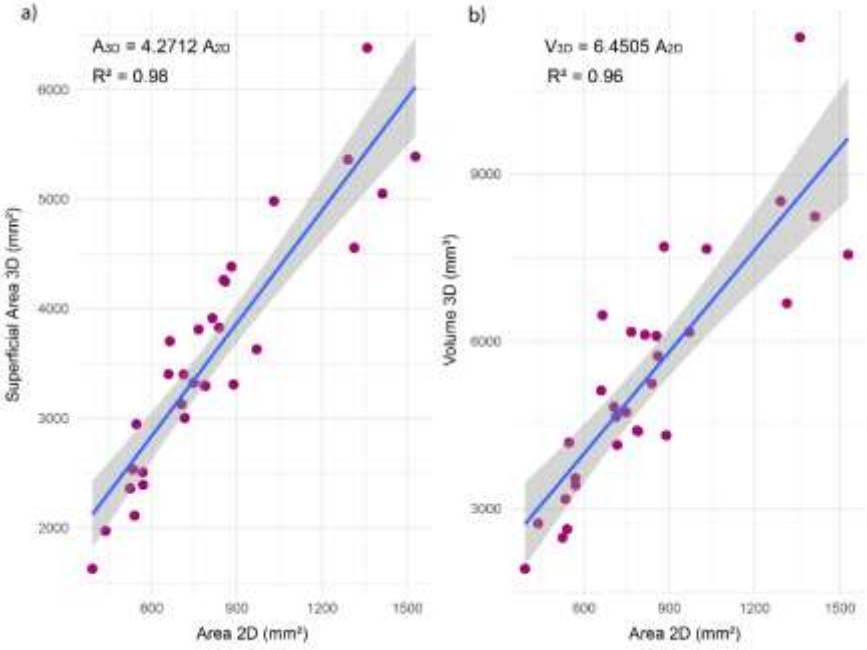


Fig.2.1.9. Linear models and equations between Area measured in 2D and (a) Superficial Area measured in 3D and (b) Volume measured in 3D

2.1.4. Discussion

The present study has characterized the morphological composition of a rhodolith bed in the continental shelf of the Menorca Channel (western Mediterranean). This area was selected due to its good conservation status, with a well-developed rhodolith bed (i.e., above 50% rhodolith coverage over 304 Km^2), and adjacent locations with decreasing rhodolith cover alternating with detritic sands (Barberá et al. 2012a; de Juan et al. 2023). It is common to find in rhodolith beds a variable quantity of dead rhodoliths and their fragments accompanying the live rhodoliths (Bracchi and Basso 2012). Our results generally show proportions of dead rhodoliths ranging from 5 to 20% in most samples (except for those from the Adjacent Habitat station S18). These values are similar to those found by Rendina et al. (2020) and support the hypothesis that the rhodolith bed in the Menorca Channel is in a good environmental condition. Despite branched forms predominate in all stations, we observed small-scale heterogeneity in the proportions of growth forms and of morphotypes. The heterogeneity observed agrees with previous studies in the Mediterranean (i.e, Bracchi et al. 2022) and particularly in the Menorca Channel (Farriols et al. 2022). In general, the proportion of branched growth forms, and particularly the proportion of morphotype A, was highest in the Core Habitat.

The differences in proportion of morphotypes between stations cannot be attributed to differences in sediment granulometry. The sediment below the rhodolith bed was coarse, with the sand fraction (grain size > 63 µm) comprising at least 50% of the sample in all stations and over 80% in S13, L1 and S5. In S15 and S18 the gravel fraction (grain size > 2 mm) comprised around 40% of the sample. This granulometry is typical of Mediterranean rhodolith beds (de Juan et al. 2013), although dominance of fine sediments (grain size < 63 µm, Bracchi et al. 2022; Ingrassia et al. 2023) or coarser sediments, including fractions larger than 20 mm (del Río et al. 2022), have been reported in Mediterranean rhodolith beds. Our findings corroborate the conclusions drawn by Cabanellas-Reboredo et al. (2017), indicating that, at the scale of a rhodolith bed, sediment granulometry has limited explanatory power regarding variations in rhodolith morphology. However, at larger spatial scales, coarse sediments are indicative of low sediment input from terrestrial origin, which is expected around Mediterranean islands. High currents predominating in the area (Moranta et al. 2014) would also prevent the deposition of fine sediments.

The specimens from the Core Habitat were larger and with more interstitial spaces, even considering the praline morphologies. It is likely that rhodoliths at the edge of the Core Habitat exhibit lower complexity, due to suboptimal environmental conditions combined with being exposed, directly or indirectly, to trawling. Interestingly, a decrease in morphotype A from S13 (in the Core Habitat and within the cables zone) to the edge of the Core Habitat and exclusion zone in S18 was observed suggesting that this morphotype is a potential candidate indicator of the conservation status of the habitat. Both natural and anthropogenic processes may be responsible for increased fragmentation of

branched growth form, resulting in smaller and less ramified (more solid) branched rhodoliths (Barberá et al.2012a, 2012b). Branched rhodoliths exhibited a greater degree of branching and had higher interstitial space (IS) in samples from the Core Habitat, suggesting that good environmental condition of the rhodolith bed contributes to maintain the architectural complexity of this habitat. Habitat complexity is significant for enhancing local species richness (de Juan et al. 2013). The spaces between branches provide microhabitats for diverse assemblages of other algae, epiphytes and invertebrates including sponges, cnidarians or bryozoans (Phillips, 2023) (see examples found in Supplementary Material –**Fig.2.1.S6**). As such the rhodolith bed community in the protected Core Habitat, characterized by high diversity of rhodolith morphotypes, could be viewed as the reference for a good environmental condition. This holds significant implications for local conservation management, as often, such reference or baseline points are scarce (Lindeboom et al. 1995).

Owing to legislation prohibiting trawling within the cables' exclusion zone, there is a high degree of certainty that the Core Habitat has experienced no physical disturbances since the early 1970s. Initial examination of the data from both Core and Adjacent Habitat stations suggest a correlation between the condition of rhodolith beds and their level of protection. However, our study was not designed to assess this relationship. Extending sampling over a gradient of trawling intensity, with enough spatial coverage to incorporate environmental variability (e.g., see Hinz et al. 2009), would contribute to assess potential variability in rhodolith morphology linked to trawling activity. While our study supports that trawling has not impacted the rhodolith bed in the Core Habitat within the cables' exclusion zone, it cannot attribute the composition of Adjacent Habitat solely to anthropogenic impacts. This recognition is important, considering that high small-scale heterogeneity within rhodolith beds (de Juan et al. 2023) may not exclusively result from fishing pressure (Jardim et al. 2022). Natural environmental factors such as depth, sediment grain size, bottom geomorphology and bottom currents (Illa-López et al. 2023; Pérez-Peris et al. 2023) can influence the density, dimensions and composition of rhodolith beds, independent of human intervention (Peña et al. 2014; Veras et al. 2020).

The morphological complexity of the rhodolith is a key driver for the high faunistic and floristic diversity of rhodolith beds (Fredericq et al. 2019; Grabara et al. 2018; Teichert et al. 2014). Our results also support the idea proposed by Jardim et al. (2022) for using the rhodolith interstitial space (or Solidity as equivalent indicator) as proxy for habitat complexity. The high correlation identified between 2D and 3D metrics for morphotype A demonstrates that 2D metrics may yield useful indicators that are faster to obtain and that are potentially effective to be incorporated in the routine monitoring of rhodolith beds. 3D measurements resulted to be time-consuming and they can be estimated to a good approximation through 2D metrics if 2D to 3D conversions have been estimated previously. Moreover, we recommend using the linear relations between measures as a method to rapidly obtain a total photosynthetic surface. This measure is important for calculating the photosynthesis rates for the branched growth forms, as well as to obtain the rhodolith volume and quantify the calcium carbonate

production (Dulin et al. 2020). Similar conclusions were reached by House et al. (2018) comparing 2D and 3D metrics across different morphologies of scleractinian corals: although 3D metrics of surface area and volume are more precise, 2D metrics scaled consistently with 3D metrics in corals, providing convenient and fast measurements of ecological function.

The study of algal physiology commonly uses dry weight to standardize indicators such as biomass of epiphytes by unit mass of rhodoliths or to estimate respiration and production (photosynthesis). However, in multi-specific rhodolith beds, as in our case study, it is often difficult to individualise different morphologies (as shown in the results of the discriminant analysis). Individual weight may vary among morphologies, for the same longitudinal size, and even within individuals of the same morphology because of the weight of organisms forming the nucleus of some rhodoliths (bryozoans, polychaetes, some boring organisms) (see an example in **Fig.2.1.10**) (Pérez-Peris et al. 2023). For these reasons we propose using the area corresponding to the thallus surface in 3D as a more realistic measurement to estimate metabolic rates or to standardize cryptofaunal abundance. Rhodolith volume is an important measure related to carbon retention and is a metric that can only be obtained with sufficient precision with 3D measurements. Simple methods based on the equation of an ellipsoid (Teichert et al. 2014) or water displacement (Amado-Filho et al. 2007) have low precision and limited general application.

In conclusion, the intricate morphological diversity observed between and within rhodolith species, their role as habitat for benthic organisms, coupled with their potential significant role as carbon reservoirs, make them suitable candidates for biomonitoring the environmental condition of deep biogenic habitats. Key measures of morphological complexity, as well as assessing parameters such as photosynthetic surface and carbonate volume, could be valuable indicators of the rhodolith bed condition. This research contributes to our comprehensive understanding of how the structural complexity of rhodoliths enhances ecosystem functioning, emphasizing the ongoing importance of advancing our knowledge and developing additional morphological indicators for these ecologically valuable species.

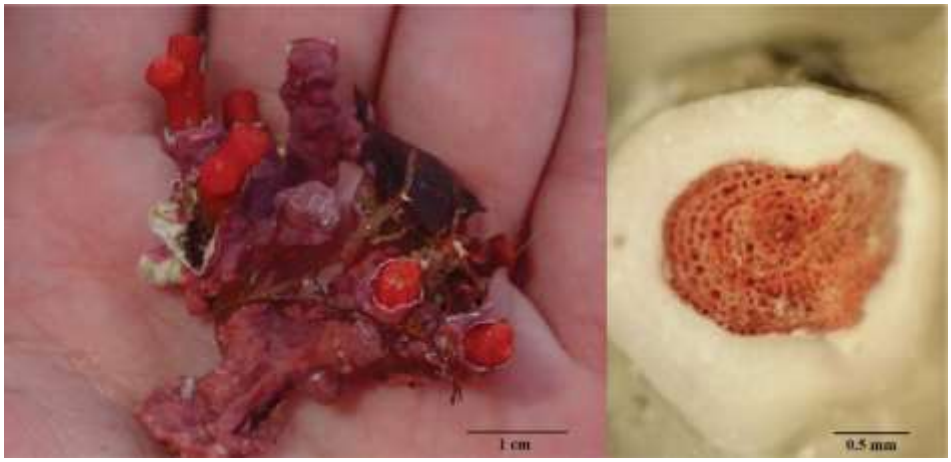


Fig.2.1.10. (Left) Red calcareous algae growing and completely covering a bryozoan. (Right) broken branch of a rhodolith from morphology A, with a bryozoan found inside

Acknowledgments

The authors are very thankful to Laia Illa-López and Géraldine Pérez for their back up during the field sampling and classification and also to Julia Castro for her support on creating the 3D digital twins of the rhodoliths. This work is developed on the framework of the EU H2020 project "MaCoBioS" (contract nº 869710). This work is contributing to the ICM's 'Center of Excellence' Severo Ochoa (CEX2019-000928-5) and to the 'Maria de Maeztu' accredited to the IMEDEA (CEX2021-001198) **SdJ** was supported by a Ramón y Cajal postdoctoral grant funded by the Ministry of Science and Innovation (Plan Estatal I+D+I, 2017- 2020; grant no. RyC2020-029062-I). **AC** is enrolled in the PhD programme in Marine Sciences at the University of Barcelona.

References

Amado-Filho, G.M., Maneveldt, G., Manso, R.C.C., Marins-Rosa, B.V., Pacheco, M.R. & Guimarães, S.M.P.B. (2007). Structure of rhodolith beds from 4 to 55 meters Deep along the southern coast of Espírito Santo State, Brazil. *Ciencias Marinas*, 33(4): 399-410. http://doi.org/10.7773/cm.v33i4.1148.

Amado-Filho, G.M., Bahia, R.G., Pereira-Filho, G.H. & Longo, L.L. (2017). South Atlantic Rhodolith Beds: Latitudinal Distribution, Species Composition, Structure and Ecosystem Functions, Threats and Conservation Status. In: Risonema-Rodríguez R, Nelson W, Aguirre J (eds). *Rhodolith/Maërl Beds: A Global Perspective*. Coastal Research Library, Chapter 12: 299–317. Coastal Research Library. Cham: Springer International Publishing, 2017. https://doi.org/10.1007/978-3-319-29315-8_12.

Ballesteros, E. (1988). Composición y estructura de los fondos de maërl de Tossa de Mar (Gerona, España). *Collectanea Botanica* (Barcelona), 17(2): 161-82. https://doi.org/10.3989/collectbot.1989.v17.137.

Barberá, C., Moranta, J., Ordines, F., Ramón, M., de Mesa, A., Díaz-Valdés, M., Grau, A.M. & Massutí, E. (2012a). Biodiversity and Habitat Mapping of Menorca Channel (Western Mediterranean): Implications for Conservation. *Biodiversity and Conservation*, 21(3): 701–28. https://doi.org/10.1007/s10531-011-0210-1.

Barberá, C., Comalada, N., Joher, S., Valls-Mir, M., Díaz-Valdés, M. & Moranta, J. (2012b). Analysis of morphological characteristics of rhodoliths as indicator of habitat complexity and fishing effects. XVII Simposio Ibérico de Estudios de Biología Marina (11/09/2012 - 14/09/2012, Donosti, Spain). *Revista de Investigación Marina*, 19(6), 346. http://hdl.handle.net/10261/324037.

Basso, D., Lorenza, B., Ramos-Esplá, A.A. & Salomidi, M. (2017). Mediterranean Rhodolith Beds. In: Risonema-Rodríguez R, Nelson W, Aguirre J (eds*) Rhodolith/Maërl Beds: A Global Perspective.* Coastal Research Library, vol 15. Springer, Cham, pp: 281-298. https://doi.org/10.1007/978-3-319-29315-8_11.

Basso, D., Babbini, L., Kaleb, S., Bracchi, V.A. & Falace, A. (2016). Monitoring Deep Mediterranean Rhodolith Beds. *Aquatic Conservation: Marine and Freshwater Ecosystems*, 26 (3): 549–61. https://doi.org/10.1002/aqc.2586.

Bernard, G., Romero-Ramirez, A., Tauran, A., Pantalos, M., Deflandre, B., Grall, J. & Grémare, A. (2019). Declining Maerl Vitality and Habitat Complexity across a Dredging Gradient: Insights from in Situ Sediment Profile Imagery (SPI). *Scientific Reports*, 9(1): 16463. https://doi.org/10.1038/s41598-019-52586-8.

Blake, C., Maggs, C. & Reimer, P. (2007). Use of radiocarbon dating to interpret past environments of maerl beds. *Ciencias Marinas*, 33(4): 385-397. https://doi.org/10.7773/cm.v33i4.1187.

Bordehore, C., Ramos-Esplá, A.A. & Riosmena-Rodríguez, R. (2003). Comparative Study of Two Maerl Beds with Different Otter Trawling History, Southeast Iberian Peninsula. *Aquatic Conservation: Marine and Freshwater Ecosystems*, 13: S43-S54. https://doi.org/10.1002/aqc.567.

Bosence, D.W.J. (1983). Description and Classification of Rhodoliths (Rhodoids, Rhodolites). In: *Peryt TM (eds) Coated Grains*. Springer, Berlin, Heidelberg. https://doi.org/10.1007/978-3-642-68869-0_19.

Boyé, A., Thiébaut, E., Grall, J., Legendre, P., Broudin, C., Houbin, C., Le Garrec, V., Maguer, M., Droual, G. & Gauthier, O. (2019). Trait-Based Approach to Monitoring Marine Benthic Data along 500 Km of Coastline. *Diversity and Distributions*, 25(12): 1879–96. https://doi.org/10.1111/ddi.12987.

Bracchi, V.A. & Basso, D. (2012). The contribution of calcareous algae to the biogenic carbonates of the continental shelf: Pontian Islands, Tyrrhenian Sea, Italy. *Geodiversitas*, 34, 61–77. https://doi.org/10.5252/g2012n1a4.

Bracchi, V.A., Caronni, S., Meroni, A.N., Gottfried-Burguett, E., Atzori, F., Cadoni, N., Marchese, F. & Basso, D. (2022). Morphostructural Characterization of the Heterogeneous Rhodolith Bed at the Marine Protected Area 'Capo Carbonara' (Italy) and Hydrodynamics. *Diversity*, 14(1): 51. https://doi.org/10.3390/d14010051.

Cabanellas-Reboredo, M., Mallol, S., Barberá, C., Vergés, A., Díaz, D. & Goñi, R. (2017). Morpho-Demographic Traits of Two Maërl-Forming Algae in Beds with Different Depths and Fishing Histories. *Aquatic Conservation: Marine and Freshwater Ecosystems*, 1:13. https://doi.org/10.1002/aqc.2827.

Carvalho, V.F., Assis, J., Serrão, E.A., Nunes, J.M., Anderson, A.B., Batista, M.B., Barufi, J.B., Silva, J., Pereira, S.M.B. & Horta, P.A. (2020). Environmental Drivers of Rhodolith Beds and Epiphytes Community along the South Western Atlantic Coast. *Marine Environmental Research*, 154:104827. https://doi.org/10.1016/j.marenvres.2019.104827.

da Silva, A.R. (2021). biotools: Tools for Biometry and Applied Statistics in Agricultural Science. R package version 4.2. https://cran.r-project.org/package=biotools.

de Juan, S., Ospina-Alvarez, A., Hinz, H., Moranta, J. & Barberá, C. (2023). The Continental Shelf Seascape: A Network of Species and Habitats. *Biodiversity and Conservation*, 32. https://doi.org/10.1007/s10531-023-02552-8.

de Juan, S., Lo Iacono, C. & Demestre, M. (2013). Benthic Habitat Characterisation of Soft-Bottom Continental Shelves: Integration of Acoustic Surveys, Benthic Samples and Trawling Disturbance Intensity. *Estuarine, Coastal and Shelf Science*, 117:199-209. https://doi.org/10.1016/j.ecss.2012.11.012.

del Río, J., Ramos, D.A., Sánchez-Tocino, L., Peñas, J. & Braga, J.C. (2022). The Punta de La Mona Rhodolith Bed: Shallow-Water Mediterranean Rhodoliths (Almuñecar, Granada, Southern Spain). *Frontiers in Earth Science*, 10:884685. https://doi.org/10.3389/feart.2022.884685.

Dulin, T., Avnaim-Katav, S., Sisma-Ventura, G., Bialik, O.M. & Angel, D.L. (2020). Rhodolith Beds along the Southeastern Mediterranean Inner Shelf: Implications for Past Depositional

Environments. *Journal of Marine Systems*, 201103241. https://doi.org/10.1016/j.jmarsys.2019.103241.

European Parliament. Council directive 1992/43/EC Conservation of natural habitats and of wild fauna and flora. Off. J. Eur. Union 1992, L206, 7–50.

Farriols, M.T., Irlinger, C., Ordines, F., Palomino, D., Marco-Herrero, E., Soto-Navarro, J., Jordà, G., Mallol, S., Díaz, D., Martínez-Carreño, N., Díaz, J.A., Fernandez-Arcaya, U., Joher, S., Ramírez-Amaro, S., de la Ballina, N.R., Vázquez, J.T. & Massutí, E. (2022). Recovery Signals of Rhodoliths Beds since Bottom Trawling Ban in the SCI Menorca Channel (Western Mediterranean). *Diversity*, 14(1): 20. https://doi.org/10.3390/d14010020.

Fedorov, A., Beichel, R., Kalpathy-Cramer, J., Finet, J., Fillion-Robin, J.C., Pujol, S., Bauer, C., Jennings, D., Fennessy, F.M., Sonka, M., Buatti, J., Aylward, S.R., Miller, J.V., Pieper, S. & Kikinis, R. (2012). 3D Slicer as an Image Computing Platform for the Quantitative Imaging Network. *Magnetic Resonance Imaging*, 30(9):1323-41. https://doi.org/10.1016/j.mri.2012.05.001.

Figueiredo, M.A.O., Santos de Menezes, K., Costa-Paiva, E.M., Paiva, P.C. & Ventura, C.R.R. (2007). Experimental evaluation of rhodoliths as living substrata for infauna at the Abrolhos Bank, Brazil. *Ciencias Marinas*, 33(4): 427-440. https://doi.org/10.7773/cm.v33i4.1221

Fredericq, S., Krayesky-Self, S., Sauvage, T., Richards, J., Kittle, R., Arakaki, N., Hickerson, E. & Schmidt, W.E. (2019). The Critical Importance of Rhodoliths in the Life Cycle Completion of Both Macro- and Microalgae, and as Holobionts for the Establishment and Maintenance of Marine Biodiversity. *Frontiers in Marine Science*, 5:502. https://doi.org/10.3389/fmars.2018.00502.

Foster, M.S., McConnico, L.M., Lundsten, L., Wadsworth, T., Kimball, T., Brooks, L., Medina-López, M., Riosmena-Rodriguez, R., Hernández-Carmona, G., Vásquez-Elizondo, R.M., Johnson, S. & Steller, D.L. (2007). Diversity and Natural History of a Lithothamnion Muelleri-Sargassum Horridum Community in the Gulf of California. *Ciencias Marinas*, 33: 367–84. https://doi.org/10.7773/cm.v33i4.1174.

Gabara, S.S., Hamilton, L., Edwards, M.S. & Steller, D.L. (2018). Rhodolith structural loss decreases abundance, diversity, and stability of benthic communities at Santa Catalina Island, CA. *Marine Ecology Progress Series*, 595: 71-88. https://doi.org/10.3354/meps12528.

Gagnon, P., Matheson, K. & Stapleton, M. (2012). Variation in Rhodolith Morphology and Biogenic Potential of Newly Discovered Rhodolith Beds in Newfoundland and Labrador (Canada). *Botanica Marina*, 55(1): 85–99. https://doi.org/10.1515/bot-2011-0064.

Hinz, H., Prieto, V. & Kaiser, M.J. (2009). Trawl Disturbance on Benthic Communities: Chronic Effects and Experimental Predictions. *Ecological Applications*, 19(3): 761–73. https://doi.org/10.1890/08-0351.1.

House, J.E., Brambilla, V., Bidaut, L.M., Christie, A.P., Pizarro, O., Madin, J.S. & Dornelas, M. (2018). Moving to 3D: Relationships between Coral Planar Area, Surface Area and Volume. *PeerJ*, 6: e4280.https://doi.org/10.7717/peerj.4280.

Illa-López, L., Cabrito, A., de Juan, S., Maynou, F. & Demestre, M. (2023). Distribution of Rhodolith Beds and Their Functional Biodiversity Characterisation Using ROV Images in the Western Mediterranean Sea. *Science of The Total Environment*, 905: 167270. https://doi.org/10.1016/j.scitotenv.2023.167270.

Ingrassia, M., Pierdomenico, M., Casalbore, D., Falese, F.G. & Chiocci, F.L. (2023). A Review of Rhodolith/Maerl Beds of the Italian Seas. *Diversity*, 15(7). https://doi.org/10.3390/d15070859.

Jardim, V.L., Gauthier, O., Toumi, C. & Grall, J. (2022). Quantifying Maerl (Rhodolith) Habitat Complexity along an Environmental Gradient at Regional Scale in the Northeast Atlantic. *Marine Environmental Research*, 181:105768. https://doi.org/10.1016/j.marenvres.2022.105768.

Kamenos, N.A., Geoffrey Moore, P. & Hall-Spencer, J.M. (2004). Nursery-Area Function of Maerl Grounds for Juvenile Queen Scallops Aequipecten Opercularis and Other Invertebrates. *Marine Ecology Progress Series*, 274: 183–89. https://doi.org/10.3354/meps274183

Kleiber, C. & Zeileis, A. (2022). AER: Applied Econometrics with R. R package version 1.2-10. https://CRAN.R-project.org/package=AER.

Kooijman, S.A.L.M. (2010). Dynamic Energy Budget Theory for Metabolic Organisation. Cambridge University Press, Cambridge.

Korkmaz, S., Goksuluk, D. & Zararsiz, G. (2014). MVN: An R Package for Assessing Multivariate Normality. *The R Journal*, 6(2): 151. https://doi.org/10.32614/RJ-2014-031.

Lindeboom, H.J. (1995). Protected Areas in the North Sea: An Absolute Need for Future Marine Research. *Helgoländer Meeresuntersuchungen*, 49(1):591–602. https://doi.org/10.1007/BF02368384.

Massutí, E., Sánchez-Guillamón, O., Farriols, M.T., Palomino, D., Frank, A., Bárcenas, P., Rincón, B, Martínez-Carreño, N., Keller, S., López-Rodríguez, C., Díaz, J.A., López-González, N., Marco-Herrero, E., Fernandez-Arcaya, U., Valls, M., Ramírez-Amaro, S., Ferragut, F., Joher, S., Ordinas, F. & Vázquez, J.T. (2022). Improving Scientific Knowledge of Mallorca Channel

Seamounts (Western Mediterranean) within the Framework of Natura 2000 Network. *Diversity*, 14(1). https://doi.org/10.3390/d14010004.

Meihoub-Berlandi, R., Figueiredo, M.A.O. & Paiva, P.C. (2012). Rhodolith Morphology and the Diversity of Polychaetes Off the Southeastern Brazilian Coast. *Journal of Coastal Research*, 28(1): 280–87. https://doi.org/10.2112/11T-00002.1.

Méndez Trejo, M.D.C., Neill, K.F., Twist, B.A. & Nelson, W.A. (2021). Cryptofauna associated with rhodoliths: Diversity is species-specific and influenced by habitat. *Marine Ecology*, 42:12647. https://doi.org/10.1111/maec.12647

Moranta, J., Barberá, C., Druet Vélez, M., Díaz-Valdés, M., Zaragoza, N., Tello-Antón, M.O., López-Jurado, J.L., Balbín, R., Flexas, M.D.M., Fernández, M., Hidalgo, M., Domínguez, M., Quetglas, A., Goñi, R., Mallol, S., Sánchez-Delgado, F., Ambroso, S. & Comalada, N. (2014). Caracterización ecológica de la plataforma continental (50-100 m) del canal de Menorca. Informe final área LIFE+ INDEMARES (LIFE07/NAT/E/000732). Instituto Español de Oceanografía-Centro Oceanográfico de Baleares (Palma). Coordinación: Fundación Biodiversidad, Palma, 504 pág. Available online at http://hdl.handle.net/10261/318214.

Nelson, W.A. (2009). Calcified Macroalgae - Critical to Coastal Ecosystems and Vulnerable to Change: A Review. *Marine and Freshwater Research*, 60(8): 787–801. https://doi.org/10.1071/MF08335.

Oksanen, J., Simpson, G., Blanchet, F., Kindt, R., Legendre, P., Minchin, P., O'Hara, R., Solymos, P., Stevens, M., Szoecs, E., Wagner, H., Barbour, M., Bedward, M., Bolker, B., Borcard, D., Carvalho, G., Chirico, M., De Caceres, M., Durand, S., Evangelista, H., FitzJohn, R., Friendly, M., Furneaux, B., Hannigan, G., Hill, M., Lahti, L., McGlinn, D., Ouellette, M., Ribeiro Cunha, E., Smith, T., Stier, A., Ter Braak, C. & Weedon, J. (2022). vegan: Community Ecology Package. R package version 2.6-4. Available online at https://CRAN.R-project.org/package=vegan.

Peña, V., Bárbara, I., Grall, J., Maggs, C.A. & Hall-Spencer, J.M. (2014). The Diversity of Seaweeds on Maerl in the NE Atlantic. *Marine Biodiversity*, 44(4): 533-51. https://doi.org/10.1007/s12526-014-0214-7.

Pérez-Peris, I., Navarro-Mayoral, S., de Esteban, M.C., Tuya, F., Peña, V., Barbara, I., Neves, P., Ribeiro, C., Abreu, A., Grall, J., Espino, F., Echedey Bosch, N., Haroun, R. & Otero-Ferrer, F. (2023). Effect of Depth across a Latitudinal Gradient in the Structure of Rhodolith Seabeds and Associated Biota across the Eastern Atlantic Ocean. *Diversity*, 15(1): 103. https://doi.org/10.3390/d15010103.

Phillips, J. (2023). *The Lives of Seaweeds: A Natural History of Our Planet's Seaweeds and Other Algae*. Princeton University Press. ISBN: 9780691230177.

Puig, P., Martín, J., Masqué, P. & Palanques, A. (2015). Increasing sediment accumulation rates in La Fonera (Palamós) submarine canyon axis and their relationship with bottom trawling activities. *Geophysical Research Letters*, 42:8106-8113. https://doi.org/10.1002/2015GL065052.

R Core Team. (2022). R: A Language and Environment for Statistical Computing. R Foundation for Statistical Computing, Vienna, Austria. Available online at https://www.R-project.org/.

Rendina, F., Kaleb, S., Caragnano, A., Ferrigno, F., Appolloni, L., Donnarumma, L., Fulvio Russo, G., Sandulli, R., Roviello, V. & Falace, A. (2020). Distribution and Characterization of Deep Rhodolith Beds off the Campania Coast (SW Italy, Mediterranean Sea). *Plants*, 9 (8): 985. https://doi.org/10.3390/plants9080985.

Riosmena-Rodríguez, R., Nelson, W. & Aguirre, J. (Eds.) (2017). *Rhodolith/Maërl Beds: A Global Perspective*, Vol. 15. Springer International Publishing. https://doi.org/10.1007/978-3-319-29315-8.

Schneider, C.A., Rasband, W.S. & Eliceiri, K.W. (2012). NIH Image to ImageJ: 25 years of image analysis. *Nature Methods*, 9, 671-675. https://doi.org/10.1038/nmeth.2089.

Steller, D.L., Riosmena-Rodríguez, R., Foster, M.S. & Roberts, C.A. (2003). Rhodolith Bed Diversity in the Gulf of California: The Importance of Rhodolith Structure and Consequences of Disturbance. *Aquatic Conservation: Marine and Freshwater Ecosystems*, 13: S5-S20. https://doi.org/10.1002/aqc.564.

Stelzer, P.S., Mazzuco, A.C.A., Gomes, L.E., Martins, J., Netto, S. & Bernardino, A.F. (2021). Taxonomic and functional diversity of benthic macrofauna associated with rhodolith beds in SE Brazil. *PeerJ*, 9:11903 https://doi.org/10.7717/peerj.11903.

Tauran, A., Dubreuil, J., Guyonnet, B. & Grall, J. (2020). Impact of Fishing Gears and Fishing Intensities on Maerl Beds: An Experimental Approach. *Journal of Experimental Marine Biology and Ecology*, 533: 151472. https://doi.org/10.1016/j.jembe.2020.151472.

Teichert, S. (2014). Hollow Rhodoliths Increase Svalbard's Shelf Biodiversity. *Scientific Reports*, 4(1):6972. https://doi.org/10.1038/srep06972.

Venables, W.N. & Ripley, B.D. (2002). Modern Applied Statistics with S, Fourth edition. Springer, New York. ISBN 0-387-95457-0, https://www.stats.ox.ac.uk/pub/MASS4/.

Veras, P.C., Pierozzi-Jr, I., Lino, J.B., Amado-Filho, G.M., Senna, A.R., Santos, C.S.G., Moura, R.L., Passos, F.D., Giglio, V.J. & Pereira-Filho, G.H. (2020). Drivers of Biodiversity Associated with Rhodolith Beds from Euphotic and Mesophotic Zones: Insights for Management and

Conservation. *Perspectives in Ecology and Conservation* 18(1): 37–43. https://doi.org/10.1016/j.pecon.2019.12.003.

Wei, T. & Simko, V. (2021). R package 'corrplot': Visualization of a Correlation Matrix. (Version 0.92). Available online at https://github.com/taiyun/corrplot.

FUNDING

The authors acknowledge funding from the EU H2020 project "MaCoBioS" (contract nº 869710).

AUTHOR INFORMATION

Authors and Affiliations

Institut de Ciències del Mar (ICM-CSIC), Passeig Marítim de la Barceloneta 37-49, Barcelona, Spain

Andrea Cabrito & Francesc Maynou

Institut Mediterrani d'Estudis Avançats (IMEDEA-CSIC), Carrer Miquel Marquès 21, Esporles, Spain

Silvia de Juan & Hilmar Hinz

Contributions

AC: Conceptualization, Methodology, Formal analysis, Writing – original draft, Writing – review & editing, Visualization. **SdJ:** Conceptualization, Writing – review & editing. **HH:** Conceptualization, Writing – review & editing. **FM:** Conceptualization, Methodology, Formal analysis, Writing – original draft, Writing – review & editing, Funding acquisition.

Corresponding author

Correspondence to Andrea Cabrito, cabrito@icm.csic.es

ETHICS DECLARATIONS

Conflict of interest

The authors declare no conflict of interest.

Data availability

Data will be made available on request.

Supplementary material

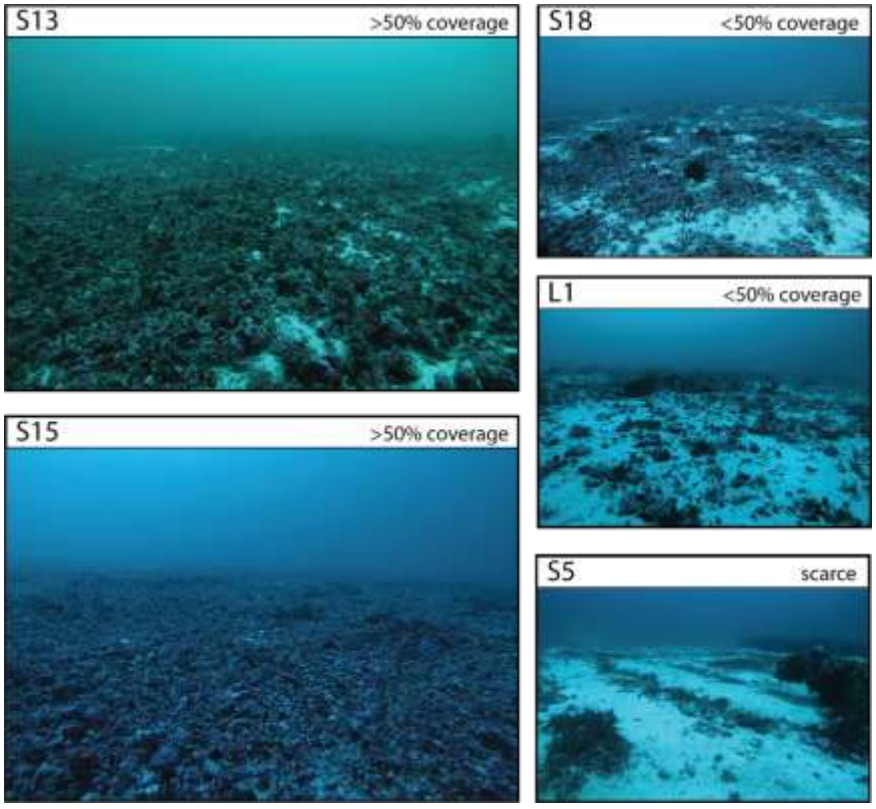


Fig.2.1.S1. Images captured by cameras launched at each station used to check the cover of rhodoliths

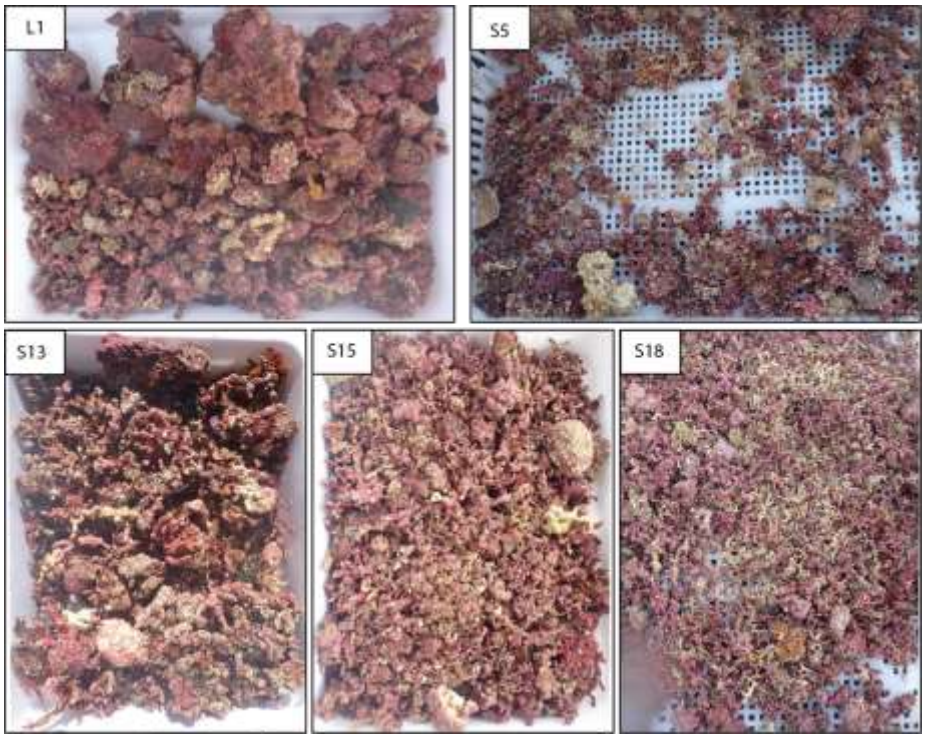


Fig.2.1.S2. Example of a dredge for each station



Fig.2.1.S3. Images of the 30 individual rhodoliths selected for the 2D/3D study

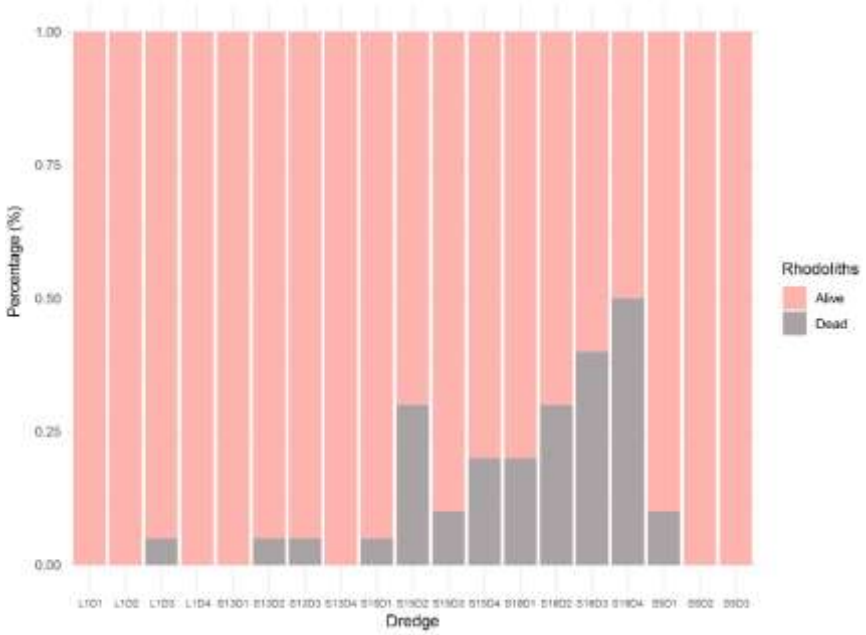


Fig.2.1.S4. Proportions of dead rhodoliths found in each dredge

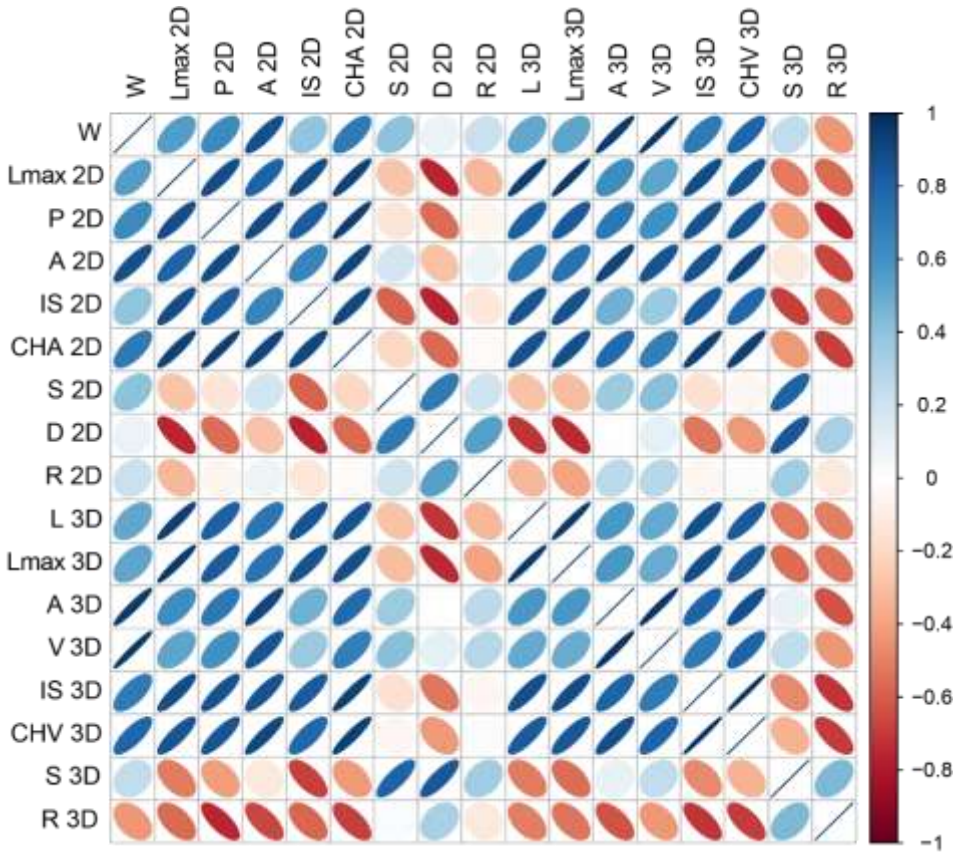


Fig.2.1.S5. Pearson correlations between 2D and 3D measurements

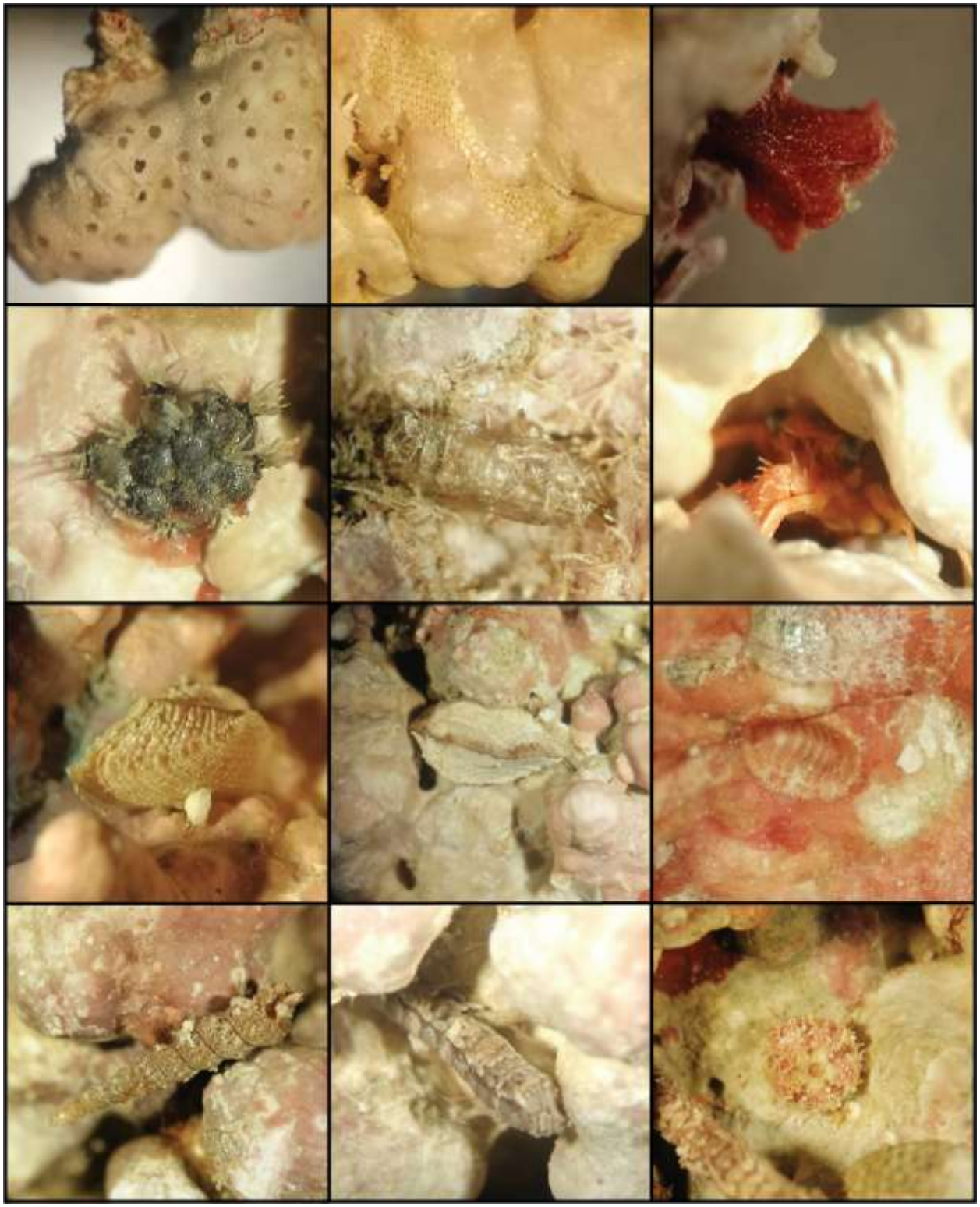


Fig.2.1.S6. Example of cryptofauna found between interstitial spaces in branched forms

Table 2.1.S1: Proportions of morphologies and growth forms in the study area

	Station	S5			S13				S15				S18				L1				
	Dredge	D1	D2	D3	D1	D2	D3	D4	D1	D2	D3	D4	D1	D2	D3	D4	D1	D2	D3	D4	TOTAL
Branched	A	1	0	2	42	41	34	56	40	47	76	33	2	4	0	0	8	1	6	0	*393*
	B	0	0	0	29	15	20	34	108	33	60	0	84	0	73	41	47	5	17	4	*570*
	C	0	0	0	0	16	18	22	134	67	95	110	169	322	255	153	45	45	4	0	*1455*
	D	116	33	86	0	0	0	0	3	0	0	0	0	0	0	22	0	0	0	3	*263*
Praline	E	0	0	0	15	32	0	13	37	76	24	116	76	57	39	0	36	17	14	0	*552*
	F	30	1	42	0	0	0	0	0	0	0	0	0	19	0	2	0	0	29	0	*123*
	G	2	0	0	0	0	26	0	0	2	0	15	0	0	18	1	0	0	0	0	*64*
Boxwork	H	0	1	0	6	11	7	19	67	24	4	29	0	28	23	13	12	10	43	16	*313*
	I	2	0	0	15	8	0	5	0	0	7	0	36	0	0	0	44	5	9	13	*144*
	TOTAL	*151*	*35*	*130*	*107*	*123*	*105*	*149*	*389*	*249*	*266*	*303*	*367*	*430*	*408*	*232*	*192*	*83*	*122*	*36*	3877

Table 2.1.S2: Random selected, measured and weighted rhodoliths

	S5	S13	S15	S18	L1	Total
A	1	5	5	5	5	*21*
B	0	5	5	5	5	*20*
C	2	5	5	5	5	*22*
D	12	1	2	5	0	*20*
E	0	6	6	6	4	*22*
F	7	1	4	3	5	*20*
G	1	6	5	6	3	*21*
H	1	5	4	5	6	*21*
I	3	5	4	5	5	*22*
Total	*27*	*39*	*41*	*44*	*38*	**189**

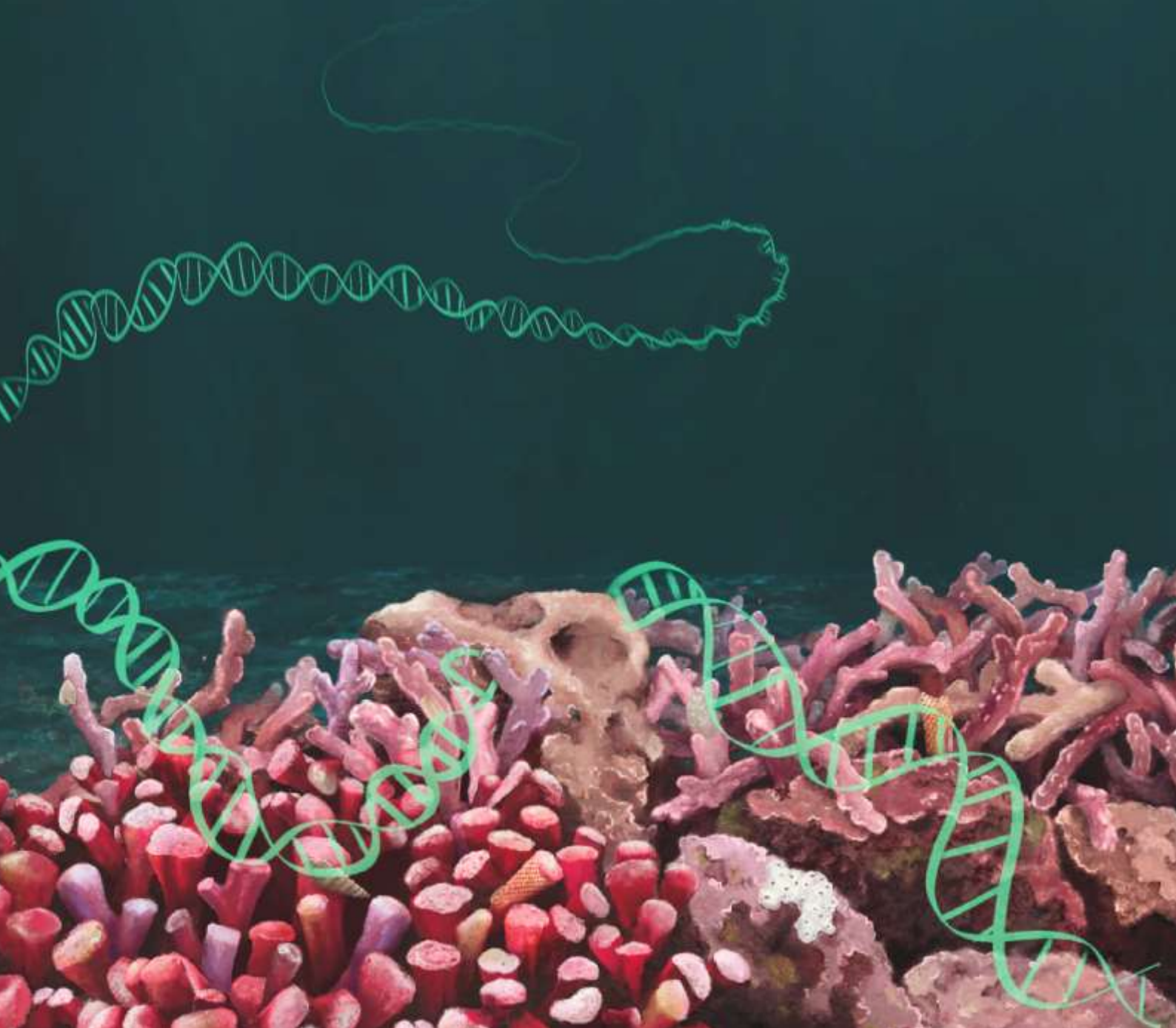
Table 2.1.S3: 2D-3D measurements in 30 rhodoliths from morphotype A

Site	Code	W (gr)	Feret-2D (mm)	P-2D (mm)	A-2D (mm^2)	IS-2D (mm^2)	CHA-2D (mm^2)	S-2D	D-2D	R-2D	L-3D (mm)	Feret-3D (mm)	A-3D (mm^2)	Vol-3D (mm^3)	IS-3D (mm^3)	CHV-3D (mm^3)	S-3D	R-3D
S13	rod01	14.48	65.98	318.40	1291.55	898.38	2189.93	0.58	0.26	0.82	39.21	64.23	5362.23	8517.53	30439.48	38957.02	0.22	0.39
S13	rod02	11.82	85.68	375.42	1313.61	1330.69	2644.31	0.49	0.19	0.43	46.35	75.35	4556.28	6685.52	38091.05	44776.57	0.15	0.39
S13	rod03	11.22	54.81	287.14	970.07	452.20	1422.27	0.68	0.29	0.63	30.38	53.46	3629.24	6168.41	15235.34	21403.75	0.29	0.46
S13	rod04	13.75	68.89	297.11	1030.79	1102.16	2132.94	0.48	0.25	0.93	37.03	61.55	4982.04	7660.13	31915.26	39575.40	0.19	0.39
S13	rod05	9.21	47.85	242.19	837.74	504.85	1342.60	0.62	0.31	0.87	28.32	50.88	3827.79	5243.44	17289.84	22533.28	0.23	0.40
S15	rod06	11.49	44.39	220.36	853.75	417.87	1271.62	0.67	0.36	0.82	25.64	46.13	4261.93	6098.49	16324.61	22423.10	0.27	0.40
S15	rod07	8.36	46.12	248.73	785.75	606.85	1392.60	0.56	0.32	0.88	22.39	42.15	3300.43	4398.77	13171.78	17570.55	0.25	0.42
S15	rod08	10.10	45.96	203.07	747.60	435.87	1183.47	0.63	0.34	0.81	24.48	43.54	3322.90	4731.14	11364.73	16095.87	0.29	0.44
S15	rod09	4.98	42.81	222.32	523.92	379.54	903.46	0.57	0.29	0.61	23.89	42.56	2360.24	2476.70	11607.10	14083.81	0.18	0.39
S15	rod10	13.88	85.61	380.15	1528.93	1050.45	2579.38	0.59	0.20	0.42	39.84	72.12	5388.93	7557.70	34894.76	42452.47	0.18	0.36
S13	rod11	18.26	59.41	291.93	1359.23	734.74	2093.98	0.64	0.32	0.81	31.75	56.26	6381.20	11454.98	31195.98	42650.96	0.27	0.41
S13	rod12	8.32	47.58	282.65	888.68	533.66	1422.34	0.62	0.31	0.90	26.20	47.27	3308.97	4315.26	13703.31	18018.57	0.24	0.40
S13	rod13	16.93	73.70	330.34	1412.67	828.70	2241.37	0.63	0.25	0.50	36.49	63.92	5050.74	8240.61	27294.15	35534.75	0.23	0.41
S13	rod14	8.54	55.60	221.15	704.95	420.12	1125.08	0.62	0.26	0.42	31.69	54.71	3128.58	4825.84	14516.96	19342.81	0.25	0.46
S13	rod15	5.86	48.50	203.03	533.86	367.30	901.16	0.59	0.27	0.41	26.18	49.85	2533.43	3171.41	10895.90	14067.31	0.23	0.43
S15	rod16	6.26	44.30	203.00	568.84	458.09	1026.93	0.55	0.30	0.87	25.25	42.53	2507.08	3545.70	11018.06	14563.76	0.24	0.47
S15	rod17	7.78	47.21	178.39	546.52	298.72	845.23	0.64	0.30	0.44	31.02	50.81	2946.33	4184.77	11937.66	16122.42	0.26	0.45
S15	rod18	8.67	52.05	245.87	713.04	543.70	1256.74	0.57	0.28	0.69	28.21	49.84	3398.97	4649.62	15813.34	20462.96	0.23	0.41
S15	rod19	9.12	43.99	197.08	659.83	251.40	911.23	0.72	0.34	0.74	24.20	41.88	3402.35	5118.06	10543.34	15661.40	0.33	0.45
S15	rod20	12.07	45.84	184.33	765.59	158.68	924.27	0.82	0.36	0.49	25.08	47.01	3810.96	6169.83	11321.29	17491.12	0.35	0.46
S13	rod21	10.71	46.74	189.75	664.34	369.54	1033.88	0.64	0.34	0.82	27.92	48.18	3703.62	6469.84	14736.22	21206.06	0.31	0.48
S13	rod22	10.22	55.30	261.95	858.93	657.28	1516.21	0.56	0.28	0.71	30.60	57.21	4248.30	5738.78	26830.28	32569.05	0.18	0.38
S13	rod23	8.94	59.40	278.44	716.49	928.86	1645.35	0.43	0.25	0.53	34.81	60.51	3002.25	4144.11	15150.06	19294.16	0.21	0.43
S13	rod24	7.27	55.85	200.01	569.77	726.81	1296.59	0.44	0.25	0.54	28.78	55.79	2392.32	3418.93	15756.04	19174.98	0.18	0.48
S13	rod25	11.29	46.67	241.64	813.90	444.85	1258.76	0.64	0.34	0.67	26.62	48.28	3913.45	6119.77	16384.02	22503.80	0.27	0.44
S15	rod26	4.17	42.59	158.68	391.49	495.10	886.59	0.44	0.27	0.58	26.01	43.84	1625.88	1921.33	8427.76	10349.09	0.19	0.48
S15	rod27	14.66	45.58	231.62	881.00	358.72	1239.72	0.71	0.39	0.82	25.63	46.04	4383.88	7699.53	13725.90	21425.43	0.36	0.45
S15	rod28	5.37	42.95	164.10	437.77	377.45	815.22	0.53	0.29	0.57	25.00	45.88	1971.54	2734.67	8223.53	10958.20	0.25	0.51
S15	rod29	5.58	51.04	224.26	540.06	625.47	1165.53	0.46	0.25	0.51	25.77	48.89	2111.20	2631.18	9565.64	12196.81	0.22	0.45
S15	rod30	9.39	60.06	278.27	789.62	825.14	1614.77	0.49	0.25	0.40	34.15	61.23	3294.93	4388.91	26907.68	31296.59	0.14	0.41

2.2. CHAPTER II: Taxonomic complexity and conservation implications of Mediterranean mesophotic rhodoliths beds.

Andrea Cabrito, Francesc Maynou, Silvia de Juan and Viviana Peña

Submitted to Aquatic conservation. Freshwater and Marine coastal ecosystems.



Abstract

Rhodolith beds are bioconstructions made by coralline algae (Rhodophyta: Corallinophycidae) and are ecologically important worldwide as they provide habitat supporting diverse biocenoses. However, conservation efforts are limited by gaps in our knowledge of their spatial distribution and species composition. On-going scientific research at mesophotic depths (60-80 m depth) of the Menorca Channel, western Mediterranean, shows that rhodolith beds host a wide variety of morphologies and multiple coexisting rhodolith-forming species. However, knowledge on their taxonomy is deficient. By integrating traditional taxonomy with molecular analysis, our study reveals that at least 15 different species of coralline red algae belonging to three orders (Hapalidiales, Corallinales and Sporolithales) contribute as rhodolith-forming species in this area. These findings confirm the presence of cryptic diversity in mesophotic habitats and emphasize that, unlike Habitats Directive based on two species predominant in NE Atlantic waters (*Lithothamnion corallioides* and *Phymatolithon calcareum*), effective conservation in the Mediterranean must recognize the multi-species and morphologically complex nature of rhodolith beds —an insight made possible by the critical use of molecular data.

Keywords: coralline red algae, maërl, *psb*A, *rbc*L, species delimitation, multi-species rhodoliths

Correspondence:

Andrea Cabrito (ORCID:0000-0002-3429-5201). Institut de Ciències del Mar (ICM-CSIC), Barcelona 08003, Spain. Email: cabrito@icm.csic.es

2.2.1. Introduction

Coralline algae (Corallinophycidae, Rhodophyta) are globally widespread, from the intertidal zones to deeper mesophotic areas (Riosmena-Rodríguez et al., 2017). They are characterized by having calcite deposited in their cell walls and exhibit a wide variety of morphologies, from encrusting to free-living forms (Jardim et al., 2025). Free-living forms consist on unattached nodules that form dense aggregations on the seafloor, known as rhodoliths or maërl beds (RBs) across tropical to Arctic waters (Hetzinger et al., 2023; Rebelo et al., 2021; Teichert, 2014). RBs create complex three-dimensional structures that enhance seabed heterogeneity (Cabrito et al., 2024a) and provide essential habitats, including nursery grounds for commercial species (Hall-Spencer et al., 2003; Costa et al., 2020; Cabrito et al., 2024b). RBs also contribute to the global carbon budget through carbon production and sequestration within sediments (Bulleri et al., 2024). Despite their ecological importance, RBs are threatened by different anthropogenic activities such as bottom trawling, which fractures rhodoliths and smothers them under fine sediments (Barbera et al., 2003). Additionally, as calcifying organisms with slow growth rates (ca. 1 mm per year for temperate rhodolith-forming species) (Adey & McKibbin 1970; Blake & Maggs, 2003; Potin et al., 1990), they are particularly vulnerable to the effects of ocean warming and acidification (Trégarot et al., 2024).

RBs are classified as vulnerable habitats and included in various protective regulations. The European Union Habitats Directive (92/43/EEC of 21 May 1992), based mainly on scientific knowledge from Atlantic areas of Europe, mandates the conservation of two key rhodolith-forming species: *Phymatolithon calcareum* (Pallas) W.H. Adey & D.L. McKibbin ex Woelkering & L.M. Irvine and *Lithothamnion corallioides* (P. Crouan & H. Crouan) P. Crouan & H. Crouan. These two species are traditionally considered the most widely distributed species in European rhodolith and maërl beds. Mediterranean RBs (generally under the denomination of “maërl”) have been included in the Marine Strategy Framework Directive (MSFD, 2008/56/EC) as habitats of special interest. Other endemic Mediterranean species, such as *Lithothamnion minervae* Basso, 1995, *Lithothamnion valens* Foslie, 1909 and *Lithophyllum racemus* (Lamarck) Foslie, 1901 are also listed for protection in the European Red List of Habitats under habitat type A5.51 “Rhodolith beds in the Mediterranean” (European Commission, 2016). National legislation may additionally recognize certain species of coralline algae as protected, such as certain species of Rhodophyta in Spanish legislation (Royal Decree RD 139/2011 of 4 February 2011 or Order AAA/75/2012 of 12 January 2012).

In the Mediterranean Sea, RBs are mainly found in mesophotic zones, between 40 and 80 meters, but can occur from the subtidal to 150 meters depth (Jacquotte, 1962; Ballesteros, 1988; Basso et al., 2017). They thrive in mesotrophic to oligotrophic conditions with moderate bottom currents that prevent fine sediment deposition (Basso et al., 2017). Mapping their distribution in the Mediterranean is complex, largely due to their deep occurrence, which limits the availability of information (Illa-López et al., 2023). However, available information associate RBs with islands, capes, submarine plateaus, terraces

and channels, where terrestrial sediment input is low (Basso et al., 2017; Rendina et al., 2020; Bracchi et al., 2022). Martin et al. (2014) compiled published data and developed distribution models for this habitat, showing that many areas in the Mediterranean provide optimal conditions for the presence of RBs (see Martin et al., 2014 – Figure 4). Several large RBs (hundreds of km^2) have been described in the Mediterranean basin (such as the Menorca Channel RB: Cabrito et al., 2024a and Malta RB: Tabone et al., 2024).

Mediterranean RBs are known for their multispecific composition and diversity in growth forms, which make them unique and more diverse in coralline algae than Atlantic RBs (Basso et al., 2017; Dulin et al., 2020). Recent studies have highlighted the high diversity of rhodolith-forming species and morphospecies in Mediterranean RBs, as well as a significant variability in species composition across different localities, driven by different environmental factors (Cabanellas-Reboredo et al., 2018; Rendina et al., 2020b; Cabrito et al., 2024a). Basso et al. (2017) reviewed scientific publications from 1885 to 2013, listing 18 species of red calcareous algae in Mediterranean RBs, with 15 species belonging to the coralline algae orders Sporolithales, Hapalidiales, and Corallinales, and three to the order Peyssonneliales. These species are identified as rhodolith-forming species but many of them are also known as encrusting on rock and boulders or even as epiphytes of shelled animals. In addition to this list, several other identifications and taxonomic updates have expanded the total count to 19 coralline algae species (**Table 2.2.1**). Recent studies from the Western Mediterranean show that a single RB can host between 4 and 13 species (Chimienti et al., 2020; Rendina et al., 2020; Ingrassia et al., 2023)—with the shallow Punta de la Mona bed in Granada, Spain, harboring up to 25 morphospecies (22 identified to species level) (del Río et al., 2022)—and that Mediterranean beds also have a rich fossil record of coralline algae dating back at least 140 million years to Albian deposits (Rindi et al., 2019; Aguirre & Braga, 2024).

The study of RBs is complicated not only due to their multi-species composition, but also by the diverse morphological forms they exhibit. Many calcareous red algae exhibit a crustose, encrusting growth form (**Table 2.2.1** and references therein). Some of them can grow independently forming branched and praliné monospecific rhodoliths or coexist with other species, growing attached on substrates forming multi-species boxwork rhodoliths (Basso, 1998). In the last two decades, phycologists increasingly rely on molecular tools for species identification. Carro et al. (2014) demonstrated the effectiveness of DNA barcoding in accurately assessing rhodolith diversity, highlighting the importance of molecular tools in distinguishing coexisting species with convergent morphologies. The integrative taxonomy combining morpho-anatomical identification with molecular analyses is crucial and is increasingly being used to accurately assess the diversity of rhodolith-forming species (Pardo et al., 2014; Peña et al., 2014; Giorgi et al., 2024; Min-Khant-Kyaw et al., 2024; Gabrielson et al., 2023a; Richards et al., 2022).

In this study, we aim to identify the diversity of rhodolith-forming species in the extensive RB of the Menorca Channel by combining morphological and molecular analyses. We focus exclusively on coralline red algae with particular emphasis on free-living rhodolith-forming species. This work builds on a previous study that investigated the morphological complexity of rhodoliths in this area (Cabrito et al., 2024a). Our goal is to provide a comprehensive account of habitat-forming species to support their inclusion in protection measures for these vulnerable and ecologically significant Mediterranean habitats.

Table 2.2.1. List of red calcareous algae cited in the literature as rhodoliths in the Mediterranean. Note that not all the species are confirmed based on both molecular and morpho-anatomic evidences. Modified from Basso et al. (2017).

Order, Family (Guiry & Guiry 2025)	SPECIES	GROWTH-FORM
Order Peyssonneliales		
Fam. Peyssonneliaceae	*Peyssonnelia heteromorpha* (Zanardini) Athanasiadis (as *P. polymorpha* (Zanardini) Schmitz in Basso et al. 2017)	Free-living forming rhodoliths (Ballesteros, 1994)
	Peyssonnelia rosa-marina Boudouresque & Denizot	Free-living forming rhodoliths (Ballesteros, 1994)
	Peyssonnelia crispata Boudouresque & Denizot	Free-living forming rhodoliths (Ballesteros, 1994)
Order Sporolithales		
	Sporolithon mediterraneum Heydrich	Unattached forming rhodoliths (Cabrito et al., 2025)
Order Corallinales		
Fam. Corallinaceae		
	Lithophyllum dentatum (Kützing) Foslie	Encrusting or unattached forming rhodoliths (Rindi et al., 2019)
	Lithophyllum incrustans Philippi	Encrusting or unattached forming rhodoliths (Rindi et al., 2019)
	Lithophyllum racemus (Lamarck) Foslie	Unattached, forming rhodoliths (Rindi et al., 2019)
	Lithophyllum pseudoracemus Caragnano, Rodondi & Rindi	Unattached, forming rhodoliths (Caragnano et al., 2020)
	Lithophyllum stictiforme (Areschoug) Hauck	Typically encrusting forming the coralligenous (Rindi et al., 2019) but also reported as unattached forming rhodoliths (Bracchi et al., 2019). Currently recognized as a species complex (Pezzolesi et al., 2019)
	Neogoniolithon brassica-florida (Harvey) Setchell & Mason	Encrusting or unattached forming rhodoliths (Rindi et al., 2019)
	Neogoniolithon mamillosum (Hauck) Setchell & L.R. Mason (currently regarded as synonym of *Neogoniolithon hauckii* (Rothpletz) R.A.Townsend Huisman)	Encrusting (Hetzinger et al., 2023) or unattached forming rhodoliths (Rendina et al., 2020)
	Spongites fruticulosus Kützing	Encrusting or unattached forming rhodoliths (Rindi et al., 2019)
Order Hapalidiales		
Fam. Hapalidiaceae		
	Lithothamnion corallioides (Crouan et Crouan) Crouan & Crouan	Unattached forming rhodoliths (Rindi et al., 2019)
	Lithothamnion minervae Basso	Unattached forming rhodoliths (Rindi et al., 2019)
	Lithothamnion valens Foslie	Unattached forming rhodoliths (Rindi et al., 2019)
	Mesophyllum philippii (Foslie) Adey	Encrusting or unattached forming rhodoliths (Rindi et al., 2019)

Mesophyllum macroblastum (Foslie) W.H. Adey	Encrusting or unattached forming rhodoliths (Peña et al. 2015a)
Mesophyllum sphaericum Peña, Bárbara, Adey, Riosmena Rodríguez & Choi	Unattached forming rhodoliths, occasionally encrusting (Rindi et al., 2019; Peña et al., 2015a)
Phymatolithon calcareum (Pallas) Adey & McKibbin	Unattached forming rhodoliths, occasionally encrusting (Rindi et al., 2019)
Phymatolithon lusitanicum V. Peña	Unattached forming rhodoliths (Peña et al., 2015b; Rindi et al., 2019)
Phymatolithon lenormandii (Areschoug) W.H. Adey	Encrusting (Rindi et al., 2019) but also reported as unattached forming rhodoliths (Bracchi et al., 2019)
Roseolithon crispatum (Hauck) P.W.Gabrielson, Maneveldt, Hughey & V.Peña	Encrusting or unattached forming rhodoliths (Coutinho et al., 2021; Gabrielson et al., 2023)

2.2.2. Methodology

2.2.2.1. Study area

The environmental conditions around the Balearic Islands (low terrigenous input and high-water transparency) allow rhodoliths to grow at greater depths than in other Mediterranean locations. Our study case, the Menorca Channel, contains the largest RB identified in the Mediterranean, covering an area of 304 km^2 at depths of 50-80 m (Barberá et al., 2012; de Juan et al., 2023; Cabrito et al., 2024a). This RB is in a well conservation status as this area has been historically protected from bottom trawling thanks to the presence of underwater cables (Barberá et al., 2012; Cabrito et al., 2024a). Moreover, the entire channel was designated as a Site of Community importance (SCI ESZZ16002) within the Natura 2000 network in 2014 (Farriols et al., 2022) due to the presence of a wide range of habitats of conservation interest.

2.2.2.2. Specimen collection and preservation

The samples used in this study were obtained in summer 2022 and used in Cabrito et al. (2024a) for morphometric measurements. Collection sites were located in five stations of the Menorca Channel RB (Balearic Islands, Spain). Samples were collected using a Naturalist Dredge (frame 45 x 18.5 cm, fitted to a 1 mm mesh bag). Nineteen valid dredges were recovered (four dredges per station, five stations, see Cabrito et al., 2024a for details on sampling collection). The field sampling strategy was designed to obtain a representation of the 9 rhodolith morphologies identified, classified in three growth forms (branched, praliné and boxwork). For this study, a random selection of four individuals for each morphotype and for each dredge were selected, when possible. This selection resulted in up to four individuals, if available, from each morphotype (up to nine morphotypes) identified in the four dredges collected at the five stations. As a result of this selection, a total of 475 specimens were photographed, air-dried and stored in zip bags with silica gel for future analysis.

For this study, a subset of 120 specimens was selected as it represented the minimum sample necessary to include all morphotypes and sampling points. In some rhodoliths, especially in those of the boxwork

morphology, more than one species was found coexisting. For this study, priority was given to rhodoliths that appeared to be formed by a single species.

2.2.2.3. Morpho-anatomical examination

Scanning electron microscopy (SEM) was performed using the microscopes JSM 6400 (Jeol, Japan) and Hitachi S-3500N (Hitachi High-Technologies Co., Japan) at a WD of 14 mm. Thalli fragments were mounted on both carbon and aluminum stubs using carbon tape as adhesive and were coated with a 15 nm gold layer using Quorum Q150R S sputter coater (Quorum Technologies Ltd.).

SEM was used to explore main anatomical structures considered diagnostic for the identification of coralline algae, including the thallus construction (monomerous – coaxial or non-coaxial - or dimerous), the presence of cell fusions or secondary pit connections between cortical cells of adjacent filaments, the shape of epithallial cells and size of subepithallial cells. Additionally, when present, reproductive structures (conceptacles, sori) were also examined. These features are key to supporting molecular identification and enhancing the robustness of taxonomic identification. For this purpose, we followed the guide of Mediterranean coralline algae by Bressan & Babbini (2003) and consulted descriptions of rhodoliths species recorded in this area (Caragnano et al., 2020; Gabrielson et al., 2023).

2.2.2.4. DNA extraction, PCR amplification and sequencing

A total of 120 specimens were cleaned from epiphytes under a stereomicroscope and selected surfaces were sanded with the use of a rotary hand tool (Dremel) to obtain powder from the epithelial cell layer for DNA extraction. Genomic DNA was extracted using a NucleoSpin® Tissue kit (Macherey-Nagel, GmbH and Co, KG, Germany), following the manufacturer's protocol. Fragments of *psb*A gene (which encodes photosystem II reaction center protein D1 gene) and *rbc*L gene (which encodes the large subunit of the enzyme ribulose-1,5-bisphosphate carboxylase/oxygenase) were PCR-amplified using the primer pairs *psb*A-F1/*psb*A-R1 (Yoon et al., 2002) and two overlapping primer combinations F57-R1150 and F753-RrbcS-start (Freshwater & Rueness, 1994; Gabrielson et al., 2023a), respectively. The PCR reaction was made by using the Supreme NZYTaq II 2x Colourless Master Mix (NZYtech) and following the thermal profiles used by Peña et al. (2015b) for the *psb*A locus and Saunders & Moore (2013) for the *rbc*L. All PCR products were purified and sequenced by Sanger method by GenoScreen (GenoScreen Innovative Genomics, France). Once the sequences were received, they were assembled, aligned and trimmed using MEGA v.6 (Tamura et al., 2013). All the sequences obtained were submitted to GenBank (accession numbers listed in **Table 2.2.S1**).

2.2.2.5. Phylogenetic and molecular species delimitation analyses

To increase the taxonomic coverage of the study, GenBank sequences that matched our sequences with more than 95% of identity using BLAST (Altschul et al., 1990) were included. In addition, whenever possible, the type species of genera and species publicly available in GenBank were included

(Supplementary Material - **Table 2.2.S1**). For both markers (*psb*A and *rbc*L), *Corallinapetra gabrielii* (order Corallinapetrales) was used as outgroup.

Three datasets were constructed. One for *psb*A marker and two for *rbc*L marker. It was decided to generate two data sets for *rbc*L because, in this study, long sequences of this marker were obtained (around 1300 bp) but most of the sequences available in GenBank are shorter fragments. For example, the lectotype of *Roseolithon crispatum* has only 117 bp, causing that not all the sequences had an overlapping region. Therefore, the *rbc*L matrix was divided into a first dataset including our sequences with those from GenBank with a minimum size of 1300 bp and another dataset with all selected sequences from Genbank and those from this study trimmed to a total length of 294 bp.

Phylogenetic relationships were inferred with maximum likelihood (ML) using IQ-TREE v2.2.0 (Nguyen et al., 2015). Bayesian inference (BI) was applied with MrBayes v3.2.7a (Ronquist et al., 2012). Models of sequence evolution were selected using the Akaike Information Criterion (AIC) obtained in ModelFinder in PhyloSuite (Zhang et al., 2020). For the three matrices, the selected model was GTR+F+I+G. ML analyses were performed for 1000 standard bootstraps generations. For the BI analyses, two parallel runs, with four Markov Chain Monte Carlo chains were run for 2,000,000 generations and sampled every 1,000 generations, in which the initial 25% of sampled data were discarded as burn-in and stationary and p files from each run were checked in Tracer v.1.7.2 (Rambaut et al., 2018) to ensure that effective sample sizes were >200 for all parameters.

Both ML and BI analysis of *psb*A and *rbc*L were performed using PhyloSuite software (Zhang et al., 2020; Xiang et al., 2023). The resulting trees were visualized and edited by Interactive Tree Of Life (iTOL) v5 online tool (Letunic & Bork, 2024). Finally, a coalescent phylogenetic inference analysis was performed in BEAST v.2.7.3 (Bouckaert et al. 2019) to obtain an ultrametric trees. The input file was created using BEAUti, the site model was set based on the ModelFinder results and the clock model was set to relaxed log-normal models (Drummond et al. 2006). The prior for the species tree model was set to the Yule model adding a prior that considers every species but the outgroup *Corallinapetra gabrielii* as a monophyletic group. For each analysis, a Markov Chain of 100 million generations was run, sampling every 10,000 generations, and stopped when converging. Chain convergence was examined with Tracer v.1.7.2 (Rambaut et al. 2018) to ensure that the ESS values were over 200. The initial 25% of tree configurations was discarded as burn-in, and the maximum credibility tree was obtained using TreeAnnotator.

Three common species delimitation methods were applied to each matrix: (i) Assemble Species by Automatic Partitioning (ASAP; Puillandre et al. 2021), (ii) Bayesian Poisson Tree Processes (bPTP; Zhang et al. 2013), and the (iii) Generalized Mixed Yule Coalescent approach (GMYC; Fujisawa and Barraclough, 2013). The ASAP method was performed using *p*-distances on the web server (https://bioinfo.mnhn.fr/abi/public/asap/). The input matrices were the *psb*A and *rbc*L FASTA

alignments, and only the partition with the lowest ASAP score was considered. To run both bPTP and GMYC analysis, the Maximum Credibility Tree transformed into Newick format through FigTree v.1.4.3 (Rambaut 2010) and was submitted to the species delimitation portal (http://species.h-its.org). Only the ML solution of the bPTP analysis was considered, as it was consistent with the results obtained through the other methods. For GMYC, both the single and multi-threshold approaches were considered.

The asymptotic diversity of rhodolith forming species was estimated by extrapolating the species accumulation curve to the double of the observed sample size (N= 2 x 69 from *psb*A sequences) using the methods in the iNEXT R package (Hsieh et al. 2016).

2.2.3. Results

2.2.3.1. Molecular species delimitation analyses

DNA extraction was successful in 85 out of 120 specimens. The *psb*A fragment was successfully amplified and sequenced for 82 out of 85 DNA samples (96.5% amplification success). After eliminating epiphyte contamination and poor-quality sequences, 69 correctly amplified sequences were obtained. These 69 sequences included 30 distinct haplotypes of 890 bp. The *rbc*L fragment was successfully amplified and sequenced for 35 out of 35 DNA samples (100% amplification success). After removing epiphyte contamination and poor-quality sequences, 28 correctly amplified sequences were obtained. These 28 sequences included 20 distinct haplotypes of 1332 bp.

Considering that for *psb*A interspecific divergences are usually greater than 2.5% (Torrano-Silva et al., 2018; Ramos et al., 2025), a 3% threshold is generally sufficient to discriminate distinct species in coralline algae. After the species delimitation analyses (**Fig.2.2.1**), at least 15 putative species have been detected (eight Hapalidiales, one Sporolithales, and five Corallinales). Most of them are well-resolved across the four species delimitation analyses and have strong posterior probability support at the nodes (>0.99) (**Fig.2.2.1**). However, only six out of the 15 detected species can be confirmed molecularly, as they have sequenced type specimens or high-quality and well-identified sequences previously available: *Sporolithon mediterraneum*, *Lithothamnion corallioides*, *Phymatolithon lusitanicum*, *Lithophyllum nitorum*, *Lithophyllum racemus*, and *Lithophyllum pseudoracemus* (uncorrected *p*-distances <1% in all cases). Additionally, a lack of available sequences in the database matching our sequences in different clades was observed. This prevents molecular confirmation of some species but allows the exclusion of others. As shown in **Fig.2.2.1**, this is the case for *Lithothamnion* cf. *valens* (identified based on morphology), *Lithothamnion* cf. *minervae*, *Lithothamnion* sp.1, *Lithothamnion* sp.2, *Spongites* sp.1, and *Spongites* sp.2. Finally, two more uncertain clades were obtained, where the four species delimitation analyses yielded conflicting results. A large number of samples clustered in a single clade with sequences identified as *Phymatolithon* sp., separated from

Phymatolithon calcareum (uncorrected *p*-distances: 1.2 – 1.5%), despite ASAP and mGMYC identified them as the same species, *P. calcareum*. A similar situation occurs with the *Roseolithon* clade, where ASAP and bPTP resolve the specimen S5X3 as a different species from the rest (uncorrected *p*-distances : 2.8% in all cases), while sGMYC and mGMYC resolved them as the same species (**Fig.2.2.1**).

Considering that interspecific divergence for *rbc*L observed in coralline algae varies considerably depending on the coralline group (Torrano-Silva et al., 2018 reported values of 0.9%-12%) and high values are common, as for example, interspecific divergences of > 6.4% in *Lithophyllum* species from Brazil (Torrano-Silva et al., 2018), the results obtained with this marker are easier to interpret together with those of *psb*A. The larger *rbc*L sequences obtained in this study (~1300 bp) did not match through BLAST with closely related species (Supplementary Material - **Fig.2.2.S1**), leaving some clades taxonomically unresolved. Using this *rbc*L matrix, 11 putative species were detected, of which only for *Lithothamnion corallioides* and *Phymatolithon lusitanicum* the identifications were considered reliable because they have valid long reference sequences for this marker. Additionally, in this case, the clade identified as *Phymatolithon* sp. is separated from *P. calcareum* (uncorrected *p*-distances: 2.8%) across all four analyses, indicating that it may represents a different species within the genus *Phymatolithon*.

The results of the analyses performed with the short *rbc*L fragment (Supplementary Material - **Fig.2.2.S2**) do not differ significantly from those presented above, but the inclusion of short sequences from some generitypes has increased the robustness of the analyses, leading to the detection of 13 putative species. In this case, our *Sporolithon* (specimen S13G11), identified as *S. mediterraneum* with *psb*A, could be a different species (uncorrected *p*-distance: 6.3%) according to all four analyses. Moreover, by including the neotype sequence of *P. calcareum*, it becomes evident that our samples form a distinct clade (uncorrected *p*-distances: 2.7%), supporting their identification as *Phymatolithon* sp. Finally, consistent results were obtained for the identification of *Roseolithon crispatum* including the lectotype sequence, but in this case, the specimen S5X3, which is identified as *R. crispatum* with *psb*A, could be a different species (uncorrected *p*-distance: 4.3%) according to all four analyses.

With a sequencing effort for *psb*A of 69 specimens, sufficient diversity of rhodolith-forming species is captured (**Fig.2.2.S3**). The detection of the maximum expected diversity of ca. 18 (17.6) species would require expanding the sampling beyond 150 sequenced specimens. However, with less than half of that number, most of the possible species are already represented.

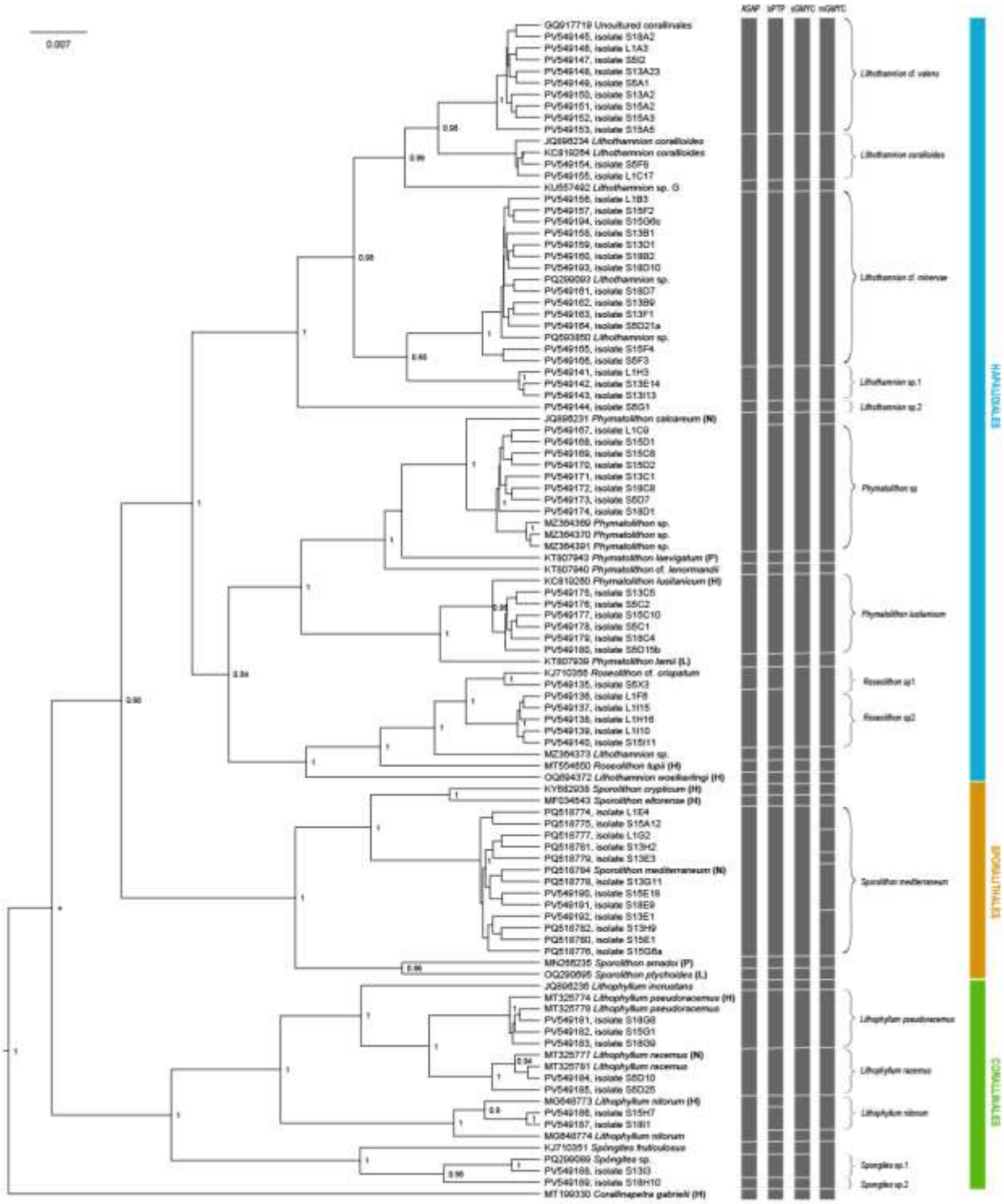


Fig.2.2.1. Summary of species delimitation analyses obtained with the *psb*A database, depicted over the coalescent analyses obtained through BEAST. Numbers in the nodes refer to the posterior probabilities from the coalescent analysis. Posterior probabilities of < 0.8 were not recorded. Asterisks designate clades that were set up as monophyletic for the coalescent analysis. Vertical grey lines summarized the results from ASAP, bPTP, sGMYC and mGMYC.

2.2.3.2. Morpho-anatomical study

The morpho-anatomical examination of representative specimens per taxa delimited in the molecular analyses, together with the consultation of taxonomic literature of Mediterranean coralline algae, as well as the guide by Bressan and Babbini (2003), supported most of the molecular identifications.

Sporolithales

Sporolithon mediterraneum Heydrich

Twelve rhodoliths of *Sporolithon mediterraneum* were identified through *psb*A molecular analysis (uncorrected *p*-distance with neotype sequence: 0%). Although the results of *rbc*L (Supplementary Material – **Fig.2.2.S2**) suggest a different species, the identification is confirmed by morpho-anatomical examination, as the collected specimens exhibited the same characters described for *S. mediterraneum* and those distinguishing it from *S. ptychoides* (Cabrito et al., 2025). The specimens were found forming rhodoliths with maximum length of 2.9-8.4 cm. The five specimens examined, showed a monomerous thallus construction with rectangular hypothallial cells. Epithallial cells are flared and disposed in a single layer, subepithallial cells are isodiametric, cortical cells are long and rectangular with presence of cell fusions and secondary pit connections (Supplementary Material - **Fig.2.2.S4B**). Tetrasporangia (empty) in individual, calcified compartments subtended by a single stalk cell, and with 5-6 calcified paraphyses interspersed among them (Supplementary Material - **Fig.2.2.S4C**); pores of each tetrasporangium are surrounded by 9-12 (N = 5 specimens examined) rosette cells (Supplementary Material - **Fig.2.2.S4D**).

Hapalidiales

Genus *Lithothamnion*

Nine rhodoliths identified with *psb*A as *Lithothamnion* cf. *valens* have been the largest in size (4.5-10.1 cm in maximum length) among the branched rhodoliths. Rhodoliths have wide branches and protrusions (**Fig.2.2.2A, B, C**). In longitudinal section, concentric bands of more or less thick-walled, heavily calcified cells are clearly visible (**Fig.2.2.2D**). Epithallial cells are flared and distributed in one-three layers (**Fig.2.2.2E, F**). The subepithallial cells are rounded to rectangular, as long as the immediately following cortical cells, which have a similar rounded to rectangular morphology (**Fig.2.2.2E, F**). Abundant cell fusions are observed between cortical cells of adjacent filaments (**Fig.2.2.2E, F**). Gametangial nor tetra/bisporangial conceptacles could be observed. The vegetative morpho-anatomical characters observed fit with those provided in Bressan and Babbini (2003) for *L. valens*.

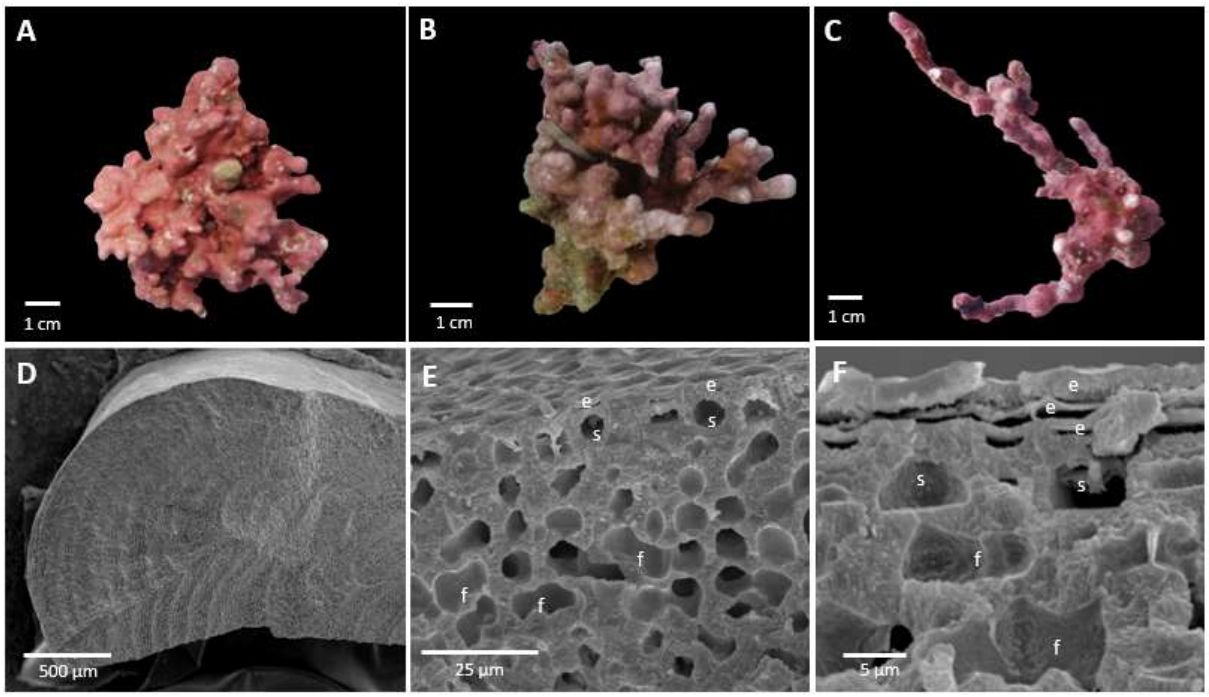


Fig.2.2.2. (A,B,C) Examples of specimens collected and identified as *Lithothamnion* cf. *valens*. (D) Longitudinal section of a branch with concentric bands. (E,F) Vertical sections showing epithallial flared cells in one-three layers (e), subepithallial cells (s) and numerous cell fusions (f). D-F : SEM.

Morpho-anatomical analysis confirmed that the rhodoliths specimens identified as *L. corallioides* and *Lithothamnion* sp.1 belong to the genus *Lithothamnion* as they all present the main common characteristics of this genus such as flared epithallial cells, rounded subepithallial cells longer or as long as the following cortical cells (Supplementary Material –**Fig.2.2.S.5**) and numerous cell fusions between cortical cells contiguous filaments (Supplementary Material - **Fig.2.2.S.5** and **Fig.2.2.S6**). The two rhodoliths identified as *L. corallioides* measured 2-2.5 cm in maximum length while the two rhodoliths identified as *Lithothamnion* sp.1 measured 2.8-3.3 cm of maximum length. In the case of *L. corallioides*, in addition to the molecular support (for both molecular markers), the specimens explored fit the description of Bressan and Babbini (2003), highlighting the rectangular spindle-shaped cortical cells with dimensions of 14-23 µm length x 4-7 µm width (measured in 20 cells of one individual) (Supplementary Material - **Fig.2.2.S.5C**). *Lithothamnion* sp.1 could only be confirmed at genus level.

The 13 rhodolith specimens of *L.* cf. *minervae* that cluster within the same clade as another Mediterrnean rhodoliths collection published as *Lithothamnion* sp. (GenBank accession numbers: PQ299093 and PQ593850, but morpho-anatomically similar to *L. minervae*). The rhodoliths ranged from 2.1-5.9 cm of maximum length, with generally small and short branches (**Fig.2.2.3**). It has a pluristratified cortex, with rectangular to ovoid cells. Epithallial cells are flared and subepithallial cells are rounded and as long as cells subtending them. (**Fig.2.2.3F**) and numerous cell fusions between cells of contiguous filaments (**Fig.2.2.3D, E, F**). Protrusions at the apex of branches could be observed under magnification, but gametangial or tetra/bisporangial conceptacles were not observed (**Fig.2.2.3B, C**).

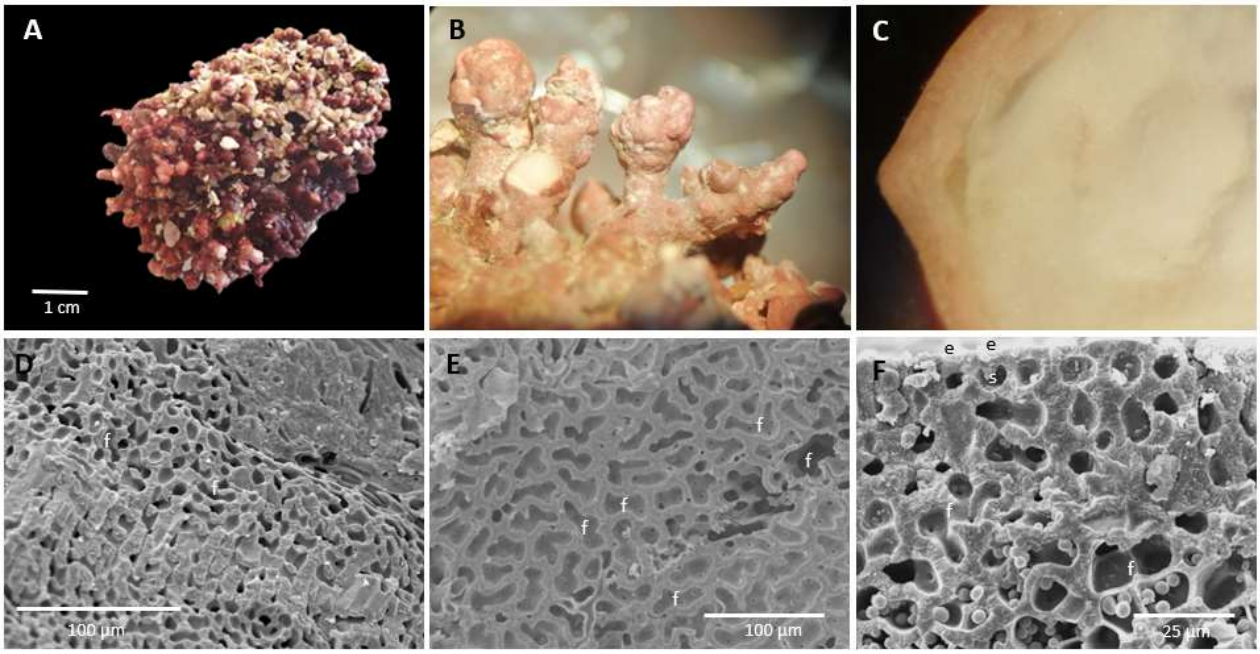


Fig.2.2.3. (A) Praliné rhodoliths identified **as** *Lithothamnion* cf. *minervae*. (B,C) Detail of protrusions under binocular microscope. (D) Vertical and (E) longitudinal sections showing numerous cell fusions (f). (F) Vertical section showing epithallial cells (e) and subepithallial cells (s). D-F: SEM.

Genus *Phymatolithon*

Molecular analysis separates our clade of *Phymatolithon* sp. from *P. calcareum*, and morpho-anatomical examination confirmed that rhodoliths specimens showed diagnostic characters described for this genus. *Phymatolithon* sp. consisted on eight rhodoliths with maximum length of 2.5-4.9 cm. Construction is monomerous, non-coaxial. Epithallial cells have a domed shape, subepithallial cells are shorter than cortical cells subtending them. Cortical cells are highly calcified, and joined by cell fusions. Gametangial or tetra/bisporangial conceptacles were not observed (Supplementary Material - **Fig.2.2.S7**).

With regards to *Phymatolithon lusitanicum*, morpho-anatomical examination confirms the molecular results, which are well-supported as their clades include the neotype and holotype of the respective species. The six rhodoliths of *P. lusitanicum* have a maximum length of 2-5.3 cm. Epithallial cells have a flattened shape, subepithallial cells are shorter than cortical cells subtending them, and cortical cells are highly calcified, and joined by cell fusions. Gametangial or tetra/bisporangial conceptacles were not observed (Supplementary Material -**Fig.2.2.S8**).

Gennus *Roseolithon*

For the *psb*A results the specimen S5X3 appears in the same cluster as a *Roseolithon* cf. *crispatum* and the clade formed by the rest of the specimens in a separate clade for two species delimitation analysis (uncorrected *p*-distance: 2.8%), in the analysis of the short *rbc*L fragment that includes the lectotype,

Roseolithon crispatum is grouped with the rest of the specimens molecularly confirming them as *R. crispatum* and leaving the specimen S5X3 as a distinct species (uncorrected *p*-distance: 3.4-4.3%). The morpho-anatomical examination of the specimen S5X3 supports the hypothesis that it is *R. crispatum*, as it exhibits a very characteristic morphology where the thallus grows in a lamellar form, ending in cone-shaped apices, with weak adherence and free margins (**Fig.2.2.S9A, B, D),** as described by Bressan and Babbini (2003) for *R. crispatum* (as *Lithothamnion crispatum*). This distinctive morphology has not been observed in any other species. Epithallial cells could not be clearly observed in cross-section, but on the surface, they appear polygonal with diameters of approximately 10 µm as it is also provided in Bressan & Babbini (2003) (**Fig.2.2.S9D**). Subepithallial cells are rectangular to ovoid and are as long as cortical cells subtending them (**Fig.2.2.S9C**). No gametangial or tetra/bisporangial conceptacles were observed. Given the inconsistency with the results of *rbc*L, the identification as *Roseolithon* sp.1 is maintained.

The other five *Roseolithon* specimens measured 3-6.5 cm of maximum length and appeared as boxwork rhodoliths with hardly any ramifications. The morpho-anatomical examination of the specimen selected, suggests that it may be a female gametophyte according to the shape of the uniporate conceptacle observed, which is likely to be carposporangial (Supplementary Material - **Fig.2.2.S10B**). In cross-section, epithallial cells are flared, subepithallial cells that are either as long as or longer than the following cortical cells subtending them, and cell fusions between cortical cells of adjacent filament cells are present (Supplementary Material - **Fig.2.2.S10C**). These characters align with the description of the genus *Roseolithon* (Coutinho et al. 2022). Although the *rbc*L results place these specimens in the same clade as the lectotype of *R. crispatum*, given the lack of consistency with the observed morphology, their identification as *Roseolithon* sp.2 is maintained.

Order Corallinales

Genus Lithophyllum

Lithophyllum nitorum was confirmed through morpho-anatomical exploration, as diagnostic characters observed does not contradict the description by Peña et al. (2018). Both specimens identified as *L. nitorum* were boxwork rhodoliths of 4.7-6 cm of maximum length. Slightly convex to flattened epithallial cells were observed, although Peña et al. (2018) described them as mostly flattened. Additionally, the subepithallial cells were noticeably shorter than the following cortical cells (**Fig.2.2.4C**), and secondary pit connections between cortical cells of contiguous filaments were observed (**Fig.2.2.4D**). Furthermore, as described by Peña et al. (2018), numerous slightly raised sori of uniporate sporangial conceptacles were observed on the surface, and in cross-section, zonately divided tetrasporangia were visible (**Fig.2.2.4B**). Although the calcified columella was not observed in this case, the overall description aligns with Peña et al. (2018).

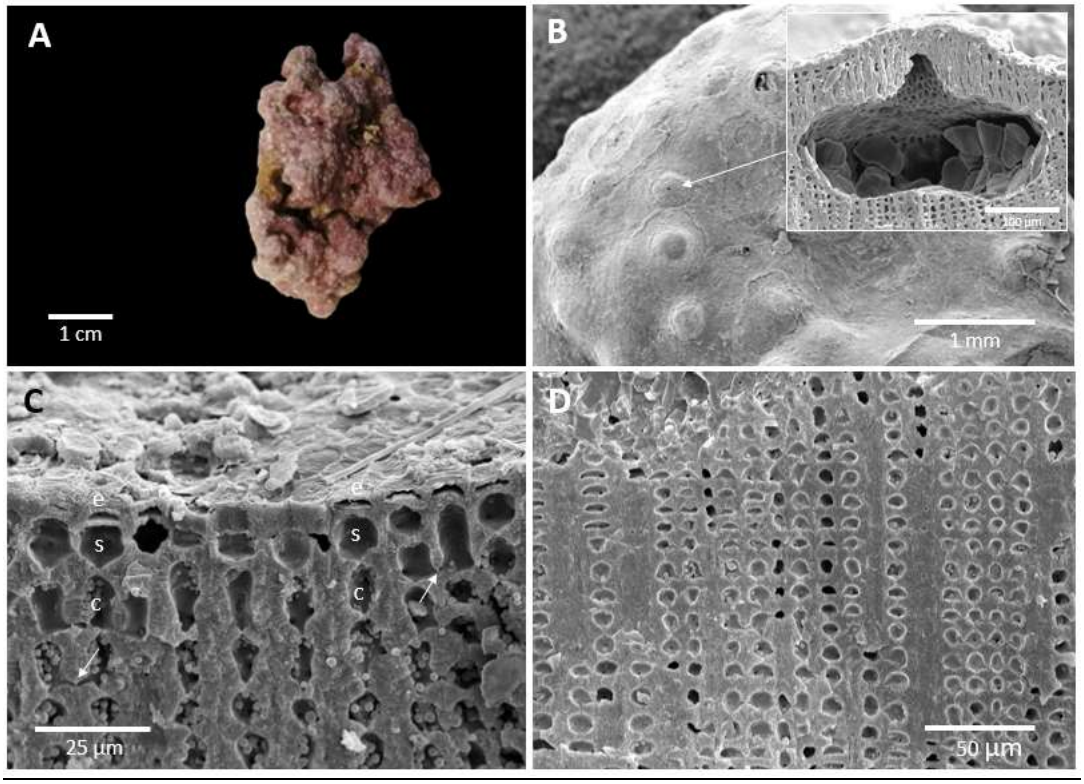


Fig.2.2.4. (A) Boxwork specimen of *Lithophyllum nitorum*. (B) Raised sori of uniporate sporangial conceptacle on surface with a zoom in a cross-section of the conceptacle with zonately divided tetrasporangia inside. (C) Vertical section showing convex to flattened epithallial cells (e), subepithallial cells (s), cortical cells (c) and secondary pit connections (arrows). (D) Vertical section of the thallus showing secondary pit connections. B-D: SEM.

The identification of *Lithophyllum racemus* and *L. pseudoracemus* is well supported by both molecular analyses and morpho-anatomy. *Lithophyllum pseudoracemus* was described recently by Caragnano et al. (2020), and at the moment there is no known morphological character that would allow the distinction between the two species.

Rhodoliths of *Lithophyllum racemus* are small (2.9-3.2 cm in maximum length) and rounded with short branches. This rhodoliths showed a dimerous construction, 1-2 layers of flattened epithallial cells were observed, with elongated subepithallial and cortical cells of contiguous filaments joined by secondary pit connections. Gametangial or sporangial conceptacles were not observed (Supplementary Material – **Fig.2.2.S11**). These characters are consistent with the description provided in Caragnano et al. (2020). Same morpho-anatomical characters were observed in *L. pseudoracemus* (Supplementary Material – **Fig.2.2.S12**). The specimens of *L. pseudoracemus* are spherical with short portuberances and measured 2.5-3.6 cm of maximum length. However, in this case, sporangial uniporate conceptacles containing zonate tetrasporangia were also observed (Supplementary Material –**Fig.2.2.S11B**). Nevertheless, in one specimen (S18G9), which molecularly clusters within the *L. pseudoracemus* clade, uniporate sporangial conceptacle were observed empty but with an elliptical shape of 358 µm x 117 µm and a

slightly calcified columella (Supplementary Material –**Fig.2.2.S12D**); this particular shape and measures coincide with those given to *L. racemus* in Bressan & Babbini (2003; sporangial uniporate conceptacles of 225-300 µm in diameter x 70-180 µm in height).

Genus *Spongites*

Specimen S13I3 molecularly identified as *Spongites* sp. 1 was not morpho-anatomically examined. For *Spongites* sp.2, only epithallial cells that appear rectangular or dome-shaped have been observed, although they are not clearly distinguishable. Solitary trichocytes which are diagnostic of this genus were also not observed (Supplementary Material - **Fig.2.2.S13B**). However, numerous cell fusions between cells of adjacent filaments were noted (Supplementary Material - **Fig.2.2.S13D**). No gametangial or tetra/bisporangial conceptacles were observed.

2.2.3.3. Morphotypes and depth distribution

Sampling limitations may prevent confirming species absence at certain depths, their presence is confirmed where they have been found. In this sense, the results confirm the presence of *Lithothamnion* cf. *valens*, *L. corallioides*, *L.* cf. *minervae* and *Phymatolithon* sp. throughout the depth range studied. Similarly, *Lithophyllum nitorum* and *L. pseudoracemus* can be confirmed only at a depth of 56-58.8 m. Some species such as *Lithothamnion* sp.2, *Roseolithon* sp.1 and *Lithophyllum racemus*, were only detected in the shallower zone (48 m), although their representation is very low with only one sequenced specimen. *Roseolithon* sp.2 was confirmed at a depth of 58.8-74 m. *Spongites* sp.1 and *Spongites* sp.2 were found with only one individual represented at depths of 62 m and 56 m, respectively. *Sporolithon mediterraneum*, which is highly represented in this study, was detected from 56 m depth onwards. *Lithothamnion* sp.1 was detected only in the deepest areas between 62 and 74 m with a representation of three sequenced specimens (**Table 2.2.2**).

Sporolithon mediterraneum has been found in high representation as a rhodoliths-forming species, mostly described by Cabrito et al. (2024a) as praline-type morphotypes G and E, although its encrusting form has occasionally been observed in boxwork-type rhodoliths (morphotype H). Within the Hapalidiales, the genus *Lithothamnion* has been found in a wide variety of morphologies with representation in both branched, praliné and boxwork forms depending on the species. *L.* cf. *valens* has always appeared forming very large branched rhodoliths (morphotype A, see Cabrito et al., 2024a). In contrast, *L. corallioides* and *L.*cf. *minervae* are mostly represented by branched morphotypes although they are also found in praliné morphotypes together with *Lithothamnion* sp.1 and *Lithothamnion* sp.2. The only *Lithothamnion* found forming crusts in boxwork rhodoliths was *Lihtothamnion* sp.1 (**Table 2.2.2**). The two identified species of the genus *Phymatolithon* were found forming branched rhodoliths. For the genus *Roseolithon,* two species may have been identified, one of them mainly grows in boxwork rhodoliths while the other one forms praliné rhodoliths (**Table 2.2.2**). Finally, among the Corallinales, all three growth forms were found to be represented with *Lithophyllum racemus* forming branched

rhodoliths (type D) and *L. pseudoracemus* forming praliné rhodoliths (type G), while *L. nitorum* as well as *Spongites* sp1 and *Spongites* sp.2 were found growing on boxwork rhodoliths (**Table 2.2.2**).

Table 2.2.2. List of the species found in this study, the depth at which they were found and the morphology with which they were classified.

SPECIES	**COLLECTION DEPTH**	**MORPHOLOGIES FOUND** Based on Cabrito et al. (2024a)
Sporolithon mediterraneum	From 56 m to 74 m depth	praliné (G, E), occasionally boxwork (H)
Lithothamnion cf *valens*	From 48.5 m to 74 m depth	branched (A)
Lithothamnion corallioides	From 48.5 m to 74 m depth	branched (C) and praliné (F)
Lithothamnion sp.1	From 62 m to 74 m depth	boxwork (H,I) and praliné (E)
Lithothamnion cf *minervae*	From 48.5 m to 74 m depth	branched (B,D) and praliné (F)
Lithothamnion sp.2	At 48.5 m depth	praliné (G)
Phymatolithon sp	From 48.5 m to 74 m depth	branched (C, D)
Phymatolithon lusitanicum	From 48.5 m to 62 m depth	branched (C, D)
Roseolithon sp.1	At 48.5 m depth	praliné (X)
Roseolithon sp.2	From 58.8 m to 74 m depth	boxwork (H, I), occasionally praliné (F)
Lithophyllum nitorum	From 56 to 58.8 m depth	boxwork (H, I)
Lithophyllum pseudoracemus	From 56 to 58.8 m depth	praliné (G)
Lithophyllum racemus	At 48.5 m depth	branched (D)
Spongites sp.1	At 62 m depth	boxwork (I)
Spongites sp.2	At 56 m depth	boxwork (H)

This study aimed to include (as far as possible) only monospecific rhodoliths. Nevertheless, species associations forming rhodoliths were observed, both of the praliné type and especially in boxwork structures (see example in Supplementary Material –**Fig.2.2.S14**). Among the rhodoliths sequenced in this study, only the praliné specimen S15G6 (ICMCBMR000672) was sequenced twice due to the suspicion of hosting two co-occurring species. The *psb*A results may indicate an association of *Sporolithon mediterraneum* with *Lithothamnion* cf. *minervae* (**Fig.2.2.1**).

Finally, considering the proportions of morphotypes reported in Cabrito et al. (2024a) (see Supplementary Material –**Fig.2.2.S15**) and the species founded in this study (**Table 2.2.2**), given that the most abundant morphotype in the study area is morphotype C, representing 37.53% of the rhodoliths, it is formed by at least three species: *Lithothamnion corallioides, Phymatolithon lusitanicum* and *Phymatolithon* sp. On the other hand, morphotype A (10.14% of the total number of rhodoliths), corresponds only to *Lithothamnion* cf. *valens* and is found in abundance in the central and better preserved part of the habitat, making it one of the most abundant species in the Menorca Channel. *Sporolithon mediterraneum* also appears to be well represented in the Menorca Channel, as it has been found forming three different morphotypes described in Cabrito et al. (2024a), and across the entire bathymetric range (see **Table 2.2.2** and Supplementary Material –**Fig.2.2.S15**). These observations support the idea that the Menorca Channel RB is highly multispecific without a clear predominance of any one species.

2.2.4. Discussion

The deepest known RBs occur in the Mediterranean Sea, with the deepest recorded at 150 m in the Balearic Islands (Aguilar et al., 2009). Their depth makes them difficult to access and study, resulting in limited knowledge of their actual species composition. In the present study, conducted in the Menorca Channel, 15 species were identified, a number that slightly exceeds the number 4 – 13 species typically reported per RB in the Western Mediterranean, depending on the locality (Bracchi et al., 2019; Chimienti et al., 2020; Rendina et al., 2020; Ingrassia et al., 2023). Previous research in the nearby Mallorca channel reported at least five rhodolith-forming species: *Lithothamnion valens, L. corallioides, Phymatolithon calcareum, Lithophyllum racemus* and *Spongites fruticulosus* (Joher et al., 2023). These identifications were based on morphological characteristics, emphasizing the importance of molecular techniques to improve species identification.

The lack of match through BLAST obtained in the two molecular markers for some of our sequences, especially in the genus *Lithothamnion*, suggests the existence of numerous cryptic species endemic to the Mediterranean with a restricted distribution, as also observed by Pezzolesi et al. (2019) for *Lithophyllum strictiforme*. The genus *Lithothamnion* is the most diverse genus found in this study area with five different species identified. Two of them, *L.* cf. *valens* and *L.* cf. *minervae* are known to be endemic to the Mediterranean and have been partially identified thanks to morpho-anatomical analysis or matched through BLAST with other GenBank sequences identified under the same taxon. The type materials described for both species have been sequenced without success to date, so their identifications cannot yet be confirmed. The detection of two other unassigned *Lithothamnion* species suggests that there may be at least two more species that may be endemic to the Mediterranean, one of which was identified at 74 m depth.

Although the two protected species (*Lithothamnion corallioides* and *Phymatolithon calcareum*) are considered globally distributed and abundant in the European coasts, Basso et al. (2016) underlined that in Mediterranean BRs they may be absent or in small proportions relative to the total number of species that form the BRs. Our results align with Basso's statement; although we detected *L. corallioides*, *P. calcareum* was not found. However, other species of the same genus (*P. lusitanicum* and *Phymatolithon* sp) were detected across a wide bathymetric range, from 48 to 62 m and 74 m depth, respectively.

Further analysis of the morpho-anatomical characteristics of *Roseolithon* specimens, as well as obtaining *psb*A sequences from the type material of *R. crispatum*, would allow us to clarify which of the two *Roseolithon* clades detected in this study actually corresponds to *R. crispatum*, the only species of the genus *Roseolithon* described in the Mediterranean to date (Gabrielson et al., 2023a). Our study provides new information on the depth distribution of the genus *Roseolithon*, whose distribution is still poorly understood. Additionally, it confirms the presence of *R. crispatum* through both molecular and morpho-anatomical data, although from different specimens. These could belong to the same species,

as the uncorrected p-distances for both psbA (2.8%) and rbcL (3.4–4.3%) are not particularly high. However, it is also possible that they reflect the existence of a genetically diverse species complex. This finding suggests that the species diversity of the genus *Roseolithon* in the Mediterranean may be greater than previously suspected.

Although the results of the short *rbc*L fragment of *Sporolithon mediterraneum* do not match the neotype described in Cabrito et al. (2025), it is known that the interspecific divergence considered in coralline algae for *rbc*L is usually higher than 3% (e.g. Gabrielson et al., 2011 used >4%). Thus, because the results of *psb*A are consistent and morpho-anatomical characters are clear and matches perfectly the neotype, its identification is confirmed.

Lithophyllum racemus is described as another Mediterranean paleoendemic species (Basso et al., 1996). Caragnano et al. (2022) investigates the high crypticism among Mediterranean *Lithophyllum* species and described a new species, *L. pseudoracemus*. In this study both species were found and confirmed at depths between 48-58.8 m matching the depth distribution ranges described in Caragnano et al. (2022). This study also confirmed the presence of *L. nitorum* that was also found at 56-58.8 m depth. To date, this species was only identified through morphology at depths ranging 37-46 m in the Cantabrian Sea (Adey & Adey, 1973) and, in the Mediterranean, it has only been recorded at shallower areas, 9-24 m depth (Peña et al., 2018; Del Río et al., 2022). Our finding contributes to the distribution data of this species, confirming that it can be found at greater depths than previously expected. Finally, among the two *Spongites* species found in this study, neither corresponds to *Spongites fruticulosus*, the only *Spongites* species described in the Mediterranean to date (Basso et al., 2017; Rindi et al., 2019). Although we do not have sequences from the type material of this species, Rösler et al. (2016) designated the epitype of *S. fruticulosus* based on other molecular markers and indicated that voucher PCO142664 (GenBank *psb*A: KJ710351) from Greece used in Peña et al. (2014) is conspecific to the epitype. *Spongites* sp.1 matched through Blast with a *Spongites* sequence from a praliné rhodolith found in Sicily at 51 m depth, which was neither identified as *S. fruticulosus*. Thus, the species found here for *Spongites* would be well separated from *S. fruticulosus* with *psb*A (2-6% of uncorrected *p*-distances). This study suggest that the diversity of *Spongites* in the Mediterranean is greater than previously described and that there may be at least two endemic species of this genus.

The high diversity of rhodolith-forming species identified in this study, align with the diversity expected in the Mediterranean which is known to be one of the regions with a highest rhodolith-forming species diversity (Rebelo et al., 2021). The multi-species character of Mediterranean RBs and the high endemism of species, emphasizes the importance of conservation of coralline algal to prevent extinctions (Ramos et al., 2024). Thus, conservation measures should include an update of the taxonomic lists of Mediterranean species, for example in the Habitats Directive to consider not only the wide distributed *P. calcareum* and *L. corallioides* but also the endemic ones. Additionally, the high

crypticism observed among rhodolith-forming species in our study, also invites to re-evaluate the identifications of some species using a combined approach including morpho-anatomical and molecular analyses. It emphasizes the importance of sampling and studying mesophotic Mediterranean RBs to further complete databases and expand knowledge on the distribution of species that are important for conservation planning and management.

Acknowledgments

The authors are very thankful to Laia Illa-López and Géraldine Pérez for their backup during the field sampling and classification and also to Fernando Ángel Fernández Álvarez (FAFA) for his support in running the BEAST models. This study was partly funded by research projects "Macobios" (EU H2020 contract nº 869710) and "RhodoMed" (Spanish Ministry of Science grant nº PID2023-146998OB-C22). This work contributes to the ICM's 'Center of Excellence' Severo Ochoa (CEX2019-000928-5) and to the 'Maria de Maeztu' accredited to the IMEDEA (CEX2021-001198). **AC** is enrolled in the PhD program in Marine Sciences at the University of Barcelona. **SdJ** was supported by a Ramon y Cajal postdoctoral grant funded by the Ministry of Science and Innocation (Plan Estatal I+D+I, 2017-2020; grant no. RyC2020-029062-I).

FUNDING

The authors acknowledge funding from the EU H2020 project "MaCoBioS" (contract nº 869710).

CONTRIBUTIONS

AC: Conceptualization, Methodology, Formal analysis, Writing – original draft, Writing – review & editing, Visualization. **FM:** Conceptualization, Writing – review & editing. **SdJ:** Conceptualization, Writing – review & editing. **VP:** Conceptualization, Methodology, Formal analysis, Writing – review & editing, Visualization.

ETHICS DECLARATIONS

Conflict of interest

The authors declare no conflict of interest.

Data availability

Data will be made available on request.

References

Adey, W.H. & Adey, P.J. (1973). Studies on the biosystematics and ecology of the Epilithic Crustose Corallinaceae of the British Isles. *British Phycological Journal*, *8*(4), 343–407. https://doi.org/10.1080/00071617300650381.

Adey, W.H. & McKibbin, D.L. (1970). Studies on the Maerl Species *Phymatolithon calcareum* (Pallas) nov. comb. and *Lithothamnium coralloides* Crouan in the Ria de Vigo. *Botanica Marina*, *13*(2), 100-106. https://doi.org/10.1515/botm.1970.13.2.100.

Aguilar, R., Pastor, X., de la Torriente, A. & Garcia, S. (2009). Deep-sea coralligenous beds observed with ROV on four seamounts in the Western Mediterranean. *UNEP-MAP-RAC/SPA, Proceedings of the 1st Mediterranean Symposium on the Conservation of the Coralligenous and Others Calcareous Bio-Concretions. Tabarka, Tunis: CAR/ASP Publishing*, 147–149.

Aguirre, J. & Braga, J. C. (2024). Rhodolith Beds in a Shifting World: A Palaeontological Perspective. *Aquatic Conservation: Marine and Freshwater Ecosystems*, *34*(11), e70015. https://doi.org/10.1002/aqc.70015.

Altschul, S.F., Gish, W., Miller, W., Myers, E.W. & Lipman, D.J. (1990). Basic local alignment search tool. *J Mol Biol* 215:403–410.

Ballesteros, E. (1988). Composición y estructura de los fondos de *maërl* de Tossa de Mar (Gerona, España). *Collectanea Botanica*, *17*(2), Article 2. https://doi.org/10.3989/collectbot.1989.v17.137.

Barberá, C., Bordehore, C., Borg, J.A., Glémarec, M., Grall, J., Hall-Spencer, J.M., de la Huz, Ch., Lanfranco, E., Lastra, M., Moore, P.G., Mora, J., Pita, M.E., Ramos-Esplá, A.A., Rizzo, M., Sánchez-Mata, A., Seva, A., Schembri, P.J. & Valle, C. (2003). Conservation and management of northeast Atlantic and Mediterranean maerl beds. *Aquatic Conservation: Marine and Freshwater Ecosystems*, *13*(S1), S65–S76. https://doi.org/10.1002/aqc.569.

Barberá, C., Mallol, S., Vergés, A., Cabanellas-Reboredo, M., Díaz, D. & Goñi, R. (2017). Maerl beds inside and outside a 25-year-old no-take area. *Marine Ecology Progress Series*, *572*, 77–90. https://doi.org/10.3354/meps12110.

Barberá, C., Moranta, J., Ordines, F., Ramón, M., de Mesa, A., Díaz-Valdés, M., Grau, A. M. & Massutí, E. (2012). Biodiversity and habitat mapping of Menorca Channel (western Mediterranean): Implications for conservation. *Biodiversity and Conservation*, *21*(3), 701–728. https://doi.org/10.1007/s10531-011-0210-1.

Basso, D. (1998). Deep rhodolith distribution in the Pontian Islands, Italy: A model for the paleoecology of a temperate sea. *Palaeogeography, Palaeoclimatology, Palaeoecology*, *137*(1), 173–187. https://doi.org/10.1016/S0031-0182(97)00099-0.

Basso, D. (2012). Carbonate production by calcareous red algae and global change. *Geodiversitas*, *34*(1), 13–33. https://doi.org/10.5252/g2012n1a2.

Basso, D., Babbini, L., Kaleb, S., Bracchi, V.A. & Falace, A. (2016). Monitoring deep Mediterranean rhodolith beds. *Aquatic Conservation: Marine and Freshwater Ecosystems*, *26*(3), 549–561. https://doi.org/10.1002/aqc.2586.

Basso, D., Babbini, L., Ramos-Esplá, A.A. & Salomidi, M. (2017). Mediterranean Rhodolith Beds. In R. Riosmena-Rodríguez, W. Nelson, & J. Aguirre (Eds.), *Rhodolith/Maërl Beds: A Global Perspective* (pp. 281–298). Springer International Publishing. https://doi.org/10.1007/978-3-319-29315-8_11.

Basso, D., Fravega, P. & Vannucci, G. (1996). Fossil and living corallinaceans related to the mediterranean endemic speciesLithophyllum racemus (Lamarck)Foslie. *Facies*, *35*(1), 275–292. https://doi.org/10.1007/BF02536965.

Blake, C. & Maggs, C.A. (2003). Comparative growth rates and internal banding periodicity of maerl species (Corallinales, Rhodophyta) from northern Europe. *Phycologia*, *42*(6), 606–612. https://doi.org/10.2216/i0031-8884-42-6-606.1.

Bouckaert, R., Vaughan, T.G., Barido-Sottani, J., Duchêne, S., Fourment, M., Gavryushkina, A., Heled, J., Jones, G., Kühnert, D., Maio, N.D., Matschiner, M., Mendes, F.K., Müller, N.F., Ogilvie, H. A., Plessis, L. du, Popinga, A., Rambaut, A., Rasmussen, D., Siveroni, I., Suchard, M.A., Wu, C.H., Xie, D., Zhang, C., Stadler, T. & Drummond, A.J. (2019). BEAST 2.5: An advanced software platform for Bayesian evolutionary analysis. *PLOS Computational Biology*, *15*(4), e1006650. https://doi.org/10.1371/journal.pcbi.1006650.

Bracchi, V.A., Angeletti, L., Marchese, F., Taviani, M., Cardone, F., Hajdas, I., Grande, V., Prampolini, M., Caragnano, A., Corselli, C. & Basso, D. (2019). A resilient deep-water rhodolith bed off the Egadi Archipelago (Mediterranean Sea) and its actuopaleontological significance. *Alpine and Mediterranean Quaternary*, *32*(2), 131–150. https://doi.org/10.26382/AMQ.2019.09.

Bressan, G. & Babbini L. (2003). Biodiversità marina delle coste Italiane: Corallinales del Mar Mediterraneo: Guida all deteminazione. In *Biologia Marina Mediterranea* (Vol. 10, pp. 1–237). S.I.B.M.

Bulleri, F., Schubert, N., Hall-Spencer, J.M., Basso, D., Burdett, H.L., Francini-Filho, R.B., Grall, J., Horta, P.A., Kamenos, N. A., Martin, S., Nannini, M., Neves, P., Olivé, I., Peña, V., Ragazzola, F., Ribeiro, C., Rinde, E., Sissini, M., Tuya, F. & Silva, J. (2024). Positive species interactions

structure rhodolith bed communities at a global scale. *Biological Reviews*, brv.13148. https://doi.org/10.1111/brv.13148.

Cabanellas-Reboredo, M., Mallol, S., Barberá, C., Vergés, A., Díaz, D. & Goñi, R. (2018). Morpho-demographic traits of two maërl-forming algae in beds with different depths and fishing histories. *Aquatic Conservation: Marine and Freshwater Ecosystems*, *28*(1), 133–145. https://doi.org/10.1002/aqc.2827.

Cabrito, A., Kaleb, S., Peña, V. & Falace, A. (2025). Neotypification of the *Sporolithon mediterraneum* Heydrich (Sporolithales, Corallinophycidae, Rhodophyta) and the status of *Sporolithon* in the Mediterranean Sea. *Aquatic Botany*, *197*, 103839. https://doi.org/10.1016/j.aquabot.2024.103839.

Cabrito, A., de Juan, S., Hinz, H. & Maynou, F. (2024a). Morphological insights into the three-dimensional complexity of rhodolith beds. *Marine Biology*, *171*(6), 127. https://doi.org/10.1007/s00227-024-04437-y.

Cabrito, A., Maynou, F., Simide, R., Mouillot, D., Lossent, J. & de Juan, S. (2024b). Non-extractive fish diversity assessment in Mediterranean rhodolith beds. *Aquatic Conservation: Marine and Freshwater Ecosystems*, *34*(6), e4212. https://doi.org/10.1002/aqc.4212.

Caragnano, A., Rodondi, G., Basso, D., Peña, V., le Gall, L. & Rindi, F. (2020). Circumscription of Lithophyllum racemus (Corallinales, Rhodophyta) from the western Mediterranean Sea reveals the species Lithophyllum pseudoracemus sp. Nov. *Phycologia*, *59*(6), 584–597. https://doi.org/10.1080/00318884.2020.1829348.

Carro, B., Lopez, L., Peña, V., Bárbara, I. & Barreiro, R. (2014). DNA barcoding allows the accurate assessment of European maerl diversity: A Proof-of-Concept study. *Phytotaxa*, *190*(1), 176. https://doi.org/10.11646/phytotaxa.190.1.12.

Chimienti, G., Rizzo, L., Kaleb, S., Falace, A., Fraschetti, S., Giosa, F.D., Tursi, A., Barbone, E., Ungaro, N. & Mastrototaro, F. (2020). Rhodolith Beds Heterogeneity along the Apulian Continental Shelf (Mediterranean Sea). *Journal of Marine Science and Engineering*, *8*(10), 813. https://doi.org/10.3390/jmse8100813.

Costa, A.C.P., Garcia, T.M., Paiva, B.P., Ximenes Neto, A.R. & Soares, M. de O. (2020). Seagrass and rhodolith beds are important seascapes for the development of fish eggs and larvae in tropical coastal areas. *Marine Environmental Research*, *161*, 105064. https://doi.org/10.1016/j.marenvres.2020.105064.

de Juan, S., Ospina-Alvarez, A., Hinz, H., Moranta, J. & Barberá, C. (2023). The continental shelf seascape: A network of species and habitats. *Biodiversity and Conservation, 32*, 1271–1290. https://doi.org/10.1007/s10531-023-02552-8.

Del Río, J., Ramos, D.A., Sánchez-Tocino, L., Peñas, J. & Braga, J. C. (2022). The Punta de la Mona Rhodolith Bed: Shallow-Water Mediterranean Rhodoliths (Almuñecar, Granada, Southern Spain). *Frontiers in Earth Science, 10*, 884685. https://doi.org/10.3389/feart.2022.884685.

Drummond, A.J., Ho, S.Y.W., Phillips, M.J. & Rambaut, A. (2006). Relaxed Phylogenetics and Dating with Confidence. *PLoS Biology 4*(5): e88. https://doi.org/10.1371/journal.pbio.0040088.

Dulin, T., Avnaim-Katav, S., Sisma-Ventura, G., Bialik, O. M. & Angel, D. L. (2020). Rhodolith beds along the southeastern Mediterranean inner shelf: Implications for past depositional environments. *Journal of Marine Systems, 201*, 103241. https://doi.org/10.1016/j.jmarsys.2019.103241.

European Commission: Directorate-General for Environment, European red list of habitats – Results for terrestrial and freshwater habitats, Publications Office, 2016, https://data.europa.eu/doi/10.2779/782848.

Farriols, M. T., Irlinger, C., Ordines, F., Palomino, D., Marco-Herrero, E., Soto-Navarro, J., Jordà, G., Mallol, S., Díaz, D., Martínez-Carreño, N., Díaz, J. A., Fernandez-Arcaya, U., Joher, S., Ramírez-Amaro, S., R. de la Ballina, N., Vázquez, J.-T. & Massutí, E. (2022). Recovery Signals of Rhodoliths Beds since Bottom Trawling Ban in the SCI Menorca Channel (Western Mediterranean). *Diversity*, *14*(1), Article 1. https://doi.org/10.3390/d14010020.

Freshwater, D. W. & Rueness, J. (1994). Phylogenetic relationships of some European Gelidium (Gelidiales, Rhodophyta) species, based on rbcL nucleotide sequence analysis. *Phycologia*, 33(3), 187–194.

Fujisawa, T. & Barraclough, T. G. (2013). Delimiting species using single-locus data and the Generalized Mixed Yule Coalescent approach: A revised method and evaluation on simulated data sets. *Systematic Biology*, 62(5), 707–724. https://doi.org/10.1093/sysbio/syt033.

Gabrielson, P. W., Miller, K.A. & Martone, P.T. (2011). Morphometric and molecular analyses confirm two distinct species of Calliarthron (Corallinales, Rhodophyta), a genus endemic to the northeast Pacific. *Phycologia*, 50(3), 298–316. https://doi.org/10.2216/10-42.1.

Gabrielson, P.W., Maneveldt, G.W., Hughey, J.R. & Peña, V. (2023a). Taxonomic contributions to Hapalidiales (Corallinophycidae, Rhodophyta): *Boreolithothamnion* gen. nov., *Lithothamnion*

redefined and with three new species and *Roseolithon* with new combinations. *Journal of Phycology*, 59(4), 751–774. https://doi.org/10.1111/jpy.13353.

Gabrielson, P.W., Hughey, J.R., Peña, V., Richards, J L., Saunders, G.W., Twist, B., Farr, T. & Nelson, W.A. (2023b). Asia Pacific *Sporolithon* (Corallinophycidae, Rhodophyta) species revised based on DNA sequencing of type specimens and including *S. crypticum sp. Nov.*, *S. immotum sp. Nov*. And *S. nodosum sp. Nov. Phycologia*, 62(6), 593–607. https://doi.org/10.1080/00318884.2023.2225309.

Giorgi, A., Monti, M., Maggioni, D., Gabrielson, P. W., Steneck, R.S., Kocot, K. & Olson, J.B. (2024). DNA sequencing reveals higher taxonomic diversity of coralline algae (Corallinales and Hapalidiales, Rhodophyta) in the tropical western North Atlantic that complicates ecological studies. *Botanica Marina*, 67(6), 561–586. https://doi.org/10.1515/bot-2024-0021.

Guiry, M.D. & Guiry, G.M. 24 February 2024. AlgaeBase. World-wide electronic publication, National University of Ireland, Galway. https://www.algaebase.org; searched on 23 April 2025.

Hall-Spencer, J.M., Grall, J., Moore, P.G. & Atkinson, R.J.A. (2003). Bivalve fishing and maerl-bed conservation in France and the UK retrospect and prospect. *Aquatic Conservation: Marine and Freshwater Ecosystems*, 13(S1), S33–S41. https://doi.org/10.1002/aqc.566.

Hetzinger, S., Grohganz, M., Halfar, J., Hathorne, E., Ballesteros, E. & Kersting, D. K. (2023). Elemental cycles in the coralline alga Neogoniolithon hauckii as a recorder of temperature variability in the Mediterranean Sea. *Frontiers in Marine Science*, 10. https://doi.org/10.3389/fmars.2023.1151592.

Hsieh, T.C., Ma, K.H. & Chao, A. 2016. iNEXT: an R package for rarefaction and extrapolation of species diversity (Hill numbers). *Methods in Ecology and Evolution* 7: 1451-1456. doi: 10.1111/2041-210X.12613.

Illa-López, L., Cabrito, A., de Juan, S., Maynou, F. & Demestre, M. (2023). Distribution of rhodolith beds and their functional biodiversity characterisation using ROV images in the western Mediterranean Sea. *Science of The Total Environment*, 905, 167270. https://doi.org/10.1016/j.scitotenv.2023.167270.

Ingrassia, M., Pierdomenico, M., Casalbore, D., Falese, F. G. & Chiocci, F. L. (2023). A Review of Rhodolith/Maerl Beds of the Italian Seas. *Diversity*, 15(7). https://doi.org/10.3390/d15070859.

Jacquotte, R. (1962). Etude des fonds de maërl de Méditerranée. *Recueil des Travaux de la Station Marine d'Endoume, 26*(41), 141–216.

Jardim, V. L., Grall, J., Barros-Barreto, M.B., Bizien, A., Benoit, T., Braga, J. C., Brodie, J., Burel, T., Cabrito, A., Diaz-Pulido, G., Gagnon, P., Hall-Spencer, J.M., Helias, M., Horta, P.A., Joshi, S., Kamenos, N. A., Kolzenburg, R., Krieger, E. C., Legrand, E., Page, T.M., Peña, V., Ragazzola, F., Rasmusson, L.M., Rendina, F., Schubert, N., Silva, J., Tâmega, F.T.S., Tauran, A. & Burdett, H.L. (2025). A Common Terminology to Unify Research and Conservation of Coralline Algae and the Habitats They Create. *Aquatic Conservation: Marine and Freshwater Ecosystems*, 35(3), e70121. https://doi.org/10.1002/aqc.70121.

Joher, S., Martínez, S. & Rodríguez-Prieto, C. (2023). Bionomic study of the detritic bottoms dominated by macroalgae from the southern coast of Mallorca (Balearic Islands). *Botanica Marina*, 66(1), 37–51. https://doi.org/10.1515/bot-2022-0043.

Letunic, I. & Bork, P. (2024). Interactive Tree of Life (iTOL) v6: Recent updates to the phylogenetic tree display and annotation tool. *Nucleic Acids Research*, gkae268. https://doi.org/10.1093/nar/gkae268.

Martin, C.S., Giannoulaki, M., De Leo, F., Scardi, M., Salomidi, M., Knittweis, L., Pace, M.L., Garofalo, G., Gristina, M., Ballesteros, E., Bavestrello, G., Belluscio, A., Cebrian, E., Gerakaris, V., Pergent, G., Pergent-Martini, C., Schembri, P.J., Terribile, K., Rizzo, L., Ben Souissi, J., Bonacorsi, M., Guarnieri, G., Krzelj, M., Macic, V., Punzo, E., Valavanis, V. & Fraschetti, S. (2014). Coralligenous and maërl habitats: Predictive modelling to identify their spatial distributions across the Mediterranean Sea. *Scientific Reports*, 4(1), 5073. https://doi.org/10.1038/srep05073.

Martin, S. & Hall-Spencer, J.M. (2017). Effects of Ocean Warming and Acidification on Rhodolith/Maërl Beds. In R. Riosmena-Rodríguez, W. Nelson, & J. Aguirre (Eds.), *Rhodolith/Maërl Beds: A Global Perspective* (pp. 55–85). Springer International Publishing. https://doi.org/10.1007/978-3-319-29315-8_3.

McCoy, S.J. & Kamenos, N.A. (2015). Coralline algae (Rhodophyta) in a changing world: Integrating ecological, physiological, and geochemical responses to global change. *Journal of Phycology*, 51(1), 6–24. https://doi.org/10.1111/jpy.12262.

Min-Khant-Kyaw, Kato, A., Adachi, K., Iryu, Y. & Baba, M. (2024). Coralline red algal species diversity at a shallow rhodolith bed in warm-temperate Japan, including two new species of

Roseolithon (Hapalidiales, Corallinophycidae). *Phycologia*, 63(6), 520–533. https://doi.org/10.1080/00318884.2024.2421269.

Nguyen, L.T., Schmidt, H.A., von Haeseler, A. & Minh, B.Q. (2015). IQ-TREE: A fast and effective stochastic algorithm for estimating maximum-likelihood phylogenies. *Molecular Biology and Evolution*, 32(1), 268–274. https://doi.org/10.1093/molbev/msu300.

Pardo, C., López, L., Peña, V., Hernández-Kantún, J., Le Gall, L., Bárbara, I. & Barreiro, R. (2014). A Multilocus Species Delimitation Reveals a Striking Number of Species of Coralline Algae Forming Maerl in the OSPAR Maritime Area. *PLoS ONE*, 9(8), e104073. https://doi.org/10.1371/journal.pone.0104073.

Peña, V., De Clerck, O., Afonso-Carrillo, J., Ballesteros, E., Bárbara, I., Barreiro, R. & Le Gall, L. (2015a). An integrative systematic approach to species diversity and distribution in the genus *Mesophyllum* (Corallinales, Rhodophyta) in Atlantic and Mediterranean Europe. *European Journal of Phycology*, 50(1), 20–36. https://doi.org/10.1080/09670262.2014.981294

Peña, V., Hernandez-Kantun, J.J., Adey, W.H., & Le Gall, L. (2018). Assessment of Coralline Species Diversity in the European Coasts Supported by Sequencing of Type Material: The Case Study of *Lithophyllum nitorum* (Corallinales, Rhodophyta). *Cryptogamie, Algologie*, 39(1), 123–137. https://doi.org/10.7872/crya/v39.iss1.2018.123.

Peña, V., Pardo, C., López, L., Carro, B., Hernandez-Kantun, J., Adey, W.H., Bárbara, I., Barreiro, R., & Le Gall, L. (2015b). *Phymatolithon lusitanicum* sp. nov. (Hapalidiales, Rhodophyta): The Third Most Abundant Maerl-Forming Species in the Atlantic Iberian Peninsula. *Cryptogamie, Algologie*, 36(4), 429–459. https://doi.org/10.7872/crya/v36.iss4.2015.429.

Peña, V., Rousseau, F., De Reviers, B. & Le Gall, L. (2014). First assessment of the diversity of coralline species forming maerl and rhodoliths in Guadeloupe, Caribbean using an integrative systematic approach. *Phytotaxa*, 190(1), 190. https://doi.org/10.11646/phytotaxa.190.1.13.

Pezzolesi, L., Peña, V., Le Gall, L., Gabrielson, P.W., Kaleb, S., Hughey, J.R., Rodondi, G., Hernandez-Kantun, J.J., Falace, A., Basso, D., Cerrano, C. & Rindi, F. (2019). Mediterranean *Lithophyllum stictiforme* (Corallinales, Rhodophyta) is a genetically diverse species complex: Implications for species circumscription, biogeography and conservation of coralligenous habitats. *Journal of Phycology*, 55(2), 473–492. https://doi.org/10.1111/jpy.12837.

Potin, P., Floch, J.Y., Augris, C. & Cabioch, J. (1990). Annual growth rate of the calcareous red alga Lithothamnion corallioides (Corallinales, Rhodophyta) in the Bay of Brest, France. *Hydrobiologia*, 204(1), 263–267. https://doi.org/10.1007/BF00040243.

Puillandre, N., Brouillet, S. & Achaz, G. (2021). ASAP: Assemble species by automatic partitioning. *Molecular Ecology Resources*, 21(2), 609–620. https://doi.org/10.1111/1755-0998.13281.

Rambaut A. 2010. FigTree v1.3.1. (http://tree.bio.ed.ac.uk/software/figtree/).

Rambaut A., Drummond A.J., Xie D., Baele G. & Suchard M.A. (2018). Posterior summarisation in Bayesian phylogenetics using Tracer 1.7. *Systematic Biology*. syy032. https://doi.org/10.1093/sysbio/syy032.

Ramos, D.A.E., Del Río, J., Peñas, J., Peña, V. & Braga, J. C. (2024). Cryptic Diversity of Mediterranean (Corallinales, Corallinophycidae, Rhodophyta). *Aquatic Conservation: Marine and Freshwater Ecosystems*, 34(10), e4255. https://doi.org/10.1002/aqc.4255.

Ramos, D.A.E., Parenden, D., Abas, A.R.E.P., Santiañez, W.J.E., Torres, A.F., Mushlihah, H., Schürholz, D., Peña, V. & Braga, J.C. (2025). Molecular diversity of reef-associated crustose coralline algae (Corallinophycidae, Rhodophyta) of the Spermonde Archipelago, Indonesia. *Phycologia*, 64(1), 40–54. https://doi.org/10.1080/00318884.2025.2469031.

Rebelo, A.C., Johnson, M.E., Rasser, M.W., Silva, L., Melo, C.S. & Ávila, S.P. (2021). Global biodiversity and biogeography of rhodolith-forming species. *Frontiers of Biogeography*, 13(1). https://doi.org/10.21425/F5FBG50646.

Rendina, F., Kaleb, S., Caragnano, A., Ferrigno, F., Appolloni, L., Donnarumma, L., Russo, G. F., Sandulli, R., Roviello, V. & Falace, A. (2020). Distribution and characterization of deep rhodolith beds off the campania coast (SW Italy, mediterranean sea). *Plants*, 9(8), 1–17. Scopus. https://doi.org/10.3390/plants9080985.

Richards, J., Kittle, R.P., Schmidt, W.E., Sauvage, T., Gurgel, C.F.D., Gabriel, D. & Fredericq, S. (2022). Assessment of Rhodolith Diversity in the Northwestern Gulf of Mexico Including the Description of Sporolithon gracile sp. Nov. (Sporolithales, Rhodophyta), and Three New Species of Roseolithon (Hapalidiales, Rhodophyta). *Frontiers in Marine Science*, 9, 906679. https://doi.org/10.3389/fmars.2022.906679.

Rindi, F., Braga, J.C., Martin, S., Peña, V., Le Gall, L., Caragnano, A. & Aguirre, J. (2019). Coralline Algae in a Changing Mediterranean Sea: How Can We Predict Their Future, if We Do Not Know Their Present? *Frontiers in Marine Science*, 6, 723. https://doi.org/10.3389/fmars.2019.00723.

Riosmena-Rodríguez, R., Nelson, W. & Aguirre, J. (Eds.). (2017). *Rhodolith/Maërl Beds: A Global Perspective* (Vol. 15). Springer International Publishing. https://doi.org/10.1007/978-3-319-29315-8.

Ronquist, F., Teslenko, M., van der Mark, P., Ayres, D.L., Darling, A., Höhna, S., Larget, B., Liu, L., Suchard, M.A. & Huelsenbeck, J.P. (2012). MrBayes 3.2: Efficient Bayesian phylogenetic inference and model choice across a large model space. *Systematic Biology*, 61(3), 539–542. https://doi.org/10.1093/sysbio/sys029.

Saunders, G.W. & Moore, T.E. (2013). *Refinements for the amplification and sequencing of red algal DNA barcode and RedToL phylogenetic markers: A summary of current primers, profiles and strategies*. 28(1), 31–43. https://doi.org/10.4490/algae.2013.28.1.031.

Tabone, L., Knittweis, L., Aguilar, R., Alvarez, H., Borg, J.A., Garcia, S., Schembri, P.J. & Evans, J. (2024). Habitat characterization, anthropogenic impacts and conservation of rhodolith beds off southeastern Malta. *Aquatic Conservation: Marine and Freshwater Ecosystems*, 34(4), e4148. https://doi.org/10.1002/aqc.4148.

Tamura, K., Stecher, G., Peterson, D., Filipski, A. & Kumar, S. (2013). MEGA6: Molecular Evolutionary Genetics Analysis version 6.0. *Molecular Biology and Evolution*, 30(12), 2725–2729. https://doi.org/10.1093/molbev/mst197.

Teichert, S. (2014). Hollow rhodoliths increase Svalbard's shelf biodiversity. *Scientific Reports*, 4(1), Article 1. https://doi.org/10.1038/srep06972.

Trégarot, E., D'Olivo, J.P., Botelho, A.Z., Cabrito, A., Cardoso, G O., Casal, G., Cornet, C.C., Cragg, S.M., Degia, A.K., Fredriksen, S., Furlan, E., Heiss, G., Kersting, D.K., Maréchal, J.-P., Meesters, E., O'Leary, B.C., Pérez, G., Seijo-Núñez, C., Simide, R., van der Geest, M. & de Juan, S. (2024). Effects of climate change on marine coastal ecosystems – A review to guide research and management. *Biological Conservation*, 289, 110394. https://doi.org/10.1016/j.biocon.2023.110394.

Torrano-Silva, B.N., Vieira, B.R., Riosmena-Rodríguez, R. & Oliveira, M.C. (2018). Guidelines for DNA barcoding of coralline algae, focusing on Lithophylloideae (Corallinales) from Brazil. *Botanica Marina*, 61(2), 127–140. https://doi.org/10.1515/bot-2017-0040.

Woelkerling, W.J. (1985). A taxonomic reassessment of Spongites (Corallinaceae, Rhodophyta) based on studies of Kützing's original collections. *British Phycological Journal*. https://doi.org/10.1080/00071618500650151.

Xiang, C.Y., Gao, F., Jakovlić, I., Lei, H.P., Hu, Y., Zhang, H., Zou, H., Wang, G.T. & Zhang, D. (2023). Using PhyloSuite for molecular phylogeny and tree-based analyses. *IMeta*, 2(1), e87. https://doi.org/10.1002/imt2.87.

Yoon, H.S., Hackett, J.D. & Bhattacharya, D. (2002). A single origin of the peridinin- and fucoxanthin-containing plastids in dinoflagellates through tertiary endosymbiosis. *Proceedings of the National Academy of Sciences of the United States of America*, 99(18), 11724–11729. https://doi.org/10.1073/pnas.172234799.

Zhang, D., Gao, F., Jakovlić, I., Zou, H., Zhang, J., Li, W.X. & Wang, G.T. (2020). PhyloSuite: An integrated and scalable desktop platform for streamlined molecular sequence data management and evolutionary phylogenetics studies. *Molecular Ecology Resources*, 20(1), 348–355. https://doi.org/10.1111/1755-0998.13096.

Zhang, J., Kapli, P., Pavlidis, P. & Stamatakis, A. (2013). A general species delimitation method with applications to phylogenetic placements. *Bioinformatics (Oxford, England)*, 29(22), 2869–2876. https://doi.org/10.1093/bioinformatics/btt499.

Supplementary Material

Table 2.2.S1. List of specimens sequenced or used in phylogenetic and species delimitation analyses.

Species	**Field Number**	**Collection Data**	GenBank Accession number ***psb*A**	***rbc*L**
Sporolithon mediterraneum Heydrich, 1899.		Italy: Gorgona Island, Thyrrenian Sea. 2018. leg: C.Cecchi. Herbarium voucher: TSB_SPR MDT 1a . **Neotype.**	PQ518784	PQ518785
S. mediterraneum	L1E4	Spain: Menorca Channel, Balearic Islands. 28.vii.2022. Leg. A. Cabrito. MaCoBioS Project – CANAL IV Fieldwork. Herbarium voucher: MA-Algae 11277.	PQ518774	
S.mediterraneum	L1G2	Spain: Menorca Channel, Balearic Islands. 28.vii.2022. Leg. A. Cabrito. MaCoBioS Project – CANAL IV Fieldwork. Herbarium voucher: BC-997459.	PQ518777	
S. mediterraneum	S15E18	Spain: Menorca Channel, Balearic Islands. 29.vii.2022. Leg. A. Cabrito. MaCoBioS Project – CANAL IV Fieldwork. Herbarium voucher: ICMCBMR000710.	PV549190	
S.mediterraneum	S15A12	Spain: Menorca Channel, Balearic Islands. 29.vii.2022. Leg. A. Cabrito. MaCoBioS Project – CANAL IV Fieldwork. Herbarium voucher: BC-997460.	PQ518775	
S. mediterraneum	S13G11	Spain: Menorca Channel, Balearic Islands. 3.viii.2022. Leg. A. Cabrito. MaCoBioS Project – CANAL IV Fieldwork. Herbarium voucher: BC-997461.	PQ518778	PV549195
S. mediterraneum	S13H2	Spain: Menorca Channel, Balearic Islands. 3.viii.2022. Leg. A. Cabrito. MaCoBioS Project – CANAL IV Fieldwork. Herbarium voucher: MA-Algae 11276.	PQ518781	
S. mediterraneum	S15E1	Spain: Menorca Channel, Balearic Islands. 29.vii.2022. Leg. A. Cabrito. MaCoBioS Project – CANAL IV Fieldwork. Herbarium voucher: MA-Algae 11278.	PQ518780	
S. mediterraneum	S13H9	Spain: Menorca Channel, Balearic Islands. 3.viii.2022. Leg. A. Cabrito. MaCoBioS Project – CANAL IV Fieldwork. Herbarium voucher: BC-997462.	PQ518782	
S. mediterraneum	S18E9	Spain: Menorca Channel, Balearic Islands. 1.viii.2022. Leg. A. Cabrito. MaCoBioS Project – CANAL IV Fieldwork. Herbarium voucher: ICMCBMR000711.	PV549191	

S. mediterraneum	S13E3	Spain: Menorca Channel, Balearic Islands. 3.viii.2022. Leg. A. Cabrito. MaCoBioS Project – CANAL IV Fieldwork. Herbarium voucher: ICMCBMR000673	PQ518779	
S. mediterraneum	S15G6a	Spain: Menorca Channel, Balearic Islands. 29.vii.2022. Leg. A. Cabrito. MaCoBioS Project – CANAL IV Fieldwork. Herbarium voucher: ICMCBMR000672.	PQ518776	
S. mediterraneum	S13E1	Spain: Menorca Channel, Balearic Islands. 3.viii.2022. Leg. A. Cabrito. MaCoBioS Project – CANAL IV Fieldwork. Herbarium voucher: ICMCBMR000712.	PV549192	
Sporolithon crypticum G. W. Saunders,J.L. Richards & P.W. Gabrielson, 2023.		Australia: Western Australia, Windy Harbour. 8.xi.2010. leg. G.W. Saunders & K. Dixon. Voucher : GWS024693. **Holotype.**	KY682938	KY682907
Sporolithon amadoi J.L.Richards & R.G.Bahia, 2019.	5_4_18_4_2	USA: Gulf of Mexico, Ewing Bank, Offshore Louisiana. 4.v.2018, 70 m depth. Leg. J.Richards & S.Fredericq. Voucher: LAF_7256. **Paratype.**	MN266235	MN258542
Sporolithon eltorense J.L.Richards & P.W.Gabrielson, 2017		Egypt : El Tor, Gulf of Suez, 1-2 m depth. 8.v.2012. leg. T.Sauvage, W.E.Schmidt & D.Gabriel. Voucher : NCU_606659. **Holotype.**	MF034543	MG051269
Sporolithon ptychoides Heydrich, 1897.		Egypt: El Tor, Gulf of Suez. Leg: Anonymous. Herbarium voucher: TRH_C19-3412. **Lectotype.**		KY994119
S. ptychoides		Egypt: El Tor. 8.v.2012. Leg: T. Sauvage, W. Schmidt & D. Gabriel. Herbarium voucher: NCU:606663.	OQ290695	
Uncultured Corallinales		France: Banyuls sur Mer, Cap Béart. 1.viii.2007. Leg: Bittner,L. Herbarium voucher: LBC0072	GQ917719	
Lithothamnion cf. *valens*	S15A3	Spain: Menorca Channel, Balearic Islands. 29.vii.2022. Leg. A. Cabrito. MaCoBioS Project – CANAL IV Fieldwork. Herbarium voucher: ICMCBMR000708.	PV549152	PV549196
L. cf. *valens*	S18A2	Spain: Menorca Channel, Balearic Islands. 1.viii.2022. Leg. A. Cabrito. MaCoBioS Project – CANAL IV Fieldwork. Herbarium voucher: ICMCBMR000701.	PV549145	PV549197
L. cf. *valens*	L1A3	Spain: Menorca Channel, Balearic Islands. 28.vii.2022. Leg. A. Cabrito. MaCoBioS Project – CANAL IV Fieldwork. Herbarium voucher: ICMCBMR000702.	PV549146	

L. cf. *valens*	S15A2	Spain: Menorca Channel, Balearic Islands. 29.vii.2022. Leg. A. Cabrito. MaCoBioS Project – CANAL IV Fieldwork. Herbarium voucher: ICMCBMR000707.	PV549151	PV549198
L. cf. *valens*	S13A2	Spain: Menorca Channel, Balearic Islands. 3.viii.2022. Leg. A. Cabrito. MaCoBioS Project – CANAL IV Fieldwork. Herbarium voucher: ICMCBMR000706.	PV549150	
L. cf. *valens*	S13A23	Spain: Menorca Channel, Balearic Islands. 3.viii.2022. Leg. A. Cabrito. MaCoBioS Project – CANAL IV Fieldwork. Herbarium voucher: ICMCBMR000704.	PV549148	
L. cf. *valens*	S5A1	Spain: Menorca Channel, Balearic Islands. 2.viii.2022. Leg. A. Cabrito. MaCoBioS Project – CANAL IV Fieldwork. Herbarium voucher: ICMCBMR000705.	PV549149	
L. cf. *valens*	S5I2	Spain: Menorca Channel, Balearic Islands. 2.viii.2022. Leg. A. Cabrito. MaCoBioS Project – CANAL IV Fieldwork. Herbarium voucher: ICMCBMR000703.	PV549147	
L. cf. *valens*	S15A5	Spain: Menorca Channel, Balearic Islands. 29.vii.2022. Leg. A. Cabrito. MaCoBioS Project – CANAL IV Fieldwork. Herbarium voucher: ICMCBMR000709.	PV549153	
Lithothamnion muelleri Lenormand ex Rosanoff, 1866		Australia: Victoria, Western Port Bay. 1851. Leg: W.H. Harvey. Voucher: CN unnumbered. **Lectotype.**		MT199336
Lithothamnion woelkerlingi P.W.Gabrielson & Maneveldt, 2023		Australia: South Australia, Yorke Peninsula, Shell Bay, 23.xi.2011. leg. P. W. Gabrielson. Herbarium voucher: NCU659225. **Holotype.**	OQ694372	OQ694373
Lithothamnion corallioides (P.Crouan & H.Crouan) P.Crouan & H.Crouan 1867		France: Bay of Brest, Subtidal , -6.2m. Muddy bottoms. 20.vii.2010. leg. J.Grall & J.Hernandez. Herbarium voucher: GALW15750	JQ896234	
L. corallioides		France (Britany). 8.iii.2011. Leg: Jacques Grall. Herbarium voucher: SANT-Algae 37963.	KC819264	
L. corallioides		France: La Rochelle. 22.vii.2011. leg. Jourde J. Voucher : LCor11.		NC_072660 (extracted from plastid genome)
L. corallioides	L1C17	Spain: Menorca Channel, Balearic Islands. 28.vii.2022. Leg. A. Cabrito. MaCoBioS Project – CANAL IV Fieldwork. Herbarium voucher: ICMCBMR000714.	PV549155	PV549199

L. corallioides	S5F8	Spain: Menorca Channel, Balearic Islands. 2.viii.2022. Leg. A. Cabrito. MaCoBioS Project – CANAL IV Fieldwork. Herbarium voucher: ICMCBMR000713.	PV549154	
Lithothamnion sp.G from Richards et al., 2016.		USA: Ewing Bank Louisiana. 26.viii.2012. Leg: J. Richards. Voucher: LAF6548	KU557492	
Lithothamnion sp.1	L1H3	Spain: Menorca Channel, Balearic Islands. 28.vii.2022. Leg. A. Cabrito. MaCoBioS Project – CANAL IV Fieldwork. Herbarium voucher: ICMCBMR000732.	PV549141	
Lithothamnion sp.1	S13I13	Spain: Menorca Channel, Balearic Islands. 3.viii.2022. Leg. A. Cabrito. MaCoBioS Project – CANAL IV Fieldwork. Herbarium voucher: ICMCBMR000734.	PV549143	PV549200
Lithothamnion sp.1	S13E14	Spain: Menorca Channel, Balearic Islands. 3.viii.2022. Leg. A. Cabrito. MaCoBioS Project – CANAL IV Fieldwork. Herbarium voucher: ICMCBMR000733.	PV549142	PV549201
Lithothamnion sp.		Italy: Sicily, Capo Gallo. 1.v.2023. Leg: Nadine Schubert. Voucher: VPF02221	PQ299093	
Lithothamnion sp.		Spain: Punta de la Mona, Almunecar. V.2020. Leg: J. Del Rio, J. Pena. Voucher ¿???	PQ593850	
Lithothamnion cf. *minervae*	L1B3	Spain: Menorca Channel, Balearic Islands. 28.vii.2022. Leg. A. Cabrito. MaCoBioS Project – CANAL IV Fieldwork. Herbarium voucher: ICMCBMR000715.	PV549156	
L. cf. *minervae*	S13F1	Spain: Menorca Channel, Balearic Islands. 3.viii.2022. Leg. A. Cabrito. MaCoBioS Project – CANAL IV Fieldwork. Herbarium voucher: ICMCBMR000722.	PV549163	PV549202
L. cf. *minervae*	S13B1	Spain: Menorca Channel, Balearic Islands. 3.viii.2022. Leg. A. Cabrito. MaCoBioS Project – CANAL IV Fieldwork. Herbarium voucher: ICMCBMR000717.	PV549158	
L. cf. *minervae*	S13D1	Spain: Menorca Channel, Balearic Islands. 3.viii.2022. Leg. A. Cabrito. MaCoBioS Project – CANAL IV Fieldwork. Herbarium voucher: ICMCBMR000718.	PV549159	
L. cf. *minervae*	S5D21a	Spain: Menorca Channel, Balearic Islands. 2.viii.2022. Leg. A. Cabrito. MaCoBioS Project – CANAL IV Fieldwork. Herbarium voucher: ICMCBMR000723.	PV549164	
L. cf. *minervae*	S15F2	Spain: Menorca Channel, Balearic Islands. 29.vii.2022. Leg. A. Cabrito. MaCoBioS Project – CANAL IV Fieldwork. Herbarium voucher: ICMCBMR000716.	PV549157	

L. cf. *minervae*	S18B2	Spain: Menorca Channel, Balearic Islands. 1.viii.2022. Leg. A. Cabrito. MaCoBioS Project – CANAL IV Fieldwork. Herbarium voucher: ICMCBMR000719.	PV549160	
L. cf. *minervae*	S18D7	Spain: Menorca Channel, Balearic Islands. 1.viii.2022. Leg. A. Cabrito. MaCoBioS Project – CANAL IV Fieldwork. Herbarium voucher: ICMCBMR000720.	PV549161	PV549203
L. cf. *minervae*	S13B9	Spain: Menorca Channel, Balearic Islands. 3.viii.2022. Leg. A. Cabrito. MaCoBioS Project – CANAL IV Fieldwork. Herbarium voucher: ICMCBMR000721.	PV549162	PV549204
L. cf. *minervae*	S18D10	Spain: Menorca Channel, Balearic Islands. 1.viii.2022. Leg. A. Cabrito. MaCoBioS Project – CANAL IV Fieldwork.	PV549193	
L. cf. *minervae*	S15G6c	Spain: Menorca Channel, Balearic Islands. 29.vii.2022. Leg. A. Cabrito. MaCoBioS Project – CANAL IV Fieldwork. Herbarium voucher: ICMCBMR000672.	PV549194	
L. cf. *minervae*	S5F3	Spain: Menorca Channel, Balearic Islands. 2.viii.2022. Leg. A. Cabrito. MaCoBioS Project – CANAL IV Fieldwork. Herbarium voucher: ICMCBMR000725.	PV549166	
L. cf. *minervae*	S15F4	Spain: Menorca Channel, Balearic Islands. 29.vii.2022. Leg. A. Cabrito. MaCoBioS Project – CANAL IV Fieldwork. Herbarium voucher: ICMCBMR000724.	PV549165	
Lithothamnion sp.2	S5G1	Spain: Menorca Channel, Balearic Islands. 2.viii.2022. Leg. A. Cabrito. MaCoBioS Project – CANAL IV Fieldwork. Herbarium voucher: ICMCBMR000735.	PV549144	
Phymatolithon calcareum (Pallas) W.H. Adey & D.L. McKibbin ex Woelkering & L.M. Irvine 1986		United Kingdom: Falmouth, England. 11.xii.1983. Leg: W.F. Farnham. Voucher: BM000712373. **Neotype.**	JQ896231	KX020487
P. calcareum		France: Trevignon, French Brittany. 13.v.2011. leg. T.Wilfried & Y.Fontana. Voucher: Tre04.		NC_072659 (extracted from plastid genome)
Phymatolithon sp.		Portugal: Madeira, Porto Santo, Baixa das Bicudas. 21.xi.2018. Leg: P. Neves & C. Ribeiro. Voucher: VPF01512	MZ364391	
Phymatolithon sp.		Portugal: Madeira, Porto Santo, Baixa das Bicudas. 9.i.2019. Leg: P. Neves & C. Ribeiro. Voucher: VPF01537	MZ364369	

Phymatolithon sp.		Portugal: Madeira, Porto Santo, Baixa das Bicudas. 21.ix.2018. Leg: P. Neves & C. Ribeiro. Voucher: VPF01495	MZ364370	
Phymatolithon sp.1	L1C9	Spain: Menorca Channel, Balearic Islands. 28.vii.2022. Leg. A. Cabrito. MaCoBioS Project – CANAL IV Fieldwork. Herbarium voucher: ICMCBMR000736.	PV549167	PV549205
Phymatolithon sp.1	S18D1	Spain: Menorca Channel, Balearic Islands. 1.viii.2022. Leg. A. Cabrito. MaCoBioS Project – CANAL IV Fieldwork. Herbarium voucher: ICMCBMR000743.	PV549174	PV549129
Phymatolithon sp.1	S5D7	Spain: Menorca Channel, Balearic Islands. 2.viii.2022. Leg. A. Cabrito. MaCoBioS Project – CANAL IV Fieldwork. Herbarium voucher: ICMCBMR000742.	PV549173	PV549216
Phymatolithon sp.1	S13C1	Spain: Menorca Channel, Balearic Islands. 3.viii.2022. Leg. A. Cabrito. MaCoBioS Project – CANAL IV Fieldwork. Herbarium voucher: ICMCBMR000740.	PV549171	PV549206
Phymatolithon sp.1	S15D1	Spain: Menorca Channel, Balearic Islands. 29.vii.2022. Leg. A. Cabrito. MaCoBioS Project – CANAL IV Fieldwork. Herbarium voucher: ICMCBMR000737.	PV549168	PV549130
Phymatolithon sp.1	S15C8	Spain: Menorca Channel, Balearic Islands. 29.vii.2022. Leg. A. Cabrito. MaCoBioS Project – CANAL IV Fieldwork. Herbarium voucher: ICMCBMR000738.	PV549169	PV549207
Phymatolithon sp.1	S15D2	Spain: Menorca Channel, Balearic Islands. 29.vii.2022. Leg. A. Cabrito. MaCoBioS Project – CANAL IV Fieldwork. Herbarium voucher: ICMCBMR000739.	PV549170	PV549208
Phymatolithon sp.1	S18C8	Spain: Menorca Channel, Balearic Islands. 1.viii.2022. Leg. A. Cabrito. MaCoBioS Project – CANAL IV Fieldwork. Herbarium voucher: ICMCBMR000741.	PV549172	PV549209
Phymatolithon cf. lenormandii (Areschoug) W.H.Adey 1966		Spain: Asturias, Cadavedo. 3.viii.2011. Leg: V. Peña. Herbarium voucher: SANT-Algae 29500.	KT807940	
Phymatolithon laevigatum (Foslie) Foslie 1898		Germany: Helgoland. 29.i.1894. Leg: Kuckuck, P. Herbarium voucher: PC0145173. **Paratype.**	KT807943	
Phymatolithon lusitanicum V. Peña 2015		Spain: Con de Pego, Ría de Vigo, Galicia. 5.iv.2011. Leg: Bárbara, I., Barreiro, R., Peña, V., Published in Pardo et al. (2014) as Phymatolithon sp.3. Herbarium voucher: SANT-Algae 29522. **Holotype.**	KC819260	

P. lusitanicum		Spain: Isla Toralla, Ria de Vigo. 1.xii.1967. Leg: W.H.Adey. Voucher: 36		MH274807
P. lusitanicum	S13C5	Spain: Menorca Channel, Balearic Islands. 3.viii.2022. Leg. A. Cabrito. MaCoBioS Project – CANAL IV Fieldwork. Herbarium voucher: ICMCBMR000744.	PV549175	
P.lusitanicum	S5D15b	Spain: Menorca Channel, Balearic Islands. 2.viii.2022. Leg. A. Cabrito. MaCoBioS Project – CANAL IV Fieldwork. Herbarium voucher: ICMCBMR000749.	PV549180	
P. lusitanicum	S5C2	Spain: Menorca Channel, Balearic Islands. 2.viii.2022. Leg. A. Cabrito. MaCoBioS Project – CANAL IV Fieldwork. Herbarium voucher: ICMCBMR000745.	PV549176	
P. lusitanicum	S15C10	Spain: Menorca Channel, Balearic Islands. 29.vii.2022. Leg. A. Cabrito. MaCoBioS Project – CANAL IV Fieldwork. Herbarium voucher: ICMCBMR000746.	PV549177	
P. lusitanicum	S18C4	Spain: Menorca Channel, Balearic Islands. 1.viii.2022. Leg. A. Cabrito. MaCoBioS Project – CANAL IV Fieldwork. Herbarium voucher: ICMCBMR000748.	PV549179	PV549210
P. lusitanicum	S5C1	Spain: Menorca Channel, Balearic Islands. 2.viii.2022. Leg. A. Cabrito. MaCoBioS Project – CANAL IV Fieldwork. Herbarium voucher: ICMCBMR000747.	PV549178	PV549211
Phymatolithon purpureum (P.Crouan & H.Crouan) Woelkerling & L.M.Irvine 1986		Ireland: Forty Foot beach Sandycove Dublin. 7.v.2014. Leg: J.G. Lee & T.O. Cho. Voucher: CUK11903		MH900244
Phymatolithon lamii (Me.Lemoine) Y.M.Chamberlain 1991		France: St. Servan, Pointe de Cancaval, Rance. 1930. Leg: Lami, R. Herbarium voucher: PC0719024. **Lectotype.**	KT807939	
Roseolithon tupii L.M.Coutinho & Barros-Barreto 2021		Brazil: Ceará, Icapuí, Praia Ponta Grossa, 3.vi.2016, 0.5–2 m depth, leg. L. M. Coutinho. **Holotype.**	MT554650	
R. tupii		Brazil: Bahia, Santa Cruz de Cabrália, Coroa Vermelha, 16.ix.2012, no habitat data, leg. C. Azevedo & F. Nauer. Voucher????		MW316626
Roseolithon crispatum (Hauck) P.W.Gabrielson, Maneveldt, Hughey & V.peña 2023		Croatia: Rovinj (Rovigno), no date, dredged 25 m, leg. F. Hauck. Herbarium voucher: L;943,7-75. **Lectotype.**		OQ694375
R. cf. crispatum			KJ710356	

Roseolithon sp.1	S5X3	Spain: Menorca Channel, Balearic Islands. 2.viii.2022. Leg. A. Cabrito. MaCoBioS Project – CANAL IV Fieldwork. Herbarium voucher: ICMCBMR000726.	PV549135	PV549131
Roseolithon rhodolapidosum J.L.Richards & Fredericq 2022		USA: Sackett Bank, offshore Louisiana. 7.ix.2014. Leg: J.Richards, S.Fredericq. Voucher: LAF_6956B		ON394006
Roseolithon sabulosum Min-Khant-Kyaw, A.Kato & M.Baba 2024		Japan: Shirasu, Minami-Arima, Nagasaki Prefecture. 21.iv.2023. Leg: Min-Khant-Kyaw & A. Kato. Voucher: SAP 115691. **Holotype.**		LC822439
R. sabulosum		Japan: Shirasu, Minami-Arima, Nagasaki Prefecture. 21.iv.2023. Leg: Min-Khant-Kyaw & A. Kato.		LC822442
Roseolithon sp.2	L1F6	Spain: Menorca Channel, Balearic Islands. 28.vii.2022. Leg. A. Cabrito. MaCoBioS Project – CANAL IV Fieldwork. Herbarium voucher: ICMCBMR000727.	PV549136	
Roseolithon sp.2	L1H16	Spain: Menorca Channel, Balearic Islands. 28.vii.2022. Leg. A. Cabrito. MaCoBioS Project – CANAL IV Fieldwork. Herbarium voucher: ICMCBMR000729.	PV549138	
Roseolithon sp.2	L1I10	Spain: Menorca Channel, Balearic Islands. 28.vii.2022. Leg. A. Cabrito. MaCoBioS Project – CANAL IV Fieldwork. Herbarium voucher: ICMCBMR000730.	PV549139	PV549212
Roseolithon sp.2	L1I15	Spain: Menorca Channel, Balearic Islands. 28.vii.2022. Leg. A. Cabrito. MaCoBioS Project – CANAL IV Fieldwork. Herbarium voucher: ICMCBMR000728.	PV549137	
Roseolithon sp.2	S15I11	Spain: Menorca Channel, Balearic Islands. 29.vii.2022. Leg. A. Cabrito. MaCoBioS Project – CANAL IV Fieldwork. Herbarium voucher: ICMCBMR000731.	PV549140	PV549213
Lithothamnion sp. 3 from Neves et al., 2021.		Portugal: Madeira, Madeira, Canical (Pedra d Eira). 9.i.2019. Leg: P.Neves, C. Ribeiro. Voucher: VPF01545	MZ364373	
Lithophyllum nitorum W.H. Adey & P.J. Adey 1973		UK: Port Erin Harbour, Isle of Man. Herbarium voucher: US 70-10B. **Holotype.**	MG648773	
L. nitorum		Spain: Ons, Ría de Pontevedra, Galicia. 7.iv.2011. Leg: I. Bárbara, R. Barreiro, V. Peña. Herbarium voucher: SANT-Algae 31426.	MG648774	
L. nitorum	S18I1	Spain: Menorca Channel, Balearic Islands. 1.viii.2022. Leg. A. Cabrito. MaCoBioS Project – CANAL IV Fieldwork. Herbarium voucher: ICMCBMR000756.	PV549187	PV549132

L. nitorum	S15H7	Spain: Menorca Channel, Balearic Islands. 29.vii.2022. Leg. A. Cabrito. MaCoBioS Project – CANAL IV Fieldwork. Herbarium voucher: ICMCBMR000755.	PV549186	PV549133
Lithophyllum incrustans Philippi 1837		Italy: Sicily. Herbarium voucher: L 943.10.34. **Lectotype.**		KR708575
Lithophyllum incrustans		France: Bay of Brest, Brittany. 20.vii.2010. Leg: J. Grall & J. Hernandez. Herbarium voucher: GALW15746.		KR708543
L. incrustans		France : Marseille. 18.xi.2004. Leg: C.A. Maggs. Herbarium voucher: GALW015735	JQ896236	
Lithophyllum pseudoracemus Caragnano, Rodondi & Rindi 2020		Italy: Gallinara Island, Ligurian Sea. 11.vi.2015. Leg: Carlo Cerrano. Herbarium voucher: FI 058886. **Holotype.**	MT325774	
L. pseudoracemus		Italy: Pontian Islands. 27.vii.2016. Leg: Valentina Bracchi. Herbarium voucher: FI 058890.	MT325778	
L. pseudoracemus	S15G1	Spain: Menorca Channel, Balearic Islands. 29.vii.2022. Leg. A. Cabrito. MaCoBioS Project – CANAL IV Fieldwork. Herbarium voucher: ICMCBMR000751.	PV549182	PV549214
L. pseudoracemus	S18G8	Spain: Menorca Channel, Balearic Islands. 1.viii.2022. Leg. A. Cabrito. MaCoBioS Project – CANAL IV Fieldwork. Herbarium voucher: ICMCBMR000750.	PV549181	PV549215
L. pseudoracemus	S18G9	Spain: Menorca Channel, Balearic Islands. 1.viii.2022. Leg. A. Cabrito. MaCoBioS Project – CANAL IV Fieldwork. Herbarium voucher: ICMCBMR000752.	PV549183	
Lithophyllum racemus (Lamarck) Foslie 1901		Italy: Capri, Gulf of Naples. 1990. Leg: local fisherman. Herbarium voucher: FI 058887. **Neotype.**	MT325777	
L. racemus		Italy: Pontian Islands. 27.vii.2016. Leg: Valentina Bracchi. Herbarium voucher: FI 058894.	MT325781	
L. racemus	S5D10	Spain: Menorca Channel, Balearic Islands. 2.viii.2022. Leg. A. Cabrito. MaCoBioS Project – CANAL IV Fieldwork. Herbarium voucher: ICMCBMR000753.	PV549184	
L. racemus	S5D25	Spain: Menorca Channel, Balearic Islands. 2.viii.2022. Leg. A. Cabrito. MaCoBioS Project – CANAL IV Fieldwork. Herbarium voucher: ICMCBMR000754.	PV549185	PV549134

Spongites fruticulosus		Grece: Rhodos Island. 7.ix.2011. Leg: Le Gall, L. Herbarium voucher: PC0142664.	KJ710351	
Spongites sp.		Italy: Sicily, Capo Gallo. 1.v.2023. Leg: Nadine Schubert. Voucher: VPF02223	PQ299089	
Spongites sp.		Indonesia: Sulawesi, Spermonde Archipelago, Kapoposang. 1.ix.2022. Leg: A. Pratama. Voucher: SA300C		PQ416990
Spongites sp.		Indonesia: Sulawesi, Spermonde Archipelago, Kapoposang. 5.viii.2022. Leg: D.Ramos. Voucher: SA070C		PQ416973
Spongites sp.1	S13I3	Spain: Menorca Channel, Balearic Islands. 3.viii.2022. Leg. A. Cabrito. MaCoBioS Project – CANAL IV Fieldwork. Herbarium voucher: ICMCBMR000757.	PV549188	
Spongites sp.2	S18H10	Spain: Menorca Channel, Balearic Islands. 1.viii.2022. Leg. A. Cabrito. MaCoBioS Project – CANAL IV Fieldwork. Herbarium voucher: ICMCBMR000758.	PV549189	PV549217
Corallinapetra gabrielii (Foslie) S.Y.Jeong, W.A.Nelson, B.Y.Won & T.O.Cho 2021 - Holotype		Australia: Ocean Beach, Phillip Island, Victoria. Iv.1905. Leg: Gabriel. Voucher: TRH B15-2362.	MT199330	MT199335

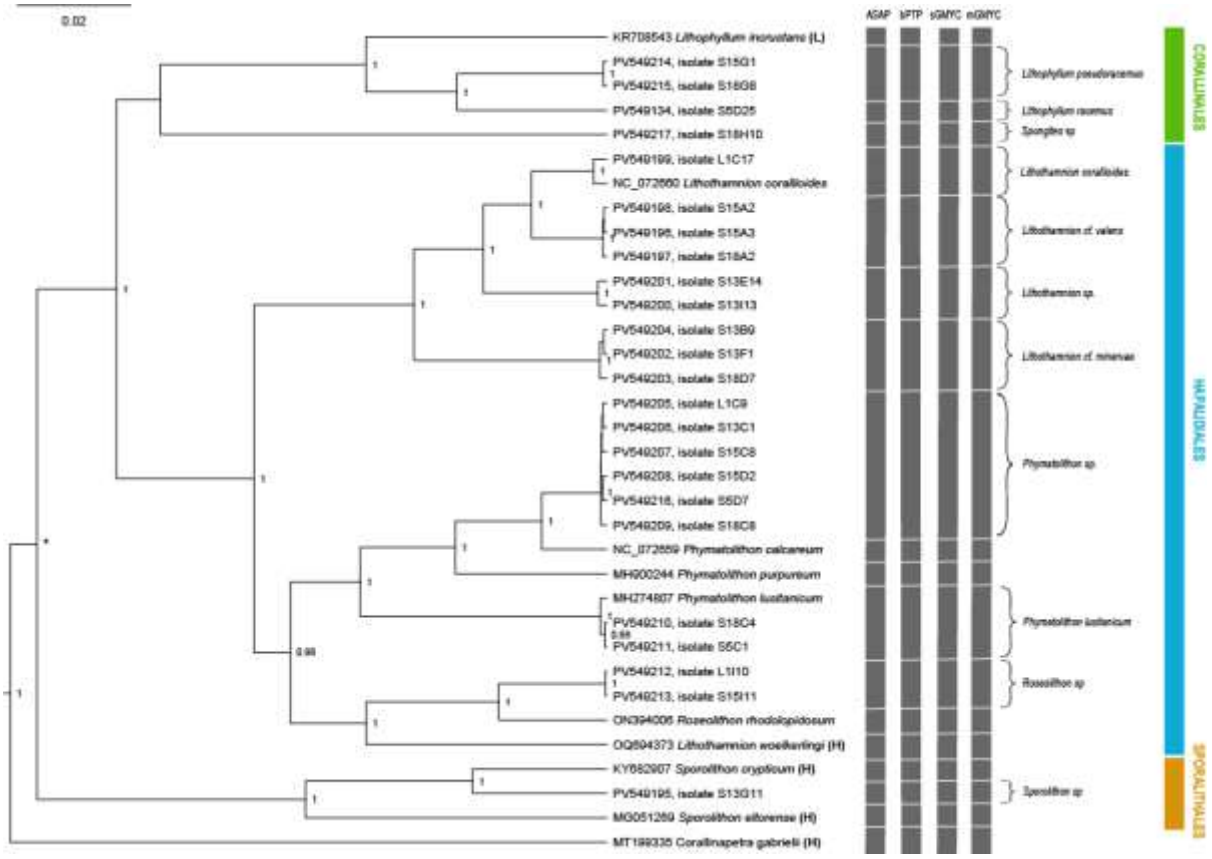


Fig.2.2.S1. Summary of species delimitation analyses obtained with the long *rbc*L database, depicted over the coalescent analyses obtained through BEAST. Numbers in the nodes refer to the posterior probabilities from the

coalescent analysis. Posterior probabilities of < 0.8 were not recorded. Asterisks designate clades that were set up as monophyletic for the coalescent analysis. Vertical grey lines summarized the results from ASAP, bPTP, sGMYC and mGMYC.

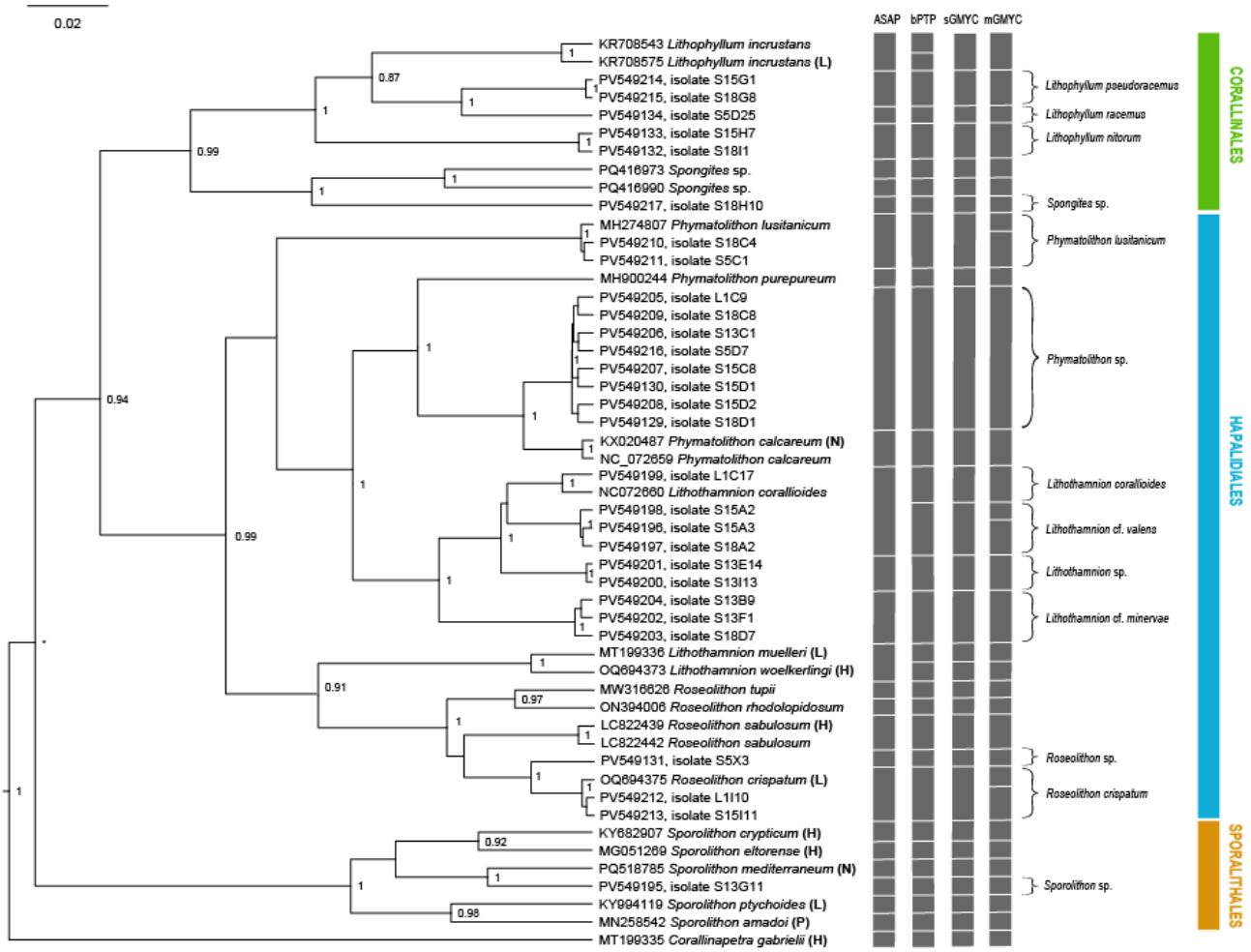


Fig.2.2.S2. Summary of species delimitation analyses obtained with the short rbcL database, depicted over the coalescent analyses obtained through BEAST 2.6.4 (Bouckaert et al.2019). Numbers in the nodes refer to the posterior probabilities from the coalescent analysis. Posterior probabilities of < 0.8 were not recorded. Asterisks designate clades that were set up as monophyletic for the coalescent analysis. Vertical grey lines summarized the results from ASAP, bPTP, sGMYC and mGMYC.

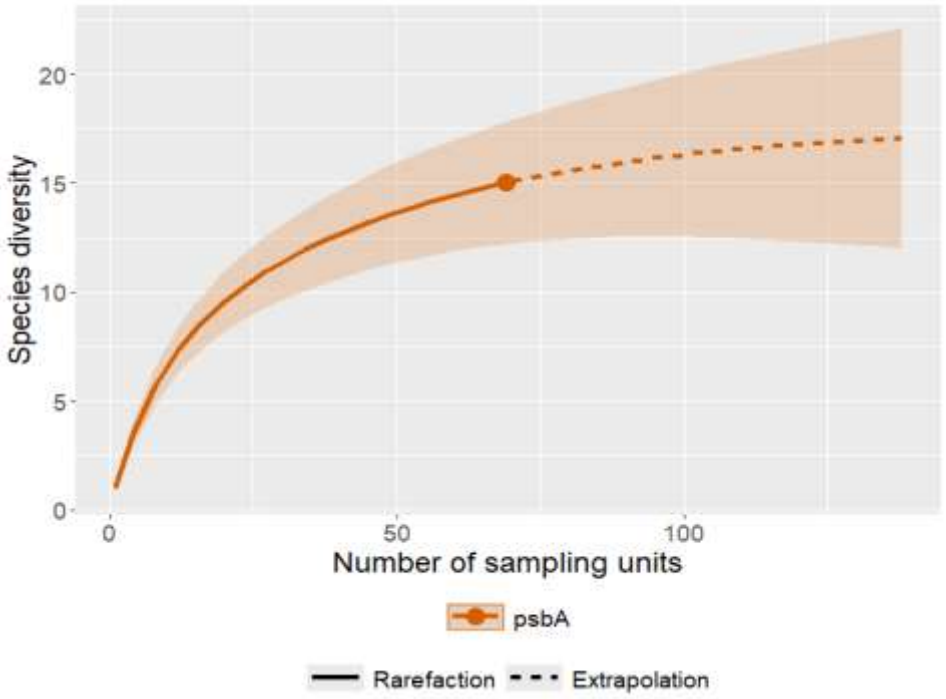


Fig.2.2.S3. Rarefraction curve of species accumulation.

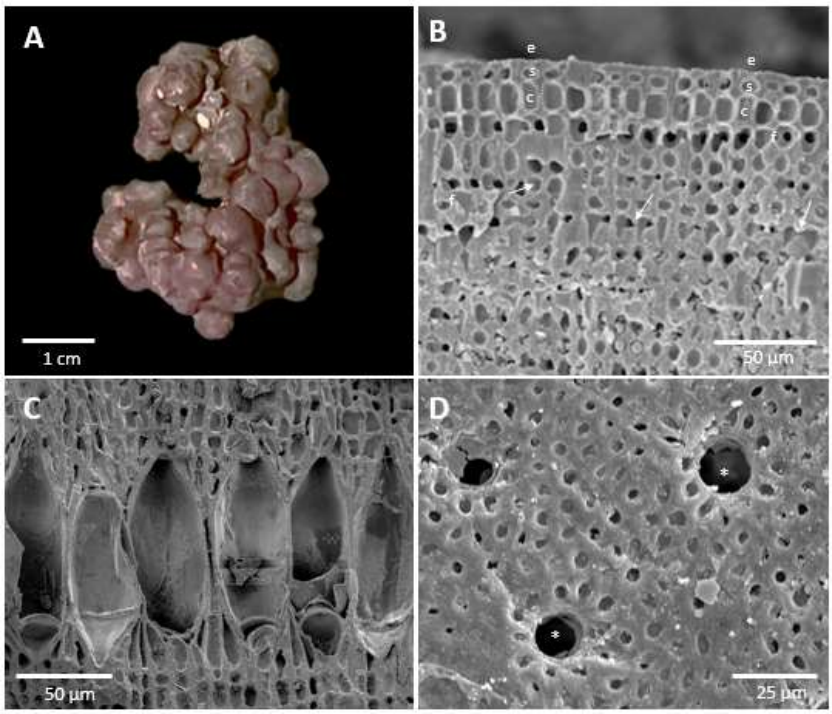


Fig.2.2.S4. (A) Example of praliné specimen collected identified as *Sporolithon mediterraneum*. (B) Vertical section showing flared epithallial cells (e), isodiametric subepithallial cells (s), long cortical cells (c), cell fusions (f) and secondary pit connections (arrows). (C) Vertical sections of empty tetrasporangial compartments subtended by a single stalk cell, and with calcified paraphyses interspersed among them. (D) Surface view of tetrasporangial sori with pores (asterisks) surrounded by rosette cells. B-D: SEM.

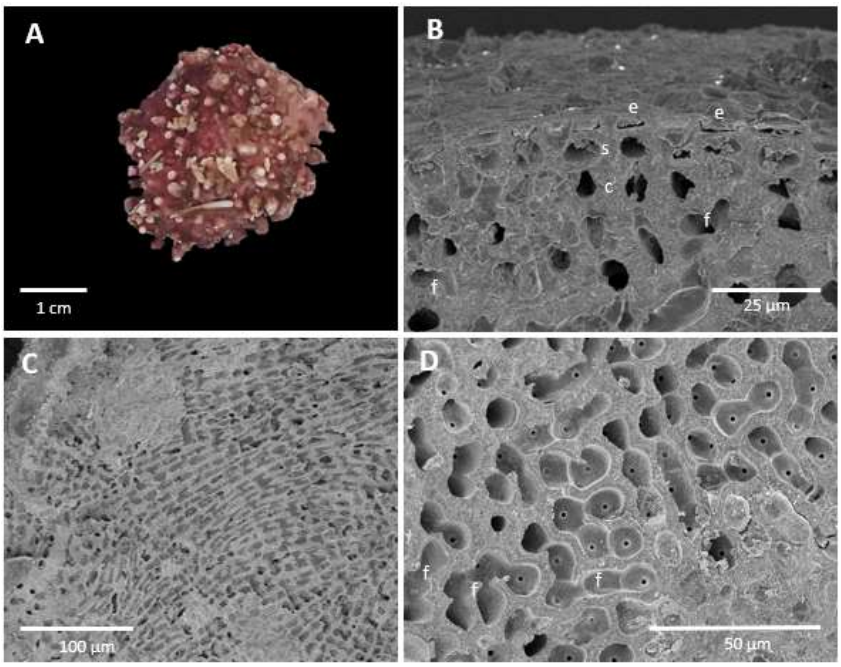


Fig.2.2.S.5. (A) Praliné rhodolith specimen identified as *Lithothamnion corallioides.*(B) Vertical section showing flared epithallial cells (e), rounded subepithallial cells (s) and cortical (c) cells with cell fusions (f). (C) Longitudinal section showing the rectangular spindle-shaped cortical cells. (D) Transversal section of a branch showing numerous cell fusions (f). B-D: SEM.

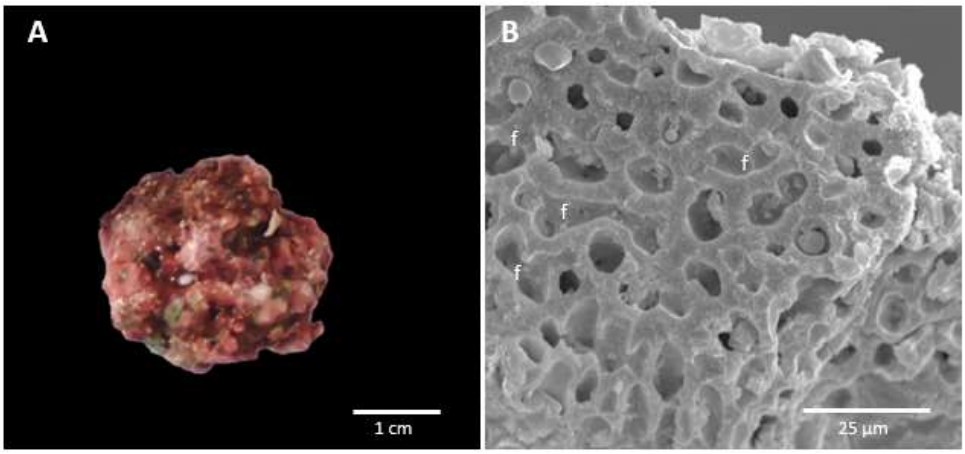


Fig.2.2.S6. (A) Small boxwork rhodolith specimen collected identified as *Lithothamnion* sp.1. (B) SEM of vertical section showing abundant cell fusions between cortical cells of contiguous filaments (f).

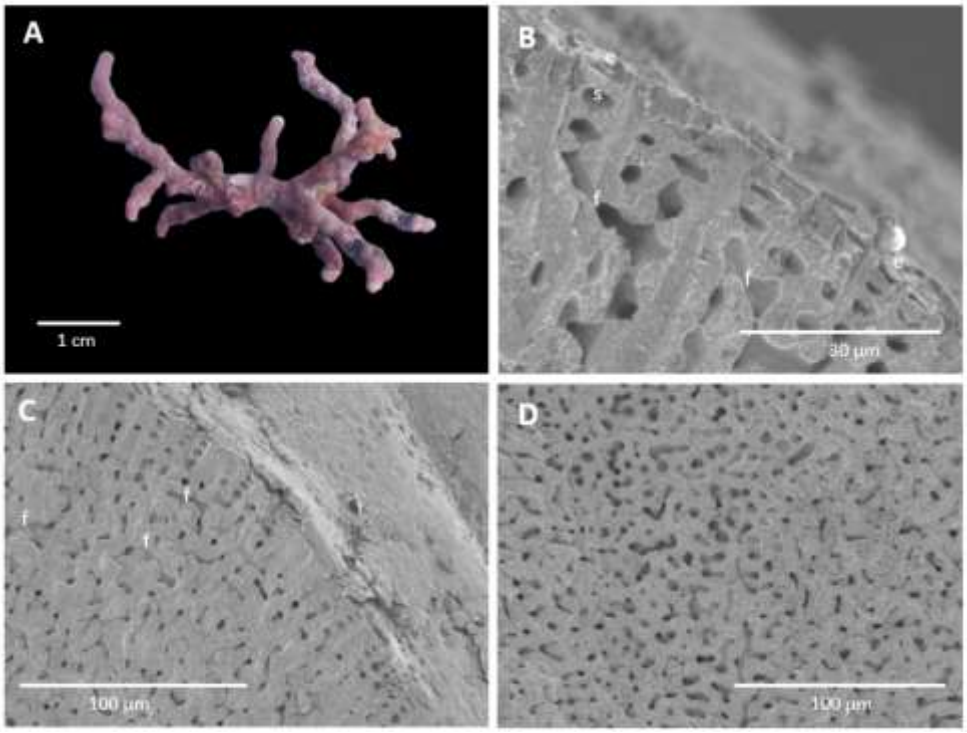


Fig.2.2.S7. (A) Branched rhodolith specimen of *Phymatolithon* sp. (B) Vertical section showing dome-shaped epithallial cells (e), short subepithallial cells (s) and cell fusions (f) between cortical cells of adjacent filaments. (C) Highly calcified vertical section showing filaments of cortical cells and cell fusions (f). (D) Section of a branch showing monomerous, non-coaxial construction. B-D: SEM.

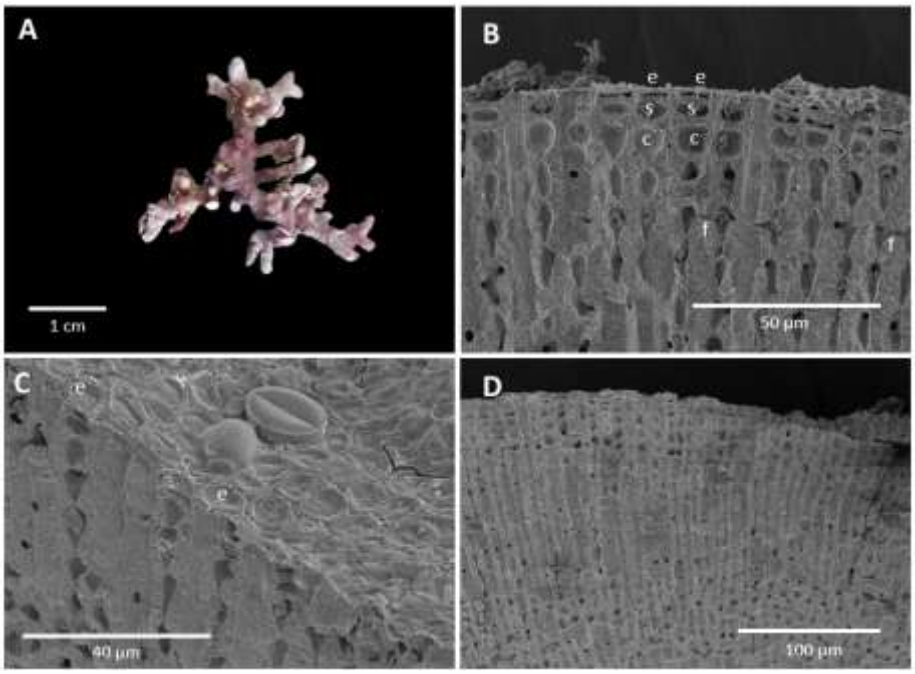


Fig.2.2.S8. (A) Branched rhodoliths specimen of *Phymatolithon lusitanicum*. (B-D) SEM Vertical sections showing flattened epithallial cells (e), subepithallial cells (s) shorter than cells subtending them, and cortical cells (c) of contiguous filaments joined by cell fusions (f).

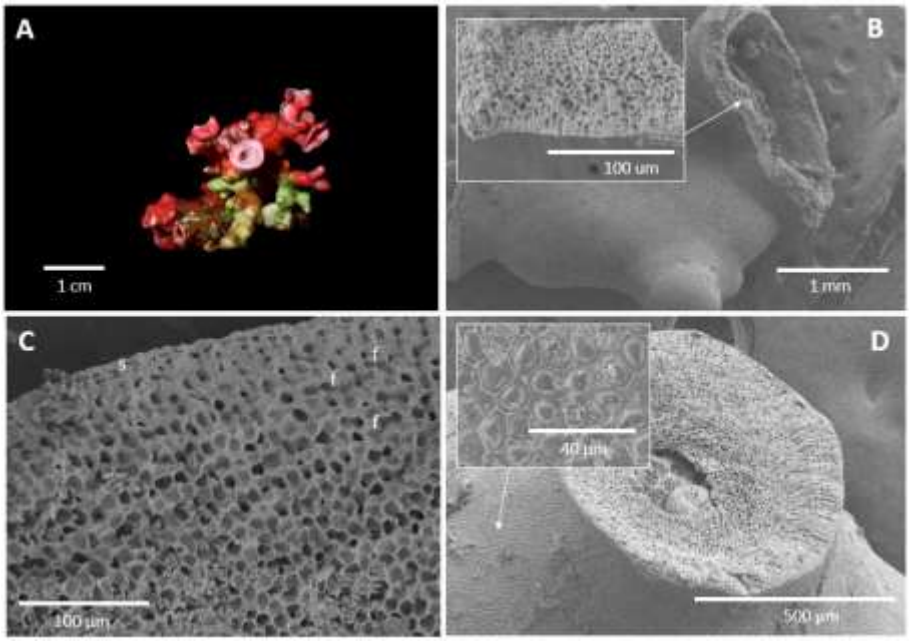


Fig.2.2.S9. (A) S5X3 specimen of *Roseolithon* sp1. Thallus growing in a lamellar form, ending in cone-shaped apices, with weak adherence and free margin. Vertical section showing subepithallial (s) cells as long as cortical cells subtending them and cell fusions (f). (D) A cone-shaped apex and superficial view of epithallial cells. B-D: SEM.

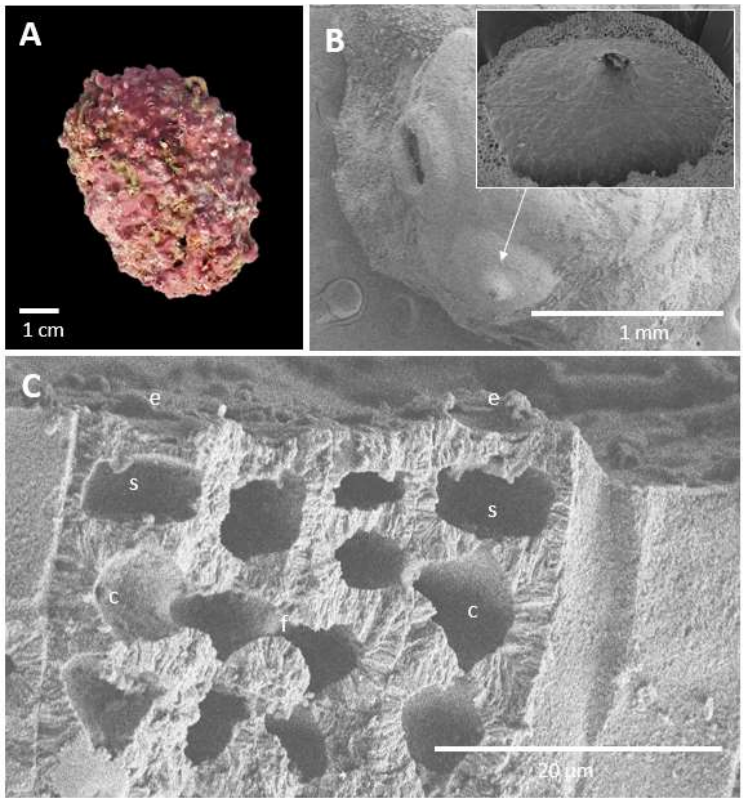


Fig.2.2.S10. (A) Boxwork rhodoliths identified as *Roseolithon* sp2. (B) Surface view showing a protruding uniporate conceptacle, probably carposporangial. (C) Transversal section showing flared epithallial cells (e),

subepithallial cells as long or longer than cortical cells subtending them (s) and cell fusions between cortical cells of adjacent filaments (c). B-C: SEM.

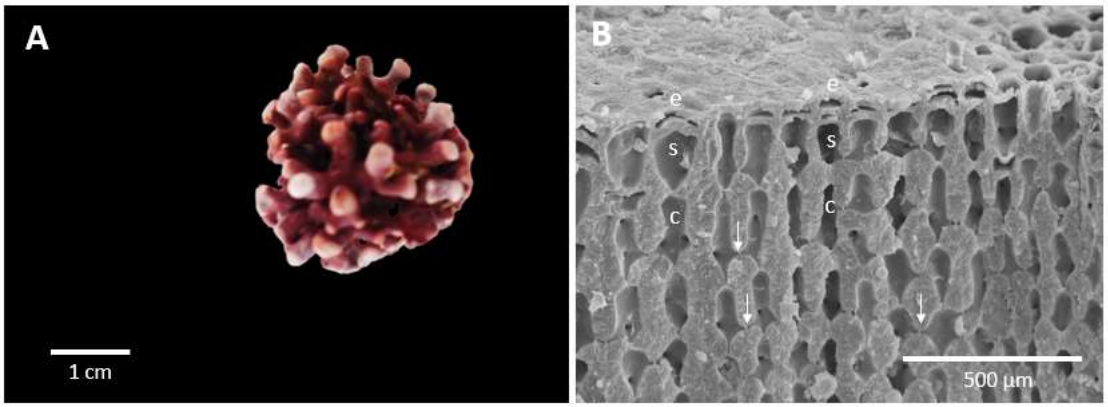


Fig.2.2.S11. (A) Branched specimen identified as *Lithophyllum racemus*. (B) SEM vertical section showing 1-2 layers of flattened to rounded epithallial cells (e), elongated subepithallial (s) and cortical (c) cells joined by secondary pit connections (arrows).

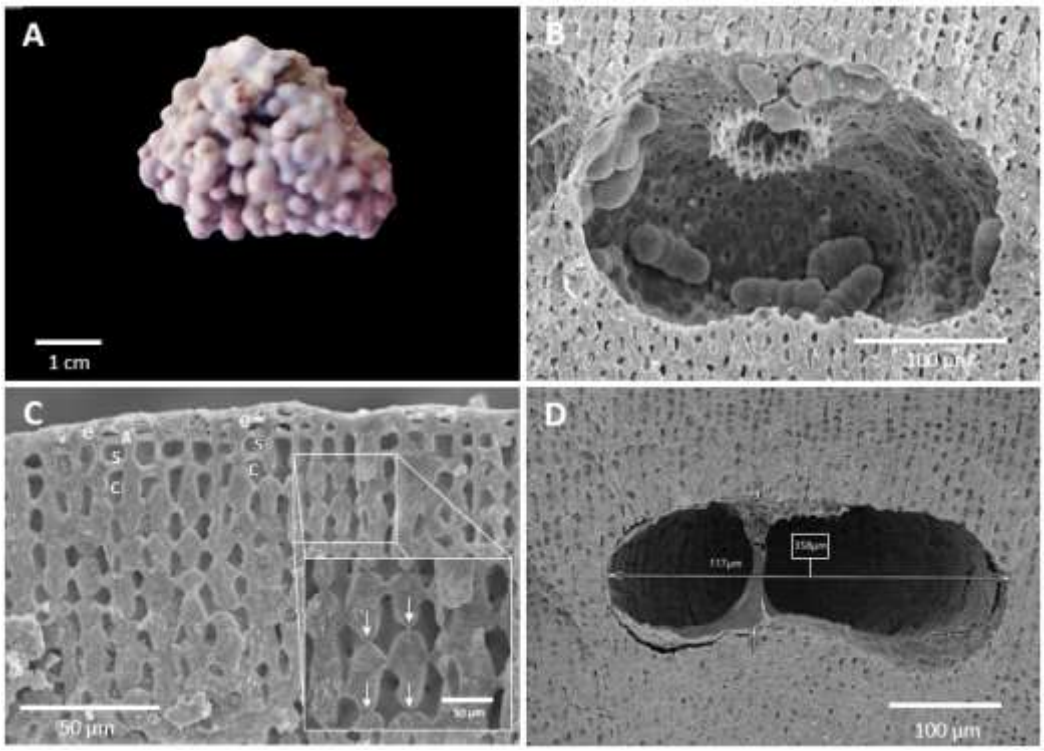


Fig.2.2.S12. (A) Praliné specimen identified as *Lithophyllum pseudoracemus*. (B) Vertical section of a uniporate sporangial conceptacle containing zonate tetrasporangia (tetraspores, i-iv). (C) Vertical section showing 1-2 layers of rounded epithallial cells (e), elongated subepithallial cells (s) and cortical cells (c) joined by secondary pit connections (arrows). (D) Vertical section of an empty uniporate conceptacle with a slightly calcified central columnella. B-D: SEM.

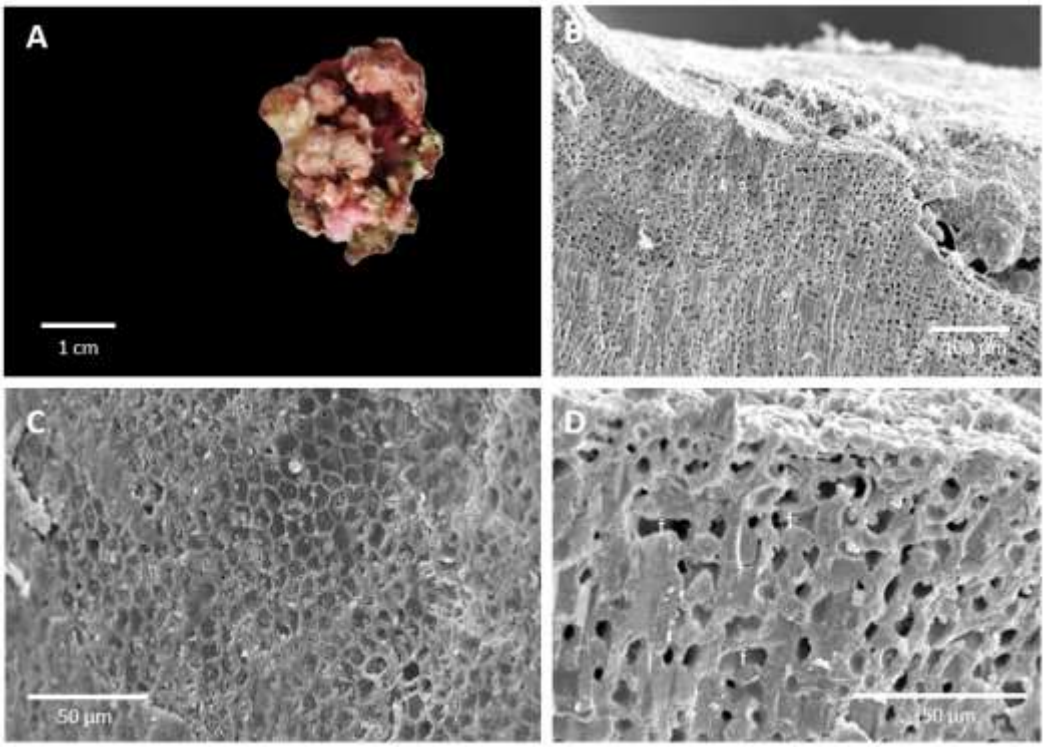


Fig.2.2.S13. (A) Boxwork rhodolith specimen identified as *Spongites* sp.1. (B) Vertical section of the thallus. (C) Surface view of epithallial cells. (D) Vertical section showing cell fusions between cortical cells of contiguous filaments (f). B-D: SEM.

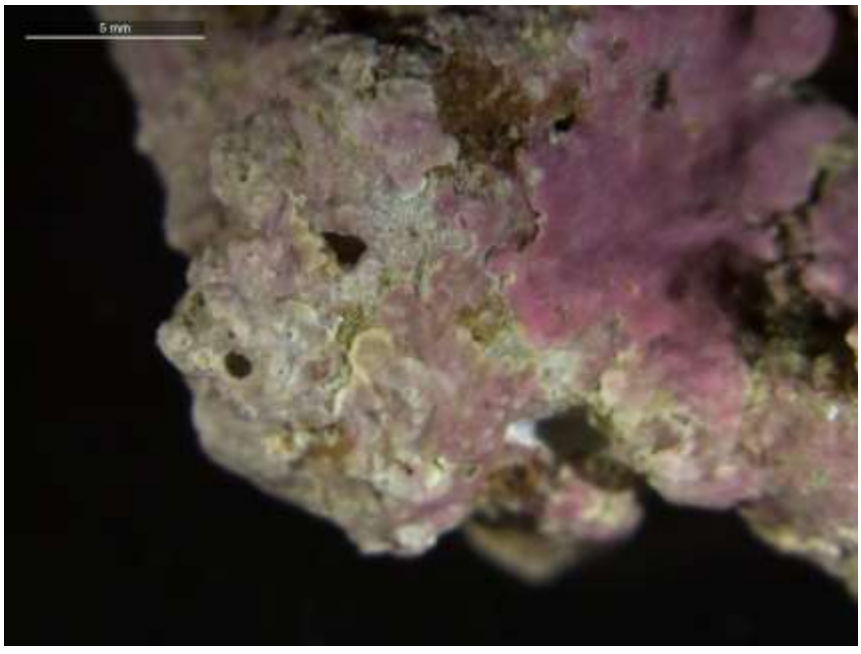


Fig.2.2.S14. Example of a boxwork rhodoliths specimen formed by more than one species.

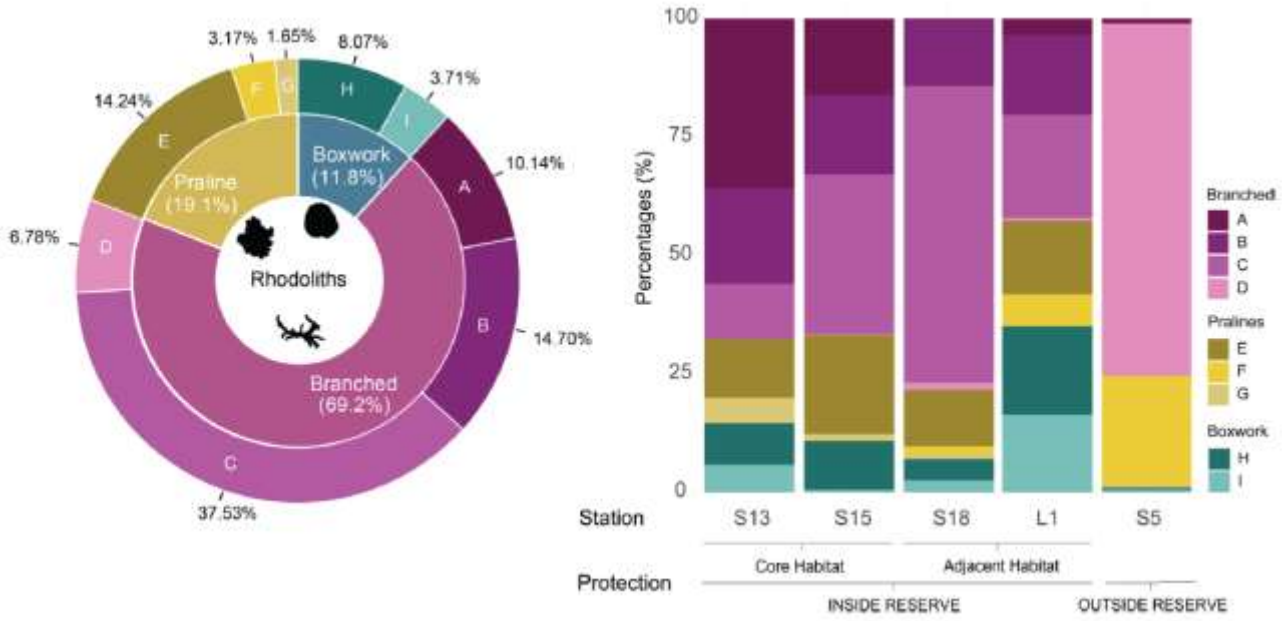


Fig.2.2.S15. Proportions of morphotypes of rhodoliths in the Menorca Channel. Extracted from Cabrito et al. (2024a).

2.3. **CHAPTER III**: Neotypification of the *Sporolithon mediterraneum* Heydrich (Sporolithales, Corallinophycidae, Rhodophyta) and the status of *Sporolithon* in the Mediterranean Sea.

Andrea Cabrito, Sara Kaleb, Viviana Peña, Annalisa Falace

Cabrito, A., *Kaleb, S., Peña, V., Falace, A. (2025). Neotypification of the* Sporolithon mediterraneum *Heydrich (Sporolithales, Corallinophycidae, Rhodophyta) and the status of* Sporolithon *in the Mediterranean Sea. Aquatic Botany, 197, 103839. https://doi.org/10.1016/j.aquabot.2024.103839.*



Abstract

A neotype specimen is designated for the coralline alga *Sporolithon mediterraneum* Heydrich (Sporolithales, Corallinophycidae, Rhodophyta) and critically examined here, since the original holotype specimen apparently has been destroyed. The neotype specimen was collected in a mesophotic rhodolith bed near Gorgona Island (Tyrrhenian Sea, Mediterranean). Additional specimens were collected in a rhodolith bed in the Menorca Channel (Western Mediterranean) and were used to confirm the identification of the neotype. Molecular analyses of *psb*A and *rbc*L with all *Sporolithon* species for which there are currently sequence data, including *S. ptychoides* and *S. molle* supported the designation of this neotype and the circumscription of this Mediterranean species. Additional specimens from Menorca Channel were resolved as conspecific based on *psb*A sequences. The morpho-anatomical data presented indicated that *S. mediterraneum* can be also distinguished from the type species *Sporolithon ptychoides* Heydrich and *Sporolithon molle* (Heydrich) Heydrich, the only two other species previously reported from the Mediterranean Sea, by the occurrence of 5-6 cell paraphyses and larger stalk cells. A consideration of the status of *Sporolithon* in the Mediterranean region is also discussed.

Key words: coralline algae; taxonomy; morpho-anatomy; *psb*A, *rbc*L; rhodoliths

Correspondence:

Andrea Cabrito (ORCID:0000-0002-3429-5201). Institut de Ciències del Mar (ICM-CSIC), Barcelona 08003, Spain. Email: cabrito@icm.csic.es

2.3.1. Introduction

Coralline algae of the genus *Sporolithon* Heydrich (Sporolithales, Corallinophycidae, Rhodophyta) are distributed worldwide, from shallow (1–1.5 m deep) (Basso et al., 2009; Richards et al., 2017) to the lower end of the mesophotic zone (178 m) (Richards et al., 2018). As ecosystem engineers, *Sporolithon* spp. play an important ecological role by contributing to the formation of structurally complex and species-rich marine habitats (i.e, coral reefs, rhodolith beds) (Littler, 1973; Keats & Chamberlain, 1993; Basso et al., 2009; Farr et al., 2009; Amado-Filho et al., 2012; Richards et al., 2017; 2018; 2022; Maneveldt et al., 2017; Fredericq et al., 2019; Leão et al., 2020; Gabrielson et al., 2023). Recent studies have shown that Sporolithon species may also play a critical role in the completion of the life cycle of macro- and microalgae (Fredericq et al., 2019) and in the settlement of coral larvae (Abdul Wahab et al., 2023).

Due to the cryptic diversity of these taxa, it has been emphasized that morpho-anatomical analyses must be combined with DNA sequencing techniques to correctly identify *Sporolithon* species, including type material (Richards et al., 2017; 2022; Gabrielson et al., 2023).

Currently, 31 species of *Sporolithon* are taxonomically recognized (Gabrielson et al., 2023; Guiry & Guiry, 2024), of which only three have been identified in the Mediterranean region, based on morpho-anatomical characters alone, namely *Sporolithon molle* (Heydrich) Heydrich (Di Geronimo & Giaccone 1994) (Di Geronimo & Giaccone, 1994), *Sporolithon mediterraneum* Heydrich (Heydrich, 1899; Lemoine, 1939 as *Archaeolithothamnion mediterraneum* (Heydrich) Foslie; Hamel & Lemoine, 1953 as *A. mediterraneum*, Giaccone et al. 1985) and the type species *Sporolithon ptychoides* Heydrich (Alongi et al., 1996; Bressan & Babbini, 2003; Cormaci et al., 2017).

Based on a critical evaluation of the literature data, Alongi et al. (1996) and Cormaci et al. (2017) considered *S. molle* as a taxon excludendum and *S. mediterraneum* as conspecific with *S. ptychoides*, the latter being the only Mediterranean species of this genus. Instead, Guiry & Guiry (2024), following Athanasiadis (2016), treat *S. mediterraneum* as a distinct species.

Sporolithon mediterraneum was described by Heydrich (1899) (pag. 227) based on a specimen reportedly collected by Dr. Francotte in the Gulf of Naples (Italy, Tyrrhenian Sea, Mediterranean Sea). The type specimen described by Heydrich has been destroyed and it is noteworthy that, according to Hamel & Lemoine (1953) (pag.76), it was actually dredged by Dr. Schleicher in the Gulf of Villefranche (Alongi et al., 1996). Moreover, the specimen collected from the Balearic Islands, and described as *A. mediterraneum* by Lemoine (1939) and Hamel & Lemoine (1953), does not correspond to the genus *Sporolithon* according to the observations of Alongi et al. (1996).

Richards et al. (2017), based on comparative analyses of DNA sequences from *Sporolithon* type specimens showed that DNA sequences of specimens called *S. ptychoides* from other parts of the world

(Brazil, Hawaii, New Caledonia) did not match the lectotype sequence of *S. ptychoides* described from El Tor, Gulf of Suez. In addition, these authors hypothesized that specimens from the Mediterranean Sea that are designated as *S. ptychoides* based on morpho-anatomy are likely a different species. Similarly, based on the lectotype sequence of *S. molle* from El Tor, Gulf of Suez, Gabrielson et al. (2023) confirmed an additional record for Mozambique (Juan de Nova Island) and the misapplication of this name for Brazilian collection.

Herein, based on DNA sequences and morpho-anatomical data, a specimen from a mesophotic rhodolith bed of the Tyrrhenian Sea is described and designated as the neotype of *Sporolithon mediterraneum* since it agrees with the original description by Heydrich (1899). This neotype is also compared with conspecific specimens collected in a rhodolith bed in the Menorca Channel (Western Mediterranean) (**Fig.2.3.S1**). Finally, the status of *Sporolithon* in the Mediterranean is discussed.

2.3.2. Methodology

2.3.2.1. Examined Specimens

Collections from mesophotic rhodolith beds were conducted in the Tyrrhenian Sea and Menorca Channel, Mediterranean Sea, in 2018 and 2022 by scuba diving or naturalist dredge, between 50-75 m depth. Ten specimens identified as *Sporolithon* were carefully measured, photographed and subsequently air-dried and preserved in zip bags with silica gel for morpho-anatomical and molecular analyses.

2.3.2.2. Morpho-anatomical analyses

For the Tyrrhenian neotype specimen (TSB_SPR MDT 1a, the herbarium acronym follows the Index Herbariorum online, continuously updated (Thiers, 2024)), scanning electron microscopy was performed with a Zeiss Gemini300 Scanning Electron Microscope (SEM) at a working distance (WD) between 8 and 11 mm. Rhodolith fragments were mounted on aluminium stubs and coated with a thin chromium layer using Quorum Q150T ES coater. For the specimens collected in the Menorca Channel (**Fig.2.3.S1**), scanning electron microscopy was performed using the microscopes JSM 6400 (Jeol, Japan) and Hitachi S-3500N (Hitachi High-Technologies Co., Japan) at a WD of 14 mm. Rhodolith fragments were mounted on both carbon and aluminium stubs using carbon tape as adhesive and were coated with a 15 nm gold layer using Quorum Q150R S sputter coater (Quorum Technologies Ltd.). Cell size was measured using SEM micrographs according to Irvine & Chamberlain (1994). Twenty cells of each vegetative cell type (epithallial, perithallial and hypothallial) were measured in the Gorgona specimen and in five of the nine Menorca Channel individuals. For the reproductive features (sporangial chamber, talk cells) and for the paraphyses, the measurements were made on 2 to 8 sporangial compartments per specimen. Samples used for light microscopy were decalcified in 10% nitric acid, and cryostatic frozen sections were prepared with a cryomicrotome (Leica CM3050 S).

2.3.2.3. DNA sequencing and analyses

A fragment of each preserved specimen was cleaned under a stereomicroscope and selected surfaces were ground for DNA extraction. Genomic DNA was extracted using a NucleoSpin® Tissue kit (Macherey-Nagel, GmbH and Co. KG, Germany), following the manufacturer's protocol. The *psb*A locus was PCR-amplified for all specimens by using the primer pair *psb*A-F1/*psb*A-R1 (Yoon et al., 2002) and the Supreme NZYTaq II 2x Colourless Master Mix (NZYtech) following the thermal profile for PCR reactions used by Peña et al. (2015). The *rbc*L sequence of the specimen of the Tyrrhenian Sea was obtained with the primer combination F1150Cor - RbcS-Start yielding a fragment trimmed to 293 bp (1172-1464) and followed Saunders & Moore (2013) for amplification. PCR products were purified and sequenced by the Sanger method by GenoScreen (GenoScreen Innovative Genomics, France) and by the molecular biology service of Universidade da Coruña (Spain). Sequences were assembled, aligned and trimmed using MEGA v.6 (Tamura et al., 2013) or SeaView version 4 (Gouy et al., 2010), and were submitted to GenBank (accession numbers listed in **Table 2.3.S1**). Two data sets were built for each for gene (*psb*A, *rbc*L), comprising sequences obtained in this study and GenBank sequences publicly available for Sporolithon species. The Rhodogorgonales taxa Rhodogorgon carriebowensis J.N. Norris & Bucher 1989, R. ramosissima J.N. Norris & Bucher 1989 and Renouxia marerubra D. Gabriel, J.N. Norris & Fredericq 2019 were used as outgroup (**Table 2.3.S1**).

Phylogenetic relationships were inferred with maximum likelihood (ML) using IQ-TREE v2.2.0 (Nguyen et al., 2015) or MEGA v.6 software (Tamura et al., 2013). Bayesian Inference (BI) was obtained using MrBayes v3.2.7a (Ronquist et al., 2012). Models of sequence evolution were estimated using the Akaike Information Criterion (AIC) and the Bayesian Information Criterion (BIC) obtained in jModeltest 2.1.3 (Darriba et al., 2012) and with ModelFinder in PhyloSuite (Zhang et al., 2020). ML of the *psb*A alignment was performed under a generalized time-reversible GTR+F model for 1000 standard bootstraps. BI for the *psb*A alignments were performed under a generalized time-reversible GTR+F model (two parallel runs, with four Markov Chain Monte Carlo method for two million generations), in which the initial 20% of sampled data were discarded as burn-in. Both ML and BI analysis of *psb*A were performed using PhyloSuite software (Zhang et al., 2020; Xiang et al., 2023). The resulting trees were visualized and edited by Interactive Tree Of Life (iTOL) v5 (Letunic & Bork, 2024) online tool. For the *rbc*L alignment, ML was performed under a generalized time-reversible with invariant sites heterogeneity model (GTR+I+G); BI was performed under the same model (GTR+I+G) with four Markov Chain Monte Carlo method for 10 million generations, and tree sampling every 1000 generations.

2.3.3. Results

The *psb*A alignment of 29 sequences, ranged from 508 to 862 base pairs (bp), and consisted of 22 haplotype sequences with 251 variable sites and 186 parsimonious informative sites. The uncorrected

p-distance within the Mediterranean specimens was among 0 – 0.6%. Both ML and BI of *psb*A data were congruent in resolving the Mediterranean specimens as conspecific, and as an independent lineage from other *Sporolithon* species (**Fig.2.3.1**). Both ML and BI analysis resolved the Mediterranean Sporolithon in a clade encompassing *S. howei, S. franciscanum, S. crypticum* and *S. eltorense*.

The *rbc*L alignment comprised 35 sequences, ranging from 260 to 297 bp, with 114 variable sites. Both ML and BI resolved the Mediterranean *Sporolithon* as a separate lineage from remaining *Sporolithon*, most of them represented by type specimens, including *S. ptychoides* and *S. molle* both described originally from El Tor, Gulf of Suez, and reported for the Mediterranean based on morpho-anatomical characters. The sequenced Mediterranean species is resolved in a clade containing *S. franciscanum, S. eltorense, S. dimotum, S. crypticum* and *S. sibogae* although with weak or no support by the analyses (**Fig.2.3.2**).

Given that the *psb*A and *rbc*L sequences circumscribed a Mediterranean species of Sporolithon, we propose, according to Article 9.8 of the International Code of Nomenclature for algae, fungi, and plants (Turland et al., 2018), the specimen from the Gorgona rhodolith bed as the neotype of S. mediterraneum (TSB_SPR MDT 1a).

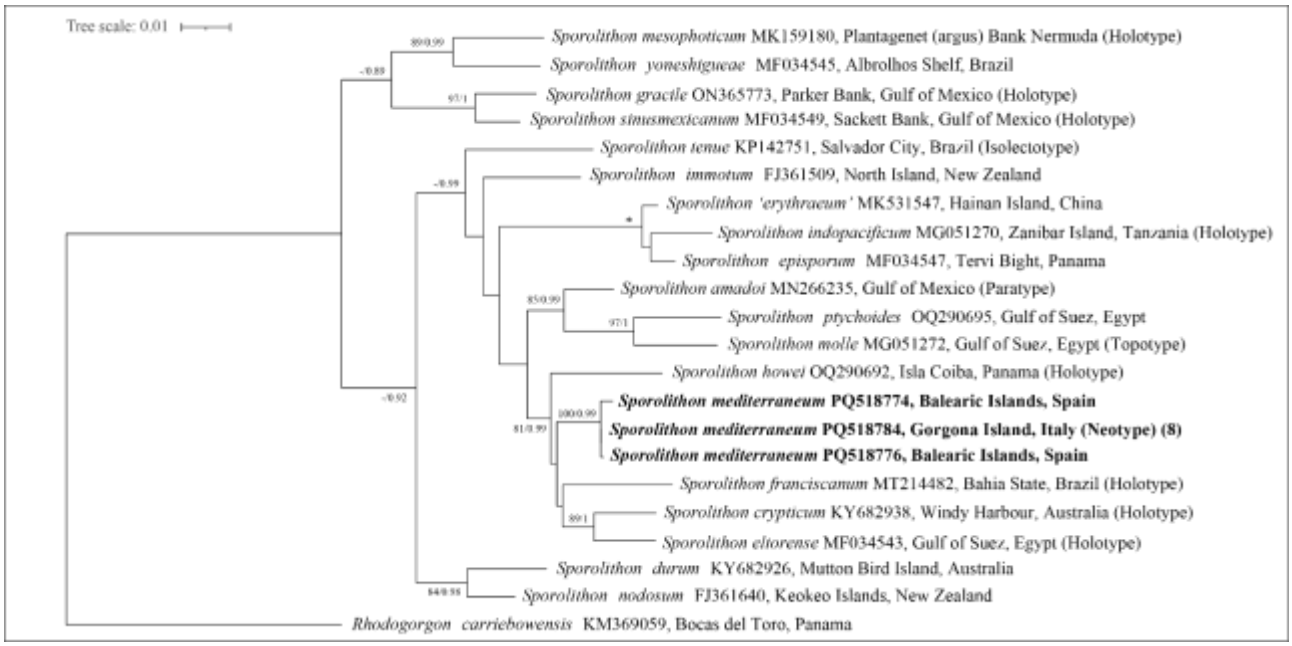


Fig.2.3.1. Phylogenetic tree inferred from ML and BI analyses of *psb*A sequences of *Sporolithon*. In bold, the neotype of *Sporolithon mediterraneum* representing a group of eight individuals sharing the same haplotype and two other haplotypes from Menorca Channel. Bootstrap ML values > 75% and posterior probabilities > 0.70 from BI are shown for each node. *Rhodogorgon carriebowensis* was used as outgroup. Specific epithets of names not linked to type specimen are in single quotes.

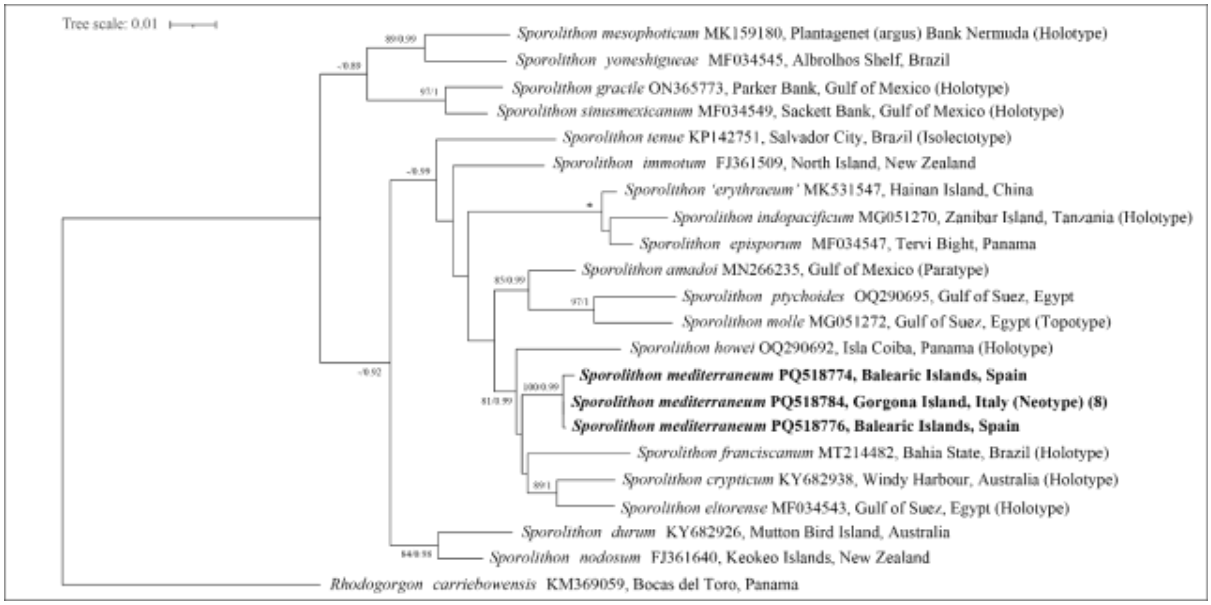


Fig.2.3.2. Phylogenetic tree inferred from ML and BI analyses of *rbc*L sequences of *Sporolithon*. In bold, the neotype of *Sporolithon mediterraneum*. Bootstrap ML values > 60% and posterior probabilities > 0.60 from BI are shown for each node. *Rhodogorgon ramosissima* were used as outgroup. Specific epithets of names not linked to type specimen are in single quotes.

***Sporolithon mediterraneum* Heydrich**

Homotypic synonyms: Archaeolithothamnion mediterraneum (Heydrich) Foslie 1901 (Foslie, 1900); *Peyssonnelia mediterranea (Heydrich)* Foslie 1905

Neotype: TSB_SPR MDT 1a. Sampled on a rhodolith bed, 50m deep, leg. Enrico Cecchi. Tetrasporophyte.

Collection date: 2018.

*DNA sequences: psb*A GenBank Accession #PQ518784; *rbc*L GenBank Accession #PQ518785.

Neotype locality: Gorgona island, Tyrrhenian Sea, Italy (43°25'21.385 N, 9°53'24.327 E).

Additional collections: Voucher BC-997461 (psbA GenBank Accession #PQ518778), Menorca Channel, Balearic Sea, Spain, 62 m depth, leg. Andrea Cabrito, 03/08/2022, tetrasporophyte. Voucher BC-997462 (*psb*A GenBank Accession #PQ518782), Menorca Chanel, Balearic Sea, Spain, 62 m depth, leg. Andrea Cabrito, 03/08/2022, tetrasporophyte. Voucher MA-Algae 11276 (*psb*A GenBank Accession #PQ518781), Menorca Chanel, Balearic Sea, Spain, 62 m depth, leg. Andrea Cabrito, 03/08/2022, tetrasporophyte. Voucher ICMCBMR000673 (*psb*A GenBank Accession #PQ518779), Menorca Chanel, Balearic Sea, Spain, 62 m depth, leg. Andrea Cabrito, 03/08/2022, tetrasporophyte. Voucher MA-Algae 11278 (*psb*A GenBank Accession #PQ518780), Menorca Chanel, Balearic Sea, Spain, 58 m depth, leg. Andrea Cabrito, 29/07/2022, tetrasporophyte. Voucher BC-997460 (*psb*A GenBank Accession #PQ518775), Menorca Chanel, Balearic Sea, Spain, 58.6 m depth, leg. Andrea Cabrito, 29/07/2022, tetrasporophyte. Voucher ICMCBMR000672 (*psb*A GenBank Accession #PQ518776), Menorca Chanel, Balearic Sea, Spain, 58.6 m depth, leg. Andrea Cabrito, 29/07/2022,

reproductive features not observed. Voucher BC-997459 (*psb*A GenBank Accession #PQ518777), Menorca Chanel, Balearic Sea, Spain, 74 m depth, leg. Andrea Cabrito, 28/07/2022, tetrasporophyte. Voucher MA-Algae 11277 (*psb*A GenBank Accession #PQ518774), Menorca Chanel, Balearic Sea, Spain, 74 m depth, leg. Andrea Cabrito, 28/07/2022, tetrasporophyte.

Habit and vegetative anatomy:

Thallus encrusting, smooth to warty, forming a rhodolith (**Fig.2.3.3A**). The rhodolith is formed by two superimposed layers of thalli, both belonging to S. mediterraneum. The one from the upper layer is the neotype described here. Thallus construction monomerous, with a 3-5 cells-layered non-coaxial hypothallium (**Fig.2.3.3B**). Hypothallial cells rectangular, 28.7-35.6 µm long and 3.9-4.9 µm wide. Perithallial cells 6.8-12.6 µm long and 5.9-10 µm wide. Adjacent hypothallial and perithallial cells linked by cell fusions and secondary pit connections (**Fig.2.3.3C,D**). Intercalary meristematic cells isodiametric or more flattened, 2-5.8 µm long and 7.3-11.7 µm wide (**Fig.2.3.3D**). Epithallium consists of a single layer of cells with thick, heavily calcified cell walls and a small trapezoidal lumen, 1.8-2.8 µm long and 6.7-10.8 µm wide (**Fig.2.3.3D**).

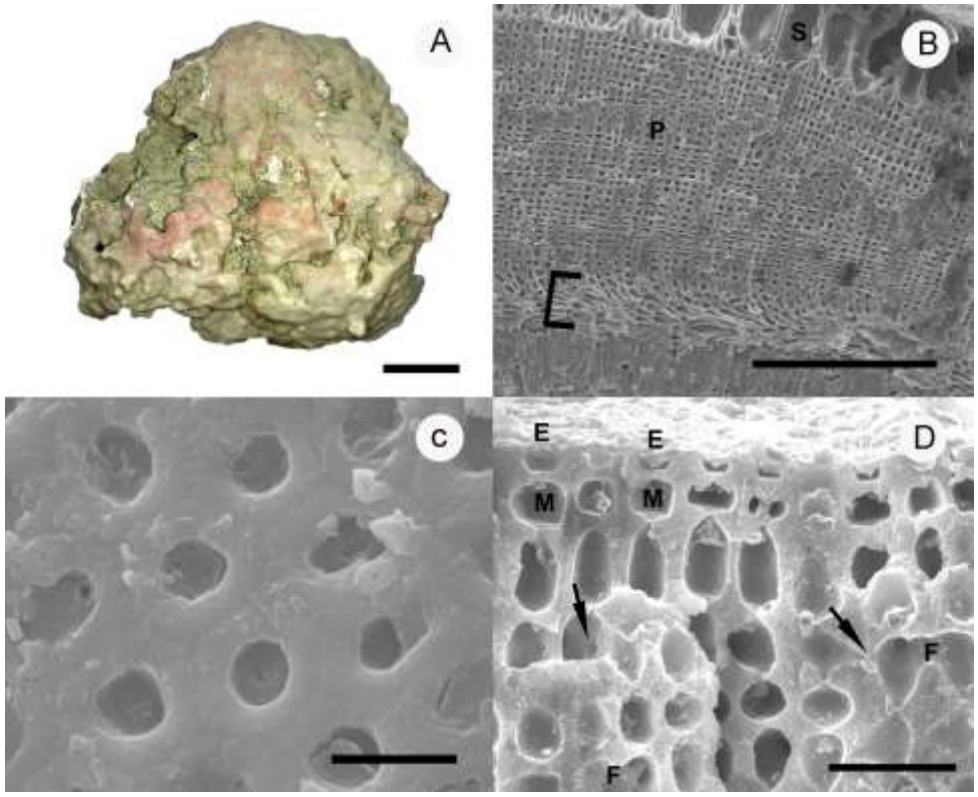


Fig.2.3.3. *Sporolithon mediterraneum* Neotype (TSB_SPR MDT 1a). a. Thallus habit. Scale bar: 2 cm. b. Scanning electron micrograph (SEM) of a vertical fracture of the upper thallus with non-coaxial hypothallium (bracket), perithallial filaments (P), and a sorus with tetrasporangia (S). Scale bar: 200 µm. c. Epithallus in surface view with rounded cells. Scale bar: 10 µm. d. SEM of vertical section showing armored epithallial cells (E), isodiametric meristematic cells (M), perithallial cells with cell fusions (F) and secondary pit connections (arrows). Scale bar: 20 µm.

Reproduction:

Tetrasporangia in calcified compartments grouped in sori. Sori protrude above the surrounding thallus surface (**Fig.2.3.4A,B**). Tetrasporangial pores in surface view 10.3-13.8 in diameter, surrounded by 9–12 rosette cells (N= 20, **Fig.2.3.4C**). Tetrasporangial compartments elliptical to "lemon-shaped" 39–56 µm in diameter and 75–108 µm in height (N= 8) (**Fig.2.3.4D**), subtended by a single triangular stalk cell 21.9-25.5 µm long x 24.2-35.9 µm wide (N= 8) (**Fig.2.3.4D,E**). Tetrasporangial compartments borne among a layer of elongated cells and are separated by 0–3 vegetative calcified filaments (paraphyses) (**Fig.2.3.4D**). Paraphyses consist of 5–6 cells that are mainly clavate, roundish only in the apical part of the filament. Tetrasporocytes (**Fig.2.3.4E,F**) develop into cruciate tetrasporangia (**Fig.2.3.4G**). Tetrasporangial compartments unshed and buried after spore release.

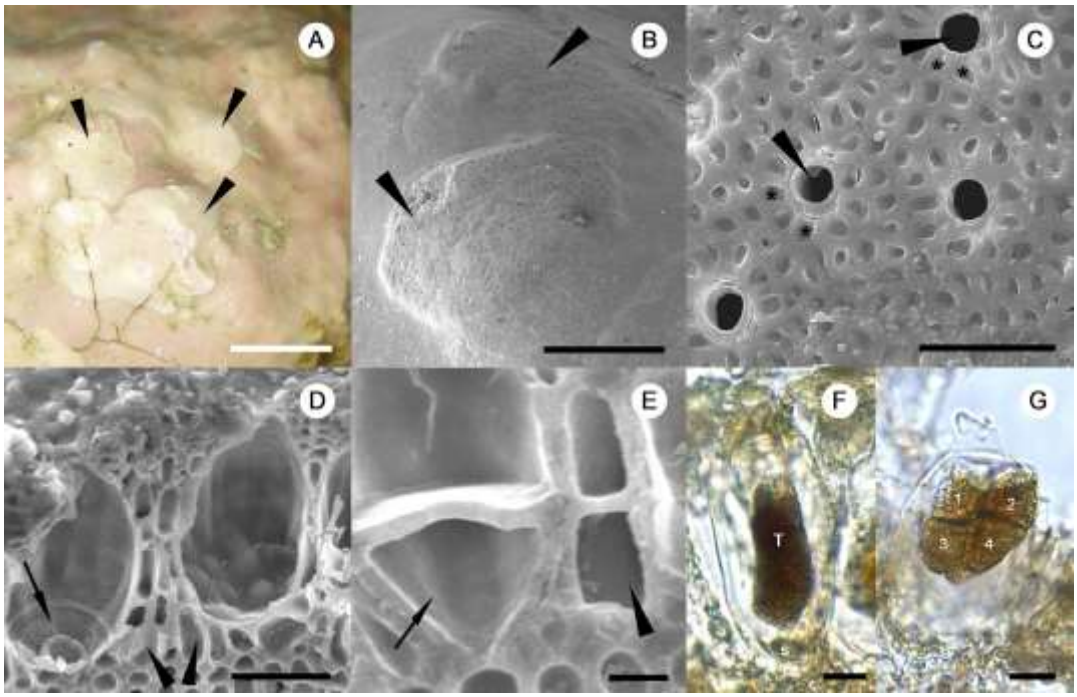


Fig.2.3.4. *Sporolithon mediterraneum* neotype (SPR_MDT 1a). a. Raised tetrasporangial sori in surface view (arrowheads). Scale bar: 500 µm. b. Scanning electron micrograph (SEM) of thallus surface with two adjacent tetrasporangial sori (arrowheads). Scale bar: 400 µm. c. SEM of tetrasporangial pores (arrowheads) and rosette cells (asterisks). Scale bar: 40 µm. d. SEM of tetrasporangial compartments subtended by a single stalk cell (arrow) and chambers with a basal layer of elongated cells. Paraphyses formed by 5-6 cells (arrowheads). Scale bar: 50 µm. e. SEM of tetrasporangial compartments in transverse section with a large triangular stalk cell (arrow) and clavate cells of a bordering paraphysis (arrowhead). Scale bar: 10 µm. f. Longitudinal section through a tetrasporangial compartment showing a tetrasporocyte (T) with stalk cell (S). Scale bar: 15 µm. g. Longitudinal section of a cruciate tetrasporangium (1-4). Scale bar: 15 µm.

2.3.4. Discussion

The specimen of *Sporolithon* from Gorgona can be distinguished from *S. ptychoides* and *S. molle* previously reported from the Mediterranean Sea based on a combination of anatomical features. The

ML and BI phylogenetic analyses of the *psb*A and *rbc*L sequences indicate that it is a distinct species compared to *S. ptychoides* and *S. molle*. We refer to the specimen from Gorgona as the *neotype* of *S. mediterraneum* since it is consistent with the description of the species by Heydrich (1899).

In the generic description of *Sporolithon* (Verheij, 1993), the number of cells in the paraphyses between the tetrasporangia has diagnostic value at the species level. The neotype differs from *S. ptychoides* and *S. molle* by the presence of paraphyses consisting of 5-6 cells, which are shorter than in the latter species, and by larger stalk cells (**Table 2.3.1**, **Fig.2.3.5**).

The paraphyses of *S. ptychoides* and *S. molle* consist of 3 elongate cells (Heydrich, 1897) (p. 68, Fig.2). While the number of cells forming the paraphyses in *S. mediterraneum* was not mentioned in the protologue, Heydrich (1899) described these cells as more clavate and thicker compared to those in *S. ptychoides*, and roundish at the top of the filament. The field-collected specimen of *S. ptychoides* from the type locality, with a sequence that matches the lectotype, has 3-4 celled paraphyses (Richards et al., 2017). The paraphyses of *S. molle* are also 3-4 celled (Richards et al., 2017). In contrast, all specimens from the Mediterranean region identified as *S. ptychoides* to date have 4-6 cells in the paraphyses (Alongi et al., 1996; Bressan & Babbini, 2003).

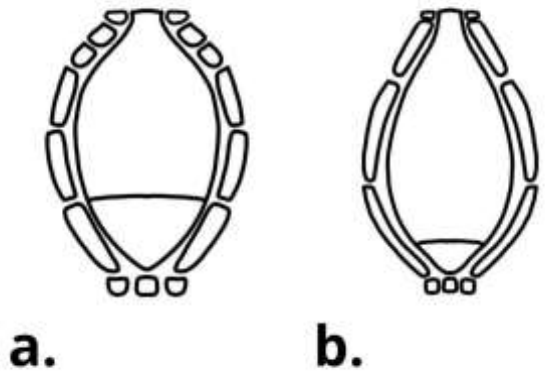


Fig.2.3.5. Tetrasporangial compartments and the bordering paraphyses in *Sporolithon*. (**a**) *S. mediterraneum* with 5-6 celled paraphyses and a larger stalk cell (> 20x20 μm). (b) *S. ptychoides* and *S. molle* with 3-4 celled paraphyses and a smaller stalk cell (< 20x20 μm).

According to Richards et al. (2017), reports of *S. ptychoides* and *S. molle* based on morpho-anatomy are likely incorrect and their worldwide distribution needs to be reevaluated. Indeed, several specimens identified as *S. ptychoides* after DNA sequencing did not match any sequence of *S. ptychoides* from El Tor, Egypt. Alongi et al. (1996) considered the specimens they examined from the Mediterranean to be conspecific and belonging to *S. ptychoides* since the size of the tetrasporangia fell within the range of *S. ptychoides*, which may indeed be considered a useful feature for some *Sporolithon* species (Verheij,

1993). Nevertheless, there is no substantial difference between the three species in this respect (**Table 2.3.1**). Moreover, the tetrasporangial compartments in the *neotype* and the other Mediterranean specimens are comparable in size to the measurements reported by Heydrich (1899) for *S. mediterraneum*. In addition to the number of cells in paraphyses, another feature that we consider diagnostic to distinguish S. *mediterraneum* (i.e., our samples) and the Mediterranean specimens (Alongi et al., 1996; Bressan & Babbini, 2003) from *S. ptychoides* and *S. molle* is the size of the stalk cell, which is larger than 20x20 μm in the former and smaller in the latter (**Table 2.3.1**).

Richards et al. (2017) demonstrated the co-occurrence at the same type locality (El Tor, Red Sea) of two species (*i.e. S. ptychoides* and *S. molle*) that are distinguishable based on sequenced markers (i.e., *rbc*L, *psb*A, UPA, COI, LSU, *tuf*A), despite the lack of distinctive morpho-anatomical characters. We cannot exclude that the specimens from the Mediterranean previously described as *S. ptychoides* also belong to different species. However, considering the confined nature of the Mediterranean basin and that the other Mediterranean specimens share all diagnostic characters with the neotype of *S. mediterraneum*, it is likely that most or all those specimens are conspecific. Currently, *S. mediterraneum* is the only confirmed species of the genus *Sporolithon* in the Mediterranean region.

The identification of *S. mediterraneum* and the morpho-anatomical characters that distinguish it from *S. ptychoides* and *S. molle* will enable us to detect records of these species in the eastern Mediterranean, in case they become established. As with other marine organisms from the Red Sea, these species have the potential to enter the Mediterranean through the Canal of Suez, a phenomenon known as Lessepsian migration, which has already been observed in other rhodophycean species (Galil, 2009; Manghisi et al., 2012; Nahor et al., 2022). Therefore, they are species of special interest because their presence may indicate shifts in their distribution due to climate change and warming waters. The detection and monitoring of these species will contribute to provide critical insights into the biogeographical changes occurring in the Mediterranean basin and help in assessing the broader impacts of environmental changes on marine ecosystems (Israel & Einav, 2017). This underscores the need for ongoing surveillance and research to track these shifts and develop appropriate conservation strategies.

Finally, the records of fossil Sporolithales found in the Mediterranean and mostly described as *S. ptychoides* [48–51] could also belong to *S. mediterraneum*. For example, in Braga and Bassi (Braga & Bassi, 2007; Aguirre et al., 2012; Quaranta et al., 2012; Simone et al., 2012) could belong to *S. mediterraneum*. For example, in Braga & Bassi (Braga & Barri, 2007) (Fig.6B), we observed more than 3-4 cellular paraphyses and therefore it is probably *S. mediterraneum* rather than *S. ptychoides*.

With these findings we highlight the importance of an integrated approach that combines traditional morpho-anatomical studies with DNA sequencing in the study of coralline algae.

Table 2.3.1. Characters to differentiate *S. mediterraneum* from *Sporolithon* species previously reported from the Mediterranean and other related taxa based on *psb*A

Character	*S. mediterraneum Holotype* (Heydrich 1899)	*S. mediterraneum Neotype* (this study)	Alongi et al. 1996 as *S. ptychoides*,	Bressan and Babbini 2003 as *S. ptychoides*	*S. molle* (Verheij 1993, Richards et al. 2017)	*S. ptychoides* (Heydrich 1897, Richards et al. 2017)
Type Locality	Gulf of Naples or more likely Gulf of Villefranche[1], (Mediterranean)	Gorgona Island (Tyrrhenian Sea, Mediterranean)	Island of Vulcano, Cannizzaro, Island of Comino (Mediterranean)	Canale di Sicilia, (Mediterranean)	El Tor (Egypt, Red Sea)	El Tor (Egypt, Red Sea)
Tetra/bisporangial chamber height (µm)	120 µm	75-108 µm	85-130 µm	86-100 µm	75-78 µm[4]	100 µm
Tetra/bisporangial chamber diameter (µm)	65 µm	39-58 µm	40-60 µm	39-51 µm	33-40 µm[4]	40 µm
Stalk cell height (µm)	ND	21.9-25.5 µm	ND	22.7 µm[3]	10–18.75 µm	10–17 µm
Stalk cell diameter (µm)	ND	24.2-35.9 µm	ND	23.8 µm[3]	14–19.5 µm	10–20 µm
Number of paraphyses between tetra/bisporangial chambers	ND	0-3	0-5[2]	ND	0-2[5]	1-3
Number of cells in paraphyses between tetra/bisporangial chambers	ND	5-6	4-6	4-6	3-4	3-4
Tetra/bisporangial chamber pore diameter (µm)	ND	10.3-13.8	12-15	12	6-10.8	ND
Number of rosette cells surrounding tetra/bisporangial chamber pore	ND	9-12		8-11	9-12	ND
Tetra/bisporangial chambers buried	ND	Yes	Yes	Yes	Yes	Yes
DNA sequence data available for type specimen(s)	ND	Yes	No	No	Yes	Yes

[1] See Introduction for detail on Holotype locality, [2] Observed from Alongi [20], [3] Measured from Bressan and Babbini [21], [4] Measured from Verheij [42] Lectotype
[5] Observed from figure 6 in Richards[2].

Acknowledgments

The authors are very thankful to SEM service from ICM-CSIC and Davide Porrelli from CIMA-UNITS for the images taken during the study and to the MaCoBioS project CANAL IV fieldwork for collecting the samples from Menorca Channel. The authors would also like to thank Sofia Comis for the technical drawing of the tetrasporangial compartments. This work is contributing to the ICM's 'Center of Excellence' Severo Ochoa (CEX2019-000928-5). **AC** is enrolled in the PhD programme in Marine Sciences at the University of Barcelona.

References

Abdul Wahab, M.A., Ferguson, S., Snekkevik, V.K., McCutchan, G., Jeong, S., Severati, A., Randall, C.J., Negri, A.P. & Diaz-Pulido, G. (2023). Hierarchical settlement behaviours of coral larvae to common coralline algae. *Scientific Reports, 13*, 5795. https:// doi.org/10.1038/s41598-023-32676-4.

Aguirre, J., Braga, J.C., Martín, J.M. & Betzler, C. (2012). Palaeoenvironmental and stratigraphic significance of Pliocene rhodolith beds and coralline algal bioconstructions from the Carboneras Basin (SE Spain). *Geodiversitas, 34*, 115–136. https://doi.org/10.5252/g2012n1a7.

Alongi, G., Cormaci, M. & Furnari, G. (1996). On the occurence of Sporolithon ptychoides Heydrich (Corallinales, Sporolithaceae, Rhodophyta) in the Mediterranean sea. *Cryptogamie Algologie, 17*, 131–137.

Amado-Filho, G.M., Moura, R.L., Bastos, A.C., Salgado, L.T., Sumida, P.Y., Guth, A.Z., Francini-Filho, R.B., Pereira-Filho, G.H., Abrantes, D.P., Brasileiro, P.S., Bahia, R.G., Leal, R.N., Kaufman, L., Kleypas, J.A., Farina, M. & Thompson, F.L. (2012). Rhodolith beds are major CaCO3 bio-factories in the tropical South West Atlantic. *PLoS ONE 7*, e35171. https://doi.org/10.1371/journal.pone.0035171.

Athanasiadis, A. (2016) Phycologia Europaea Rhodophyta. Thessaloniki: Published and distributed by the author. Vol. I. pp. [i]-xxxxviii, 1-762.

Basso, D., Nalin, R. & Nelson, C.S. (2009). Shallow-Water Sporolithon Rhodoliths from North Island (New Zealand). *PALAIOS 24*, 92–103. Available at: 〈http://www.jstor.or g/stable/27670583〉.

Braga, J.C. & Bassi, D. (2007). Neogene history of Sporolithon Heydrich (Corallinales, Rhodophyta) in the Mediterranean region. *Palaeogeography. Palaeoclimatology. Palaeoecology, 243*, 189–203. https://doi.org/10.1016/j.palaeo.2006.07.014.

Bressan, G. & Babbini, L. (2003). Biodiversit`a marina delle coste Italiane: Corallinales del Mar Mediterraneo: guida all deteminazione. *Biologia Marina Mediterranea*. S.I.B.M., pp. 1–237.

Cormaci, M., Furnari, G. & Alongi, G. (2017). Flora marina bentonica del Mediterraneo: Rhodophyta (Rhodymeniophycidae escluse). *Bullettin of the Gioenia Academy of Natural Sciences of Catania, 50*, FP1–FP391.

Darriba, D., Taboada, G.L., Doallo, R. & Posada, D. (2012). jModelTest 2: more models, new heuristics and parallel computing. *Nature Methods, 9*. https://doi.org/10.1038/ nmeth.2109, 772–772.

Di, Geronimo R. & Giaccone, G. (1994). Le alghe calcaree nel detritico costiero di Lampedusa (Isole Pelagie). *Bullettin of the Gioenia Academy of Natural Sciences of Catania,* 27, 5–25.

Farr, T., Broom, J., Hart, D., Neill, K. & Nelson, W. (2009). Common coralline algae of northern New Zealand: an identification guide. *NIWA Information Series, No 70*. ISSN 1174- 264X.

Foslie, M. (1900). Revised systematical survey of the Melobesieae. *Det Kongelige Norske videnskabers selskabs skrifter, 5*, 1–22.

Foslie, M. (1905). A new squamariacea from the Adriatic and the Mediterranean. *Det Kongelige Norske videnskabers selskabs skrifter, 1*, 1–9. , 1 fig.

Fredericq, S., Krayesky-Self, S., Sauvage, T., Richards, J., Kittle, R., Arakaki, N., Hickerson, E. & Schmidt, W.E. (2019). The critical importance of rhodoliths in the life cycle completion of both macro- and microalgae, and as holobionts for the establishment and maintenance of marine biodiversity. *Frontiers in Marine Science, 5*, 502. https://doi.org/10.3389/fmars.2018.00502.

Gabriel, D., Draisma, S.G.A., Schils, T., Schmidt, W.E., Sauvage, T., Harris, D.J., Norris, J.N. & Fredericq, S. (2019). Quite an oddity: new worldwide records of *Renouxia* (Rhodogorgonales, Rhodophyta), including *R. marerubra* sp. nov. *European Journal of Phycology, 55*, 197–206.

Gabrielson, P.W., Hughey, J.R., Pe˜na, V., Richards, J.L., Saunders, G.W., Twist, B., Farr, T. & Nelson, W.A. (2023). Asia Pacific *Sporolithon* (Corallinophycidae, Rhodophyta) species revised based on DNA sequencing of type specimens and including *S. crypticum* sp. nov., *S. immotum* sp. nov. and *S. nodosum* sp. nov. *Phycologia, 62*, 593–607. https://doi.org/10.1080/00318884.2023.2225309.

Galil, B.S. (2009). Taking stock: inventory of alien species in the Mediterranean sea. *Biological Invasions, 11*, 359–372. https://doi.org/10.1007/s10530-008-9253-y.

Giaccone, G., Colonna, P., Graziano, C., Mannino, A., Tornatore, E., Cormaci, M., Furnari, G. & Scammacca, B. (1985). Revisione della flora marina di Sicilia e isole minori. *Bullettin of the Gioenia Academy of Natural Sciences of Catania, 18,* 537–781.

Gouy, M., Guindon, S. & Gascuel, O. (2010). SeaView version 4: A multiplatform graphical user interface for sequence alignment and phylogenetic tree building. *Molecular Biology and Evolution, 27,* 221–224. https://doi.org/10.1093/molbev/msp259.

Guiry, M.D. & Guiry, G.M. (2024). AlgaeBase. World-wide electronic publication, National University of Ireland, Galway. Listing the World's Algae, AlgaeBase. 〈https://www. algaebase.org/〉. Accessed 29 Oct 2024.

Hamel, G. & Lemoine, M. (1953). Corallinac´ees de France et d'Afrique du Nord. *Archives du Museum National d'Histoire Naturelle de Paris, série 7,* 1: 15-138, 23 plates.

Heydrich, F. (1897). Corallinaceae, insbesondere Melobesieae. *Berichte der Deutschen Botanischen Gesellschaft, 15,* 34–70. , 3 figs, pl III.

Heydrich, F. (1899). Einige neue Melobesien des Mittelmeeres. . *Berichte der Deutschen Botanischen Gesellschaft, 17,* 221–227.

Irvine, L.M. & Chamberlain, Y.M. (1994). Seaweeds of the British Isles. Volume 1. Rhodophyta. Part 2B. Corallinales, Hildenbrandiales. vii, 276p. :986-986. *Journal of the Marine Biological Association of the United Kingdom, 74* (4). https://doi.org/10.1017/S0025315400090342.

Israel, A. & Einav, R. (2017). Alien seaweeds from the Levant basin (Eastern Mediterranean Sea), with emphasis to the Israeli shores. *Israel Journal of Plant Sciences,* 1–12. https://doi.org/ 10.1080/07929978.2016.1257091.

Keats, D.W. & Chamberlain, Y.M. (1993). *Sporolithon ptychoides* Heydrich and *S. episporum* (Howe) Dawson: two crustose coralline red algae (Corallinales, Sporolithaceae) in South Africa. *South African Journal of Botany, 59,* 541–550. https://doi.org/10.1016/S0254-6299 (16)30701-3.

Leão, L.A.S., Bahia, R.G., Jesionek, M.B., Adey, W.H., Johnson, G., Salgado, L.T. & Pereira, R.C. (2020). *Sporolithon franciscanum* sp. nov. (Sporolithales, Rhodophyta), a new rhodolith-forming species from Northeast Brazil. *Diversity, 12,* 199. https://doi. org/10.3390/d12050199.

Lemoine, M. (1939). Les algues calcaires fossiles de l'Algérie. *Matériaux pour la carte géologique de l'Algérie, Série Paléontologique, 9,* 1–131. , pls 1–3.

Letunic, I. & Bork, P. (2024). Interactive Tree of Life (iTOL) v6: recent updates to the phylogenetic tree display and annotation tool. *Nucleic Acids Research gkae 268*. https:// doi.org/10.1093/nar/gkae268.

Littler, M.M. (1973). The population and community structure of Hawaiian fringing-reef crustose Corallinaceae (Rhodophyta, Cryptonemiales). *Journal of Experimental Marine Biology and Ecology, 11,* 103–120. https://doi.org/10.1016/0022-0981(73)90050-6.

Maneveldt, G.W., Gabrielson, P.W. & Kangwe, J. (2017). *Sporolithon indopacificum* sp. nov. (Sporolithales, Rhodophyta) from tropical western Indian and western Pacific oceans: First report, confirmed by DNA sequence data, of a widely distributed species of *Sporolithon*. *Phytotaxa, 326*, 115. https://doi.org/10.11646/phytotaxa.326.2.3.

Manghisi, A., Bertuccio, C., Armeli, Minicante S., Fiore, V., Le, Grall L., Genovese, G. & Morabito, M. (2012). Identifying alien macroalgae through DNA barcodes: the case of Hypnea cornuta (Cystocloniaceae, Rhodophyta). *Transitional Waters Bulletin, 5*. https://doi. org/10.1285/i1825229Xv5n1p42.

Nahor, O., Luzzatto-Knaan, T. & Israel, A. (2022). A new genetic lineage of Asparagopsis taxiformis (Rhodophyta) in the Mediterranean Sea: as the DNA barcoding indicates a recent Lessepsian introduction. *Frontiers in Marine Science, 9*. https://doi.org/10.3389/ fmars.2022.873817.

Nguyen, L.-T., Schmidt, H.A., von Haeseler, A. & Minh, B.Q. (2015). IQ-TREE: a fast and effective stochastic algorithm for estimating maximum-likelihood phylogenies. *Molecular Biology and Evolution, 32*, 268–274. https://doi.org/10.1093/molbev/msu300.

Norris, J.N. & Bucher (1989). *Rhodogorgon*, an anamolous new red algal genus from the Caribbean Sea. *Proceedings of the Biological Society of Washington, 102*, 1050–1066.

Peña, V., De Clerck, O., Afonso-Carrillo, J., Ballesteros, E., B´arbara, I., Barreiro, R. & Le Gall, L. (2015). An integrative systematic approach to species diversity and distribution in the genus Mesophyllum (Corallinales, Rhodophyta) in Atlantic and Mediterranean Europe. *European Journal of Phycology, 50*, 20–36. https://doi.org/10.1080/ 09670262.2014.981294.

Quaranta, F., Tomassetti, L., Vannucci, G. & Brandano, M. (2012). Coralline algae as environmental indicators: a case study from the Attard member (Chattian, Malta). *Geodiversitas, 34*, 151–166. https://doi.org/10.5252/g2012n1a9.

Richards, J., Kittle, R.P., Schmidt, W.E., Sauvage, T., Gurgel, C.F.D., Gabriel, D. & Fredericq, S. (2022). Assessment of rhodolith diversity in the Northwestern Gulf of Mexico including the description of Sporolithon gracile sp. nov. (Sporolithales, Rhodophyta), and three new species of Roseolithon (Hapalidiales, Rhodophyta). *Frontiers in Marine Science, 9*, 906679. https://doi.org/10.3389/fmars.2022.906679.

Richards, J.L., Sauvage, T., Schmidt, W.E., Fredericq, S., Hughey, J.R. & Gabrielson, P.W. (2017). The coralline genera Sporolithon and Heydrichia (Sporolithales, Rhodophyta) clarified by sequencing type material of their generitypes and other species. *Journal of Phycology, 53*, 1044–1059. https://doi.org/10.1111/jpy.12562.

Richards, J.L., Gabrielson, P.W. & Schneider, C.W. (2018). *Sporolithon mesophoticum* sp. nov. (Sporolithales, Rhodophyta) from Plantagenet Bank off Bermuda at a depth of 178 m. *Phytotaxa 385*, 67. https://doi.org/10.11646/phytotaxa.385.2.2.

Ronquist, F., Teslenko, M., van der Mark, P., Ayres, D.L., Darling, A., Höhna, S., Larget, B., Liu, L., Suchard, M.A. & Huelsenbeck, J.P. (2012). MrBayes 3.2: efficient Bayesian phylogenetic inference and model choice across a large model space. *Systematic Biology, 61*, 539–542. https://doi.org/10.1093/sysbio/sys029.

Saunders, G.W. & Moore, T.E. (2013). Refinements for the amplification and sequencing of red algal DNA barcode and RedToL phylogenetic markers: a summary of current primers, profiles and strategies. *ALGAE 28,* 31–43. https://doi.org/10.4490/ algae.2013.28.1.031.

Simone, L., Carannante, G., Bassi, D. & Cherchi, A. (2012). Rudist-bearing rhodalgal facies in the post-Turonian recovery of peri-Tethyan carbonate systems: a case history from the Nurra region (northwestern Sardinia, Italy). *Geodiversitas 34*, 167–187. https:// doi.org/10.5252/g2012n1a10.

Tamura, K., Stecher, G., Peterson, D., Filipski, A. & Kumar, S. (2013). MEGA6: Molecular Evolutionary Genetics Analysis version 6.0. *Molecular Biology and Evolution, 30*, 2725–2729. https:// doi.org/10.1093/molbev/mst197.

Thiers B.M. (2024). Index Herbariorum. Available online： https://sweetgum.nybg.org/science/ih/. Accessed 29 Oct 2024.

Turland, N.J., Wiersema, J.H., Barrie, F.R., Greuter, W., Hawksworth, D.L., Herendeen, P.S., Knapp, S., Kusber, W.-H., Li, D.-Z., Marhold, K., May, T.W., McNeill, J., Monro, A.M., Prado, J., Price, M.J. & Smith, G.F. (2018). International Code of Nomenclature for algae, fungi, and plants (Shenzhen Code) adopted by the Nineteenth International Botanical Congress Shenzhen, China, July 2017. Regnum Vegetabile 159 (eds.). Koeltz Botanical Books, Glashütten. https://doi.org/ 10.12705/Code.2018.

Verheij, E. (1993). The genus Sporolithon (Sporolithaceae fam. nov., Corallinales, Rhodophyta) from the Spermonde Archipelago, Indonesia. *Phycologia 32*, 184–196. , 27 figs, 3 tables.

Xiang, C.-Y., Gao, F., Jakovli´c, I., Lei, H.-P., Hu, Y., Zhang, H., Zou, H., Wang, G.-T. & Zhang, D. (2023). Using PhyloSuite for molecular phylogeny and tree-based analyses. *iMeta 2*, e87. https://doi.org/10.1002/imt2.87.

Yoon, H.S., Hackett, J.D. & Bhattacharya, D. (2002). A single origin of the peridinin- and fucoxanthin-containing plastids in dinoflagellates through tertiary endosymbiosis. *Proceedings of the National Academy of Sciences of the United States of America 99*, 11724–11729. https://doi.org/10.1073/ pnas.172234799.

Zhang, D., Gao, F., Jakovli´c, I., Zou, H., Zhang, J., Li, W.X. & Wang, G.T. (2020). PhyloSuite: An integrated and scalable desktop platform for streamlined molecular sequence data management and evolutionary phylogenetics studies. *Molecular Ecology Resources*, *20*, 348‑355. https://doi.org/10.1111/1755-0998.13096.

Supplementary Material

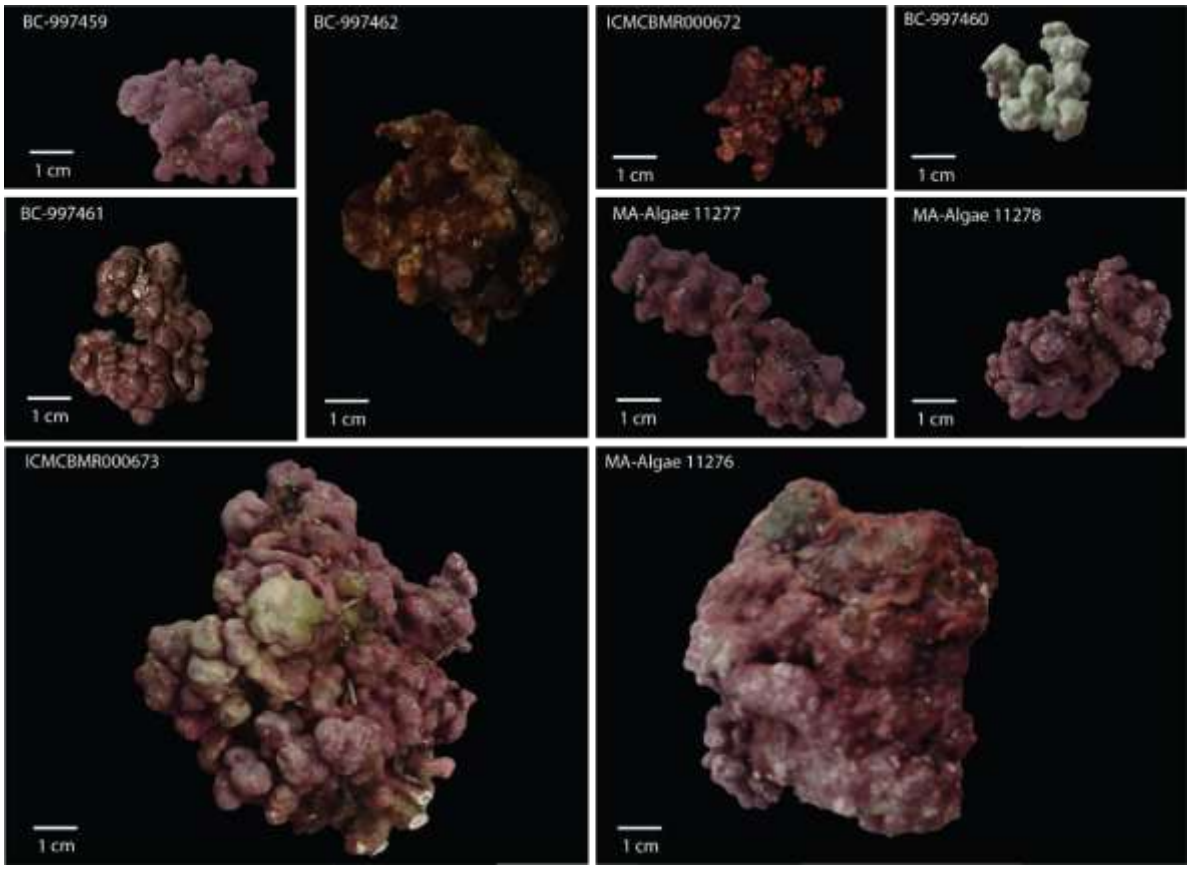


Fig.2.3.S1. Complementary collection of S. mediterraneum from Menorca Channel, Balearic Sea, Spain.

Table 2.3.S1. List of specimens of *Sporolithon* sequenced or used in phylogenetic analyses.

Species	Collection Data	GenBank Accession	
		***psb*A**	***rbc*L**
***Sporolithon mediterraneum* Heydrich, 1899. - Neotype**.	Gorgona Island, Thyrrenian Sea , Italy (Mediterranean), 2018, rhodolith, 50 m depth, leg. C.Cecchi. Voucher: TSB_SPR MDT 1a .	PQ518784	PQ518785
Sporolithon mediterraneum	Menorca Channel, Balearic Islands, Spain (Mediterranean), 28.vii.2022, rhodolith, 74 m depth, leg. A. Cabrito. MaCoBioS Project – CANAL IV Fieldwork. Voucher: BC-997459.	PQ518777	
Sporolithon mediterraneum	Menorca Channel, Balearic Islands, Spain (Mediterranean), 29.vii.2022, rhodolith, 58.6 m depth, leg. A. Cabrito. MaCoBioS Project – CANAL IV Fieldwork. Voucher: BC-997460.	PQ518775	
Sporolithon mediterraneum	Menorca Channel, Balearic Islands, Spain (Mediterranean), 3.viii.2022, rhodolith, 62 m depth, leg. A. Cabrito. MaCoBioS Project – CANAL IV Fieldwork. Voucher: BC-997461.	PQ518778	
Sporolithon mediterraneum	Menorca Channel, Balearic Islands, Spain (Mediterranean), 3.viii.2022, rhodolith, 62 m depth, leg. A. Cabrito. MaCoBioS Project – CANAL IV Fieldwork. Voucher: BC-997462.	PQ518782	
Sporolithon mediterraneum	Menorca Channel, Balearic Islands, Spain (Mediterranean), 29.vii.2022,	PQ518776	

	rhodolith, 58.6 m depth, leg. A. Cabrito. MaCoBioS Project – CANAL IV Fieldwork. Voucher: ICMCBMR000672.		
Sporolithon mediterraneum	Menorca Channel, Balearic Islands, Spain (Mediterranean), 3.viii.2022, rhodolith, 62 m depth, leg. A. Cabrito. MaCoBioS Project – CANAL IV Fieldwork. Voucher: ICMCBMR000673.	PQ518779	
Sporolithon mediterraneum	Menorca Channel, Balearic Islands, Spain (Mediterranean), 3.viii.2022, rhodolith, 62 m depth, leg. A. Cabrito. MaCoBioS Project – CANAL IV Fieldwork. Voucher: MA-Algae 11276.	PQ518781	
Sporolithon mediterraneum	Menorca Channel, Balearic Islands, Spain (Mediterranean), 28.vii.2022, rhodolith, 74 m depth, leg. A. Cabrito. MaCoBioS Project – CANAL IV Fieldwork. Voucher: MA-Algae 11277.	PQ518774	
Sporolithon mediterraneum	Menorca Channel, Balearic Islands, Spain (Mediterranean), 29.vii.2022, rhodolith, 58 m depth, leg. A. Cabrito. MaCoBioS Project – CANAL IV Fieldwork. Voucher: MA-Algae 11278.	PQ518780	
Sporolithon amadoi J.L.Richards & R.G. Bahia. 2019. - Paratype.	Gulf of Mexico, Ewing Bank, Offshore Louisiana, USA. 4.v.2018, 70 m depth, leg. J.Richards & S. Fredericq. Voucher: LAF_7256_Field_number_5_4_18_4_2.	MN266235	MN258542

Sporolithon crypticum G. W. Saunders,J.L. Richards & P.W. Gabrielson, 2023. – Holotype.	Australia: Western Australia, Windy Harbour. 8.xi.2010. leg. G.W. Saunders & K. Dixon. Voucher : GWS024693.	KY682938	KY682907
Sporolithon dimotum (Foslie & M.Howe) Yamaguishi-Tomita ex M.J.Wynne, 1986. – Holotype.	Puerto Rico: Lemon Bay near Guanica. 27.vi.1903. leg. M.A. Howe. Voucher: NY_900043(Howe2667).	-	KY994131
Sporolithon durum (Foslie) R.A.Townsend & Woelkerling, 1995. – Lectotype.	Australia: South Australia,Cape Jaffa. Leg. A. Engelhart. Voucher: TRH:C19-3381.	-	OQ290680
Sporolithon durum	Australia: Western Australia, Mutton Bird I. 6.xi.2010. leg. G.W. Saunders & K. Dixon. Voucher: GWS024261	KY682926	KY682902
Sporolithon durum	Australia: South Australia, Gravel Bay. 24.xi.2011. leg. P.W. Gabrielson. Voucher: NCU:657550	-	OQ290681
Sporolithon durum	Australia: South Australia, King George Beach. 26.ii.2011. leg. G. Belton. Voucher: AD:A92272.		OQ290682
Sporolithon durum	Australia: South Australia, Coombra. 17.xii.2010. leg. G. Belton. Voucher: NCU:597130.	-	OQ290683
Sporolithon durum	Australia: Western Australia, Cape LeGrand. 10.xii.2012. leg. K. Dixon & G. Belton. Voucher: NCU:594351.	-	OQ290684
Sporolithon eltorense J.L.Richards & P.W.Gabrielson, 2017. – Holotype.	Egypt: El Tor, Gulf of Suez, 1-2 m depth. 8.v.2012. leg. T. Sauvage, W.E. Schmidt & D. Gabriel. Voucher: NCU_606659.	MF034543	MG051269

Sporolithon episoredion (W.H.Adey, R.A.Townsend & Boykins) Verheij, 1992. – Holotype.	USA: Hawai'I, St. Rogatien Bank. leg: D. Child. Voucher: US:190909.	-	OQ290685
Sporolithon episporum (M.Howe) E.Y.Dawson, 1960. – Holotype.	Panama: Point Toro, near Colon, low water mark to several meters depth. 7.i.1910. leg. M.A. Howe. Voucher: NY_900041.		KY994125
Sporolithon episporum	Panama: Bocas del Toro, 3 m Depth. 13.vii.2008. leg. K. Miklasz. Voucher: NCU_598843.	MF034547	
Sporolithon erythraeum (Rothpletz) Kylin, 1956.	China: Hainan Sanya Luhuitou fringing reef. 23.v.2016. leg. Hu Qunju & Xiao Yunzhu. Voucher: SY:1602.	MK531547	MK531545
Sporolithon franciscanum L.A.S.Leão & Bahia 2020. – Holotype.	Brazil: Aracaju, Sergipe. 2.ii.2011. Leg. L.C.S Fontes J.R. Santos L.A. Santos J.B.S., Mendonca & M.S. Santos. Voucher: RB 797665.	MT214482	
S. franciscanum. - Paratype	Brazil: Bahia State, Abrolhos Continental Shelf. 11.iii.2012. leg. Amado Filho Guillermo. Voucher: GM AF5		KP142786
Sporolithon gracile J.L.Richards, Kittle & Fredericq 2022. – Holotype.	Gulf of Mexico, USA: Parker Bank, offshore Louisiana, 92 m depth. 20.v.2019. leg. R.P.KittleIII, S.Fredericq, W.E.Schmidt. Voucher: LAF_7382	ON365773	ON365775
Sporolithon howei (Me.Lemoine) N.Yamaguishi-Tomita ex M.J.Wynne, 1986. - Holotype.	Panama: Isla Coiba. Leg. C. Crossland. Voucher: PC:0731949.	OQ290692	

Sporolithon immotum T.J. Farr & W.A.Nelson, 2023.	New Zealand: North Island, Raglan, Whale Bay. 1.ii.2006. Voucher: WELT A029451.	FJ361509	KM369123
Sporolithon immotum	Australia: Victoria, Glaneuse Reef. 29.x.2011. Leg. P.W.Gabrielson. Voucher: NCU:600682.	OQ290693	OQ290686
Sporolithon immotum	Australia: South Australia, Salmon Bay. 18.xi.2011. Leg. P.W.Gabrielson & K. Dixon. Voucher: NCU:597121	OQ290694	OQ290687
Sporolithon indopacificum G.W.Maneveldt & P.W.Gabrielson, 2017. – Holotype.	Tanzania: Zanzibar Island, Chwaka Bay. 6.vi.2016. Leg. J. Kangwe, J. Nene & K. Mohammed. Voucher: L:3964509.	MG051270	MG051266
Sporolithon molle (Heydrich) Heydrich, 1897. – Lectotype.	Egypt: El Tor, Gulf of Suez. Leg. Anonymous. Voucher: C_A92529.	-	KY994121
S. mole - Topotype	Egypt: Gulf of Suez, El Tor. 8.v.2012. Leg: T. Sauvage, W. E. Schmidt & K. Gabriel. Voucher: NCU:606657.	MG051272	KY994120
S. molle (S. crassiramosum)	France: Juan de Nova Island, Mozambique. Leg: Voeltzkow. Voucher: TRH:C19-3376.	-	OQ290679
Sporolithon mesophoticum J.L.Richards, P.W.Gabrielson & C.W.Schneider, 2018. – Holotype.	Bermuda. 26.ix.2016. Leg: Craig W. Schneider. Voucher: NCU 658543.	MK159180	MK159181
Sporolithon nodosum T.J.Farr & W.A.Nelson, 2023.	New Zealand: North Island, Northland, Cavalli Passage, between Motumuka and Keokeo Islands.	FJ361640	

Sporolithon ptychoides Heydrich, 1897. – Lectotype-	Egypt: El Tor, Gulf of Suez. Leg: Anonymous. Voucher: TRH_C19-3412.	-	KY994119
Sporolithon ptychoides	Egypt: El Tor. 8.v.2012. Leg: T. Sauvage, W. Schmidt & D. Gabriel. Voucher: NCU:606663.	OQ290695	KY994118
Sporolithon sp.	Australia: 'The Docks' Jervis Bay, New South Wales. 16.iii.2000. Voucher: LTB21140.	-	KM369121
Sporolithon schmidtii (Foslie) G.D.Gordon, Masaki & Akioka, 1976. – Holotype.	Thailand: Ko Kahdat. Leg: J. Schmidt. Voucher: TRH:C19-3421.	-	OQ290688
Sporolithon sinusmexicanum J.L.Richards & Fredericq, 2018. - Holotype.	Gulf of Mexico, USA: Offshore Louisiana, Sackett Bank, 65-68 m depth. 7.ix.2014. Leg: J. Richards. Voucher: LAF_6956A.	MF034549	KY994126
Sporolithon sibogae (Weber Bosse & Foslie) P.C.Silva, 1987. – Lectotype.	Indonesia: Sulu Archipelago, Pearl Bank. Voucher: TRH:C19-3426.	-	OQ290689
Sporolithon tenue Bahia, Amado-Filho, Maneveldt & W.H.Adey, 2013. – Isolectotype.	Brazil: Bahia State, off Salvador City. 8.ii.2012. Leg: Ricardo Bahia. Voucher: US 170943.	KP142751	KP142785
Sporolithon timorense (Foslie) P.C.Silva, 1987. – Isolectotype.	Indonesia: Pulau Sailus-besar. Voucher: L:935.207-13.	-	OQ290690
Sporolithon yoneshigueae Bahia, Amado-Filho, Maneveldt & W.H.Adey, 2015.	Brazil. Leg: T.B.A. Voucher: T.B.A.1.	MF034545	KY994122
Renouxia marerubra D. Gabriel, J.N. Norris & Fredericq, 2019.	Egypt: Hurghada, 10 m depth.13.v.2012. Leg: D. Gabriel, T.	-	MK174342

	Sauvage & W.E. Schmidt. Voucher: LAF6170.		
Rhodogorgon carriebowensis J.N.Norris & Bucher, 1989.	Panama: Isla Zapatilla, Bocas del Toro archipelago. 8.viii.2010. Voucher: TBA.	KM369059	
Rhodogorgon ramosissima' J.N.Norris & Bucher 1989	Jamaica: east side of Discovery Bay, St. Ann Parish. 13.iii.2003. Leg: C. Pueschel & H. Verbruggen. Voucher: HV434.	-	KC134341

2.4. **CHAPTER IV**: Non-extractive fish diversity assessment in Mediterranean rhodolith beds.

Andrea Cabrito, Francesc Maynou, Remy Simide, David Mouillot, Julie Lossent, Silvia de Juan

***Cabrito, A.**, Maynou, F., Simide, R., Mouillot, D., Lossent, J. & de Juan, S. (2024). Non-extractive fish diversity assessment in Mediterranean rhodolith beds. Aquatic Conservation: Marine and Freshwater Ecosystems, 34(6), e4212. https://doi.org/10.1002/aqc.4212*



Abstract

Rhodolith beds, recognized as biodiversity hotspots with high ecological and conservation importance, face local anthropic pressures, including trawl fishing. However, monitoring the diversity associated to this sensitive biogenic habitat in the deep waters of the Mediterranean Sea is challenging. Traditional monitoring, such as experimental trawling and trammel nets, are extractive and have sampling limitations in providing comprehensive diversity inventories. In this work, we explore three alternative techniques (still video cameras, eDNA and bioacoustics) to monitor fish assemblages associated to rhodolith beds in the Menorca Channel at 45-80 m depth. Ten sites were surveyed with eDNA and 66 fish taxa were identified, including endangered sharks and cryptic species. The Molecular Operational Taxonomic Units (MOTUs) richness varied significantly according to habitat heterogeneity, being higher in homogeneous bottoms, and to exposure to trawling, with higher richness in non-exposed areas. Bioacoustics, though limited by a reduced library of fish sounds, detected differences in sound richness between habitat types and the highest abundance of sounds was recorded in the areas with the greatest small-scale habitat heterogeneity. Underwater video revealed limitations in species detection but proved effective for characterizing small-scale habitat type and heterogeneity. In summary, each technique provides valuable information at different spatial scales and levels of detail. To assess the feasibility of these techniques for long term monitoring, we explored their capabilities and limitations in terms of costs, survey logistics and data output.

Key words: Passive acoustic monitoring, eDNA, stationary video, innovative biodiversity monitoring, Rhodolith beds, biogenic habitats

Correspondence:

Andrea Cabrito (ORCID:0000-0002-3429-5201). Institut de Ciències del Mar (ICM-CSIC), Barcelona 08003, Spain. Email: cabrito@icm.csic.es

2.4.1. Introduction

Rhodolith beds are distributed worldwide from tropical to polar regions (Fragkopoulou et al., 2021), extending from the lower infralittoral to 40 m depth in the North Atlantic region (Peña et al., 2014), and reaching 100 m depth in the western Mediterranean (Barberá et al., 2012). They are habitats of high ecological and conservation interest (Habitats Directive, 92/43/EEC) and are recognized as global biodiversity hotspots (Riosmena-Rodríguez et al., 2017; Tuya et al., 2023). Rhodolith beds have been described as nursery areas for fish, including economically important species (Hall-Spencer et al., 2003; Riosmena-Rodríguez 2017; Costa et al., 2020).

Despite the recognized ecological importance of rhodolith beds, their protection is deficient (Tuya et al., 2023). Globally, they face multiple local pressures, including trawl fishing (de Juan et al., 2013), increased sedimentation, and epiphytic algae overgrowth (Legrand et al., 2017; Fragkopoulou et al., 2021). Impacts on rhodolith beds are expected to intensify with warming and acidification of the oceans (Tregarot et al., 2023).

In the Mediterranean, the distribution and conservation status of rhodolith beds are still poorly known, hindering the implementation of adequate conservation plans, although advances have been made in some locations (e.g., Sciberras et al., 2009; Barberá et al., 2012; Romagnoli et al., 2021; Maggio et al., 2022). In this context, identifying and monitoring rhodolith beds that are in a good ecological condition is urgent.

Fish species composition and abundance are considered relevant indicators of anthropogenic pressures on marine ecosystems (Dalongeville et al., 2022; Pinna et al., 2023), and are being used by the EU Marine Strategy Framework Directive (e.g., descriptors 1 and 3).

Traditional methods for monitoring demersal fish, such as towed fishing gears or epibenthic sledges, imply physical disturbance of the seabed and a limited deployment in time and space (de Juan et al., 2020). Recently, remotely operated vehicles (ROVs) have been used to monitor deep marine habitats (Kuhnz et al., 2022), including rhodolith beds (Illa-López et al., 2023; Demestre et al., 2024). This non-extractive technique enables a more precise estimation of motile megafauna, such as fish, compared to fishing nets, as mobile fauna often evade capture by these nets (López-Garrido et al., 2020). However, species identification remains challenging due to the speed of the ROV and the quality of images (Illa-López et al., 2023).

In this work, we explore three different techniques to monitor the presence of rhodolith beds and their associated fish diversity in the Mediterranean:

I. **Stationary bait-less cameras.** Several studies used different types of video recording (i.e., baited cameras or stereo-cameras) to identify and measure fish (Cappo et al., 2003; Letessier et al., 2015). Video imaging is also used to characterize abiotic (e.g. substrate, rugosity, slope) and biotic habitats

(e.g., coral reefs, seagrass) (de Juan et al., 2015; Loh et al., 2019; Kuhnz et al., 2022), including coverage by rhodoliths (Illa-López et al., 2023). However, a limitation is the video quality caused by water transparency, along with constrains related to the duration of the analysed video footage.

II. **Environmental DNA (eDNA) metabarcoding.** This method is particularly useful for providing biodiversity inventories, especially in marine areas where sampling across entire taxonomic groups or habitats is expensive or challenging (e.g. Muff et al., 2023). Also, eDNA metabarcoding has proved effective for evidencing the diversity of cryptobenthic fish in complex habitats (Mathon et al., 2023), where traditional methods such as Underwater Video Census (UVC) are intrinsically limited (Polanco-Fernández et al., 2021). One limitation of eDNA application in offshore, open waters is the persistence of viable DNA for 2-3 days (depending on temperature) in the water mass (Collins et al., 2018; Caza-Allard et al., 2021). This DNA can be subject to transport by currents, which may affect the interpretation of the results (Collins et al., 2018).

III. **Passive Acoustic Monitoring.** The sounds emitted by fish and other marine animals can be proxies for local biodiversity (Mooney et al., 2020). Indices of "acoustic" diversity can be relevant indicators of habitat conservation status as observed in coralligenous habitats of the Western Mediterranean (Di Iorio et al., 2021). Passive acoustic techniques have the advantage of providing extensive spatial and temporal coverage. For example, Di Iorio et al. (2021) developed a long-term monitoring approach of fish soundscapes on seagrass beds, encompassing up to 3 years of sampling and covering an area of 3 hectares. Interestingly, changes in the soundscape have been linked to human disturbance (Rabin and Greene, 2002), which is relevant for the monitoring of ecological conditions of marine ecosystems. An anticipated drawback is the current limitation of sound libraries, which can accurately detect only a small number of taxa at low taxonomic level (See Supplementary Material - **Table 2.4.S1**).

Previous works have combined two techniques to monitor fish biodiversity. For example, Sato et al. (2021) combined data from eDNA with acoustic echo sounder surveys, Mueller et al. (2006) analysed data from video and acoustic cameras, Stat et al. (2019) and Mirimim et al. (2021) combined underwater video and eDNA. Some studies, such as Aglieri et al. (2020), combined eDNA analysis with underwater video census, baited remote underwater video, and small-scale fisheries sampling to investigate their efficiency and complementarity in assessing fish diversity in shallow depths. Nevertheless, to our knowledge, no published study has explored the relevance and complementarity of the three techniques (I-III) explained above in deep marine ecosystems, with all the challenges it entails. In this study, we applied these three non-extractive and non-destructive techniques to monitor fish diversity in a well-preserved Mediterranean rhodolith bed, ranging from approximately 50 m to 100 m depth. Furthermore, we compared our findings with a reference species list obtained from previous trawling and ROV

surveys in the area. Additionally, we evaluated the cost-effectiveness of each technique in terms of economic cost and personnel requirements, as well as the characteristics of the output data.

2.4.2. Methodology

Study area

The Menorca Channel is located in the western Mediterranean, between the islands of Mallorca and Menorca, comprising a total of 335,353.6 hectares with a maximum depth of 100 m (Moranta et al., 2014). The transparency of its waters enables photosynthesis up to its maximum depth, facilitating the development of a diverse community of algae, including free-living nodules of red calcareous algae that accumulates as rhodolith beds (de Juan et al., 2023).

The area has remained in a good conservation status thanks to a relatively low fishing effort. Fishing with trammel nets is routinely practised in the Channel, however, trawl fishing has historically been low compared to other Mediterranean areas (Barberá et al., 2003). Moreover, there are areas off limits to trawl fishing in coastal waters shallower than 50 m. Trawl fishing is restricted in the central part of the channel due to the presence of an underwater cable installed in the 1970s. In 2016 a trawling ban was extended throughout the Menorca Channel (Order AAA/1479/2016 of 7 September, https://www.boe.es/eli/es/o/2016/09/07/aaa1479/con).

Sampling protocols and Data processing

Eleven sampling stations were selected based on exposure to trawling and substrate type. Rhodoliths coverage was extracted from previous studies (Moranta et al., 2014) (**Fig.2.4.1a**). These stations are between 45 and 80 m depth. Two "trawl fishing exposure" levels were identified based on Vessel Monitoring System (VMS) data available at the Global Fishing Watch organisation (https://globalfishingwatch.org) and on the protection history of the area: (i) "Not exposed", which includes all stations within the trawling exclusion zone i.e., cables (S13 and S01) and areas within the trawling ban limits (S15, S21 and S26), and areas shallower than 50 m where trawling is not allowed (S04 and S05); (ii) "Exposed", which includes areas open to trawling activities (L2) and areas under the influence of trawling, i.e., stations where trawling was allowed before the 2016 ban and now are at the edge of the exclusion zone (S18, S16 and S10) (**Fig.2.4.1b**). These sampling stations also have distinctive habitat characteristics-(**Fig.2.4.1**; Moranta et al., 2014). In four stations rhodolith coverage is higher than 50% (S01, S13, S15, S18), while in four stations rhodolith coverage is between 25 and 50% (S10, S16, S26 and L2). Three stations (S21, S04 and S05) with sparse rhodolith presence (coverage <10%) were added to the study to test the hypothesis that rhodolith beds are biologically richer and more diverse habitats (Barberá et al., 2003).

The three non-extractive techniques were planned for the eleven stations (**Fig.2.4.1**), although technical failures in the use of the devices restricted sampling at some stations. This resulted in a total of eight

stations sampled with all three techniques. At least two of the three techniques were deployed at the remaining stations.

Sampling spanned from July 2021 to July 2022. Initially, 10 stations were sampled for eDNA and 5 for bioacoustics in July 2021. Video deployment to characterize the habitat took place in October 2021. In July 2022, an additional 5 stations were added for bioacoustics and the video recordings of four stations (L2, S10, S18, and S26) were redeployed due to the low quality obtained in October 2021. We considered potential interannual variability by sampling species presence for eDNA and bioacoustics within the same month, thereby minimizing any variations. Subsequently, we decided to utilize video recordings not only for characterizing the habitat but also for assessing the technique's ability to detect fish species. We took into consideration the seasonal variability in fish communities when interpreting the results. Despite logistical challenges during fieldwork, this multi-method approach promises valuable insights into monitoring fish communities.

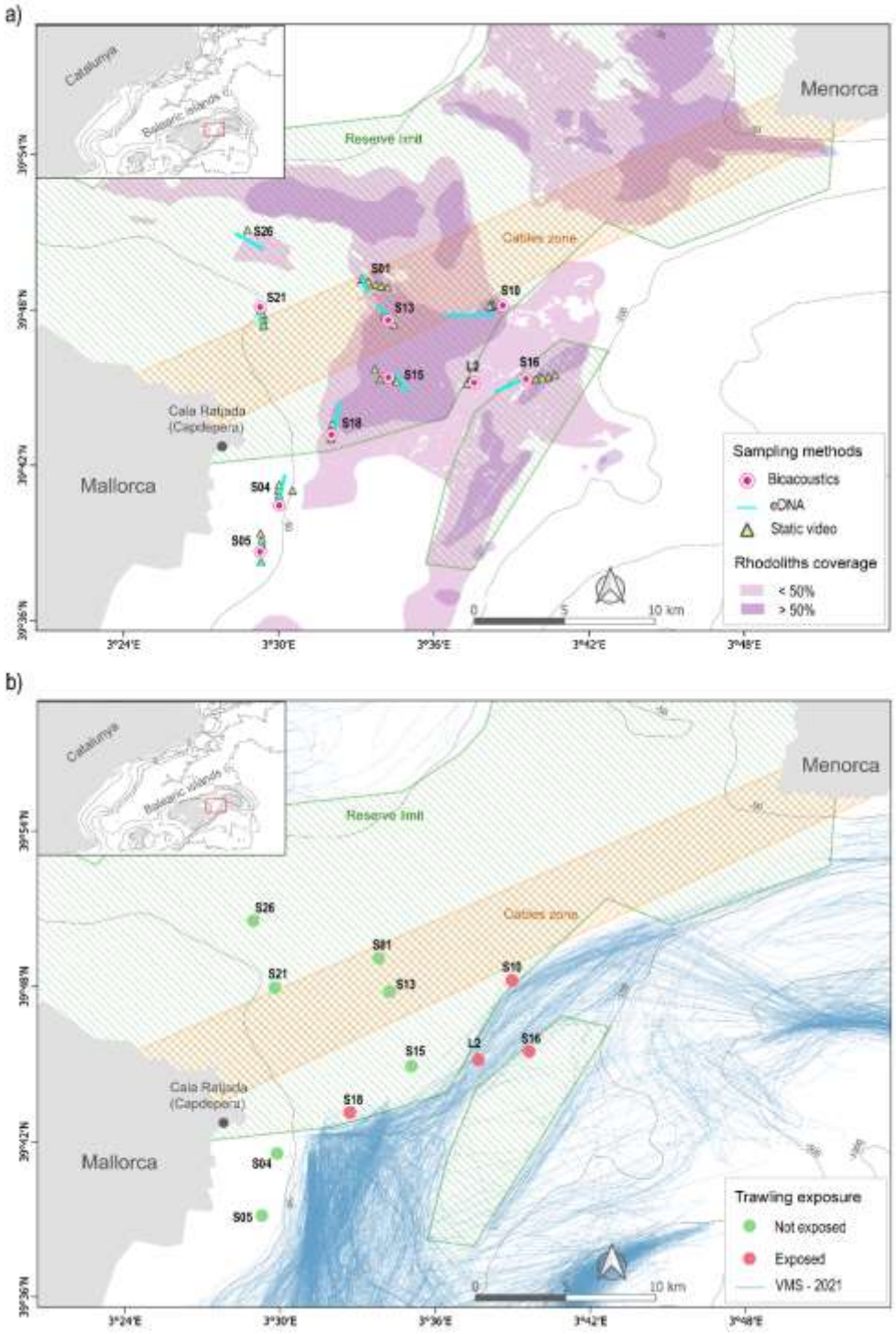


Fig.2.4.1. Map of the sampling stations in the Menorca channel. (**a**) Locations of the sampling stations where any of the three techniques were deployed. Rhodolith coverage, extracted from Moranta et al. (2014), is represented in different purple intensities, the white areas correspond to the sandy stations with sparse rhodoliths. (**b**) Fishing tracks of the trawl fleet (corresponding to 2021) and identification of the sampling stations exposed (red) or not exposed (green) to trawling. Green hatching shows the area protected from fishing by the marine reserve declared in 2016

2.4.2.1. Underwater video survey: small-scale habitat characterization and species detection

Five camera sets separated by *ca*. 350 m were deployed at each station for recording 30-40 minutes of video. In S5 and S26 stations only 3 and 1 (respectively) video sets were deployed due to time constrains. The video system was mounted on a tripod equipped with two Go-Pro7 cameras (resolution of 1920x1440 HD) inside watertight enclosures designed to withstand high pressure.

The video footage was visually analysed following 3 steps: (i) The first 20 minutes with good quality of the image were selected (i.e., without the pitching that the swell sometimes caused on the tripods). (ii) The selected video sample (20') was visually inspected to characterise the habitat type. This was done by systematically describing the type of substrate (considering the predominant type of sediment, mainly gravel and sand), the percentage of rhodoliths coverage, presence of macroalgae (e.g. *Laminaria*) and signals of biotic activity (e.g. tracks or mounds). Then, applying the rhodolith coverage criteria, a habitat type was assigned to each sample. (iii). A second visualisation of the video sample was made using the Kinovea software to register the presence of fish species. Fish were noted and identified to the lowest taxonomic level possible. All the fish identified in the sample were noted only one time, considering presence/absence. In addition, the presence of groups that could not be identified and/or counted was noted as categorical data (e.g., "school of fish").

Data analyses

Video samples were analysed to provide a semi-quantitative estimation of the small-scale biophysical heterogeneity. Habitats were classified into three types: (i) rhodolith beds, with more than 50% of rhodolith coverage, (ii) detritic biogenic habitats with less than 50% of rhodolith cover, and (iii) detritic biogenic habitats with less than 10% of rhodolith cover. In a second stage, a more detailed description of the biophysical elements identified at each sampling station was performed, considering the presence of other habitat components and sediment features. For this, we considered (i) the presence of other algae such as *Peyssonnelia rosa-marina, Osmundaria volubilis* and *Laminaria rodriguezii* that contribute to increase the biogenic habitat complexity; (ii) the presence of marks and traces of biological activity on the sediments as indicators of bioturbation; and (iii) the presence of patches and discontinuities in the biogenic habitat as an indicator of small-scale heterogeneity.

Then, the 3-5 video samples obtained in each station were reviewed to identify the diversity of fish. We calculated the richness of fish taxa by combining the identified species at each station. However, due to the sampling limitations (two distinct time periods), no statistical tests were conducted. Therefore, the richness results obtained from this technique are considered solely for comparative purposes with the species detection capabilities of the other techniques.

2.4.2.2. Environmental DNA metabarcoding: fish biodiversity

To assess fish richness with DNA metabarcoding, water samples were collected in 10 stations (**Fig.2.4.1**). Samples were obtained by towing a water pump at *ca*. 5 m above the seabed during 45 min, filtering 45 l of seawater. The water pump was fitted to a 0.2 µm polyethersulfone filter that retains small DNA fragments released by all organisms in their close environment (Miya, 2022). In each station, two replicates were obtained. The filtered eDNA was then transported to the laboratory. At all stages, a strict contamination control protocol was followed (see Mathon et al., 2023). eDNA extraction was performed following the protocols by Juhel et al. (2020) and Pont et al. (2018). The teleost-specific 12S mitochondrial rRNA primer pair (Valentini et al., 2016) was used for the amplification of metabarcode sequences. The primers were 5' labelled with a unique tag allowing the assignment of sequences to the samples during the bioinformatic analysis. Twelve PCR replicates per sample were performed (Mathon et al., 2023) and an average of 650,000 sequence reads were obtained per sample in the raw data.

The reads were processed using clustering and post-clustering cleaning to remove errors and estimate the number of species using Molecular Operational Taxonomic Units (MOTUs) (Mathon et al., 2023). First, reads were assembled using *vsearch* (Rognes et al., 2016), then demultiplexed and trimmed using CUTADAPT (Martin, 1994) and clustering was performed using SWARM v.2 (Mahé et al., 2015) with d = 1, which corresponds to a maximum of 1 mismatch between neighbouring pairs of sequences within each cluster. Taxonomic assignment of MOTUs was carried out using the Lower Common Ancestor (LCA) algorithm *ecotag* implemented in the Obitools toolkit (Boyer et al., 2016) and the European Nucleotide Archive (ENA) as a reference database (release 143, March 2020), supplemented by Mathon et al. (2023) custom reference database.

For each station and replicate, we obtained the read abundance of MOTUs, which cannot be directly linked to in situ taxon abundance (Sanchez et al., 2022). Therefore, MOTU abundances were converted to a presence/absence matrix of MOTUs by sampling station. A first correction was made aimed at eliminating false positives, by setting the number of reads assigned to a certain MOTU to zero if they represented less than 3% of the total abundance of that MOTU (following Wangensteen and Turón, 2017). Then, a second adjustment was made by joining the two replicates of each station. For this purpose, all MOTUs, even if they were only detected in one of the two filters, were considered as present.

Data analyses

Fish richness was estimated from the MOTUs presence/absence matrix extracted from the eDNA samples. In this case, this measurement is a count of the number of different MOTUs present in each station. To test whether trawling exposure, habitat type and habitat heterogeneity explain significant differences in MOTUs Richness, Kruskal-Wallis comparisons of means were performed using

kruskal.test from the *stats* R package. No attempt was made at exploring the interaction among explanatory factors due to the low number of samples. Significant differences were assumed when the probability level was lower than p=0.1.

To explore variability in species composition (based on MOTU as proxy) between stations, a non-metric multidimensional scaling analysis was carried out based on Jaccard similarity index and using *metaMDS* in the *vegan* R package. To test whether the distribution of MOTUs across stations is related to trawling exposure, habitat type or habitat heterogeneity, an analysis of variance (PERMANOVA, with 999 permutations) was performed using the *adonis2* function from *vegan* R package. Due to the sampling characteristics, the factors have been considered as independent, without interaction. Then, to determine which species characterized each level of trawling exposure and each level of habitat type, we calculated the strength of association between species and site group membership using the *strassoc* function from the *indicspecies* R package (De Cáceres, 2022).

2.4.2.3. Bioacoustic monitoring: fish soundscape - fish activity

Data were acquired using an HTI-92-WB hydrophone (High Tech Inc., USA) with a sensitivity of –155 +/-3 dB re 1 V/µPa and flat frequency response from 5 Hz to 50 kHz connected to a SDA14 compact autonomous recorder (RTSys®, France). The acquisition chain is fully calibrated. The device, which acquired sounds continuously at a 78 kHz sampling rate and 24-bit resolution, was bottom-moored with the hydrophone 1 m above the seafloor. At each recording date, the recorder was deployed in the afternoon and recovered the next day. Recordings were made during the night because most temperate fish predominantly vocalise nocturnally (Picciulin et al., 2012, Bolgan et al., 2019) and interference with anthropogenic noise is largely reduced.

The mooring was deployed at the 10 stations, but successful recordings were obtained from only 9 stations (**Fig.2.4.1**). Audio files from 5 pm to 9 am were divided into 10 seconds snapshots that were converted into 10-s spectrograms (Fast Fourier Transform [FFT] resolution 11 Hz, Kaiser window 180 dB, 85% overlap). These spectrograms were classified using a custom-built MATLAB® (version R2014b) interface that allowed identification of potential fish sounds by an expert. The 15 types of fish sounds recovered were classified into 6 categories (see Supplementary Material **Fig.2.4.S1**) following Desiderà et al. (2019) (Supplementary Material **Table 2.4.S1**). Some categories (1, 2, 3 and 4) refer to fish species (or genera) that emit well-studied types of sound that can be taxonomically classified. Other categories (5 and 6) are related to groups of fish that emit characteristic and similar sounds that cannot be directly linked to a specific taxon. It should be noted that the same species may emit more than one type of sound depending on its activity, and these sounds are grouped in the corresponding category (e.g., category 4 for all sounds emitted by *Epinephelus marginatus).*

For each 10-s interval the number of different sound types were counted and pooled in one-hour bins. The number of sounds were pooled per station.

Data analyses

The total abundance of sounds (number of vocalizations/h), as well as the abundance of each category of sounds, were calculated per station, as an index of total and specific fish activity in the area. In addition, the number of sounds with different origins (i.e., different species or different activities within the same species) was calculated as a sound richness index. To test whether trawling exposure, habitat type and habitat heterogeneity explain significant differences in sounds Richness and in the abundance of sounds Kruskal-Wallis comparisons of means were performed using *kruskal.test* from the *stats* R package. No attempt was made at exploring the interaction among explanatory factors due to the low number of samples. Significant differences were assumed when the probability level was lower than p=0.1.

2.4.2.4. Complementarity between techniques

Due to the nature of data acquisition, i.e., the temporal and the spatial scales that each technique encompasses, the different datasets are not directly comparable. Nevertheless, the three techniques provided different proxies for the biodiversity of fish associated with the rhodolith bed under study, suggesting that they might be complementary in exploring fish communities from different perspectives; however, the feasibility of the technique for long-term monitoring has not been proved.

In order to analyse complementarity between the three techniques, a Friedman rank test (R package 'stats') was performed with the relative richness from the eight stations where the three techniques were successfully. A pairwise Wilcoxon test was performed to check which techniques differed from each other. Relative richness was calculated as the ratio of the number of MOTUs, sounds or taxa detected at each station (by each technique) to the total number of MOTUs, sounds or taxa detected by each technique (in the whole study).

An assessment of the advantages and disadvantages of the techniques was conducted. For this, a qualitative comparison was made between the three non-extractive techniques and a traditional extractive technique used in previous projects, a "Grande Ouverture Verticale" trawl net (GOC, Ordines and Massutí, 2009; Moranta et al., 2014). Information was extracted from fieldwork conducted in the Menorca Channel during the projects MaCoBioS (See Supplementary Material **Table 2.4.S7a**, **Table 2.4.S7b**, **Table 2.4.S7c** and **Table 2.4.S7d**) and INDEMARES (Moranta et al., 2014). MaCoBioS fieldwork information combined with expert knowledge was used to score various aspects of the monitoring techniques, such as the economic cost and personnel requirements of the technique (i.e. investment of time and personnel as well as fieldwork costs, analysis costs or processing time), the ability to obtain information on fish diversity (i.e. species inventories, detection of vulnerable or cryptic

species and recording of biological activity), the ability to obtain information at the seascape (i.e. spatial scale, habitat composition or habitat heterogeneity), and their destructiveness to the marine environment.

All statistical analyses were carried out in R version 3.6.3 (R Core Team 2020).

2.4.3. Results

2.4.3.1. Habitat characterisation by underwater video

A total of forty-seven video samples were analysed (i.e., between 3-5 video samples in each station, **Fig.2.4.1**) and the description of the habitat type in each station was summarized in Table 2.4.1. In S26, only one video could be recovered due to time limitation, therefore, the video was only used to describe the habitat type and rhodolith coverage, which was expected to be <50% but turned out to be <10%.

Based on visual examination of video images, three levels of rhodolith coverage at the site scale were identified (Supplementary Material - **Fig.2.4.S2a,b,c**). A 100% rhodolith coverage (i.e., rhodolith bed) was identified in S13, within the cables protected area. This rhodolith bed might extend to the north reaching S01; however, a habitat transition was observed at the edge of the cables' exclusion zone. In this area, the rhodoliths coverage decreased progressively and S01 was characterised by high spatial heterogeneity between replicates (at the scale of 350 m). To the south, the rhodolith bed extended to S15, within the protected area, and up to S18 at the limits of protection. In the deeper stations, at the edge of the protected area (S16 and S10), the density of rhodoliths decreased. In this area the substrate was characterized as biogenic habitat with less than 50% rhodolith coverage. The shallower stations, S21, S04 and S05, were characterised by biogenic detrital beds with less than 10% of rhodoliths. In addition, high habitat heterogeneity at a small-scale was observed in S05 due to the presence of rocky outcrops covered with algae and sessile organisms (Supplementary Material- **Fig.2.4.S2d**). A total of 14 fish taxa could be identified through video visualization in the ten stations (Supplementary Material - **Table 2.4.S3**). Having images of the same point from two different seasonal periods allowed us to verify that both the number and types of taxa remained consistent.

Table 2.4.1. Habitat description extracted from video footage in each study site.

Station	Depth (m)	Habitat	Description for each station
S10	70	Sand with < 50% of rhodolith cover	Sand with < 50% of rhodolith coverage and algae. Presence of mounds (sign of bioturbation). Homogeneity between replicates.
S16	71.2	Sand with < 50% of rhodolith cover	Sand with < 50% of rhodolith coverage, high algae cover with *Laminaria* fronds. Presence

			of mounds (sign of bioturbation). **Heterogeneity** between replicates.
S01	62	Rhodolith bed	Transition between habitats. From sand with < 50% of rhodolith coverage to rhodolith bed. Presence of *Peyssonnelia* and *Laminaria* fronds. **Heterogeneity** between replicates.
S13	62	Rhodolith bed	100% rhodolith coverage. Presence of *Peyssonnelia* and *Laminaria* fronds. Homogeneity between replicates.
S15	58.8	Rhodolith bed	100% rhodolith coverage. Presence of *Peyssonnelia* and *Osmundaria.* Homogeneity between replicates.
S18	56	Rhodolith bed	100% rhodolith coverage. Presence of *Osmundaria* and high amount of dead sea urchins. Presence of mounds (sign of bioturbation). **Heterogeneity** between replicates
S21	51	Sand with < 10% of rhodolith cover	Sand with ripples and less than 10% rhodolith cover and sparse algae. Homogeneity between replicates.
S04	48	Sand with < 10% of rhodolith cover	Sand with < 10% of rhodolith coverage with algae and presence of *Osmundaria*. Presence of animal tracks (sign of bioturbation). Homogeneity between replicates.
S05	48.5	Sand with < 10% of rhodolith cover	Sand with < 10% of rhodolith coverage with algae and *Osmundaria*. Presence of ripples and rocks with algae. Presence of animal tracks (sign of bioturbation). **Heterogeneity** between replicates.
L2	65.6	Sand with < 50% of rhodolith cover	Sand with < 50% of rhodolith with a full cover by *Laminaria*. Homogeneity between replicates.
S26	65	Sand with < 10% of rhodolith cover	Sand with < 10% of rhodolith coverage. Only one replicate hampered the assessment of heterogeneity.

2.4.3.2. Fish diversity with environmental DNA

The 20 eDNA samples (10 stations x 2 replicates) yielded a total of 2,374,169 sequence reads (average 118,708.45 per sample) that could be assigned to known fish taxa in the reference database (European Nucleotide Archive - www.ebi.ac.uk/ena/browser/home). In most cases, the MOTU could be associated with a fish species, although in some cases the attribution could be made only at the level of genus or closely related genera. A total of 66 different taxa were identified, 58 from the subclass Teleostei (bony fish) and 8 from the subclass Elasmobranch (cartilaginous fish) (see Supplementary Material – **Table 2.4.S4**).

The results of the Kruskal-Wallis test indicate that MOTUs richness varied significantly according to trawling exposure ($X^2 = 3.776$, df = 1, *p*-value = 0.052). Habitat heterogeneity was also significant, with higher richness in stations with homogeneous substrate ($X^2 = 3.84$, df = 1, *p*-value = 0.050). No significant differences were detected for MOTU richness between habitat types ($X^2 = 2.209$, df = 2, *p*-value = 0.331), although there is a general tendency of higher MOTUs richness in sandy sites with less than 10% rhodolith cover (**Fig.2.4.2**).

The MOTU composition across stations was also affected by these factors, as evidenced by the PERMANOVA significance levels for: trawling exposure (F = 2.863, df = 1, *p*-value = 0.001), the habitat type (F = 1.653, df = 2, *p*-value = 0.022) and the habitat heterogeneity (F = 1.470, df = 2, *p*-value = 0.066). The interaction could not be assessed due to the limited number of samples (**Fig.2.4.3**).

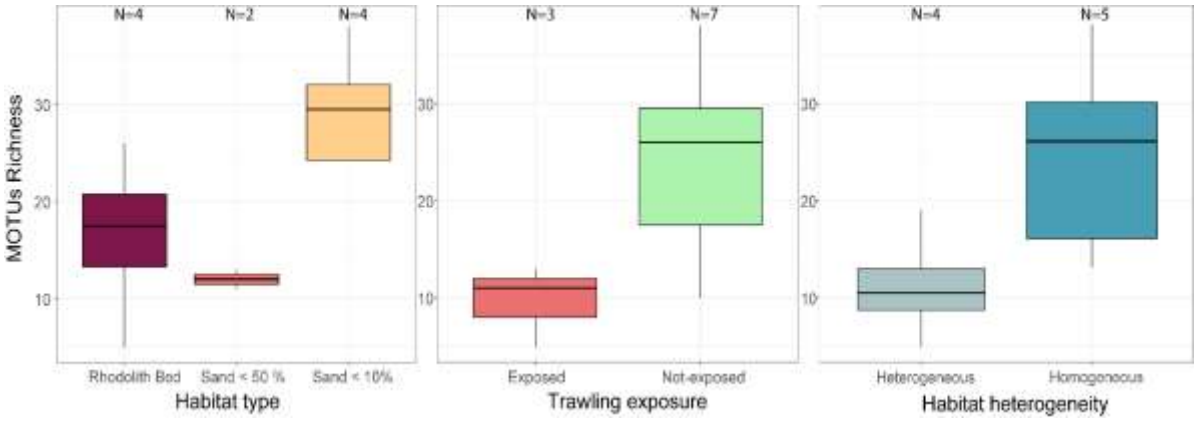


Fig.2.4.2. Richness of MOTUs detected with eDNA in the study area. From left to right, samples identified by type of habitat, by exposure to trawling activity and by the habitat heterogeneity.

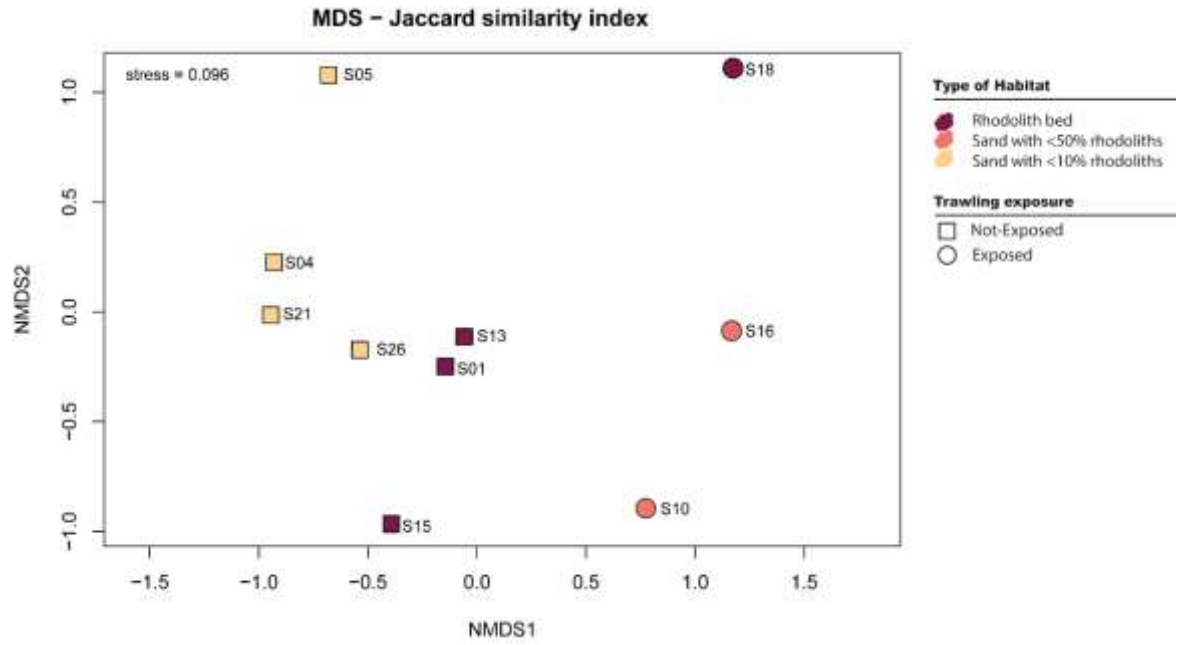


Fig.2.4.3. Multidimensional Scaling (MDS) based on Jaccard similarity index of fish species data identified through eDNA metabarcoding in the 10 sampling stations.

The highest similarity between stations (55%) occurred for the relatively shallow stations S04 and S21 that were characterised by sand with < 10% of rhodolith coverage. The second pair of stations with highest similarity (45%) were the not-exposed rhodolith beds in S13 and S01. These two pairs of stations are relatively close in the multivariate space (**Fig.2.4.3**) together with S26 which is sandy and not-exposed.

The most represented species (MOTUs) within the not-exposed areas include species of commercial interest, such as sparids, and benthic fishes such as *Uranoscopus scaber*, as well as the rainbow wrasse *Coris julis* (see Supplementary Material - **Table 2.4.S5**). Cryptic species such as *Corcyrogobius liechtensteini* or *Crystallogobius linearis*, were found among the 10 most characteristic species of the rhodolith bed. In addition, protected, endangered and threatened species of elasmobranchs such as *Myliobatis aquila*, *Prionace glauca* or *Pteroplatytrygon violacea* were found both over rhodolith beds and sandy bottoms with less than 50% of rhodolith cover. In sandy bottoms with less than 10% of rhodolith coverage, there was a predominance of species typically associated with sandy habitats (e.g., *Buenia affinis, Gobius cruentatus or Chelidonichthys obscurus)* (see Supplementary Material - **Table 2.4.S5**).

2.4.3.3. Bioacoustic monitoring: fish sounds

A total of 15 different sound types were detected in the nine sampling stations: one sound type classified as *Ophidion rochei*, two sound types as *Sciaena umbra*, one type as *Scorpaena* spp., four types as *Epinephelus marginatus*, two types as HF fishes, and five types classified as other fishes.

The results of the Kruskal-Wallis test revealed significant differences at the 0.1 significance level among the various habitat types (X^2 = 5.262, df = 2, *p*-value = 0.072). However, despite this finding, the pairwise Wilcoxon post hoc test failed to identify any differences among the three groups (*p*-value > 0.1 in all comparisons). Statistical tests indicated that there were no significant differences in sound richness associated with either trawling exposure (X^2 = 1.593, df = 1, *p*-value = 0.207) or habitat heterogeneity (X^2 = 0.071, df = 1, *p*-value = 0.790).

We also estimated the abundance of sounds of the six sound categories included in Supplementary Material Table 2.4.S1. The mean of total sound abundance was higher in stations with high habitat heterogeneity (205 sounds/h) compared to homogeneous areas (107.92 sounds/h) (see Supplementary Material - **Table 2.4.S**). The results for Kruskal-Wallis test revealed significant differences at the 0.1 significance level for the habitat heterogeneity (X^2 = 3.267, df = 1, *p*-value = 0.071) but no significant differences were found among habitat type or for trawling exposure (*p*-value > 0.1).

The stations with the highest sound abundances were those exhibiting high small-scale habitat heterogeneity, such as S5 and S18 (**Fig.2.4.4**). However, stations with high sound abundance were generally found in sand with less than 10% rhodolith coverage (S5 and S21), and with less than 50% rhodolith coverage (S10 and S16).

High frequency fishes (HF Fish) were represented, and had the higher abundance, only in stations characterised by sand with < 50% of rhodoliths. *Ophidion rochei* was the most heard species in the area and its sounds were registered within rhodolith beds and sand with less than 10% of rhodoliths. In these sandy stations, *Sciaena umbra* was also commonly heard. Species from the Scorpaenidae family were detected mostly in rhodolith beds and Groupers mostly in coastal and heterogeneous stations (**Fig.2.4.4**).

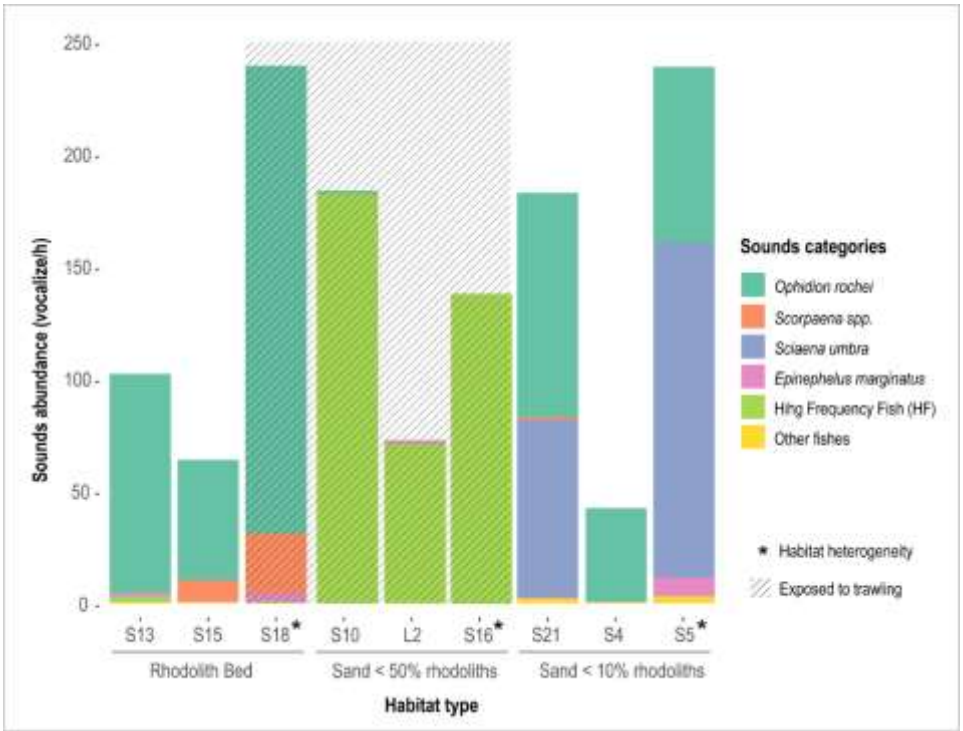


Fig.2.4.4. Barplot of the abundance of the 6 sound categories measured as the number of vocalizations / h at each station. Rhodolith coverage levels are indicated below together with habitat heterogeneity. The stations exposed to trawling are texturised with lines.

2.4.3.4. Comparative feasibility and cost-effectiveness of monitoring approaches

Considering the relative richness as a proxy for diversity, there was variability in the number of fishes identified with the three different techniques, and there was also high variability across the stations (see Supplementary Material - **Fig.2.4.S3**). The station with highest diversity recorded with any of the 3 techniques was station S21. The results for the other stations were variable. In general, S16 exhibited a low diversity.

The results of the Friedman rank test were statistically significant ($X^2 = 9.484$, df = 2, *p*-value = 0.009), indicating that the three techniques did not detect richness in the same ranking. The post-hoc Wilcoxon test showed that acoustic and video did not provide different richness rankings (*p*-value = 1.0), while eDNA and acoustic (*p*-value = 0.041) and eDNA and video (*p*-value = 0.023) did differ in richness ranking.

Environmental DNA detected the highest number of total taxa, with 66 detected taxa (S = 5-38 per station). In comparison, video (14 total taxa, S= 2-8 per station) and bioacoustics (15 types of sounds but only 4 categories assigned to taxa and S= 2-8 sound types per station) techniques are very limited (see Supplementary Material - **Table 2.4.S**). No taxon was detected by all three techniques simultaneously. Those taxa that were detected with two of the three techniques were not always detected in the same station, e.g. *Coris julis* was detected with eDNA at stations S13, S21 and S04 and with

video at stations S10 and S05. Only *Serranus cabrilla* was detected in a relatively high number of stations with video and eDNA simultaneously (see Supplementary Material - **Table 2.4.S6**). Some species were detected with only one of the three techniques, such as *Ophidion rochei* that was only detected with bioacoustics, *Aphia minuta* detected only with video, and 35 species detected only with eDNA (see Supplementary Material - **Table 2.4.S6**).

The qualitative comparison, grounded in fieldwork conducted in the study area, of the feasibility and cost-effectiveness of three techniques highlighted variations in the limitations, data acquisition, and costs associated with fieldwork activities and data analysis for each technique (see Supplementary Material - **Table 2.4.S7a**, **Table 2.4.S7b**, **Table 2.4.S7c** and **Table 2.4.S7d**). In comparison with sampling with towed nets, video images, bioacoustics and eDNA are innovative non-extractive techniques that are less expensive in terms of fieldwork operative costs (i.e., they do not require a large research vessel), time and personnel requirements. Bioacoustics and eDNA have higher costs in terms of data analyses (e.g., currently externalised to private laboratories). On the other hand, static video allows us to get information on habitat composition and heterogeneity. Bioacoustics and video resulted to be more useful for detecting biological activity while eDNA is more effective for detecting cryptic and vulnerable species (**Fig.2.4.5**).

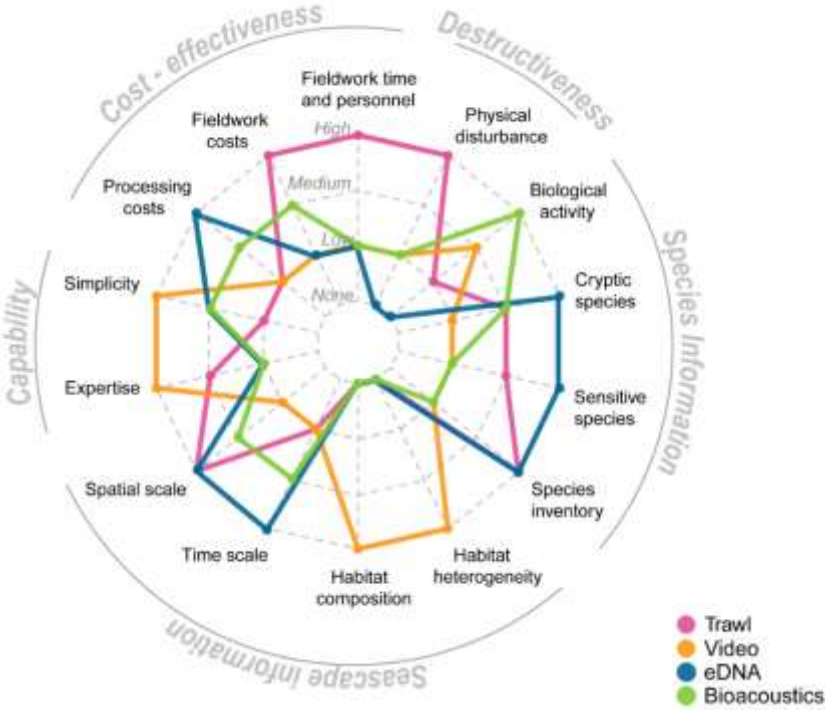


Fig.2.4.5. Qualitative comparison in terms of costs and time requirements and in extraction of species and ecosystem information between an extractive sampling technique (Trawl of type "GOC": Chalut à Grand Ouverture Verticale) and the three non-extractive sampling techniques. The information is based on expert knowledge and supported by costs and information extracted from the fieldwork of the MaCoBioS and Indemares projects.

2.4.4. Discussion

The present study investigates the efficacy of three non-destructive and non-extractive techniques for monitoring fish diversity in a Mediterranean rhodolith bed, each offering unique insights across different scales and levels of detail. Among these techniques, environmental DNA (eDNA) stands out for its ability to detect a wide array of species. However, caution is warranted in interpreting results, as diversity is inferred from the presence of DNA fragments in the water mass, potentially influenced by the amount of material contributed by different species and by environmental factors such as hydrodynamics. The effectiveness of the other two techniques is limited; although video recordings are useful for habitat characterization, their low quality restricts fish identification. Bioacoustics shows promise but would necessitate investment in reference databases to enhance its utility. The results, despite the limited number of stations and the techniques intrinsic limitations, suggest an interplay of factors driving the diversity of fish over rhodolith beds, including exposure to trawling, habitat type and small-scale habitat heterogeneity. The station with the highest recorded fish diversity using the three techniques was characterized by homogeneous detrital sediments, containing less than 10% rhodoliths. This location, sheltered from trawling, is relatively shallow and situated near the coast. The results for the other stations were variable, and fish diversity followed different patterns depending on the technique selected. The highest values recorded with bioacoustics were observed at a shallow station not exposed to trawling and characterised by habitat heterogeneity. This area featured regions densely populated by rhodolith beds alternating with patches of sand, each with less than 50% rhodolith coverage. Similarly, both video and eDNA methods detected elevated taxa richness at another shallow station characterized by detrital bottoms, situated near the boundaries of the 50-meter trawling exclusion zone. In contrast, the deeper area exposed to trawling exhibited lower diversity overall. The stations within the rhodolith bed did not exhibit a particularly high fish diversity.

This study explores the capabilities and limitations of the three techniques for monitoring fish diversity. We could only identify a few fish taxa to the species level from the video samples. The low cost, bait-less imaging system used was easy to deploy but the duration of the recordings and the image quality were limited. The more video time analysed, the more species would be detected; however, the probability of species passing in front of the camera during the video recording also needs to be considered (see Supplementary Material – **Fig.2.4.S4a,b** as examples). In addition, factors such as the species' cryptic nature (see Supplementary Material - **Fig.2.4.S4** as example) and the diminished light in deep waters further influence species detectability. This likely explains the observed lower species count in rhodolith beds compared to sandy stations, attributed to the cryptic nature of many species inhabiting rhodolith beds (e.g. *Corcyrogobius liechtensteini, Speleogobius trigloides* and *Odondebuenia balearica* detected in rhodolith beds by eDNA). The problem of detectability has already been documented for UVC in coral reefs (Polanco-Fernández et al. 2021) and for remotely operated vehicles (ROV) in rhodolith beds (Illa-López et al., 2023). While the other techniques rely on indirect

detection methods, such as DNA fragments or sounds, images provide direct and irrefutable evidence of species presence, reducing the possibility of false positives. Additionally, still video proves effective in characterising the biophysical habitat and discerning habitat heterogeneity at the site scale, essential for providing context for the application of other techniques.

In contrast, eDNA metabarcoding identified a high number of fish taxa in the study area. In a previous project covering the entire Menorca Channel (Moranta et al., 2014), 30 species of fish (teleost and elasmobranchs) were detected using ROV, while 90 species were detected with a trawling net "GOC". In the present study, focusing on the rhodolith bed within the channel (**Fig.2.4.1**), eDNA surveys detected 66 fish species (58 teleost species and 8 elasmobranchs). Of these species, 64% were common to the inventory obtained with the ROV, while only 42% of the species were also identified with the trawl survey. This evidences that eDNA is more effective for detecting fish species than the other non-extractive techniques tested, including the previously used ROV. At the same time, eDNA detected almost half of the diversity that was detected with the trawling net, although a full comparison cannot be made because we sampled only 10 stations on the rhodolith bed while the trawl survey covered a diversity of habitats (Moranta el al., 2014).

Significant differences in species composition between habitat types and fishing exposure were observed using eDNA. These findings align with expected hypotheses, such as observing greater correlation with commercial species in unfished areas, and more cryptic species associated with rhodolith bottoms (e.g., *Speleogobius trigloides* and *Crystallogobius linearis*). Additionally, notable higher fish diversity (MOTUs) was found in both unfished zones and homogeneous habitats. These results suggest that eDNA is not only effective in detecting numerous fish species but also valuable for monitoring fish communities in relation to habitat heterogeneity and protection measures. eDNA metabarcoding was also effective for detecting endangered fish species such as elasmobranchs. These findings align with results reported in other studies, such as He et al. (2023), Polanco-Fernández et al. (2021), or Juhel et al. (2018), supporting the idea that eDNA is a good approach for fast and cost-effective monitoring of highly diverse ecosystems. Given the approximate 2-3 days lifespan of DNA in temperate water, the captured sample spans a temporal scale of several days (Caza-Allard et al., 2021), and therefore it could be influenced not only by the hydrodynamics of the area (e.g., bottom currents) but also by the dynamics of the species (e.g. gregarious or solitary behaviour). This variability is particularly pertinent for the large pelagic species observed, underscoring the need for cautious interpretation of results. It is important to note that data for benthic species should be the most accurate due to their sedentary nature. On the other hand, while this method still presents challenges in accurately quantifying species abundance (Wong et al., 2022), it proves valuable for detecting a diverse set of species in our study area, including cryptobenthic species. Aglieri et al., (2020) showed that eDNA monitoring may go beyond the identification of taxonomic entities and be applied to ecological studies

of functional diversity, providing more robust results than sampling with fishing nets or baited underwater video.

The third technique, bioacoustics, shows promise for fish monitoring in the Mediterranean rhodolith bed; however, it remains in the early stages of development. This technique only detected a maximum of 15 different types of sounds that were classified into 6 categories; four of these categories could be associated to a species or genus, whereas the other two lack referent information in the database and significantly reduces the total number of species this technique could potentially detect. Still, this technique provides unique information as sound richness is the variety of sounds detected, representing a blend of various species emitting distinct sounds during different biological activities, such as vocalizations linked to the courtship, territorial defence or warning sounds. The sounds detected include both unique sounds from the same species and distinct sounds from different species. Therefore, sound richness can be understood as a proxy of "activity diversity". When sound richness is lower, the habitat is more sonically homogeneous either because the sounds are emitted by few different species or because few biological activities are taking place. Conversely, when sound richness is high, the habitat is sonically heterogeneous, hosting either a greater number of fish species or a greater variety of different activities. On the other hand, sound abundance, representing the number of recorded sounds, whether similar or diverse, serves as a proxy for the 'activity abundance' or 'functionality' of the habitat (Mooney et al., 2020). This suggests that acoustic richness and abundance are indicative of the habitat's support for fish breeding activity (Mooney et al., 2020).

Significant differences in sound richness among various habitat types were observed, although the limited data set prevented us to test the specific habitat types where these differences occurred. The highest abundance of sounds was recorded in heterogeneous habitats such as the limits of rhodolith beds, sandy bottoms with rocky outcrops, and sandy bottoms with less than 10% rhodolith coverage, possibly because they serve as preferred feeding habitats. These areas may foster a greater diversity of prey due to the presence of various habitats at small scales. As observed by de Juan et al. (2023), it is the combination of habitats that increases the total diversity of invertebrates in the area, which are potential prey for many fish species. In addition, some of these heterogeneous stations are also among the stations with the highest richness. These findings suggest that this technique could prove useful for detecting changes in sound richness across different habitat types with the availability of more comprehensive libraries in the future.

Implications for conservation

The present study explores three non-extractive techniques for monitoring deep biogenic habitats, emphasizing their efficiency in demanding fewer resources and personnel compared to traditional methods like the trawling nets. Therefore, these techniques provide a feasible alternative for monitoring marine habitats that are vulnerable to invasive sampling.

There exists a trade-off between non-destructiveness and the effectiveness of recording the species composition. In this study, the availability of fish DNA databases enabled eDNA to compile species lists independently of taxonomist's or local fishing knowledge (McDevitt et al., 2019). Therefore, regular fish monitoring through eDNA could provide indicators related to the conservation status of the area (Dalongeville et al., 2022). On the other hand, in terms of contextualising the study area by assessing the habitat composition, video proves effective as it enables the detection of changes in algae coverage or composition, facilitating seascape monitoring. Finally, despite limited fish sound libraries in the Mediterranean, bioacoustics technique is suitable for detecting species behaviour and the presence of some cryptobenthic species, such as *Ophidion rochei*, which might elude detection by other methods.

Based on our findings and despite the difficulties in comparing the techniques and the limitations when interpreting results, we advocate the implementation of a monitoring program that utilizes the three non-extractive techniques to document fish species associated with deep habitats like Mediterranean rhodolith beds. This program should aim to assess the temporal dynamics of fish presence and activity in the area over time. However, further development in data analysis is required. For example, the development of more automatic identification of images (e.g., Catalán et al., 2023); the use of more than one molecular marker for eDNA in order to maximize the detection success of the technique (Polanco-Fernández et al., 2021); and the development of extensive libraries of sound-producing species that are still unidentified (Di Iorio et al., 2021). This strategic focus aims to facilitate the future generation of species lists and inventories, encompassing not only fish but also invertebrates, without the necessity of destructive sampling methods.

Acknowledgments

The authors are very thankful to Ewan Trégarot, Cindy Cornet, Loïc Sanchez, Raphael Seguin, Géraldine Pérez and Laia Illa-López for their indispensable assistance during the sampling and also to Giulia Cortinovis for her support on video analysis. This work is developed on the framework of the EU H2020 project "MaCoBioS" (contract nº 869710). This work is contributing to the ICM's 'Center of Excellence' Severo Ochoa (CEX2019-000928-5) and to the 'Maria de Maetzu' accredited to the IMEDEA (CEX2021-001198) **SdJ** was supported by a Ramon y Cajal postdoctoral grant funded by the Ministry of Science and Innovation (Plan Estatal I+D+I, 2017- 2020; grant no. RyC2020-029062-I). **AC** is enrolled in the PhD programme in Marine Sciences at the University of Barcelona.

FUNDING

The authors acknowledge funding from the EU H2020 project "MaCoBioS" (contract nº 869710).

CONTRIBUTIONS

AC: Conceptualization, Methodology, Formal analysis, Writing – original draft, Writing – review & editing, Visualization. **FM:** Conceptualization, Methodology, Formal analysis, Writing – review &

editing. **RS:** Conceptualization, Writing – review & editing. **DM:** Conceptualization, Writing – review & editing. **JL:** Conceptualization, Writing – review & editing. **SdJ:** Conceptualization, Methodology, Formal analysis, Writing – review & editing.

ETHICS DECLARATIONS

Conflict of interest

The authors declare no conflict of interest.

Data availability

Data will be made available on request.

References

Aglieri, G., Baillie, C., Mariani, S., Cattano, C., Calò, A., Turco, G., Spatafora, D., Di Franco, A., Di Lorenzo, M., Guidetti, P. & Milazzo, M. (2020). Environmental DNA Effectively Captures Functional Diversity of Coastal Fish Communities. *Molecular Ecology 30*(13): 3127–39. https://doi.org/10.1111/mec.15661.

Barberá, C., Moranta, J., Ordines, F., Ramón, M., de Mesa, A., Díaz-Valdés, M., Grau, A.M. & Massutí, E. (2012). Biodiversity and Habitat Mapping of Menorca Channel (Western Mediterranean): Implications for Conservation. *Biodiversity and Conservation 21*(3): 701–28. https://doi.org/10.1007/s10531-011-0210-1.

Bolgan, M., Soulard, J., Di Iorio, L., Gervaise, C., Lejeune, P., Gobert, S. & Parmentier, E. (2019). The Sea Chordophones Make the Mysterious /Kwa/: Emitter Identification of the Dominating Fish Sound in Mediterranean Seagrass Meadows. *Journal of Experimental Biology*, jeb.196931. https://doi.org/10.1242/jeb.196931.

Boyer, F., Mercier, C., Bonin, A.E., Le Bras, Y., Taberlet, P. & Coissac, E. (2016). OBITOOLS: a UNIX-inspiredsoftware package for DNA Metabarcoding. *Molecular Ecology Resources, 16*: 176–182. https://doi.org/10.1111/1755-0998.12428.

Cappo, M., Harvey, E., Malcolm, H. & Speare, P. (2003). Potential of Video Techniques to Monitor Diversity, Abundance and Size of Fish in Studies of Marine Protected Areas. In J. P. Beumer, A. Grant, & D. C. Smith (Eds.), *Aquatic protected areas. What works best and how do we know?* (Cairns ed., Vol. 1, pp. 455-464). University of Queensland.

Catalán, I.A., Álvarez-Ellacuría, A., Lisani, J.L., Sánchez, J., Vizoso, G., Heinrichs-Maquilón, A.E., Hinz, H., Alós, J., Signarioli, M., Aguzzi, J., Francescangeli, M. & Palmer, M. (2023). Automatic

Detection and Classification of Coastal Mediterranean Fish from Underwater Images: Good Practices for Robust Training. *Frontiers in Marine Science 10*.

Caza-Allard, I., Laporte, M., Côté, G., April, J. & Bernatchez, L. (2021). Effect of biotic and abiotic factors on the production and degradation of fish environmental DNA: An experimental evaluation. *Environmental DNA 4*: 453-468. https://doi.org/10.1002/edn3.266.

Collins, R.A., Wangensteen, O.S., O'Gorman, E.J., Mariani, S., Sims, D.W. & Genner, M.J. (2018). Persistence of Environmental DNA in Marine Systems. *Communications Biology 1*, no. 1: 185. https://doi.org/10.1038/s42003-018-0192-6.

Costa, A.C.P., Garcia, T.M., Paiva, B.P., Neto, A.R.X. & de Oliveira Soares, M. (2020). Seagrass and rhodolith beds are important seascapes for the development of fish eggs and larvae in tropical coastal areas. *Marine Environmental Research 161*: 105064. https://doi.org/10.1016/j.marenvres.2020.105064.

Dalongeville, A., Boulanger, E., Marques, V., Charbonnel, E., Hartmann, V., Santoni, M.C., Deter, J., Valentini, A., Lenfant, P., Boissery, P., Dejean, T., Velez, V., Pichot, F., Sanchez, L., Arnal, V., Bockel, T., Delaruelle, G., Holon, F., Milhau, T., Romant, L., Manel, S. & Mouillot, D. (2022). Benchmarking Eleven Biodiversity Indicators Based on Environmental DNA Surveys: More Diverse Functional Traits and Evolutionary Lineages inside Marine Reserves. *Journal of Applied Ecology 59*, no. 11: 2803–13. https://doi.org/10.1111/1365-2664.14276.

De Cáceres, M. & Jansen, M. & De Caceres, F.M.M. (2022). *Indicator species analysis using 'indicspecies'*.

de Juan, S., Ospina-Alvarez, A., Hinz, H., Moranta, J. & Barberá, C. (2023). The Continental Shelf Seascape: A Network of Species and Habitats. *Biodiversity and Conservation 32*. https://doi.org/10.1007/s10531-023-02552-8.

de Juan, S., Hinz, H., Sartor, P., Vitale, S., Bentes, L., Bellido, J.M., Musumeci, C., Massi, D., Gancitano, V. & Demestre, M. (2020). Vulnerability of Demersal Fish Assemblages to Trawling Activities: A Traits-Based Index. *Frontiers in Marine Science 7*. https://doi.org/10.3389/fmars.2020.00044.

de Juan, S., Lo Iacono, C. & Demestre, M. (2013). Benthic Habitat Characterisation of Soft-Bottom Continental Shelves: Integration of Acoustic Surveys, Benthic Samples and Trawling Disturbance Intensity. *Estuarine, Coastal and Shelf Science 117*:199-209. https://doi.org/10.1016/j.ecss.2012.11.012.

de Juan, S., Hewitt, J., Thrush, S. & Freeman, D. (2015). Standardising the Assessment of Functional Integrity in Benthic Ecosystems. *Journal of Sea Research 98*: 33–41. https://doi.org/10.1016/j.seares.2014.06.001.

Demestre, M., Soto, S., Durán, R., García del Arco, J.A., Cabrito, A., Illa-Lopez, L., Maynou, F., Sánchez, P., García-de-Vinuesa, A. & Emelianov, M. (2024). Reconstruction of the Maërl Habitat to Better Understand Its Ecological Integrity. *Science of The Total Environment 912*: 168752. https://doi.org/10.1016/j.scitotenv.2023.168752.

Desiderà, E., Guidetti, P., Panzalis, P., Navone, A., Valentini-Poirrier, C.A., Boissery, P., Gervaise, C. & Di Iorio, L. (2019). Acoustic Fish Communities: Sound Diversity of Rocky Habitats Reflects Fish Species Diversity. *Marine Ecology Progress Series 608*: 183–97. https://doi.org/10.3354/meps12812.

Di Iorio, L., Audax, M., Deter, J., Holon, F., Lossent, J., Gervaise, C. & Boissery, P. (2021). Biogeography of Acoustic Biodiversity of NW Mediterranean Coralligenous Reefs. *Scientific Reports 11*:16991. https://doi.org/10.1038/s41598-021-96378-5.

European Parliament. Council directive 1992/43/EC Conservation of natural habitats and of wild fauna and flora. Off. J. Eur. Union 1992, L206, 7–50.

Fragkopoulou, E., Serrão, E.A., Horta, P.A., Koerich, G. & Assis, J. (2021). Bottom Trawling Threatens Future Climate Refugia of Rhodoliths Globally. *Frontiers in Marine Science* 7:594537. https://doi.org/10.3389/fmars.2020.594537.

Hall-Spencer, J.M., Grall, J., Moore, P.G. & Atkinson, R.J.A. (2003). Bivalve Fishing and Maerl-Bed Conservation in France and the UK-Retrospect and Prospect. *Aquatic Conservation: Marine and Freshwater Ecosystems, 13*: S33–41. https://doi.org/10.1002/aqc.566.

He, X., Jeffery, N.W., Stanley, R.R.E., Hamilton, L.C., Rubidge, E.M. & Abbott, C.L. (2023). EDNA metabarcoding enriches traditional trawl survey data for monitoring biodiversity in the marine environment. *ICES Journal of Marine Science, 80*(5): 1529-1538. https://doi.org/10.1093/icesjms/fsad083

Hernandez-Kantun, J.J., Rindi, F., Adey, W.H., Heesch, S., Peña, V., Le Gall, L. & Gabrielson, P.W. (2015). Sequencing Type Material Resolves the Identity and Distribution of the Generitype *Lithophyllum Incrustans*, and Related European Species *L. Hibernicum* and *L. Bathyporum* (Corallinales, Rhodophyta). Edited by C. Lane. *Journal of Phycology 51*, no. 4: 791–807. https://doi.org/10.1111/jpy.12319.

Hewitt, J.E., Wang, D., Francis, M., Lundquist, C. & Duffy, C. (2015). Evaluating Demersal Fish Richness as a Surrogate for Epibenthic Richness in Management and Conservation. *Diversity and Distributions 21*(8): 901–12. https://doi.org/10.1111/ddi.12336.

Illa-López, L., Cabrito, A., de Juan, S., Maynou, F. & Demestre, M. (2023). Distribution of Rhodolith Beds and Their Functional Biodiversity Characterisation Using ROV Images in the Western

Mediterranean Sea. *Science of The Total Environment 905:* 167270. https://doi.org/10.1016/j.scitotenv.2023.167270.

Juhel, J.B., Utama, R.S., Marques, V., Vimono, I.B., Sugeha, H.Y., Kadarusman Pouyaud, L., Dejean, T., Mouillot, D, & Hocdé, R. (2020). Accumulation curves of environmental DNA sequences predict coastal fish diversity in thecoral triangle. *Proceedings of the Royal Society, B287*: 20200248. http://dx.doi.org/10.1098/rspb.2020.0248.

Juhel, J.B., Laurent, V., Mouillot, D., Kulbicki, M., Letessier, T.B., Meeuwig, J.J. & Wantiez, L. (2018). Reef accessibility impairs the protection of sharks. *Journal of Applied Ecology, 55*(2): 673-683. https://doi.org/10.1111/1365-2664.13007

Kuhnz, L.A., Gilbane, L., Cochrane, G.R. & Paull, C.K. (2022). Multi-Factor Biotopes as a Method for Detailed Site Characterization in Diverse Benthic Megafaunal Communities and Habitats in Deep-Water off Morro Bay, California. *Deep Sea Research Part I: Oceanographic Research Papers 190*: 103872. https://doi.org/10.1016/j.dsr.2022.103872.

Legrand, E., Riera, P., Lutier, M., Coudret, J., Grall, J. & Martin, S. (2017). Species Interactions Can Shift the Response of a Maerl Bed Community to Ocean Acidification and Warming. *Biogeosciences 14*, no. 23: 5359–76. https://doi.org/10.5194/bg-14-5359-2017.

Letessier, T.B., Juhel, J.B., Vigliola, L. & Meeuwig, J.J. (2015). Low-Cost Small Action Cameras in Stereo Generates Accurate Underwater Measurements of Fish. *Journal of Experimental Marine Biology and Ecology 466:* 120–26. https://doi.org/10.1016/j.jembe.2015.02.013.

Loh, T.L., Archer, S.K. & Dunham, A. (2019). Monitoring program design for data-limited marine biogenic habitats: A structured approach. *Ecology and Evolution, 9*:73467359. https://doi.org/10.1002/ece3.5261.

López-Garrido, P.H., Barry, J.P., González-Gordillo, J.I. & Escobar-Briones, E. (2020). ROV's Video Recordings as a Tool to Estimate Variation in Megabenthic Epifauna Diversity and Community Composition in the Guaymas Basin. *Frontiers in Marine Science*, 7: 154. https://doi.org/10.3389/fmars.2020.00154.

Maechler, M., Rousseeuw, P., Croux, C., Todorov, V., Ruckstuhl, A., Salibian-Barrera, M., Verbeke, T., Koller, M., Conceicao, E.L.T. & Di Palma, M.A. (2022). Robustbase: basic robust statistics. R package v.0.95-0. [WWW document] URL http://CRAN.R-project.org/package=robustbase. [accessed 28 November 2023].

Maggio, T., Perzia, P., Pazzini, A., Campagnuolo, S., Falautano, M., Mannino, A.M., Allegra, A. & Castriota, L. (2022). Sneaking into a Hotspot of Biodiversity: Coverage and Integrity of a

Rhodolith Bed in the Strait of Sicily (Central Mediterranean Sea). *Journal of Marine Science and Engineering*, *10*, no. 12: 1808. https://doi.org/10.3390/jmse10121808.

Mahé, F., Rognes, T., Quince, C., de Vargas, C. & Dunthorn, M. (2015). Swarm v2: highly-scalable and high-resolution amplicon clustering. *PeerJ*, *3*, 1–12. Retrieved from https://peerj.com/articles/1420.

Martin, M. (1994). Cutadapt removes adapter sequences from high- throughput sequencing reads. *EMBnet.Journal*, *17*(1), 10–1 2.

Mathon, L., Marques, V., Manel, S., Albouy, C., Andrello, M., Boulanger, E., Deter, J., Hocdé, R., Leprieur, F., Letessier, T.B., Loiseau, N., Maire, E., Valentini, A., Vigiola, L., Baletaud, F., Bessudo, S., Dejean, T., Faure, N., Guerin, P.E., Jucker, M., Juhel, J.B., Kadarusman Polanco, A.F., Pouvaud, L., Schwörer, D., Thompson, K.F., Troussellier, M., Sugeha, H.Y., Velez, L., Zhang, X., Zhong, W., Pellissier, L. & Mouillot, D. (2023). The Distribution of Coastal Fish EDNA Sequences in the Anthropocene. *Global Ecology and Biogeography*.13698. https://doi.org/10.1111/geb.13698.

McDevitt, A.D., Guimarães Sales, N., Browett, S.S., Sparnenn, A.O., Mariani, S., Wangensteen, O.S., Coscia, I., Benvenuto, C. (2019). Environmental DNA Metabarcoding as an Effective and Rapid Tool for Fish Monitoring in Canals. *Journal of Fish Biology* *95*(2): 679–82. https://doi.org/10.1111/jfb.14053.

Mirimin, L., Desmet, S., López Romero, D., Fernandez Fernandez, S., Miller, D.L., Mynott, S., Gonzalez Brincau, A., Stefanni, S., Berry, A., Gaughan, P. & Aguzzi, J. (2021). Don't Catch Me If You Can – Using Cabled Observatories as Multidisciplinary Platforms for Marine Fish Community Monitoring: An in Situ Case Study Combining Underwater Video and Environmental DNA Data. *Science of The Total Environment* *773*: 145351. https://doi.org/10.1016/j.scitotenv.2021.145351.

Miya, M. (2022). Environmental DNA Metabarcoding: A Novel Method for Biodiversity Monitoring of Marine Fish Communities. *Annual Review of Marine Science* *14*, no. 1: 161–85. https://doi.org/10.1146/annurev-marine-041421-082251.

Mooney, T.A., Di Iorio, L., Lammers, M., Lin, T.H., Nedelec, S.L., Parsons, M., Radford, C., Urban, E. & Stanley, J. (2020). Listening forward: approaching marine biodiversity assessments using acoustic methods. *Royal Society Open Science*, *7*: 201287. http://dx.doi.org/10.1098/rsos.201287.

Moranta, J., Barberá, C., Druet Vélez, M., Díaz-Valdés, M., Zaragoza, N., Tello-Antón, M.O., López-Jurado, J.L., Balbín, R., Flexas, M.D.M., Fernández, M., Hidalgo, M., Domínguez, M., Quetglas, A., Goñi, R., Mallol, S., Sánchez-Delgado, F., Ambroso, S. & Comalada, N. (2014). Caracterización ecológica de la plataforma continental (50-100 m) del canal de Menorca.

Informe final área LIFE+ INDEMARES (LIFE07/NAT/E/000732). Instituto Español de Oceanografía-Centro Oceanográfico de Baleares (Palma). Coordinación: Fundación Biodiversidad, Palma, 504 pág. Available online at http://hdl.handle.net/10261/318214.

Mueller, R.P., Brown, R.S., Hop, H. & Moulton, L. (2006). Video and Acoustic Camera Techniques for Studying Fish under Ice: A Review and Comparison. *Reviews in Fish Biology and Fisheries 16*: 213–26. https://doi.org/10.1007/s11160-006-9011-0.

Muff, M., Jaquier, M., Marques, V., Ballesta, L., Deter, J., Bockel, T., Hocdé, R., Juhel, J.B., Boulanger, E., Guellati, N., Polanco-Fernández, A., Valentini, A., Dejean, T., Manel, S., Albouy, C., Durville, P., Mouillot, D., Holon, F. & Pellissier, L. (2023). Environmental DNA Highlights Fish Biodiversity in Mesophotic Ecosystems. *Environmental DNA* 5, no. 1: 56–72. https://doi.org/10.1002/edn3.358.

Ordines, F. & Massutí, E. (2009). Relationships between Macro-epibenthic Communities and Fish on the Shelf Grounds of the Western Mediterranean. *Aquatic Conservation: Marine and Freshwater Ecosystems 19*(4): 370–83. https://doi.org/10.1002/aqc.969.

Peña, V., Bárbara, I., Grall, J., Maggs, C.A. & Hall-Spencer, J.M. (2014). The Diversity of Seaweeds on Maerl in the NE Atlantic. *Marine Biodiversity*, *44*(4): 533-51. https://doi.org/10.1007/s12526-014-0214-7.

Picciulin, M., Sebastianutto, L., Codarin, A., Calcagno, G. & Ferrero, E.A. (2012). Brown Meagre Vocalization Rate Increases during Repetitive Boat Noise Exposures: A Possible Case of Vocal Compensation. *The Journal of the Acoustical Society of America* 132, no. 5: 3118–24. https://doi.org/10.1121/1.4756928.

Pinna, M., Zangaro, F., Saccomanno, B., Scalone, C., Bozzeda, F., Fanini, L. & Specchia, V. (2023). An Overview of Ecological Indicators of Fish to Evaluate the Anthropogenic Pressures in Aquatic Ecosystems: From Traditional to Innovative DNA-Based Approaches. *Water 15*: 949. https://doi.org/10.3390/w15050949.

Polanco-Fernández, A., Marques, V., Fopp, F., Juhel, J.B., Borrero-Pérez, G.E., Cheutin, M.C., Dejean, T., González Corredor, J.D., Acosta-Chaparro, A., Hocdé, R., Eme, D., Maire, E., Spescha, M., Valentini, A., Manel, S., Mouillot, D., Albouy, C. & Pellissier, L. (2021). Comparing environmental DNA metabarcoding and underwater visual census to monitor tropical reef fishes. *Environmental DNA*, *3*:142-156. https://doi.org/10.1002/ edn3.140.

Pont, D., Rocle, M., Valentini, A., Civade, R., Jean, P., Maire, A., Roset, N., Schabuss, M., Zornig, H. & Dejean, T. (2018). Environmental DNA reveals quantitative patterns of fish biodiversity in large

rivers despite its downstream transportation. *Scientific Reports 8*, 10361. https://doi.org/10.1038/s41598-018-28424-8.

R Core Team (2022). R: A Language and Environment for Statistical Computing. R Foundation for Statistical Computing, Vienna, Austria. Available online at https://www.R-project.org/.

Rabin, L.A. & Greene, C.M. (2002). Changes to Acoustic Communication Systems in Human-Altered Environments. *Journal of Comparative Psychology* 116: 137–41. https://doi.org/10.1037/0735-7036.116.2.137.

Riosmena-Rodríguez, R., Nelson, W., Aguirre, J. (Eds.) (2017). *Rhodolith/Maërl Beds: A Global Perspective*, Vol. 15. Springer International Publishing. https://doi.org/10.1007/978-3-319-29315-8.

Robert, K., Jones, D.O.B. & Huvenne, V.A.I. (2014). Megafaunal distribution and biodiversity in a heterogeneous landscape: The iceberg-scoured Rockall Bank, NE Atlantic. *Marine Ecology Progress Series, 501*: 67-88. https://doi.org/10.3354/meps10677.

Rognes, T., Flouri, T., Nichols, B., Quince, C. & Mahé, F. (2016). VSEARCH: a versatile open source tool for metagenomics. *PeerJ*.

Romagnoli, B., Grasselli, F., Costantini, F., Abbiati, M., Romagnoli, C., Innangi, S., Di Martino, G. & Tonielli, R. (2021). Evaluating the Distribution of Priority Benthic Habitats through a Remotely Operated Vehicle to Support Conservation Measures off Linosa Island (Sicily Channel, Mediterranean Sea). *Aquatic Conservation: Marine and Freshwater Ecosystems, 31*: 1686–99. https://doi.org/10.1002/aqc.3554.

Sanchez, L., Boulanger, E., Arnal, V., Boissery, P., Dalongeville, A., Dejean, T., Deter, J., Guellati, N., Holon, F., Juhel, J.B., Lenfant, P., Leprieur, F., Valentini, A., Manel, S. & Mouillot, D. (2022). Ecological indicators based on quantitative eDNA metabarcoding: the case of marine reserves. *Ecological Indicators 140*:108966. https://www.sciencedirect.com/science/article/pii/S1470160X2200437X?via%3Dihub.

Sciberras, M., Rizzo, M., Mifsud, J., Camilleri, K., Borg, J.A., Lanfranco, E. & Schembri, P. (2009). Habitat Structure and Biological Characteristics of a Maerl Bed off the Northeastern Coast of the Maltese Islands (Central Mediterranean). *Marine Biodiversity, 39*: 251–64. https://doi.org/10.1007/s12526-009-0017-4.

Sato, M., Inoue, N., Nambu, R., Furuichi, N., Imaizumi, T. & Ushio, M. (2021). Quantitative Assessment of Multiple Fish Species Around Artificial Reefs Combining Environmental DNA Metabarcoding and Acoustic Survey. *Scientific Reports* 11: 19477. https://doi.org/10.1038/s41598-021-98926-5.

Stat, M., John, J., Di Battista, J.D., Newman, S.J., Bunce, M. & Harvey, E.S. (2019). Combined Use of EDNA Metabarcoding and Video Surveillance for the Assessment of Fish Biodiversity. *Conservation Biology 33*: 196–205. https://doi.org/10.1111/cobi.13183.

Thorson, J.T. & Barnett, L.A.K. (2017). Comparing Estimates of Abundance Trends and Distribution Shifts Using Single- and Multispecies Models of Fishes and Biogenic Habitat. Edited by Emory Anderson. *ICES Journal of Marine Science, 74*(5): 1311–21. https://doi.org/10.1093/icesjms/fsw193.

Trégarot, E., D'Olivo, J.P., Botelho, A.Z., Cabrito, A., Cardoso, G.O., Casal, G., Cornet, C.C., Cragg, S.M., Degia, A.K., Fredriksen, S., Furlan, E., Heiss, G., Kersting, D.K., Maréchal, J.P., Meesters, E., O'Leary, B.C., Pérez, G., Seijo-Núñez, C., Simide, R., van der Geest, M. & de Juan, S. (2023). Effects of climate change on marine coastal ecosystems – A review to guide research and management. *Biological conservation***.** https://doi.org/10.1016/j.biocon.2023.110394.

Tuya, F., Schubert, N., Aguirre, J., Basso, D., Bastos, E.O., Berchez, F., Bernardino, A.F., Bosch, N.E., Burdett, H., Espino, F., Fernández-Gárcia, C., Francini-Filho, R.B., Gagnon, P., Hall-Spencer, J.M., Haroun, R., Hofmann, L.C., Horta, P.A., Kamenos, N.A., Le Gall, L., Magris, R.A., Martin, S., Nelson, W.A., Neves, P., Olivé, I., Otero-Ferrer, F., Peña, V., Pereira-Filho, G.H., Ragazzola, F., Rebelo, A.C., Ribeiro, C., Rinde, E., Schoenrock, K., Silva, J., Sissini, M.N. & Tâmega, F.T.S. (2023). Levelling-up Rhodolith-Bed Science to Address Global-Scale Conservation Challenges. *Science of The Total Environment 892*: 164818. https://doi.org/10.1016/j.scitotenv.2023.164818.

Valentini, A., Taberlet, P., Miaud, C., Civade, R., Herder, J., Thomsen, P.F., Bellemain, E., Besnard, A., Coissac, E., Boyer, F., Gaboriaud, C., Jean, P., Poulet, N., Roset, N., Copp, G.H., Geneiz, P., Pont, D., Argillier, C., Baudoin, J.M., Peroux, T., Crivelli, A.J., Olivier, A., Acqueberge, M., Le Brun, M., Moller, P.R., Willerslev, E. & Dejean, T. (2016). Next-Generation Monitoring of Aquatic Biodiversity Using Environmental DNA Metabarcoding. *Molecular Ecology 25*(4): 929–42. https://doi.org/10.1111/mec.13428.

Wangensteen, O.S. & Turón, X. (2017). Metabarcoding techniques for assessing biodiversity of marine animal forests. *Marine animal forests. The ecology of benthic biodiversity hotspots*, 1, 445–503. https://doi.org/10.1007/978-3-319-17001-5_53-1.

Wong, M.K.W., Nobata, S., Ito, S.I. & Hyodo, S. (2022). Development of species-specific multiplex real-time PCR assays for tracing the small pelagic fishes of North Pacific with environmental DNA. *Environmental DNA 4*(3): 510-522. https://doi.org/10.1002/edn3.275.

Supplementary Material

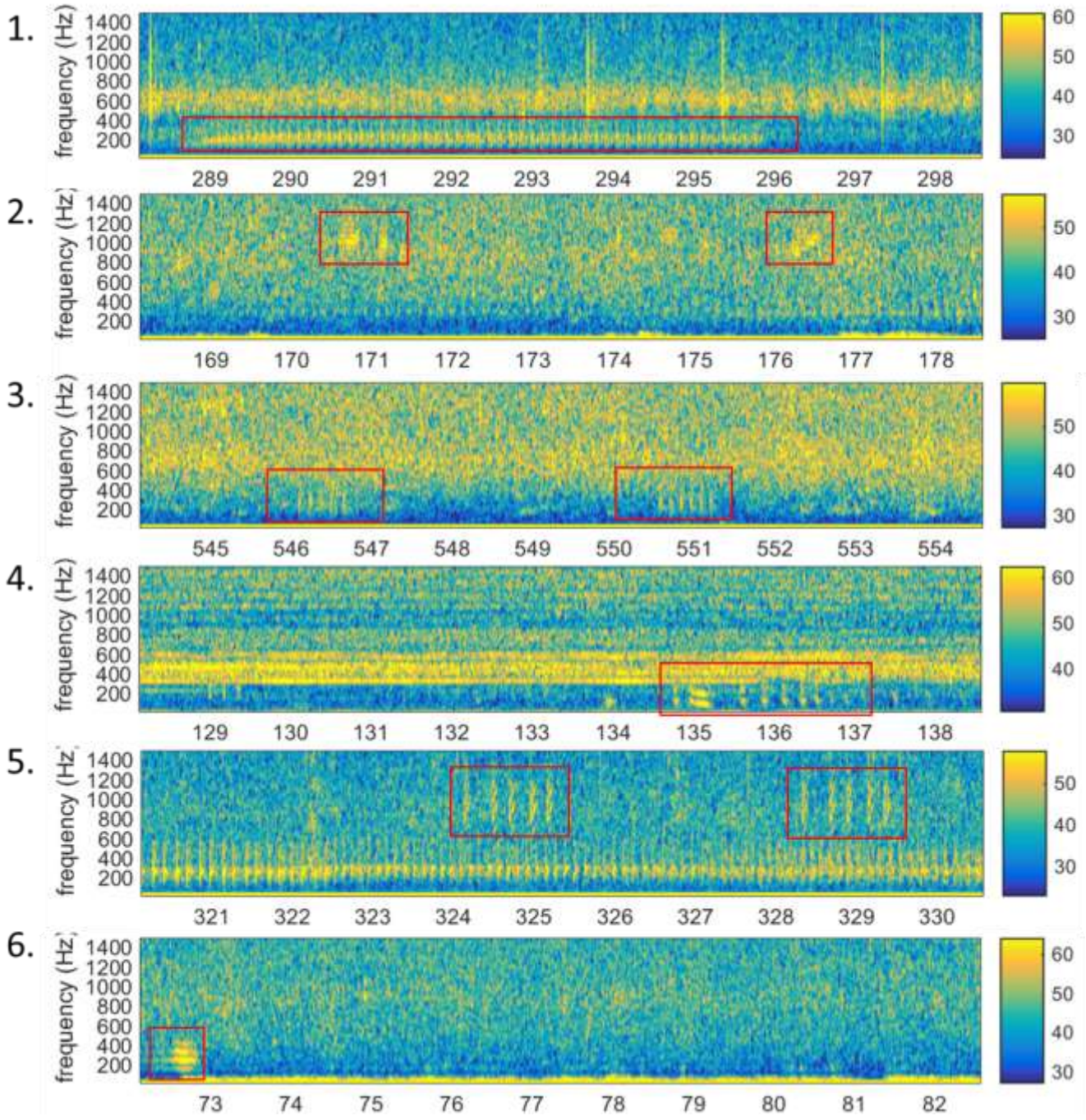


Fig.2.4.S1. Spectrograms of 10 s with from the top to the bottom (**1**) one acoustic signature emitted by *Ophidion rochei* (**2**) two call of *Scorpaena* spp, (**3**) two R-calls of brown meager, (**4**) one downsweep series of a grouper, (**5**) two "High Frequency" cals typical of Mediterranean coralligenous habitat and (**6**) one call of another, undetermined species.

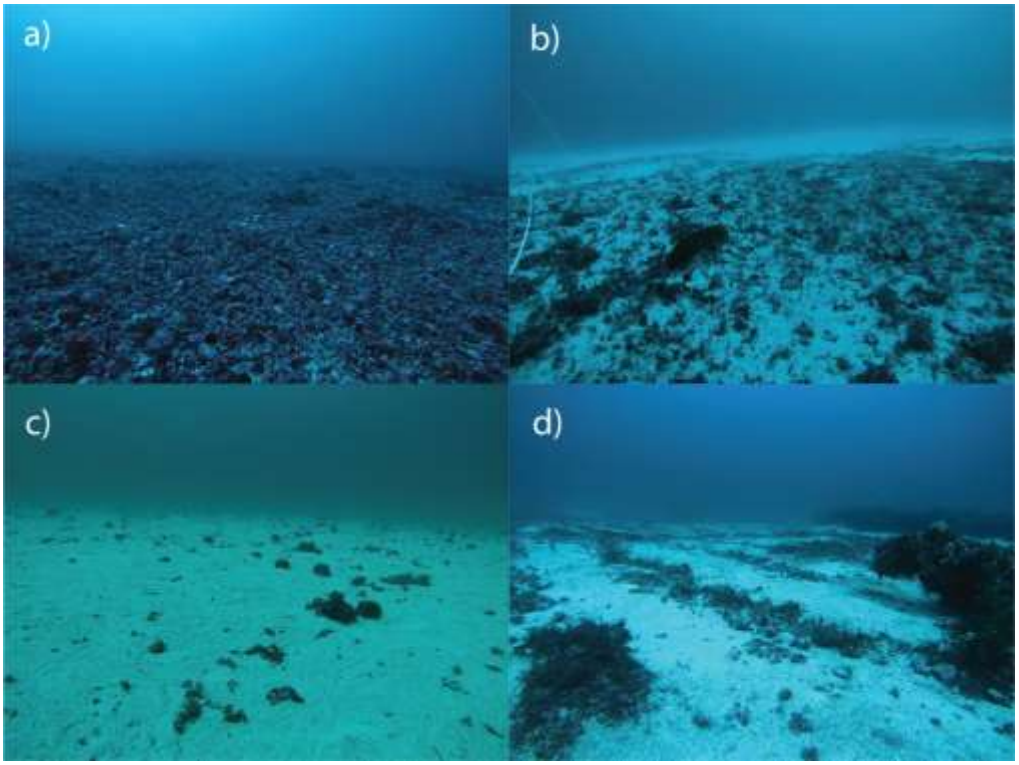


Fig.2.4.S2. Habitat types detected in the study area with the static video. (**a**) Rhodolith bed (100% rhodolith coverage), (**b**) sand with <50% of rhodolith cover, (**c**) sand with <10% rhodolith cover and (**d**) heterogeneous habitat with rocky outcrops.

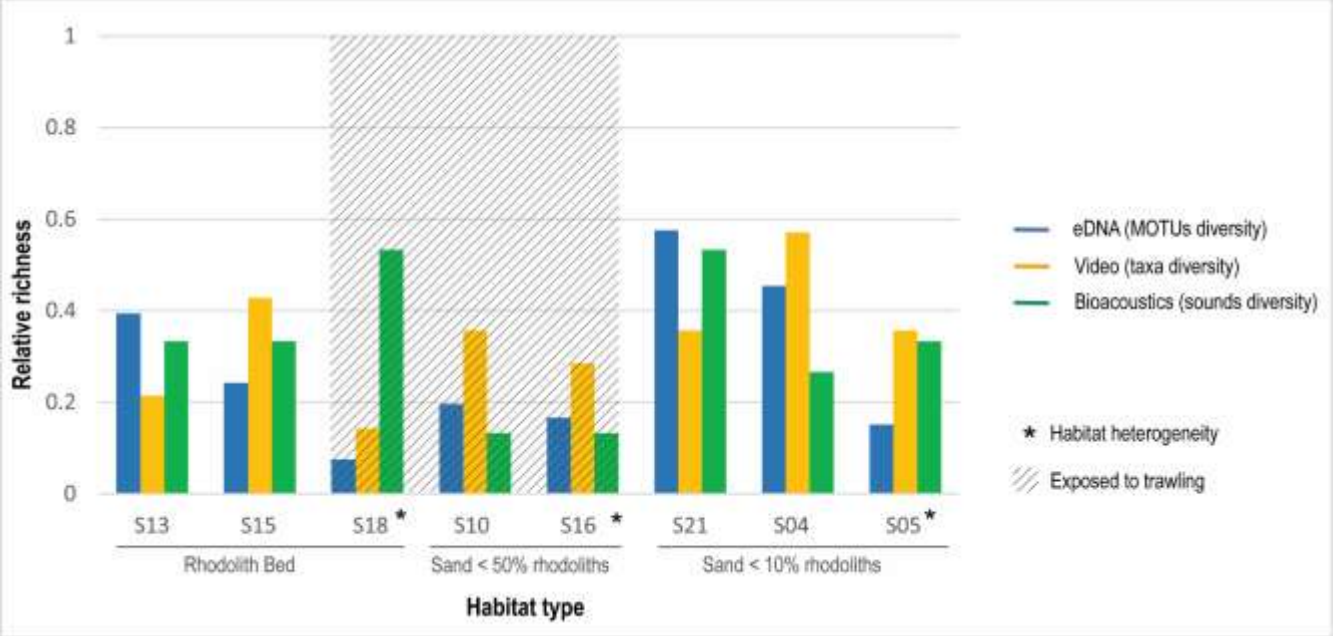


Fig.2.4.S3. Relative richness values per station estimated with the three different techniques, data normalised to maximum value detected per technique. In blue fish richness detected with eDNA (index of MOTUs diversity), in orange the richness detected through 20 minutes of video and in green richness of sounds (index of fish sounds diversity).

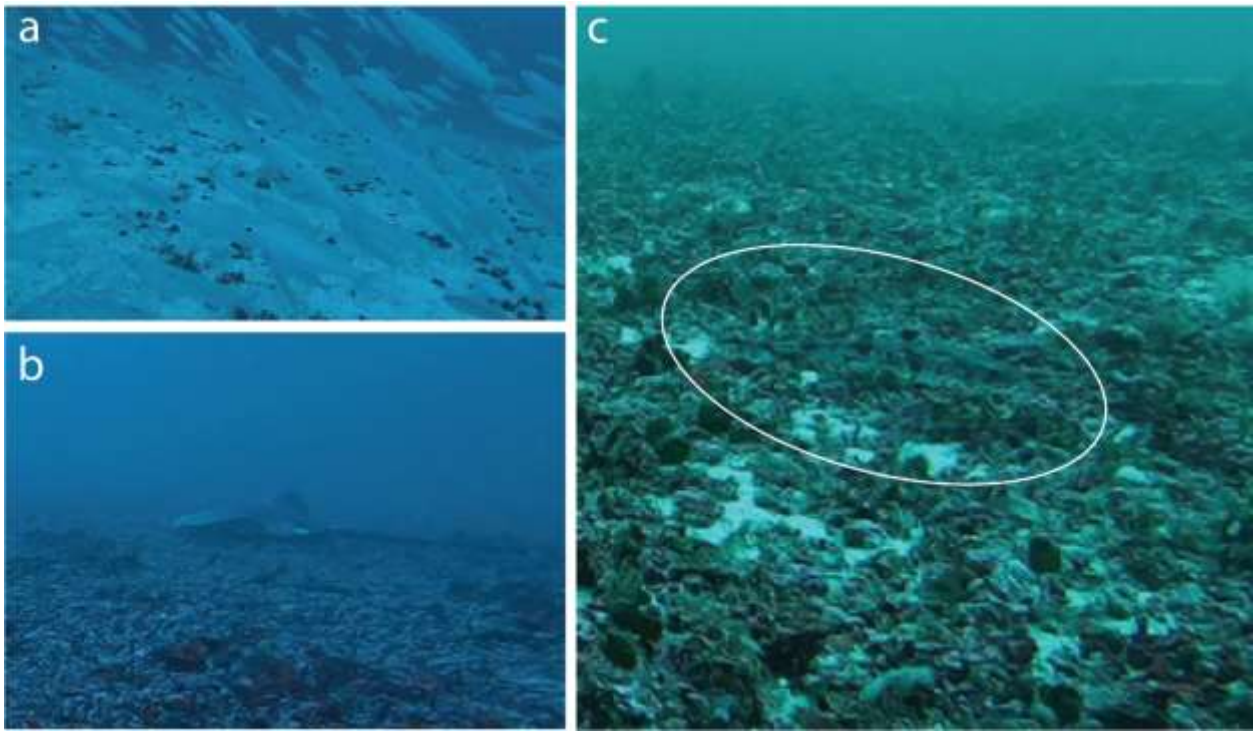


Fig.2.4.S4. Examples of species observed with video imaging: (**a**) shoal of *Spicara* sp., (**b**) Ray passing in front of the camera, (**c**) *Scyliorhinus canicula* camouflaged with the bottom.

Table 2.4.S1. Sounds fish categories from Desiderà et al. (2019). Categories 1 to 4 include types of sounds that can be assigned to a species or genus. Category 5 includes high frequency sounds recorded from Mediterranean coralligenous bottoms, while category 6 includes sounds emitted by other fishes.

Category	Emitted by	Reference
1	*Ophidion rochei* (Roche's cusk-eel)	Kéver et al. (2016)
2	*Scorpaena* spp. (Scorpion fish)	Bolgan et al. (2019)
3	*Sciaena umbra* (Brown meagre)	Picciulin et al. (2013)
4	*Epinephelus marginatus* (Dusky grouper)	Bertucci et al. (2015), Desiderà et al. (2019)
5	HF (High Frequency) (typical in coralligenous reefs)	Di Iorio et al. (2021)
6	Other fish	

Table 2.4.S2: Summary of the means, maximum and minimum values obtained for fish richness, fish sound richness and abundance of sounds for each of the three techniques used on the three considered factors: Rhodolith coverage, habitat heterogeneity (both factors defined after video sampling analysis) and trawling exposure (Fig.2.4.1).

		VIDEO				eDNA				ACOUSTICS						
		Richness (S) of fish taxa				Richness (S) of fish MOTUs				Richness (S) of fish sounds				Abundance of sounds per hour n° of vocalizations / h		
		N	Mean	max	min	*N*	Mean	max	min	*N*	Mean	max	min	Mean	max	min
RHODOLITH COVERAGE	*Rhodolith Bed (S01, S13, S15, S18)*	4	4.25	6	2	4	16.5	26	5	3	6	8	5	135.1	239.3	63.9
	Detrital biogenic <50% (S10, S16, L2)	3	5	6	4	2	12	13	11	3	2.67	4	2	131.43	183.7	72.6
	Detrital biogenic <10% (S04, S05, S21, S26)	3	6	8	5	4	26	38	10	3	5.67	8	4	154.67	238.8	42.4
TRAWLING EXPOSURE	*Not-Exposed (S21, S01, S13, S15, S04, S05, S26)*	6	5.5	8	3	7	23.57	38	10	5	5.4	8	4	126	238.8	42.4
	Exposed (S10, S16, S18, L2)	4	4.25	6	2	3	9.67	13	5	4	4	8	2	158.4	239.3	72.6
HABITAT HETEROGENEITY	*Homogeneity (S10, S13, S15, S18, S21, S04)*	6	5.5	8	3	5	24.6	38	13	6	4.67	8	2	107.92	183.7	42.4
	Heterogeneity (S01, S16, L2, S05)	4	4.25	6	2	4	11.25	19	5	3	5	8	2	205.37	239.3	138

Table 2.4.S3. Taxa identified through video analysis at the lowest taxonomic level (LTL). * (Species of commercial interest in Balearic Islands).

Class	Family	Taxon
Actinopterygii	Gobiidae	*Aphia* cf. *minuta*
Actinopterygii	Gobiidae	Gobid
Actinopterygii	Sparidae	*Boops boops*
Actinopterygii	Sparidae	*Dentex dentex* *
Actinopterygii	Sparidae	Fish
Actinopterygii	Sparidae	Shoal of fishes
Actinopterygii	Labridae	*Coris julis*
Actinopterygii	Serranidae	*Serranus cabrilla*
Actinopterygii	Serranidae	*Serranus hepatus*
Actinopterygii	Serranidae	*Serranus* sp.
Actinopterygii	Pleuronectidae	Flat fish
Actinopterygii	Trachinidae	*Trachinus* sp.
Chondrichthyes	Dasyatidae	*Dasyatis pastinaca*
Chondrichthyes	Scyliorhinidae	*Scyliorhinus canicula**

Table 2.4.S4. Teleost and chondrichthyes taxa recovered by eDNA according to reference database. * (Species of commercial interest), * (Vulnerable species), * (Cryptic species).

Class	Order	Family	Taxon
Actinopterygii	Anguilliformes	Congridae	*Conger conger* *
		Muraenidae	*Muraena helena*
	Aulopiformes	Synodontidae	*Synodus saurus*
	Blenniiformes	Blenniidae	*Blennius ocellaris*
	Carangiformes	Carangidae	*Seriola dumerili**
			*Trachurus picturatus**
			Trachurus sp. *
	Clupeiformes	Clupeidae	*Sardina pilchardus* *
			Sardinella aurita
		Engraulidae	*Engraulis encrasicolus* *
	Gobiiformes	Gobiidae	*Buenia affinis**
			Corcyrogobius liechtensteini *
			Crystallogobius linearis *
			Gobius cruentatus
			Gobius xanthocephalus
			Lebetus guilleti *
			Odondebuenia balearica *
			Pseudaphya ferreri *
			Speleogobius trigloides *
	Istiophoriformes	Xiphiidae	*Xiphias gladius* *
	Kurtiformes	Apogonidae	*Apogon imberbis*
	Labriformes	Labridae	*Coris julis*
			Symphodus sp.
			Xyrichtys novacula *
	Myctophiformes	Myctophidae	*Ceratoscopelus maderensis*
			Lampanyctus crocodilus
	Perciformes	Scorpaenidae	*Scorpaena notata* *
			Scorpaena porcus *
			Scorpaena scrofa *
		Serranidae	*Anthias anthias*
			Epinephelus marginatus **
			Serranus cabrilla

			Serranus hepatus
		Trachinidae	*Trachinus draco*
			Trachinus radiatus
		Triglidae	*C. obscurus / T. lastoviza*
	Pleuronectiformes	Bothidae	*Arnoglossus laterna*
			Bothus podas
	Scombriformes	Scombridae	*Auxis sp.* *
			Euthynnus alletteratus *
			Scomber colias *
			Thunnus thynnus **
	Spariformes	Centracanthidae	*Spicara maena*
		Sparidae	*B. boops / O. melanura*
			D. dentex / P. auriga / P. pagrus *
			Diplodus vulgaris *
			Pagellus acarne *
			Pagellus bogaraveo *
			Pagellus erythrinus *
			Spondyliosoma cantharus *
	Syngnathiformes	Dactylopteridae	*Dactylopterus volitans*
		Mullidae	*Mullus barbatus* *
			Mullus surmuletus *
		Syngnathidae	*Syngnathus acus* *
	Uranoscopiformes	Ammodytidae	*Gymnammodytes semisquamatus* *
		Uranoscopidae	*Uranoscopus scaber*
	-	Pomacentridae	*Chromis chromis*
	-	Sciaenidae	*Sciaena umbra* *
Chondrichthyes	Carcharhiniformes	Carcharhinidae	*Prionace glauca* *
		Scyliorhinidae	*Scyliorhinus canicula* **
	Myliobatiformes	Dasyatidae	*Dasyatis pastinaca* **
			Pteroplatytrygon violacea *
		Myliobatidae	*Myliobatis aquila* *
	Rajiformes	Rajidae	*Raja brachyura* *
			Raja asterias / Raja clavata
	Torpediniformes	Torpedinidae	*Torpedo marmorata* *

Table 2.4.S5. The 10 most represented species in each level of rhodolith coverage, in each level of habitat complexity and in each level of trawling exposure.

Rhodolith bed	**sand < 50% rhodoliths**	**sand < 10% rhodoliths**
Corcyrogobius liechtensteini	*Trachurus picturatus*	*Xyrichtys novacula*
Speleogobius trigloides	*Xiphias gladius*	*Scorpaena scrofa*
Trachins radiatus	*Lampanyctus crocodilus*	*C.obscurus_T.lastoviza*
Myliobatis aquila	*Arnoglossus laterna*	*Pagellus erythrinus*
Engraulis encrasicolus	*Pagellus bogaraveo*	*Gobius cruentatus*
Odondebuenia balearica	*Prionace glauca*	*Apogon imberbis*
Scorpaena notata	*Pteroplatytrygon violacea*	*Spìcara maena*
Pagellus acarne	*Trachurus sp.*	*Gymmnammodytes semisquamatus*
Crystallgobius linearis	*Scomber colias*	*Sciaena umbra*
Diplodus vulgaris	*Euthynnus alletteratus*	*Raja brachyura*
Heterogeneous habitat	**Homogeneous habitat**	
Serranus hepatus	*Crystallogobius linearis*	
Xiphias gladius	*Engraulis encrasicolus*	
Pagellus bogaraveo	*Conger conger*	
Syngnathus acus	*Sardinella aurita*	
Prionace glauca	*Pseudaphya ferreri*	
Anthias anthias	*Diplodus vulgaris*	
Sardina pilchardus	*Scorpaena notata*	
Gobius cruentatus	*Pagellus acarne*	
Apogon imberbis	*Scyliorhinus canicula*	
Spicara maena	*Muraena helena*	
Not Exposed stations	**Exposed stations**	
Diplodus vulgaris	*Euthynnus alletteratus*	
Pagellus erythrinus	*Trachurus picturatus*	
B.boops / O.melanura	*Xiphias gladius*	
Coris julis	*Lampanyctus crocodilus*	
Serranus cabrilla	*Arnoglossus laterna*	
D.dentex / P. auriga / P.pagrus	*Pagellus bogaraveo*	
Spondyliosoma cantharus	*Prionace glauca*	
Uranoscopus scaber	*Pteroplatytrygon violacea*	
Conger conger	*Trachurus sp*	
Synodus saurus	*Scomber colias*	

Table 2.4.S6. Species detected in the eight sites where all three techniques were performed.

Method	Sps	S13	S15	S18	S16	S10	S21	S4	S5
eDNA	*Anthias anthias*	1		1	1		1	1	1
Video	*Aphia* cf. *minuta* .		1					1	
eDNA	*Apogon imberbis*						1	1	
eDNA	*Arnoglossus laterna*					1			
eDNA	*B. boops, O. melanura*	1	1		1	1	1	1	1
Video	*Boops boops*	1							
eDNA	*Blennius ocellaris*						1		
eDNA	*Bothus podas*								1
eDNA	*Buenia affinis*	1					1	1	1
eDNA	*C. obscurus, T. lastoviza*						1	1	
eDNA	*Ceratoscopelus maderensis*						1		
eDNA	*Chromis chromis*						1	1	1
eDNA	*Conger conger*	1	1				1	1	
eDNA	*Corcyrogobius liechtensteini*	1							
eDNA	*Coris julis*	1					1	1	
Video	*Coris julis*					1			1
eDNA	*Crystallogobius linearis*	1	1			1	1	1	
eDNA	*Dactylopterus volitans*						1		
eDNA	*Dasyatis pastinaca*		1				1	1	
Video	*Dasyatis pastinaca*		1						
eDNA	*D. dentex / P. auriga / P. pagrus*	1					1	1	
Video	*Dentex dentex.*							1	
eDNA	*Diplodus vulgaris*	1	1				1	1	
eDNA	*Epinephelus marginatus*						1		
Acoustic	*Epinephelus* spp.	1	1	1	1		1		1
Video	Fish	1	1		1		1	1	1
Video	Flat fish							1	
Video	Gobid		1			1	1	1	
eDNA	*Gobius cruentatus*						1	1	
eDNA	*Gymnammodytes semisquamatus*							1	1
eDNA	*Lampanyctus crocodilus*					1			
eDNA	*Lebetus guilleti*	1							
eDNA	*Mullus surmuletus*	1		1			1	1	
eDNA	*Myliobatis aquila*		1						
eDNA	*Odondebuenia balearica*	1	1	1			1		
Acoustic	*Ophidion rochei*	1	1	1		1	1	1	1
eDNA	*Pagellus acarne*	1	1						
eDNA	*Pagellus erythrinus*	1	1			1	1	1	1
eDNA	*Prionace glauca*				1				
eDNA	*Pseudaphya ferreri*	1	1			1	1	1	
eDNA	*Pteroplatytrygon violacea*					1			
eDNA	*Raja brachyura*							1	
eDNA	*Raja asterias / Raja clavata*	1						1	
eDNA	*Sciaena umbra*							1	

Acoustic	*Sciaena Umbra*	1					1	1	1
eDNA	*Scorpaena notata*	1				1			
eDNA	*Scorpaena porcus*						1		
eDNA	*Scorpaena scrofa*							1	
Acoustic	Scorpaenidae		1	1			1		
eDNA	*Scyliorhinus canicula*		1				1		
Video	*Scyliorhinus canicula*		1	1	1	1			
eDNA	*Serranus cabrilla*	1	1				1	1	
Video	*Serranus cabrilla*		1		1		1	1	1
eDNA	*Serranus hepatus*			1			1	1	
Video	*Serranus hepatus*			1	1			1	
Video	*Serranus* spp						1		
Video	Shoal of fishes	1				1			1
eDNA	*Speleogobius trigloides*		1						
eDNA	*Spicara maena*						1	1	
eDNA	*Spondyliosoma cantharus*	1					1	1	
eDNA	*Symphodus* sp.	1					1		
eDNA	*Syngnathus acus*							1	
eDNA	*Synodus saurus*						1	1	
eDNA	*Torpedo marmorata*						1	1	
eDNA	*Trachinus draco*						1	1	
Video	*Trachinus* spp.					1	1	1	1
eDNA	*Uranoscopus scaber*	1						1	1
eDNA	*Xyrichtys novacula*						1	1	1

Table 2.4.S7a. Qualitative assessment for trawl sampling. Information based on expert knowledge and supported by information extracted from the fieldwork of the Indemares project.

			TRAWL (x 10 stations)		
	Requirements	**Description**	Expert knowledge		*Qualitative value*
Capability	**Simplicity**	Degree of being easily done (sampling technique)	*Experience is recommended.*		*Low*
	Expertise	Technical expertise in species identification	*Some taxonomic expertise*		*Medium*
	Spatial scale	Spatial extent of ecological processes detected	*Depending on the transect length, 1km minimum*		*High*
Seascape information	**Time scale**	Sampling timeframe	*Instantaneous (snapshot)*		*Low*
	Habitat composition	Relative proportions of habitat elements	*No information available*		*None*
	Habitat heterogeneity	Detection of small-scale heterogeneity	*No information available*		*None*
Species information	**Species inventory**	Ability to detect number of species	*For benthic monitoring*		*High*
	Sensitive species	Ability to detect vulnerable species	*Selective sampling gear*		*Medium*
	Cryptic species	Ability to detect cryptic species	*Selective sampling gear*		*Medium*
	Biological activity	Ability to detect biological activities	*You could infer activity from catchability*		*Low*
Intrusiveness	**Physical disturbance**	Level of seafloor disturbance	*Trawling gear impact and damage the seafloor*		*High*
Cost – effectiveness	**Fieldwork time and personnel**	Time	*3 days full time*		*High*
		Personnel	*4 scientists + ship crew*		
		Sampling time	*8h shifts*		
	Fieldwork cost	Eur. Personnel	*3 days x 4 scientist x 50 EUR/day*	600 EUR	*High*
		Eur. Ship/Boat	*Oceanographic vessel 3 days x 5,000 EUR/Day*	15,000 EUR	
		Eur. Material	*10% amortization of 6,000 EUR (trawl price)*	600 EUR	
		EUR TOTAL		**16,200 EUR**	
	Processing cost	Eur. Processing	*Introducing data 10h x 30 EUR/h*	300 EUR	*Low*
	TOTAL MONETARY COSTS CAMPAIGN			**TOTAL = 16,500 EUR**	**High**

Table 2.4.S7b. Qualitative assessment for static video sampling. Information based on expert knowledge and supported by information extracted from the fieldwork of the MaCoBioS project.

			STATIC VIDEO (x 10 stations)		
	Requirements	**Description**	Expert knowledge		Qualitative value
Capability	**Simplicity**	Degree of being easily done (sampling technique)	*Easy to deploy cameras*		High
	Expertise	Technical expertise in species identification	*Taxonomic expertise*		High
	Spatial scale	Spatial extent of ecological processes detected	*With high transparency, 5 meters from the camera.*		Low
Seascape information	**Time scale**	Sampling timeframe	*Instantaneous (20' video)*		Low
	Habitat composition	Relative proportions of habitat elements	*You have a real vision of the habitat sampled*		High
	Habitat heterogeneity	Detection of small-scale heterogeneity	*Detection of within/between sites habitat patchiness*		High
Species information	**Species inventory**	Ability to detect number of species	*Limited to the video frame*		Low
	Sensitive species	Ability to detect vulnerable species	*Low*		Low
	Cryptic species	Ability to detect cryptic species	*Low*		Low
	Biological activity	Ability to detect biological activities	*Ability to detect activities and movement signals*		Medium
Intrusiveness	**Physical disturbance**	Level of seafloor disturbance	*Static contact with the seabed*		Low
Cost – effectiveness	**Fieldwork time and personnel**	Time	*3 days part time*		Low
		Personnel	*2 scientists + ship crew*		
		Sampling time	*10 ' Deployment + 30' waiting + 20 ' recover*		
	Fieldwork cost	Eur. Personnel	*3 days x 2 scientist x 50 EUR/Day*	300 EUR	
		Eur. Ship/Boat	*Scientific small boat. 3 days x 375 EUR/Day*	1,125 EUR	
		Eur. Material	*10% amortization of 3,200 EUR (tripod+go pros)*	320 EUR	
		EUR TOTAL		**1,745 EUR**	
	Processing cost	Eur. Processing	*Video visualization 10h x 30 EUR/h*	300 EUR	Low
	TOTAL MONETARY COSTS CAMPAIGN			**TOTAL = 2,045 EUR**	**Low**

Table 2.4.S7c. Qualitative assessment for eDNA sampling. Information based on expert knowledge and supported by information extracted from the fieldwork of the MaCoBioS project.

			eDNA (x 10 stations)		
	Requirements	**Description**	*Expert knowledge*		*Qualitative value*
Capability	**Simplicity**	Degree of being easily done (sampling technique)	*Water sampling isn't so difficult*		Medium
	Expertise	Technical expertise in species identification	*Data provided by external service*		Low
	Spatial scale	Spatial extent of ecological processes detected	*Due to the hydrodinamics, 3-5 km between stations*		High
Seascape information	**Time scale**	Sampling timeframe	*2-3 days of detectability*		High
	Habitat composition	Relative proportions of habitat elements	*No information available*		None
	Habitat heterogeneity	Detection of small-scale heterogeneity	*No information available*		None
Species information	**Species inventory**	Ability to detect number of species	*High detectability*		High
	Sensitive species	Ability to detect vulnerable species	*High*		High
	Cryptic species	Ability to detect cryptic species	*High*		High
Intrusiveness	**Biological activity**	Ability to detect biological activities	*No biological activity can be detected*		None
	Physical disturbance	Level of seafloor disturbance	*No contact with the seabed*		None
Cost – effectiveness	**Fieldwork time and personnel**	Time	*5 days part time*		Low
		Personnel	*2 scientists + ship crew*		
		Sampling time	*20 ' Deployment + 45' waiting + 20 ' recover*		
	Fieldwork cost	Eur. Personnel	*5 days x 2 scientist x 50 EUR/Day*	500 EUR	Low
		Eur. Ship/Boat	*Scientific small boat. 5 days x 375 EUR/Day*	1,875 EUR	
		Eur. Material	*10% amortization of 20,000 EUR (water pump)*	2,000 EUR	
		EUR TOTAL		**4,375 EUR**	
	Processing cost	Eur. Processing	*Sequencing 2x10 samples 10,660 eur*	10,660 EUR	High
	TOTAL MONETARY COSTS CAMPAIGN			**TOTAL = 15,035 EUR**	**High**

Table 2.4.S7d. Qualitative assessment for bioacoustic sampling. Information based on expert knowledge and supported by information extracted from the fieldwork of the MaCoBioS project.

			BIOACOUSTICS (x 10 stations)		
	Requirements	**Description**	*Expert knowledge*		*Qualitative value*
Capability	**Simplicity**	Degree of being easily done (sampling technique)	*Easy to deploy hydrophones*		Medium
	Expertise	Technical expertise in species identification	*Data provided by external service*		Low
	Spatial scale	Spatial extent of ecological processes detected	*Depending on the environmental conditions between 50 m and 300 m*		Medium
Seascape information	**Time scale**	Sampling timeframe	*12 h of recording*		Medium
	Habitat composition	Relative proportions of habitat elements	*No information available*		None
	Habitat heterogeneity	Detection of small-scale heterogeneity	*No information available*		None
Species information	**Species inventory**	Ability to detect number of species	*Low detectability but potential for development*		Low
	Sensitive species	Ability to detect vulnerable species	*Low*		Low
	Cryptic species	Ability to detect cryptic species	*Cryptobenthic species and nocturn species*		Medium
	Biological activity	Ability to detect biological activities	*Sounds for reproduction, feeding, communication*		High
Intrusiveness	**Physical disturbance**	Level of seafloor disturbance	*Static contact with the seabed*		Low
Cost – effectiveness	**Fieldwork time and personnel**	Time	*10 days part time*		Low
		Personnel	*2 scientists + ship crew*		
		Sampling time	*20 ' Recover + 20' Deployment (all night waiting)*		
	Fieldwork cost	Eur. Personnel	*10 days x 2 scientist x 50 EUR/Day*	1,000 EUR	Medium
		Eur. Ship/Boat	*Scientific small boat. 10 days x 375 EUR/Day*	3,750 EUR	
		Eur. Material	*Rental of microphone set*	2,200 EUR	
		EUR TOTAL		**6,950 EUR**	
	Processing Cost	Eur. Processing	*Sound analysis*	6,000 EUR	Medium
	TOTAL MONETARY COSTS CAMPAIGN			**TOTAL = 12,950 EUR**	**High**

REFERENCES:

Bertucci, F., Lejeune, P., Payrot, J. & Parmentier, E. (2015). Sound production by dusky grouper *Epinephelus marginatus* at spawning aggregations sites. *Journal of Fish Biology, 87*: 400-421. https://doi.org/10.1111/jfb.12733.

Kéver, L., Lejeune, P., Michel, L.N. & Parmentier, E. (2016). Passive acoustic recording of Ophidion rochei calling activity in Calvi Bay (France). *Marine Ecology, 37*: 1315−1324. https://doi.org/10.1111/maec.12341.

2.5. Summary of the results

The previous four chapters (from 2.1 to 2.4) included the methodologies, results, and discussions related to the principal axes of this thesis. This results section begins with the description of the morphological diversity of rhodoliths in the Menorca Channel and the study of their three-dimensional characteristics, as an approach to assess habitat complexity (2.1). It then continues with the molecular and taxonomic identification of rhodolith-forming species diversity (2.2 and 2.3). It concludes with the assessment of the effectiveness of three non-intrusive techniques for monitoring the fish diversity associated with these habitats as a proxy for the assessment of the environmental status of RBs and their contribution to marine biodiversity (2.4).

A summary of the major findings and results found in these chapters is provided below:

Chapter I: Morphological insights into the three-dimensional complexity of rhodolith beds.

This chapter provides novel information on **morphological rhodoliths composition** of the Menorca Channel focusing on **2D and 3D key morphological parameters**. These parameters included the **maximum Feret diameter, area, weight, perimeter, circularity, solidity, roudness, shape coefficient** and the **interstitial space** among others.

The study found that dead (bleached) rhodoliths were mostly low (<20%), with some stations showing higher percentages. The rhodoliths had predominantly branched forms (69.2%). The proportions and representation of morphotypes showed significant variations between stations, particularly in the Adjacent Habitat. The rhodoliths accumulated over sediments composed of mostly gravel (85%). Growth forms distributions varied, with branched forms being the most abundant and consistent growth form across stations, while non-branched and boxwork forms showed more variation, especially across stations within the Core Habitat. Station-specific differences in morphotype abundance were thus observed, indicating heterogeneity within the rhodolith bed. This study emphasizes the diversity and spatial distribution of rhodoliths growth forms. The results indicate that boxwork forms were larger and heavier, whereas branched rhodoliths, which characterize the Core Habitat, had greater interstitial space and overall size. Although growth curves showed similar allometric rates, boxwork forms remained significantly heavier than branched rhodoliths of the same length.

A linear discriminant analysis (LDA) was done with the aim of building a classifier to predict growth forms using easily measurable variables. The first axis (96.6% variance) separated solid, rounded rhodoliths (pralines, boxwork) from branched forms, while the second axis (3.37%) distinguished longer from shorter rhodoliths. The model correctly classified 63.15% of cases, improving to 69.5% with repeated testing. Branched forms were best classified (88.13% accuracy), whereas misclassifications mainly occurred between praline and boxwork forms, with boxwork often mistaken for praline (40.87%) and vice versa (30.73%).

A 3D model was created for 30 rhodoliths with the aim of stablish the correlations between 2D and 3D measurements. The analysis revealed strong correlations between 2D and 3D shape metrics. Linear models showed high correlations (R = 0.99 for area, R = 0.98 for volume), with 3D area being 4.27 times the 2D area and volume 6.45 times the 2D area. These equations allow for estimating ecologically meaningful 3D quantities from simpler 2D measurements, facilitating analysis.

Chapter II: Taxonomic complexity and conservation implications of Mediterranean mesophotic rhodoliths beds.

This chapter identified the **main putative species** of rhodoliths in the Menorca Channel by combining morpho-anatomical exploration and molecular analysis. Focusing on the importance of multispecific rhodoliths beds in the Mediterranean, this study emphasizes on the **importance to advance on conservation priorities** of this habitat.

In order to identify the species that are forming the rhodoliths in the study area through molecular data and species delimitation analysis, the *psb*A and *rbc*L molecular markers were amplified and sequenced. Then, morpho-anatomical exploration of some specimens was carried out to corroborate the identifications. DNA was successfully extracted from 85 out of 120 specimens. The *psb*A fragment was amplified and sequenced in 82 of these (96.5% success), resulting in 69 high-quality sequences after removing contaminations and poor-quality sequences, representing 30 distinct haplotypes (890 bp). The *rbc*L fragment was successfully amplified in all 35 tested samples (100% success), yielding 28 clean sequences representing 20 haplotypes (1332 bp). The *rbc*L data were split because this study produced long sequences (~1300 bp), while most *rbc*L sequences in GenBank are shorter. As a result, one *rbc*L dataset included only long sequences (≥1300 bp), and a second dataset included all sequences trimmed to 294 bp to ensure alignment compatibility.

Analyses of *psb*A identified at least 15 putative species, with strong support across most methods. However, only six could be molecularly confirmed through reference sequences: *Sporolithon mediterraneum, Lithothamnion corallioides, Phymatolithon lusitanicum, Lithophyllum nitorum, L. racemus,* and *L. pseudoracemus*. Several other clades lacked close matches in databases but could be distinguished from known species based on sequence data and morpho-anatomical exploration. These include *Lithothamnion* cf. *valens, L.* cf. *minervae, Lithothamnion* sp.1, *Lithothamnion* sp.2, *Spongites* sp.1, *and Spongites* sp.2. Two clades remained uncertain due to inconsistent delimitation results, notably the *Phymatolithon* and *Roseolithon* groups, where methods differed in species boundaries despite genetic distances of 1–3% (the 3% threshold is generally sufficient to discriminate distinct species in coralline algae). Sequencing of 69 *psb*A samples captured most species diversity. Although the estimated maximum diversity is 18 (17.6) species (requiring over 150 samples), the current effort already captures the majority of rhodolith-forming species with less than half that number.

The long *rbc*L sequences (~1300 bp) revealed 11 putative species, but many clades remained taxonomically unresolved due to lack of close matches in BLAST results. Only *Lithothamnion corallioides* and *Phymatolithon lusitanicum* could be reliably identified using valid long reference sequences. Considering that a conservative cut-off value would be 2.5-3% to suggest different species with *rbc*L marker, a distinct *Phymatolithon* clade, separated from *P. calcareum* by 2.8% (*p*-distance), suggests a different species for this genus clarifying the results obtained for *psb*A. The short *rbc*L dataset (294 bp) improved taxonomic resolution, detecting 13 putative species. Notably, the sample identified as *Sporolithon mediterraneum* with *psb*A appeared to be a different species from the neotype described in the Chapter III (6.3% *p*-distance), but, considering that interspecific divergence for *rbc*L could be higher than 3% in some groups of coralline algae and because the morpho-anatomic exploration fit perfectly the neotype, the species is confirmed. The inclusion of the *P. calcareum* neotype further confirmed the hypothesis that our *Phymatolithon* samples are a distinct species (2.7% *p*-distance). Consistent results also supported the distinction between *Roseolithon crispatum* and *Roseolithon* sp.1 (S5X3), with a 4.3% *p*-distance and suggest that *Roseolithon* sp.2 is *R. crispatum*.

Morpho-anatomically, it could be confirmed that most of the species showed the main distinctive characters described in their original descriptions (e.g. *S. mediterraneum, L. racemus, L.pseudoracemus, L. nitorum* or *L. corallioides*). However, due to the lack of observation of key characters, such as conceptacles and reproductive structures in many genera or the presence of trichocystes in the genus *Spongites*, many of the taxa could only be identified morphologically at the genus level. Furthermore, the particular characteristics described for *Roseolithon crispatum* were identified in a specimen of *Roseolithon* sp.1, while molecularly it appears to be distinct from the clade which with *rbc*L is resolved as *R. crispatum*, leaving the identification of this species unresolved.

Lithothamnion cf. *valens, L. corallioides, L*. cf. *minervae,* and *Phymatolithon* sp. were found throughout the entire depth range. *L. nitorum* and *L. pseudoracemus* were only recorded at 56–58.8 m, while *Lithothamnion* sp.2, *Roseolithon* sp.1, and *L. racemus* appeared exclusively at 48 m with minimal representation. *Roseolithon* sp.2 occurred at depths between 58.8–74 m. *Spongites* sp.1 and sp.2 were each represented by a single specimen at 62 m and 56 m, respectively. *Sporolithon mediterraneum*, abundant in the study, was found from 56 m onward.

Some species associations were observed, particularly in boxwork and praliné types. One praliné rhodolith (S15G6) was sequenced twice, revealing a possible co-occurrence of *Sporolithon mediterraneum* and *Lithothamnion* cf. *minervae*. Finally, based on morphotype proportions reported by Cabrito et al. (2024a), the most abundant rhodolith morphotype (C, 37.53%) is formed by at least *Lithothamnion corallioides, Phymatolithon lusitanicum*, and *Phymatolithon* sp. Morphotype A (10.14%) is exclusively formed by *Lithothamnion* cf. *valens,* found mainly in the well-preserved central zone of the habitat. *Sporolithon mediterraneum* is also widely represented, forming three morphotypes

across the full depth range. These findings highlight the high species diversity of rhodolith beds in the Menorca Channel, with no single species clearly dominating the community.

Chapter III: Neotypification of the *Sporolithon mediterraneum* Heydrich (Sporolithales, Corallinophycidae, Rhodophyta) and the status of *Sporolithon* in the Mediterranean Sea.

As a result of the exploration and identification of rhodolith-forming species in the previous chapter, the **neotype** of *Sporolithon mediterraneum* is **designated** in this study since the original type specimen (the holotype) was lost. This study provides **new relevant information on the morpho-anatomical characters and molecular sequences** of the species. Finally, the status of *Sporolithon* in the Mediterranean Sea is discussed.

A specimen suspected to be a different species from *Sporolithon ptychoides* (the *Sporolithon* species expected to be found in the Mediterranean) was identified on Gorgona Island at the same time that several specimens were also identified in the study area of the thesis, the Menorca Channel. To confirm whether it was a different species, molecular analyses were conducted using two different markers (*psb*A and *rbc*L), along with morpho-anatomical analyses. The *psb*A alignment of 29 sequences revealed 22 haplotypes with 251 variable sites, showing low genetic divergence (0-0.6%) within all Mediterranean specimens. Phylogenetic analyses confirmed these as a distinct lineage within the *Sporolithon* genera, related to *S. howei, S. franciscanum, S. crypticum* and *S. eltorense*. The *rbc*L alignment (35 sequences) similarly supported the Mediterranean *Sporolithon* as a separate lineage. Based on these findings, the Gorgona rhodoliths bed specimen is proposed as the neotype of *Sporolithon mediterraneum*, following taxonomic guidelines.

The habit and vegetative anatomy analyses of the specimen designated as the neotype of *Sporolithon mediterraneum*, showed that the thallus has a monomerous construction with 3-5 cell-layered non-coaxial hypothallium. Hypothallial cells are rectangular, while perithallial cells are smaller and linked by cell fusions and secondary pit connections. The intercalary meristematic cells vary in shape, and the epithallium consist of a single layer of thick-walled, heavily calcified cells with a trapezoidal lumen.

For the reproductive structures, it was observed that the tetrasporangia were housed in calcified compartments grouped into sori that protrude above the thallus surface. Tetrasporangial pores are 10.3–13.8 µm in diameter, surrounded by 9–12 rosette cells. The compartments are elliptical to lemon-shaped and subtended by a single large (more than 20x20 µm) triangular stalk cell. They are embedded among elongated cells and separated by 5-6 calcified vegetative filaments (paraphyses). Tetrasporocytes develop into cruciate tetrasporangia, and after spore release, the compartments remain buried within the thallus.

These morphological characteristics contributed to the description of the neotype of this species. Furthermore, although many of the characteristics described for *S. mediterraneum* are shared with other

Sporolithon species, such as *S. ptychoides* and *S. molle*, the number of paraphyses surrounding the tetrasporangial compartments and the size of the stalk cell were defined as distinguishing characters of *S. mediterraneum*, as it has a greater number of paraphyses and larger stalk cells compared to other species of this genus.

Chapter IV: Non-extractive fish diversity assessment in Mediterranean rhodoliths beds.

In this chapter, three alternative non-intrusive techniques (**eDNA, bioacoustics** and still **video cameras**) were explored to monitor fish assemblages associated with rhodoliths beds in the Menorca Channel. By integrating these methods, this study **provides novel insights into their combined applicability and performance** in a mesophotic environment. Additionally, it offers the **first data on the cost-effectiveness and efficiency** of this monitoring approach, comparing our results with traditional trawling and ROV surveys.

The analysis included a total of 47 video samples from 10 stations, revealing three levels of rhodolith coverage between and within stations. A 100% rhodolith coverage was found within the cable-protected area. The rhodoliths cover decreased with distance to the cable-exclusion area. Deeper stations had <50% coverage, while shallower sites had <10%, with some stations showing high habitat heterogeneity due to rocky outcrops. The visual inspection of the video allowed the identification of fourteen fish taxa, confirming species presence.

The 20 eDNA samples, collected close to the seabed at the same 10 stations (2 replicates per station), yielded 2,374,169 sequence reads, identifying 66 fish taxa, including 58 bony fish and 8 cartilaginous fish. MOTU richness was significantly influenced by trawling exposure and habitat heterogeneity, with higher richness in stations with homogeneous substrates. Habitat type did not significantly affect MOTU richness. The most common species in non-exposed to trawling areas included commercial fish, such as sparids, and benthic fishes such as *Uranoscopus scaber*. In addition, protected, endangered and threatened species of elasmobranch such as *Myliobatis aquila*, *Prionace glauca* or *Pteroplatrygon violacea* were found both over RBs and sandy bottoms with less than 50% or rhodoliths cover. Sandy bottoms with low rhodolith coverage (<10%) were dominated by species typical of sandy habitats, such as *Gobius cruentatus* or *Buenia affinis*.

Fifteen sound types were detected across the nine stations that were surveyed with this technique, including species like *Ophidion rochei* and *Sciaena umbra*. Habitat type showed marginal significance for sound diversity (at the 0.1 significance level), without any differences detected among the three groups of habitat type. No significant differences were found for trawling exposure or habitat heterogeneity in sound diversity. On the other hand, stations with high habitat heterogeneity had greater sound abundance (at the 0.1 significance level) and no differences in sound abundances were detected for habitat type or trawling exposure. Even so, some patterns in the provenance of sounds according to taxon were detected. *O. rochei* was the most common sound in the whole area. In sandy stations, *S.*

umbra was commonly heard and species from *Scorpaenidae* family were detected mostly in RBs. High frequency fishes were represented by higher abundances only in stations characterized by sand with < 50% of rhodoliths coverage. Stations with small scale-heterogeneity had higher representation of sound emitted by Groupers.

The study highlights the variability in fish diversity detected with three different techniques across stations. eDNA identified the most taxa (66), followed by video (14) and bioacoustics (15). The techniques showed different effectiveness: eDNA excelled in detecting cryptic species, while video and bioacoustics were more suitable for detecting biological activity. Cost-effectiveness also varied; video was the least expensive, while bioacoustics and eDNA had higher analysis costs. These techniques proved complementary, providing valuable insights for monitoring diverse marine environments. Therefore, in this study, a combined monitoring to assess the associated fish diversity as a proxy for environmental status is proposed.

SECTION III

SUMMARY OF DISCUSSIONS

The main objective of this thesis is to improve our knowledge of deep RBs in the Mediterranean, focusing on their structural complexity, species composition, and role as habitat providers. Additionally, with the generated knowledge, this thesis aims to propose innovative and non-intrusive monitoring methodologies to inform specific conservation strategies for these habitats. I have focused on the Menorca Channel as the study area, as it hosts the most extensive RB in the Mediterranean and it is in a good conservation status due to its relatively low level of human impact and partial protection.

In this **Section III**, I summarize the discussions presented in the different chapters (**Section II**, from 2.1 to 2.4), structured around three main axes. I begin by examining the morphological and structural complexity of the studied RB, highlighting the methods used to assess their three-dimensional habitat complexity. Next, I analyze the species composition of coralline algae that form these RBs in the Menorca Channel, highlight their high diversity and importance in the context of habitat protection regulations. Finally, I evaluate the effectiveness of three innovative and non-intrusive techniques for detecting fish diversity associated with these habitats, and consider their potential for long-term monitoring, particularly in recognizing RBs as key habitat providers.

Rhodoliths of varying forms are growing and accumulating in the study area over coarse sediments, as typically reported for Mediterranean RBs (de Juan et al., 2013). Coarse sediments, at large scales, are indicative of slow sediment input from terrestrial origin, which is often observed around Mediterranean islands, particularly in areas with moderate bottom currents that prevent the deposition of fine sediments (Moranta et al., 2014). Results showed that, within my study area, the differences in proportions of morphotypes and growth forms between stations cannot be attributed to differences in sediment granulometry. These findings are in accordance to the conclusions drawn by Cabanellas-Reboredo et al. (2017), indicating that, at the scale of a RB, sediment granulometry has limited explanatory power regarding variations in rhodoliths morphologies. Additionally, it is common to find a variable quantity of dead rhodoliths and fragments accompanying the live rhodoliths (Bracchi and Basso 2012). However, the presence of RBs with a higher percentage of live, intact, and structurally well-formed rhodoliths (branched, unbroken, and larger in size) is assumed to indicate better environmental conditions. In the study area, between 5 to 20% of dead rhodoliths were found in most samples, providing similar results to Rendina et al. (2020), and lending support to the hypothesis that the RBs in Menorca Channel are in a good environmental status. Despite branched forms were predominant in all stations, small-scale heterogeneity in the proportions of growth forms and morphotypes was observed in agreement with previous studies in the Mediterranean (Bracchi et al., 2022), and particularly in the study area (Farriols et al., 2022). This heterogeneity of morphotypes align with the multi-specific character of Mediterranean RBs.

Within the Core Habitat of the Menorca Channel, rhodoliths were larger and exhibited greater interstitial space. In contrast, rhodoliths in the Adjacent Habitat displayed lower structural complexity

probably due to suboptimal environmental conditions and exposure – either directly or indirectly – to trawling. From the nine morphotypes identified in the study area, a decline in morphotype A was observed from the Core Habitat toward the habitat's edge and the exclusion zone, suggesting that this morphotype could serve as a potential indicator of habitat conservation status.

Since trawling has been prohibited within the Menorca Channel cables' exclusion zone since the early 1970s, it is highly likely that the Core Habitat has remained undisturbed by this activity for decades. Preliminary data from both Core and Adjacent Habitat stations suggest a potential relationship between RB condition and protection status, although this study was not specifically designed to evaluate that link. While our findings suggest that trawling has not impacted the RB within the Core Habitat's exclusion zone, they cannot confirm that the composition of the Adjacent Habitat is solely the result of human activities. Small-scale heterogeneity within RBs can result from multiple factors beyond fishing pressure (Jardim et al., 2022), and variations in rhodoliths density, size and composition can also be influenced by natural environmental variables such as depth, bottom currents and seafloor geomorphology (Illa-López et al., 2023; Veras et al., 2020; Peña et al., 2014).

After observing the high morphological diversity of rhodoliths from the Menorca Channel, a high diversity of rhodolith-forming species was expected. In this study, a total of 15 different species were identified—an amount that matches or slightly exceeds the number of species found in other Western Mediterranean RBs, where recent studies report between 4 and 13 species per bed, depending on the locality (Bracchi et al., 2019; Chimienti et al., 2020; Rendina et al., 2020; Ingrassia et al., 2023). In this chapter, the species identification was carried out with a combined approach using molecular (two markers: *psb*A and *rbc*L) and morpho-anatomical techniques. The results revealed a higher diversity than that reported by Joher et al. (2023) in a similar area, the Mallorca Channel, where identifications were based solely on morphology. This highlights the importance of combining morpho-anatomic and molecular techniques to avoid underestimating the diversity of rhodolith-forming species in the multi-specific Mediterranean RBs.

The lack of BLAST matches for some sequences - particularly within the genus *Lithothamnion* - suggests the presence of numerous cryptic species endemic to the Mediterranean, as also noted by Pezzolesi et al. (2019). In addition, the lack of sequenced type materials of some described species makes their identification difficult. Therefore, in addition to providing a large number of sequences of Mediterranean species, this thesis has contributed to the neotypification of *Sporolithon mediterraneum* by providing relevant information on its morpho-anatomy, as well as providing neotype sequences for both *psb*A and *rbc*L.

The results obtained showed that, among the Hapalidiales, *Lithothamnion* was the most diverse genus in the study area, with five species identified. Two of them, *L.* cf. *valens* and *L.* cf. *minervae*, are known Mediterranean endemics and were partially identified, as the type materials have not been successfully

sequenced. The detection of two other unidentified *Lithothamnion* species, one of them at 74 m depth, indicates the possible existence of at least two other endemic species in the region. In addition, although the two protected species, *Lithothamnion corallioides* and *Phymatolithon calcareum*, are considered globally widespread and abundant, in this thesis only *L. corallioides* was detected. This support the observation of Basso et al. (2016) who noted that this common species may be absent, or present in low proportions, in Mediterranean RBs. Moreover, instead of *P. calcareum*, another species within the same genus—*Phymatolithon lusitanicum* and *Phymatolithon* sp.—were found across a wide bathymetric range (48–62 m and 74 m, respectively). To date, the only *Roseolithon* species detected in the Mediterranean is *R. crispatum* (Gabrielson et al., 2023a). Our results detect the presence of two different species of *Roseolithon* that need further analysis to be identified, but it is not excluded that one of them belongs to *R. crispatum* as it was confirmed through molecular and morpho-anatomical data from different specimens. The two clades could belong to the same species as the uncorrected *p*-distances for both markers are not particularly high. However, it is also possible that they reflect the existence of a genetically diverse species complex.

Among the Corallinales, three species from genus *Lithophyllum* were detected and confirmed. The paleoendemic Mediterranean species *L. racemus* and the cryptic *L. pseudoracemus* were confirmed at 48-58.8 m depth, consistent with previously reported depth ranges for this species by Caragnano et al. (2020). Additionally, *L. nitorum* was identified at 56–58.8 m depth—being the first molecular confirmation of its presence at such depths, extending its known distribution beyond the shallower records from the Cantabrian Sea (Adey & Adey, 1973) and Mediterranean Sea (Del Río et al., 2022). Regarding the genus *Spongites*, neither of the two species found in the Menorca Channel corresponds to *S. fruticulosus*, the only *Spongites* species formally described in the Mediterranean (Basso et al., 2017; Rindi et al., 2019). One species, *Spongites* sp.1, matched a GenBank sequence from Sicily that was also not identified as *S. fruticulosus*. These findings suggest that *Spongites* diversity in the Mediterranean is underestimated and may include at least two additional endemic species.

Among the Sporolithales, only one species has been found in the study area. *Sporolithon mediterraneum* was identified in a bathymetric range from 56 to 74 m and was found forming free-living praline rhodoliths and attached to boxwork rhodoliths. The same specimens contributed to confirming the designation of a neotype for this species, discovered on Gorgona Island (Italy), by providing consistent morpho-anatomical and molecular evidence. The Gorgona specimen and those from the Menorca Channel differ from *S. ptychoides* and *S. molle*, previously recorded in the Mediterranean Sea, based on a distinct combination of anatomical characteristics. Phylogenetic analyses using ML and BI methods on *psb*A and *rbc*L sequences confirm that it represents a separate species from *S. ptychoides* and *S. molle*. Given its agreement with Heydrich's original description, we designate the Gorgona specimen as the neotype of *S. mediterraneum*. This neotype was used in this study, where more specimens of *Sporolithon mediterraneum* were identified morphologically and molecularly with *psb*A. Species

delimitation results with *rbc*L showed high interspecific divergence (>6%) between the Menorca Channel specimens and the neotype previously described.

These results showed that in the genus *Sporolithon*, paraphysis cell number and stalk cell size are key traits for species identification. The neotype of *S. mediterraneum* differs from *S. ptychoides* and *S. molle* by having shorter paraphyses (5–6 cells) and larger stalk cells (>20×20 μm). In contrast, *S. ptychoides* and *S. molle* typically have paraphysis composed of 3–4 elongated cells and smaller stalk cells (Richards et al., 2017; Heydrich, 1897). Although early descriptions of *S. mediterraneum* did not specify paraphysis details, Mediterranean specimens previously identified as *S. ptychoides* (Alongi et al., 1996; Bressan & Babbini, 2003) often show traits more consistent with *S. mediterraneum*.

Molecular data further suggest misidentifications: Richards et al. (2017) found that many specimens labeled as *S. ptychoides* do not match the reference sequence from the type locality in Egypt. Additionally, tetrasporangial size—previously used as a distinguishing character—does not clearly differentiate among these three species (*S. ptychoides*, *S. molle* and *S. mediterraneum*). Richards et al. (2017) confirmed the coexistence of *S. ptychoides* and *S. molle* in the Red Sea using multiple genetic markers, but such diversity is not yet supported at the molecular level in the Mediterranean. Therefore, given shared morphological traits and geographical confinement, most Mediterranean specimens previously identified as *S. ptychoides* likely belong to *S. mediterraneum*, currently the only confirmed *Sporolithon* species in the region.

Identifying *S. mediterraneum* and its distinguishing morpho-anatomical traits from *S. ptychoides* and *S. molle* will help detect potential records of these species in the eastern Mediterranean. As with other Red Sea organisms, they could enter through the Suez Canal via Lessepsian migration, a process already observed in other rhodophytes (Galil, 2009; Manghisi et al., 2012; Nahor et al., 2022). Their presence could signal biogeographical shifts driven by climate change, highlighting the importance of ongoing monitoring to assess environmental impacts on Mediterranean ecosystems (Israel & Einav, 2017).

A high diversity of rhodolith-forming species was detected in alignment with what was expected for the morphological diversity observed in the study area. These findings are also consistent with the known richness of the Mediterranean, one of the most diverse regions for these species (Rebelo et al., 2021). The multi-species nature and high endemism of Mediterranean RBs highlight the need for conservation strategies that prevent local extinctions (Ramos et al., 2024). Conservation policies, such as the Habitats Directive, should be updated to include not only widely distributed species like *P. calcareum* and *L. corallioides*, but also Mediterranean endemics. The strong crypticism observed in this study calls for re-evaluating species identifications using both morphological and molecular approaches. Therefore, the study of mesophotic RBs is essential to improve species databases and support effective conservation and management strategies.

The structural complexity of rhodoliths plays a crucial role in supporting the high diversity of fauna and flora within RBs (Fredericq et al., 2019; Teichert, 2014), as the spaces between branches create microhabitats for various algae, epiphytes, and invertebrates (Phillips, 2023). The interstitial space (IS), calculated as the difference between the area of the convex hull and the area of rhodoliths in 2D, or as the difference between the volume of the convex hull and the volume of the rhodoliths in 3D, is the actual available space that a rhodolith (especially branched ones) offer as substrate or shelter for other species. Results showed that in the Core Habitat, branched rhodoliths displayed greater branching complexity and higher interstitial space (in 2D), indicating that favorable environmental conditions help maintain habitat three-dimensional complexity. Thus, in accordance with our results as well as Jardim et al. (2022) conclusions, IS is a reliable proxy for habitat complexity. Therefore, the RB community within the protected Core Habitat can be considered a reference site for assessing good environmental conditions.

The strong correlation found between 2D and 3D metrics for morphotype A (identified as *Lithothamnion* cf. *valens*) suggests that 2D measurements can act as effective, time-efficient and practical tool for routine monitoring of RBs. This align with House et al. (2018) conclusions where 2D measurements, despite being less precise than 3D ones, provided consistent and scalable estimates of ecological functions in scleractinian corals. Additionally, we recommend employing linear 2D/3D relationships between different measurements to estimate total photosynthetic surface for determining photosynthesis rates in complex branched morphologies, as well as for calculating rhodolith volume and quantifying calcium carbonate production (Dulin et al., 2020).

In RBs formed by multiple species and morphotypes, distinguishing between morphologies can be challenging. Rhodoliths of the same shape and longitudinal size, could vary in weight due to differences in internal composition (the presence of a nuclei formed by other organisms for example) (Pérez-Peris et al., 2023). Therefore, we recommended using the 3D surface area of the thallus as a more accurate metric for estimating metabolic rates and standardizing cryptofaunal abundance, rather than relying on dry weight. Additionally, rhodolith volume, which plays a key role in carbon retention, requires accurate 3D measurements to be reliably assessed because methods based on simple approximations (i.e., ellipsoid equation (Teichert et al. 2014) or water displacement (Amado-Filho et al., 2007)), lack the necessary precision and are not broadly applicable across diverse rhodolith morphologies.

Given the ecological relevance of rhodolith structural complexity, the vulnerability of these habitats, and their difficult access due to the depth at which they are found, the following section explores innovative, non-intrusive techniques for monitoring fish diversity as an indicator of the role of RBs as large-scale habitat providers (seascape).

During this work, I assessed the strengths and limitations of the three techniques for monitoring fish diversity. Video recordings, while offering direct evidence of species presence and useful habitat

characterization, were limited by short duration and low image quality, which reduced species detectability—especially for cryptic species and in low-light conditions. These limitations have been already documented for UVCs and ROVs (Polanco Fernández et al., 2021; Illa-López et al., 2023) and likely explain the lower species counts observed in rhodolith habitats compared to sandy areas. Unlike eDNA and bioacoustics, which rely on indirect evidence and may lead to false positives, video provides verifiable species observations. In contrast, eDNA metabarcoding proved highly effective in detecting fish diversity in the Menorca Channel's RB, identifying 66 species—more than ROV surveys and nearly half of those found by broader trawl surveys (Moranta et al., 2014).

Despite environmental DNA proved the most effective of the three techniques for detecting a wide range of fish species, its interpretation is limited by environmental factors and DNA transport. eDNA integrates data over several days and can be influenced by hydrodynamics and species behavior, nevertheless, it proves particularly reliable for detecting benthic, low-mobility species. Despite limitations in estimating abundance, results suggest that eDNA is a powerful and, cost-effective tool for biodiversity monitoring and assessing functional diversity (He et al., 2023; Polanco-Fernández et al., 2021; Aglieri et al., 2020; Juhel et al., 2018). Bioacoustics showed potential for monitoring fish in Mediterranean RBs, but it is still in early development. The technique detected up to 15 sound types, categorized into six groups, with four linked to specific species or genera. However, two categories lacked sufficient reference data, limiting the number of species it can detect. Sound richness, which reflects the variety of sounds from different species and biological activities (like courtship or territorial defense), serves as a proxy for "activity diversity." High sound richness indicates a more diverse and active habitat, while low richness suggests sonically homogeneous habitat. Sound abundance, representing the number of sounds recorded, is linked to habitat functionality, particularly fish breeding activity (Mooney et al., 2020). Significant differences in sound richness were observed among habitat types, with higher abundance recorded in heterogeneous habitats like RB limits and rocky outcrops, which may support greater prey diversity. These findings suggest bioacoustics could be a valuable tool for detecting changes in habitat conditions, especially with enhanced sound libraries in the future.

Despite methodological constraints, results suggest that fish diversity over RBs is influenced by trawling exposure, habitat type, and small-scale heterogeneity. The highest diversity was observed in a shallow, trawling-sheltered site with detrital sediments and low rhodoliths cover. Other shallow sites near trawling exclusion zones also showed high diversity; however, this depended on the technique. In contrast, deeper, trawled areas and RBs themselves did not show particularly high fish diversity. The combination of eDNA, video and bioacoustics offers a less invasive alternative and complementary approach to monitor vulnerable marine habitats. While non-destructive methods may limit precise estimates of species composition or abundance, they provide valuable insights into biodiversity and functional roles. eDNA, for instance, can generate species inventories without relying on taxonomic expertise, while video is effective for assessing habitat composition and bioacoustics can detect

behavior and cryptic often missed by the other tools. The study advocates for the integration of all three techniques into a comprehensive monitoring program for deep habitats like Mediterranean RBs. Further improvements in data analysis, image identification, eDNA markers, and acoustic libraries will enhance the effectiveness of these methods and advance towards non-destructive sampling. In future work, I plan to apply the same techniques to characterise and monitor benthic fauna associated with RBs aiming to better understand the ecosystem services provided by RBs.

The integration of these three non-invasive techniques to monitor fish diversity associated to RBs, combined with regular assessment of structural complexity and taxonomic composition of rhodolith-forming species, will allow us to track changes in the seabed resulting from environmental pressures (e.g. Climate Change) or conservation measures (e.g. trawling ban). The data obtained (ranging from morphometrics and rhodolith-forming species composition to associated biodiversity) provide indirect but valuable indicators of the health and potential functionality of these habitats.

To conclude, this thesis—centered on the largest RB identified in the Mediterranean—has significantly advanced our understanding of these unique habitats. It revealed a high diversity of morphotypes and species forming the RB, many of which are potentially threatened by human activities, such as bottom trawling and by the impacts of climate change. The exhaustive species inventory provided here contributes valuable knowledge that should inform protection schemes under the Habitats and Species Directives. Furthermore, the findings highlight the essential role of RBs as habitat providers, underscoring the need for long-term monitoring using non-intrusive techniques to safeguard these ecologically important yet vulnerable habitats in the Mediterranean Sea.

3.4. References of Section III

Adey, W. H. & Adey, P. J. (1973). Studies on the biosystematics and ecology of the Epilithic Crustose Corallinaceae of the British Isles. *British Phycological Journal*, *8*(4), 343–407. https://doi.org/10.1080/00071617300650381.

Aglieri, G., Baillie, C., Mariani, S., Cattano, C., Calò, A., Turco, G., Spatafora, D., Di Franco, A., Di Lorenzo, M., Guidetti, P. & Milazzo, M. (2020). Environmental DNA Effectively Captures Functional Diversity of Coastal Fish Communities. *Molecular Ecology 30*(13): 3127–39. https://doi.org/10.1111/mec.15661.

Alongi, G., Cormaci, M. & Furnari, G. (1996). On the occurence of Sporolithon ptychoides Heydrich (Corallinales, Sporolithaceae, Rhodophyta) in the Mediterranean sea. *Cryptogamie. Algologie*, *17*(2), 131–137.

Amado-Filho, G.M., Maneveldt, G., Manso, R.C.C., Marins-Rosa, B.V., Pacheco, M.R. & Guimarães, S. (2007). Structure of rhodolith beds from 4 to 55 meters deep along the southern coast of Espírito Santo State, Brazil. *Ciencias Marinas*, *33*(4), Article 4. https://doi.org/10.7773/cm.v33i4.1148.

Basso, D., Babbini, L., Kaleb, S., Bracchi, V. A. & Falace, A. (2016). Monitoring deep Mediterranean rhodolith beds. *Aquatic Conservation: Marine and Freshwater Ecosystems*, *26*(3), 549–561. https://doi.org/10.1002/aqc.2586.

Basso, D., Babbini, L., Ramos-Esplá, A.A. & Salomidi, M. (2017). Mediterranean Rhodolith Beds. In R. Riosmena-Rodríguez, W. Nelson, & J. Aguirre (Eds.), *Rhodolith/Maërl Beds: A Global Perspective* (pp. 281–298). Springer International Publishing. https://doi.org/10.1007/978-3-319-29315-8_11.

Bracchi, V.A. & Basso, D. (2012) The contribution of calcareous algae to the biogenic carbonates of the continental shelf: Pontian Islands, Tyrrhenian Sea, Italy. *Geodiversitas*, *34*, 61–77. https://doi.org/10.5252/g2012n1a4.

Bracchi, V.A., Angeletti, L., Marchese, F., Taviani, M., Cardone, F., Hajdas, I., Grande, V., Prampolini, M., Caragnano, A., Corselli, C. & Basso, D. (2019). A resilient deep-water rhodolith bed off

the Egadi Archipelago (Mediterranean Sea) and its actuopaleontological significance. *Alpine and Mediterranean Quaternary*, *32*(2), 131–150. https://doi.org/10.26382/AMQ.2019.09.

Bracchi, V.A., Caronni, S., Meroni, A.N., Burguett, E.G., Atzori, F., Cadoni, N., Marchese, F. & Basso, D. (2022). Morphostructural Characterization of the Heterogeneous Rhodolith Bed at the Marine Protected Area "Capo Carbonara" (Italy) and Hydrodynamics. *Diversity*, *14*(1), Article 1. https://doi.org/10.3390/d14010051.

Bressan, G. & Babbini L. (2003). Biodiversità marina delle coste Italiane: Corallinales del Mar Mediterraneo: Guida all deteminazione. In *Biologia Marina Mediterranea* (Vol. 10, pp. 1–237). S.I.B.M.

Cabanellas-Reboredo, M., Mallol, S., Barberá, C., Vergés, A., Díaz, D. & Goñi, R. (2018). Morpho-demographic traits of two maërl-forming algae in beds with different depths and fishing histories. *Aquatic Conservation: Marine and Freshwater Ecosystems*, *28*(1), 133–145. https://doi.org/10.1002/aqc.2827.

Caragnano, A., Rodondi, G., Basso, D., Peña, V., le Gall, L. & Rindi, F. (2020). Circumscription of *Lithophyllum racemus* (Corallinales, Rhodophyta) from the western Mediterranean Sea reveals the species *Lithophyllum pseudoracemus* sp. Nov. *Phycologia*, *59*(6), 584–597. https://doi.org/10.1080/00318884.2020.1829348.

Chimienti, G., Rizzo, L., Kaleb, S., Falace, A., Fraschetti, S., Giosa, F.D., Tursi, A., Barbone, E., Ungaro, N. & Mastrototaro, F. (2020). Rhodolith Beds Heterogeneity along the Apulian Continental Shelf (Mediterranean Sea). *Journal of Marine Science and Engineering*, *8*(10), 813. https://doi.org/10.3390/jmse8100813.

de Juan, S., Lo Iacono, C. & Demestre, M. (2013). Benthic habitat characterisation of soft-bottom continental shelves: Integration of acoustic surveys, benthic samples and trawling disturbance intensity. *Estuarine, Coastal and Shelf Science*, *117*, 199–209. https://doi.org/10.1016/j.ecss.2012.11.012.

Del Río, J., Ramos, D.A., Sánchez-Tocino, L., Peñas, J. & Braga, J.C. (2022). The Punta de la Mona Rhodolith Bed: Shallow-Water Mediterranean Rhodoliths (Almuñecar, Granada, Southern Spain). *Frontiers in Earth Science*, *10*, 884685. https://doi.org/10.3389/feart.2022.884685.

Dulin, T., Avnaim-Katav, S., Sisma-Ventura, G., Bialik, O.M. & Angel, D.L. (2020). Rhodolith beds along the southeastern Mediterranean inner shelf: Implications for past depositional environments. *Journal of Marine Systems*, *201*, 103241. https://doi.org/10.1016/j.jmarsys.2019.103241.

Farriols, M.T., Irlinger, C., Ordines, F., Palomino, D., Marco-Herrero, E., Soto-Navarro, J., Jordà, G., Mallol, S., Díaz, D., Martínez-Carreño, N., Díaz, J.A., Fernandez-Arcaya, U., Joher, S., Ramírez-Amaro, S., de la Ballina, N.R., Vázquez, J.T. & Massutí, E. (2022). Recovery Signals of Rhodoliths Beds since Bottom Trawling Ban in the SCI Menorca Channel (Western Mediterranean). *Diversity*, *14*(1), Article 1. https://doi.org/10.3390/d14010020.

Fredericq, S., Krayesky-Self, S., Sauvage, T., Richards, J., Kittle, R., Arakaki, N., Hickerson, E. & Schmidt, W.E. (2019). The Critical Importance of Rhodoliths in the Life Cycle Completion of Both Macro- and Microalgae, and as Holobionts for the Establishment and Maintenance of Marine Biodiversity. *Frontiers in Marine Science*, *5*, 502. https://doi.org/10.3389/fmars.2018.00502.

Gabrielson, P.W., Maneveldt, G.W., Hughey, J.R. & Peña, V. (2023). Taxonomic contributions to Hapalidiales (Corallinophycidae, Rhodophyta): Boreolithothamnion gen. nov., Lithothamnion redefined and with three new species and Roseolithon with new combinations. *Journal of Phycology*, *59*(4), 751–774. https://doi.org/10.1111/jpy.13353.

Galil, B.S. (2009). Taking stock: Inventory of alien species in the Mediterranean sea. *Biological Invasions*, *11*(2), 359–372. https://doi.org/10.1007/s10530-008-9253-y.

He, X., Jeffery, N.W., Stanley, R.R.E., Hamilton, L.C., Rubidge, E.M. & Abbott, C.L. (2023). EDNA metabarcoding enriches traditional trawl survey data for monitoring biodiversity in the marine environment. *ICES Journal of Marine Science*, *80*(5): 1529-1538. https://doi.org/10.1093/icesjms/fsad083.

Heydrich, F. (1897). *Corallinaceae, insbesondere Melobesieae. 15*, 34–70, 3 figs, pl III.

House, J.E., Brambilla, V., Bidaut, L.M., Christie, A.P., Pizarro, O., Madin, J.S. & Dornelas, M. (2018). Moving to 3D: Relationships between coral planar area, surface area and volume. *PeerJ*, *6*, e4280. https://doi.org/10.7717/peerj.4280.

Illa-López, L., Cabrito, A., de Juan, S., Maynou, F. & Demestre, M. (2023). Distribution of rhodolith beds and their functional biodiversity characterisation using ROV images in the western Mediterranean Sea. *Science of The Total Environment*, *905*, 167270. https://doi.org/10.1016/j.scitotenv.2023.167270.

Ingrassia, M., Pierdomenico, M., Casalbore, D., Falese, F.G. & Chiocci, F.L. (2023). A Review of Rhodolith/Maerl Beds of the Italian Seas. *Diversity*, *15*(7). Scopus. https://doi.org/10.3390/d15070859.

Israel, A. & Einav, R. (2017). Alien seaweeds from the Levant basin (Eastern Mediterranean Sea), with emphasis to the Israeli shores. *Israel Journal of Plant Sciences*, 1–12. https://doi.org/10.1080/07929978.2016.1257091.

Jardim, V.L., Gauthier, O., Toumi, C. & Grall, J. (2022). Quantifying maerl (rhodolith) habitat complexity along an environmental gradient at regional scale in the Northeast Atlantic. *Marine Environmental Research*, *181*, 105768. https://doi.org/10.1016/j.marenvres.2022.105768.

Joher, S., Martínez, S. & Rodríguez-Prieto, C. (2023). Bionomic study of the detritic bottoms dominated by macroalgae from the southern coast of Mallorca (Balearic Islands). *Botanica Marina*, *66*(1), 37–51. https://doi.org/10.1515/bot-2022-0043.

Juhel, J.B., Laurent, V., Mouillot, D., Kulbicki, M., Letessier, T.B., Meeuwig, J.J. & Wantiez, L. (2018). Reef accessibility impairs the protection of sharks. *Journal of Applied Ecology*, *55*(2): 673-683. https://doi.org/10.1111/1365-2664.13007.

Manghisi, A., Bertuccio, C., Armeli Minicante, S., Fiore, V., Gall, L., Genovese, G. & Morabito, M. (2012). Identifying alien macroalgae through DNA barcodes: The case of *Hypnea cornuta* (Cystocloniaceae, Rhodophyta). *Transitional Water Bulletin*, *5*. https://doi.org/10.1285/i1825229Xv5n1p42.

Mooney, T.A., Di Iorio, L., Lammers, M., Lin, T.H., Nedelec, S.L., Parsons, M., Radford, C., Urban, E. & Stanley, J. (2020). Listening forward: Approaching marine biodiversity assessments using acoustic methods. *Royal Society Open Science*, *7*(8), 201287. https://doi.org/10.1098/rsos.201287.

Moranta, J., Barberá, C., Druet Vélez, M., Díaz-Valdés, M., Zaragoza, N., Tello-Antón, M.O., López-Jurado, J.L., Balbín, R., Flexas, M. del M., Fernández, M., Hidalgo, M., Domínguez, M., Quetglas, A., Goñi, R., Mallol, S., Sánchez-Delgado, F., Ambroso, S. & Comalada, N. (2014). *Caracterización ecológica de la plataforma continental (50-100 m) del canal de Menorca*. https://digital.csic.es/handle/10261/318214.

Nahor, O., Luzzatto-Knaan, T. & Israel, Á. (2022). A new genetic lineage of Asparagopsis taxiformis (Rhodophyta) in the Mediterranean Sea: As the DNA barcoding indicates a recent Lessepsian introduction. *Frontiers in Marine Science*, *9*. https://doi.org/10.3389/fmars.2022.873817

Peña, V., Bárbara, I., Grall, J., Maggs, C.A. & Hall-Spencer, J.M. (2014). The diversity of seaweeds on maerl in the NE Atlantic. *Marine Biodiversity*, *44*(4), 533–551. https://doi.org/10.1007/s12526-014-0214-7.

Pérez-Peris, I., Navarro-Mayoral, S., de Esteban, M.C., Tuya, F., Peña, V., Barbara, I., Neves, P., Ribeiro, C., Abreu, A., Grall, J., Espino, F., Bosch, N.E., Haroun, R. & Otero-Ferrer, F. (2023). Effect of Depth across a Latitudinal Gradient in the Structure of Rhodolith Seabeds and Associated Biota across the Eastern Atlantic Ocean. *Diversity*, *15*(1), 103. https://doi.org/10.3390/d15010103.

Pezzolesi, L., Peña, V., Le Gall, L., Gabrielson, P.W., Kaleb, S., Hughey, J.R., Rodondi, G., Hernandez-Kantun, J.J., Falace, A., Basso, D., Cerrano, C. & Rindi, F. (2019). Mediterranean *Lithophyllum stictiforme* (Corallinales, Rhodophyta) is a genetically diverse species complex: Implications for species circumscription, biogeography and conservation of coralligenous habitats. *Journal of Phycology*, *55*(2), 473–492. https://doi.org/10.1111/jpy.12837.

Phillips, J. A. (2023). *The Lives of Seaweeds: A Natural History of Our Planet's Seaweeds and Other Algae*. Princeton University Press.

Polanco Fernández, A., Marques, V., Fopp, F., Juhel, J.B., Borrero-Pérez, G.H., Cheutin, M.C., Dejean, T., González Corredor, J.D., Acosta-Chaparro, A., Hocdé, R., Eme, D., Maire, E., Spescha, M., Valentini, A., Manel, S., Mouillot, D., Albouy, C. & Pellissier, L. (2021). Comparing environmental DNA metabarcoding and underwater visual census to monitor tropical reef fishes. *Environmental DNA*, *3*(1), 142–156. https://doi.org/10.1002/edn3.140.

Ramos, D.A.E., Del Río, J., Peñas, J., Peña, V. & Braga, J.C. (2024). Cryptic Diversity of Mediterranean (Corallinales, Corallinophycidae, Rhodophyta). *Aquatic Conservation: Marine and Freshwater Ecosystems*, *34*(10), e4255. https://doi.org/10.1002/aqc.4255.

Rebelo, A.C., Johnson, M.E., Rasser, M.W., Silva, L., Melo, C.S. & Ávila, S.P. (2021). Global biodiversity and biogeography of rhodolith-forming species. *Frontiers of Biogeography*, *13*(1). https://doi.org/10.21425/F5FBG50646.

Rendina, F., Kaleb, S., Caragnano, A., Ferrigno, F., Appolloni, L., Donnarumma, L., Russo, G.F., Sandulli, R., Roviello, V. & Falace, A. (2020). Distribution and Characterization of Deep Rhodolith Beds off the Campania coast (SW Italy, Mediterranean Sea). *Plants*, *9*(8), Article 8. https://doi.org/10.3390/plants9080985.

Richards, J.L., Sauvage, T., Schmidt, W.E., Fredericq, S., Hughey, J.R. & Gabrielson, P.W. (2017). The coralline genera *Sporolithon* and *Heydrichia* (Sporolithales, Rhodophyta) clarified by sequencing type material of their generitypes and other species. *Journal of Phycology*, *53*(5), 1044–1059. https://doi.org/10.1111/jpy.12562.

Rindi, F., Braga, J.C., Martin, S., Peña, V., Le Gall, L., Caragnano, A. & Aguirre, J. (2019). Coralline Algae in a Changing Mediterranean Sea: How Can We Predict Their Future, if We Do Not Know Their Present? *Frontiers in Marine Science*, *6*, 723. https://doi.org/10.3389/fmars.2019.00723.

Teichert, S. (2014). Hollow rhodoliths increase Svalbard's shelf biodiversity. *Scientific Reports*, *4*(1), Article 1. https://doi.org/10.1038/srep06972.

Veras, P.C., Pierozzi-Jr, I., Lino, J.B., Amado-Filho, G.M., de Senna, A.R., Santos, C.S.G., Leão de Moura, R., Passos, F.D., Giglio, V.J. & Pereira-Filho, G.H. (2020). Drivers of bio -diversity associated with rhodolith beds from euphotic and mesophotic zones: insights for managementand conservation. *Perspectectives in Ecology and Conservation, 18*:37–43. https://doi.org/10.1016/j.pecon.2019.12.003.

SECTION IV

SUMMARY OF CONCLUSIONS

The main conclusions derived from the present Ph.D. thesis are:

1. The specimens of rhodoliths sampled in the center of the most extensive RB described in the Mediterranean, and located in our study area, the Menorca Channel, were larger and with more interstitial spaces (IS) than rhodoliths at the edges of this RB. It is likely that the lower complexity of rhodoliths at the edge of the Core Habitat are a consequence of suboptimal environmental conditions combined with being exposed, directly or indirectly, to trawling.

2. Among the nine different rhodolith morphotypes identified, morphotype A (consisting exclusively of *Lithothamnion* cf. *valens*) was common throughout the study area. However, its complexity decreased from the RB Core to the adjacent areas, suggesting that it is a potential candidate indicator of the conservation status of the habitat. In addition, due to the structural complexity of rhodoliths observed in the Core Habitat, this can be considered a reference site for assessing good environmental conditions.

3. The three-dimensional complexity of the habitat is given by the three-dimensional complexity of the rhodoliths that form it. Thus, the interstitial space between the branches of the branching morphologies is a reliable proxy for the study of the habitat structural complexity.

4. The observed strong correlation between 2D and 3D data reinforces previous findings in other benthic organisms and highlights the potential of using functional relationships between dimensions to estimate key ecological functions, including photosynthetic surface area, rhodolith volume, and calcium carbonate production.

5. A total of 15 different rhodolith-forming species were found in the Menorca Channel RB. Of these, six were confidentially identified to species level, while two are provisionally assigned as candidate species due to the lack of available type sequences. The remaining specimens were identified to the genus level. These findings expand the list of rhodolith-forming species in the Mediterranean, providing valuable information on their depth distribution, and enhance molecular reference databases for the region.

6. Among the Hapalidiales, *Lithothamnion* was the most diverse genus with five species identified. The common and currently protected *L. corallioides* was the only species confirmed with certainty. The presence of the endemic species *L.* cf. *valens* and *L.* cf. *minervae* is suspected, while two additional *Lithothamnion* species were detected, one occurring at a depth of 74 m. The well-known and also protected *Phymatolithon calcareum* was not detected, but *P.*

lusitanicum and a distinct *Phymatolithon* were confirmed in the area. Additionally, two possible *Roseolithon* species were detected, one of which is likely *R. crispatum*.

7. Among the Corallinales, *Lithophyllum racemus*, *L. pseudoracemus* and *L. nitorum* were detected. This study provides the first confirmation of *L. nitorum* at 56-58.8 m depth, extending its known distribution beyond shallower records from the Cantabrian and Mediterranean Seas. Two different species from the genus *Spongites* were detected; however, although *S. fruticulosus* was expected to be found, none of them belongs to this species.

8. Among the Sporolithales, only one species was found in the study area: *Sporolithon mediterraneum*. This species was confirmed, and a neotype was designed based on a specimen collected from Gorgona Island (Italy), which matches the original description by Heydrich 1899. *S. mediterraneum* is, therefore, the only *Sporolithon* species currently confirmed in the Mediterranean region.

9. Although the species of the genus *Sporolithon* are morphologically very similar, diagnostic characters, such as the number of cells in the paraphyses between the tetrasporangia and the size of the stalk cells, can be used to distinguish *S. mediterraneum* from *S. ptychoides* and *S.molle*. Thus, previous records of other *Sporolithon* species in the Mediterranean could also correspond to *S. mediterraneum.*

10. The lack of matches through BLAST in the two molecular markers used, suggests the presence of numerous cryptic and endemic species in the Mediterranean. Misidentifications are common when species-level identification only relies on morpho-anatomical characteristics. Therefore, an integrated approach that combines traditional morpho-anatomical with molecular analysis is essential for accurate identification in coralline algae species.

11. The detection and monitoring of these species can provide critical insights into biogeographical changes occurring in the Mediterranean basin, and support the assessment of broader environmental impacts on marine ecosystems. The multi-species composition and high endemism of Mediterranean RBs highlight the need for conservation strategies aimed at preventing local extinctions.

12. Mediterranean RBs deserve priority in conservation efforts due to their role as habitat providers, their morphological complexity, and, above all, their high species diversity. Despite their ecological importance, many of the most prevalent Mediterranean species are not currently recognized under the Habitats Directive, highlighting the need for its revision. Conservation policies should expand their scope to include not only widely distributed European species such

as *P. calcareum* and *L. corallioides*, but also Mediterranean endemic species, in order to ensure comprehensive habitat protection.

13. The fragility and ecological importance of RBs make it imperative to study their biological diversity with non-intrusive techniques. The availability of fish DNA databases has enabled the compilation of species lists independently of taxonomists or local fishing knowledge through the use of eDNA. Therefore, regular fish monitoring through eDNA could provide indicators related to the conservation status of the area.

14. In terms of contextualizing the study area by assessing the habitat composition, video survey proved effective as it enabled the detection of changes in algae coverage or composition, facilitating seascape monitoring. Nevertheless, it is less useful for fish species identification.

15. Bioacoustics technique is suitable for detecting species behavior and the presence of some cryptobenthic species which might elude detection by other methods. Moreover, sound abundances serve as a proxy for the 'activity abundance' or 'functionality' of the habitat.

16. These techniques provide a feasible alternative for monitoring marine habitats that are vulnerable to invasive sampling. Nevertheless, further development in data bases and data analysis is required. This strategic focus aims to facilitate the future generation of species lists and inventories, encompassing not only fish but also invertebrates, without the necessity of destructive sampling methods.

17. With regular information on the morphological and three-dimensional structure of the habitat, the species composition of the RBs, as well as information on the presence and activity of the associated biodiversity (both fish and invertebrates), we can indirectly assess the state of health and functionality of these vulnerable habitats. Thus, we advocate periodic monitoring based on non-intrusive techniques with complementary and punctual sampling with small dredges at points of interest.

SECTION V

SUMMARY OF CONTRIBUTIONS

This section contains a summary of the four chapters that belongs to this doctoral thesis, along with a brief explanation of the Ph.D. candidate's contribution in each of them. The original published papers corresponding to these chapters can be found in Appendix I. Additionally, the author has chosen to include summaries of other papers and her contribution to them. Although these articles are not part of the core thesis, as she was not the lead author, they were developed contemporaneously and have helped the candidate formulate related and applied questions within the thesis, as well as gain background knowledge for its writing. The original papers can be found in Appendix II.

Contributions to the Thesis Chapters:

- **Chapter 2.1.**
  Morphological insights into the three-dimensional complexity of rhodolith beds.
  Andrea Cabrito, Silvia de Juan, Hilmar Hinz, Francesc Maynou
  Marine Biology, 171(6), 127 (2024).
  https://doi.org/10.1007/s00227-024-04437-y

  The Ph.D. candidate conceived the idea for this paper as one of the main chapters of the thesis. The candidate formulated the hypothesis, and designed the sampling strategy. Additionally, responsibility was taken for deploying the dredges during fieldwork, collecting the rhodoliths, classifying them morphologically, and taking all relevant morphological measurements.
  The 3D models of the rhodoliths were created by Hilmar Hinz and Maria del Mar Gil, with support from the Ph.D. candidate. Francesc Maynou took the lead in developing the script for extracting tridimensional measurements from these models; however, the candidate was the sole responsible of running all the models, curating the data, and designing the statistical analyses for both 2D and 3D data. All figures and photographs included in this chapter were created by the candidate. The manuscript was written by the candidate, and all rounds of revision and responses to the journal reviewers were coordinated by her, taking on the role of corresponding author. Throughout the process, supervision was provided by Silvia de Juan and Francesc Maynou.

- **Chapter 2.2.**
  Taxonomic complexity and conservation implications of Mediterranean mesophotic rhodoliths beds.
  Andrea Cabrito, Silvia de Juan, Francesc Maynou, Viviana Peña
  Submitted to Aquatic Conservation: Marine and Freshwater Ecosystems

  The Ph.D. candidate conceived the idea for this study, formulating the relevant hypotheses. The sampling design and laboratory protocols necessary to obtain the results were developed by the

candidate. To achieve this, the candidate conducted a research stay in University of La Coruña (Galicia-Spain) to learn from expert and co-author Viviana Peña. In Barcelona, the candidate replicated and adapted the protocols to the study needs, adjusting them iteratively until they proved effective.

All laboratory work was carried out by the PhD candidate, and the sequences were sent to GenoScreen for sequencing. Once the results were obtained, and under the supervision of Viviana Peña, the PhD candidate performed sequence curation, followed by molecular phylogenetic analyses and species delimitation. The PhD candidate conducted multiple microscopy sessions to capture all the images presented in the chapter, and assembled the relevant figures. The manuscript was written under the supervision of thesis advisors Silvia de Juan and Francesc Maynou.

- **Chapter 2.3.**
  Neotypification of the *Sporolithon mediterraneum* Heydrich (Sporolithales, Corallinophycidae, Rhodophyta) and the status of *Sporolithon* in the Mediterranean Sea.
  Andrea Cabrito, Sara Kaleb, Viviana Peña, Annalisa Falace
  Aquatic Botany, 197, 103839 (2025).
  https://doi.org/10.1016/j.aquabot.2024.103839

  Right place, right time! During the development of the second chapter, evidence of this species was found among the Ph.D. candidate's samples. After contacting the co-authors of this chapter—Sara Kaleb, Annalisa Falace, and Viviana Peña—it was discovered that they were working on the same species, of which they had only one specimen, intended to be the neotype. With their work at a standstill, the contribution of specimens from the Menorca Channel led to a proposal for the Ph.D. candidate to resume and complete the study, providing an opportunity for a first independent collaboration with other researchers.

  Molecular analyses were conducted again, incorporating the newly available samples. Specimens were examined under SEM, photographed, and some of the study's figures were assembled. Although the manuscript was already in progress, a thorough review was carried out, the introduction and results section were completed with information extracted from the new analyses, and the discussion was structured accordingly. Additionally, the revisions and responses to the journal reviewers were handled, taking on the role of corresponding author.

- **Chapter 2.4.**
  Non-extractive fish diversity assessment in Mediterranean rhodolith beds.
  Andrea Cabrito, Francesc Maynou, Remy Simide, David Mouillot, Julie Lossent, Silvia de Juan

Aquatic Conservation: Marine and Freshwater Ecosystems, 34(6), e4212 (2024). https://doi.org/10.1002/aqc.4212

In this case, the Ph.D. candidate did not design the sampling or the hypotheses of the study, as these were original to the European project (MaCoBioS) that has supported the candidate throughout the doctoral work. During the sampling, the candidate was responsible for everything related to the deployment of the underwater cameras and provided support to the eDNA and bioacoustic samplings. The bioacoustic and the eDNA data were processed by external companies (Chorus and SpyGen, respectively), while the candidate processed the videos and obtained the corresponding data.

Once the data from the external companies were received, the candidate was responsible for curating the data and subsequently designing the statistical strategy to achieve the study objectives. The candidate also leads the writing of the manuscript, as well as the handling of the necessary revisions for the journal and responding to the reviewers, assuming the role of corresponding author. The entire process was supervised by her advisors, Silvia de Juan and Francesc Maynou.

Other Contributions:

- **Distribution of rhodolith beds and their functional biodiversity characterisation using ROV images in the western Mediterranean Sea**

  Laia Illa-López, Andrea Cabrito, Sílvia de Juan, Francesc Maynou, Montserrat Demestre

  Science of the Total Environment 905, 167270 (2023)

  https://doi.org/10.1016/j.scitotenv.2023.167270

  In this study, which was completed during the development of the doctoral thesis, the Ph.D. candidate analyzed the videos obtained with the ROV, extracted species diversity and frequency data from the videos, and designed and conducted the statistical analyses related to species diversity. Additionally, she developed the results and discussion sections related to species diversity for the manuscript. She participated in the revision of the manuscript and in the creation of figures, as well as the graphical abstract.

  This study helped the Ph.D. candidate gain background knowledge on rhodolith beds in the Mediterranean and the species diversity they harbor, allowing her to formulate questions and strategies for developing her thesis.

- **Reconstruction of the Maërl habitat to better understand its ecological integrity.**

  Montserrat Demestre, Sara Soto, Ruth Durán, José Antonio García del Arco, Andrea Cabrito, Laia Illa-López, Francesc Maynou, Pilar Sánchez, Alfredo García-de-Vinuesa, Mickail Emelianov

  Science of the Total Environment 912, 168752 (2024)

  https://doi.org/10.1016/j.scitotenv.2023.168752

  Once again, the Ph.D. candidate was responsible for analyzing the ROV videos in this study focused on a rhodolith bed on the continental shelf of Blanes. Additionally, she designed and conducted all the statistical analyses related to species diversity data. She organized and created several of the figures for the manuscript and contributed to the writing of the results and discussion sections.

  Similar to the previous study, participation in this research allowed the Ph.D. candidate to gain background knowledge on rhodolith beds, the species diversity they support, as well as the potential use of cameras for monitoring them.

- **Effects of climate change on marine coastal ecosystems – A review to guide research and management**

  Ewan Trégarot, Juan Pablo D'Olivo, Andrea Zita Botelho, Andrea Cabrito, Gabriel O. Cardoso, Gema Casal, Cindy C. Cornet, Simon M.Cragg, A. Karima Degia, Stein Fredriksen, Elisa Furlan, Georg Heiss, Diego K. Kersting, Jean-Philippe Maréchal, Erik Meesters, Bethan C. O'Leary, Géraldine Pérez, Cristina Seijo-Nuñez, Rémy Simide, Matthijs van der Geest, Silvia de Juan.

  Biological Conservation 289, 110394 (2024)

  https://doi.org/10.1016/j.biocon.2023.110394

  As a result of the European project (MaCoBioS) that supported this thesis, the Ph.D. candidate participated in this study, where she contributed to the literature review and conducted the analysis of maërl beds data from the Mediterranean. Additionally, she assisted in designing the figures presented, and contributed to the writing of sections related to Mediterranean maërl beds.

  This study allowed the Ph.D. candidate to gain background knowledge for the thesis, particularly regarding the vulnerability of these habitats to climate change and anthropogenic pressures.

- **A common terminology to unify research and conservation of coralline algae and the habitats they create**

  Victor L. Jardim, Jacques Grall, Anaëlle Bizien, Juan C. Braga, Juliet Brodie, Thomas Burel, Andrea Cabrito, Guillermo Diaz-Pulido, Jason M. Hall-Spencer, Mathieu Helias, Paulo Horta, Siddhi Joshi, Nick A. Kamenos, Regina Kolzenburg, Erik C. Krieger, Erwann Legrand, Tessa M. Page, Viviana Peña, Federica Ragazzola, Lina M. Rasmusson, Francesco Rendina, Nadine Schumbert, João Silva, Federico T.S. Tâmega, Adeline Tauran, Thomas Benoit, Heidi L. Burdett.

  Marine and Freshwater Ecosystems 35(3), e70121 (2025).

  https://doi.org/10.1002/aqc.70121

  This work is the conclusion of one of the workshops the Ph.D. candidate attended during the 7th International Coralline Algae Meeting, Umea, Sweden (September 2023). The candidate's contribution was to participate in the discussion on the terminology of this group of algae and how to resolve it for unification during the meeting, as well as in the drafting and revision of the manuscript. It was her second independent collaboration and the first in a study with so many authors involved.

  This work helped the candidate clarify terms related to the development and nomenclature of these algae groups, allowing her to design and develop the introduction to her thesis with clear terminology.

APPENDIX I.

ORIGINAL PUBLISHED PAPERS AND DRAFTS BELONGING TO THIS THESIS.



Marine Biology (2024) 171:127
https://doi.org/10.1007/s00227-024-04437-y

ORIGINAL PAPER

Morphological insights into the three-dimensional complexity of rhodolith beds

Andrea Cabrito[1] · **Silvia de Juan**[2] · **Hilmar Hinz**[2] · **Francesc Maynou**[1]

Received: 26 November 2023 / Accepted: 8 April 2024 / Published online: 3 May 2024
© The Author(s) 2024

Abstract
The ecological importance of rhodolith beds stems from their role as structurally complex three-dimensional habitat formed by free-living red calcareous algae. Their structural singularity is due to the great variety of complex and branching morphologies exhibited by rhodoliths that create interstitial spaces and increase their surface area. This increases the ecological niches for cryptofauna and provide refuge for a high number of organisms, which is why rhodolith beds are considered biodiversity hotspots. In this work, we studied a rhodolith bed located in the Menorca Channel, formed by several species of red calcareous algae that exhibit a great variety of morphologies and form an extensive and heterogeneous habitat. This study explored the morphological diversity of the rhodolith bed, comparing the 'Core Habitat' (within the center of the bed with the highest densities of rhodoliths) with the boundaries or 'Adjacent Habitat' where rhodolith density was lower. Our results show that all rhodolith growth forms (branched, pralines and boxwork) in the Core Habitat had higher interstitial space and were larger than the ones from adjacent zones. Moreover, we explored the three-dimensional techniques to study the morphological characteristics that have historically been studied in two dimensions. This study contributes to the knowledge of morphological diversity in well-preserved rhodolith beds from continental shelves in the western Mediterranean Sea and reinforces the use of three-dimensional measurements, specifically the interstitial space of branched rhodoliths, to provide more accurate data on habitat complexity.

Keywords Coralline algae · Red calcareous algae · Biodiversity · Morphometrics · Mediterranean Sea

Introduction

Rhodoliths are free-living, long-lived, and slow-growing non-geniculate calcareous algae (Rhodophyta: Corallinaceae, also known as maërl). They accumulate as rhodolith beds in subtidal areas characterized by coarse, detritic sediments consisting of gravels and clean sands (Illa-López et al. 2023). They are distributed globally (Riosmena-Rodríguez et al. 2017) in environments where bottom currents prevent their burial by finer sediment, and where irradiance is low but still adequate for photosynthesis (Peña et al. 2014; Carvalho et al. 2020). In consequence, the depth limit of rhodolith beds is determined by the optical properties of the water body (transparency, turbidity, sediment load), affecting the quality and intensity of light reaching the seabed (Basso et al. 2017). In Mediterranean islands, rhodoliths thrive at great depths, reaching 100 m in the Mediterranean western basin (Ballesteros 1988; Barberá et al. 2012a) and reported at a maximum depth of 137 m for the Mallorca channel in the Balearic Islands (Massutí et al. 2022).

Rhodolith beds build hard, three-dimensional complex structures that provide substrate for other algae and invertebrates (Bordehore et al. 2003; Teichert 2014). These organisms are often referred to as ecosystem engineers (Nelson 2009). Rhodoliths can acquire various complex morphologies, from highly branched to massive round thalli (Bosence 1983). Therefore, they provide a greater array of microhabitats at different scales, from the interstitial spaces between branches (Bernard et al. 2019; Fredericq et al. 2019; Boyé et al. 2019) to the seascape level by increasing habitat heterogeneity (Amado-Filho et al.

Responsible Editor: F. Bulleri.

✉ Andrea Cabrito
cabrito@icm.csic.es

[1] Institut de Ciències del Mar (ICM-CSIC), Passeig Marítim de La Barceloneta 37-49, Barcelona, Spain

[2] Institut Mediterrani d'Estudis Avançats (IMEDEA-CSIC), Carrer Miquel Marquès 21, Esporles, Spain

2017). In consequence, the accumulation of rhodoliths over sandy sediments contributes to increase the local and regional biodiversity (Bernard et al. 2019; de Juan et al. 2023).

Previous studies identified a relationship between rhodolith morphological complexity and the associated biodiversity. In particular, the diversity of cryptofauna is related to thallus size, growth form and structural complexity (Kamenos et al. 2004; Steller et al. 2003; Figueiredo et al. 2007), with higher diversity associated with highly branched forms (Steller et al. 2003; Foster et al. 2007; Meihoub-Berlandi et al. 2012; Méndez Trejo et al. 2021). High density of rhodoliths also favors higher benthic fauna richness (Veras et al. 2020), while larger sizes of rhodoliths seem to facilitate reproduction and feeding in fishes and invertebrates (Steller et al. 2003; Gagnon et al. 2012).

Physical processes such as sedimentation or turbulence can affect rhodolith morphology and, therefore, their associated communities (Pérez-Peris et al. 2023). Trawl or dredge fishing contribute to increased sedimentation rates (Puig et al. 2015) and to physical damage of the rhodolith (e.g., breaking or chipping) (Cabanellas-Reboredo et al. 2017; Gabara et al. 2018). Rhodolith beds have a high conservation value; they are included in the European "Habitats Directive" (Council Directive 92/43/EEC). However, in the Mediterranean, they continue to face threats from trawling activities (de Juan et al. 2013) and current protection measures are often inadequate. Due to their slow growth (of the order of 1 mm yr^{-1}, Blake et al. 2007) rhodoliths exhibit exceptionally low renewal rates, which can result in slow recovery trajectories (Tauran et al. 2020).

This study focuses on rhodoliths from a well-preserved rhodolith bed in the Menorca Channel (Balearic Islands, Western Mediterranean, 3°45′ E, 39°75′ N) (Barberá et al. 2012a). The main objective of the study is to describe and measure the morphology of rhodoliths as a proxy for habitat structural complexity. By analyzing samples from the well-preserved rhodolith bed, this study (1) analyzes the diversity of rhodolith morphologies; (2) determines the allometric growth curve for each of the major morphologies; (3) produces a discriminant rule to classify rhodoliths based on few morphometric measurements; (4) compares 2D with 3D measurements of branched rhodoliths to examine whether simple, relatively easy to measure 2D metrics would be sufficient to describe the morphometry of a naturally occurring 3D object. This is relevant because, given the intricate three-dimensional growth pattern of rhodoliths, 2D metrics may lack the precision and accuracy needed to effectively describe their shape or interstitial space. This estimation is important, as it is directly linked to the ecological functions facilitated by rhodoliths, which inherently exist in three dimensions.

The understanding of the structural complexity of rhodolith beds, achieved by exploring objectives 1–4, is essential for deducing their functional importance (Stelzer et al. 2021) and to improve their protection and preservation status globally (del Río et al. 2022).

Methodology

Study area

The study area is located in the Menorca Channel between 45 and 80 m depth (Fig. 1) and was selected based on previous studies (Moranta et al. 2014) that identified a well-developed and preserved rhodolith bed that alternates with detritic bottoms and biogenic assemblages formed by other species of algae (de Juan et al. 2023). The Menorca Channel was declared a European Site of Community Importance (LIC ESZZ16002) in 2016, including a trawling ban for most of the channel. Moreover, the presence of underwater communication cables crossing the channel delimits an exclusion area that has been protected from trawling for more than five decades.

The presence of the cables' exclusion zone, a gently sloping continental shelf (reaching a maximum depth of 100 m), and the prevalence of strong bottom currents create optimal conditions for the development of rhodolith beds. As a consequence, the study area includes the largest identified rhodolith bed in the region, which has an extension of 304 km^2 (Fig. 1). As the distance from this bed increases, the depth increases toward the south-east and decreases toward the coast (west), with the north-west area being influenced by the sandy platform of the Bay of Alcudia (Fig. 1). In addition to the variation of these environmental factors, the density of rhodoliths decreases as the distance from the center of the rhodolith bed increases, hereafter referred to as Core Habitat (Fig. 1).

We assessed the variation of rhodolith morphology in relation to the distance to the Core Habitat. Five sampling stations were deployed from the center to the periphery of the rhodolith bed (or Core Habitat). Sampling stations were thus classified into: (1) "Core Habitat", including samples within the cable zone at 69 m depth (S13) and in the trawl exclusion area close to the cable zone at 58.8 m depth (S15), where rhodolith cover is typically > 50%; (2) "Adjacent Habitat", including samples far from the cables zone at 56 and 74 m depth (S18 and L1, respectively), where rhodolith cover is less than 50%, and "outside the reserve area" at 48.5 m depth (S5), where rhodoliths are scarce (Fig. 1). The percentage cover of rhodoliths at each station was extracted from Moranta et al. (2014), where a spatially structured survey was conducted to estimate the habitats distribution in the channel. To verify the rhodolith coverage at a small scale

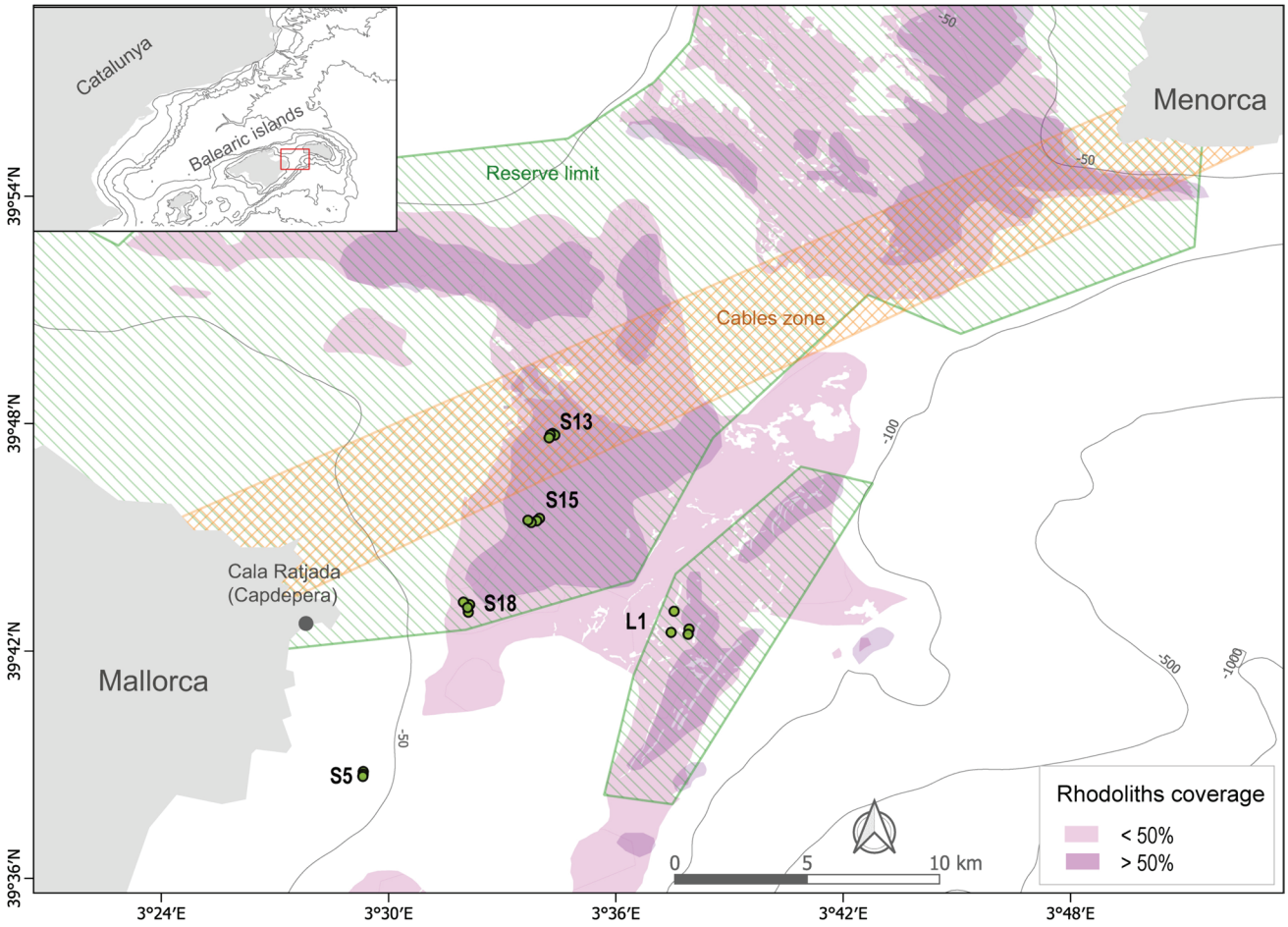


Fig. 1 Map of the study area in the Menorca Channel, showing the positions of the dredges (green dots). Area limited by the cables zone ("Cables zone" in the figure, established in 1971) and the "Trawl Exclusion Reserve" (declared 2016, green cross-hatch). Source: INDEMARES (Moranta et al. 2014)

(1–10 m), additional video images were obtained using still cameras (see Supplementary Material—Fig. S1).

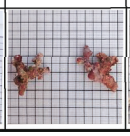
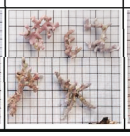
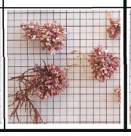
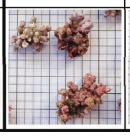
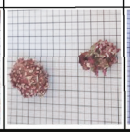
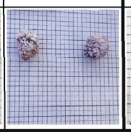
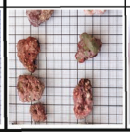
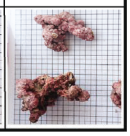
Data acquisition

We collected four samples per station using a "Naturalist" Dredge (frame 45 × 18.5 cm, fitted to a 1 mm mesh bag) in summer 2022. Nineteen valid samples were recovered, as only 3 dredges could be collected in S5 (example in Supplementary Material—Fig. S2). For each sample, a volume of approximately 7000 cm^3 of the content was systematically extracted, distributed in a tray and photographed. The proportion of live and dead rhodoliths was visually estimated on board for each tray.

The rhodoliths were classified into nine morphotypes (A to I), described based on the six used in Barberá et al. (2012b) with some modifications that further divided heterogeneous groups (Table 1). These nine morphotypes belong to the three main rhodolith categories or growth forms according to Basso et al. (2016): "Branched" (Br), "Praline" (PR) and "Bowork" (Bo). The rhodoliths were grouped by morphotypes, photographed on a graduated white board and dry stored. A total of 3877 rhodoliths were counted in the photographs (see Supplementary Material Table S1). The number and frequency of the morphotypes (A to I) and growth forms in each sample were estimated from the photographs.

A sample of 100 g of sediment extracted from each dredge was stored for granulometry analysis, while the remaining content of the dredges was returned to the sea. A subsample of 20 g of sediment was used for the analysis of grain size. The granulometry was analyzed using a laser diffraction particle size analyzer (HORIBA LA-950V2) after disaggregation and removal of the biogenic fraction (10% H_2O_2 solution) and dispersion in an ultrasonic bath.

Table 1 Rhodolith growth forms (top) and description of morphotypes defined in the finer classification (A to I)

MORPHOTYPES	BRANCHED				PRALINES			BOXWORK	
	Large size with wide branching	Small size, less and short branching	Small size with slender branches	Many short branches. Spherical	Rough, bumpy and quite irregular	Rounded with small protusions or short branches	Rounded with many thick and smooth protusions	Rounded and incrusted in other subtratum	Irregular form, incrusted in other subtratum
	A	B	C	D	E	F	G	H	I
									

2D measurements

From the rhodolith samples (i.e., 3877 rhodoliths photographed on board), five individuals for each morphotype per station (when possible) were selected and set aside. This selection resulted in a total of 189 rhodoliths belonging to the nine morphotypes (Supplementary Material Table S2). These 189 rhodoliths were photographed individually to obtain 2D morphological metrics. A total of 15 metrics were obtained for each rhodolith. The *maximum* and *minimum axis of the fitted ellipse* (A_{max} and A_{min}, mm), the *surface of the projected area* (A, mm^2), *convex hull area* (CHA, mm^2), *shape perimeter* (P, mm), the *angle* (a, °), the *Feret length* (L_{max}, mm) and *Feret's angle* (Fa, °) were obtained measuring the rhodolith shape and estimating the convex hull of the shape. These metrics were obtained using the default measurement routines in ImageJ 1.52a software (Schneider et al. 2012), except for *CHA* which was obtained with the plugin "Hull and Circle" v.2.1b contributed by A. Karperien (http://imagej.net/ij/plugins/hull-circle.html).

In addition, the dimensionless metrics *circularity* (C), *roundness* (R), *aspect ratio* (AR) and *solidity* (S) were automatically determined by ImageJ program according to the following formulas:

$$C = 4\pi \frac{A}{P^2},$$

$$R = 4\frac{A}{\pi A_{max}^2},$$

$$AR = \frac{A_{max}}{A_{min}},$$

$$S = \frac{A}{CHA}.$$

Finally, three additional metrics were obtained:

1. the *interstitial space* (IS, mm^2) as the missing space (area) between the convex hull area and the rhodolith surface area:

$$IS = CHA - A,$$

2. the individual dry weight (W, g) and
3. the *shape coefficient* (D, Kooijman 2010) extracted from:

$$D = \sqrt[3]{\frac{W}{2.71\, L_{max}{}^3}},$$

with $d = 2.71$ g/cm^3 being the density of calcite.

2D/3D measurements in branched morphotype A

Given that the difference between 2 and 3D metrics is likely to be more noticeable in the branched growth form, this analysis focuses only on morphotype A. We subsampled a new set of 30 rhodoliths (from the stored dry sample) classified as branched (morphotype A) and collected in the stations S13 and S15 (Supplementary Material Fig. S3). The 30 rhodoliths were photographed and dry weighed individually. Then, the images were processed through ImageJ as described in the previous section. To compare the 2D and 3D information extracted, the measurements assessed are subscripted "2D": the *maximum ellipse axis* ($A_{max\text{-}2D}$), the *maximum Feret diameter* ($L_{max\text{-}2D}$), the *perimeter* (P_{2D}), the *surface area* (A_{2D}), *the convex hull area* (CHA_{2D}), the *roundness* (R_{2D}), the *solidity* (S_{2D}) and the *interstitial space* (IS_{2D}).

For 3D measurements, digital twins of selected rhodoliths were created using high-precision blue light 3D scanner (Revopoint MINI) with a precision of up to 0.02 mm and the associated programs Revoscan and Revostudio (www.revopoint3d.com). For each 3D model twin, the *surface area* (A_{3D}, mm^2), the *maximum length from the center of mass* (L_{3D}, mm), the *volume* (V_{3D}, mm^3) and the *convex hull volume* (CHV_{3D}, mm^3) were calculated using an ad hoc R

script based on libraries Rvcg, geometry and MeshesTools, while *the maximum Feret diameter* ($L_{max\text{-}3D}$) and the *roundness* (R_{3D}) were obtained using Slicer program v. 5.2.2 (Fedorov et al. 2012). With these measurements, the 3D *interstitial space* (IS_{3D}, mm^3) was calculated as the difference between the volume of the convex hull and the volume of the rhodolith:

$$IS_{3D} = CHV_{3D} - V_{3D}.$$

The solidity in 3D (S_{3D}) was calculated with the relation between the 3D rhodolith volume and the 3D convex hull volume:

$$S_{3D} = \frac{V_{3D}}{CHV_{3D}}.$$

Finally, we obtained a matrix of 17 metrics (8 from 2D, 8 from 3D and the weight) measured for the 30 rhodolith samples (see Supplementary Material Table S3).

Statistical analysis

Morphological rhodolith composition of the study area

Differences in the proportion of growth forms (Br, Pr and Bo) between Core Habitat and Adjacent Habitat stations were analyzed with PERMANOVA, with a model design including "Station" nested within Habitat factor with two levels (Core and Adjacent Habitat). Both factors were treated as fixed factors. The proportions were arcsin transformed for this analysis. The routine adonis2 of R package *vegan* was used (Oksanen et al. 2022).

2D: General measurements analysis

After removing nine outliers (determined through exploratory data analysis with the aid of boxplots), 180 measured rhodoliths were used to fit several models. Firstly, a regression model was performed to assess the *W*/*L* relation, with *L* corresponding to the Feret's diameter, by linearizing the allometric growth equation:

$$W = aL_{max}^{b}.$$

This was done for the pool of 180 rhodoliths and for each category or growth form (Br, Bo, Pr) separately. Then, to evaluate the significance of the difference in the values of the *a* and *b* parameter of this relation between the three growth forms, we performed a generalized linear model (GLM) from package *stats* (R Core Team 2022) fitted with a Gaussian distribution with logarithm link. To examine the possibility of overdispersion in the data, we performed a dispersion test from the package *AER* (Kleiber and Zeileis 2022).

2D: Multivariate analyses

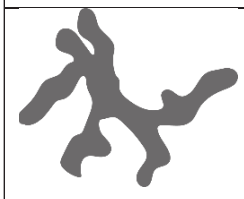
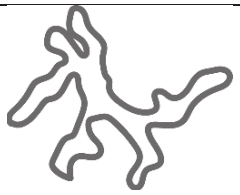
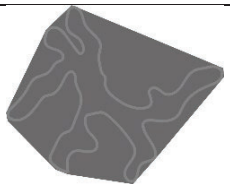
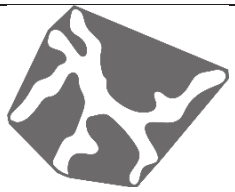
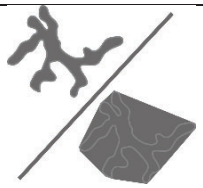
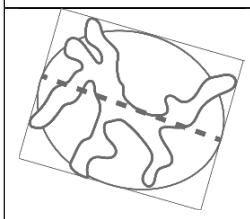
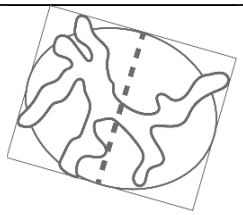
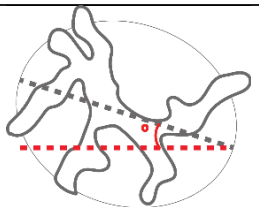
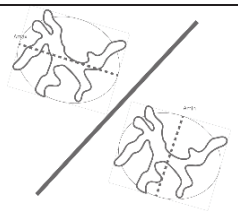
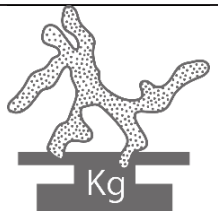
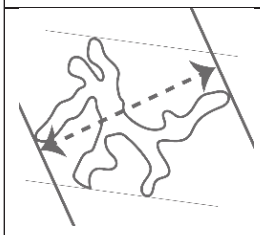
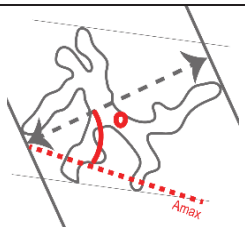
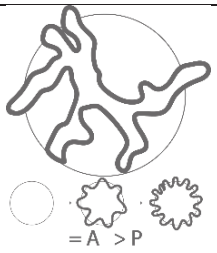
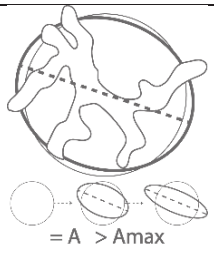
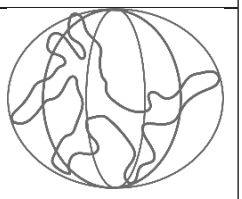
A PCA was performed on the full 2D metrics data set to reduce the number of variables while preserving the maximum variance possible of the original data set. This reduction in dimensionality facilitates visualization and data interpretation. Function prcomp from the R *stats* package was used. To accomplish that, we standardized all 15 morphometric variables measured from the 180 rhodoliths (Table 2).

To examine how these variables perform as morphology classifiers, we selected the less correlated variables based on the Pearson correlation test from package *corrplot* (Wei and Simko 2021) to perform a linear discriminant analysis (LDA) from package *MASS* (Venables and Ripley 2002). The numeric variables used in the model were: *maximum Feret diameter* (L_{max}), *roundness* (*R*) and *solidity* (*S*) and the classification factor was the growth form (Br, Pr and Bo). To fit the model, the variable L_{max} was log transformed, and solidity and roundness were arcsin transformed. With these transformations, the assumptions for LDA of multivariate normality and homoscedasticity between groups were met. Multivariate normality of the metrics by morphology was not rejected according to the Royston's multivariate normality test (p value = 0.05 for branched; p value = 0.40 for pralines and p value = 0.88 for boxwork), using the *MVN* package (Korkmaz et al. 2014). The hypothesis of homoscedasticity could not be rejected based on Box's *M*-test for homogeneity of covariances matrices ($X^2 = 18.562$, df = 12, p value = 0.0996) of the *biotools* package (da Silva 2021). The matrix of 180 individuals was randomly re-sampled to split the data into a training data matrix (70%) to train the model, and a test data matrix (30%) to test the model. To achieve better prediction accuracy, this process was repeated a total of 100 times.

2D/3D morphotype A measurement analysis

With the matrix of 17 morphological variables (8 in 2D, 8 in 3D and the weight), a Pearson correlation test was performed from package *corrplot* (Wei and Simko 2021) to assess the correlation between the two measurements. Furthermore, considering the total available surface area and the volume as key morphological measurements of high biological interest for metabolic or growth studies, linear models from package 'stats' were fitted between the surface area measured in 2D (A_{2D}) and in 3D (A_{3D}) and between the surface area measured in 2D (A_{2D}) and the total volume measured in 3D (V_{3D}).

Table 2 Graphical representation of the 15 morphometric variables measured

Area (*A*)	**Perimeter (*P*)**	**ConvexHull Area (*CHA*)**	**Interstitial Space (*IS*)**	**Solidity (*S*)**
				
Maximum axis (A_{max})	**Minimum axis (A_{min})**	**Angle (*a*)**	**Aspect Ratio (*AR*)**	**Weight (*W*)**
				
Feret diameter (L_{max})	**Feret angle (F_a)**	**Circularity (*C*)**	**Roundness (*R*)**	**Shape coefficient (*D*)**
				

All statistical analyses were computed in R (R Core Team 2022) under version 4.2.1.

Results

Morphological rhodolith composition of the study area

The proportion of dead (bleached) rhodoliths was predominantly low (< 20%) with exceptions found in three samples from station L1 and two samples from stations S5 and S13 that had no dead rhodoliths, while three samples from S18 had higher percentages, one reaching 50% coverage by dead rhodoliths (Supplementary Material Fig. S4).

All stations exhibited similar sediment compositions, primarily gravel (85% or higher), with minimal silt and clay (never exceeding 15%). Branched forms predominated in 50–90% of the samples, with lower proportions of pralines (5–40%) and boxwork (0–30%). However, variations in rhodolith morphologies were observed within samples collected at the same station, suggesting high small-scale heterogeneity. The Adjacent Habitat station L1 was very heterogeneous, and boxwork forms were more prevalent in several samples (Fig. 2).

Of the 3877 rhodoliths photographed, 69.2% were branched, 19.1% pralines and 11.8% boxwork (Fig. 3, left panel). From these, the most abundant morphotypes were the branched types C (37.53%), B (14.70%) and A (10.14%), and praline E (14.24%) (see Table 1 for reference to the morphotypes). The proportions and representation of rhodolith morphotypes remained consistent across the two habitats (PERMANOVA $p(F) = 0.211$); however, the PERMANOVA test identified significant effects of the factor station within habitat (PERMANOVA $p(F) = 0.003$).

At S5, the dominant morphotypes were branched (D) and praline (F), which were scarce at other stations. These differences likely stem from the habitat, as S5 is characterized by sand with scattered rhodoliths, and it is considered outside the rhodolith bed. Consequently, S5 was excluded from the statistical analyses conducted in this section and the subsequent one.

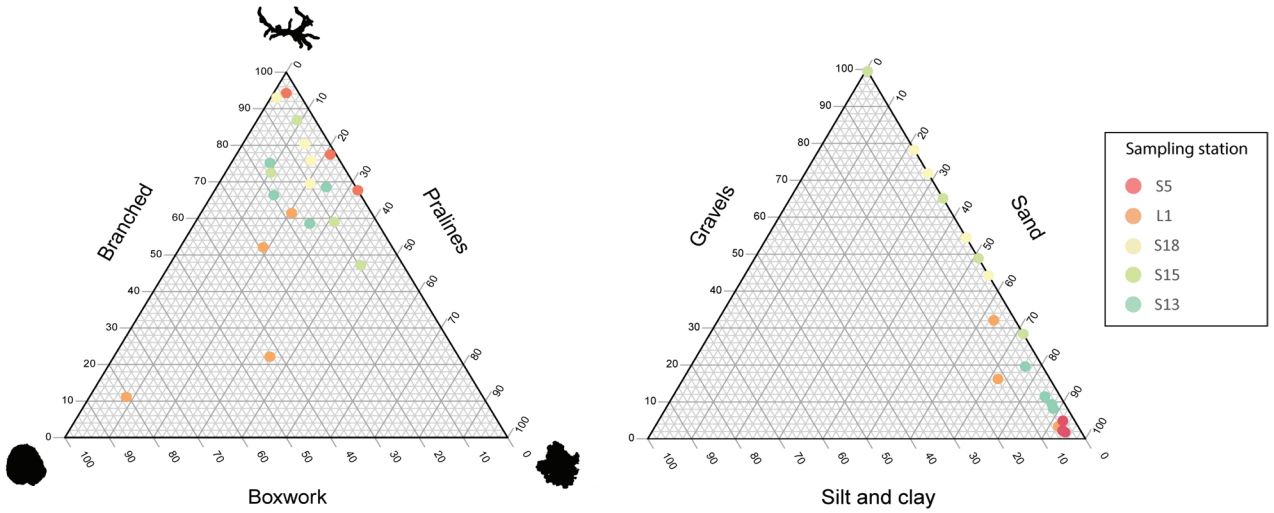


Fig. 2 Ternary plot of sediment composition showing the proportion of gravels, sand, silt and clay (right) and ternary plot of rhodolith growth forms composition showing the proportion of branched, pralines and boxwork rhodoliths (left). Each dredge was represented and color coded following the stations sampled

The stations within the Core Habitat exhibited more consistent proportions of morphologies compared to those in the Adjacent Habitat. Specifically, the dominant branched morphotype A decreased in abundance from station S13 to S15 and further to L1, where it was absent, while the branched morphotype C remained consistently abundant across all stations, with the highest representation observed at adjacent station S18. The non-branched morphotypes were never dominant, but appeared relatively frequently in station L1. The praline morphotype E was represented equally in all stations. The praline morphotype G occurred mostly in the stations from Core Habitat. The boxwork growth forms (morphotypes H and I) were proportionally represented in all core and adjacent stations except in S15 where mophotype H was predominant.

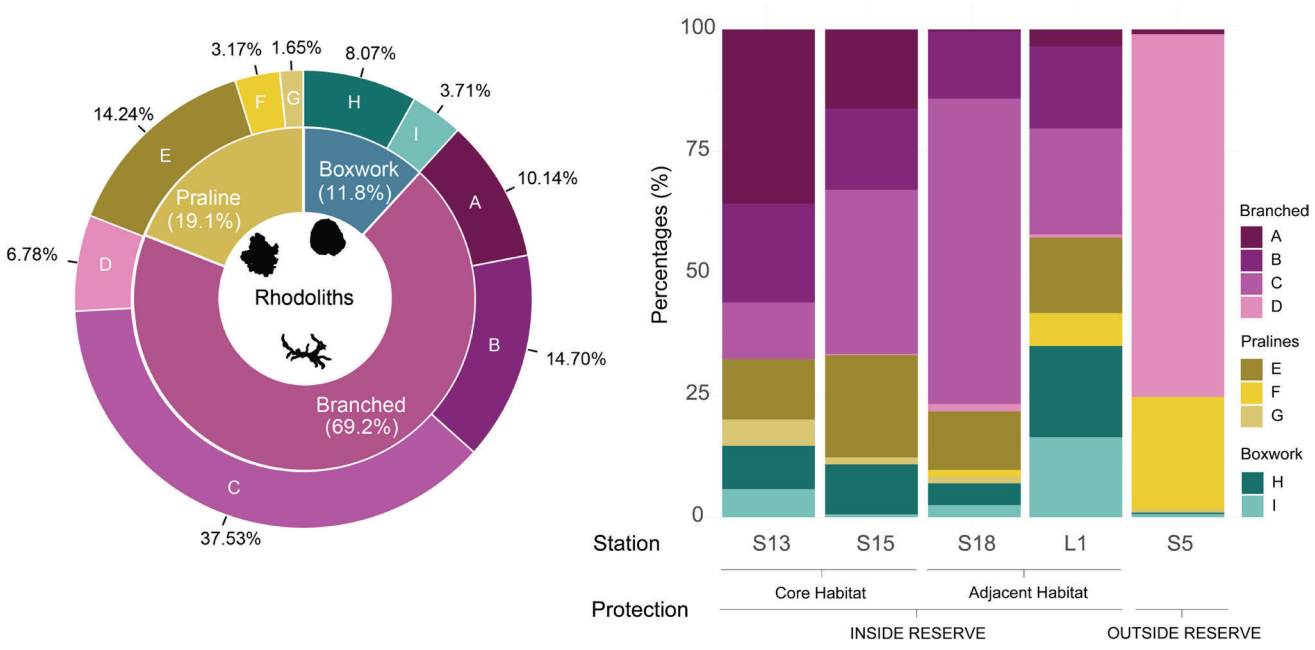


Fig. 3 Total proportions of each growth form (Br, Pr and Bo) considering all stations together (left). Percentage of morphotypes (A to I) coverage in each station (right)

2D morphological measurements

The PCA revealed the main morphometric variables describing the 2D rhodolith shape. These results showed that 46.7% of the variance could be explained by the first dimension, while the second dimension explained 25.2% of the variance. Figure 4 shows that the most differentiated group is the one formed by the branched forms. Praline and boxwork overlapped in the biplot.

The variables *maximum Feret diameter* (L_{max}), *area* (*A*) and *convex hull area* (*CHA*), *weight* (*W*) and the *maximum* and *minimum ellipse axis* (A_{max} and A_{min}) were highly correlated and their variability is represented by the first dimension (PCA *X*-axis). *Shape coefficient* (*D*), *circularity* (*C*), *solidity* (*S*) and *roundness* (*R*) were also correlated and defined by the second dimension (PCA *Y*-axis). *Aspect ratio* (*AR*) and *roundness* (*R*) were negatively correlated, indicating that branched forms have lower roundness (and higher aspect ratio) than pralines and boxwork rhodoliths.

Because of the high correlation between several shape measurements, only a representative subset (L_{max}, *IS*, *W*, *A*, *D* and *P*) was used to examine differences between samples recovered from the Core Habitat and the Adjacent Habitat (Fig. 5). Boxwork growth forms tended to be bigger, longer and heavier than praline and these than branched forms (Fig. 5). Moreover, there was a clear effect of the Core Habitat in terms of interstitial space, maximum Feret diameter and area. These metrics had greater values in all growth forms in the stations within the Core Habitat compared to the stations from the Adjacent Habitat.

The allometric growth curves ($W = a\ L^b$) were estimated for each rhodolith growth form based on the linear models fitted for the relationship between weight and the L_{max} (Fig. 6). The parameter *a* was significantly different between boxwork and branched curves (p value < 0.001), but not between praline and branched curves (p value $= 0.097$). The parameter *b* showed no significant differences between growth forms. Therefore, the three groups showed a similar allometric growth rate, despite the groups having significantly different weights for the same length. The test for overdispersion was significant (p value < 0.001), but with a low value of dispersion 1.80.

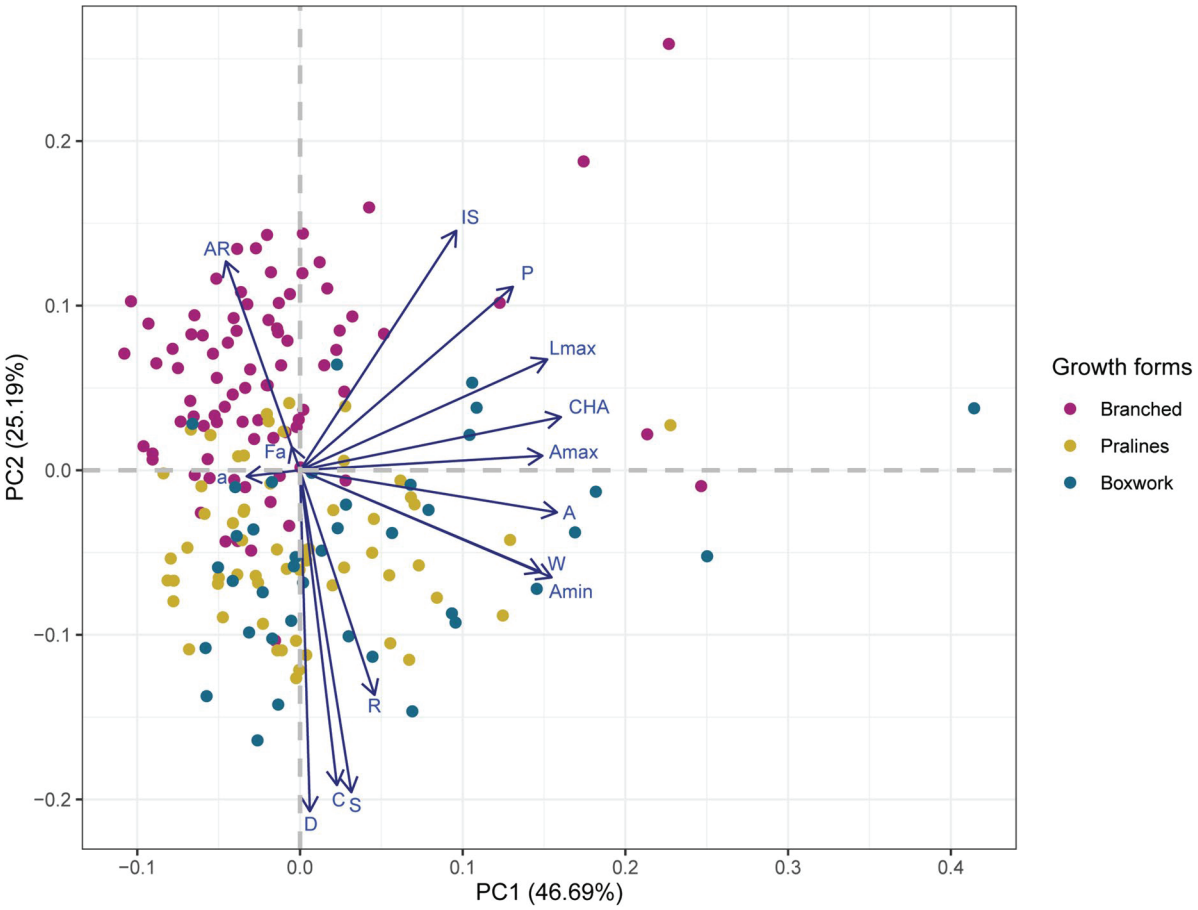


Fig. 4 Principal components analysis (PCA) of individual rhodolith metrics from the Menorca Channel. *A* area, *a* angle, A_{max} maximum ellipse axis, A_{min} minimum ellipse axis, *AR* aspect ratio, *C* circularity, *CHA* convex hull area, *D* shape coefficient, *Fa* Feret angle, *IS* interstitial space, L_{max} maximum Feret diameter, *P* perimeter, *R* roundness, *S* solidity, *W* weight

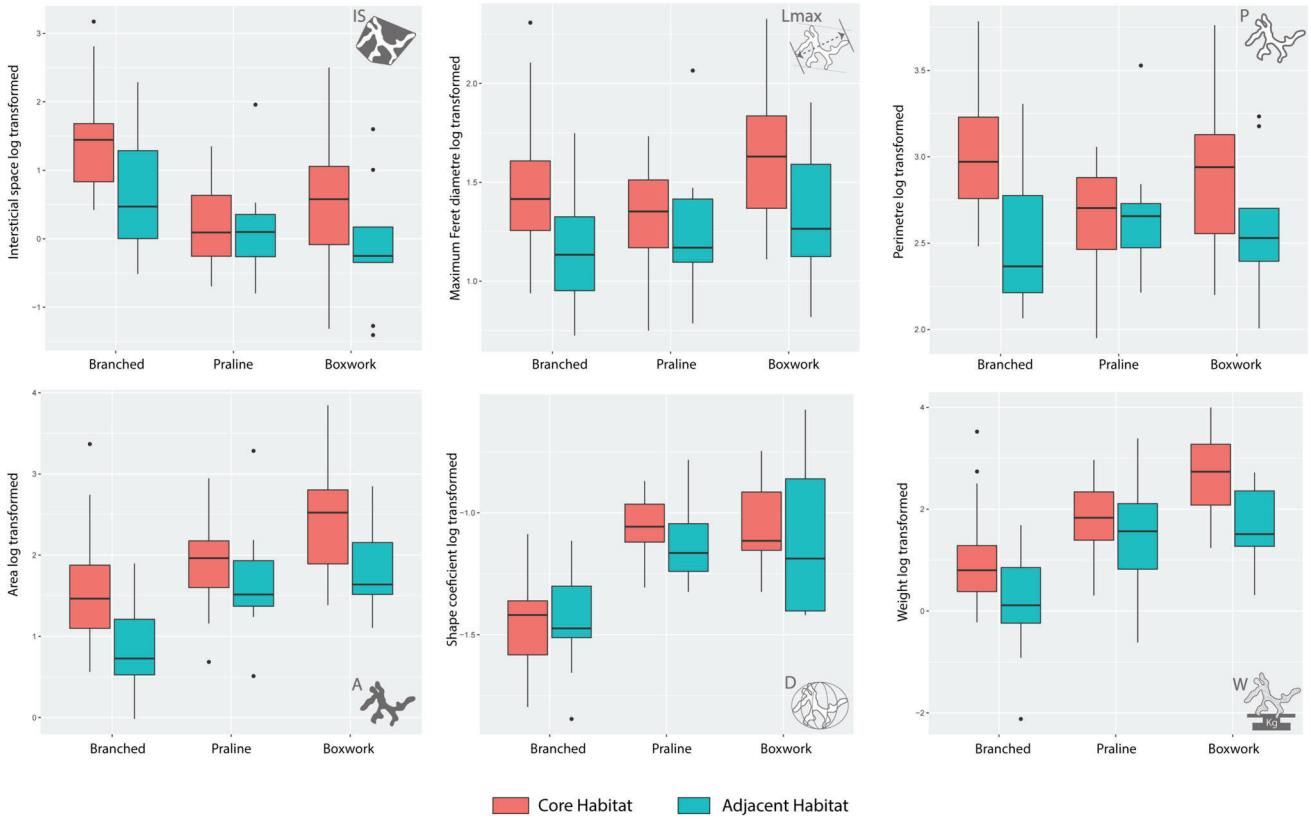


Fig. 5 Boxplots for a subset of six morphological variables both in Core Habitat and in Adjacent Habitat for the three growth forms of rhodoliths. From left to right at the top: interstitial space (*IS*), maximum Feret diameter (L_{max}) and perimeter (*P*). From left to right at the bottom: area (*A*), shape coefficient (*D*) and weight (*W*). All variables were log transformed

Discriminant analysis

A linear discriminant analysis was used to build a classifier to predict growth forms from a set of relatively easy to measure variables. The results of the LDA showed that, although the three groups had a large degree of overlap, they can be statistically distinguished. The variables with the greatest weight in defining the first dimension of the LDA were the *roundness* (*R*) and the *solidity* (*S*), while the *maximum Feret diameter* (L_{max}) had the greatest weight in the second dimension. The first LDA axis explained 96.6% of the variance. This first direction separates the rhodoliths with greatest solidity (less branching), roundness and relatively large L_{max} in the positive axis, from the rhodoliths with less *S* (more branching) and less *R* in the negative axis. The second LDA dimension explained the rest of the variance (3.37%), driven by L_{max}, with longer rhodoliths in the positive axis and shorter in the negative one. Thus, the first dimension separates the largest, most rounded and solid rhodoliths (both pralines and boxwork growth forms) from the branched forms (Fig. 7). The classification equations based on *maximum Feret diameter*, *roundness* and *solidity* are:

$$\text{LDA1}: 1.996\left[L_{max}\right] + \mathbf{0.252}\,[\mathbf{R}] + \mathbf{0.274}\,[\mathbf{S}],$$

$$\text{LDA2}: \mathbf{21.232}\,[\mathbf{L_{max}}] + 0.123\,[R] + 0.147\,[S].$$

Applying the estimation model to the data test, we found that the classification rate was correct in 63.15% of the cases. After reproducing the analysis 100 times and running the predictive model, the classification rate for a new rhodolith was 69.5%, with the percentages of success for each growth form being different (Table 3). The best classified form was always branched with 88.13% of success. The more common misclassification was obtained when classifying a boxwork as a praline (40.87% of times) or a praline as a boxwork (30.73% of times).

3D morphological measurements in a subset of morphotype A

A 3D model twin of the complete rhodolith shape (Fig. 8) and its corresponding measurements were obtained for 30 rhodoliths. The correlation test showed that both sets of

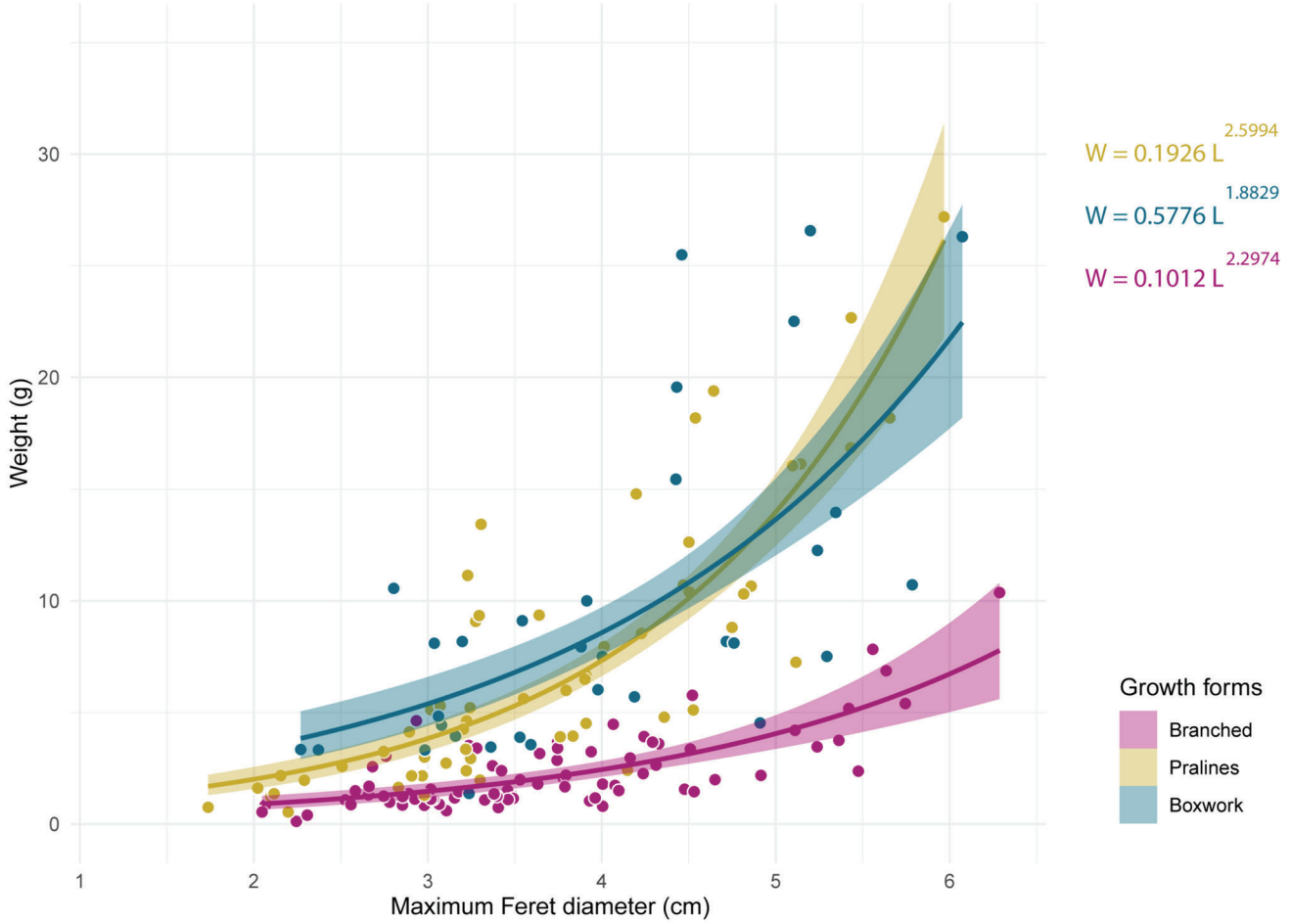


Fig. 6 Rhodolith allometric growth curves, representing the relation between L_{max} and W for each morphotype or growth form

metrics (2D vs. 3D) are highly correlated (Supplementary Material Fig. S5), especially a metric on two different dimensions (e.g., area 2D and area 3D), but also between metrics in the same dimension (e.g., perimeter 2D with area 2D).

The linear models (with intercept at 0) fitted between 2 and 3D area and between 2D area and the volume showed that both sets were highly correlated ($R = 0.99$ and $R = 0.98$, respectively) (Fig. 9). The 3D area resulted in 4.27 times the 2D area (Fig. 9a), while the volume was 6.45 times the 2D area (Fig. 9b). These equations can be useful in estimating the ecologically meaningful quantities (area, volume) in 3D from their equivalent quantities in 2D, which are much easier to measure.

Discussion

The present study has characterized the morphological composition of a rhodolith bed in the continental shelf of the Menorca Channel (western Mediterranean). This area was selected due to its good conservation status, with a well-developed rhodolith bed (i.e., above 50% rhodolith coverage over 304 km^2), and adjacent locations with decreasing rhodolith cover alternating with detritic sands (Barberá et al. 2012a; de Juan et al. 2023). It is common to find in rhodolith beds a variable quantity of dead rhodoliths and their fragments accompanying the live rhodoliths (Bracchi and Basso 2012). Our results generally show proportions of dead rhodoliths ranging from 5 to 20% in most samples (except for those from the Adjacent Habitat station S18). These values are similar to those found by Rendina et al. (2020) and support the hypothesis that the rhodolith bed in the Menorca Channel is in a good environmental condition. Despite that branched forms predominate in all stations, we observed small-scale heterogeneity in the proportions of growth forms and of morphotypes. The heterogeneity observed agrees with previous studies in the Mediterranean (i.e., Bracchi et al. 2022) and particularly in the Menorca Channel (Farriols et al. 2022). In general, the proportion of branched growth forms, and particularly

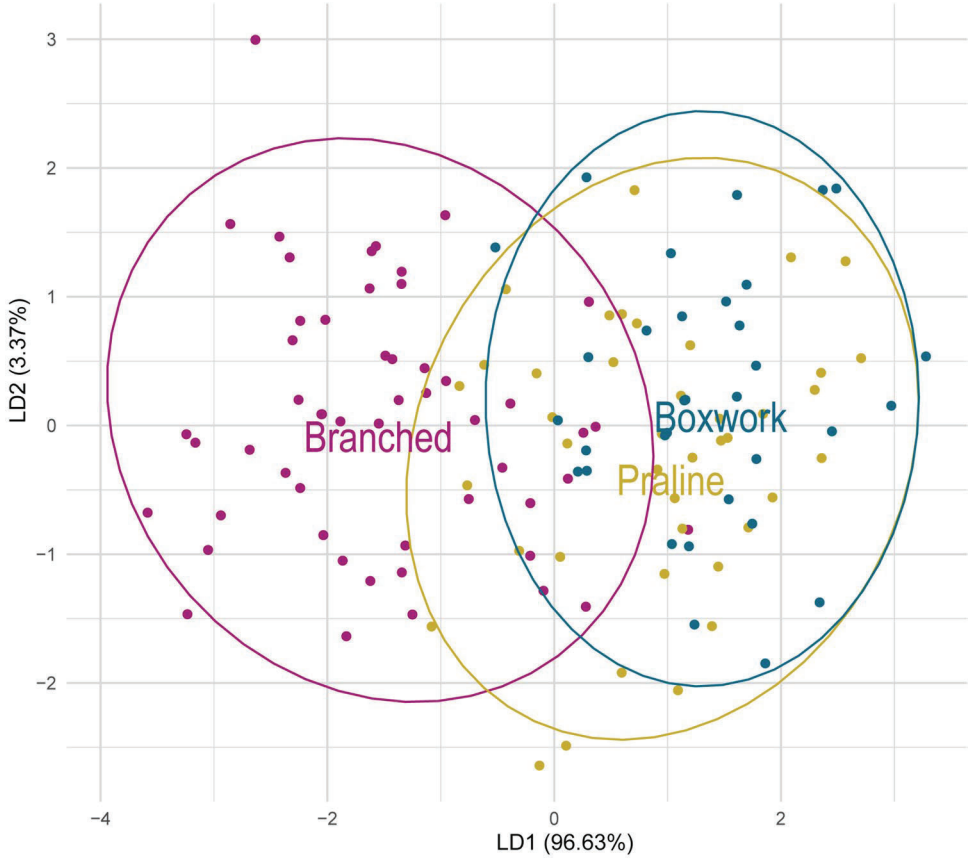


Fig. 7 Representation of the linear discriminant analysis (LDA)

Table 3 Table of predictions when classifying rhodoliths according to the variables considered in the LDA

	Predicted class		
Real Class	Branched	Praline	Bowork
Branched	0.8813	0.096	0.0225
Praline	0.1364	0.5563	0.3073
Boxwork	0.0608	0.4087	0.5304

the proportion of morphotype A, was highest in the Core Habitat.

The differences in the proportion of morphotypes between stations cannot be attributed to differences in sediment granulometry. The sediment below the rhodolith bed was coarse, with the sand fraction (grain size > 63 µm) comprising at least 50% of the sample in all stations and over 80% in S13, L1 and S5. In S15 and S18, the gravel fraction (grain size > 2 mm) comprised around 40% of the sample. This granulometry is typical of Mediterranean rhodolith beds (de Juan et al. 2013), although dominance of fine sediments (grain size < 63 µm, Bracchi et al. 2022; Ingrassia et al. 2023) or coarser sediments, including fractions larger than 20 mm (del Río et al. 2022), have been reported in Mediterranean rhodolith beds. Our findings corroborate the conclusions drawn by Cabanellas-Reboredo et al. (2017), indicating that, at the scale of a rhodolith bed, sediment granulometry has limited explanatory power regarding variations in rhodolith morphology. However, at larger spatial scales, coarse sediments are indicative of low sediment input from terrestrial origin, which is expected around Mediterranean islands. High currents predominating in the area (Moranta et al. 2014) would also prevent the deposition of fine sediments.

The specimens from the Core Habitat were larger and with more interstitial spaces, even considering the praline morphologies. It is likely that rhodoliths at the edge of the Core Habitat exhibit lower complexity, due to suboptimal environmental conditions combined with being exposed, directly or indirectly, to trawling. Interestingly, a decrease in morphotype A from S13 (in the Core Habitat and within the cables zone) to the edge of the Core Habitat and exclusion zone in S18 was observed suggesting that this morphotype is a potential candidate indicator of the conservation status of the habitat. Both natural and anthropogenic processes may be responsible for increased fragmentation of branched growth form, resulting in smaller and less ramified (more solid) branched rhodoliths (Barberá et al. 2012a, b). Branched rhodoliths exhibited a greater degree of branching and had higher interstitial space (IS) in samples

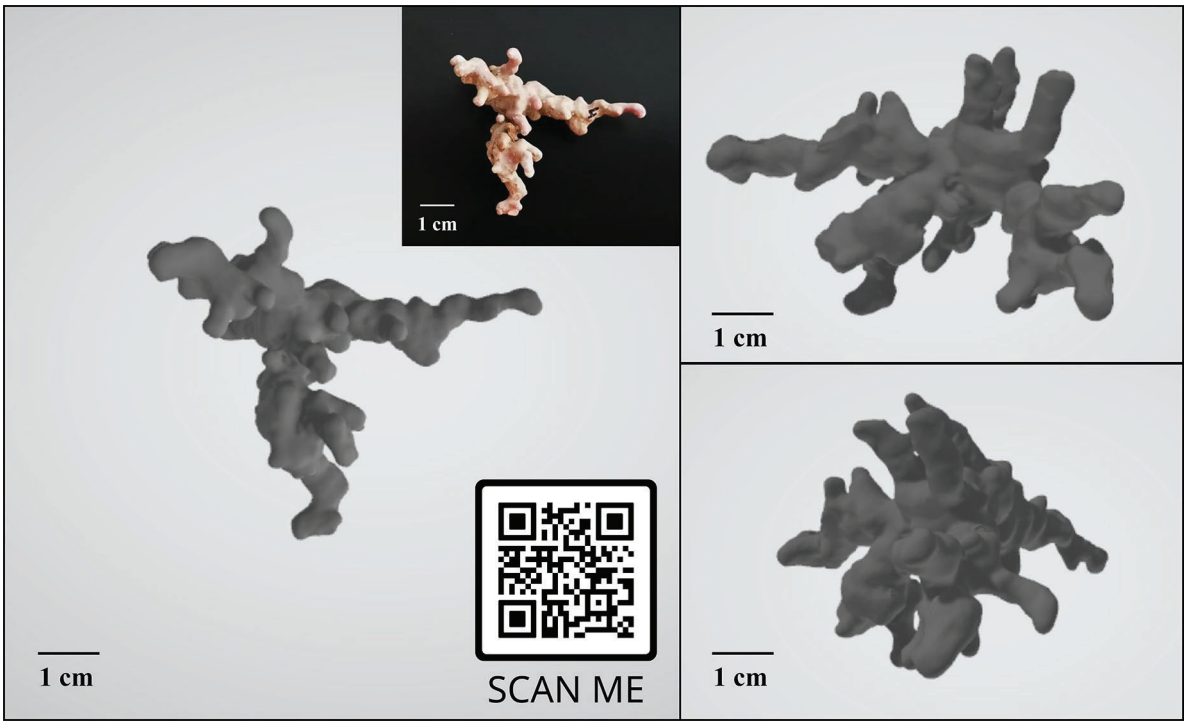


Fig. 8 Example of 3D model twin from a morphotype A rhodolith. 3D model view scanning the QR

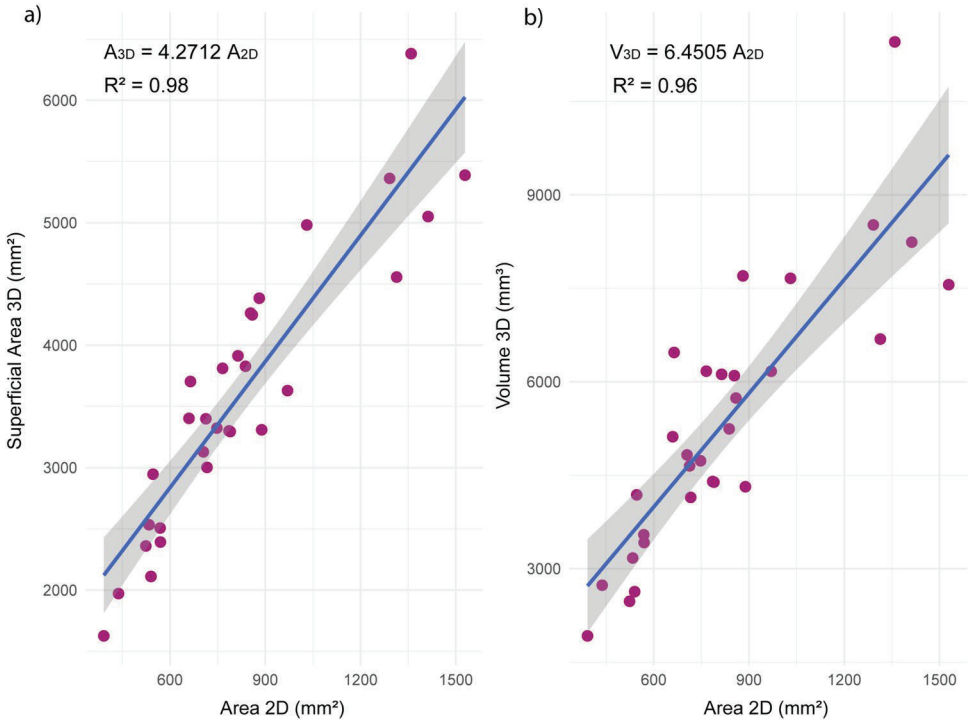


Fig. 9 Linear models and equations between area measured in 2D and (**a**) superficial area measured in 3D and (**b**) volume measured in 3D

from the Core Habitat, suggesting that good environmental condition of the rhodolith bed contributes to maintain the architectural complexity of this habitat. Habitat complexity is significant for enhancing local species richness (de Juan et al. 2013). The spaces between branches provide microhabitats for diverse assemblages of other algae, epiphytes

and invertebrates including sponges, cnidarians or bryozoans (Phillips 2023) (see examples found in Supplementary Material—Fig.S6). As such, the rhodolith bed community in the protected Core Habitat, characterized by high diversity of rhodolith morphotypes, could be viewed as the reference for a good environmental condition. This holds significant implications for local conservation management, as often, such reference or baseline points are scarce (Lindeboom 1995).

Owing to legislation prohibiting trawling within the cables exclusion zone, there is a high degree of certainty that the Core Habitat has experienced no physical disturbances since the early 1970s. Initial examination of the data from both Core and Adjacent Habitat stations suggest a correlation between the condition of rhodolith beds and their level of protection. However, our study was not designed to assess this relationship. Extending sampling over a gradient of trawling intensity, with enough spatial coverage to incorporate environmental variability (e.g., see Hinz et al. 2009), would contribute to assess potential variability in rhodolith morphology linked to trawling activity. While our study supports that trawling has not impacted the rhodolith bed in the Core Habitat within the cables exclusion zone, the composition of Adjacent Habitat cannot be attributed solely to anthropogenic impacts. This recognition is important, considering that high small-scale heterogeneity within rhodolith beds (de Juan et al. 2023) may not exclusively result from fishing pressure (Jardim et al. 2022). Natural environmental factors such as depth, sediment grain size, bottom geomorphology and bottom currents (Illa-López et al. 2023; Pérez-Peris et al. 2023) can influence the density, dimensions and composition of rhodolith beds, independent of human intervention (Peña et al. 2014; Veras et al. 2020).

The morphological complexity of the rhodolith is a key driver for the high faunistic and floristic diversity of rhodolith beds (Fredericq et al. 2019; Gabara et al. 2018; Teichert 2014). Our results also support the idea proposed by Jardim et al. (2022) for using the rhodolith interstitial space (or solidity as equivalent indicator) as proxy for habitat complexity. The high correlation identified between 2 and 3D metrics for morphotype A demonstrates that 2D metrics may yield useful indicators that are faster to obtain and potentially effective to be incorporated in the routine monitoring of rhodolith beds. 3D measurements resulted to be time-consuming and can be estimated to a good approximation through 2D metrics if 2D to 3D conversions have been estimated previously. Moreover, we recommend using the linear relations between measures as a method to rapidly obtain a total photosynthetic surface. This measure is important for calculating the photosynthesis rates for the branched growth forms, as well as to obtain the rhodolith volume and quantify the calcium carbonate production (Dulin et al. 2020). Similar conclusions were reached by House et al. (2018) comparing 2D and 3D metrics across different morphologies of scleractinian corals: although 3D metrics of surface area and volume are more precise, 2D metrics scaled consistently with 3D metrics in corals, providing convenient and fast measurements of ecological function.

The study of algal physiology commonly uses dry weight to standardize indicators such as biomass of epiphytes by unit mass of rhodoliths or to estimate respiration and production (photosynthesis). However, in multi-specific rhodolith beds, as in our case study, it is often difficult to individualize different morphologies (as shown in the results of the discriminant analysis). Individual weight may vary among morphologies, for the same longitudinal size, and even within individuals of the same morphology because of the weight of organisms forming the nucleus of some rhodoliths (bryozoans, polychaetes, some boring organisms) (see an example in Fig. 10) (Pérez-Peris et al. 2023). For these reasons, we propose using the area corresponding to the thallus surface in 3D as a more realistic measurement to estimate metabolic rates or to standardize cryptofaunal abundance. Rhodolith volume is an important measure related to carbon retention and is a metric that can only be obtained with sufficient precision with 3D measurements. Simple methods based on the equation of an ellipsoid (Teichert 2014) or water displacement (Amado-Filho et al. 2007) have low precision and limited general application.

In conclusion, the intricate morphological diversity observed between and within rhodolith species, their role as habitat for benthic organisms, coupled with their potential significant role as carbon reservoirs, make them suitable candidates for biomonitoring the environmental condition of deep biogenic habitats. Key measures of morphological complexity, as well as assessing parameters such as photosynthetic surface and carbonate volume, could be valuable indicators of the rhodolith bed condition. This research contributes to our comprehensive understanding of how the structural complexity of rhodoliths enhances ecosystem functioning, emphasizing the ongoing importance of advancing our knowledge and developing additional morphological indicators for these ecologically valuable species.

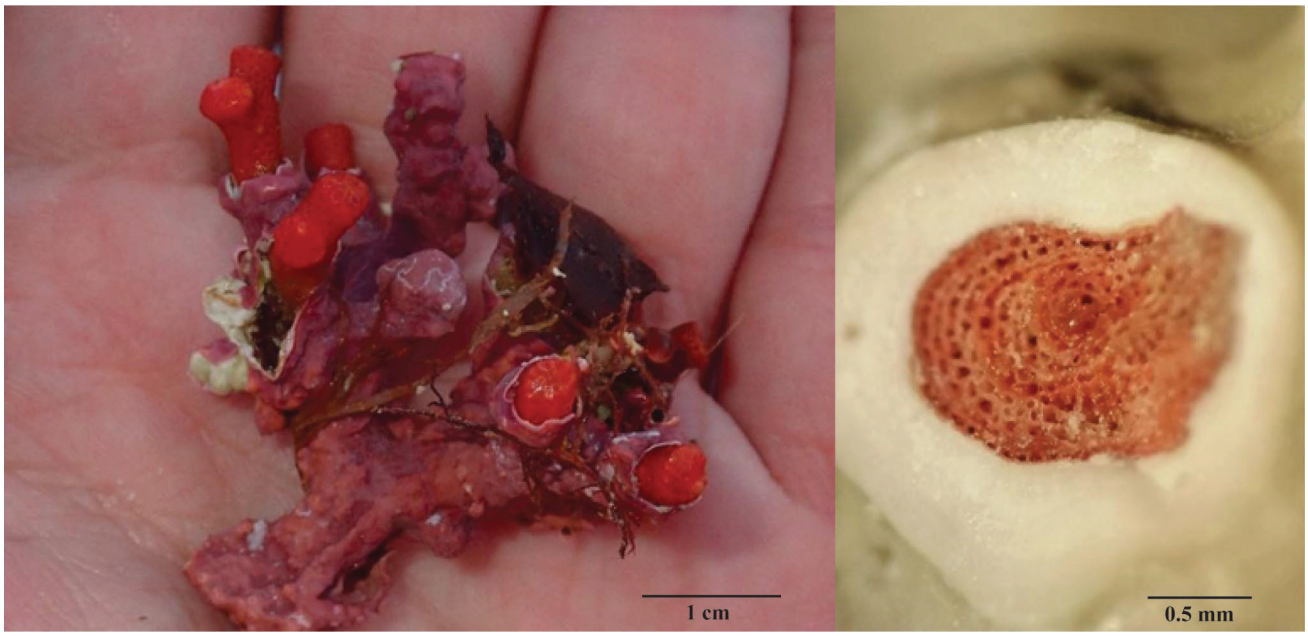


Fig. 10 (Left) Red calcareous algae growing and completely covering a bryozoan. (Right) broken branch of a rhodolith from morphology A, with a bryozoan found inside

Supplementary Information The online version contains supplementary material available at https://doi.org/10.1007/s00227-024-04437-y.

Acknowledgements The authors are very thankful to Laia Illa-López and Géraldine Pérez for their backup during the field sampling and classification and also to Julia Castro for her support in creating the 3D digital twins of the rhodoliths. This work is developed on the framework of the EU H2020 project "MaCoBioS" (contract no. 869710). This work contributes to the ICM's 'Center of Excellence' Severo Ochoa (CEX2019-000928-5) and to the 'Maria de Maeztu' accredited to the IMEDEA (CEX2021-001198). **SdJ** was supported by a Ramón y Cajal postdoctoral grant funded by the Ministry of Science and Innovation (Plan Estatal I+D+I, 2017- 2020; grant no. RyC2020-029062-I). **AC** is enrolled in the PhD program in Marine Sciences at the University of Barcelona.

Author contributions **AC:** conceptualization, methodology, formal analysis, writing—original draft, writing—review and editing, visualization. **SdJ:** conceptualization, writing—review and editing. **HH:** conceptualization, writing—review and editing. **FM:** conceptualization, methodology, formal analysis, writing—original draft, writing—review and editing, funding acquisition.

Funding Open Access funding provided thanks to the CRUE-CSIC agreement with Springer Nature.

Data availability Data will be made available on request.

Declarations

Conflict of interest The authors declare no conflict of interest.

Open Access This article is licensed under a Creative Commons Attribution 4.0 International License, which permits use, sharing, adaptation, distribution and reproduction in any medium or format, as long as you give appropriate credit to the original author(s) and the source, provide a link to the Creative Commons licence, and indicate if changes were made. The images or other third party material in this article are included in the article's Creative Commons licence, unless indicated otherwise in a credit line to the material. If material is not included in the article's Creative Commons licence and your intended use is not permitted by statutory regulation or exceeds the permitted use, you will need to obtain permission directly from the copyright holder. To view a copy of this licence, visit http://creativecommons.org/licenses/by/4.0/.

References

Amado-Filho GM, Maneveldt G, Manso RCC, Marins-Rosa BV, Pacheco MR, Guimarães SMPB (2007) Structure of rhodolith beds from 4 to 55 meters deep along the southern coast of Espírito Santo State, Brazil. Cienc Mar 33(4):399–410. https://doi.org/10.7773/cm.v33i4.1148

Amado-Filho GM, Bahia RG, Pereira-Filho GH, Longo LL (2017) South Atlantic Rhodolith Beds: latitudinal distribution, species composition, structure and ecosystem functions, threats and conservation status. Chapter 12. In: Risonema-Rodríguez R, Nelson W, Aguirre J (eds) Rhodolith/Maërl Beds: a global perspective. Coastal Research Library, Springer International, Cham, pp 299–317. https://doi.org/10.1007/978-3-319-29315-8_12

Ballesteros E (1988) Composición y estructura de los fondos de maërl de Tossa de Mar (Gerona, España). Collect Bot (barcelona) 17(2):161–182. https://doi.org/10.3989/collectbot.1989.v17.137

Barberá C, Moranta J, Ordines F, Ramón M, de Mesa A, Díaz-Valdés M, Grau AM, Massutí E (2012a) Biodiversity and habitat mapping of Menorca Channel (Western Mediterranean): implications for conservation. Biodivers Conserv 21(3):701–728. https://doi.org/10.1007/s10531-011-0210-1

Barberá C, Comalada N, Joher S, Valls-Mir M, Díaz-Valdés M, Moranta J (2012b) Analysis of morphological characteristics

of rhodoliths as indicator of habitat complexity and fishing effects. XVII Simposio Ibérico de Estudios de Biología Marina (11/09/2012-14/09/2012, Donosti, Spain). Revista de Investigación Marina 19(6):346. http://hdl.handle.net/10261/324037

Basso D, Babbini L, Kaleb S, Bracchi VA, Falace A (2016) Monitoring deep mediterranean rhodolith beds. Aquat Conserv Mar Freshw Ecosyst 26(3):549–561. https://doi.org/10.1002/aqc.2586

Basso D, Lorenza B, Ramos-Esplá AA, Salomidi M (2017) Mediterranean Rhodolith Beds. In: Risonema-Rodríguez R, Nelson W, Aguirre J (eds) Rhodolith/Maërl Beds: a global perspective. Coastal Research Library, vol 15. Springer, Cham, pp 281–298. https://doi.org/10.1007/978-3-319-29315-8_11

Bernard G, Romero-Ramirez A, Tauran A, Pantalos M, Deflandre B, Grall J, Grémare A (2019) Declining Maerl vitality and habitat complexity across a dredging gradient: insights from in situ sediment profile imagery (SPI). Sci Rep 9(1):16463. https://doi.org/10.1038/s41598-019-52586-8

Blake C, Maggs C, Reimer P (2007) Use of radiocarbon dating to interpret past environments of maerl beds. Cienc Mar 33(4):385–397. https://doi.org/10.7773/cm.v33i4.1187

Bordehore C, Ramos-Esplá AA, Riosmena-Rodríguez R (2003) Comparative study of two maerl beds with different otter trawling history, Southeast Iberian Peninsula. Aquat Conserv Mar Freshw Ecosyst 13:S43–S54. https://doi.org/10.1002/aqc.567

Bosence DWJ (1983) Description and classification of rhodoliths (Rhodoids, Rhodolites). In: Peryt TM (ed) Coated grains. Springer, Berlin, Heidelberg. https://doi.org/10.1007/978-3-642-68869-0_19

Boyé A, Thiébaut E, Grall J, Legendre P, Broudin C, Houbin C, Le Garrec V, Maguer M, Droual G, Gauthier O (2019) Trait-based approach to monitoring marine benthic data along 500 km of coastline. Divers Distrib 25(12):1879–1896. https://doi.org/10.1111/ddi.12987

Bracchi VA, Basso D (2012) The contribution of calcareous algae to the biogenic carbonates of the continental shelf: Pontian Islands, Tyrrhenian Sea, Italy. Geodiversitas 34:61–77. https://doi.org/10.5252/g2012n1a4

Bracchi VA, Caronni S, Meroni AN, Gottfried-Burguett E, Atzori F, Cadoni N, Marchese F, Basso D (2022) Morphostructural characterization of the heterogeneous rhodolith bed at the marine protected area 'Capo Carbonara' (Italy) and hydrodynamics. Diversity 14(1):51. https://doi.org/10.3390/d14010051

Cabanellas-Reboredo M, Mallol S, Barberá C, Vergés A, Díaz D, Goñi R (2017) Morpho-demographic traits of two maërl-forming algae in beds with different depths and fishing histories. Aquat Conserv Mar Freshw Ecosyst 1:13. https://doi.org/10.1002/aqc.2827

Carvalho VF, Assis J, Serrão EA, Nunes JM, Anderson AB, Batista MB, Barufi JB, Silva J, Pereira SMB, Horta PA (2020) Environmental drivers of rhodolith beds and epiphytes community along the South Western Atlantic Coast. Mar Environ Res 154:104827. https://doi.org/10.1016/j.marenvres.2019.104827

da Silva AR (2021) biotools: Tools for biometry and applied statistics in agricultural science. R package version 4.2. https://cran.r-project.org/package=biotools

de Juan S, Lo Iacono C, Demestre M (2013) Benthic habitat characterisation of soft-bottom continental shelves: integration of acoustic surveys, benthic samples and trawling disturbance intensity. Estuar Coast Shelf Sci 117:199–209. https://doi.org/10.1016/j.ecss.2012.11.012

de Juan S, Ospina-Alvarez A, Hinz H, Moranta J, Barberá C (2023) The continental shelf seascape: a network of species and habitats. Biodivers Conserv 32:1271–1290. https://doi.org/10.1007/s10531-023-02552-8

del Río J, Ramos DA, Sánchez-Tocino L, Peñas J, Braga JC (2022) The Punta de La Mona Rhodolith Bed: shallow-water Mediterranean Rhodoliths (Almuñecar, Granada, Southern Spain). Front Earth Sci 10:884685. https://doi.org/10.3389/feart.2022.884685

Dulin T, Avnaim-Katav S, Sisma-Ventura G, Bialik OM, Angel DL (2020) Rhodolith Beds along the Southeastern Mediterranean inner shelf: implications for past depositional environments. J Mar Syst 201:103241. https://doi.org/10.1016/j.jmarsys.2019.103241

European Parliament (1992) Council directive 1992/43/EC conservation of natural habitats and of wild fauna and flora. Off J Eur Union L206:7–50

Farriols MT, Irlinger C, Ordines F, Palomino D, Marco-Herrero E, Soto-Navarro J, Jordà G, Mallol S, Díaz D, Martínez-Carreño N, Díaz JA, Fernandez-Arcaya U, Joher S, Ramírez-Amaro S, de la Ballina NR, Vázquez JT, Massutí E (2022) Recovery signals of rhodoliths beds since bottom trawling ban in the SCI Menorca Channel (Western Mediterranean). Diversity 14(1):20. https://doi.org/10.3390/d14010020

Fedorov A, Beichel R, Kalpathy-Cramer J, Finet J, Fillion-Robin JC, Pujol S, Bauer C, Jennings D, Fennessy FM, Sonka M, Buatti J, Aylward SR, Miller JV, Pieper S, Kikinis R (2012) 3D Slicer as an image computing platform for the quantitative imaging network. Magn Reson Imaging 30(9):1323–1341. https://doi.org/10.1016/j.mri.2012.05.001

Figueiredo MAO, Santos de Menezes K, Costa-Paiva EM, Paiva PC, Ventura CRR (2007) Experimental evaluation of rhodoliths as living substrata for infauna at the Abrolhos Bank. Brazil Ciencias Marinas 33(4):427–440. https://doi.org/10.7773/cm.v33i4.1221

Fredericq S, Krayesky-Self S, Sauvage T, Richards J, Kittle R, Arakaki N, Hickerson E, Schmidt WE (2019) The critical importance of rhodoliths in the life cycle completion of both macro- and microalgae, and as holobionts for the establishment and maintenance of marine biodiversity. Front Mar Sci 5:502. https://doi.org/10.3389/fmars.2018.00502

Foster MS, McConnico LM, Lundsten L, Wadsworth T, Kimball T, Brooks L, Medina-López M, Riosmena-Rodriguez R, Hernández-Carmona G, Vásquez-Elizondo RM, Johnson S, Steller DL (2007) Diversity and natural history of a Lithothamnion Muelleri-Sargassum Horridum community in the Gulf of California. Cienc Mar 33:367–384. https://doi.org/10.7773/cm.v33i4.1174

Gabara SS, Hamilton L, Edwards MS, Steller DL (2018) Rhodolith structural loss decreases abundance, diversity, and stability of benthic communities at Santa Catalina Island, CA. Mar Ecol Prog Ser 595:71–88. https://doi.org/10.3354/meps12528

Gagnon P, Matheson K, Stapleton M (2012) Variation in rhodolith morphology and biogenic potential of newly discovered rhodolith beds in Newfoundland and Labrador (Canada). Bot Mar 55(1):85–99. https://doi.org/10.1515/bot-2011-0064

Hinz H, Prieto V, Kaiser MJ (2009) Trawl disturbance on benthic communities: chronic effects and experimental predictions. Ecol Appl 19(3):761–773. https://doi.org/10.1890/08-0351.1

House JE, Brambilla V, Bidaut LM, Christie AP, Pizarro O, Madin JS, Dornelas M (2018) Moving to 3D: relationships between coral planar area, surface area and volume. PeerJ 6:e4280. https://doi.org/10.7717/peerj.4280

Illa-López L, Cabrito A, de Juan S, Maynou F, Demestre M (2023) Distribution of rhodolith beds and their functional biodiversity characterisation using ROV images in the Western Mediterranean Sea. Sci Total Environ 905:167270. https://doi.org/10.1016/j.scitotenv.2023.167270

Ingrassia M, Pierdomenico M, Casalbore D, Falese FG, Chiocci FL (2023) A review of rhodolith/maerl beds of the Italian Seas. Diversity 15(7):859. https://doi.org/10.3390/d15070859

Jardim VL, Gauthier O, Toumi C, Grall J (2022) Quantifying maerl (Rhodolith) habitat complexity along an environmental gradient at regional scale in the Northeast Atlantic. Mar Environ Res 181:105768. https://doi.org/10.1016/j.marenvres.2022.105768

Kamenos NA, Geoffrey Moore P, Hall-Spencer JM (2004) Nursery-area function of maerl grounds for Juvenile Queen Scallops Aequipecten Opercularis and other invertebrates. Mar Ecol Prog Ser 274:183–189. https://doi.org/10.3354/meps274183

Kleiber C, Zeileis A (2022) AER: applied econometrics with R. R package version 1.2-10. https://CRAN.R-project.org/package=AER

Kooijman SALM (2010) Dynamic energy budget theory for metabolic organisation. Cambridge University Press, Cambridge

Korkmaz S, Goksuluk D, Zararsiz G (2014) MVN: an R package for assessing multivariate normality. R J 6(2):151. https://doi.org/10.32614/RJ-2014-031

Lindeboom HJ (1995) Protected areas in the North Sea: an absolute need for future marine research. Helgoländer Meeresuntersuchungen 49(1):591–602. https://doi.org/10.1007/BF02368384

Massutí E, Sánchez-Guillamón O, Farriols MT, Palomino D, Frank A, Bárcenas P, Rincón B, Martínez-Carreño N, Keller S, López-Rodríguez C, Díaz JA, López-González N, Marco-Herrero E, Fernandez-Arcaya U, Valls M, Ramírez-Amaro S, Ferragut F, Joher S, Ordinas F, Vázquez JT (2022) Improving scientific knowledge of Mallorca channel seamounts (Western Mediterranean) within the framework of Natura 2000 network. Diversity 14(1):4. https://doi.org/10.3390/d14010004

Meihoub-Berlandi R, Figueiredo MAO, Paiva PC (2012) Rhodolith morphology and the diversity of polychaetes off the Southeastern Brazilian Coast. J Coastal Res 28(1):280–287. https://doi.org/10.2112/11T-00002.1

Méndez Trejo MDC, Neill KF, Twist BA, Nelson WA (2021) Cryptofauna associated with rhodoliths: diversity is species-specific and influenced by habitat. Mar Ecol 42:12647. https://doi.org/10.1111/maec.12647

Moranta J, Barberá C, Druet Vélez M, Díaz-Valdés M, Zaragoza N, Tello-Antón MO, López-Jurado JL, Balbín R, Flexas MDM, Fernández M, Hidalgo M, Domínguez M, Quetglas A, Goñi R, Mallol S, Sánchez-Delgado F, Ambroso S, Comalada N (2014) Caracterización ecológica de la plataforma continental (50–100 m) del canal de Menorca. Informe final área LIFE+ INDEMARES (LIFE07/NAT/E/000732). Instituto Español de Oceanografía-Centro Oceanográfico de Baleares (Palma). Coordinación: Fundación Biodiversidad, Palma, p 504. http://hdl.handle.net/10261/318214

Nelson WA (2009) Calcified macroalgae—critical to coastal ecosystems and vulnerable to change: a review. Mar Freshw Res 60(8):787–801. https://doi.org/10.1071/MF08335

Oksanen J, Simpson G, Blanchet F, Kindt R, Legendre P, Minchin P, O'Hara R, Solymos P, Stevens M, Szoecs E, Wagner H, Barbour M, Bedward M, Bolker B, Borcard D, Carvalho G, Chirico M, De Caceres M, Durand S, Evangelista H, FitzJohn R, Friendly M, Furneaux B, Hannigan G, Hill M, Lahti L, McGlinn D, Ouellette M, Ribeiro Cunha E, Smith T, Stier A, Ter Braak C, Weedon J (2022) vegan: Community Ecology Package. R package version 2.6-4. https://CRAN.R-project.org/package=vegan

Peña V, Bárbara I, Grall J, Maggs CA, Hall-Spencer JM (2014) The diversity of seaweeds on maerl in the NE Atlantic. Mar Biodiv 44(4):533–551. https://doi.org/10.1007/s12526-014-0214-7

Pérez-Peris I, Navarro-Mayoral S, de Esteban MC, Tuya F, Peña V, Barbara I, Neves P, Ribeiro C, Abreu A, Grall J, Espino F, Echedey Bosch N, Haroun R, Otero-Ferrer F (2023) Effect of depth across a latitudinal gradient in the structure of rhodolith seabeds and associated biota across the Eastern Atlantic Ocean. Diversity 15(1):103. https://doi.org/10.3390/d15010103

Phillips J (2023) The lives of seaweeds: a natural history of our planet's seaweeds and other algae. Princeton University Press, Princeton, NJ. ISBN: 9780691230177

Puig P, Martín J, Masqué P, Palanques A (2015) Increasing sediment accumulation rates in La Fonera (Palamós) submarine canyon axis and their relationship with bottom trawling activities. Geophys Res Lett 42:8106–8113. https://doi.org/10.1002/2015GL065052

R Core Team (2022) R: a language and environment for statistical computing. R Foundation for Statistical Computing, Vienna, Austria. https://www.R-project.org/

Rendina F, Kaleb S, Caragnano A, Ferrigno F, Appolloni L, Donnarumma L, Fulvio Russo G, Sandulli R, Roviello V, Falace A (2020) Distribution and characterization of deep rhodolith beds off the Campania Coast (SW Italy, Mediterranean Sea). Plants 9(8):985. https://doi.org/10.3390/plants9080985

Riosmena-Rodríguez R, Nelson W, Aguirre J (2017) Rhodolith/Maërl beds: a global perspective, vol 15. Springer International, Cham. https://doi.org/10.1007/978-3-319-29315-8

Schneider CA, Rasband WS, Eliceiri KW (2012) NIH Image to ImageJ: 25 years of image analysis. Nat Methods 9:671–675. https://doi.org/10.1038/nmeth.2089

Steller DL, Riosmena-Rodríguez R, Foster MS, Roberts CA (2003) Rhodolith bed diversity in the Gulf of California: the importance of rhodolith structure and consequences of disturbance. Aquat Conserv Mar Freshw Ecosyst 13:S5–S20. https://doi.org/10.1002/aqc.564

Stelzer PS, Mazzuco ACA, Gomes LE, Martins J, Netto S, Bernardino AF (2021) Taxonomic and functional diversity of benthic macrofauna associated with rhodolith beds in SE Brazil. PeerJ 9:11903. https://doi.org/10.7717/peerj.11903

Tauran A, Dubreuil J, Guyonnet B, Grall J (2020) Impact of fishing gears and fishing intensities on maerl beds: an experimental approach. J Exp Mar Biol Ecol 533:151472. https://doi.org/10.1016/j.jembe.2020.151472

Teichert S (2014) Hollow rhodoliths increase Svalbard's Shelf biodiversity. Sci Rep 4(1):6972. https://doi.org/10.1038/srep06972

Venables WN, Ripley BD (2002) Modern applied statistics with S, 4th edn. Springer, New York. ISBN 0-387-95457-0. https://www.stats.ox.ac.uk/pub/MASS4/

Veras PC, Pierozzi-Jr I, Lino JB, Amado-Filho GM, Senna AR, Santos CSG, Moura RL, Passos FD, Giglio VJ, Pereira-Filho GH (2020) Drivers of biodiversity associated with rhodolith beds from euphotic and mesophotic zones: insights for management and conservation. Perspect Ecol Conserv 18(1):37–43. https://doi.org/10.1016/j.pecon.2019.12.003

Wei T, Simko V (2021) R package 'corrplot': visualization of a correlation matrix. (Version 0.92). https://github.com/taiyun/corrplot

Publisher's Note Springer Nature remains neutral with regard to jurisdictional claims in published maps and institutional affiliations.

Aquatic Botany 197 (2025) 103839

Contents lists available at ScienceDirect

Aquatic Botany

journal homepage: www.elsevier.com/locate/aquabot

Neotypification of the *Sporolithon mediterraneum* Heydrich (Sporolithales, Corallinophycidae, Rhodophyta) and the status of *Sporolithon* in the Mediterranean Sea

Andrea Cabrito [a,b,*], Sara Kaleb [c], Viviana Peña [d], Annalisa Falace [c]

[a] Institut de Ciències del Mar (ICM-CSIC), Passeig Marítim de la Barceloneta 37-49, Barcelona, Spain
[b] Facultat de Ciències de la Terra, Universitat de Barcelona, Barcelona, Spain
[c] Department Life Sciences, University of Trieste, Via Licio Giorgieri 10, Trieste 34127, Italy
[d] BioCost Research Group, Faculty of Sciences, University of A Coruña, rúa da Fraga 10, A Coruña 15008, Spain

ARTICLE INFO

Keywords:
Coralline algae
Taxonomy
Morpho-anatomy
*psb*A, *rbc*L
Rhodoliths

ABSTRACT

A neotype specimen is designated for the coralline alga *Sporolithon mediterraneum* Heydrich (Sporolithales, Corallinophycidae, Rhodophyta) and critically examined here, since the original holotype specimen apparently has been destroyed. The neotype specimen was collected in a mesophotic rhodolith bed near Gorgona Island (Tyrrhenian Sea, Mediterranean). Additional specimens were collected in a rhodolith bed in the Menorca Channel (Western Mediterranean) and were used to confirm the identification of the neotype. Molecular analyses of *psb*A and *rbc*L with all *Sporolithon* species for which there are currently sequence data, including *S. ptychoides* and *S. molle* supported the designation of this neotype and the circumscription of this Mediterranean species. Additional specimens from Menorca Channel were resolved as conspecific based on *psb*A sequences. The morpho-anatomical data presented indicated that *S. mediterraneum* can be also distinguished from the type species *Sporolithon ptychoides* Heydrich and *Sporolithon molle* (Heydrich) Heydrich, the only two other species previously reported from the Mediterranean Sea, by the occurrence of 5–6 cell paraphyses and larger stalk cells. A consideration of the status of *Sporolithon* in the Mediterranean region is also discussed.

1. Introduction

Coralline algae of the genus *Sporolithon* Heydrich (Sporolithales, Corallinophycidae, Rhodophyta) are distributed worldwide, from shallow (1–1.5 m deep) (Basso et al., 2009; Richards et al., 2017) to the lower end of the mesophotic zone (178 m) (Richards et al., 2018). As ecosystem engineers, *Sporolithon* spp. play an important ecological role by contributing to the formation of structurally complex and species-rich marine habitats (i.e, coral reefs, rhodolith beds) (Basso et al., 2009; Richards et al., 2017, 2022, 2018; Littler, 1973; Keats and Chamberlain, 1993; Farr et al., 2009; Amado-Filho et al., 2012; Maneveldt et al., 2017; Fredericq et al., 2019; Leão et al., 2020; Gabrielson et al., 2023). Recent studies have shown that *Sporolithon* species may also play a critical role in the completion of the life cycle of macro- and microalgae (Fredericq et al., 2019) and in the settlement of coral larvae (Abdul Wahab et al., 2023).

Due to the cryptic diversity of these taxa, it has been emphasized that morpho-anatomical analyses must be combined with DNA sequencing techniques to correctly identify *Sporolithon* species, including type material (Richards et al., 2017, 2022; Gabrielson et al., 2023).

Currently, 31 species of *Sporolithon* are taxonomically recognized (Gabrielson et al., 2023; Guiry and Guiry, 2024), of which only three have been identified in the Mediterranean region, based on morpho-anatomical characters alone, namely *Sporolithon molle* (Heydrich) Heydrich (Di and Giaccone, 1994), *Sporolithon mediterraneum* Heydrich (Heydrich, 1899; Lemoine, 1939) as *Archaeolithothamnion mediterraneum* (Heydrich) Foslie; (Hamel and Lemoine, 1953) as *A. mediterraneum,* (Giaccone et al., 1985)) and the type species *Sporolithon ptychoides* Heydrich (Alongi et al., 1996; Bressan and Babbini, 2003; Cormaci et al., 2017).

Based on a critical evaluation of the literature data, Alongi (Alongi et al., 1996) and Cormaci (Cormaci et al., 2017) considered *S. molle* as a *taxon excludendum* and *S. mediterraneum* as conspecific with *S. ptychoides*, the latter being the only Mediterranean species of this

* Corresponding author at: Institut de Ciències del Mar (ICM-CSIC), Passeig Marítim de la Barceloneta 37-49, Barcelona, Spain.
E-mail address: cabrito@icm.csic.es (A. Cabrito).

https://doi.org/10.1016/j.aquabot.2024.103839
Received 10 June 2024; Received in revised form 31 October 2024; Accepted 22 November 2024
Available online 30 November 2024
0304-3770/© 2024 The Authors. Published by Elsevier B.V. This is an open access article under the CC BY-NC-ND license (http://creativecommons.org/licenses/by-nc-nd/4.0/).

genus. Instead, Guiry and Guiry (Guiry and Guiry, 2024), following Athanasiadis (Athanasiadis, 2016), treat *S. mediterraneum* as a distinct species.

Sporolithon mediterraneum was described by Heydrich (Heydrich, 1899) (pag. 227) based on a specimen reportedly collected by Dr. Francotte in the Gulf of Naples (Italy, Tyrrhenian Sea, Mediterranean Sea). The type specimen described by Heydrich has been destroyed and it is noteworthy that, according to Hamel and Lemoine (Hamel and Lemoine, 1953) (pag.76), it was actually dredged by Dr. Schleicher in the Gulf of Villefranche (Alongi et al., 1996). Moreover, the specimen collected from the Balearic islands, and described as *A. mediterraneum* by Lemoine (Lemoine, 1939) and Hamel and Lemoine (Hamel and Lemoine, 1953), does not correspond to the genus *Sporolithon* according to the observations of Alongi (Alongi et al., 1996).

Richards (Richards et al., 2017), based on comparative analyses of DNA sequences from *Sporolithon* type specimens showed that DNA sequences of specimens called *S. ptychoides* from other parts of the world (Brazil, Hawaii, New Caledonia) did not match the lectotype sequence of *S. ptychoides* described from El Tor, Gulf of Suez. In addition, these authors hypothesized that specimens from the Mediterranean Sea that are designated as *S. ptychoides* based on morpho-anatomy are likely a different species. Similarly, based on the lectotype sequence of *S. molle* from El Tor, Gulf of Suez, Gabrielson (Gabrielson et al., 2023) confirmed an additional record for Mozambique (Juan de Nova Island) and the misapplication of this name for Brazilian collection.

Herein, based on DNA sequences and morpho-anatomical data, a specimen from a mesophotic rhodolith bed of the Tyrrhenian Sea is described and designated as the neotype of *Sporolithon mediterraneum* since it agrees with the original description by Heydrich (Heydrich, 1899). This neotype is also compared with conspecific specimens collected in a rhodolith bed in the Menorca Channel (Western Mediterranean) (Fig. S1). Finally, the status of *Sporolithon* in the Mediterranean is discussed.

2. Materials and methods

2.1. Examined specimens

Collections from mesophotic rhodolith beds were conducted in the Tyrrhenian Sea and Menorca Channel, Mediterranean Sea, in 2018 and 2022 by scuba diving or naturalist dredge, between 50 and 75 m depth. Ten specimens identified as *Sporolithon* were carefully measured, photographed and subsequently air-dried and preserved in zip bags with silica gel for morpho-anatomical and molecular analyses.

2.2. Morpho-anatomical analyses

For the Tyrrhenian neotype specimen (TSB_SPR MDT 1a, the herbarium acronym follows the Index Herbariorum online, continuously updated (Thiers, 2024)), scanning electron microscopy was performed with a Zeiss Gemini300 Scanning Electron Microscope (SEM) at a working distance (WD) between 8 and 11 mm. Rhodolith fragments were mounted on aluminium stubs and coated with a thin chromium layer using Quorum Q150T ES coater. For the specimens collected in the Menorca Channel (Fig. S1), scanning electron microscopy was performed using the microscopes JSM 6400 (Jeol, Japan) and Hitachi S-3500N (Hitachi High-Technologies Co., Japan) at a WD of 14 mm. Rhodolith fragments were mounted on both carbon and aluminium stubs using carbon tape as adhesive and were coated with a 15 nm gold layer using Quorum Q150R S sputter coater (Quorum Technologies Ltd.). Cell size was measured using SEM micrographs according to Irvine and Chamberlain (Irvine and Chamberlain, 1994). Twenty cells of each vegetative cell type (epithallial, perithallial and hypothallial) were measured in the Gorgona specimen and in five of the nine Menorca Channel individuals. For the reproductive features (sporangial chamber, talk cells) and for the paraphyses, the measurements were made on 2–8 sporangial compartments per specimen. Samples used for light microscopy were decalcified in 10 % nitric acid, and cryostatic frozen sections were prepared with a cryomicrotome (Leica CM3050 S).

2.3. DNA sequencing and analyses

A fragment of each preserved specimen was cleaned under a stereomicroscope and selected surfaces were ground for DNA extraction. Genomic DNA was extracted using a NucleoSpin® Tissue kit (Macherey-Nagel, GmbH and Co. KG, Germany), following the manufacturer's protocol. The *psb*A locus was PCR-amplified for all specimens by using the primer pair *psb*A-F1/*psb*A-R1 (Yoon et al., 2002) and the Supreme NZYTaq II 2x Colourless Master Mix (NZYtech) following the thermal profile for PCR reactions used by Peña (Peña et al., 2015). The *rbc*L sequence of the specimen of the Tyrrhenian Sea was obtained with the primer combination F1150Cor - RbcS-Start yielding a fragment trimmed to 293 bp (1172–1464) and followed Saunders and Moore (Saunders and Moore, 2013) for amplification. PCR products were purified and sequenced by the Sanger method by GenoScreen (GenoScreen Innovative Genomics, France) and by the molecular biology service of Universidade da Coruña (Spain). Sequences were assembled, aligned and trimmed using MEGA v.6 (Tamura et al., 2013) or SeaView version 4 (Gouy et al., 2010), and were submitted to GenBank (accession numbers listed in Table S1). Two data sets were built for each for gene (*psb*A, *rbc*L), comprising sequences obtained in this study and GenBank sequences publicly available for *Sporolithon* species. The Rhodogorgonales taxa *Rhodogorgon carriebowensis* J.N. Norris and Bucher, 1989 (Norris and Bucher, 1989), *R. ramosissima* J.N. Norris and Bucher, 1989 (Norris and Bucher, 1989) and *Renouxia marerubra* D.Gabriel, J.N. Norris & Fredericq 2019 (Gabriel et al., 2019) were used as outgroup (Table S1).

Phylogenetic relationships were inferred with maximum likelihood (ML) using IQ-TREE v2.2.0 (Nguyen et al., 2015) or MEGA v.6 software (Tamura et al., 2013). Bayesian Inference (BI) was obtained using MrBayes v3.2.7a (Ronquist et al., 2012). Models of sequence evolution were estimated using the Akaike Information Criterion (AIC) and the Bayesian Information Criterion (BIC) obtained in jModeltest 2.1.3 (Darriba et al., 2012) and with ModelFinder in PhyloSuite (Zhang et al., 2020). ML of the *psb*A alignment was performed under a generalized time-reversible GTR+F model for 1000 standard bootstraps. BI for the *psb*A alignments were performed under a generalized time-reversible GTR+F model (two parallel runs, with four Markov Chain Monte Carlo method for two million generations), in which the initial 20 % of sampled data were discarded as burn-in. Both ML and BI analysis of *psb*A were performed using PhyloSuite software (Zhang et al., 2020; Xiang et al., 2023). The resulting trees were visualized and edited by Interactive Tree Of Life (iTOL) v5 (Letunic and Bork, 2024) online tool. For the *rbc*L alignment, ML was performed under a generalized time-reversible with invariant sites heterogeneity model (GTR+I+G); BI was performed under the same model (GTR+I+G) with four Markov Chain Monte Carlo method for 10 million generations, and tree sampling every 1000 generations.

3. Results

The *psb*A alignment of 29 sequences, ranged from 508 to 862 base pairs (bp), and consisted of 22 haplotype sequences with 251 variable sites and 186 parsimonious informative sites. The uncorrected p-distance within the Mediterranean specimens was among 0 – 0.6 %. Both ML and BI of *psb*A data were congruent in resolving the Mediterranean specimens as conspecific, and as an independent lineage from other *Sporolithon* species (Fig. 1). Both ML and BI analysis resolved the Mediterranean *Sporolithon* in a clade encompassing *S. howei, S. franciscanum, S. crypticum* and *S. eltorense*.

The *rbc*L alignment comprised 35 sequences, ranging from 260 to 297 bp, with 114 variable sites. Both ML and BI resolved the Mediterranean *Sporolithon* as a separate lineage from remaining *Sporolithon,*

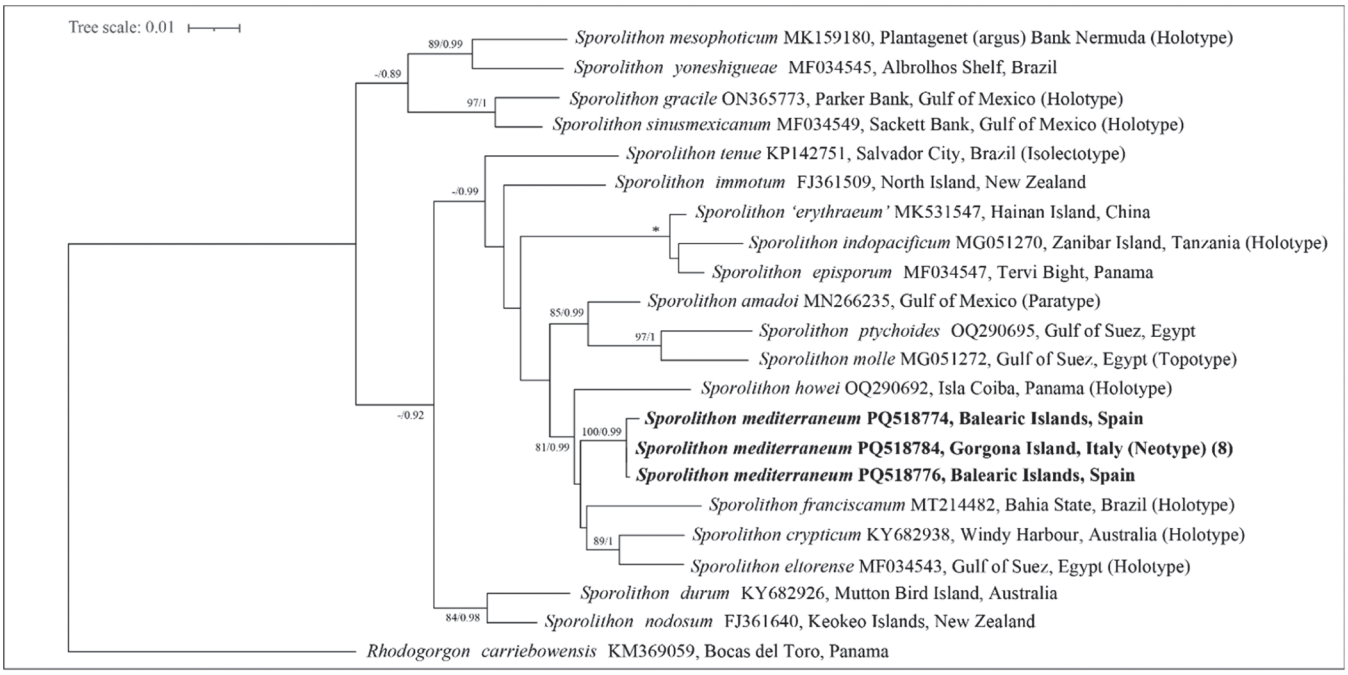


Fig. 1. *Phylogenetic tree inferred from ML and BI analyses of* psb*A sequences of* Sporolithon*. In bold, the neotype of* Sporolithon mediterraneum representing a group of eight individuals sharing the same haplotype and two other haplotypes from Menorca Channel. Bootstrap ML values > 75 % and posterior probabilities > 0.70 from BI are shown for each node. Rhodogorgon carriebowensis was used as outgroup. Specific epithets of names not linked to type specimen are in single quotes.

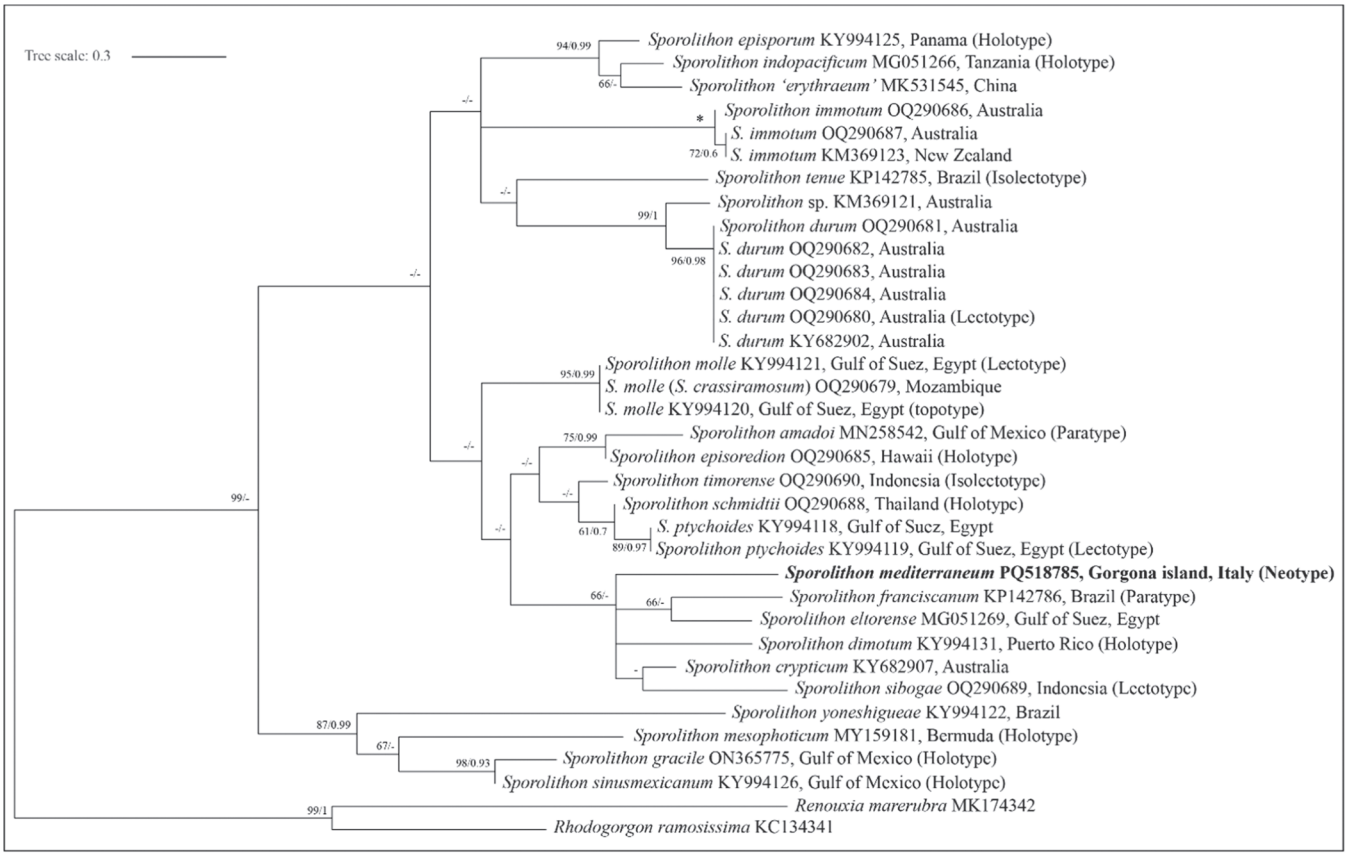


Fig. 2. *Phylogenetic tree inferred from ML and BI analyses of* rbc*L sequences of* Sporolithon*. In bold, the neotype of* Sporolithon mediterraneum. Bootstrap ML values > 60 % and posterior probabilities > 0.60 from BI are shown for each node. Renouxia marerubra and Rhodogorgon ramosissima were used as outgroup. Specific epithets of names not linked to type specimen are in single quotes.

most of them represented by type specimens, including *S. ptychoides* and *S. molle* both described originally from El Tor, Gulf of Suez, and reported for the Mediterranean based on morpho-anatomical characters. The sequenced Mediterranean species is resolved in a clade containing *S. franciscanum, S. eltorense, S. dimotum, S. crypticum and S. sibogae* although with weak or no support by the analyses (Fig. 2).

Given that the *psb*A and *rbc*L sequences circumscribed a Mediterranean species of *Sporolithon*, we propose, according to Article 9.8 of the International Code of Nomenclature for algae, fungi, and plants (Turland et al., 2018), the specimen from the Gorgona rhodolith bed as the neotype of *S. mediterraneum* (TSB_SPR MDT 1a).

3.1. *Sporolithon mediterraneum Heydrich*

Homotypic synonyms: Archaeolithothamnion mediterraneum (Heydrich) Foslie 1901 (Foslie, 1900); *Peyssonnelia mediterranea (Heydrich)* (Foslie, 1905)

Neotype: TSB_SPR MDT 1a. Sampled on a rhodolith bed, 50 m deep, *leg.* Enrico Cecchi. Tetrasporophyte.

Collection date: 2018.

*DNA sequences: psb*A GenBank Accession #PQ518784; *rbc*L GenBank Accession #PQ518785.

Neotype locality: Gorgona island, Tyrrhenian Sea, Italy (43°25'21.385 N, 9°53'24.327 E).

Additional collections: Voucher BC-997461 (*psb*A GenBank Accession #PQ518778), Menorca Channel, Balearic Sea, Spain, 62 m depth, *leg.* Andrea Cabrito, 03/08/2022, tetrasporophyte. Voucher BC-997462 (*psb*A GenBank Accession #PQ518782), Menorca Chanel, Balearic Sea, Spain, 62 m depth, *leg.* Andrea Cabrito, 03/08/2022, tetrasporophyte. Voucher MA-Algae 11276 (*psb*A GenBank Accession #PQ518781), Menorca Chanel, Balearic Sea, Spain, 62 m depth, *leg.* Andrea Cabrito, 03/08/2022, tetrasporophyte. Voucher ICMCBMR000673 (*psb*A GenBank Accession #PQ518779), Menorca Chanel, Balearic Sea, Spain, 62 m depth, *leg.* Andrea Cabrito, 03/08/2022, tetrasporophyte. Voucher MA-Algae 11278 (*psb*A GenBank Accession #PQ518780), Menorca Chanel, Balearic Sea, Spain, 58 m depth, *leg.* Andrea Cabrito, 29/07/2022, tetrasporophyte. Voucher BC-997460 (*psb*A GenBank Accession #PQ518775), Menorca Chanel, Balearic Sea, Spain, 58.6 m depth, *leg.* Andrea Cabrito, 29/07/2022, tetrasporophyte. Voucher ICMCBMR000672 (*psb*A GenBank Accession #PQ518776), Menorca Chanel, Balearic Sea, Spain, 58.6 m depth, *leg.* Andrea Cabrito, 29/07/2022, reproductive features not observed. Voucher BC-997459 (*psb*A GenBank Accession #PQ518777), Menorca Chanel, Balearic Sea, Spain, 74 m depth, *leg.* Andrea Cabrito, 28/07/2022, tetrasporophyte. Voucher MA-Algae 11277 (*psb*A GenBank Accession #PQ518774), Menorca Chanel, Balearic Sea, Spain, 74 m depth, *leg.* Andrea Cabrito, 28/07/2022, tetrasporophyte.

3.1.1. *Habit and vegetative anatomy*

Thallus encrusting, smooth to warty, forming a rhodolith (Fig. 3A). The rhodolith is formed by two superimposed layers of thalli, both belonging to *S. mediterraneum*. The one from the upper layer is the neotype described here. Thallus construction monomerous, with a 3–5 cells-layered non-coaxial hypothallium (Fig. 3B). Hypothallial cells rectangular, 28.7–35.6 µm long and 3.9–4.9 µm wide. Perithallial cells 6.8–12.6 µm long and 5.9–10 µm wide. Adjacent hypothallial and perithallial cells linked by cell fusions and secondary pit connections (Fig. 3C). Intercalary meristematic cells isodiametric or more flattened, 2–5.8 µm long and 7.3–11.7 µm wide (Fig. 3C). Epithallium consists of a single layer of cells with thick, heavily calcified cell walls and a small trapezoidal lumen, 1.8–2.8 µm long and 6.7–10.8 µm wide (Fig. 3C).

3.1.2. *Reproduction*

Tetrasporangia in calcified compartments grouped in sori. Sori

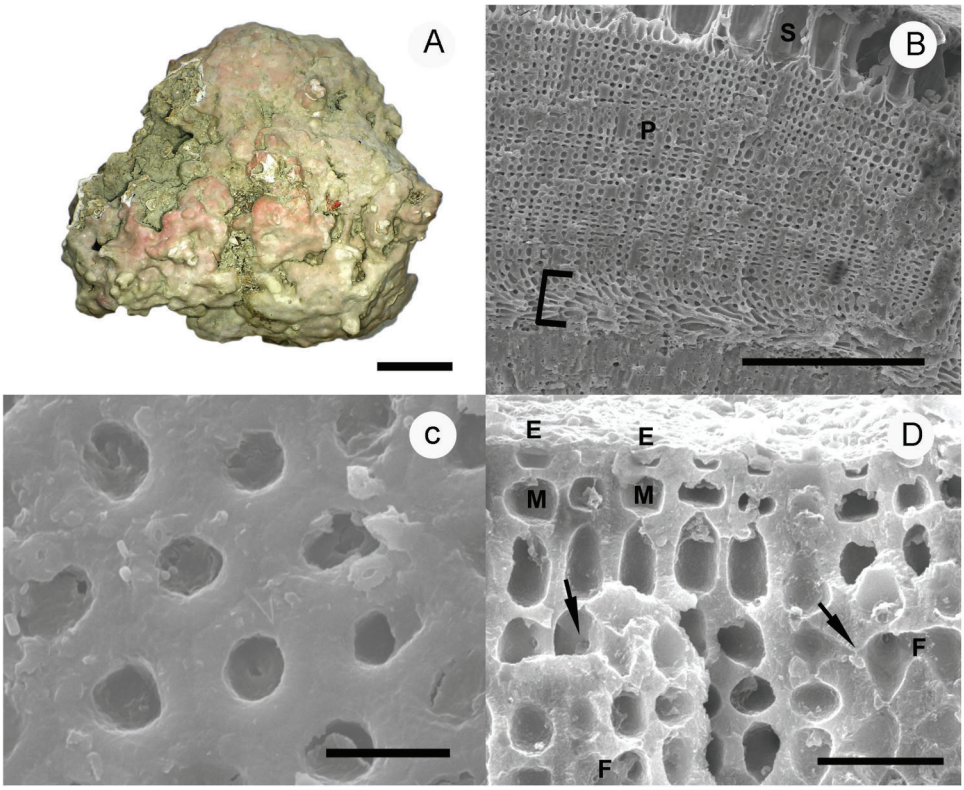


Fig. 3. *Sporolithon mediterraneum Neotype* (TSB_SPR MDT 1a). **a.** Thallus habit. Scale bar: 2 cm. **b.** Scanning electron micrograph (SEM) of a vertical fracture of the upper thallus with non-coaxial hypothallium (bracket), perithallial filaments (P), and a sorus with tetrasporangia (S). Scale bar: 200 µm. **c.** Epithallus in surface view with rounded cells. Scale bar: 10 µm. **d.** SEM of vertical section showing armored epithallial cells (E), isodiametric meristematic cells (M), perithallial cells with cell fusions (F) and secondary pit connections (arrows). Scale bar: 20 µm.

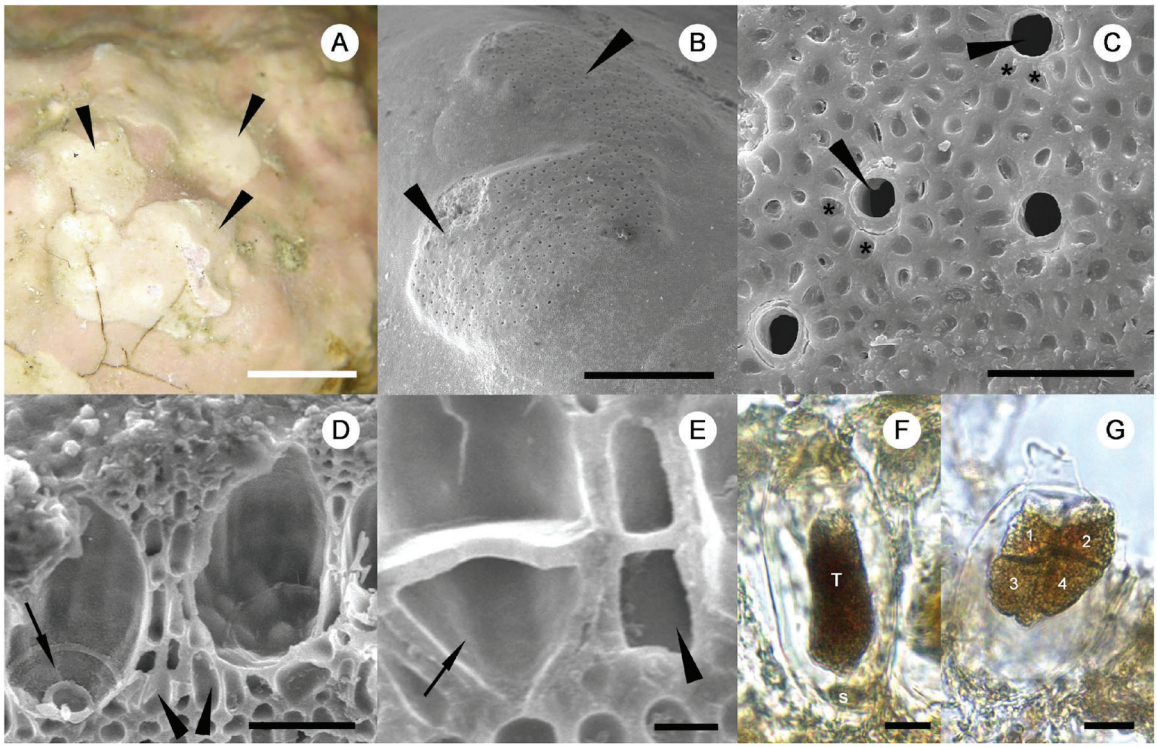


Fig. 4. *Sporolithon mediterraneum* neotype (SPR_MDT 1a). **a.** Raised tetrasporangial sori in surface view (arrowheads). Scale bar: 500 μm. **b.** Scanning electron micrograph (SEM) of thallus surface with two adjacent tetrasporangial sori (arrowheads). Scale bar: 400 μm. **c.** SEM of tetrasporangial pores (arrowheads) and rosette cells (asterisks). Scale bar: 40 μm. **d.** SEM of tetrasporangial compartments subtended by a single stalk cell (arrow) and chambers with a basal layer of elongated cells. Paraphyses formed by 5–6 cells (arrowheads). Scale bar: 50 μm. **e.** SEM of tetrasporangial compartments in transverse section with a large triangular stalk cell (arrow) and clavate cells of a bordering paraphysis (arrowhead). Scale bar: 10 μm. **f.** Longitudinal section through a tetrasporangial compartment showing a tetrasporocyte (T) with stalk cell (S). Scale bar: 15 μm. **g.** Longitudinal section of a cruciate tetrasporangium (1−4). Scale bar: 15 μm.

protrude above the surrounding thallus surface (Fig. 4A, 4B). Tetrasporangial pores in surface view 10.3–13.8 in diameter, surrounded by 9–12 rosette cells (N = 20, Fig. 2C). Tetrasporangial compartments elliptical to "lemon-shaped" 39–56 μm in diameter and 75–108 μm in height (N = 8) (Fig. 4D), subtended by a single triangular stalk cell 21.9–25.5 μm long x 24.2–35.9 μm wide (N = 8) (Figs. 4D, 4E). Tetrasporangial compartments borne among a layer of elongated cells and are separated by 0–3 vegetative calcified filaments (paraphyses) (Fig. 4D). Paraphyses consist of 5–6 cells that are mainly clavate, roundish only in the apical part of the filament. Tetrasporocytes (Fig. 4E, F) develop into cruciate tetrasporangia (Fig. 4G). Tetrasporangial compartments unshed and buried after spore release.

4. Discussion

The specimen of *Sporolithon* from Gorgona can be distinguished from *S. ptychoides* and *S. molle* previously reported from the Mediterranean Sea based on a combination of anatomical features. The ML and BI phylogenetic analyses of the *psb*A and *rbc*L sequences indicate that it is a distinct species compared to *S. ptychoides* and *S. molle*. We refer to the specimen from Gorgona as the *neotype* of *S. mediterraneum* since it is consistent with the description of the species by Heydrich (Heydrich, 1899).

In the generic description of *Sporolithon* (Verheij, 1993), the number of cells in the paraphyses between the tetrasporangia has diagnostic value at the species level. The neotype differs from *S. ptychoides* and *S. molle* by the presence of paraphyses consisting of 5–6 cells, which are shorter than in the latter species, and by larger stalk cells (Table 1, Fig. 5).

The paraphyses of *S. ptychoides* and *S. molle* consist of 3 elongate cells (Heydrich, 1897) (p. 68, Fig. 2). While the number of cells forming the paraphyses in *S. mediterraneum* was not mentioned in the protologue, Heydrich (Heydrich, 1899) described these cells as more clavate and thicker compared to those in *S. ptychoides*, and roundish at the top of the filament. The field-collected specimen of *S. ptychoides* from the type locality, with a sequence that matches the lectotype, has 3–4 celled paraphyses (Richards et al., 2017). The paraphyses of *S. molle* are also 3–4 celled (Richards et al., 2017). In contrast, all specimens from the Mediterranean region identified as *S. ptychoides* to date have 4–6 cells in the paraphyses (Alongi et al., 1996; Bressan and Babbini, 2003).

According to Richards (Richards et al., 2017), reports of *S. ptychoides* and *S. molle* based on morpho-anatomy are likely incorrect and their worldwide distribution needs to be reevaluated. Indeed, several specimens identified as *S. ptychoides* after DNA sequencing did not match any sequence of *S. ptychoides* from El Tor, Egypt. Alongi (Alongi et al., 1996) considered the specimens they examined from the Mediterranean to be conspecific and belonging to *S. ptychoides* since the size of the tetrasporangia fell within the range of *S. ptychoides*, which may indeed be considered a useful feature for some *Sporolithon* species (Verheij, 1993). Nevertheless, there is no substantial difference between the three species in this respect (Table 1). Moreover, the tetrasporangial compartments in the *neotype* and the other Mediterranean specimens are comparable in size to the measurements reported by Heydrich (Heydrich, 1899) for *S. mediterraneum*. In addition to the number of cells in paraphyses, another feature that we consider diagnostic to distinguish S. *mediterraneum* (i.e., our samples) and the Mediterranean specimens (Alongi et al., 1996; Bressan and Babbini, 2003) from *S. ptychoides* and *S. molle* is the size of the stalk cell, which is larger than 20 × 20 μm in the former and smaller in the latter (Table 1).

Richards (Richards et al., 2017) demonstrated the co-occurrence at the same type locality (El Tor, Red Sea) of two species (*i.e. S. ptychoides* and *S. molle*) that are distinguishable based on sequenced markers (i.e.,

Table 1
Characters to differentiate *S. mediterraneum* from *Sporolithon* species previously reported from the Mediterranean and other related taxa based on *psb*A.

Character	*S. mediterraneum Holotype* (Heydrich, 1899)	*S. mediterraneum Neotype* (this study)	Alongi et al. (1996) as *S. ptychoides*,	Bressan and Babbini, (2003) as *S. ptychoides*	*S. molle* (Verheij, 1993, Richards et al. 2017)	*S. ptychoides* (Heydrich, 1897, Richards et al. 2017)
Type Locality	Gulf of Naples or more likely Gulf of Villefranche[1,] (Mediterranean)	Gorgona Island (Tyrrhenian Sea, Mediterranean)	Island of Vulcano, Cannizzaro, Island of Comino (Mediterranean)	Canale di Sicilia, (Mediterranean)	El Tor (Egypt, Red Sea)	El Tor (Egypt, Red Sea)
Tetra/bisporangial chamber height (μm)	120 μm	75–108 μm	85–130 μm	86–100 μm	75–78 μm[4]	100 μm
Tetra/bisporangial chamber diameter (μm)	65 μm	39–58 μm	40–60 μm	39–51 μm	33–40 μm[4]	40 μm
Stalk cell height (μm)	ND	21.9–25.5 μm	ND	22.7 μm[3]	10–18.75 μm	10–17 μm
Stalk cell diameter (μm)	ND	24.2–35.9 μm	ND	23.8 μm[3]	14–19.5 μm	10–20 μm
Number of paraphyses between tetra/ bisporangial chambers	ND	0–3	0–5[2]	ND	0–2[5]	1–3
Number of cells in paraphyses between tetra/bisporangial chambers	ND	5–6	4–6	4–6	3–4	3–4
Tetra/bisporangial chamber pore diameter (μm)	ND	10.3–13.8	12–15	12	6–10.8	ND
Number of rosette cells surrounding tetra/ bisporangial chamber pore	ND	9–12		8–11	9–12	ND
Tetra/bisporangial chambers buried	ND	Yes	Yes	Yes	Yes	Yes
DNA sequence data available for type specimen(s)	ND	Yes	No	No	Yes	Yes

[1] See Introduction for detail on Holotype locality,
[2] Observed from Alongi (Alongi et al., 1996),
[3] Measured from Bressan and Babbini (Bressan and Babbini, 2003),
[4] Measured from Verheij (Verheij, 1993) Lectotype
[5] Observed from figure 6 in Richards (Richards et al., 2017).

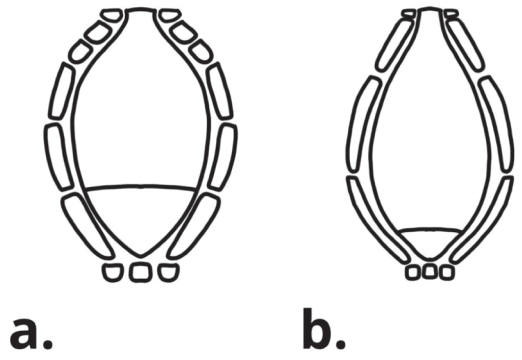


Fig. 5. Tetrasporangial compartments and the bordering paraphyses in *Sporolithon*. (**a**) *S. mediterraneum* with 5–6 celled paraphyses and a larger stalk cell (> 20 ×20 μm). (b) *S. ptychoides* and *S. molle* with 3–4 celled paraphyses and a smaller stalk cell (< 20 ×20 μm).

*rbc*L, *psb*A, UPA, COI, LSU, *tuf*A), despite the lack of distinctive morpho-anatomical characters. We cannot exclude that the specimens from the Mediterranean previously described as *S. ptychoides* also belong to different species. However, considering the confined nature of the Mediterranean basin and that the other Mediterranean specimens share all diagnostic characters with the neotype of *S. mediterraneum*, it is likely that most or all those specimens are conspecific. Currently, *S. mediterraneum* is the only confirmed species of the genus *Sporolithon* in the Mediterranean region.

The identification of *S. mediterraneum* and the morpho-anatomical characters that distinguish it from *S. ptychoides* and *S. molle* will enable us to detect records of these species in the eastern Mediterranean, in case they become established. As with other marine organisms from the Red Sea, these species have the potential to enter the Mediterranean through the Canal of Suez, a phenomenon known as Lessepsian migration, which has already been observed in other rhodophycean species (Galil, 2009; Manghisi et al., 2012; Nahor et al., 2022). Therefore, they are species of special interest because their presence may indicate shifts in their distribution due to climate change and warming waters. The detection and monitoring of these species will contribute to provide critical insights into the biogeographical changes occurring in the Mediterranean basin and help in assessing the broader impacts of environmental changes on marine ecosystems (Israel and Einav, 2017). This underscores the need for ongoing surveillance and research to track these shifts and develop appropriate conservation strategies.

Finally, the records of fossil Sporolithales found in the Mediterranean and mostly described as *S. ptychoides* (Braga and Bassi, 2007; Aguirre et al., 2012; Quaranta et al., 2012; Simone et al., 2012) could also belong to *S. mediterraneum*. For example, in Braga and Bassi (Braga and Bassi, 2007) (Fig. 6B), we observed more than 3–4 cellular paraphyses and therefore it is probably *S. mediterraneum* rather than *S. ptychoides*.

With these findings we highlight the importance of an integrated approach that combines traditional morpho-anatomical studies with DNA sequencing in the study of coralline algae.

Funding statement

There was no funding allocated to this study.

CRediT authorship contribution statement

Andrea Cabrito: Writing – review & editing, Visualization, Validation, Formal analysis, Conceptualization. **Sara Kaleb:** Writing – review & editing, Writing – original draft, Visualization, Validation, Supervision, Formal analysis, Conceptualization. **Viviana Peña:** Writing – review & editing, Writing – original draft, Visualization, Validation, Formal analysis, Conceptualization. **Annalisa Falace:** Writing – original draft, Visualization, Formal analysis, Conceptualization.

Declaration of Competing Interest

The authors declare that they have no known competing financial or personal interests.

Acknowledgements

The authors are very thankful to SEM service from ICM-CSIC and Davide Porrelli from CIMA-UNITS for the images taken during the study and to the MaCoBioS project CANAL IV fieldwork for collecting the samples from Menorca Channel. The authors would also like to thank Sofia Comis for the technical drawing of the tetrasporangial compartments. This work is contributing to the ICM's 'Center of Excellence' Severo Ochoa (CEX2019–000928–5). **AC** is enrolled in the PhD programme in Marine Sciences at the University of Barcelona.

Appendix A. Supporting information

Supplementary data associated with this article can be found in the online version at doi:10.1016/j.aquabot.2024.103839.

Data Availability

Data will be made available on request. Data is available on GenBank. The neotype has been deposited in TSB, four specimens from Menorca Channel in BC, three in MA and two in ICMCBMR.

References

Abdul Wahab, M.A., Ferguson, S., Snekkevik, V.K., McCutchan, G., Jeong, S., Severati, A., Randall, C.J., Negri, A.P., Diaz-Pulido, G., 2023. Hierarchical settlement behaviours of coral larvae to common coralline algae. Sci. Rep. 13, 5795. https://doi.org/10.1038/s41598-023-32676-4.

Aguirre, J., Braga, J.C., Martín, J.M., Betzler, C., 2012. Palaeoenvironmental and stratigraphic significance of Pliocene rhodolith beds and coralline algal bioconstructions from the Carboneras Basin (SE Spain). Geodiversitas 34, 115–136. https://doi.org/10.5252/g2012n1a7.

Alongi, G., Cormaci, M., Furnari, G., 1996. On the occurence of *Sporolithon ptychoides* Heydrich (Corallinales, Sporolithaceae, Rhodophyta) in the Mediterranean sea. Cryptogam. Algol. 17, 131–137.

Amado-Filho, G.M., Moura, R.L., Bastos, A.C., Salgado, L.T., Sumida, P.Y., Guth, A.Z., Francini-Filho, R.B., Pereira-Filho, G.H., Abrantes, D.P., Brasileiro, P.S., Bahia, R.G., Leal, R.N., Kaufman, L., Kleypas, J.A., Farina, M., Thompson, F.L., 2012. Rhodolith beds are major $CaCO_3$ bio-factories in the tropical South West Atlantic. PLoS ONE 7, e35171. https://doi.org/10.1371/journal.pone.0035171.

Athanasiadis A. (2016) Phycologia Europaea Rhodophyta. Thessaloniki: Published and distributed by the author. Vol. I. pp. [i]-xxxxviii, 1-762.

Basso, D., Nalin, R., Nelson, C.S., 2009. Shallow-Water *Sporolithon* Rhodoliths from North Island (New Zealand). PALAIOS 24, 92–103. Available at: ⟨http://www.jstor.org/stable/27670583⟩.

Braga, J.C., Bassi, D., 2007. Neogene history of *Sporolithon* Heydrich (Corallinales, Rhodophyta) in the Mediterranean region. Palaeogeogr. Palaeoclim. Palaeoecol. 243, 189–203. https://doi.org/10.1016/j.palaeo.2006.07.014.

Bressan, G., Babbini, L., 2003. Biodiversità marina delle coste Italiane: Corallinales del Mar Mediterraneo: guida all deteminazione. Biologia Marina Mediterranea. S.I.B.M., pp. 1–237

Cormaci, M., Furnari, G., Alongi, G., 2017. Flora marina bentonica del Mediterraneo: Rhodophyta (Rhodymeniophycidae escluse). Bullettin Gioenia Acad. Nat. Sci. Catania 50, FP1–FP391.

Darriba, D., Taboada, G.L., Doallo, R., Posada, D., 2012. jModelTest 2: more models, new heuristics and parallel computing. Nat. Methods 9. https://doi.org/10.1038/nmeth.2109, 772–772.

Di, Geronimo R., Giaccone, G., 1994. Le alghe calcaree nel detritico costiero di Lampedusa (Isole Pelagie). Boll. Accad. Gioenia Sci. Nat. 27, 5–25.

Farr, T., Broom, J., Hart, D., Neill, K., Nelson, W., 2009. Common coralline algae of northern New Zealand: an identification guide. NIWA Inf. Ser. No 70. ISSN 1174-264X.

Foslie, M., 1900. Revised systematical survey of the Melobesieae. Det. K. Nor. Vidensk. Selsk. Skr. 5, 1–22.

Foslie, M., 1905. A new squamariacea from the Adriatic and the Mediterranean. Det. K. Nor. Vidensk. Selsk. Skr. 1, 1–9. , 1 fig.

Fredericq, S., Krayesky-Self, S., Sauvage, T., Richards, J., Kittle, R., Arakaki, N., Hickerson, E., Schmidt, W.E., 2019. The critical importance of rhodoliths in the life cycle completion of both macro- and microalgae, and as holobionts for the establishment and maintenance of marine biodiversity. Front Mar. Sci. 5, 502. https://doi.org/10.3389/fmars.2018.00502.

Gabriel, D., Draisma, S.G.A., Schils, T., Schmidt, W.E., Sauvage, T., Harris, D.J., Norris, J. N., Fredericq, S., 2019. Quite an oddity: new worldwide records of *Renouxia* (Rhodogorgonales, Rhodophyta), including R. marerubra sp. nov. Eur. J. Phycol. 55, 197–206.

Gabrielson, P.W., Hughey, J.R., Peña, V., Richards, J.L., Saunders, G.W., Twist, B., Farr, T., Nelson, W.A., 2023. Asia Pacific *Sporolithon* (Corallinophycidae, Rhodophyta) species revised based on DNA sequencing of type specimens and including *S. crypticum sp. nov., S. immotum sp. nov.* and *S. nodosum sp. nov.* Phycologia 62, 593–607. https://doi.org/10.1080/00318884.2023.2225309.

Galil, B.S., 2009. Taking stock: inventory of alien species in the Mediterranean sea. Biol. Invasions 11, 359–372. https://doi.org/10.1007/s10530-008-9253-y.

Giaccone, G., Colonna, P., Graziano, C., Mannino, A., Tornatore, E., Cormaci, M., Furnari, G., Scammacca, B., 1985. Revisione della flora marina di Sicilia e isole minori. Boll. della Accad. Gioenia di Sci. Nat. Catania 18, 537–781.

Gouy, M., Guindon, S., Gascuel, O., 2010. SeaView version 4: A multiplatform graphical user interface for sequence alignment and phylogenetic tree building. Mol. Biol. Evol. 27, 221–224. https://doi.org/10.1093/molbev/msp259.

Guiry, M.D., Guiry, G.M., 2024. AlgaeBase. World-wide electronic publication, National University of Ireland, Galway. Listing the World's Algae, AlgaeBase. ⟨https://www.algaebase.org/⟩. Accessed 29 Oct 2024.

Hamel G. and Lemoine M. (1953) Corallinacées de France et d'Afrique du Nord. Archives du Museum National d'Histoire Naturelle de Paris, série 7 1: 15-138, 23 plates.

Heydrich, F., 1897. Corallinaceae, insbesondere Melobesieae. Ber. der Dtsch. Bot. Ges. 15, 34–70. , 3 figs, pl III.

Heydrich, F., 1899. Einige neue Melobesien des Mittelmeeres. Ber. der Dtsch. Bot. Ges. 17, 221–227.

Irvine, L.M., Chamberlain, Y.M., 1994. Seaweeds of the British Isles. Volume 1. Rhodophyta. Part 2B. Corallinales, Hildenbrandiales. vii, 276p. :986-986 J. Mar. Biol. Assoc. U. Kingd. 74 (4). https://doi.org/10.1017/S0025315400090342.

Israel, A., Einav, R., 2017. Alien seaweeds from the Levant basin (Eastern Mediterranean Sea), with emphasis to the Israeli shores. Isr. J. Plant Sci. 1–12. https://doi.org/10.1080/07929978.2016.1257091.

Keats, D.W., Chamberlain, Y.M., 1993. *Sporolithon ptychoides* Heydrich and *S. episporum* (Howe) Dawson: two crustose coralline red algae (Corallinales, Sporolithaceae) in South Africa. South Afr. J. Bot. 59, 541–550. https://doi.org/10.1016/S0254-6299(16)30701-3.

Leão, L.A.S., Bahia, R.G., Jesionek, M.B., Adey, W.H., Johnson, G., Salgado, L.T., Pereira, R.C., 2020. *Sporolithon franciscanum sp. nov.* (Sporolithales, Rhodophyta), a new rhodolith-forming species from Northeast Brazil. Diversity 12, 199. https://doi.org/10.3390/d12050199.

Lemoine, M., 1939. Les algues calcaires fossiles de l'Algérie. Mat. ériaux pour la Carte Géologique De. l'Alg. érie, SéR. PaléOntol. 9, 1–131. , pls 1–3.

Letunic, I., Bork, P., 2024. Interactive Tree of Life (iTOL) v6: recent updates to the phylogenetic tree display and annotation tool. Nucleic Acids Res gkae 268. https://doi.org/10.1093/nar/gkae268.

Littler, M.M., 1973. The population and community structure of Hawaiian fringing-reef crustose Corallinaceae (Rhodophyta, Cryptonemiales). J. Exp. Mar. Biol. Ecol. 11, 103–120. https://doi.org/10.1016/0022-0981(73)90050-6.

Maneveldt, G.W., Gabrielson, P.W., Kangwe, J., 2017. *Sporolithon indopacificum sp. nov.* (Sporolithales, Rhodophyta) from tropical western Indian and western Pacific oceans: First report, confirmed by DNA sequence data, of a widely distributed species of *Sporolithon*. Phytotaxa 326, 115. https://doi.org/10.11646/phytotaxa.326.2.3.

Manghisi, A., Bertuccio, C., Armeli, Minicante S., Fiore, V., Le, Grall L., Genovese, G., Morabito, M., 2012. Identifying alien macroalgae through DNA barcodes: the case of *Hypnea cornuta* (Cystocloniaceae, Rhodophyta). Transit. Water Bull. 5. https://doi.org/10.1285/i1825229Xv5n1p42.

Nahor, O., Luzzatto-Knaan, T., Israel, Á., 2022. A new genetic lineage of *Asparagopsis taxiformis* (Rhodophyta) in the Mediterranean Sea: as the DNA barcoding indicates a recent Lessepsian introduction. Front Mar. Sci. 9. https://doi.org/10.3389/fmars.2022.873817.

Nguyen, L.-T., Schmidt, H.A., von Haeseler, A., Minh, B.Q., 2015. IQ-TREE: a fast and effective stochastic algorithm for estimating maximum-likelihood phylogenies. Mol. Biol. Evol. 32, 268–274. https://doi.org/10.1093/molbev/msu300.

Norris, J.N., Bucher, 1989. *Rhodogorgon*, an anamolous new red algal genus from the Caribbean Sea. Proc. Biol. Soc. Wash. 102, 1050–1066.

Peña, V., De Clerck, O., Afonso-Carrillo, J., Ballesteros, E., Bárbara, I., Barreiro, R., Le Gall, L., 2015. An integrative systematic approach to species diversity and distribution in the genus *Mesophyllum* (Corallinales, Rhodophyta) in Atlantic and

Mediterranean Europe. Eur. J. Phycol. 50, 20–36. https://doi.org/10.1080/09670262.2014.981294.
Quaranta, F., Tomassetti, L., Vannucci, G., Brandano, M., 2012. Coralline algae as environmental indicators: a case study from the Attard member (Chattian, Malta). Geodiversitas 34, 151–166. https://doi.org/10.5252/g2012n1a9.
Richards, J., Kittle, R.P., Schmidt, W.E., Sauvage, T., Gurgel, C.F.D., Gabriel, D., Fredericq, S., 2022. Assessment of rhodolith diversity in the Northwestern Gulf of Mexico including the description of *Sporolithon gracile sp. nov.* (Sporolithales, Rhodophyta), and three new species of *Roseolithon* (Hapalidiales, Rhodophyta). Front Mar. Sci. 9, 906679. https://doi.org/10.3389/fmars.2022.906679.
Richards, J.L., Sauvage, T., Schmidt, W.E., Fredericq, S., Hughey, J.R., Gabrielson, P.W., 2017. The coralline genera *Sporolithon* and *Heydrichia* (Sporolithales, Rhodophyta) clarified by sequencing type material of their generitypes and other species. J. Phycol. 53, 1044–1059. https://doi.org/10.1111/jpy.12562.
Richards, J.L., Gabrielson, P.W., Schneider, C.W., 2018. *Sporolithon mesophoticum sp. nov.* (Sporolithales, Rhodophyta) from Plantagenet Bank off Bermuda at a depth of 178 m. Phytotaxa 385, 67. https://doi.org/10.11646/phytotaxa.385.2.2.
Ronquist, F., Teslenko, M., van der Mark, P., Ayres, D.L., Darling, A., Höhna, S., Larget, B., Liu, L., Suchard, M.A., Huelsenbeck, J.P., 2012. MrBayes 3.2: efficient Bayesian phylogenetic inference and model choice across a large model space. Syst. Biol. 61, 539–542. https://doi.org/10.1093/sysbio/sys029.
Saunders, G.W., Moore, T.E., 2013. Refinements for the amplification and sequencing of red algal DNA barcode and RedToL phylogenetic markers: a summary of current primers, profiles and strategies. ALGAE 28, 31–43. https://doi.org/10.4490/algae.2013.28.1.031.
Simone, L., Carannante, G., Bassi, D., Cherchi, A., 2012. Rudist-bearing rhodalgal facies in the post-Turonian recovery of peri-Tethyan carbonate systems: a case history from the Nurra region (northwestern Sardinia, Italy). Geodiversitas 34, 167–187. https://doi.org/10.5252/g2012n1a10.
Tamura, K., Stecher, G., Peterson, D., Filipski, A., Kumar, S., 2013. MEGA6: Molecular Evolutionary Genetics Analysis version 6.0. Mol. Biol. Evol. 30, 2725–2729. https://doi.org/10.1093/molbev/mst197.
Thiers B.M. (2024) Index Herbariorum. ⟨https://sweetgum.nybg.org/science/ih/⟩. Accessed 29 Oct 2024.
Turland, N.J., Wiersema, J.H., Barrie, F.R., Greuter, W., Hawksworth, D.L., Herendeen, P.S., Knapp, S., Kusber, W.-H., Li, D.-Z., Marhold, K., May, T.W., McNeill, J., Monro, A.M., Prado, J., Price, M.J., Smith, G.F., 2018. International Code of Nomenclature for algae, fungi, and plants (Shenzhen Code) adopted by the Nineteenth International Botanical Congress Shenzhen, China, July 2017. Regnum Vegetabile 159 (eds.). Koeltz Botanical Books, Glashütten. https://doi.org/10.12705/Code.2018.
Verheij, E., 1993. The genus *Sporolithon* (Sporolithaceae fam. nov., Corallinales, Rhodophyta) from the Spermonde Archipelago, Indonesia. Phycologia 32, 184–196. , 27 figs, 3 tables.
Xiang, C.-Y., Gao, F., Jakovlić, I., Lei, H.-P., Hu, Y., Zhang, H., Zou, H., Wang, G.-T., Zhang, D., 2023. Using PhyloSuite for molecular phylogeny and tree-based analyses. iMeta 2, e87. https://doi.org/10.1002/imt2.87.
Yoon, H.S., Hackett, J.D., Bhattacharya, D., 2002. A single origin of the peridinin- and fucoxanthin-containing plastids in dinoflagellates through tertiary endosymbiosis. Proc. Natl. Acad. Sci. USA 99, 11724–11729. https://doi.org/10.1073/pnas.172234799.
Zhang, D., Gao, F., Jakovlić, I., Zou, H., Zhang, J., Li, W.X., Wang, G.T., 2020. PhyloSuite: An integrated and scalable desktop platform for streamlined molecular sequence data management and evolutionary phylogenetics studies. Mol. Ecol. Resour. 20, 348–355. https://doi.org/10.1111/1755-0998.13096.

Check for updates

Received: 22 December 2023 | Revised: 20 May 2024 | Accepted: 28 May 2024

DOI: 10.1002/aqc.4212

ARTICLE

WILEY

Non-extractive fish diversity assessment in Mediterranean rhodolith beds

Andrea Cabrito[1,2] | Francesc Maynou[1] | Remy Simide[3] | David Mouillot[4] | Julie Lossent[5] | Silvia de Juan[6]

[1]Institut de Ciències del Mar (ICM-CSIC), Barcelona, Spain

[2]Facultat de Ciències de la Terra, Universitat de Barcelona, Barcelona, Spain

[3]Institut océanographique Paul Ricard, Embiez island, France

[4]Université de Montpellier, Montpellier, France

[5]Institut de recherche CHORUS, Grenoble, France

[6]Institut Mediterrani d'Estudis Avançats (IMEDEA-CSIC), Esporles, Spain

Correspondence
Andrea Cabrito, Institut de Ciències del Mar (ICM-CSIC), Passeig Marítim de la Barceloneta, 37-49, 08003 Barcelona, Spain.
Email: cabrito@icm.csic.es

Funding information
The authors acknowledge funding from the EU H2020 project 'MaCoBioS' (contract no. 869710).

Abstract

1. Rhodolith beds, recognized as biodiversity hotspots with high ecological and conservation importance, face local anthropic pressures, including trawl fishing. However, monitoring the diversity associated with this sensitive biogenic habitat in the deep waters of the Mediterranean Sea is challenging.
2. Traditional monitoring methods, such as experimental trawling and trammel nets, are extractive and have sampling limitations in providing comprehensive diversity inventories. In this work, we explore three alternative techniques (still video cameras, environmental DNA [eDNA] and bioacoustics) to monitor fish assemblages associated with rhodolith beds in the Menorca Channel at 45–80 m depth.
3. Ten sites were surveyed with eDNA, and 66 fish taxa were identified, including endangered sharks and cryptic species. The molecular operational taxonomic units (MOTUs) richness varied significantly according to habitat heterogeneity, being higher in homogeneous bottoms, and to exposure to trawling, with higher richness in non-exposed areas.
4. Bioacoustics, though limited by a reduced library of fish sounds, detected differences in sound richness between habitat types, and the highest abundance of sounds was recorded in the areas with the greatest small-scale habitat heterogeneity.
5. Underwater video revealed limitations in species detection but proved effective for characterizing small-scale habitat types and heterogeneity.
6. In summary, each technique provides valuable information at different spatial scales and levels of detail. To assess the feasibility of these techniques for long-term monitoring, we explored their capabilities and limitations in terms of costs, survey logistics and data output.

KEYWORDS

biogenic habitats, eDNA, innovative biodiversity monitoring, passive acoustic monitoring, rhodolith beds, stationary video

This is an open access article under the terms of the Creative Commons Attribution-NonCommercial-NoDerivs License, which permits use and distribution in any medium, provided the original work is properly cited, the use is non-commercial and no modifications or adaptations are made.
© 2024 The Author(s). *Aquatic Conservation: Marine and Freshwater Ecosystems* published by John Wiley & Sons Ltd.

1 | INTRODUCTION

Rhodolith beds are distributed worldwide from tropical to polar regions (Fragkopoulou et al., 2021), extending from the lower infralittoral to 40 m depth in the North Atlantic region (Peña et al., 2014) and reaching 100 m depth in the Western Mediterranean (Barberá et al., 2012). They are habitats of high ecological and conservation interest (Habitats Directive, 92/43/EEC) and are recognized as global biodiversity hotspots (Riosmena-Rodríguez et al., 2017; Tuya et al., 2023). Rhodolith beds have been described as nursery areas for fish, including economically important species (Hall-Spencer et al., 2003; Riosmena-Rodríguez et al., 2017; Costa et al., 2020).

Despite the recognized ecological importance of rhodolith beds, their protection is deficient (Tuya et al., 2023). Globally, they face multiple local pressures, including trawl fishing (de Juan et al., 2013), increased sedimentation and epiphytic algae overgrowth (Fragkopoulou et al., 2021; Legrand et al., 2017). Impacts on rhodolith beds are expected to intensify with warming and acidification of the oceans (Trégarot et al., 2023).

In the Mediterranean, the distribution and conservation status of rhodolith beds are still poorly known, hindering the implementation of adequate conservation plans, although advances have been made in some locations (e.g., Barberá et al., 2012; Maggio et al., 2022; Romagnoli et al., 2021; Sciberras et al., 2009). In this context, identifying and monitoring rhodolith beds that are in good ecological condition is urgent.

Fish species composition and abundance are considered relevant indicators of anthropogenic pressures on marine ecosystems (Dalongeville et al., 2022; Pinna et al., 2023) and are being used by the EU Marine Strategy Framework Directive (e.g., Descriptors 1 and 3).

Traditional methods for monitoring demersal fish, such as towed fishing gears or epibenthic sledges, imply physical disturbance of the seabed and a limited deployment in time and space (de Juan et al., 2020). Recently, remotely operated vehicles (ROVs) have been used to monitor deep marine habitats (Kuhnz et al., 2022), including rhodolith beds (Demestre et al., 2024; Illa-López et al., 2023). This non-extractive technique enables a more precise estimation of motile megafauna, such as fish, compared with fishing nets, as mobile fauna often evade capture by these nets (López-Garrido et al., 2020). However, species identification remains challenging due to the speed of the ROV and the quality of the images (Illa-López et al., 2023).

In this work, we explore three different techniques to monitor the presence of rhodolith beds and their associated fish diversity in the Mediterranean:

I. **Stationary bait-less cameras.** Several studies used different types of video recording (i.e., baited cameras or stereo cameras) to identify and measure fish (Cappo et al., 2003; Letessier et al., 2015). Video imaging is also used to characterize abiotic (e.g., substrate, rugosity, slope) and biotic habitats (e.g., coral reefs, seagrass) (de Juan et al., 2015; Kuhnz et al., 2022; Loh et al., 2019), including coverage by rhodoliths (Illa-López et al., 2023). However, a limitation is the video quality caused by water transparency, along with constraints related to the duration of the analysed video footage.
II. **Environmental DNA (eDNA) metabarcoding.** This method is particularly useful for providing biodiversity inventories, especially in marine areas where sampling across entire taxonomic groups or habitats is expensive or challenging (e.g., Muff et al., 2023). Also, eDNA metabarcoding has proved effective for evidencing the diversity of cryptobenthic fish in complex habitats (Mathon et al., 2023), where traditional methods such as underwater video census (UVC) are intrinsically limited (Polanco-Fernández et al., 2021). One limitation of eDNA application in offshore, open waters is the persistence of viable DNA for 2–3 days (depending on temperature) in the water mass (Caza-Allard et al., 2021; Collins et al., 2018). This DNA can be subject to transport by currents, which may affect the interpretation of the results (Collins et al., 2018).
III. **Passive acoustic monitoring.** The sounds emitted by fish and other marine animals can be proxies for local biodiversity (Mooney et al., 2020). Indices of 'acoustic' diversity can be relevant indicators of habitat conservation status, as observed in coralligenous habitats of the Western Mediterranean (Di Iorio et al., 2021). Passive acoustic techniques have the advantage of providing extensive spatial and temporal coverage. For example, Di Iorio et al. (2021) developed a long-term monitoring approach for fish soundscapes on seagrass beds, encompassing up to 3 years of sampling and covering an area of 3 ha. Interestingly, changes in the soundscape have been linked to human disturbance (Rabin & Greene, 2002), which is relevant for the monitoring of ecological conditions in marine ecosystems. An anticipated drawback is the current limitation of sound libraries, which can accurately detect only a small number of taxa at a low taxonomic level (see Table S1).

Previous works have combined two techniques to monitor fish biodiversity. For example, Sato et al. (2021) combined data from eDNA with acoustic echo sounder surveys; Mueller et al. (2006) analysed data from video and acoustic cameras; Stat et al. (2019) and Mirimin et al. (2021) combined underwater video and eDNA. Some studies, such as Aglieri et al. (2020), combined eDNA analysis with UVC, baited remote underwater video and small-scale fisheries sampling to investigate their efficiency and complementarity in assessing fish diversity in shallow depths. Nevertheless, to our knowledge, no published study has explored the relevance and complementarity of the three techniques (I–III) explained above in deep marine ecosystems, with all the challenges they entail. In this study, we applied these three non-extractive and non-destructive techniques to monitor fish diversity in a well-preserved Mediterranean rhodolith bed, ranging from approximately 50 to 100 m depth. Furthermore, we compared our findings with a reference species list obtained from previous trawling and ROV surveys in the area. Additionally, we evaluated the cost-effectiveness of each technique in terms of economic cost and personnel requirements, as well as the characteristics of the output data.

10990755, 2024, 6, Downloaded from https://onlinelibrary.wiley.com/doi/10.1002/aqc.4212 by Csic Organizacion Central Om (Oficialia Mayor) (Unci), Wiley Online Library on [25/09/2024]. See the Terms and Conditions (https://onlinelibrary.wiley.com/terms-and-conditions) on Wiley Online Library for rules of use; OA articles are governed by the applicable Creative Commons License

2 | METHODOLOGY

2.1 | Study area

The Menorca Channel is located in the Western Mediterranean, between the islands of Mallorca and Menorca, and comprises a total of 335,353.6 ha with a maximum depth of 100 m (Moranta et al., 2014). The transparency of its waters enables photosynthesis up to its maximum depth, facilitating the development of a diverse community of algae, including free-living nodules of red calcareous algae that accumulate as rhodolith beds (de Juan et al., 2023).

The area has remained in good conservation status thanks to a relatively low fishing effort. Fishing with trammel nets is routinely practised in the channel; however, trawl fishing has historically been low compared with other Mediterranean areas (Barbera et al., 2003). Moreover, there are areas off limits to trawl fishing in coastal waters shallower than 50 m. Trawl fishing is restricted in the central part of the channel due to the presence of an underwater cable installed in the 1970s. In 2016, a trawling ban was extended throughout the Menorca Channel (Order AAA/1479/2016 of 7 September, https://www.boe.es/eli/es/o/2016/09/07/aaa1479/con).

2.2 | Sampling protocols and data processing

Eleven sampling stations were selected based on exposure to trawling and substrate type. Rhodolith coverage was extracted from previous studies (Moranta et al., 2014) (Figure 1a). These stations are between 45 and 80 m depth. Two 'trawl fishing exposure' levels were identified based on vessel monitoring system (VMS) data available at the Global Fishing Watch organization (https://globalfishingwatch.org) and on the protection history of the area: (i) 'Not exposed', which includes all stations within the trawling exclusion zone, that is, cables (S13 and S01) and areas within the trawling ban limits (S15, S21 and S26), and areas shallower than 50 m where trawling is not allowed (S04 and S05); (ii) 'Exposed', which includes areas open to trawling activities (L2) and areas under the influence of trawling, that is, stations where trawling was allowed before the 2016 ban and now are at the edge of the exclusion zone (S18, S16 and S10) (Figure 1b). These sampling stations also have distinctive habitat characteristics (Figure 1; Moranta et al., 2014). In four stations, rhodolith coverage is higher than 50% (S01, S13, S15 and S18), while in four stations, rhodolith coverage is between 25% and 50% (S10, S16, S26 and L2). Three stations (S21, S04 and S05) with sparse rhodolith presence (coverage <10%) were added to the study to test the hypothesis that rhodolith beds are biologically richer and more diverse habitats (Barberá et al., 2003).

The three non-extractive techniques were planned for the 11 stations (Figure 1), although technical failures in the use of the devices restricted sampling at some stations. This resulted in a total of eight stations sampled with all three techniques. At least two of the three techniques were deployed at the remaining stations.

Sampling spanned from July 2021 to July 2022. Initially, 10 stations were sampled for eDNA and five for bioacoustics in July 2021. Video deployment to characterize the habitat took place in October 2021. In July 2022, an additional five stations were added for bioacoustics, and the video recordings of four stations (L2, S10, S18 and S26) were redeployed because of the low quality obtained in October 2021. We considered potential interannual variability by sampling species presence for eDNA and bioacoustics within the same month, thereby minimizing any variations. Subsequently, we decided to utilize video recordings not only for characterizing the habitat but also for assessing the technique's ability to detect fish species. We took into consideration the seasonal variability in fish communities when interpreting the results. Despite logistical challenges during fieldwork, this multi-method approach promises valuable insights into monitoring fish communities.

2.3 | Underwater video survey: small-scale habitat characterization and species detection

Five camera sets separated by approximately 350 m were deployed at each station to record 30–40 min of video. At stations S5 and S26, only 3 and 1 video sets, respectively, were deployed due to time constraints. The video system was mounted on a tripod equipped with two Go-Pro7 cameras (resolution of 1920 × 1440 HD) inside watertight enclosures designed to withstand high pressure.

The video footage was visually analysed following three steps: (i) The first 20 min with good quality of the image were selected (i.e., without the pitching that the swell sometimes caused on the tripods). (ii) The selected video sample (20′) was visually inspected to characterize the habitat type. This was done by systematically describing the type of substrate (considering the predominant type of sediment, mainly gravel and sand), the percentage of rhodolith coverage, the presence of macroalgae (e.g., *Laminaria*) and signals of biotic activity (e.g., tracks or mounds). Then, applying the rhodolith coverage criteria, a habitat type was assigned to each sample. (iii). A second visualization of the video sample was made using the Kinovea software to register the presence of fish species. Fish were noted and identified at the lowest taxonomic level possible. All the fish identified in the sample were noted only once, considering their presence/absence. In addition, the presence of groups that could not be identified and/or counted was noted as categorical data (e.g., 'school of fish').

2.3.1 | Data analyses

Video samples were analysed to provide a semi-quantitative estimation of the small-scale biophysical heterogeneity. Habitats were classified into three types: (i) rhodolith beds, with more than 50% of rhodolith coverage; (ii) detritic biogenic habitats with less than 50% of rhodolith cover; and (iii) detritic biogenic habitats with less than 10% of rhodolith cover. In a second stage, a more detailed description of the biophysical elements identified at each sampling station was performed, considering the presence of other habitat components and sediment features. For this, we considered

10990755, 2024, 6, Downloaded from https://onlinelibrary.wiley.com/doi/10.1002/aqc.4212 by Csic Organizacion Central Om (Oficialia Mayor) (Unci), Wiley Online Library on [25/09/2024]. See the Terms and Conditions (https://onlinelibrary.wiley.com/terms-and-conditions) on Wiley Online Library for rules of use; OA articles are governed by the applicable Creative Commons License

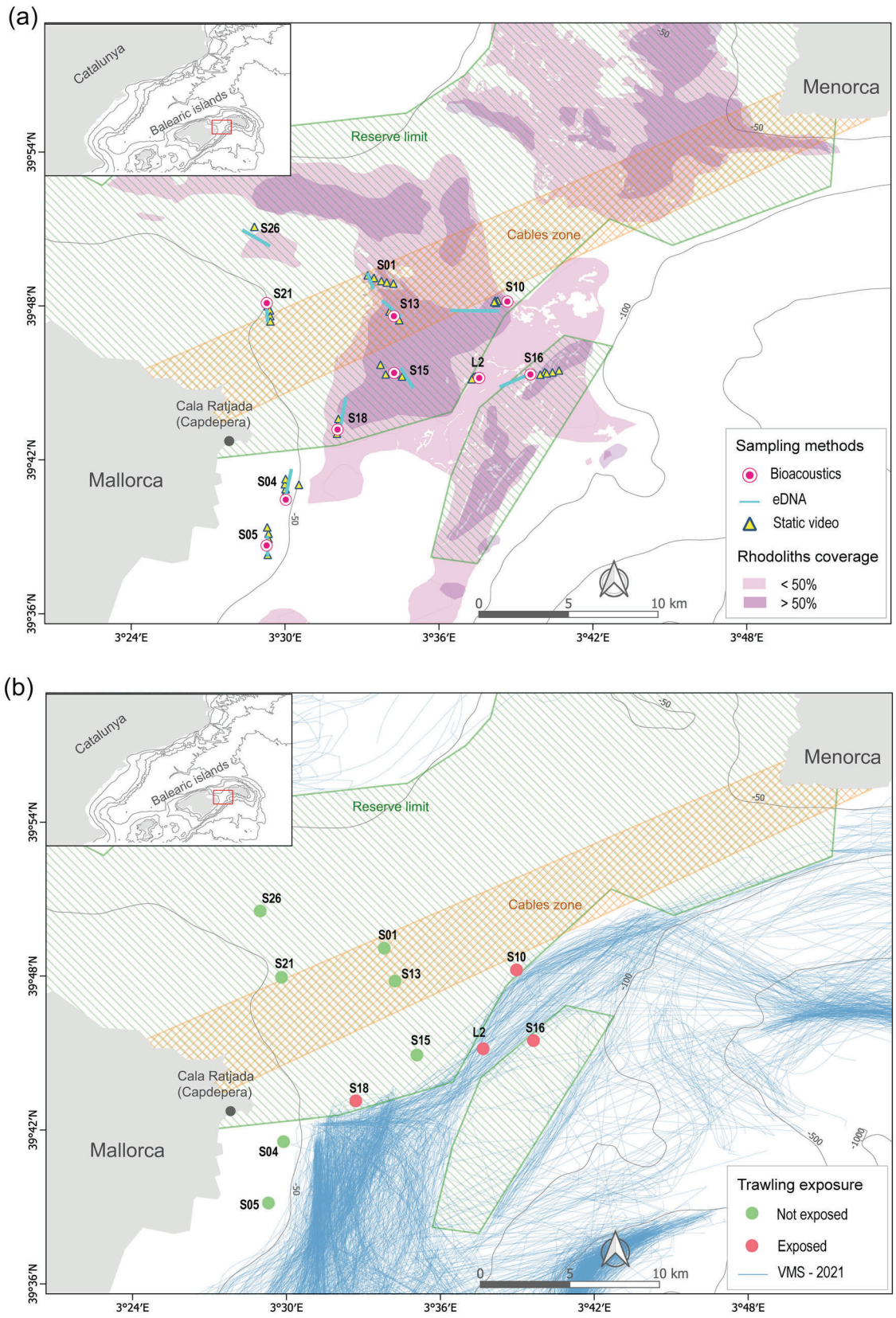


FIGURE 1 Map of the sampling stations in the Menorca Channel. (a) Locations of the sampling stations where any of the three techniques were deployed. Rhodolith coverage, extracted from Moranta et al. (2014), is represented in different purple intensities; the white areas correspond to the sandy stations with sparse rhodoliths. (b) Fishing tracks of the trawl fleet (corresponding to 2021) and identification of the sampling stations exposed (red) or not exposed (green) to trawling. Green hatching shows the area protected from fishing by the marine reserve declared in 2016.

10990755, 2024, 6, Downloaded from https://onlinelibrary.wiley.com/doi/10.1002/aqc.4212 by Csic Organizacion Central Om (Oficialia Mayor) (Unci), Wiley Online Library on [25/09/2024]. See the Terms and Conditions (https://onlinelibrary.wiley.com/terms-and-conditions) on Wiley Online Library for rules of use; OA articles are governed by the applicable Creative Commons License

(i) the presence of other algae such as *Peyssonnelia rosa-marina*, *Osmundaria volubilis* and *Laminaria rodriguezii* that contribute to increase the biogenic habitat complexity; (ii) the presence of marks and traces of biological activity on the sediments as indicators of bioturbation; and (iii) the presence of patches and discontinuities in the biogenic habitat as an indicator of small-scale heterogeneity.

Then, the 3–5 video samples obtained in each station were reviewed to identify the diversity of fish. We calculated the richness of fish taxa by combining the identified species at each station. However, due to the sampling limitations (two distinct time periods), no statistical tests were conducted. Therefore, the richness results obtained from this technique are considered solely for comparative purposes with the species detection capabilities of the other techniques.

2.4 | Environmental DNA metabarcoding: fish biodiversity

To assess fish richness with DNA metabarcoding, water samples were collected in 10 stations (Figure 1). Samples were obtained by towing a water pump approximately 5 m above the seabed for 45 min, filtering 45 L of seawater. The water pump was fitted to a 0.2 μm polyethersulfone filter that retains small DNA fragments released by all organisms in their close environment (Miya, 2022). In each station, two replicates were obtained. The filtered eDNA was then transported to the laboratory. At all stages, a strict contamination control protocol was followed (see Mathon et al., 2023). eDNA extraction was performed following the protocols by Juhel et al. (2020) and Pont et al. (2018). The teleost-specific 12S mitochondrial rRNA primer pair (Valentini et al., 2016) was used for the amplification of metabarcode sequences. The primers were 5′ labelled with a unique tag, allowing the assignment of sequences to the samples during the bioinformatic analysis. Twelve PCR replicates per sample were performed (Mathon et al., 2023) and an average of 650,000 sequence reads were obtained per sample in the raw data.

The reads were processed using clustering and post-clustering cleaning to remove errors and estimate the number of species using molecular operational taxonomic units (MOTUs) (Mathon et al., 2023). First, reads were assembled using *vsearch* (Rognes et al., 2016), then demultiplexed and trimmed using Cutadapt (Martin, 1994), and clustering was performed using SWARM v.2 (Mahé et al., 2015) with d = 1, which corresponds to a maximum of 1 mismatch between neighbouring pairs of sequences within each cluster. Taxonomic assignment of MOTUs was carried out using the lower common ancestor (LCA) algorithm *ecotag* implemented in the Obitools toolkit (Boyer et al., 2016) and the European Nucleotide Archive (ENA) as a reference database (release 143, March 2020), supplemented by the Mathon et al. (2023) custom reference database.

For each station and replicate, we obtained the read abundance of MOTUs, which cannot be directly linked to in situ taxon abundance (Sanchez et al., 2022). Therefore, MOTU abundances were converted to a presence/absence matrix of MOTUs by the sampling station. A first correction was made aimed at eliminating false positives by setting the number of reads assigned to a certain MOTU to zero if they represented less than 3% of the total abundance of that MOTU (following Wangensteen & Turón, 2017). Then, a second adjustment was made by joining the two replicates of each station. For this purpose, all MOTUs, even if they were only detected in one of the two filters, were considered as present.

2.4.1 | Data analyses

Fish richness was estimated from the MOTU presence/absence matrix extracted from the eDNA samples. In this case, this measurement is a count of the number of different MOTUs present in each station. To test whether trawling exposure, habitat type and habitat heterogeneity explain significant differences in MOTUs richness, Kruskal–Wallis comparisons of means were performed using *kruskal.test* function from the *stats* R package. No attempt was made to explore the interaction among explanatory factors due to the low number of samples. Significant differences were assumed when the probability level was lower than $p = 0.1$.

To explore variability in species composition (based on MOTU as a proxy) between stations, a non-metric multidimensional scaling analysis was carried out based on the Jaccard similarity index and using *metaMDS* in the *vegan* R package. To test whether the distribution of MOTUs across stations is related to trawling exposure, habitat type or habitat heterogeneity, an analysis of variance (PERMANOVA, with 999 permutations) was performed using the *adonis2* function from the *vegan* R package. Due to the sampling characteristics, the factors have been considered as independent, without interaction. Then, to determine which species characterized each level of trawling exposure and each level of habitat type, we calculated the strength of association between species and site group membership using the *strassoc* function from the *indicspecies* R package (De Cáceres et al., 2022).

2.5 | Bioacoustic monitoring: fish soundscape—fish activity

Data were acquired using an HTI-92-WB hydrophone (High Tech Inc., USA) with a sensitivity of −155 ±3 dB re 1 V/μPa and a flat frequency response from 5 Hz to 50 kHz, connected to an SDA14 compact autonomous recorder (RTSys®, France). The acquisition chain is fully calibrated. The device, which acquired sounds continuously at a 78 kHz sampling rate and 24-bit resolution, was bottom-moored with the hydrophone 1 m above the seafloor. On each recording date, the recorder was deployed in the afternoon and recovered the next day. Recordings were made during the night because most temperate fish predominantly vocalize nocturnally (Bolgan et al., 2019; Picciulin et al., 2012), and interference with anthropogenic noise is largely reduced.

10990755, 2024, 6, Downloaded from https://onlinelibrary.wiley.com/doi/10.1002/aqc.4212 by Csic Organizacion Central Om (Oficialia Mayor) (Unici), Wiley Online Library on [25/09/2024]. See the Terms and Conditions (https://onlinelibrary.wiley.com/terms-and-conditions) on Wiley Online Library for rules of use; OA articles are governed by the applicable Creative Commons License

The mooring was deployed at 10 stations, but successful recordings were obtained from only nine stations (Figure 1). Audio files from 5:00 PM to 9:00 AM were divided into 10-s snapshots that were converted into 10-s spectrograms (fast Fourier transform [FFT] resolution 11 Hz, Kaiser window 180 dB, 85% overlap). These spectrograms were classified using a custom-built MATLAB® (version R2014b) interface that allowed the identification of potential fish sounds by an expert. The 15 types of fish sounds recovered were classified into six categories (see Figure S1) following Desiderà et al. (2019) (Table S1). Some categories (1, 2, 3 and 4) refer to fish species (or genera) that emit well-studied types of sound that can be taxonomically classified. Other categories (5 and 6) are related to groups of fish that emit characteristic and similar sounds that cannot be directly linked to a specific taxon. It should be noted that the same species may emit more than one type of sound depending on its activity, and these sounds are grouped in the corresponding category (e.g., Category 4 for all sounds emitted by *Epinephelus marginatus*).

For each 10-s interval, the number of different sound types was counted and pooled in 1-h bins. The number of sounds was pooled per station.

2.5.1 | Data analyses

The total abundance of sounds (number of vocalizations/h), as well as the abundance of each category of sounds, were calculated per station as an index of total and specific fish activity in the area. In addition, the number of sounds with different origins (i.e., different species or different activities within the same species) was calculated as a sound richness index. To test whether trawling exposure, habitat type, and habitat heterogeneity explain significant differences in sound richness and abundance of sounds, Kruskal–Wallis comparisons of means were performed using *kruskal.test* function from the *stats* R package. No attempt was made to explore the interaction among explanatory factors due to the low number of samples. Significant differences were assumed when the probability level was lower than $p = 0.1$.

2.6 | Complementarity between techniques

Due to the nature of data acquisition, that is, the temporal and spatial scales that each technique encompasses, the different datasets are not directly comparable. Nevertheless, the three techniques provided different proxies for the biodiversity of fish associated with the rhodolith bed under study, suggesting that they might be complementary in exploring fish communities from different perspectives; however, the feasibility of the technique for long-term monitoring has not been proven.

In order to analyse complementarity between the three techniques, a Friedman rank test (R package 'stats') was performed using the relative richness from the eight stations where the three techniques were successfully applied. A pairwise Wilcoxon test was performed to check which techniques differed from each other. Relative richness was calculated as the ratio of the number of MOTUs, sounds or taxa detected at each station (by each technique) to the total number of MOTUs, sounds or taxa detected by each technique (in the whole study).

An assessment of the advantages and disadvantages of the techniques was conducted. For this, a qualitative comparison was made between the three non-extractive techniques and a traditional extractive technique used in previous projects, a 'Grande Ouverture Verticale' trawl net (GOC, Ordines & Massutí, 2009; Moranta et al., 2014). Information was extracted from fieldwork conducted in the Menorca Channel during the projects MaCoBioS (see Tables S7a–S7d) and INDEMARES (Moranta et al., 2014). MaCoBioS fieldwork information combined with expert knowledge was used to score various aspects of the monitoring techniques, such as the economic cost and personnel requirements of the technique (i.e., investment of time and personnel as well as fieldwork costs, analysis costs or processing time), the ability to obtain information on fish diversity (i.e., species inventories, detection of vulnerable or cryptic species and recording of biological activity), the ability to obtain information at the seascape (i.e., spatial scale, habitat composition or habitat heterogeneity) and their destructiveness to the marine environment.

All statistical analyses were carried out in R version 3.6.3 (R Core Team, 2022).

3 | RESULTS

3.1 | Habitat characterization by underwater video

A total of 47 video samples were analysed (i.e., between 3–5 video samples in each station, Figure 1), and the description of the habitat type in each station was summarized in Table 1. In S26, only one video could be recovered because of time limitations; therefore, the video was only used to describe the habitat type and rhodolith coverage, which was expected to be <50% but turned out to be <10%.

Based on the visual examination of video images, three levels of rhodolith coverage at the site scale were identified (Figure S2a–c). A 100% rhodolith coverage (i.e., rhodolith bed) was identified in S13, within the cable-protected area. This rhodolith bed might extend to the north, reaching S01; however, a habitat transition was observed at the edge of the cables' exclusion zone. In this area, the rhodolith coverage decreased progressively, and S01 was characterized by high spatial heterogeneity between replicates (at a scale of 350 m). To the south, the rhodolith bed extended to S15, within the protected area, and up to S18 at the limits of protection. In the deeper stations at the edge of the protected area (S16 and S10), the density of rhodoliths decreased. In this area, the substrate was characterized as a biogenic habitat with less than 50% rhodolith coverage. The shallower stations, S21,

10990755, 2024, 6, Downloaded from https://onlinelibrary.wiley.com/doi/10.1002/aqc.4212 by Csic Organizacion Central Om (Oficialia Mayor) (Unici), Wiley Online Library on [25/09/2024]. See the Terms and Conditions (https://onlinelibrary.wiley.com/terms-and-conditions) on Wiley Online Library for rules of use; OA articles are governed by the applicable Creative Commons License

TABLE 1 Habitat description extracted from video footage in each study site.

Station	Depth (m)	Habitat	Description for each station
S10	70	Sand with <50% of rhodolith cover	Sand with <50% of rhodolith coverage and algae. Presence of mounds (sign of bioturbation). Homogeneity between replicates.
S16	71.2	Sand with <50% of rhodolith cover	Sand with <50% of rhodolith coverage, high algae cover with *Laminaria* fronds. Presence of mounds (sign of bioturbation). **Heterogeneity** between replicates.
S01	62	Rhodolith bed	Transition between habitats. From sand with <50% of rhodolith coverage to rhodolith bed. Presence of *Peyssonnelia* and *Laminaria* fronds. **Heterogeneity** between replicates.
S13	62	Rhodolith bed	100% rhodolith coverage. Presence of *Peyssonnelia* and *Laminaria* fronds. Homogeneity between replicates.
S15	58.8	Rhodolith bed	100% rhodolith coverage. Presence of *Peyssonnelia* and *Osmundaria*. Homogeneity between replicates.
S18	56	Rhodolith bed	100% rhodolith coverage. Presence of *Osmundaria* and high amount of dead sea urchins. Presence of mounds (sign of bioturbation). **Heterogeneity** between replicates.
S21	51	Sand with <10% of rhodolith cover	Sand with ripples and less than 10% rhodolith cover and sparse algae. Homogeneity between replicates.
S04	48	Sand with <10% of rhodolith cover	Sand with <10% of rhodolith coverage with algae and presence of *Osmundaria*. Presence of animal tracks (sign of bioturbation). Homogeneity between replicates.
S05	48.5	Sand with <10% of rhodolith cover	Sand with <10% of rhodolith coverage with algae and *Osmundaria*. Presence of ripples and rocks with algae. Presence of animal tracks (sign of bioturbation). **Heterogeneity** between replicates.
L2	65.6	Sand with <50% of rhodolith cover	Sand with <50% of rhodolith with a full cover by *Laminaria*. Homogeneity between replicates.
S26	65	Sand with <10% of rhodolith cover	Sand with <10% of rhodolith coverage. Only one replicate hampered the assessment of heterogeneity.

S04 and S05, were characterized by biogenic detrital beds with less than 10% of rhodoliths. In addition, high habitat heterogeneity at a small scale was observed in S05 due to the presence of rocky outcrops covered with algae and sessile organisms (Figure S2d). A total of 14 fish taxa could be identified through video visualization in the 10 stations (Table S3). Having images of the same point from two different seasonal periods allowed us to verify that both the number and types of taxa remained consistent.

3.2 | Fish diversity with environmental DNA

The 20 eDNA samples (10 stations × 2 replicates) yielded a total of 2,374,169 sequence reads (average 118,708.45 per sample) that could be assigned to known fish taxa in the reference database (ENA—www.ebi.ac.uk/ena/browser/home). In most cases, the MOTU could be associated with a fish species, although in some cases, the attribution could be made only at the level of a genus or closely related genera. A total of 66 different taxa were identified, 58 from the subclass Teleostei (bony fish) and 8 from the subclass Elasmobranch (cartilaginous fish) (see Table S4).

The results of the Kruskal–Wallis test indicate that MOTUs richness varied significantly according to trawling exposure ($X^2 = 3.776$, df = 1, p-value = 0.052). Habitat heterogeneity was also significant, with higher richness in stations with homogeneous substrates ($X^2 = 3.84$, df = 1, p-value = 0.050). No significant differences were detected for MOTU richness between habitat types ($X^2 = 2.209$, df = 2, p-value = 0.331), although there is a general tendency for higher MOTUs richness in sandy sites with less than 10% rhodolith cover (Figure 2).

The MOTU composition across stations was also affected by these factors, as evidenced by the PERMANOVA significance levels for trawling exposure (F = 2.863, df = 1, p-value = 0.001), habitat type (F = 1.653, df = 2, p-value = 0.022) and habitat heterogeneity (F = 1.470, df = 2, p-value = 0.066). The interaction could not be assessed because of the limited number of samples.

The highest similarity between stations (55%) occurred for the relatively shallow stations S04 and S21 that were characterized by

10990755, 2024, 6, Downloaded from https://onlinelibrary.wiley.com/doi/10.1002/aqc.4212 by Csic Organizacion Central Om (Oficialia Mayor) (Unci), Wiley Online Library on [25/09/2024]. See the Terms and Conditions (https://onlinelibrary.wiley.com/terms-and-conditions) on Wiley Online Library for rules of use; OA articles are governed by the applicable Creative Commons License

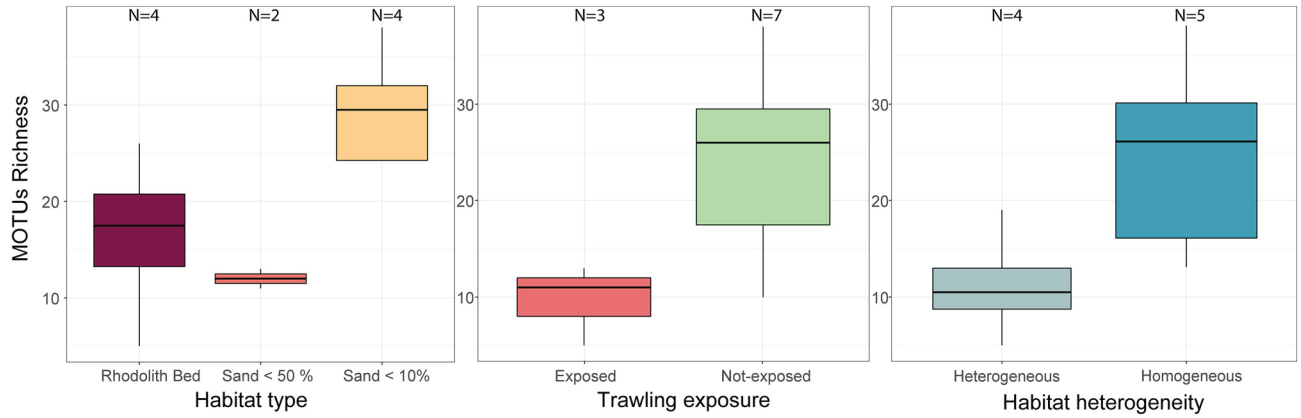


FIGURE 2 Richness of molecular operational taxonomic units (MOTUs) detected with environmental DNA (eDNA) in the study area. From left to right, samples were identified by type of habitat, exposure to trawling activity and habitat heterogeneity.

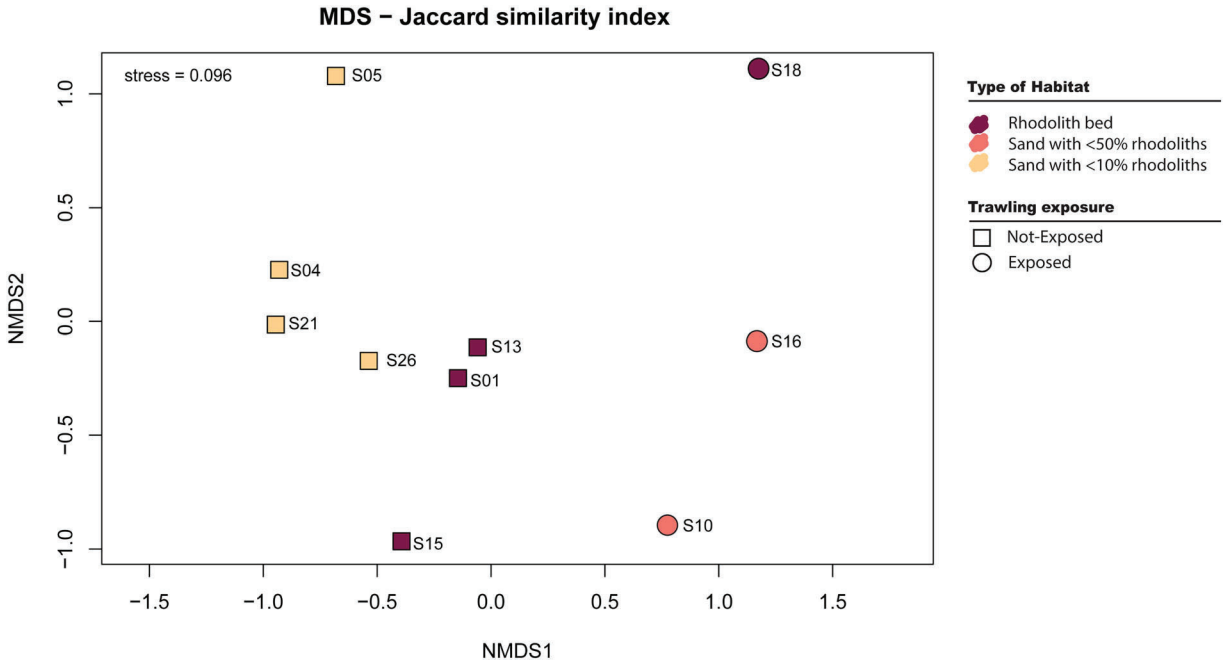


FIGURE 3 Multidimensional scaling (MDS) based on the Jaccard similarity index of fish species data identified through environmental DNA (eDNA) metabarcoding in the 10 sampling stations.

sand with <10% of rhodolith coverage. The second pair of stations with the highest similarity (45%) were the not-exposed rhodolith beds in S13 and S01. These two pairs of stations are relatively close in the multivariate space (Figure 3), together with S26, which is sandy and not exposed.

The most represented species (MOTUs) within the not-exposed areas include species of commercial interest, such as sparids, and benthic fishes such as *Uranoscopus scaber*, as well as the rainbow wrasse *Coris julis* (see Table S5). Cryptic species such as *Corcyrogobius liechtensteini* or *Crystallogobius linearis* were found among the 10 most characteristic species of the rhodolith bed. In addition, protected, endangered and threatened species of elasmobranchs such as *Myliobatis aquila*, *Prionace glauca* and *Pteroplatytrygon violacea* were found both over rhodolith beds and sandy bottoms with less than 50% of rhodolith cover. In sandy bottoms with less than 10% of rhodolith coverage, there was a predominance of species typically associated with sandy habitats (e.g., *Buenia affinis*, *Gobius cruentatus* or *Chelidonichthys obscurus)* (see Table S5).

3.3 | Bioacoustic monitoring: fish sounds

A total of 15 different sound types were detected in the nine sampling stations: one sound type classified as *Ophidion rochei*, two sound types as *Sciaena umbra*, one type as *Scorpaena* spp., four types

10990755, 2024, 6, Downloaded from https://onlinelibrary.wiley.com/doi/10.1002/aqc.4212 by Csic Organizacion Central Om (Oficialia Mayor) (Unci), Wiley Online Library on [25/09/2024]. See the Terms and Conditions (https://onlinelibrary.wiley.com/terms-and-conditions) on Wiley Online Library for rules of use; OA articles are governed by the applicable Creative Commons License

as *E. marginatus*, two types as HF fishes and five types classified as other fishes.

The results of the Kruskal–Wallis test revealed significant differences at the 0.1 significance level among the various habitat types ($X^2 = 5.262$, df = 2, p-value = 0.072). However, despite this finding, the pairwise Wilcoxon post hoc test failed to identify any differences among the three groups (p-value > 0.1 in all comparisons). Statistical tests indicated that there were no significant differences in sound richness associated with either trawling exposure ($X^2 = 1.593$, df = 1, p-value = 0.207) or habitat heterogeneity ($X^2 = 0.071$, df = 1, p-value = 0.790).

We also estimated the abundance of sounds in the six sound categories included in Table S1. The mean of total sound abundance was higher in stations with high habitat heterogeneity (205 sounds/h) compared with homogeneous areas (107.92 sounds/h) (see Table S2). The results of the Kruskal–Wallis test revealed significant differences at the 0.1 significance level for habitat heterogeneity ($X^2 = 3.267$, df = 1, p-value = 0.071), but no significant differences were found among habitat type or for trawling exposure (p-value > 0.1).

The stations with the highest sound abundances were those exhibiting high small-scale habitat heterogeneity, such as S5 and S18 (Figure 4). However, stations with high sound abundance were generally found in sand with less than 10% rhodolith coverage (S5 and S21) and with less than 50% rhodolith coverage (S10 and S16).

High-frequency fishes (HF Fish) were represented and had the highest abundance only in stations characterized by sand with less than 50% rhodoliths. *O. rochei* was the most heard species in the area, and its sounds were registered within rhodolith beds and sand with less than 10% of rhodoliths. In these sandy stations, *S. umbra* was also commonly heard. Species from the Scorpaenidae family were detected mostly in rhodolith beds, and groupers mostly in coastal and heterogeneous stations (Figure 4).

3.4 | Comparative feasibility and cost-effectiveness of monitoring approaches

Considering the relative richness as a proxy for diversity, there was variability in the number of fish identified with the three different techniques, and there was also high variability across the stations (see Figure S3). The station with the highest diversity recorded with any of the three techniques was station S21. The results for the other stations were variable. In general, S16 exhibited low diversity.

The results of the Friedman rank test were statistically significant ($X^2 = 9.484$, df = 2, p-value = 0.009), indicating that the three techniques did not detect richness in the same ranking. The post-hoc Wilcoxon test showed that acoustic and video did not provide different richness rankings (p-value = 1.0), while eDNA and acoustic (p-value = 0.041) and eDNA and video (p-value = 0.023) did differ in richness ranking.

eDNA detected the highest number of total taxa, with 66 detected taxa (S = 5–38 per station). In comparison, video (14 total taxa, S = 2–8 per station) and bioacoustics (15 types of sounds, but only four categories assigned to taxa and S = 2–8 sound types per station) techniques are very limited (see Table S2). No taxon was detected by all three techniques simultaneously. Those taxa that were detected with two of the three techniques were not always detected in the same station; for example, *C. julis* was detected with eDNA at stations S13, S21 and S04 and with video at stations S10 and S05. Only *Serranus cabrilla* was detected in a relatively high number of stations with video and eDNA simultaneously (see Table S6). Some species were detected with only one of the three techniques, such as *O. rochei*, which was only detected with bioacoustics; *Aphia minuta*, detected only with video; and 35 species, detected only with eDNA (see Table S6).

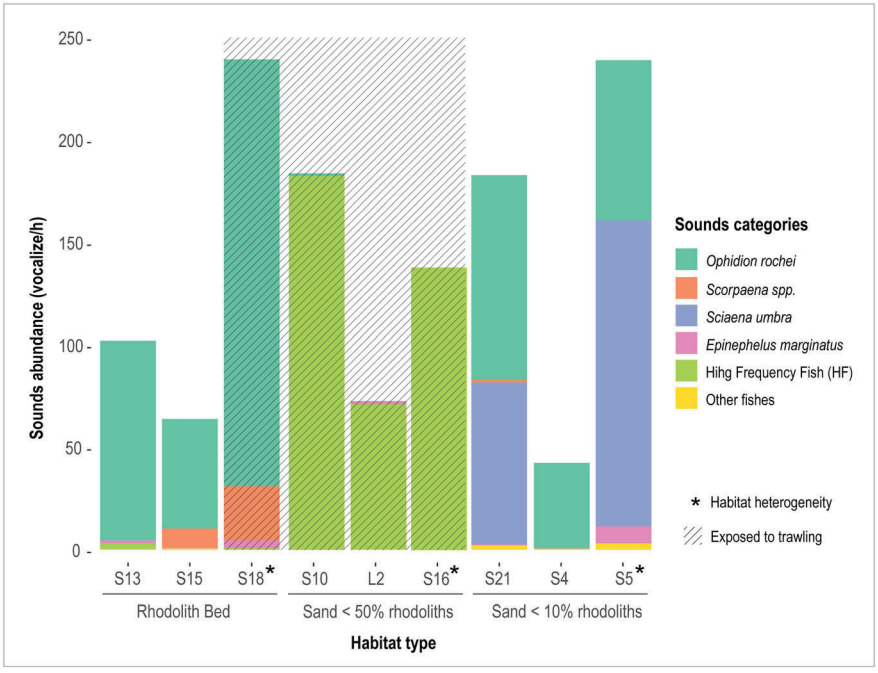


FIGURE 4 Barplot of the abundance of the six sound categories measured as the number of vocalizations/h at each station. Rhodolith coverage levels are indicated below, along with habitat heterogeneity. The stations exposed to trawling are texturised with lines.

10990755, 2024, 6, Downloaded from https://onlinelibrary.wiley.com/doi/10.1002/aqc.4212 by Csic Organizacion Central Om (Oficialia Mayor) (Unici), Wiley Online Library on [25/09/2024]. See the Terms and Conditions (https://onlinelibrary.wiley.com/terms-and-conditions) on Wiley Online Library for rules of use; OA articles are governed by the applicable Creative Commons License

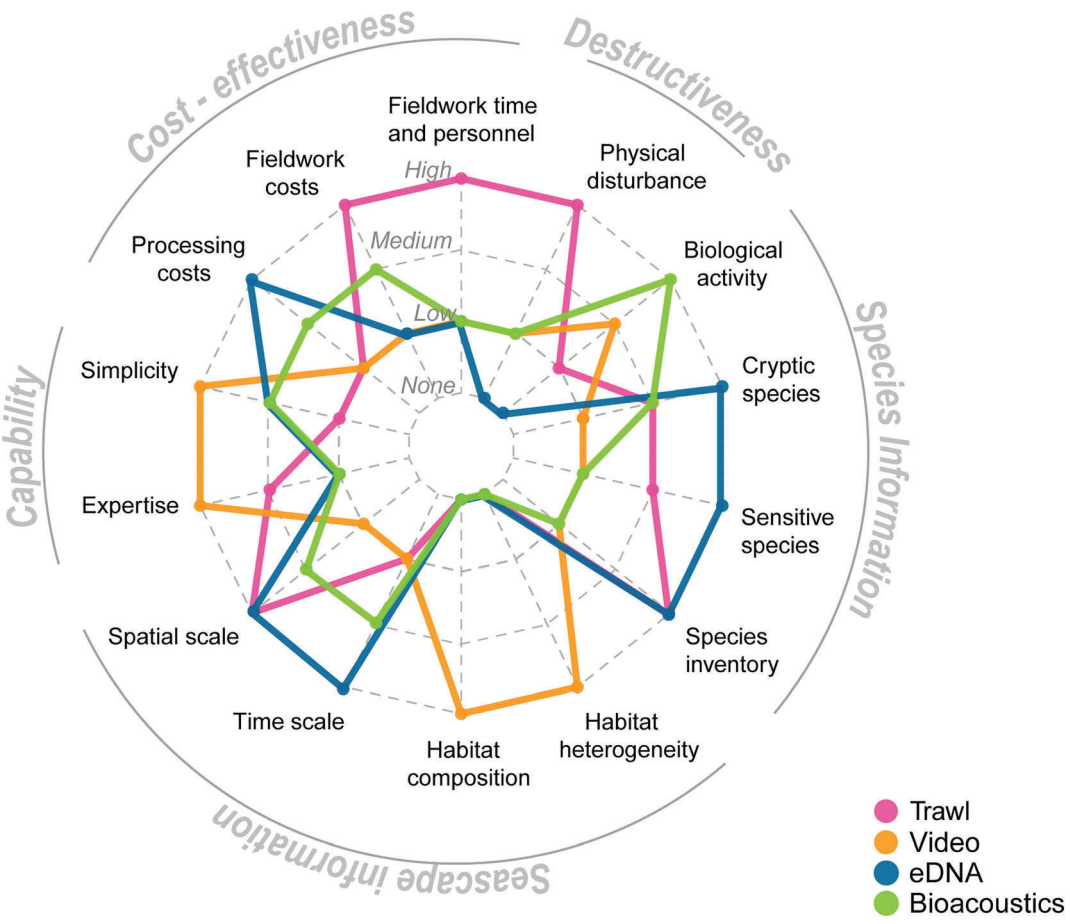


FIGURE 5 Qualitative comparison in terms of costs and time requirements and in the extraction of species and ecosystem information between an extractive sampling technique (trawl of type 'GOC': Chalut à Grand Ouverture Verticale) and the three non-extractive sampling techniques. The information is based on expert knowledge and supported by costs and information extracted from the fieldwork of the MaCoBioS and INDEMARES projects.

The qualitative comparison, grounded in fieldwork conducted in the study area, of the feasibility and cost-effectiveness of three techniques highlighted variations in the limitations, data acquisition and costs associated with fieldwork activities and data analysis for each technique (see Tables S7a–S7d). In comparison with sampling with towed nets, video images, bioacoustics and eDNA are innovative non-extractive techniques that are less expensive in terms of fieldwork operative costs (i.e., they do not require a large research vessel), time and personnel requirements. Bioacoustics and eDNA have higher costs in terms of data analyses (e.g., currently externalized to private laboratories). On the other hand, static video allows us to get information on habitat composition and heterogeneity. Bioacoustics and video proved to be more useful for detecting biological activity, while eDNA was more effective for detecting cryptic and vulnerable species (Figure 5).

4 | DISCUSSION

The present study investigates the efficacy of three non-destructive and non-extractive techniques for monitoring fish diversity in a Mediterranean rhodolith bed, each offering unique insights across different scales and levels of detail. Among these techniques, eDNA stands out for its ability to detect a wide array of species. However, caution is warranted in interpreting results, as diversity is inferred from the presence of DNA fragments in the water mass, potentially influenced by the amount of material contributed by different species and by environmental factors such as hydrodynamics. The effectiveness of the other two techniques is limited; although video recordings are useful for habitat characterization, their low quality restricts fish identification. Bioacoustics shows promise but would necessitate investment in reference databases to enhance its utility. The results, despite the limited number of stations and the technique's intrinsic limitations, suggest an interplay of factors driving the diversity of fish over rhodolith beds, including exposure to trawling, habitat type and small-scale habitat heterogeneity. The station with the highest recorded fish diversity using the three techniques was characterized by homogeneous detrital sediments, containing less than 10% rhodoliths. This location, sheltered from trawling, is relatively shallow and situated near the coast. The results for the other stations were variable, and fish diversity followed different patterns depending on the technique selected. The highest

10990755, 2024, 6, Downloaded from https://onlinelibrary.wiley.com/doi/10.1002/aqc.4212 by Csic Organizacion Central Om (Oficialia Mayor) (Unci), Wiley Online Library on [25/09/2024]. See the Terms and Conditions (https://onlinelibrary.wiley.com/terms-and-conditions) on Wiley Online Library for rules of use; OA articles are governed by the applicable Creative Commons License

values recorded with bioacoustics were observed at a shallow station not exposed to trawling and characterized by habitat heterogeneity. This area featured regions densely populated by rhodolith beds alternating with patches of sand, each with less than 50% rhodolith coverage. Similarly, both video and eDNA methods detected elevated taxa richness at another shallow station characterized by detrital bottoms, situated near the boundaries of the 50-m trawling exclusion zone. In contrast, the deeper area exposed to trawling exhibited lower diversity overall. The stations within the rhodolith bed did not exhibit a particularly high fish diversity.

This study explores the capabilities and limitations of the three techniques for monitoring fish diversity. We could only identify a few fish taxa at the species level from the video samples. The low-cost, bait-less imaging system used was easy to deploy, but the duration of the recordings and the image quality were limited. The more video time analysed, the more species would be detected; however, the probability of species passing in front of the camera during the video recording also needs to be considered (see Figure S4a,b as examples). In addition, factors such as the species' cryptic nature (see Figure S4 as an example) and the diminished light in deep waters further influence species detectability. This likely explains the observed lower species count in rhodolith beds compared with sandy stations, attributed to the cryptic nature of many species inhabiting rhodolith beds (e.g., *C. liechtensteini*, *Speleogobius trigloides* and *Odondebuenia balearica* detected in rhodolith beds by eDNA). The problem of detectability has already been documented for UVC in coral reefs (Polanco-Fernández et al., 2021) and for ROV in rhodolith beds (Illa-López et al., 2023). While the other techniques rely on indirect detection methods, such as DNA fragments or sounds, images provide direct and irrefutable evidence of species presence, reducing the possibility of false positives. Additionally, still video proves effective in characterizing the biophysical habitat and discerning habitat heterogeneity at the site scale, which is essential for providing context for the application of other techniques.

In contrast, eDNA metabarcoding identified a high number of fish taxa in the study area. In a previous project covering the entire Menorca Channel (Moranta et al., 2014), 30 species of fish (teleosts and elasmobranchs) were detected using ROV, while 90 species were detected with a trawling net ('GOC'). In the present study, focusing on the rhodolith bed within the channel (Figure 1), eDNA surveys detected 66 fish species (58 teleost species and 8 elasmobranchs). Of these species, 64% were common to the inventory obtained with the ROV, while only 42% of the species were also identified with the trawl survey. This evidence shows that eDNA is more effective for detecting fish species than the other non-extractive techniques tested, including the previously used ROV. At the same time, eDNA detected almost half of the diversity that was detected with the trawling net, although a full comparison cannot be made because we sampled only 10 stations on the rhodolith bed while the trawl survey covered a diversity of habitats (Moranta et al., 2014).

Significant differences in species composition between habitat types and fishing exposures were observed using eDNA. These findings align with expected hypotheses, such as observing a greater correlation with commercial species in unfished areas and more cryptic species associated with rhodolith bottoms (e.g., *S. trigloides* and *C. linearis*). Additionally, notable higher fish diversity (MOTUs) was found in both unfished zones and homogeneous habitats. These results suggest that eDNA is not only effective in detecting numerous fish species but also valuable for monitoring fish communities in relation to habitat heterogeneity and protection measures. eDNA metabarcoding was also effective for detecting endangered fish species, such as elasmobranchs. These findings align with results reported in other studies, such as He et al. (2023), Polanco-Fernández et al. (2021) or Juhel et al. (2018), supporting the idea that eDNA is a good approach for fast and cost-effective monitoring of highly diverse ecosystems. Given the approximate 2–3-day lifespan of DNA in temperate water, the captured sample spans a temporal scale of several days (Caza-Allard et al., 2021), and therefore it could be influenced not only by the hydrodynamics of the area (e.g., bottom currents) but also by the dynamics of the species (e.g., gregarious or solitary behaviour). This variability is particularly pertinent for the large pelagic species observed, underscoring the need for cautious interpretation of results. It is important to note that data for benthic species should be the most accurate due to their sedentary nature. On the other hand, while this method still presents challenges in accurately quantifying species abundance (Wong et al., 2022), it proves valuable for detecting a diverse set of species in our study area, including cryptobenthic species. Aglieri et al. (2020) showed that eDNA monitoring may go beyond the identification of taxonomic entities and be applied to ecological studies of functional diversity, providing more robust results than sampling with fishing nets or baited underwater video.

The third technique, bioacoustics, shows promise for fish monitoring in the Mediterranean rhodolith bed; however, it remains in the early stages of development. This technique only detected a maximum of 15 different types of sounds that were classified into six categories; four of these categories could be associated with a species or genus, whereas the other two lack referent information in the database, significantly reducing the total number of species this technique could potentially detect. Still, this technique provides unique information, as sound richness is the variety of sounds detected, representing a blend of various species emitting distinct sounds during different biological activities, such as vocalizations linked to courtship, territorial defence or warning sounds. The sounds detected include both unique sounds from the same species and distinct sounds from different species. Therefore, sound richness can be understood as a proxy for 'activity diversity'. When sound richness is lower, the habitat is more sonically homogeneous, either because the sounds are emitted by a few different species or because few biological activities are taking place. Conversely, when sound richness is high, the habitat is sonically heterogeneous, hosting either a greater number of fish species or a greater variety of different activities. On the other hand, sound abundance, representing the number of recorded sounds, whether similar or diverse, serves as a proxy for the 'activity abundance' or 'functionality' of the habitat (Mooney

10990755, 2024, 6, Downloaded from https://onlinelibrary.wiley.com/doi/10.1002/aqc.4212 by Csic Organizacion Central Om (Oficialia Mayor) (Unici), Wiley Online Library on [25/09/2024]. See the Terms and Conditions (https://onlinelibrary.wiley.com/terms-and-conditions) on Wiley Online Library for rules of use; OA articles are governed by the applicable Creative Commons License

et al., 2020). This suggests that acoustic richness and abundance are indicative of the habitat's support for fish breeding activity (Mooney et al., 2020).

Significant differences in sound richness among various habitat types were observed, although the limited data set prevented us from testing the specific habitat types where these differences occurred. The highest abundance of sounds was recorded in heterogeneous habitats such as the limits of rhodolith beds, sandy bottoms with rocky outcrops and sandy bottoms with less than 10% rhodolith coverage, possibly because they serve as preferred feeding habitats. These areas may foster a greater diversity of prey due to the presence of various habitats at small scales. As observed by de Juan et al. (2023), it is the combination of habitats that increases the total diversity of invertebrates in the area, which are potential prey for many fish species. In addition, some of these heterogeneous stations are also among the stations with the highest richness. These findings suggest that this technique could prove useful for detecting changes in sound richness across different habitat types with the availability of more comprehensive libraries in the future.

4.1 | Implications for conservation

The present study explores three non-extractive techniques for monitoring deep biogenic habitats, emphasizing their efficiency in demanding fewer resources and personnel compared with traditional methods like trawling nets. Therefore, these techniques provide a feasible alternative for monitoring marine habitats that are vulnerable to invasive sampling.

There exists a trade-off between non-destructiveness and the effectiveness of recording the species composition. In this study, the availability of fish DNA databases enabled eDNA to compile species lists independently of taxonomists' or local fishing knowledge (McDevitt et al., 2019). Therefore, regular fish monitoring through eDNA could provide indicators related to the conservation status of the area (Dalongeville et al., 2022). On the other hand, in terms of contextualizing the study area by assessing the habitat composition, video proves effective as it enables the detection of changes in algae coverage or composition, facilitating seascape monitoring. Finally, despite limited fish sound libraries in the Mediterranean, the bioacoustics technique is suitable for detecting species behaviour and the presence of some cryptobenthic species, such as *O. rochei*, which might elude detection by other methods.

Based on our findings and despite the difficulties in comparing the techniques and the limitations when interpreting results, we advocate the implementation of a monitoring programme that utilizes the three non-extractive techniques to document fish species associated with deep habitats like Mediterranean rhodolith beds. This programme should aim to assess the temporal dynamics of fish presence and activity in the area over time. However, further development in data analysis is required. For example, the development of more automatic identification of images (e.g., Catalán et al., 2023); the use of more than one molecular marker for eDNA in order to maximize the detection success of the technique (Polanco-Fernández et al., 2021); and the development of extensive libraries of sound-producing species that are still unidentified (Di Iorio et al., 2021). This strategic focus aims to facilitate the future generation of species lists and inventories, encompassing not only fish but also invertebrates, without the necessity of destructive sampling methods.

AUTHOR CONTRIBUTIONS

Andrea Cabrito: Conceptualization; methodology; data curation; writing—original draft; writing—review and editing; visualization; investigation; formal analysis. **Francesc Maynou**: Conceptualization; investigation; methodology; formal analysis; supervision; writing—review and editing. **Remy Simide**: Conceptualization; writing—review and editing; methodology. **David Mouillot**: Conceptualization; data curation; writing—review and editing. **Julie Lossent**: Conceptualization; writing—review and editing; data curation. **Silvia de Juan**: Conceptualization; methodology; formal analysis; writing—review and editing; supervision; investigation.

ACKNOWLEDGEMENTS

The authors are very thankful to Ewan Trégarot, Cindy Cornet, Loïc Sanchez, Raphael Seguin, Géraldine Pérez and Laia Illa-López for their indispensable assistance during the sampling and also to Giulia Cortinovis for her support on video analysis. Thanks also to Joan Moranta for facilitating the baseline information available in the Menorca Channel from the Life-INDEMARES project. Finally, thanks to the Ministry for Ecological Transition and Demographic Challenge for granting us the necessary permits for sampling. This work is developed within the framework of the EU H2020 project 'MaCoBioS' (contract no. 869710). This work is contributing to the ICM's 'Center of Excellence' Severo Ochoa (CEX2019-000928-5) and to the 'Maria de Maetzu' accredited to the IMEDEA (CEX2021-001198). SdJ was supported by a Ramon y Cajal postdoctoral grant funded by the Ministry of Science and Innovation (Plan Estatal I+D+I, 2017-2020; grant no. RyC2020-029062-I). AC is enrolled in the PhD programme in Marine Sciences at the University of Barcelona.

CONFLICT OF INTEREST STATEMENT

The authors declare no conflict of interest.

DATA AVAILABILITY STATEMENT

The data that support the findings of this study are available from the corresponding author upon reasonable request.

ETHICS AND PERMIT APPROVAL STATEMENT

No animal testing was performed during this study. All required permits for sampling and field studies were obtained by the authors from the appropriate authorities, as indicated in the acknowledgements.

10990755, 2024, 6, Downloaded from https://onlinelibrary.wiley.com/doi/10.1002/aqc.4212 by Csic Organizacion Central Om (Oficialia Mayor) (Unci), Wiley Online Library on [25/09/2024]. See the Terms and Conditions (https://onlinelibrary.wiley.com/terms-and-conditions) on Wiley Online Library for rules of use; OA articles are governed by the applicable Creative Commons License

REFERENCES

Aglieri, G., Baillie, C., Mariani, S., Cattano, C., Calò, A., Turco, G. et al. (2020). Environmental DNA effectively captures functional diversity of coastal fish communities. *Molecular Ecology*, 30(13), 3127–3139. https://doi.org/10.1111/mec.15661

Barbera, C., Bordehore, C., Borg, J.A., Glémarec, M., Grall, J., Hall-Spencer, J.M., et al. (2003). Conservation and management of northeast Atlantic and Mediterranean maerl beds. *Aquatic Conservation: Marine and Freshwater Ecosystems*, 13(S1), S65–S76. https://doi.org/10.1002/aqc.569

Barberá, C., Moranta, J., Ordines, F., Ramón, M., de Mesa, A., Díaz-Valdés, M. et al. (2012). Biodiversity and habitat mapping of Menorca Channel (Western Mediterranean): implications for conservation. *Biodiversity and Conservation*, 21(3), 701–728. https://doi.org/10.1007/s10531-011-0210-1

Bolgan, M., Soulard, J., Di Iorio, L., Gervaise, C., Lejeune, P., Gobert, S. et al. (2019). The sea chordophones make the mysterious/Kwa/: emitter identification of the dominating fish sound in Mediterranean seagrass meadows. *Journal of Experimental Biology*, 222(11), jeb.196931. https://doi.org/10.1242/jeb.196931

Boyer, F., Mercier, C., Bonin, A., Le Bras, Y., Taberlet, P. & Coissac, E. (2016). Obitools: a unix-inspired software package for DNA metabarcoding. *Molecular Ecology Resources*, 16(1), 176–182. https://doi.org/10.1111/1755-0998.12428

Cappo, M., Harvey, E., Malcolm, H. & Speare, P. (2003). Potential of video techniques to monitor diversity, abundance and size of fish in studies of marine protected areas. *Aquatic Protected Areas. What Works Best and How Do We Know*, 1, 455–464. https://www.semanticscholar.org/paper/Potential-of-video-techniques-to-monitor-diversity%2C-Cappo-Harvey/2b99d3f34a636dd59fce74fd87c6609a4ef0e5ed

Catalán, I.A., Álvarez-Ellacuría, A., Lisani, J.L., Sánchez, J., Vizoso, G., Heinrichs-Maquilón, A.E. et al. (2023). Automatic detection and classification of coastal Mediterranean fish from underwater images: good practices for robust training. *Frontiers in Marine Science*, 10. https://www.frontiersin.org/articles/10.3389/fmars.2023.1151758

Caza-Allard, I., Laporte, M., Côté, G., April, J. & Bernatchez, L. (2021). Effect of biotic and abiotic factors on the production and degradation of fish environmental DNA: an experimental evaluation. *Environmental DNA*, 4(2), 453–468. https://doi.org/10.1002/edn3.266

Collins, R.A., Wangensteen, O.S., O'Gorman, E.J., Mariani, S., Sims, D.W. & Genner, M.J. (2018). Persistence of environmental DNA in marine systems. *Communications Biology*, 1(1), 185. https://doi.org/10.1038/s42003-018-0192-6

Costa, A.C.P., Garcia, T.M., Paiva, B.P., Neto, A.R.X. & de Oliveira, S.M. (2020). Seagrass and rhodolith beds are important seascapes for the development of fish eggs and larvae in tropical coastal areas. *Marine Environmental Research*, 161, 105064. https://doi.org/10.1016/j.marenvres.2020.105064

Dalongeville, A., Boulanger, E., Marques, V., Charbonnel, E., Hartmann, V., Santoni, M.C. et al. (2022). Benchmarking eleven biodiversity indicators based on environmental DNA surveys: more diverse functional traits and evolutionary lineages inside marine reserves. *Journal of Applied Ecology*, 59(11), 2803–2813. https://doi.org/10.1111/1365-2664.14276

De Cáceres M, Jansen M, De Caceres FMM, (2022). *Indicator species analysis using 'indicspecies'*.

de Juan, S., Hewitt, J., Thrush, S. & Freeman, D. (2015). Standardising the assessment of functional integrity in benthic ecosystems. *Journal of Sea Research*, 98, 33–41. https://doi.org/10.1016/j.seares.2014.06.001

de Juan, S., Hinz, H., Sartor, P., Vitale, S., Bentes, L., Bellido, J.M. et al. (2020). Vulnerability of demersal fish assemblages to trawling activities: a traits-based index. *Frontiers in Marine Science*, 7. https://doi.org/10.3389/fmars.2020.00044

de Juan, S., Lo Iacono, C. & Demestre, M. (2013). Benthic habitat characterisation of soft-bottom continental shelves: integration of acoustic surveys, benthic samples and trawling disturbance intensity. *Estuarine, Coastal and Shelf Science*, 117, 199–209. https://doi.org/10.1016/j.ecss.2012.11.012

de Juan, S., Ospina-Alvarez, A., Hinz, H., Moranta, J. & Barberá, C. (2023). The continental shelf seascape: a network of species and habitats. *Biodiversity and Conservation*, 32. https://doi.org/10.1007/s10531-023-02552-8

Demestre, M., Soto, S., Durán, R., García del Arco, J.A., Cabrito, A., Illa-Lopez, L. et al. (2024). Reconstruction of the Maërl habitat to better understand its ecological integrity. *Science of the Total Environment*, 912, 168752. https://doi.org/10.1016/j.scitotenv.2023.168752

Desiderà, E., Guidetti, P., Panzalis, P., Navone, A., Valentini-Poirrier, C.A., Boissery, P. et al. (2019). Acoustic fish communities: sound diversity of rocky habitats reflects fish species diversity. *Marine Ecology Progress Series*, 608, 183–197. https://doi.org/10.3354/meps12812

Di Iorio, L., Audax, M., Deter, J., Holon, F., Lossent, J., Gervaise, C. et al. (2021). Biogeography of acoustic biodiversity of NW Mediterranean coralligenous reefs. *Scientific Reports*, 11, 16991. https://doi.org/10.1038/s41598-021-96378-5

Fragkopoulou, E., Serrão, E.A., Horta, P.A., Koerich, G. & Assis, J. (2021). Bottom trawling threatens future climate refugia of rhodoliths globally. *Frontiers in Marine Science*, 7, 594537. https://doi.org/10.3389/fmars.2020.594537

Hall-Spencer, J.M., Grall, J., Moore, P.G. & Atkinson, R.J.A. (2003). Bivalve fishing and Maerl-bed conservation in France and the UK-retrospect and prospect. *Aquatic Conservation: Marine and Freshwater Ecosystems*, 13(S1), S33–S41. https://doi.org/10.1002/aqc.566

He, X., Jeffery, N.W., Stanley, R.R.E., Hamilton, L.C., Rubidge, E.M. & Abbott, C.L. (2023). eDNA metabarcoding enriches traditional trawl survey data for monitoring biodiversity in the marine environment. *ICES Journal of Marine Science*, 80(5), 1529–1538. https://doi.org/10.1093/icesjms/fsad083

Illa-López, L., Cabrito, A., de Juan, S., Maynou, F. & Demestre, M. (2023). Distribution of rhodolith beds and their functional biodiversity characterisation using ROV images in the Western Mediterranean Sea. *Science of the Total Environment*, 905, 167270. https://doi.org/10.1016/j.scitotenv.2023.167270

Juhel, J.B., Laurent, V., Mouillot, D., Kulbicki, M., Letessier, T.B., Meeuwig, J.J. et al. (2018). Reef accessibility impairs the protection of sharks. *Journal of Applied Ecology*, 55(2), 673–683. https://doi.org/10.1111/1365-2664.13007

Juhel, J.B., Utama, R.S., Marques, V., Vimono, I.B., Sugeha, H.Y., Kadarusman, P.L. et al. (2020). Accumulation curves of environmental DNA sequences predict coastal fish diversity in thecoral triangle. *Proceedings of the Royal Society B*, 287(1930), 20200248. https://doi.org/10.1098/rspb.2020.0248

Kuhnz, L.A., Gilbane, L., Cochrane, G.R. & Paull, C.K. (2022). Multi-factor biotopes as a method for detailed site characterization in diverse benthic megafaunal communities and habitats in deep-water off Morro Bay, California. *Deep Sea Research Part I: Oceanographic Research Papers*, 190, 103872. https://doi.org/10.1016/j.dsr.2022.103872

Legrand, E., Riera, P., Lutier, M., Coudret, J., Grall, J. & Martin, S. (2017). Species interactions can shift the response of a Maerl bed community to ocean acidification and warming. *Biogeosciences*, 14(23), 5359–5376. https://doi.org/10.5194/bg-14-5359-2017

Letessier, T.B., Juhel, J.B., Vigliola, L. & Meeuwig, J.J. (2015). Low-cost small action cameras in stereo generates accurate underwater measurements of fish. *Journal of Experimental Marine Biology and Ecology*, 466, 120–126. https://doi.org/10.1016/j.jembe.2015.02.013

Loh, T.-L., Archer, S.K. & Dunham, A. (2019). Monitoring program design for data-limited marine biogenic habitats: a structured approach.

10990755, 2024, 6, Downloaded from https://onlinelibrary.wiley.com/doi/10.1002/aqc.4212 by Csic Organizacion Central Om (Oficialia Mayor) (Unci), Wiley Online Library on [25/09/2024]. See the Terms and Conditions (https://onlinelibrary.wiley.com/terms-and-conditions) on Wiley Online Library for rules of use; OA articles are governed by the applicable Creative Commons License

Ecology and Evolution, 9(12), 7346–7359. https://doi.org/10.1002/ece3.5261

López-Garrido, P.H., Barry, J.P., González-Gordillo, J.I. & Escobar-Briones, E. (2020). ROV's video recordings as a tool to estimate variation in megabenthic epifauna diversity and community composition in the Guaymas Basin. *Frontiers in Marine Science*, 7, 154. https://doi.org/10.3389/fmars.2020.00154

Maggio, T., Perzia, P., Pazzini, A., Campagnuolo, S., Falautano, M., Mannino, A.M. et al. (2022). Sneaking into a hotspot of biodiversity: coverage and integrity of a rhodolith bed in the strait of Sicily (Central Mediterranean Sea). *Journal of Marine Science and Engineering*, 10(12), 1808. https://doi.org/10.3390/jmse10121808

Mahé, F., Rognes, T., Quince, C., de Vargas, C. & Dunthorn, M. (2015). Swarm v2: highly-scalable and high-resolution amplicon clustering. *PeerJ*, 3, 1–12. https://peerj.com/articles/1420

Martin, M. (1994). Cutadapt removes adapter sequences from high-throughput sequencing reads. *EMBnet. Journal*, 17(1), 10–12.

Mathon, L., Marques, V., Manel, S., Albouy, C., Andrello, M., Boulanger, E. et al. (2023). The distribution of coastal fish eDNA sequences in the Anthropocene. *Global Ecology and Biogeography*, 32(8), 13698. https://doi.org/10.1111/geb.13698

McDevitt, A.D., Guimarães Sales, N., Browett, S.S., Sparnenn, A.O., Mariani, S., Wangensteen, O.S. et al. (2019). Environmental DNA metabarcoding as an effective and rapid tool for fish monitoring in canals. *Journal of Fish Biology*, 95(2), 679–682. https://doi.org/10.1111/jfb.14053

Mirimin, L., Desmet, S., López Romero, D., Fernandez Fernandez, S., Miller, D.L., Mynott, S. et al. (2021). Don't catch me if you can—using cabled observatories as multidisciplinary platforms for marine fish community monitoring: an *in situ* case study combining Underwater Video and environmental DNA data. *Science of the Total Environment*, 773, 145351. https://doi.org/10.1016/j.scitotenv.2021.145351

Miya, M. (2022). Environmental DNA metabarcoding: a novel method for biodiversity monitoring of marine fish communities. *Annual Review of Marine Science*, 14(1), 161–185. https://doi.org/10.1146/annurev-marine-041421-082251

Mooney, T.A., Di Iorio, L., Lammers, M., Lin, T.-H., Nedelec, S.L., Parsons, M. et al. (2020). Listening forward: approaching marine biodiversity assessments using acoustic methods. *Royal Society Open Science*, 7(8), 201287. https://doi.org/10.1098/rsos.201287

Moranta J, Barberá C, Druet Vélez M, Díaz-Valdés M, Zaragoza N, Tello-Antón MO, López-Jurado JL, Balbín R, Flexas MDM, Fernández M, Hidalgo M, Domínguez M, Quetglas A, Goñi R, Mallol S, Sánchez-Delgado F, Ambroso S, Comalada N (2014). Caracterización ecológica de la plataforma continental (50-100 m) del canal de Menorca. Informe final área LIFE+ INDEMARES (LIFE07/NAT/E/000732). Instituto Español de Oceanografía-Centro Oceanográfico de Baleares (Palma). Coordinación: Fundación Biodiversidad, Palma, 504 pág. http://hdl.handle.net/10261/318214

Mueller, R.P., Brown, R.S., Hop, H. & Moulton, L. (2006). Video and acoustic camera techniques for studying fish under ice: a review and comparison. *Reviews in Fish Biology and Fisheries*, 16, 213–226. https://doi.org/10.1007/s11160-006-9011-0

Muff, M., Jaquier, M., Marques, V., Ballesta, L., Deter, J., Bockel, T. et al. (2023). Environmental DNA highlights fish biodiversity in mesophotic ecosystems. *Environmental DNA*, 5(1), 56–72. https://doi.org/10.1002/edn3.358

Ordines, F. & Massutí, E. (2009). Relationships between macro-epibenthic communities and fish on the shelf grounds of the Western Mediterranean. *Aquatic Conservation: Marine and Freshwater Ecosystems*, 19(4), 370–383. https://doi.org/10.1002/aqc.969

Peña, V., Bárbara, I., Grall, J., Maggs, C.A. & Hall-Spencer, J.M. (2014). The diversity of seaweeds on Maerl in the NE Atlantic. *Marine Biodiversity*, 44(4), 533–551. https://doi.org/10.1007/s12526-014-0214-7

Picciulin, M., Sebastianutto, L., Codarin, A., Calcagno, G. & Ferrero, E.A. (2012). Brown meagre vocalization rate increases during repetitive boat noise exposures: a possible case of vocal compensation. *The Journal of the Acoustical Society of America*, 132(5), 3118–3124. https://doi.org/10.1121/1.4756928

Pinna, M., Zangaro, F., Saccomanno, B., Scalone, C., Bozzeda, F., Fanini, L. et al. (2023). An overview of ecological indicators of fish to evaluate the anthropogenic pressures in aquatic ecosystems: from traditional to innovative DNA-based approaches. *Water*, 15(5), 949. https://doi.org/10.3390/w15050949

Polanco-Fernández, A., Marques, V., Fopp, F., Juhel, J.B., Borrero-Pérez, G.E., Cheutin, M.C. et al. (2021). Comparing environmental DNA metabarcoding and underwater visual census to monitor tropical reef fishes. *Environmental DNA*, 3(6), 142–156. https://doi.org/10.1002/edn3.140

Pont, D., Rocle, M., Valentini, A., Civade, R., Jean, P., Maire, A. et al. (2018). Environmental DNA reveals quantitative patterns of fish biodiversity in large rivers despite its downstream transportation. *Scientific Reports*, 8, 10361. https://doi.org/10.1038/s41598-018-28424-8

R Core Team. (2022). *R: a language and environment for statistical computing*. Vienna, Austria. R Foundation for Statistical Computing. https://www.R-project.org/

Rabin, L.A. & Greene, C.M. (2002). Changes to acoustic communication systems in human-altered environments. *Journal of Comparative Psychology*, 116(2), 137–141. https://doi.org/10.1037/0735-7036.116.2.137

Riosmena-Rodríguez, R., Nelson, W. & Aguirre, J. (Eds.) (2017). *Rhodolith/Maërl beds: a global perspective*, Vol. 15: Springer International Publishing. https://doi.org/10.1007/978-3-319-29315-8

Rognes, T., Flouri, T., Nichols, B., Quince, C. & Mahé, F. (2016). VSEARCH: a versatile open source tool for metagenomics. *PeerJ*, 4. https://doi.org/10.7717/peerj.2584

Romagnoli, B., Grasselli, F., Costantini, F., Abbiati, M., Romagnoli, C., Innangi, S. et al. (2021). Evaluating the distribution of priority benthic habitats through a remotely operated vehicle to support conservation measures off Linosa Island (Sicily Channel, Mediterranean Sea). *Aquatic Conservation: Marine and Freshwater Ecosystems*, 31(7), 1686–1699. https://doi.org/10.1002/aqc.3554

Sanchez, L., Boulanger, E., Arnal, V., Boissery, P., Dalongeville, A., Dejean, T. et al. (2022). Ecological indicators based on quantitative eDNA metabarcoding: the case of marine reserves. *Ecological Indicators*, 140, 108966. https://www.sciencedirect.com/science/article/pii/S1470160X2200437X?via%3Dihub

Sato, M., Inoue, N., Nambu, R., Furuichi, N., Imaizumi, T. & Ushio, M. (2021). Quantitative assessment of multiple fish species around artificial reefs combining environmental DNA metabarcoding and acoustic survey. *Scientific Reports*, 11, 19477. https://doi.org/10.1038/s41598-021-98926-5

Sciberras, M., Rizzo, M., Mifsud, J., Camilleri, K., Borg, J.A., Lanfranco, E. et al. (2009). Habitat structure and biological characteristics of a maerl bed off the northeastern coast of the Maltese Islands (central Mediterranean). *Marine Biodiversity*, 39, 251–264. https://doi.org/10.1007/s12526-009-0017-4

Stat, M., John, J., Di Battista, J.D., Newman, S.J., Bunce, M. & Harvey, E.S. (2019). Combined use of eDNA metabarcoding and video surveillance for the assessment of fish biodiversity. *Conservation Biology*, 33(1), 196–205. https://doi.org/10.1111/cobi.13183

Trégarot, E., D'Olivo, J.P., Botelho, A.Z., Cabrito, A., Cardoso, G.O., Casal, G. et al. (2023). Effects of climate change on marine coastal ecosystems—a review to guide research and management. *Biological Conservation*, 289. https://doi.org/10.1016/j.biocon.2023.110394

Tuya, F., Schubert, N., Aguirre, J., Basso, D., Bastos, E.O., Berchez, F. et al. (2023). Levelling-up rhodolith-bed science to address global-scale

10990755, 2024, 6, Downloaded from https://onlinelibrary.wiley.com/doi/10.1002/aqc.4212 by Csic Organización Central Om (Oficialia Mayor) (Uici), Wiley Online Library on [25/09/2024]. See the Terms and Conditions (https://onlinelibrary.wiley.com/terms-and-conditions) on Wiley Online Library for rules of use; OA articles are governed by the applicable Creative Commons License

conservation challenges. *Science of the Total Environment*, 892, 164818. https://doi.org/10.1016/j.scitotenv.2023.164818

Valentini, A., Taberlet, P., Miaud, C., Civade, R., Herder, J., Thomsen, P.F. et al. (2016). Next-generation monitoring of aquatic biodiversity using environmental DNA metabarcoding. *Molecular Ecology*, 25(4), 929–942. https://doi.org/10.1111/mec.13428

Wangensteen, O.S. & Turón, X. (2017). Metabarcoding techniques for assessing biodiversity of marine animal forests. *Marine animal forests. The ecology of benthic biodiversity hotspots*, 1, 445–503. https://doi.org/10.1007/978-3-319-17001-5_53-1

Wong, M.K.W., Nobata, S., Ito, S.I. & Hyodo, S. (2022). Development of species-specific multiplex real-time PCR assays for tracing the small pelagic fishes of North Pacific with environmental DNA. *Environmental DNA*, 4(3), 510–522. https://doi.org/10.1002/edn3.275

SUPPORTING INFORMATION

Additional supporting information can be found online in the Supporting Information section at the end of this article.

How to cite this article: Cabrito, A., Maynou, F., Simide, R., Mouillot, D., Lossent, J. & de Juan, S. (2024). Non-extractive fish diversity assessment in Mediterranean rhodolith beds. *Aquatic Conservation: Marine and Freshwater Ecosystems*, 34(6), e4212. https://doi.org/10.1002/aqc.4212

10990755, 2024, 6, Downloaded from https://onlinelibrary.wiley.com/doi/10.1002/aqc.4212 by Csic Organización Central Om (Oficialia Mayor) (Unci), Wiley Online Library on [25/09/2024]. See the Terms and Conditions (https://onlinelibrary.wiley.com/terms-and-conditions) on Wiley Online Library for rules of use; OA articles are governed by the applicable Creative Commons License

APPENDIX II.

ORIGINAL PUBLISHED PAPERS AND DRAFTS THAT DO NOT FORM PART OF THIS THESIS BUT ARE LINKED.



Science of the Total Environment 905 (2023) 167270

Contents lists available at ScienceDirect

Science of the Total Environment

journal homepage: www.elsevier.com/locate/scitotenv

Distribution of rhodolith beds and their functional biodiversity characterisation using ROV images in the western Mediterranean Sea

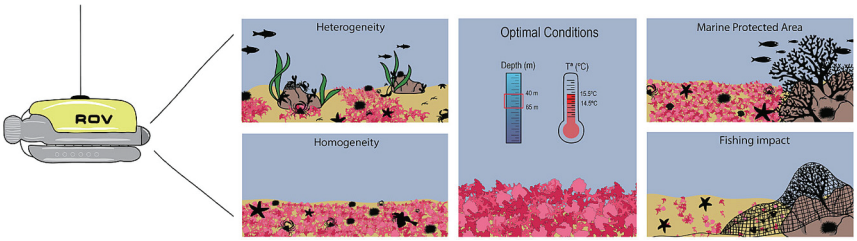
Laia Illa-López [a,*], Andrea Cabrito [a], Sílvia de Juan [b], Francesc Maynou [a], Montserrat Demestre [a]

[a] Institut de Ciències del Mar (ICM-CSIC), Passeig Marítim de la Barceloneta 37-49, Barcelona, Spain
[b] Institut Mediterrani d'Estudis Avançats (IMEDEA-CSIC), Carrer Miquel Marquès 21, Esporles, Spain

HIGHLIGHTS

- Video surveys showed that rhodoliths accumulate on coarse sediment bottoms.
- Relative abundance of rhodoliths was driven by depth and temperature.
- The optimal depth range for the occurrence of rhodoliths extended from 40 to 65 m while the temperature range was between 14.5 °C and 15.5 °C.
- Rhodolith beds on fishing grounds showed the lowest functional richness index.
- Functional richness was higher on heterogeneous sea-beds rather than on homogenous ones (higher β-diversity).

GRAPHICAL ABSTRACT



ARTICLE INFO

Guest Editor: Aridane G. Gonzalez

Keywords:
Biogenic habitat
Biological traits
Biophysical parameters
maërl beds
Species distribution models
Video monitoring

ABSTRACT

Underwater biogenic habitats composed of unattached calcified red algae, named as rhodolith or maërl beds, may extant either alive or dead, over the seabed. The accumulation of rhodoliths constitute three-dimensional structured biogenic habitats that harbour high diversity of benthic organisms. In the Mediterranean Sea, rhodolith beds can be found between ca. 50 and 100 m, increasing diversity of the continental shelf habitats and their conservation value. Despite the remarkable relevance of these habitats, information regarding their spatial distribution in the western Mediterranean is scarce. In addition, these habitats are threatened by a range of anthropogenic activities and by climate-driven changes. In this study, we explored areas with rhodoliths' occurrence from the north to the south of the east coast of Spain. By feeding video recording data into a spatial distribution model, we assessed which biophysical drivers: (i) shape the spatial variation in the abundance of rhodoliths and (ii) define the assemblages of the biological traits and functional richness of the associated epibenthic fauna recorded by video. In addition, we examined the impact of fishing activities on these habitats. Our results evidenced that 'Depth' and 'Temperature' were important environmental factors explaining rhodoliths variation, and we defined their optimal distribution range in the western Mediterranean. The biological traits approach showed significant effects of the geographical location of rhodolith beds and their small-scale spatial heterogeneity on the functional richness index. Indeed, the lowest functional richness value was observed in the area closer to trawl fishing which could be related to habitat degradation due to trawling. This study contributes to the knowledge of deep-water rhodolith beds in the western Mediterranean and reinforce the importance of rhodolith beds in continental shelves as these constitute heterogeneous seabed habitats that harbour a high species and functional diversity.

* Corresponding author.
E-mail address: illa@icm.csic.es (L. Illa-López).

https://doi.org/10.1016/j.scitotenv.2023.167270
Received 25 April 2023; Received in revised form 8 September 2023; Accepted 20 September 2023
Available online 22 September 2023
0048-9697/© 2023 The Authors. Published by Elsevier B.V. This is an open access article under the CC BY-NC-ND license (http://creativecommons.org/licenses/by-nc-nd/4.0/).

1. Introduction

Rhodolith beds are accumulations of living and dead unattached coralline algae that can cover large areas of the seafloor (Barberá et al., 2003; Neves et al., 2021). Also known as maërl beds (Foster, 2001), these complex habitats occur worldwide, from tropical to polar environments (Bosence, 1983; Foster, 2001). In European waters, they are found along the North-East Atlantic coast, from Svalbard to Portugal (Barberá et al., 2003; Peña et al., 2014) and in the Mediterranean Sea (Ballesteros, 1988). In the western Mediterranean, these beds occur from subtidal waters down to 100 m depth (Riosmena-Rodríguez et al., 2017), generally accumulating over soft sediments (de Juan et al., 2013).

Studies focused on the spatial distribution of rhodolith beds identify major environmental conditions which determine habitat structure, for instance, light, sedimentation, hydrodynamics (currents and wave turbulence) and temperature (Carvalho et al., 2020; Holz et al., 2020; Martin et al., 2014; Sañé et al., 2016; Sciberras et al., 2009; Wilson et al., 2004). In the European Atlantic waters, rhodolith beds occur from low intertidal waters down to 50 m depth in very clear waters (Peña et al., 2014). Nevertheless, in the oligotrophic Mediterranean Sea, the low terrestrial sediment input caused by the absence of large rivers allows sufficient light availability to reach greater depths (Ballesteros, 1989.; Barberá et al., 2003; Barberá et al., 2012; Foster, 2001; Joher et al., 2016). In addition, the influence of hydrodynamics and sedimentation defines the occurrence and shape the structure of rhodoliths (Bracchi et al., 2019; Foster, 2001; Sañé et al., 2016; Sciberras et al., 2009). Water motion is key to prevent the smothering of rhodoliths by fine sediments (Joshi and Farrell, 2020; Marrack, 1999; Wilson et al., 2004). However, high water movement can translocate rhodoliths and break them up, thus constraining their distribution (Marrack, 1999; Otero-Ferrer et al., 2020). Temperature is also a key driver of the geographical distribution of rhodoliths by determining the species composition at large-scale (Wilson et al., 2004).

Rhodolith algae are widely acknowledged as ecosystem engineers and hotspots of marine life that provide structural and functional complexity and supply a variety of ecosystem functions (de Juan et al., 2023; Kamenos et al., 2004; Tuya et al., 2023). The characteristic three-dimensional hard structures of rhodoliths provide refuge and nursery for juveniles of commercial species (Costa et al., 2020; Ordines and Massutí, 2009) and create microhabitats providing shelter and food for a great diversity of macrofauna, such as molluscs, crustaceans and polychaetes (Barberá et al., 2003; Foster, 2001; Kamenos et al., 2004; Sciberras et al., 2009). Moreover, rhodolith beds, as biogenic calcareous habitats, could contribute to long-term carbon sequestration and, due to their global distribution, constitute one of the most important carbonate deposits of the world (Amado-Filho et al., 2012; Martin et al., 2005, 2007).

Despite rhodolith beds have a remarkable conservation value, numerous human activities, such as bottom trawling, effluent discharges or alien species, as well as climate change-driven impacts, threaten their ecological integrity (Barberá et al., 2017; Peña et al., 2014; Rindi et al., 2019; Riosmena-Rodríguez et al., 2017). Legislation measures have been proposed to increase their conservation status and implement fishery regulations by banning trawling activities on these habitats (i.e., Barcelona Convention Decision 1999/800/EC, and Mediterranean Fisheries Regulation EC no. 1967/2006, Order AAA/2808/2012) (Barberá et al., 2017). In addition, two maërl-forming species, that have been identified in the Mediterranean, *Phymatolithon calcareum* and *Lithothamnion corallioides,* are considered species of community interest included in Annex V of the EC Habitats Directive (Council Directive 92/43/EEC) (Wilson et al., 2004).

Shifting the focus to a regional perspective, in the western Mediterranean, the current spatial distribution and occurrence of rhodolith beds largely respond to historically fishing pressure and changes in environmental conditions (Barberá et al., 2012; de Juan et al., 2013; Wilson et al., 2004). However, the lack of current and past information about rhodolith beds distribution and small-scale heterogeneity makes the assessment of their evolution in time difficult. Considering the scarce information available on western Mediterranean rhodolith beds, it is mandatory to define the limits of the parameters driving their distribution. Our working hypothesis is that the suitable area for rhodolith beds development over continental shelves is conditioned by a narrow range of variability of environmental factors. Therefore, the objective of the present study is to define which biophysical factors drive: (i) the abundance of rhodoliths and (ii) assemblages of the biological traits of the associated epibenthic biodiversity in rhodolith beds, as well as, their functional richness index in the east coast of Spain. In order to do so, soft bottoms with rhodoliths occurrence were explored using video recording, a non-intrusive technique that allows the acquisition of a diversity data in a continuous scale frame while minimizing habitat alteration (Bicknell et al., 2016; Hewitt et al., 2004).

Ecological models were applied to identify biophysical drivers shaping the variation in the abundance of rhodoliths identified in areas of the seabed through video transects. We applied Species Distribution Models (SDM), a useful tool in Ecology to describe the complex, often non-linear, relationships between species and their environment and build predictors of species distribution at multiple spatio-temporal scales (Elith and Leathwick, 2009; Morán-Ordóñez et al., 2017). Video techniques have also proven to be a good mechanism to extract information on the biological traits of the observed organisms through taxonomical expert knowledge (de Juan et al., 2015). Analysis of biological traits is an approach widely used in marine ecological studies to assess changes in communities as a response to environmental conditions and human impacts (i.e., bottom trawling) (de Juan et al., 2007). Biological traits approach can also be applied to unravel ecosystem functions in order to understand the functional role of species' assemblages and the consequences of alterations in a community (Boyé et al., 2019; de Juan et al., 2022). In this study, a biological-traits approach was applied to the list of species identified in the video footage to be analysed as a proxy of functional diversity associated to rhodolith beds. Finally, we examined the impact of fisheries on these habitats in the western Mediterranean.

2. Material and methods

2.1. Study area

To explore the drivers of rhodoliths distribution over the western Mediterranean continental shelves, we selected three study areas located between 40 and 100 m depth, along the east coast of Spain (western Mediterranean), from north to south: Continental shelf off Blanes (BL), Columbretes Islands (COL) and Cabo de Palos e Islas Hormigas (CP) (Fig. 1). These areas were selected based on previous knowledge extracted from the research projects COMSOM, FORMED and MINOUW (de Juan et al., 2013; Demestre et al., 2017; García-de-Vinuesa et al., 2018). The study areas are in different environmental contexts along the Spanish coast, including differences in the geomorphology of the continental shelf and intensity of fishing activities. Each transect was defined according to previous knowledge from experts on potential areas of rhodoliths aggregations, besides Guillén et al. (2017) provides geomorphological information on our study areas.

The study area BL is located in the shallower area of a submarine canyon in front of the port of Blanes (Catalonia, Spain) (Fig. 1). The submarine canyon is surrounded by fishing grounds ranging from 50 m down to 800 m. Considering the wide depth range, the area has a high habitat heterogeneity, with the alternation of crinoid aggregation habitats, muddy bottoms and rhodolith beds (observations from MINOUW project). This area is a productive fishing ground, where bottom trawling is the main fishing technique (García-de-Vinuesa et al., 2018).

The study area COL is located offshore the coast of Castelló (Spain) and it is around a volcanic archipelago formed by a set of three groups of islets and one main island. This area is characterized by the presence of CO_2 vents between 35 and 50 m, which determines the composition of

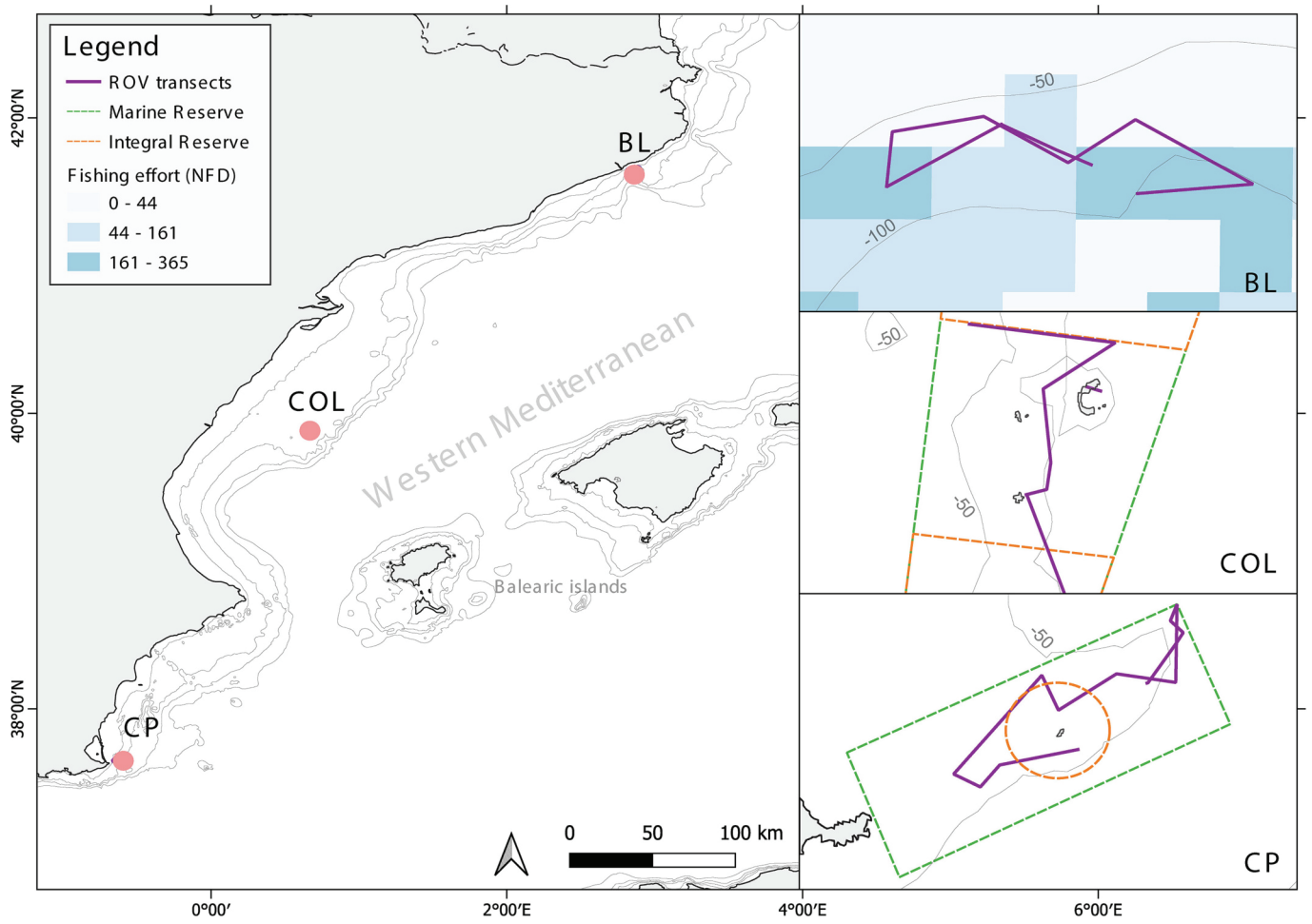


Fig. 1. Map of the studied areas along the east coast of Spain in the western Mediterranean Sea. From north to south: BL: Continental shelf off Blanes; COL: Columbretes Islands and CP: Cabo de Palos. Purple line represents the transects recorded with the ROV. (BL): Fishing effort (Number of Fishing Days x boat) for the year 2018 is represented in blue. (COL) and (CP): Green and orange dotted lines delineate the marine and the integral areas of both Marine Reserve Areas, respectively.

benthic communities and habitats (Linares et al., 2015). The entire archipelago is a Marine Natural Park since 1990 (BOE n° 97, of 23rd April 1990), where no trawl fishing is allowed, but limited artisanal fishing is permitted.

The study area CP is located in the "Cabo de Palos e Islas Hormigas" Marine Reserve (Murcia, Spain). This area is found at depths between 40 and 50 m, and it is characterized by the presence of rhodolith, gravel, sands and mud (de Juan et al., 2013). The Marine Reserve was created in 1995 (BOE n° 161, of 7th July 1995), where bottom trawling is not permitted but limited artisanal fishing in the periphery of the Marine Protected Area (MPA) can be carried out. The study area encompassed the protected and nearby unprotected area around the reserve.

2.2. Video analysis for data acquisition

The study areas were surveyed in September 2020 using a Remotely Operated Vehicle equipped with video, ROV-LIROPUS, towed by the R/V "Sarmiento de Gamboa" along the three pre-defined transects (Fig. 1). Positioning of the ROV with respect to the sea-floor was ensured by differential Global Positioning System (GPS). The ROV was equipped with high-resolution cameras, which allowed us to record georeferenced video. It was also equipped with two lasers separated by a distance of 10 cm, that allowed the estimation of organism sizes, and with data-loggers for continuous recording of temperature (°C) and depth (m). This information allowed us to calculate slope (m/min, calculated as the depth change per minute) and swept area per minute (m^2/min). The ROV moved with an average speed of 0.5 knots and toured a mean of 11 km per transect, corresponding to an average of 16 h of video recording.

The video footage was visualized using the VLC media player, a free and open-source multimedia player and framework. The information of interest was the relative rhodolith coverage along the transect, the visible fauna (fishes and invertebrates) and flora (algae), and the physical characteristics of the seabed. For this purpose, two observers visualized the videos. When an organism was detected, the video was paused and the following information was annotated:

(i) Identification and quantification of visible fauna and flora (minimum size 4 cm) at the lowest taxonomic level possible (species whenever possible).
(ii) Estimation of rhodolith coverage: the percentage of coverage was visually determined by comparing the four levels defined. These levels were: 0 - rhodolith absence -, 1 -<25 %-, 2 - ≥25 ≤ 50 %-, 3 - >50 %- (Fig. A.1).
(iii) Description of biophysical parameters:

- **Substrate type:** Visual characterization of the sediment considering the categories: sandy, muddy sand, sandy mud, mud, mixed sediment (with the presence of gravel of different sizes and shells), coarse sediment (biogenic sand and

homogenous gravel), and rocky bottoms (rock or other hard substrata) (Fig. A.2).

- **Bottom relief:** Considered flat or with the presence of ripples (Fig. A.3).
- **Presence of rocky outcrops:** Considered when there were rocky outcrops with associated fauna or flora (Fig. A.4).
- **Presence of algal cover:** Filamentous algal covering substrate (Fig. A.4).
- **Presence of fisheries** footprint, such as lost or abandoned fishing nets or trawl tracks.

2.3. Data processing

The information gathered during the video visualization were grouped into 1 min interval. The quantitative variables (occurrences of each taxon) were calculated as the total sum, while for the qualitative variables such as rhodolith coverage and the biophysical parameters, the predominant category within the minute was noted. Based on this information, two data matrices were created:

(i) Environmental data

The environmental data matrix included the rhodolith coverage, the biophysical parameters described beforehand and the environmental variables such as depth and temperature. In this step, the substrate type variable was reduced to 4 levels -Mud, Mixed sediment, Coarse sediment and Rocky or other hard substrata-. Finally, the environmental data matrix was set up by adding a last variable:

- **Number of biotopes:** the number of biotopes that appeared when grouping observations into 1 min clusters was noted as a measure of small-scale heterogeneity. For this purpose, a biotope was counted whenever substrate composition, relief and/or rhodolith cover changed significantly.

(ii) Biological traits

A species density matrix was calculated for each minute as the sum of individuals per swept area (ind/m^2). Each taxon identified in the video footage was then described considering the biological traits categories listed in Table 1. The biological traits included in the analysis were chosen for their suitability to inform on the sensitiveness of species to fishing and/or could be associated with ecosystem functions in soft bottoms (de Juan et al., 2015).

The biological traits assignation to each taxon was based on information extracted from different sources such as WoRMS (WoRMS editorial Board, 2023), Fishbase (Froese and Pauly, 2023), MarLIN (Marine Life Information Network, 2020) and its catalogue of biological traits information BIOTIC (MarLin, 2006), as well as from expert knowledge (e.g., de Juan et al., 2007; de Juan and Demestre, 2012). The information was summarized using a binary code in a conversion matrix (i.e., trait absent or present). The taxon density matrix was multiplied by the conversion matrix to obtain the biological traits density matrix for its subsequent analysis.

Table 1
List of biological traits and their levels considered to characterize large epibenthic fauna (after de Juan et al., 2015).

Biological traits	Levels
Size	Small (<1 cm), medium (1–5 cm), large (>5 cm)
Age	Annual, short, medium, long
Morphology	Arborescent, articulate, bivalved, crustose, cushion, flat, globose, stellate, turbinate, vermiform
Composition	Calcareous, chitinous, cuticle, none
Habitat	Attached, surface, subsurface
Mobility	Sessile, sedentary, crawler, swimmer
Feeding	Deposit feeder, suspension feeder, grazer, benthivorous, piscivorous, predatory opportunistic, planktivorous, primary producer

Finally, the data from both matrices was assembled at 15 min intervals, considered the optimal time interval to have sufficient representativeness of taxa for statistical analysis. For each interval the mean was calculated for the numerical variables, while for categorical variables the most abundant characteristic was selected, with the exception of the variable 'Number of biotopes'. The information provided by this variable along the 15 min was classified within 3 categories: Homogeneous, a unique biotope typology within the 15 min; 2 Biotopes, – two different biotope typologies alternate in the 15 min (e.g., muddy sands and coarse sediment with <25 % rhodoliths); and, >2 Biotopes, >2 biotope typologies alternate or appear in the 15 min-.

A description of each study area was performed by calculating the percentage of area covered by substrate type and rhodolith abundance, in order to visually define the extension of substrate type and rhodolith coverage assemblages. Then, an estimation of taxonomic biodiversity was done through the quantification in percentage of the phyla and species in each area. In order to characterize the most abundant species in each area according to substrate type and rhodolith abundance, the percentages of the three species with higher density were represented.

2.4. Statistical analysis

2.4.1. Environmental factors explaining rhodolith abundance

In order to identify the biophysical factors driving the distribution and abundance of rhodoliths over continental shelves in the study sites, we applied a species distribution model. SDMs use statistical algorithms that fit observations of species occurrence or abundance data to environmental conditions (Elith and Leathwick, 2009). The choice of statistical algorithms available to build SDMs is large, with differences in performance depending on the objective of the application (description vs prediction) (Derville et al., 2018). The model chosen was Boosted-Regression Tree (BRT) (Elith et al., 2008) a technique used to reveal important predictor variables and interactions between them (Elith and Franklin, 2017). BRT can be understood as an additive regression model in which simple tree models can be combined and fitted to provide improved predictive performance. BRTs: a) can handle different types of predictor variables (quantitative or qualitative) and accommodate missing data, and b) are able to fit complex non-linear relationships and identify interaction effects between predictors.

In order to perform the BRT model, we set 'Rhodolith abundance' as the response variable (four levels – the different levels of coverage: 0, <25 %, <50 % and >50 %). The explanatory variables considered were three categorical variables: 'Location' (three levels – the surveyed localities: BL, COL, CP), 'Relief' (two levels: Flat or Ripples), 'Substrate' (four levels – different types of substrate with more than two observations: Mud, Mixed sediment, Coarse sediment and Rocky or other hard substrata), two logical variables: 'Rocky outcrops' and 'Fishing' (two levels: Presence or Absence) and four numerical variables with 'Depth (m)', 'Temperature (°C)', 'Slope (m/min)' and 'Area (m^2/min)' (Table 2).

The model was fitted to a Poisson distribution for the response variable, using the pooled data from the three localities. For our analysis, the initial tree complexity values were 3, 4, 5, 6, 7 with learning rates values of 0.0005, 0.001, 0.005, 0.01, 0.05. We selected the optimal settings of the model by means of the number of trees (minimum of 1500 trees) and the lowest deviance coefficient (for detailed methodology and model selection criteria, Elith et al., 2008). The outputs of the model showed the contribution of each environmental variable to the overall performance of the model and helped produce partial dependency plots for each predictor (Carvalho et al., 2020). BRT models were fit using the R package '*Dismo*' (Hijmans et al., 2022).

Table 2
Explanatory variables used in the statistical analysis: BRT, multivariate model and GLM. The environmental variables were quantitative, all other variables were categorical.

Biophysical parameters	Levels			
Location	BL	COL	CP	
Rhodolith coverage	Absence	<25 %	≥25 ≤ 50 %	>50 %
Relief	Flat	Ripples		
Substrate	Mud	Mixed sediment	Coarse sediment	Rocky or other hard substrata
Number biotopes	Homogeneity	2 Biotopes	>2 Biotopes	
Algal cover	Presence or absence			
Rocky outcrops				
Fishing				
Environmental	Depth (m)	Temperature (°C)	Slope (m/min)	

2.4.2. Biological traits

2.4.2.1. Multivariate model. In order to visualize the important biophysical factors explaining the variability in biological traits composition in soft-bottoms associated with rhodoliths, the biological traits density matrix was displayed through a Canonical Correspondence Analysis (CCA), based on Jaccard Distance, from the R package '*vegan*' (Oksanen et al., 2022). Moreover, a multivariate regression model was fit using the R package '*mvabund*' (Wang et al., 2022).

For the multivariate regression model, the biological traits density was set as the response variable, while the explanatory variables were five categorical variables: 'Location' (three levels – the surveyed localities: BL, COL, CP), 'Rhodolith abundance' (four levels – the different levels of coverage: 0, <25 %, <50 %, >50 %), 'Relief' (two levels: Flat or Ripples), 'Substrate' (four levels – different types of substrate with more than two observations: Mud, Mixed sediment, Coarse sediment and Rocky or other hard substrata) and 'Number biotopes' (three levels – Homogeneity, 2 Biotopes or >2 Biotopes); three logical variables: 'Algal cover', 'Rocky outcrops' and 'Fishing' (two levels: Presence or Absence) and three numerical variables with 'Depth (m)', 'Temperature (°C)' and 'Slope (m/min)' (Table 2).

With the same biological traits' matrix, a "fourth-corner" analysis (Brown et al., 2014; Warton et al., 2015) was performed to examine the influence of biological traits on the interaction between the abundance and environmental matrices. To determine which environmental and trait variables to include in the analysis, we followed the model-based approached described in Brown et al. (2014), using the method of least absolute shrinkage and selection operator (LASSO, Hastie et al., 2009) based on penalized likelihood. The analysis was conducted with the function *traitsglm* of the R package '*mvabund*' (Wang et al., 2012), using the negative binomial as distribution function for the response matrix (taxon abundance).

2.4.2.2. Functional richness. The functional richness was calculated based on the matrix of biological traits density, for the species assemblages identified, using '*specnumber*' function from package '*vegan*' (Oksanen et al., 2022). This measure is a count of the number of different traits in a given sampling unit, in our case the functional richness index is representing only the biological traits diversity of visible benthic fauna identified in each 15 min video footage intervals.

We explored the effect of environmental variables on functional richness by performing a generalized linear model (GLM) from the R package '*stats*' (R Core Team, 2022). The stepwise approach for the selection of the best model consisted in running a full GLM with 'Richness index' introduced as the response variable and including all biophysical parameters as the explanatory variables (Table 2). The model was fitted to a Poisson distribution. Removal of all non-significant factors was done with function '*stepAIC*' from the R package '*MASS*' (Venables and Ripley, 2002). We followed a backwards model selection based on the lowest AIC. The explanatory variables that remained, at the selected model, were 'Location' (three levels – the surveyed localities: BL, COL, CP), 'Number biotopes' (three levels – Homogeneity, 2 Biotopes or >2 Biotopes), 'Algal cover' and 'Rocky outcrops' (two levels: Presence or Absence) and 'Depth (m)'. A posterior post-hoc analysis was performed with variable 'Location' from the R package '*emmeans*' (Lenth, 2022).

All analyses were computed in R (R Core Team, 2020) under version 4.2.1.

3. Results

3.1. Physical and biological description of the sites

The video transects in the three study sites resulted in 53 h – 17 h in BC and COL and 19 h in CP- of footage over ca. 39,780 m^2 of survey, of which around 13 % were coralligenous rocks. This substrate was removed from the dataset as it is characterized by coralline crustose algae, not the objective of our study. Considering the remaining video footage, a total of 34,215 m^2–12,580 m^2 in BC, 12,321 m^2 in CP and 9314 m^2 in COL-, we identified a total of 119 different organisms, belonging to eight phyla (Annelida, Arthropoda, Bryozoa, Chordata, Cnidaria, Echinodermata, Mollusca and Porifera), of which around 60 % were identified to species level. In terms of abundance, the phylum most represented in the total video footage were echinoderms with *Spatangus purpureus* (36.2 %) and *Echinaster sepositus* (13.7 %).

The site BL is characterized by biogenic sand and gravel, which represents 85 % of the area explored. About 25 % of this area, restricted to 46–56 m depth, had scattered rhodoliths (Fig. 2). Another important substrate identified in BL were muddy areas deeper than 60 m, with no evidence of rhodoliths. The most abundant species in this study area were the starfish *Echinaster sepositus* (32 %), and aggregated sponges (Porifera) (22 %), particularly found at low (<25 %) or null rhodoliths coverage in coarse sediment (Fig. 3).

The main substrate covering COL is biogenic sand and gravel with a 93 % of coverage; the remaining 7 % is covered by mixed sediments without the presence of rhodoliths (Fig. 2). Rhodolith beds were observed in the 52–68 m depth range within coarse sediment areas. In COL there was a larger extension of rhodoliths, with an abundance over 50 % detected in 22 % of the area. Considering the species' densities, the dominant species along the transect was the echinoid *Echinaster sepositus* (23 %) and species from the phylum Porifera (17 %) (Fig. 3). Crinoids are characteristic of muddy bottoms, they represented 19 % of the density, in coarse sediment with rhodoliths coverage <50 %. Finally, it is worth to highlight the specific diversity found associated with mixed sediments without rhodoliths: fish density (6.23 %) and the presence of sessile cnidaria e.g., *Pennatula phosphorea* and *Veretillum cynomorium*.

The site CP is covered in 92 % of the area by biogenic sand and gravel, whereas the remaining 8 % is characterized by the presence of rocks and other hard substrata (Fig. 2). In this rocky substrate the presence of rhodoliths is scarce, representing <25 % of the coverage. However, in coarse sediments from 40 m to 73 m depth, there is a notorious presence of rhodoliths, with variable abundance from 0 % to >50 %. In this area, a high density of rhodoliths (>50 %) is present in 17 % of the surveyed area. Considering the species densities in CP we highlight important aggregations of the sea urchin *Spatangus purpureus*

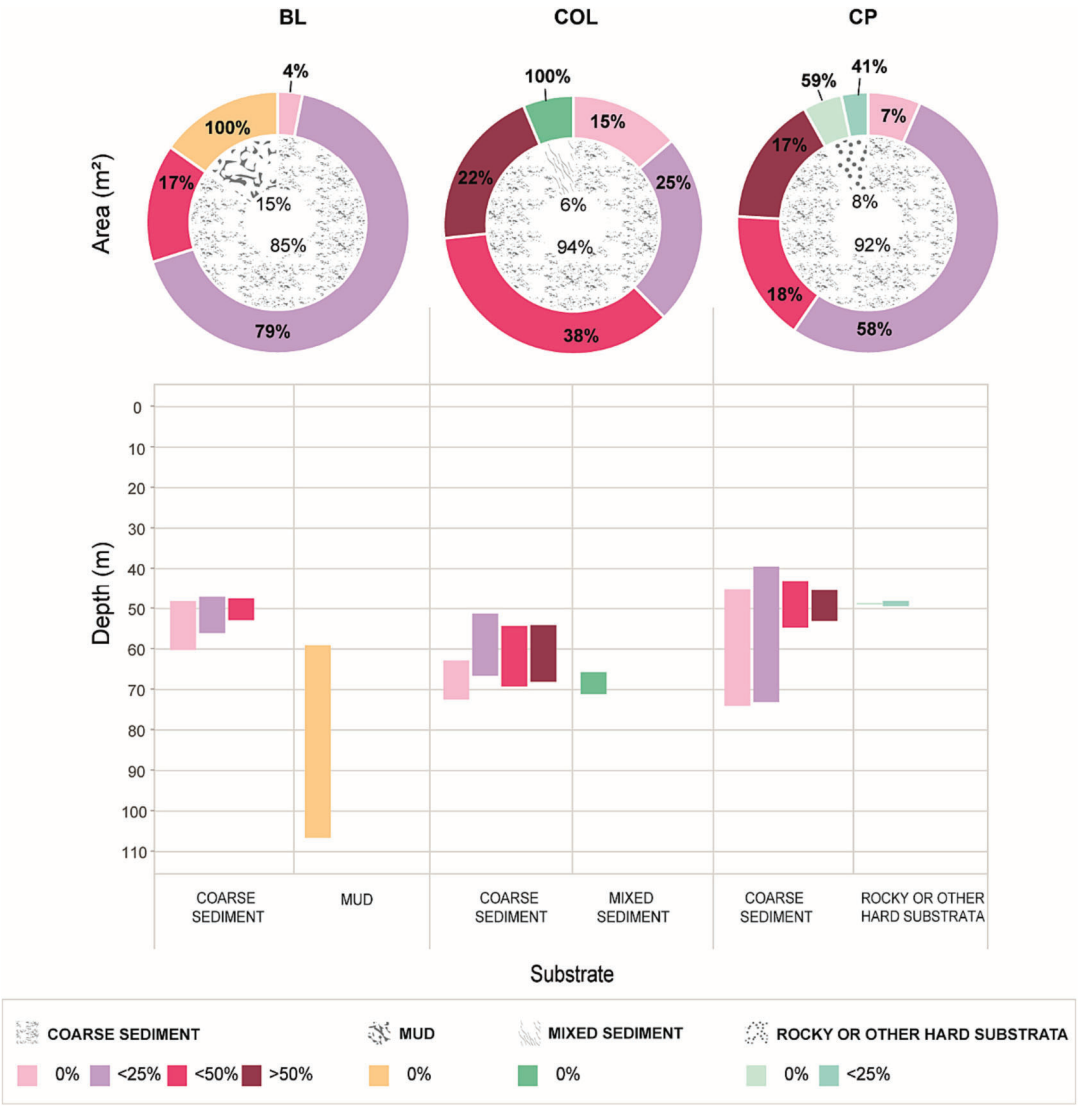


Fig. 2. Characterization of the substrate types and rhodolith abundance for each studied area. Top: Pie charts represent the percentage of area (%) covered by different levels of rhodolith coverage (outer donut) according to the predominant substrate type (inner donut) at each study site. Bottom: Depth (m) range occupied by different levels of rhodolith coverage according to the predominant substrate type at each study site. From left to right: BL. Continental shelf off Blanes; COL. Columbretes Islands; CP. Cabo de Palos.

(49 %) at sites with rhodoliths presence (<25 % to >50 %), followed by lower densities of the starfish *Echinaster sepositus* (8 %) (Fig. 3). At sites with low or null rhodolith coverage and in rocky substrates, the predominant species belonged to Porifera. Furthermore, in rocky outcrops, we highlight the presence of demersal fish (2.76 %) and the hydrozoan *Nemertesia antennina* (1.62 %).

A completed list of the organisms identified is provided in Appendices (Table A.1), as well as a set of ROV images (Fig. A.5).

3.2. Environmental factors explaining rhodolith abundance

According to the BRT model (with a tree complexity equal to 6 and a learning rate of 0.001), the two main environmental factors explaining rhodolith abundance were 'Depth' and 'Temperature', explaining 24 % and 23 % abundance variation, respectively (Fig. 4). The other biophysical parameters considered (e.g., Location, relief, substrate) contributed less to the variation explained. 'Location' explained 9 % of the variation, and represented the highest contribution of a categorical variables.

The normalized partial response of rhodolith abundance for the quantitative variables with highest contribution (depth, slope and temperature) indicated the optimal ranges for rhodolith cover in terms of relative abundances (Fig. 4). Across the three study sites, the relative rhodolith abundance was higher at depths between 40 and 65 m, while at deeper sites its abundance was drastically reduced. Higher rhodolith cover was found around slope values of 0 to 0.35 (m/min), i.e., rhodoliths tend to accumulate in flat places. Finally, temperatures around 14.5 °C were linked to a rapid increase in relative abundance of rhodoliths, but its abundance started to decrease after 15.5 °C.

Considering the categorical variables 'Location' and 'Substrate', with an explained variation of 9 % and 6 % respectively, the highest relative abundance of rhodoliths was found in COL and on bottoms dominated by coarse sediment. The lower relative rhodolith abundance was found in BL and, for 'Substrate', in muddy bottoms (Fig. 4).

3.3. Biological traits

3.3.1. Multivariate model

The CCA biplot (Fig. 5), explained about 30 % of the variance of the assemblage structure. The main variables expressed in the CCA were

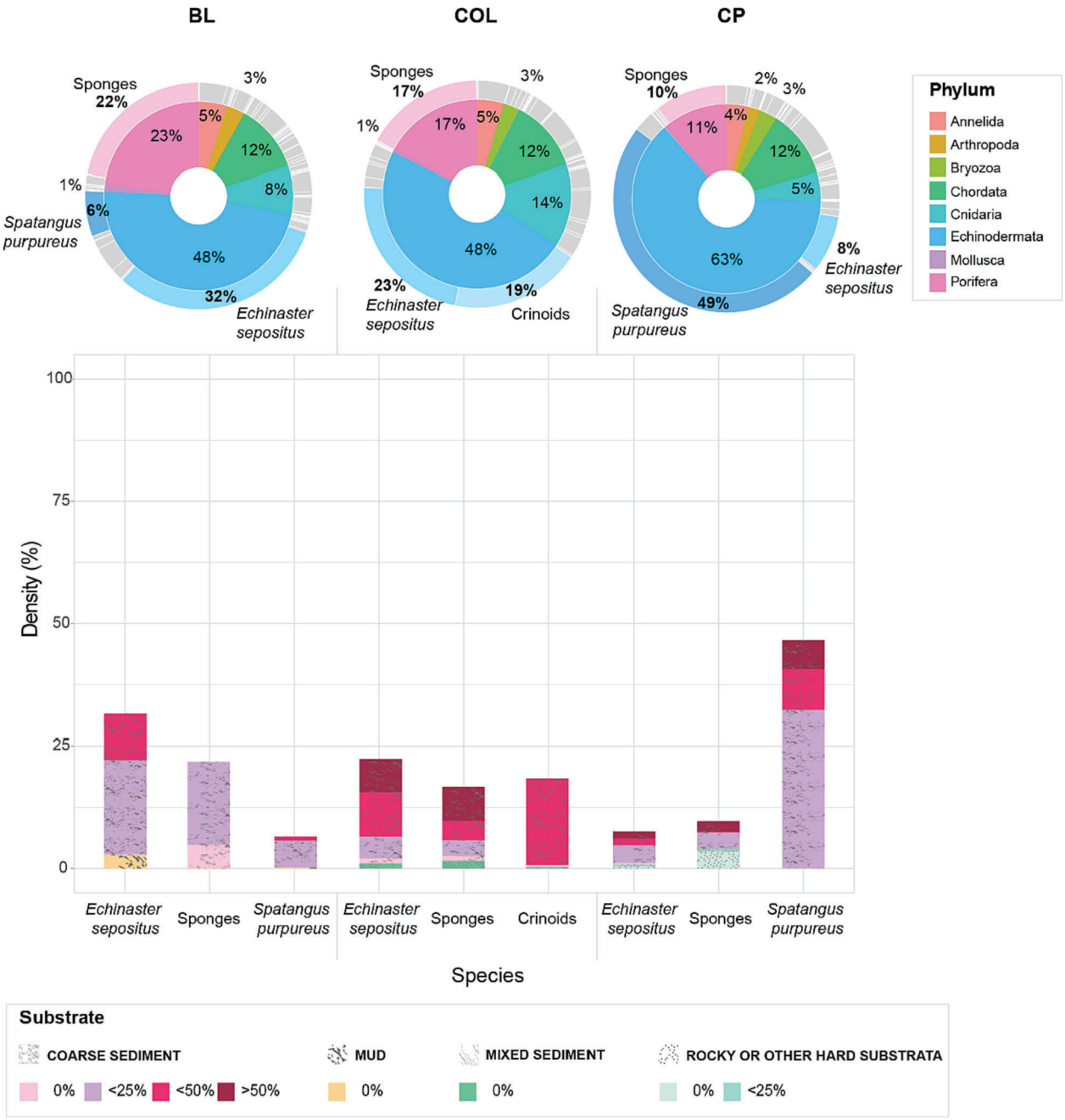


Fig. 3. Species composition according to substrate type and rhodolith abundance for each studied area. Top: Pie charts represent the percentage (%) of each phylum (inner donut) and the 3 species with higher density (outer donut) at each study site. Bottom: Bar plot represent the densities of the three most abundant species found at different levels of rhodolith coverage according to substrate type at each study site. From left to right: BL. Continental shelf off Blanes; COL. Columbretes Islands; CP. Cabo de Palos.

'Location', 'Algal cover', 'Rocky outcrops' and 'Depth', which defined some ecological groups according to biological traits distribution. Globose morphologies with grazing as a feeding strategy (e.g., represented by a grazing sea urchin), were aligned with CP station where algal cover was the highest. In addition, cushion and arborescent morphologies that live attached on the substrate, and characterized by suspension feeding strategy (e.g., from sponges to gorgonians), overlapped with the presence of rocky outcrops and hard substrate.

In the multivariate regression model the biophysical parameters explained 43 % of the biological traits' composition. The variables that had a significant explanatory power were: 'Location', 'Rhodolith abundance', 'Temperature', 'Algal cover', 'Fishing', 'Substrate', 'Rocky outcrops' and 'Number biotopes' (Table 3). In addition, the multivariate model of the interaction between species' traits and environmental variables fit with the LASSO algorithm converged after 25 iterations (AIC = −4874.12), compared to the null model of no interaction (AIC = −4775.33). This result suggests that the species variability as response to environmental factors was significantly mediated by trait variables. Similar to the CCA results, the environmental factors selected were 'Location', 'Algal cover', 'Rocky outcrops' and 'Depth'. The scaled coefficients of the species traits and environment interactions (Fig. A.6) show that most functional traits had relatively low influence on the power of environmental traits to explain the abundance of taxa. "Sessile" organisms were overrepresented in Rocky outcrops, while "crawlers" increased with depth and was less frequent in one of the sites, CP. The habitat trait "attached" was more prevalent in BL, area characterized by

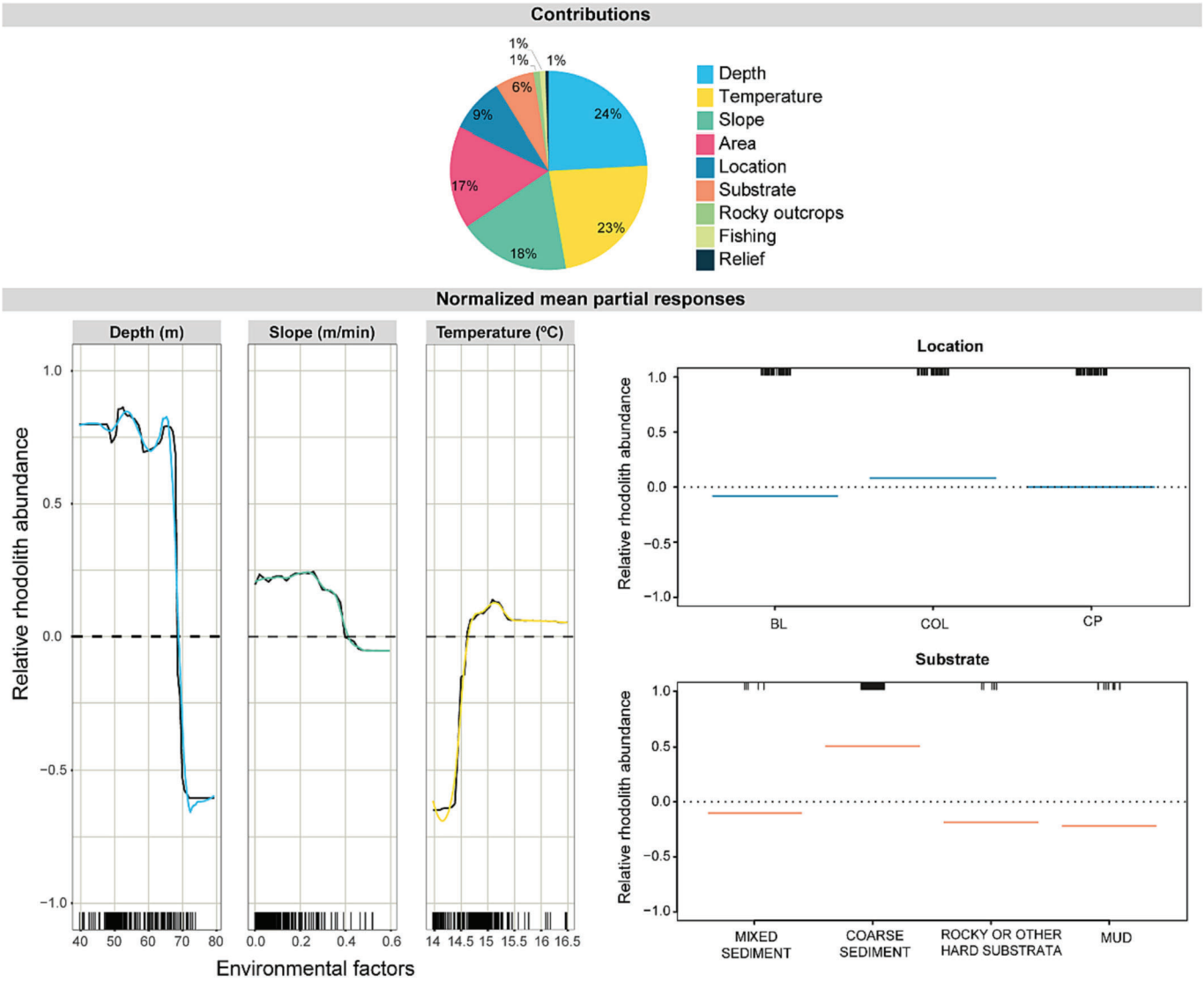


Fig. 4. Results of the selected *Boosted Regression tree* model. Top: Variance contribution of the explanatory variables in the abundance of rhodoliths. Bottom: Plots of the normalized partial responses of the relative abundance as a function of the quantitative variables of Depth (m), Slope (m/min), Temperature (°C) and the two main qualitative variables: Location and Substrate. Mean relative abundance of rhodoliths is represented by 0. Higher values represent relative abundances higher than the mean and lower values represent lower relative abundances than the mean. *Black line*: BRT result; *colored line*: smothered BRT result to facilitate visualization.

the presence of sponges and gorgonians, than in COL and neutral in CP. However, "attached" tended to be underrepresented in areas with presence of rocky outcrops, due to presence of *Calliactis parasitica* and *Suberites domuncula* in BL, which are organisms attached to hermit crabs (Fig. A.6). Long-lived organisms were more common in sites with high algal cover, whereas larger organisms were more common in the shallower site CP and decrease their presence with depth.

3.3.2. *Functional diversity*

The most parsimonious GLM included the following biophysical factors: 'Location', 'Depth', 'Algal cover', 'Rocky outcrops' and 'Number biotopes'; which explained 34 % of the variance of the functional richness index (Table 3). The most significant factors were 'Location' and 'Number biotopes'. Functional richness values from CP were higher than in COL and BL, i.e., there was a higher number of different traits in CP. Nevertheless, the post-hoc analysis revealed non-significant differences between functional richness values in the two protected study sites (CP vs COL) or between COL and BL, while there were significant differences between CP and BL (Fig. A.7). Regarding the effect of 'Number biotopes' as an approximation of small spatial heterogeneity, an increase in the functional richness index was observed from one to two biotopes. However, when the number of biotopes was higher than 2, the functional richness value decreased (Fig. A.7).

4. Discussion

Our results show that, in agreement with other studies (Carvalho et al., 2020; Fragkopoulou et al., 2021), the relative abundance of rhodoliths is driven by depth and temperature. Depth, which directly conditions light availability, determines the presence and abundance of red algae and the rhodoliths forming species. In the North Atlantic, rhodolith beds have been identified from the intertidal down to 60 m depth (Hernandez-Kantun et al., 2017; Otero-Ferrer et al., 2020; Peña et al., 2014), while in the oligotrophic Mediterranean waters they can reach 100 m (Ballesteros, 1989; Basso et al., 1996). In our study site, a higher abundance of rhodoliths was observed in a narrow temperature range, 14.5–15.5 °C, decreasing rhodolith abundance at higher temperature. These results correspond to the upper temperature range

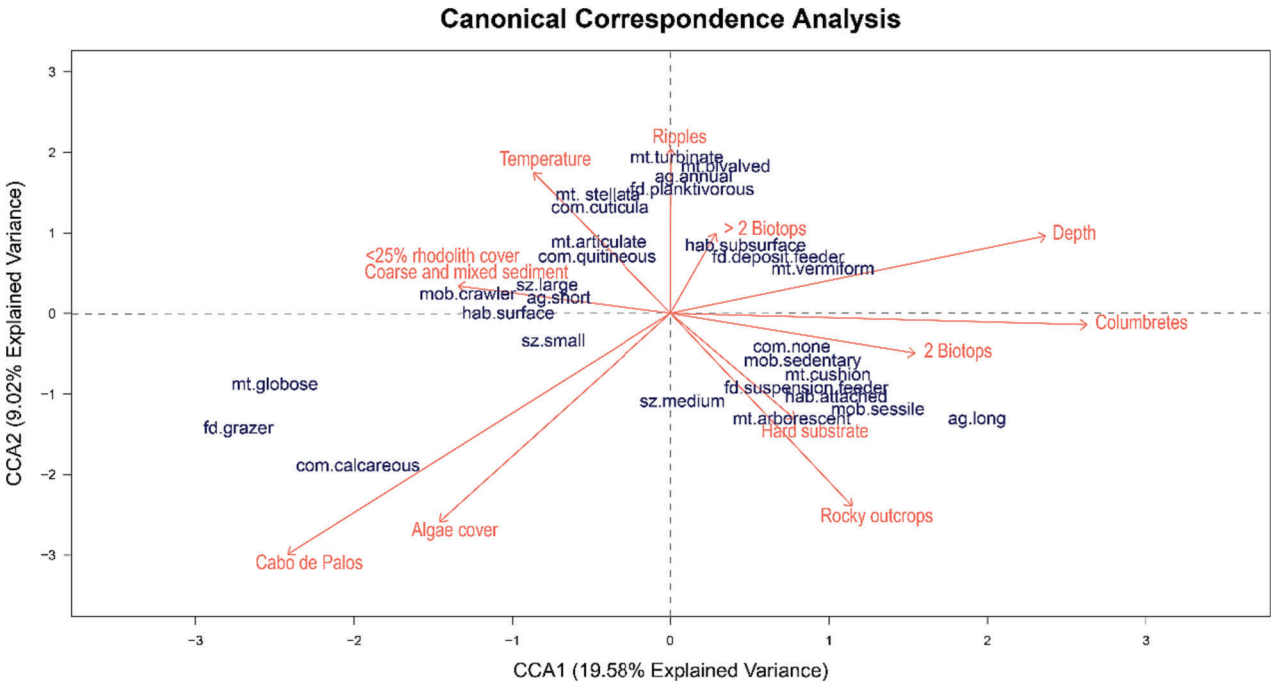


Fig. 5. Canonical Correspondence Analysis showing the position of different biological traits (blue) according to different biophysical parameters and Location (red arrows).

Table 3
Results of the statistical models applied to the multivariate biological traits matrix (top) and to functional richness index (bottom).

Model	Response variable	Explanatory variable	Df	F-value	*P*-values
Many LM	Biological traits	Location	2	802.2	<0.01
		Rhodolith coverage	3	138.8	<0.01
		Temperature	1	134.6	<0.01
		Depth	1	51.7	0.152
		Slope	1	53.0	>0.05
		Algal cover	1	150.8	<0.01
		Relief	1	28.8	>0.05
		Fishing	1	136.3	<0.01
		Substrate	3	180.9	<0.01
		Rocky outcrops	1	318.9	<0.01
		Number biotopes	2	110.5	<0.01
				X^2-value	
GLM	Functional richness index	Location	2	150.18	<0.001
		Depth	1	149.18	>0.05
		Algal cover	1	147.76	>0.05
		Rocky outcrops	1	143.06	<0.05
		Number biotopes	2	133.29	<0.01

observed in North Atlantic waters, with similar species composition distributed in shallower waters (9.6–17.6 °C, Martin et al., 2007). Nevertheless, a study in the Mediterranean reported shallow water rhodolith beds, exposed to seasonal warm temperatures as high as 25 °C (del Río et al., 2022).

On the other hand, substrate composition had relatively lower importance in the BRT analysis. However, it might be an important factor at a small spatial scale. Sediments composed of sand and coarse fractions favor the development of extensive rhodolith beds with higher coverage, often interspersed with patches of lower abundance. This patchy habitat supports higher diversity than a homogenous high rhodolith coverage (Boyé et al., 2019; de Juan et al., 2023). On the other hand, the presence of fine sediments, i.e., mud or muddy sands, restricts the occurrence of rhodoliths. In fine sediments the burial of red calcareous algae due to sediment resuspension leads to the death of the specimens; this is a consequence to the lack of light irradiance and a reduction of the water movement around rhodoliths that could reduce gaseous exchange (Wilson et al., 2004). Accordingly, hydrodynamics arises as a determinant factor for rhodoliths establishment. Currents must be intense enough to prevent the burial of rhodoliths by fine particles (Tauran et al., 2020), thus avoiding suffocation of rhodoliths. Conversely, areas with high hydrodynamics are not suitable for the settlement of rhodoliths, because wave-induced turbulence breaks rhodoliths up or sweep them outside suitable areas for rhodolith beds development (Marrack, 1999; Foster, 2001). Therefore, a delicate balance of water movement is required for the correct development of areas with a high abundance of rhodoliths (Joshi and Farrell, 2020).

Our study evidenced, that the role of fisheries footprint, e.g., trawl tracks or lost fishing gear, was apparently minor in driving rhodoliths abundance. However, when comparing rhodoliths relative abundance across the three study sites, BL was the site with lower overall rhodolith abundance, which is currently subjected to commercial trawling activities. Cabanellas-Reboredo et al. (2017) and Barberá et al. (2017) reported that off Columbretes islands (close to our COL study site) a 6-year trawl ban resulted in different morphologies and sizes of two rhodolith forming algae. However, their results did not provide evident signs of enhanced rhodolith coverage compared with adjacent areas under a longer (25 year) fish ban. Similarly, Farriols et al. (2022) discussed that recovery of rhodolith beds from trawl impact may not be evident after a 3-year ban. These results are not surprising considering the slow growth of rhodolith-forming species (ca. 1 mm per year) (Blake et al., 2007). A study previously conducted in the CP site observed a high rhodolith coverage within no-trawling areas compared to open areas (de Juan et al., 2013). Furthermore, the biodiversity associated to rhodolith beds can also be affected by trawling and dredging, resulting in changes in species composition, dominance patterns and abundance of more sensitive species (Mangano et al., 2013; Ordines et al., 2007; Tauran et al., 2020).

Rhodoliths provide shelter for small organisms within its structure, especially the branched forms, and serve as fixation points for epiphytic

algae and epibenthos, harbouring a rich microbiome (Carvalho et al., 2020; Cavalcanti et al., 2018; Fredericq et al., 2019). For instance, Boyé et al. (2019) showed that in well-preserved rhodolith beds in the Brittany coast niche diversity and functional redundancy is promoted. Indeed, alternation of biogenic and sand habitats promotes a high species diversity at the seascape, including habitat-generalists and habitat-specialist species (de Juan et al., 2023). In our study, we focused on functional richness, which links species composition with the potential ecological functions associated to rhodolith beds (de Juan et al., 2022), and observed significantly higher functional richness in the two protected study sites (CP and COL). However, functional richness was highest in patchy biotopes consisting in two types of substrates. This result reinforces the ecological notion that heterogeneous seabed habitats mighty harbour higher diversity (β-diversity) than purely homogeneous habitats (de Juan et al., 2013).

The two MPAs (CP and COL) had distinctive ecological groups with different functional roles (Fig. 5). The CP MPA was characterized by species with a high bioturbation capacity that may contribute to rhodolith mixing in the surface sediment while feeding on other benthic organisms like abundant algal cover (Sciberras et al., 2009). In the other hand, COL MPA had a high presence of sessile suspension feeders that increase the three-dimensional habitat complexity, providing refuge for benthic species and fish juveniles.

Notwithstanding the importance of video surveys to investigate deep-water habitats at small scale (Kuhnz et al., 2022), we acknowledge important limitations of the technique.

The taxonomic inventory reported by visual censuses based on data from remote video observation was inevitably biased towards larger specimens of those conspicuous species. For instance, we obtained high density values for echinoderms (*Spatangus purpureus* and *Echinaster sepositus)* and sponges, similar to those species found in another deep-water rhodolith bed in the Mediterranean Sea (Barberá et al., 2012; Bracchi et al., 2019). In contrast to low density values for other epifaunal invertebrates (e.g., *Pennatula phosphorea*, *Veretillum cynomorium*, *Nemertesia antennina*), fishes and practically no representation of crustaceans. Therefore, it is important to complement visual censuses with other non-intrusive sampling techniques, such as eDNA (Boulanger et al., 2021), which may help providing a more complete view of the biodiversity present on rhodolith beds.

5. Conclusions

The present study is an important contribution that generates baseline knowledge on deep-water rhodolith beds in the western Mediterranean Sea. The continuous non-intrusive video survey of the seafloor was essential to characterize the small-scale heterogeneity of rhodolith beds and their associated functional biodiversity. This study reinforces the link between rhodolith occurrence and abiotic drivers, such as depth and temperature and proposed an optimal environmental range for rhodoliths' occurrence in the east coast of Spain. In this area, rhodolith beds extend from 40 to 65 m depth, are more common on thick substrates and in a temperature range between 14.5 °C and 15.5 °C. Fishing activity limits the extent of these bottoms. However, there are potentially key factors in the distribution of rhodoliths, such as bottom current or suspended sediment, which were not taken into account in this study, reflected by the percentage of variance not explained by our models. Other external factors such as nutrient inputs, invasive species, or limitations in ecological connectivity between seafloor areas may also limit whether or not rhodolith extension is possible. These current gaps in the knowledge of Mediterranean maërl bed occurrence encourages scientific efforts to understand the ecological and functional importance of these habitats in the region.

CRediT authorship contribution statement

Laia Illa-López: Conceptualization, Methodology, Formal analysis, Writing – original draft, Writing – review & editing, Visualization. **Andrea Cabrito:** Conceptualization, Methodology, Formal analysis, Writing – original draft, Writing – review & editing, Visualization. **Sílvia de Juan:** Conceptualization, Writing – review & editing. **Francesc Maynou:** Conceptualization, Methodology, Formal analysis, Writing – original draft, Writing – review & editing. **Montserrat Demestre:** Conceptualization, Methodology, Writing – review & editing, Funding acquisition.

Declaration of competing interest

The authors declare that they have no known competing financial interests or personal relationships that could have appeared to influence the work reported in this paper.

Data availability

Data will be made available on request.

Acknowledgments

Authors are very thankful to Sara Soto for her back up with GIS tools. This study is developed on the framework of the I+D+I Project CriMa (RTI2018-095770-B100; MCIU/AEI/FEDER, EU). The EU project MaCoBioS (contract n° 869710) also contributed funding to this study. This work contributes to the ICM's 'Center of Excellence' Severo Ochoa (CEX2019-000928-S).

Appendix A. Supplementary data

Supplementary data to this article can be found online at https://doi.org/10.1016/j.scitotenv.2023.167270.

References

Amado-Filho, G.M., Moura, R.L., Bastos, A.C., Salgado, L.T., Sumida, P.Y., Guth, A.Z., Francini-Filho, R.B., Pereira-Filho, G.H., Abrantes, D.P., Brasileiro, P.S., Bahia, R.G., Leal, R.N., Kaufman, L., Kleypas, J.A., Farina, M., Thompson, F.L., 2012. Rhodolith beds are major $CaCO_3$ bio-factories in the tropical south West Atlantic. PloS One 7 (4), e35171. https://doi.org/10.1371/journal.pone.0035171.

Ballesteros, E., 1988. Composición y estructura de los fondos de maërl de Tossa de Mar (Gerona, España). Collect. Bot. 17 (2) https://doi.org/10.3989/collectbot.1989.v17.137.

Ballesteros, E., 1989. Contribució al coneixement algologic de la mediterrània espanyola, viii. Addicions a la flora balear. Folia Botanica Miscellanea 6, 65–70. http://hdl.handle.net/10261/98616.

Barberá, C., Bordehore, C., Borg, J.A., Glémarec, M., Grall, J., Hall-Spencer, J.M., de la Huz, Ch., Lanfranco, E., Lastra, M., Moore, P.G., Mora, J., Pita, M.E., Ramos-Esplá, A. A., Rizzo, M., Sánchez-Mata, A., Seva, A., Schembri, P.J., Valle, C., 2003. Conservation and management of northeast Atlantic and Mediterranean maërl beds. Aquat. Conserv. Mar. Freshwat. Ecosyst. 13 (S1), S65–S76. https://doi.org/10.1002/aqc.569.

Barberá, C., Moranta, J., Ordines, F., Ramón, M., de Mesa, A., Díaz-Valdés, M., Grau, A. M., Massutí, E., 2012. Biodiversity and habitat mapping of Menorca Channel (western Mediterranean): implications for conservation. Biodivers. Conserv. 21 (3), 701–728. https://doi.org/10.1007/s10531-011-0210-1.

Barberá, C., Mallol, S., Vergés, A., Cabanellas-Reboredo, M., Díaz, D., Goñi, R., 2017. Maërl beds inside and outside a 25-year-old no-take area. Mar. Ecol. Prog. Ser. 572, 77–90. https://doi.org/10.3354/meps12110.

Basso, D., Fravega, P., Vannucci, G., 1996. Fossil and living corallinaceans related to the Mediterranean endemic species *Lithophyllum racemus* (Lamarck) Foslie. Facies 35 (1), 275–292. https://doi.org/10.1007/BF02536965.

Bicknell, A.W., Godley, B.J., Sheehan, E.V., Votier, S.C., Witt, M.J., 2016. Camera technology for monitoring marine biodiversity and human impact. Front. Ecol. Environ. 14 (8), 424–432. https://doi.org/10.1002/fee.1322.

Blake, C., Maggs, C., Reimer, P., 2007. Use of radiocarbon dating to interpret past environments of maërl beds. Cienc. Mar. 33 (4), 385–397.

Bosence, D.W.J., 1983. The occurrence and ecology of recent rhodoliths—a review. In: Peryt, En T.M. (Ed.), Coated Grains. Springer, Berlin Heidelberg, pp. 225–242. https://doi.org/10.1007/978-3-642-68869-0_20.

Boulanger, E., Loiseau, N., Valentini, A., Arnal, V., Boissery, P., Dejean, T., Deter, J., Guellati, N., Holon, F., Juhel, J.-B., Lenfant, P., Manel, S., Mouillot, D., 2021. Environmental DNA metabarcoding reveals and unpacks a biodiversity conservation paradox in Mediterranean marine reserves. Proc. R. Soc. B Biol. Sci. 288 (1949), 20210112. https://doi.org/10.1098/rspb.2021.0112.

Boyé, A., Thiébaut, É., Grall, J., Legendre, P., Broudin, C., Houbin, C., Le Garrec, V., Maguer, M., Droual, G., Gauthier, O., 2019. Trait-based approach to monitoring marine benthic data along 500 km of coastline. Divers. Distrib. 25 (12), 1879–1896. https://doi.org/10.1111/ddi.12987.

Bracchi, Angeletti, L., Marchese, F., Taviani, M., Taviani, Marco, Cardone, F., Cardone, F., Irka, H., Grande, Prampolini, M., Caragnano, A., Corselli, C., Basso, D., 2019. A resilient deep-water rhodolith bed off the Egadi Archipelago (Mediterranean Sea) and its actuopaleontological significance. Alp. Mediterr. Quat. 32 (2), 131–150. https://doi.org/10.26382/amq.2019.09.

Brown, A.M., Warton, D.I., Andrew, N.R., Binns, M., Cassis, G., Gibb, H., 2014. The fourth-corner solution – using predictive models to understand how species traits interact with the environment. Methods Ecol. Evol. 5 (4), 344–352. https://doi.org/10.1111/2041-210X.12163.

Cabanellas-Reboredo, M., Mallol, S., Barberá, C., Vergés, A., Díaz, D., Goñi, R., 2017. Morpho-demographic traits of two maërl-forming algae in beds with different depths and fishing histories. Aquat. Conserv.: Mar. Freshw. Ecosyst. 28 (1), 133–145. https://doi.org/10.1002/aqc.2827.

Carvalho, V.F., Assis, J., Serrão, E.A., Nunes, J.M., Anderson, A.B., Batista, M.B., Barufi, J.B., Silva, J., Pereira, S.M.B., Horta, P.A., 2020. Environmental drivers of rhodolith beds and epiphytes community along the South Western Atlantic coast. Mar. Environ. Res. 154, 104827. https://doi.org/10.1016/j.marenvres.2019.104827.

Cavalcanti, G.S., Shukla, P., Morris, M., Ribeiro, B., Foley, M., Doane, M.P., Thompson, C. C., Edwards, M.S., Dinsdale, E.A., Thompson, F.L., 2018. Rhodoliths holobionts in a changing ocean: host-microbes interactions mediate coralline algae resilience under ocean acidification. BMC Genomics 19 (1), 701. https://doi.org/10.1186/s12864-018-5064-4.

Costa, A.C.P., Garcia, T.M., Paiva, B.P., Ximenes Neto, A.R., Soares, M. de O., 2020. Seagrass and rhodolith beds are important seascapes for the development of fish eggs and larvae in tropical coastal areas. Mar. Environ. Res. 161, 105064. https://doi.org/10.1016/j.marenvres.2020.105064.

de Juan, S., Demestre, M., 2012. A trawl disturbance indicator to quantify large scale fishing impact on benthic ecosystems. Ecol. Indic. 18, 183–190. https://doi.org/10.1016/j.ecolind.2011.11.020.

de Juan, S., Thrush, S.F., Demestre, M., 2007. Functional changes as indicators of trawling disturbance on a benthic community located in a fishing ground (NW Mediterranean Sea). Mar. Ecol. Prog. Ser. 334, 117–129. https://doi.org/10.3354/meps334117.

de Juan, S., Lo Iacono, C., Demestre, M., 2013. Benthic habitat characterisation of soft-bottom continental shelves: integration of acoustic surveys, benthic samples and trawling disturbance intensity. Estuar. Coast. Shelf Sci. 117, 199–209. https://doi.org/10.1016/j.ecss.2012.11.012.

de Juan, S., Hewitt, J., Thrush, S., Freeman, D., 2015. Standardising the assessment of functional integrity in benthic ecosystems. J. Sea Res. 98, 33–41. https://doi.org/10.1016/j.seares.2014.06.001.

de Juan, S., Bremner, J., Hewitt, J., Törnroos, A., Mangano, M.C., Thrush, S., Hinz, H., 2022. Biological traits approaches in benthic marine ecology: dead ends and new paths. Ecol. Evol. 12 (6), e9001 https://doi.org/10.1002/ece3.9001.

de Juan, S., Ospina-Alvarez, A., Hinz, H., Moranta, J., Barberá, C., 2023. The continental shelf seascape: a network of species and habitats. Biodivers. Conserv. https://doi.org/10.1007/s10531-023-02552-8.

Del Río, J., Ramos, D.A., Sánchez-Tocino, L., Peñas, J., Braga, J.C., 2022. The Punta de la Mona Rhodolith bed: shallow-water Mediterranean Rhodoliths (Almuñecar, Granada, southern Spain). Front. Earth Sci. 10. https://www.frontiersin.org/articles/10.3389/feart.2022.884685.

Demestre, M., Muntadas, A., Sánchez, P., García-de-Vinuesa, A., Mas, J., Franco, I., Duran, R., Guillen, J., 2017. Bio and anthropogenic disturbance of Maërl communities settled on subaqueous dunes on the Mar Menor continental shelf (Western Mediterranean). In: Guillén, J., Acosta, J., Chiocci, F., Palanques, A. (Eds.), Atlas of Bedforms in the Western Mediterranean. Springer, Cham. https://doi.org/10.1007/978-3-319-33940-5_33.

Derville, S., Torres, L.G., Iovan, C., Garrigue, C., 2018. Finding the right fit: comparative cetacean distribution models using multiple data sources and statistical approaches. Divers. Distrib. 24 (11), 1657–1673. https://doi.org/10.1111/ddi.12782.

Elith, J., Franklin, J., 2017. Species distribution modeling. In: En Encyclopedia of Biodiversity. Elsevier Inc., pp. 692–705. https://doi.org/10.1016/B978-0-12-384719-5.00318-X

Elith, J., Leathwick, J.R., 2009. Species distribution models: ecological explanation and prediction across space and time. Annu. Rev. Ecol. Evol. Syst. 40 (1), 677–697. https://doi.org/10.1146/annurev.ecolsys.110308.120159.

Elith, J., Leathwick, J.R., Hastie, T., 2008. A working guide to boosted regression trees. J. Anim. Ecol. 77 (4), 802–813. https://doi.org/10.1111/j.1365-2656.2008.01390.x.

Farriols, M.T., Irlinger, C., Ordines, F., Palomino, D., Marco-Herrero, E., Soto-Navarro, J., Jordà, G., Mallol, S., Díaz, D., Martínez-Carreño, N., Díaz, J.A., Fernandez-Arcaya, U., Joher, S., Ramírez-Amaro, S., R. de la Ballina, N., Vázquez, J.-T., Massutí, E., 2022. Recovery signals of rhodoliths beds since bottom trawling ban in the SCI Menorca Channel (Western Mediterranean). Diversity 14 (1), 1. https://doi.org/10.3390/d14010020.

Foster, M.S., 2001. Rhodoliths: between rocks and soft places. J. Phycol. 37 (5), 659–667. https://doi.org/10.1046/j.1529-8817.2001.00195.x.

Fragkopoulou, E., Serrão, E.A., Horta, P.A., Koerich, G., Assis, J., 2021. Bottom trawling threatens future climate refugia of rhodoliths globally. Front. Mar. Sci. 7, 594537. https://doi.org/10.3389/fmars.2020.594537.

Fredericq, S., Krayesky-Self, S., Sauvage, T., Richards, J., Kittle, R., Arakaki, N., Hickerson, E., Schmidt, W.E., 2019. The critical importance of rhodoliths in the life cycle completion of both macro- and microalgae, and as holobionts for the establishment and maintenance of marine biodiversity. Front. Mar. Sci. 5. https://www.frontiersin.org/articles/10.3389/fmars.2018.00502.

Froese, R., Pauly, D. (Eds.), 2023. FishBase. World Wide Web electronic publication. www.fishbase.org. version (02/2023).

García-de-Vinuesa, A., Sola, I., Quattrocchi, F., Maynou, F., Demestre, M., 2018. Linking trawl fleet dynamics and the spatial distribution of exploited species can help to avoid unwanted catches: the case of the NW Mediterranean fishing grounds. Sci. Mar. 82. https://doi.org/10.3989/scimar.04755.17A.

Guillén, J., Acosta, J., Chiocci, F.L., Palanques, A. (Eds.), 2017. Atlas of Bedforms in the Western Mediterranean. Springer. https://doi.org/10.1007/978-3-319-33940-5, 291 pp.

Hastie, T., Tibshirani, R., Friedman, J., 2009. The Elements of Statistical Learning: Data Mining, Inference and Prediction, 2nd edn. Springer, New York, New York.

Hernandez-Kantun, J.J., Hall-Spencer, J.M., Grall, J., Adey, W., Rindi, F., Maggs, C.A., Bárbara, I., Peña, V., 2017. North Atlantic rhodolith beds. In: Riosmena-Rodríguez, En R., Nelson, W., Aguirre, J. (Eds.), Rhodolith/Maërl Beds: A Global Perspective. Springer International Publishing, pp. 265–279. https://doi.org/10.1007/978-3-319-29315-8_10.

Hewitt, J.E., Thrush, S.F., Legendre, P., Funnell, G.A., Ellis, J., Morrison, M., 2004. Mapping of marine soft-sediment communities: integrated sampling for ecological interpretation. Ecol. Appl. 14 (4), 1203–1216. https://doi.org/10.1890/03-5177.

Hijmans, R.J., Phillips, S., Leathwick, J., Elith, J., 2022. _dismo: species distribution Modeling_. R package version 1.3-9. https://CRAN.R-project.org/package=dismo.

Holz, V., Bahia, R., Karez, C., Vieira, F., Moraes, F., Vale, N., Sudatti, D., Salgado, L., Moura, R., Amado-Filho, G., Bastos, A., 2020. Structure of rhodolith beds and surrounding habitats at the Doce River shelf (Brazil). Diversity 12 (2), 75. https://doi.org/10.3390/d12020075.

Joher, S., Ballesteros, E., Rodríguez-Prieto, C., 2016. Macroalgal-dominated coastal detritic communities from the Western Mediterranean and the northeastern Atlantic. Mediterr. Mar. Sci. 17 (2), 476–495. https://doi.org/10.12681/mms.1438.

Joshi, S., Farrell, E., 2020. Physical oceanographic drivers of geomorphology of rhodolith/maërl beds in Galway Bay, Ireland. In: Seafloor Geomorphology as Benthic Habitat, pp. 231–242. https://doi.org/10.1016/B978-0-12-814960-7.00012-9.

Kamenos, N., Moore, P., Hall-Spencer, J., 2004. Nursery-area function of maërl grounds for juvenile queen scallops *Aequipecten opercularis* and other invertebrates. Mar. Ecol. Prog. Ser. 274, 183–189. https://doi.org/10.3354/meps274183.

Kuhnz, L.A., Gilbane, L., Cochrane, G.R., Paull, C.K., 2022. Multi-factor biotopes as a method for detailed site characterization in diverse benthic megafaunal communities and habitats in deep-water off Morro Bay, California. Deep-Sea Res. I Oceanogr. Res. Pap. 190, 103872. https://doi.org/10.1016/j.dsr.2022.103872.

Lenth, R., 2022. _emmeans: estimated marginal means, aka least-squares Means_. R package version 1.8.2. https://CRAN.R-project.org/package=emmeans.

Linares, C., Vidal, M., Canals, M., Kersting, D.K., Amblas, D., Aspillaga, E., Cebrián, E., Delgado-Huertas, A., Díaz, D., Garrabou, J., Hereu, B., Navarro, L., Teixidó, N., Ballesteros, E., 2015. Persistent natural acidification drives major distribution shifts in marine benthic ecosystems. Proc. R. Soc. B: Biol. Sci. 282 (1818), 20150587. https://doi.org/10.1098/rspb.2015.0587.

Mangano, M.C., Kaiser, M.J., Porporato, E.M.D., Spanò, N., 2013. Evidence of trawl disturbance on mega-epibenthic communities in the southern Tyrrhenian Sea. Mar. Ecol. Prog. Ser. 475, 101–117. https://doi.org/10.3354/meps10115.

MarLIN, 2006. BIOTIC - Biological Traits Information Catalogue. Marine Life Information Network. Plymouth: Marine Biological Association of the United Kingdom, 20/04/2023 Available from. www.marlin.ac.uk/biotic>.

MarLIN (Marine Life Information Network), 2020. Marine Life Information Network. Plymouth: Marine Biological Association of the United Kingdom [cited 01/01/09]. Available from. www.marlin.ac.uk.

Marrack, E.C., 1999. The relationship between water motion and living rhodolith beds in the southwestern Gulf of California, Mexico. Palaios 14 (2), 159–171. https://doi.org/10.2307/3515371.

Martin, S., Clavier, J., Guarini, J.-M., Chauvaud, L., Hily, C., Grall, J., Thouzeau, G., Jean, F., Richard, J., 2005. Comparison of *Zostera marina* and maërl community metabolism. Aquat. Bot. 83 (3), 161–174. https://doi.org/10.1016/j.aquabot.2005.06.002.

Martin, S., Clavier, J., Chauvaud, L., Thouzeau, G., 2007. Community metabolism in temperate maërl beds. I. Carbon and carbonate fluxes. Mar. Ecol. Prog. Ser. 335, 19–29. https://doi.org/10.3354/meps335019.

Martin, C.S., Giannoulaki, M., De Leo, F., Scardi, M., Salomidi, M., Knittweis, L., Pace, M. L., Garofalo, G., Gristina, M., Ballesteros, E., Bavestrello, G., Belluscio, A., Cebrian, E., Gerakaris, V., Pergent, G., Pergent-Martini, C., Schembri, P.J., Terribile, K., Rizzo, L., Fraschetti, S., 2014. Coralligenous and maërl habitats: predictive modelling to identify their spatial distributions across the Mediterranean Sea. Sci. Rep. 4 (1), 5073. https://doi.org/10.1038/srep05073.

Morán-Ordóñez, A., Lahoz-Monfort, J.J., Elith, J., Wintle, B.A., 2017. Evaluating 318 continental-scale species distribution models over a 60-year prediction horizon: what factors influence the reliability of predictions? Glob. Ecol. Biogeogr. 26 (3), 371–384. https://doi.org/10.1111/geb.12545.

Neves, P., Silva, J., Peña, V., Ribeiro, C., 2021. "Pink round stones"—rhodolith beds: an overlooked habitat in Madeira archipelago. Biodivers. Conserv. 30 (12), 3359–3383. https://doi.org/10.1007/s10531-021-02251-2.

Oksanen, J., Simpson, G., Blanchet, F., Kindt, R., Legendre, P., Minchin, P., O'Hara, R., Solymos, P., Stevens, M., Szoecs, E., Wagner, H., Barbour, M., Bedward, M., Bolker, B., Borcard, D., Carvalho, G., Chirico, M., De Caceres, M., Durand, S., Evangelista, H., FitzJohn, R., Friendly, M., Furneaux, B., Hannigan, G., Hill, M., Lahti, L., McGlinn, D., Ouellette, M., Ribeiro Cunha, E., Smith, T., Stier, A., Ter

Braak, C., Weedon, J., 2022. _vegan: Community Ecology Package_. R package version 2.6-4. https://CRAN.R-project.org/package=vegan>.
Ordines, F., Massutí, E., 2009. Relationships between macro-epibenthic communities and fish on the shelf grounds of the western Mediterranean. Aquat. Conserv.: Mar. Freshw. Ecosyst. 19 (4), 370–383.
Ordines, F., Massutí, E., Quetglas, A., Moranta, J., 2007. Macro-epibenthic assemblages on the trawling grounds along the shallow continental shelf off the Balearic Islands (western Mediterranean). Rapport de la Commision Internationale pour l'Exploration Scientifique de la Mer Méditerranée 38, 561.
Otero-Ferrer, F., Cosme, M., Tuya, F., Espino, F., Haroun, R., 2020. Effect of depth and seasonality on the functioning of rhodolith seabeds. Estuar. Coast. Shelf Sci. 235, 106579. https://doi.org/10.1016/j.ecss.2019.106579.
Peña, V., Bárbara, I., Grall, J., Maggs, C.A., Hall-Spencer, J.M., 2014. The diversity of seaweeds on maërl in the NE Atlantic. Mar. Biodivers. 44 (4), 533–551. https://doi.org/10.1007/s12526-014-0214-7.
R Core Team, 2020. R: A Language and Environment for Statistical Computing. R Foundation for Statistical Computing, Vienna, Austria. URL. https://www.R-project.org/.
R Core Team, 2022. R: A Language and Environment for Statistical Computing. R Foundation for Statistical Computing, Vienna, Austria. URL. https://www.R-project.org/.
Rindi, F., Braga, J.C., Martin, S., Peña, V., Le Gall, L., Caragnano, A., Aguirre, J., 2019. Coralline algae in a changing Mediterranean Sea: how can we predict their future, if we do not know their present? Front. Mar. Sci. 6. https://www.frontiersin.org/articles/10.3389/fmars.2019.00723.
Riosmena-Rodríguez, R., Nelson, W., Aguirre, J. (Eds.), 2017. Rhodolith/Maërl Beds: A Global Perspective, Vol. 15. Springer International Publishing. https://doi.org/10.1007/978-3-319-29315-8.
Sañé, E., Chiocci, F.L., Basso, D., Martorelli, E., 2016. Environmental factors controlling the distribution of rhodoliths: an integrated study based on seafloor sampling, ROV and side scan sonar data, offshore the W-Pontine archipelago. Cont. Shelf Res. 129, 10–22. https://doi.org/10.1016/j.csr.2016.09.003.
Sciberras, M., Rizzo, M., Mifsud, J.R., Camilleri, K., Borg, J.A., Lanfranco, E., Schembri, P.J., 2009. Habitat structure and biological characteristics of a maërl bed off the northeastern coast of the Maltese islands (Central Mediterranean). Mar. Biodivers. 39 (4), 251–264. https://doi.org/10.1007/s12526-009-0017-4.
Tauran, A., Dubreuil, J., Guyonnet, B., Grall, J., 2020. Impact of fishing gears and fishing intensities on maerl beds: an experimental approach. J. Exp. Mar. Biol. Ecol. 533, 151472. https://doi.org/10.1016/j.jembe.2020.151472.
Tuya, F., Schubert, N., Aguirre, J., Basso, D., Bastos, E.O., Berchez, F., Bernardino, A.F., Bosch, N.E., Burdett, H.L., Espino, F., Fernández-Gárcia, C., Francini-Filho, R.B., Gagnon, P., Hall-Spencer, J.M., Haroun, R., Hofmann, L.C., Horta, P.A., Kamenos, N. A., Le Gall, L., Tâmega, F.T.S., 2023. Levelling-up rhodolith-bed science to address global-scale conservation challenges. Sci. Total Environ. 892, 164818. https://doi.org/10.1016/j.scitotenv.2023.164818.
Venables, W.N., Ripley, B.D., 2002. Modern Applied Statistics with S, Fourth edition. Springer, New York, ISBN 0-387-95457-0. https://www.stats.ox.ac.uk/pub/MASS4/.
Wang, Y., Neuman, U., Wright, S., Warton, D.I., 2012. mvabund: an R package for model-based analysis of multivariate abundance data. Methods Ecol. Evol. 3, 471–473.
Wang, Y., Naumann, U., Eddelbuettel, D., Wilshire, J., Warton, D., 2022. _mvabund: statistical methods for analysing multivariate abundance Data_. R package version 4.2.1. https://CRAN.R-project.org/package=mvabund.
Warton, D.I., Blanchet, F.G., O'Hara, R.B., Ovaskainen, O., Taskinen, S., Walker, S.C., Hui, F.K.C., 2015. So many variables: joint modeling in community ecology. Trends Ecol. Evol. 30 (12), 766–779. https://doi.org/10.1016/j.tree.2015.09.007.
Wilson, S., Blake, C., Berges, J.A., Maggs, C.A., 2004. Environmental tolerances of free-living coralline algae (maerl): implications for European marine conservation. Biol. Conserv. 120 (2), 279–289. https://doi.org/10.1016/j.biocon.2004.03.001.
WoRMS Editorial Board, 2023. World register of marine species. Available from. https://www.marinespecies.org. at VLIZ. Accessed 2023-04-06. doi:10.14284/170.

Science of the Total Environment 912 (2024) 168752

Contents lists available at ScienceDirect

Science of the Total Environment

journal homepage: www.elsevier.com/locate/scitotenv

Reconstruction of the Maërl habitat to better understand its ecological integrity

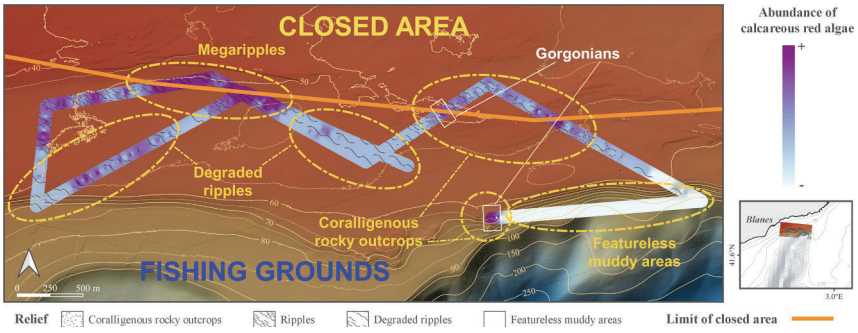
Montserrat Demestre [*], Sara Soto, Ruth Durán, José Antonio García del Arco, Andrea Cabrito, Laia Illa-Lopez, Francesc Maynou, Pilar Sánchez, Alfredo García-de-Vinuesa [1], Mickail Emelianov

Institut de Ciències del Mar, Passeig Marítim de la Barceloneta 37-49, 08003 Barcelona, Spain

HIGHLIGHTS

- Video images provide a solid basis for Maërl habitat reconstruction.
- Identification of four assemblages defined by relief and bottom sediments.
- Megaripples are the most representative assemblage with greater rhodoliths abundance.
- Combination of non-intrusive sampling allows successful assessment of Maërl's GES.
- Fragmentation due to fishing undermines resilience and ecological integrity.

GRAPHICAL ABSTRACT



ARTICLE INFO

Editor: Damia Barcelo

Keywords:
Coralligenous rocky-outcrops
Maërl bed
Non-intrusive sampling
Underwater-video images
Good environmental status
Western Mediterranean

ABSTRACT

Maërl habitats are composed of coralline red algae species that can live freely rolling on the seabed and forming nodules, the so-called rhodoliths, or incrusted forming coralligenous habitats. Maërl habitats are generally distributed in the Mediterranean at a depth of between 30 m and 70 m and are considered one of the most emblematic Mediterranean seabeds. In the present study, the complex structure of maërl habitats was investigated to i) characterise the relief features and classify the different sediments, ii) to estimate the abundance of the coralline red algae (both rhodoliths and encrusting ones) and iii) to analyse the biodiversity of the species inhabiting the habitat. Data were obtained from an approximately 11 km-long transect, using non-intrusive sampling methods, integrating information from video images collected using the Remotely Operated Vehicle LIROPUS (IEO_CSIC), and multibeam bathymetry and backscatter data. Video images were used to reconstruct (using GIS) the habitat structure and characteristics. Throughout the transect, a strong relationship between habitat characteristics and the effect of trawling activity and the geomorphology of the studied area was observed. The closed area to fishing activity showed a high abundance of rhodoliths in well-structured megaripples reliefs. Contrarily, the areas affected by fishing showed an important destructuring of the relief with a low density of rhodoliths. Last, the muddy bottoms showed areas with no characteristic features and no rhodoliths. All this information has allowed to reconstruct the maërl habitat in the Blanes continental shelf (NW

* Corresponding author.
E-mail address: montse@icm.csic.es (M. Demestre).
[1] Instituto Español de Oceanografía (IEO-CSIC), Centro Oceanográfico de Cádiz, Puerto Pesquero, Muelle de Levante 2609, 11,006 Cádiz Spain.

https://doi.org/10.1016/j.scitotenv.2023.168752
Received 11 May 2023; Received in revised form 2 August 2023; Accepted 19 November 2023
Available online 21 November 2023
0048-9697/© 2023 The Authors. Published by Elsevier B.V. This is an open access article under the CC BY-NC-ND license (http://creativecommons.org/licenses/by-nc-nd/4.0/).

Mediterranean) and analyse the fragmentation of the assemblages seen in the video to assess its good environmental status (GES), and finally to identify the level of ecological integrity of this vulnerable habitat.

1. Introduction

Coastal zones are home to important marine ecosystems that are subject to strong anthropogenic pressures and global change, with significant negative impacts on biodiversity (Thrush et al., 2012; Demestre et al., 2015; Fragkopoulou et al., 2021; Chaudhary et al., 2021; Gómez-Gras et al., 2021). In the Mediterranean, there are coastal ecosystems that constitute biodiversity 'hotspots', such as *Posidonia oceanica* meadows (Boudouresque et al., 2012; Duarte et al., 2013) and coralligenous bioconstructions, hard formations of accumulations mainly of calcareous red algae. (Ballesteros, 2006; Ballesteros et al., 2014). The Maërl seabed is one of the most representative and biodiverse examples of shallow coastal habitats on the Mediterranean continental shelf (Barberá et al., 2012; Riosmena-Rodríguez et al., 2017). Available information on their distribution and abundance in the Mediterranean is fragmentary and insufficient (Garcia-de-Vinuesa, 2021); for example, EMODnet[2] is a compilation of studies that have identified Maërl beds. Other work (Martin et al., 2014) has used predictive modelling to produce a continuous map of the entire Mediterranean. Therefore, there is an urgent need to develop a comprehensive mapping of benthic habitats to establish the most realistic distribution of Maërl habitats along the Mediterranean continental platform (Ingrassia et al., 2023).

Maërl beds are composed of rhodoliths, the unattached calcareous coralline red algae that create a hard but fragile skeleton (Lloret, 2015; Da Silva et al., 2021), and are organised in a very complex biological structure that provides ecospace in the form of three-dimensional habitats that increase local biodiversity by providing protective habitat against predators (Steller et al., 2003). Commercial important species like the red mullet, *Mullus surmuletus and M. barbatus*, benefit from more food and safe life growth periods (García-de-Vinuesa et al., 2022).

Maërl beds are considered important essential habitats that facilitate necessary services supporting important fisheries, bottom trawling and the artisanal fishing of a variety of commercial species and they also play a considerable role in carbon regulation. The impact of fishing gears, mainly trawls, on Maërl habitats may modify its structural complexity (Bordehore et al., 2003). Nevertheless, they are barely recognised as a vulnerable marine ecosystem (VME) (de Juan et al., 2020; Long et al., 2020) and need structures of protection beyond the existing regulations in the Habitats Directive (92/43/EEC 2007) on the conservation of natural habitats and of wild fauna and flora. More research is needed to understand the vulnerability of Maërl habitats and to identify pressures that may prevent them from achieving good environmental status and the right level of conservation (Rendina et al., 2022; Tuya et al., 2023).

The use of sampling methods such as underwater imaging provides information that allows marine habitats to be mapped to achieve a spatial representation of the seabed, defining its configuration, extent and condition, as well as the characteristics of its communities, which is difficult to achieve using other sampling systems (e.g. grab, dredge, trawl) (Bicknell et al., 2016; Beisiegel et al., 2017). Furthermore, multibeam echosounders (MBES) are now widely used for mapping marine habitats, mostly because they have technological capabilities (acquisition of high-resolution bathymetry, wide depth range and information on seabed texture) that are not available in other existing systems. Full coverage bathymetry allows the characterisation of the seascape by providing relevant information on the spatial distribution patterns of habitats and the relationship between seabed type and benthic habitats (Beaman et al., 2005; Holmes et al., 2008).

[2] (https://emodnet.ec.europa.eu/en/map-week-%E2%80%93-maerl-habitats)

The exact extent of the presence of Maërl in the area located in the continental shelf off the Blanes coast (NW Mediterranean) was unknown. The aim of this work is to provide new knowledge on the location and distribution of the Maërl habitats on the seabed of Blanes, to identify the structural complexity of the different relief and seabed types, and to analyse the abundance of rhodoliths and the biodiversity. The final objective of the study is to evaluate the Good Environmental Status (GES) of the Maërl habitat on the seabed of Blanes, using visual and non-intrusive sampling methods to assess its ecological integrity.

2. Methods

2.1. Study area

The study area is located on the continental shelf off the Blanes on the Catalan coast. The continental shelf is characterised by its narrowness (<4 km wide) due to the incision of the Blanes submarine canyon very close to the shoreline (Fig. 1a).

The different existing data on the three levels of information, geomorphology, biology and fishing activity in the selected area provided the necessary information to design a transect along the seabed to detect the presence of Maërl (Fig. 1, b,c).

2.1.1. Geomorphology background

The continental shelf displays numerous reliefs corresponding to infralittoral prograding wedges, small prodeltas, large morphological steps and narrow ridges interpreted as cemented beachrocks, and rocky outcrops, which appear exposed or partially covered by thick sediment layer (Lastras et al., 2011; Durán et al., 2013).

The backscatter imagery displays significant variations along and across-shelf (Durán et al., 2013, 2014). High backscatter values, displayed as light tones in the backscatter imagery (Fig. 1c), are associated to large grain sizes and rocky outcrops; whereas low backscatter values (depicted as dark tones) correspond to smaller grain sizes. On the Blanes continental shelf, backscatter intensities are medium to high over most of the continental shelf corresponding to medium and coarse with the exception of small areas of low backscatter in the inner and middle shelf associated to fine sand (Durán et al., 2013, 2017). Only close to the canyon rim and to the south of the large morphological step that extend from the Tordera prodelta to the canyon head, the seafloor is characterised by low backscatter corresponding to muddy sediments (ITGE, 1989; Díaz and Maldonado, 1990).

2.1.2. Biological and fisheries background

In the framework of some scientific projects developed prior to CRIMA (FORMED, COMSOM, MINOUW), several studies have been carried out in different areas of the continental shelf of the Mediterranean coast (Catalonia, Valencia, Murcia), providing information on the distribution, abundance and diversity of epifaunal and infaunal organisms.. With these precise data, it was possible to delimit the areas where their presence could indicate the presence of Maërl beds. This information, together with the characterisation and classification of the different types of sediment obtained from the aforementioned scientific projects, also provided valuable information for identifying the possible presence of Maërl beds in the Blanes study area. (de Juan et al., 2011; de Juan and Demestre, 2012; Muntadas et al., 2014; Demestre et al., 2017; Garcia-de-Vinuesa et al., 2018).

The studied area suffers trawl fishing activity during 6 month of the year. The fishing activity in the area adjacent to the port of Blanes revealed the presence of Maërl-related species in some fishing hauls and their total absence in others. The area with the presence of possible

Maërl beds is affected by the trawling activity of the Blanes between September and February, with the rest of the year regulated by a closed season. The main commercial species captured is red mullet (*Mullus surmuletus* and *Mullus barbatus*) (García-de-Vinuesa et al., 2022). The data on the fishing effort in the different fishing grounds visited by the trawling fleet from the port of Blanes helped to identify the potential seabeds that could be most damaged and unstructured because of to the chronic activity of the trawling fleet (Demestre et al., 1997; Demestre et al., 2000; Sánchez et al., 2004). In addition, an extensive Vessel Monitoring System (VMS) dataset extending over a long period of years from 2004 to 2021, and provided by the "General Secretariat for Fisheries of the Spanish Government", was analysed to explore the chronic fishing activity developed in the study area. The VMS is the oldest fisheries monitoring system in use and is readily available for scientific studies, which is why it was chosen to calculate fishing effort, a product that is useful for seeing where and how fishing activity is taking place in different areas. The combined analysis of all this information allowed us to design a transect 3 km from the port of Blanes of 11 km of length, with a maximum depth pf 111 m and minimum depth of 42 m, above the bottom that was a priori the most appropriate as Maërl habitat.

In order to obtain new information on the location and distribution of the Maërl habitat in the designed transect an oceanographic cruise CRIMA was carried out between 3 and 21 September 2020, on board the R/V Sarmiento de Gamboa (CSIC), The transect was imaged and mapped using ROV and multibeam systems. The video images of the 11 km length transect covered a total area of 13.8 ha. It took 3 days to film the transect and each day was filmed for 7–8 h in daylight.

3. Data processing and analysis

3.1. Bathymetric and backscatter data

High-resolution multibeam data (bathymetry and backscatter) and bottom sediment samples were used to characterise the morphology and sediment characteristics of the seabed. Swath bathymetry data were collected during the CRIMA cruise (September 2020) using an Atlas Fansweep FS-20-100 operating at a frequency of 100 kHz. Complementary swath bathymetry from a previous survey carried out during the ESPACE project (2004) using an EM 3000D from Kongsberg was considered to covering the whole continental shelf between 5 and 120 m water depth. The EM 3000D is a dual system with two sonar heads that operates at a frequency of 300 kHz. Positioning during multibeam data acquisition was by differential GPS.

Post-processing of the multibeam data from both surveys was conducted using the CARIS HIPS and SIPS Hydrographic Data Processing System©. Filtered soundings were gridded to 4-m digital elevation

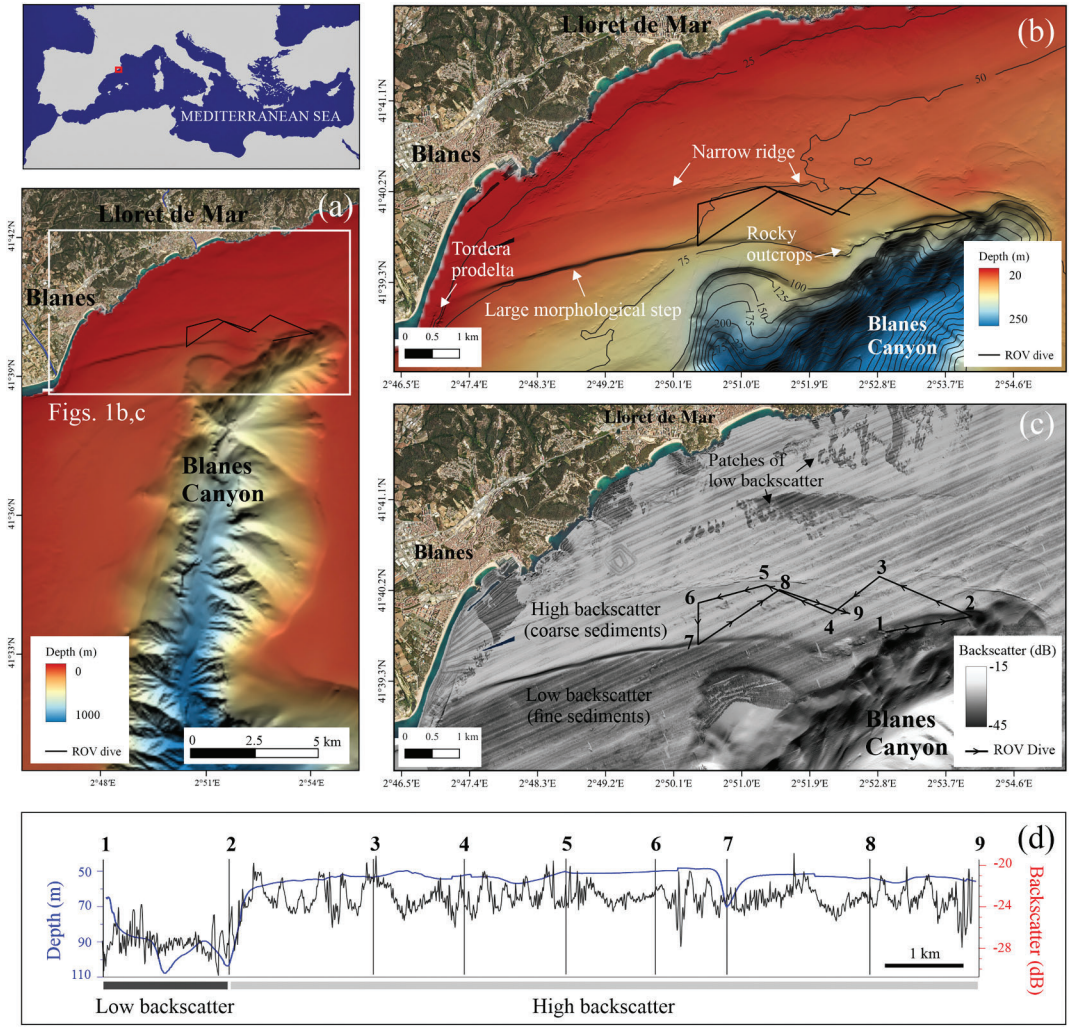


Fig. 1. (a) Shaded relief bathymetric map of the Blanes continental margin. (b) Bathymetry and (c) backscatter imagery of the Blanes continental shelf showing the location of the ROV transect. (d) Backscatter profile at the location of the ROV transect. Numbers indicate the intersection points along the transect from start to dive (point 1) to end (point 9). Note the abrupt change of backscatter from low values in the first sector of the transect located in the canyon rim (1 to 2) to high values in the continental shelf sectors.

models (DEM). Backscatter data were processed at higher resolution (1 m). Bathymetric and backscatter data were integrated into a geographic information system (QGIS) for the morphological analysis.

In addition, textural analyses were conducted on sediment samples collected in the study area during the CRIMA cruise using a Van Veen grab. A Horiba LA 950 laser diffraction particle size analyser was used to determine the grain size distribution of the sediment.

3.2. Video data

Video images from the seabed were provided by the Remotely Operated Vehicle (ROV) LIROPUS (IEO-CSIC). The LIROPUS, equipped with a Kongsberg OE14-502 A HD videocamera, facilitated video recording along the transect designed on the seabed to enable the reconstruction of the Maërl habitat of the selected study area. A total of 16 h of videos was recorded along the 11 km transect. The ROV was also equipped with a two-point laser 10 cm apart, used as a reference for the distance and size of species and for any observed object, and also with dataloggers to record the temperature and depth. An area of 13,838.64 m^2 was swept at an average speed of 0.5 knots.

All the information obtained from the video analysis and during the CRIMA cruise was organised and stored in the PostGIS geospatial database which was built under the Database Management System Postgres. This database is based on an entity-relationship schema useful for the analysis and consultation of information (PostGIS Project Steering Committee, 2023).

The processing of the video information allowed the visualization of the data obtained along the transect at the level of relief and sediment characteristics, rhodolith abundance and diversity, and species/taxa abundance. The entire video was visualised along the transect to identify: i) physical parameters such as different relief features and substrate (sediments) bottom type; ii) the distribution and abundance of the rhodoliths relating to the both the relief and the sediments, iii) and visible organisms (fauna and flora) at species level or at the lowest possible taxonomic level, and to quantify the abundance for each taxa as the sum of individuals per swept area (sum/m2). Data visualization, mapping and data analysis were carried out using the QGIS software. QGIS is a Geographic Information Systems program that also allows the connection to the database to be exploited by means of sql queries (QGIS Development Team, 2021). All the geospatial information used was projected onto the Universal Transverse Mercator reference system, datum ETRS89, zone 31 N (EPSG: 25831).

i) Relief features and sediments

The video analysis allowed the definition of the existing reliefs. The relief and background data extracted from the video analysis were mapped using QGIS along the transect following the 50 m buffer to have a more global view of the area and to be able to establish a relationship between among relief, bottom type and Maërl abundance.

In addition, we used selected frames sequences extracted from the recorded video were used to obtain 3D view models using MeshRoom software through a Photogrammetry Pipeline. Photogrammetry allows to create a mosaic image to be created with overlapping multiple images. The aims were to study and define an object with precision in terms of shape, dimensions and position. These models were useful to identify relief structures from the bottom in some interesting transect areas.

ii) Abundance and diversity of rhodoliths

The estimation of the percentages of Maërl beds along the transect was estimated by rhodoliths abundance. This was defined by analysing the video images of the abundance of rhodoliths considering the following classification: NR ("no-rhodoliths") 0 % bottom coverage by rhodoliths, LDR ("low-density rhodoliths") < 30 % coverage by rhodoliths, MDR ("medium-density rhodoliths") 30 % to 50 % coverage by rhodoliths, and HDR ("high-density rhodoliths") >50 % coverage by rhodoliths. From this classification a Multilevel B-spline algorithm for spatial interpolation of scattered data was used to obtain an abundance distribution map in the same buffer of 50 m from the transect line. The algorithm makes use of a coarse-to-fine hierarchy of control grids to generate a sequence of bicubic B-spline functions whose sum approximates the desired interpolation function (Lee et al., 1997; Russo et al., 2011). Multilevel B-Spline was chosen because it was the interpolation method that best fit with those offered by the QGIS software.

iii) Abundance of species/taxa

The ROV sampling technique can be very useful for characterising habitats by providing in situ observations of all the elements that constitute the ecosystem and how they vary along a transect (Price et al., 2019; López-Garrido et al., 2020). Despite its undisputable advantages, this technique has limitations because it is not always possible to reach the species level in terms of identification, so it has always been identified at the highest taxonomic level possible. Another limitation is that only the fauna inhabiting the upper layer of the seafloor is imaged. However, the variety of taxa found in this area was high and it was important to identify them as they are representative of each type of seabed. To this effect, the communities with the species that characterise in the study area could be identified.

Species were classified following the nomenclature used in Ballesteros et al. (2014): *dominant taxa*, those with a higher abundance than the rest and were dominating the habitat studied; *abundant* taxa, those that were abundant but not dominant; *significant taxa*, those that were in the habitat almost exclusively or with a clearly differentiated abundance and *sporadic taxa*, those that appeared with lower abundance and provided little information.

The abundance of species identified was estimated for each of the relief types as the sum of individuals per swept area (sum/m2) for each of the relief types identified. The diversity of the Maërl habitat along the transect was estimated using the specific Richness (S) and Shannon-Weiner index (H).

3.2.1. Multidimensional analysis

The ROV images of the transect were used to develop a matrix with a total of 109 points selected every 100 m characterised by the abundance of calcareous red algae, both rhodoliths and encrusting, and by the type of relief, the type of bottom sediment, the species observed and the depth. The matrix was used to test the spatial distribution and variability of these assemblages along the visualised transect.

The PRIMER statistical software was used to perform multivariate analyses of the sea bottom data (Clarke and Warwick, 1994). A cluster analysis using the Bray-Curtis similarity index was carried out using double square root transformed data, and dendrograms were made using the group average clustering method. The resulting similarity matrices were then used to perform non-metric multidimensional scaling (MDS). The ANOSIM test was used to test the similarity between samples.

3.2.2. Univariate measures of diversity

Univariate measures of diversity such as specific Richness (S) and Shannon diversity index (H′) were calculated on the different tupes of substrate and Maërl coverage. Both indices serve to reflect the diversity gradients by measuring the diversity heterogeneity (Thrush et al., 2012; Barberá et al., 2012). These measurements were obtained considering 15 min section of video where, the Richness index (S) was calculated as the number of different species observed using the *specnumber()*-function from package *vegan* (Oksanen et al., 2022) and the Shannon index was obtained through the function $H^{'} = \sum_{i=1}^{S}(p_i \, x \, lnp_i)$ where p_i represents the proportion of each species in the population. Two ANOVA model tests were performed on the Richness and Shannon indices. Then a post-hoc Tukey test from the 'stats' package (R Core Team, 2022) was

performed to examine the differences between levels of maërl coverage on the Shannon index. These statistical analyses were performed in R (R Core Team, 2022) under version 3.6.3.

3.3. Fishing effort

Fishing effort was processed using information from the Vessel Monitoring System (VMS) data and calculated to contemplate the spatial component following the methodology explained in García del Arco et al. (2015, 2016), and to map the results using QGIS. Fishing effort value was represented by a grid of 1 km^2 cells, displayed as hour/km2. This product is useful to see where and how the fishing activity occurs in the different areas. Data from VMS in three different periods 2010–2011, 2015–2016 and 2020–2021 were analysed to see the different levels of fishing and compare their impact on the Maërl bed over the years,

4. Results

The study of the seafloor following the designed transect was carried out using non-intrusive techniques with different data sets including multibeam data, sediment samples and video images using ROV acquired during the CriMa cruise.

4.1. Description and characteristics of the Maërl habitat along the transect

The reconstruction of the habitat was made possible by analysing the ROV imagery along the transect. From the video images, it was feasible to identify and estimate percentages of the relief features and characterise the different types of bottom (Table 1). Four types of main reliefs were identified: megaripples, degraded ripples, coralligenous rocky outcrops and featureless muddy areas.

The most representative relief of this Maërl habitat was the ripples with as total of 11,277.08 m^2 of the total swept area of the transect. Ripples along the transect appeared as megaripples covering an area of 5402.11 m^2 (39.04 %) and degraded ripples an area of 5874.97 m^2 (42.45 %). The megaripples occurred mainly to the north of the transect at a depth of around 50 m (Fig. 2), with heights above 20 cm, and locally up to 60 cm, and were composed of coarse sediments as evidenced by the backscatter data (high values, Fig. 1c) and bottom sediment samples. More specifically, the sediment sample collected in the area of greatest abundance of rhodoliths associated with the megaripples showed a bimodal grain size distribution, consisting of coarse sands and gravels with very low percentages of silt (< 4 %). Sand content ranged between 75 % and 85 % of the total sediment and gravels between 15 % and 25 % with a median size close to 1000 um. The degraded ripples were distributed and scattered in different areas across the video. The most characteristic sediment of this relief was poorly sorted coarse sand. The video images revealed an area located to the south of the transect with no discernible relief and is displayed in the backscatter image with low values (Fig. 1d), corresponding to muddy sediments. This area occupied 1619.08 m^2, or 11.70 % of the total swept area of the transect. Finally, the area of coralligenous rocky outcrops observed represented 6.81 % of the total transect. This is the area where there were most biocenosis with a high biodiversity located in areas dominated by sand and gravel sediments.

4.2. Reconstruction of the Maërl habitat along the transect

Fig. 2 shows the reconstruction of the seabed according to the visualised transect. Different assemblages were mainly identified depending on the type of relief and the estimated abundance of the rhodoliths along the transect. Bottom type characteristics and abundance of species (taxa) were also taken into account in each assemblage.

The estimated percentage of abundance of Maërl beds in density of rhodoliths, was calculated for each of the relief features defined above (Table 1). Megaripples occupy 39.04 % of the total swept area The higher abundance of rhodoliths (29.70 %, Table 1) was associated with megaripple formations. Degraded ripples appeared in different parts along the transect (Fig. 2) with the highest percentage of the total swept area (42.45 %, Table 1). They were mainly observed around 50-60 m depth. The higher density of rhodoliths in these assemblages corresponded to the category of low density with an occurrence of 31.40 %. However, because of their presence along the entire transect it was possible to find areas with medium density (5.36 %) even with high density (1.01 %) (Table 1). These areas of degraded ripples corresponded to areas of high backscatter, consisting of sandy and coarse sediments (Fig. 2). The distribution of these areas along the transect evidenced the existence of a transition from areas characterised by the presence of megaripples and high abundance of rhodoliths to perturbed areas of degraded ripples (Table 1). In the southern part of the transect, there was a featureless area where the density of rhodoliths was zero and the backscatter data showed the lowest values of the transect area, corresponding to muddy sediment (Fig. 1d).

Along the transect, areas of coralligenous rocky outcrops with a significant abundance of encrusting calcareous red algae were also identified. These areas represented only 6.81 % of the transect (the remaining 93.19 % had rhodoliths), but they were areas of great importance due to the biodiversity associated with them, forming interesting biocenosis areas.

Regarding the coralligenous rocky outcrops, it is important to highlight the two areas of gorgonians (*Paramuricea clavata*) observed in their surrounding areas. One area is located in the northern part, at a depth of around 50 m depth, very close to the area closed to fishing, and the other is further south at a depth of around 70 m, close to the canyon head. Both areas of gorgonians were located in rocky areas, corresponding to the eastern limit of a large ridge that extends along the mid-shelf to the canyon rim and to scattered rocks at 70 m depth close to the canyon head (Figs. 1 and 2).

Based on the information provided by the video images on the different types of reliefs- the associated bottom type, the abundance of calcareous red algae (rhodoliths and incrusting) and the species inhabiting them- it was possible to identify four assemblages that are perfectly corroborated in the MDS analysis with a stress level of 0.08 (Fig. 3). The result of the ANOSIM test shows an R value of 0.69 ($p = 0.001$), which is consistent with the four assemblages identified by the MDS.

According to the MDS, the relief of the featureless muddy areas and the coralligenous rocky outcrops were clearly separated from the other

Table 1
Density of Maërl bed as the percentage of abundance of rhodoliths (low, medium and high density) and coralligenous rocky outcrops, according to the encrusting algae (no-rhodoliths) in each of the defined reliefs (megaripples, degraded ripples, coralligenous rocky outcrops and featureless muddy area) along the transect, weighted all to the swept area.

Calcareous red algae	Rhodoliths (%)			Encrusting (%)	Swept area (%)
	Megaripples	Degraded ripples	Featureless muddy areas	Coralligenous rocky outcrop	
High-density	86.64	6.05	0.00	7.31	16.72
Medium-density	62.92	22.16	0.00	14.92	24.17
Low-density	20.47	73.04	0.61	4.34	42.99
No-rhodoliths	0.00	29.05	70.95	0.00	16.12

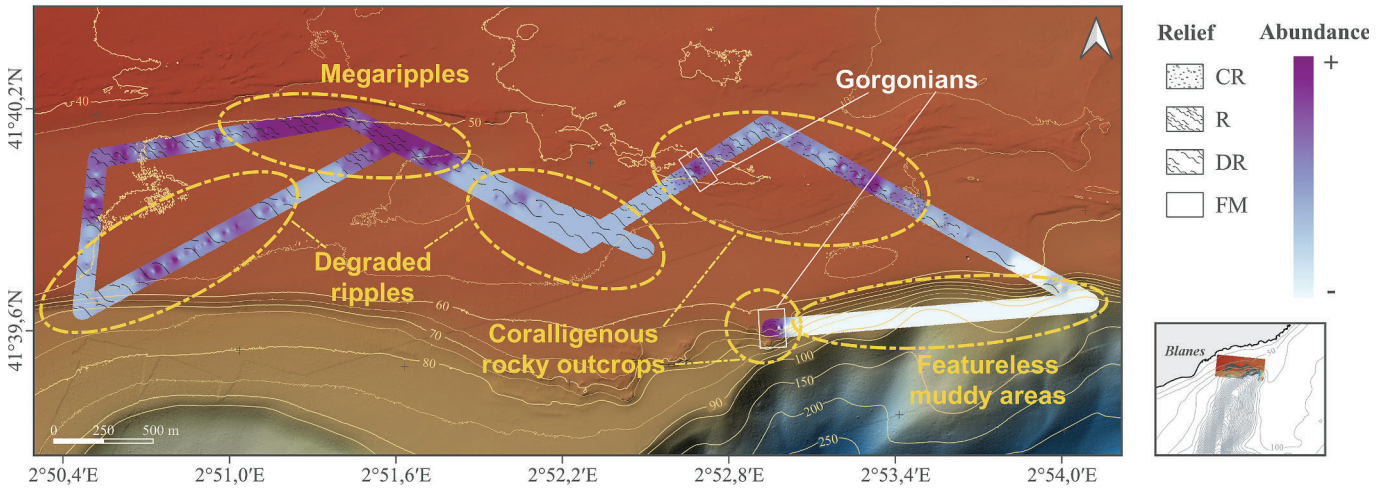


Fig. 2. Transect across the seabed of the Blanes continental shelf (NW Mediterranean) showing the distribution of the four assemblages with each type of relief identified (dashed lines): megaripples (R), degraded ripples (DR), coralligenous rocky outcrops (CR) and featureless muddy areas (FM). Intensity of colour shows the estimated abundance of rhodoliths.

reliefs, both shown at the extremes of Fig. 3. The evident separation was a consequence of the non-existence of rhodoliths in the two reliefs. Contrarily, even though they presented a clear separation, the megaripples and the degraded ripples, were still related with some connectivity due to the abundance of rhodoliths in both reliefs. This was clearly noticeable from the MDS of the existing transition of the reliefs from the megaripples to the featureless muddy area passing through the degraded ripples.

Regarding to the fishing effort in the study area ongoing and intense fishing activity has taken place there over the years. To understand the different levels of fishing impact on the Maërl bed, data from the VMS in the periods 2010–2011, 2015–2016 and 2020–2021 were analysed for identification and comparison purposes. The three fishing periods represented in Fig. 4 had a constant and chronic impact in the study area. Fishing activity takes place in the fishing ground from September to February and the rest of the year it is closed to trawlers. In the north of the transect there is a closed fishing area since 2006, where trawling is strictly not allowed.

It should be noted that the lowest fishing effort values appeared in the northern part of the transect where the megaripples were found (Fig. 4a). In turn, part of this relief is under the protection of the permanent closed area, which means that trawling activity is forbidden and there is consequently no impact on the seabed. Fishing effort in the assemblage of degraded ripples (Fig. 4b) has been of a high and constant intensity over the years causing degradation and leading to a transition from megaripples with high abundance of rhodoliths to degraded ripples where rhodoliths abundance is low. There are areas where even the degraded ripples appear in a very smooth way and where the sediments become finer (from sand to muddy sand). The coralligenous rocky outcrops offer even better natural protection due to their abrupt relief, which prevents trawlers from fishing over the rocks, resulting in lower fishing intensity. (Fig. 4 c).

4.3. Good environment status

Information from the ROV imagery was used to identify possible changes to the Maërl habitat that had caused assemblages fragmentation. The fragmentation-connectivity of the biophysical characteristics of the habitats was analysed in 15 min sections across the entire transect and the homogeneity of relief, and the type of sediment together with the level of abundance of rhodoliths and the diversity was estimated (Fig. 5).

Different homogeneous assemblages were observed along the transect being the megaripples the most representatives for this Maërl habitat with a high abundance of rhodoliths and sediment of medium and coarse sand (Fig. 5a; Table 1). Their percentage across the total transect was 39.04 %. The featureless muddy area relief was also a homogeneous assemblage characterised by the non-presence of rhodoliths and muddy sediment and patches of detritus representing 11.70 % of the total transect (Fig. 5b; Table 1). The third homogeneous assemblage corresponded to degraded ripples. Although it looked like a heterogeneous assemblage, it was in fact a background where the undulations were degraded to different degrees and where rhodoliths also appeared in densities alternating between medium and low density (Fig. 5c; Table 1). Strong fragmentation was only observed along the transect where there was a change between very different assemblages, in one direction or another, such as the change from mega undulation or degraded ripple assemblages to coralligenous rocky outcrops or to featureless and rhodolith-free muddy areas.

The ANOVA model test performed on Richness value (S) shows no significant differences (p-value = 0.159) between the different types of sediment (medium and coarse sand and muddy sands) neither between levels of Maërl coverage (p-value = 0.259). In contrast, the result of the ANOVA test for the Shannon index (H') shows significant differences between the type of substrate (p -value <0.05) and between the levels of Maërl coverage (p-value <0.05). The Shannon index has turned out to be higher in muddy sands and in areas without Maërl coverage (Fig. 6). Finally, the Tukey test shows that the differences in Shannon index for the Maërl coverage levels were found between “without Maërl” and “Low Medium cover” (p-value <0.05) and between “without Maërl” and “High cover” (p-value <0.05).

In parallel, the observed species or taxa shown in the video were classified according to the importance and abundance of each in the four assemblages, and classified as dominant, abundant, significant and secondary. Undoubtedly, the significant, or habitat building, specie in the study area is the Maërl, considering as Maërl the different species of rhodoliths. *Echinaster sepositus* was the dominant species and was present in all the assemblages. The most abundant species in the megaripples assemblage was also *E. sepositus*, with different species of hermit crabs in the degraded ripples and *Holothuria tubulosa* in the muddy areas. The coralligenous rocky outcrops was the assemblage with the highest biodiversity, with four most abundant species: *Bonellia viridis*, *Halocynthia papillosa*, *Axinella polypoides* and *Paramuricea clavata*.

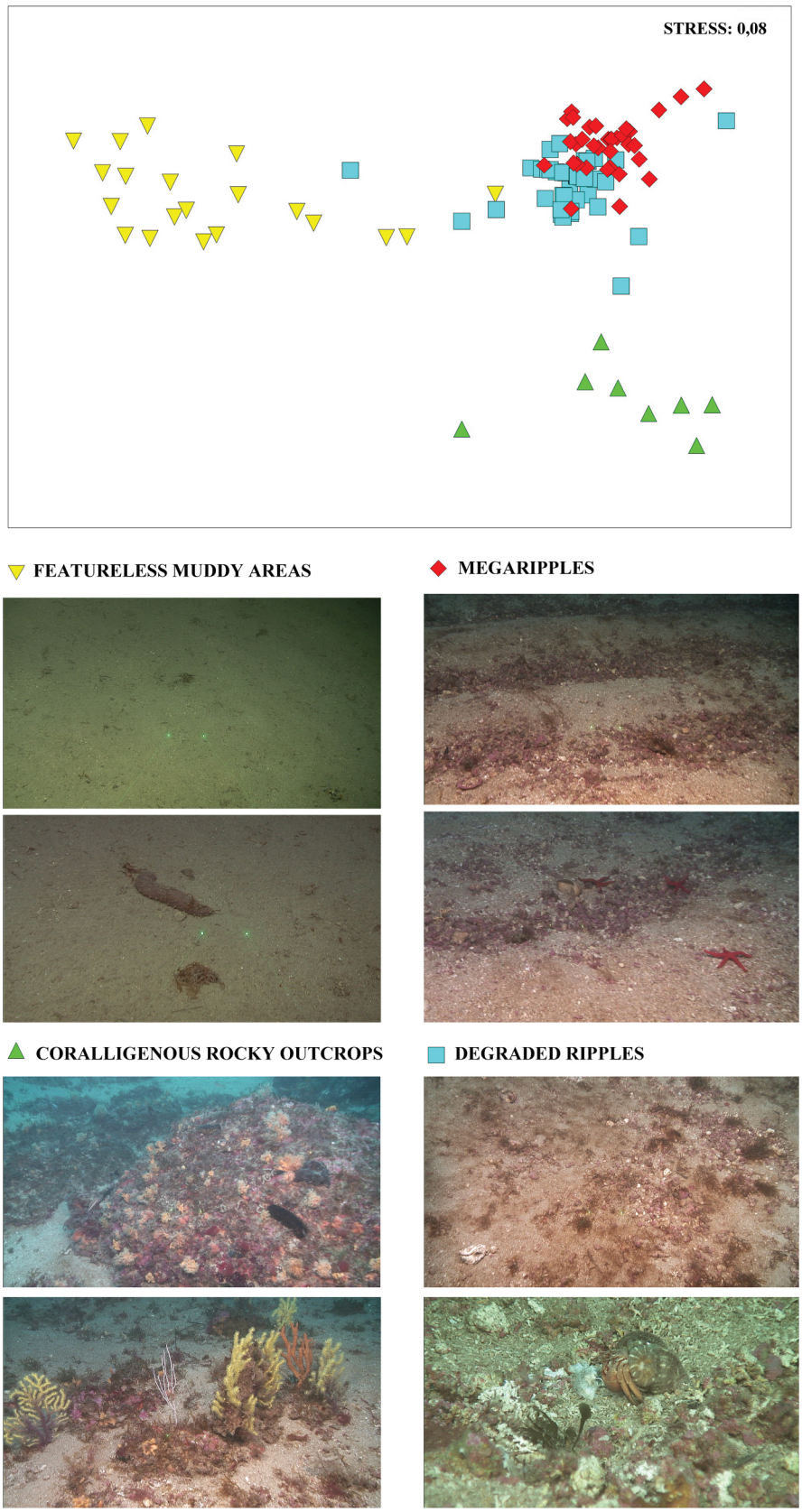


Fig. 3. MDS representation of the four assemblages identified on the seabed (megaripples, degraded ripples, coralligenous rocky outcrops and featureless mudflats) based on the analysis of the video images obtained along the transect, including some representative images of each of them.

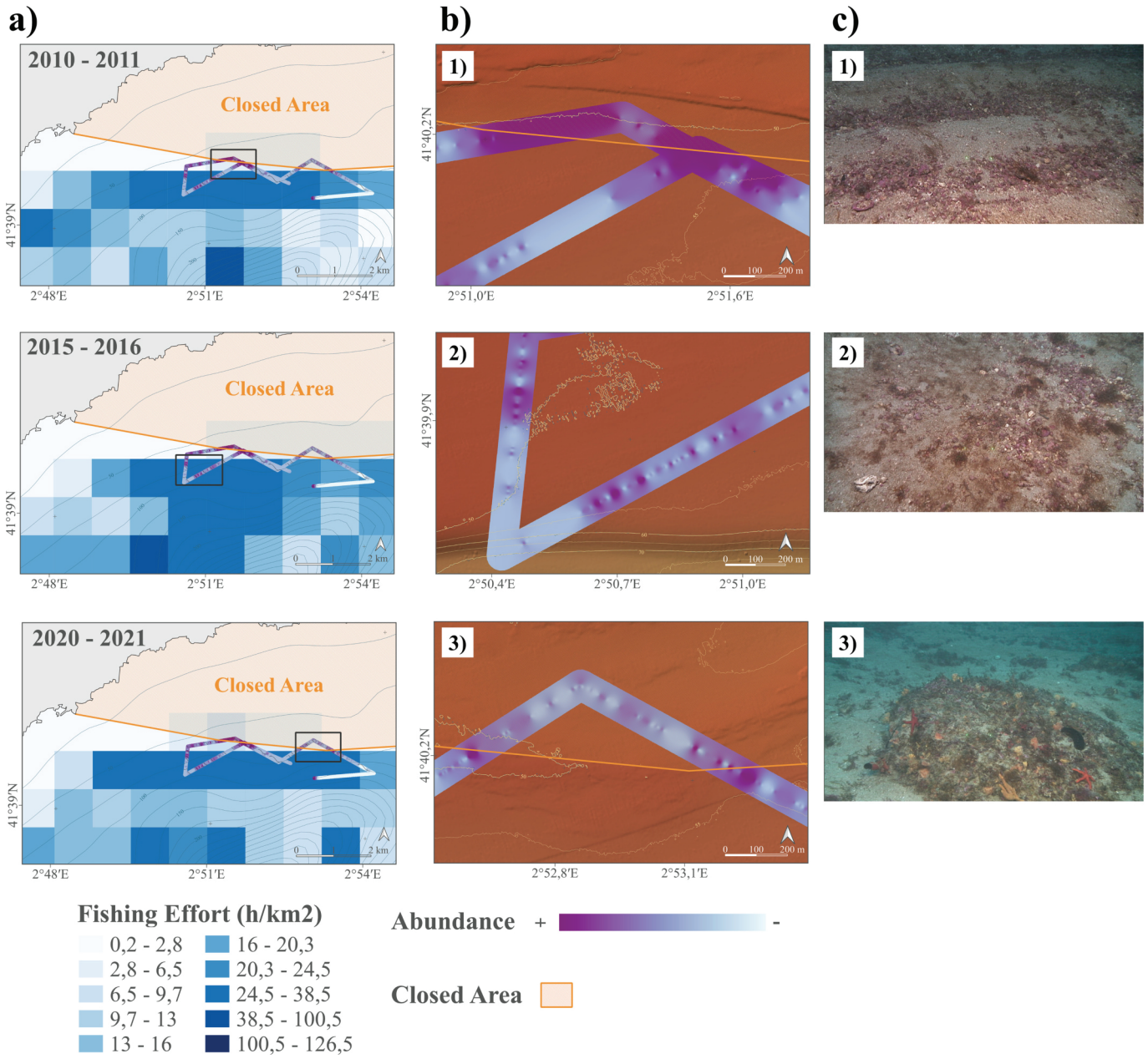


Fig. 4. a) Fishing Effort estimated by VMS information of three periods: 2010–2011, 2015–2016 and 2020–2021. b) Map showing the abundance of Maërl bed and the relief types, and c) video images of the each of the relief types: (1) Megaripples, (2) Degraded ripples and (3) Coralligeonus rocky outcrops.

5. Discussion

The most important finding of the present study was the successful characterisation and assessment of the seabed of a Maërl bed and a coral rocky outcrops using a visual and non-intrusive sampling method. Both habitats are typical Mediterranean seascapes with species bio-constructors of red calcareous algae. There are important gaps in the distribution of these habitats across the Mediterranean Sea making it very difficult to know their ecological status and progress towards achieving their ecological integrity.

The rhodoliths are coralligenous red algae assemblages responsible of forming the Maërl beds one of the most important hotspot of the biodiversity in the Mediterranean Sea. The most identified species as forming Maërl bed at Mediterranean level are *Lithothamnion corallioides* and *Phytomatholithon calcareum* (Barberá et al., 2003; Peña and Bárbara, 2004; Martin et al., 2014; Ingrassia et al., 2023). In the Blanes continental shelf, observations of light microscopy (LM) and scanning electron microscopy (SEM) from direct samples revealed the presence of a great variety of other forming Maërl bed species of red algae, including *Lithophyllum pustulatum, L. racemus, Lithothamnion sonderi, L. minervae, L. valens, Mesophyllum lichenoides, Neogoniolithon mamillosum,* and *Spongites fruticulosus*. At the same time these habitats are of great interest because they offer ecosystem services, including as food provision because several commercial species inhabiting in it (*Mullus surmuletus* and *M. barbatus*, Triglidae, *Loligo vulgaris*), and as a place as spawning, nursery and growing of both commercial and non-commercial species (García-de-Vinuesa et al., 2022; Tuya et al., 2023).

Analysis of the images of the video was feasible to identify and characterise the sea bottom and be possible to elaborate a habitat mapping. The extraction of this information allowed the identification of the physical and ecological characteristics of the habitat (Price et al., 2019; Cresswell et al., 2021). In the Blanes continental shelf, the

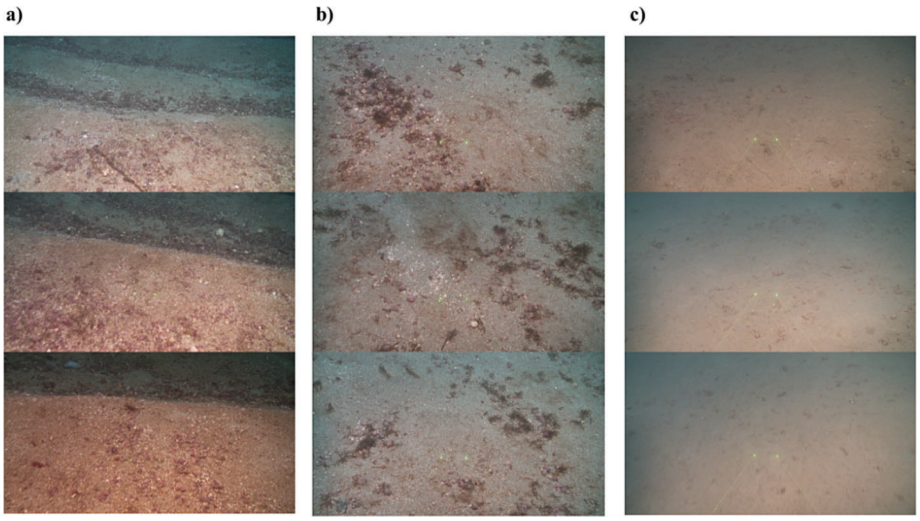


Fig. 5. Images representatives of the 15-min section: a) megaripples composed of medium and coarse sand with high abundance of rhodoliths, b) degraded ripples composed of medium and coarse sand with media and low rhodoliths abundance, c) featureless muddy area with zero rhodoliths.

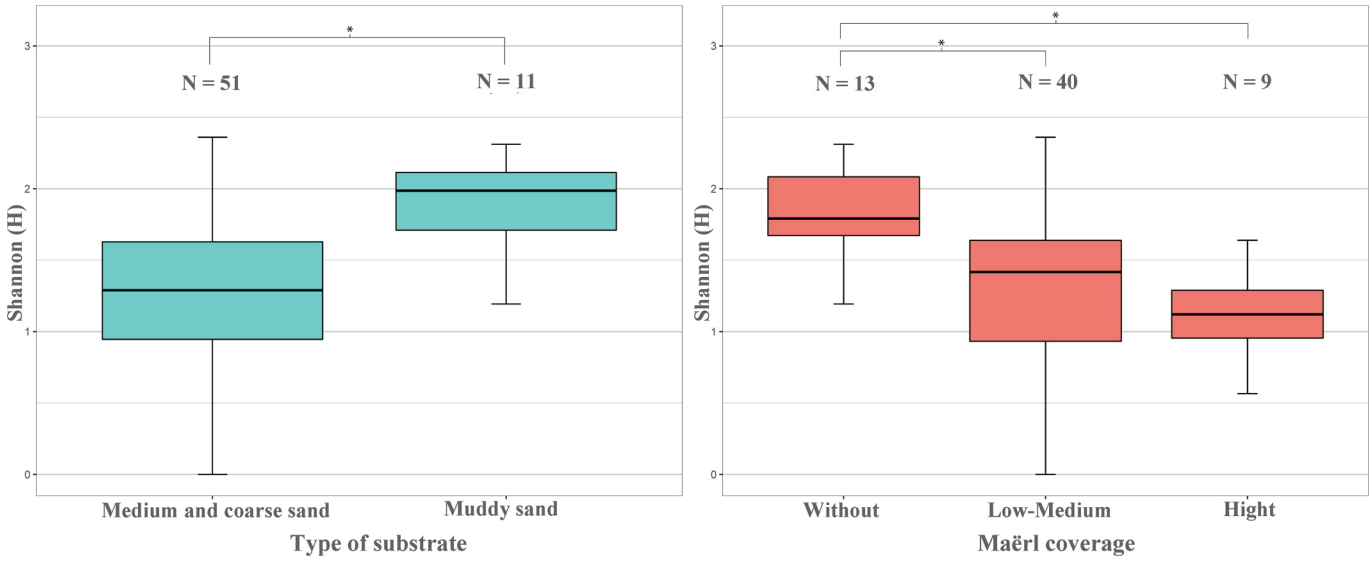


Fig. 6. Shannon (H′) index for (left) type of substrate ad (right) Maërl coverage.

distribution and characteristics of the red calcareous algae habitats observed in the video images show a strong relationship with the geomorphology and sediment characteristics of the seabed, as well as with the impact of trawling activities. The results offered four assemblages across the studied area. Well-structured Maërl beds were observed on areas of coarse sediments where megaripples develop. The distribution of Maërl is controlled by different environmental factors such as seabed characteristics (grain size), sediment input and hydrodynamics. Accordingly, Maërl beds occur in areas swept by currents (Toscano et al., 2006) or in areas with no significant energy but with reduced sediment influx (Millar and Gagnon, 2018). In the Blanes shelf the presence of Maërl habitats in the megaripples assemblage can be explained by the limited contribution of fine sediments transported by rivers and the local hydrodynamics that favours the transport of fines to other areas.

At its mouth the Tordera River releases large amounts of coarse sands (approx. 83 % of the total sediment discharge of the river) carried as bedload and fine sediment in suspension (Rovira et al., 2005; Liquete et al., 2009), that can subsequently be transported towards the southwest favoured by predominant south along-shelf currents (Durán et al., 2013). The sorting and preferential escape of fines makes the sedimentary cover of this sector of the continental shelf to be mainly sandy, as shown by the high backscatter pattern (Fig. 1d). Backscatter is high over most of the continental shelf imaged by ROV video (about -23 dB), except for the last section of the transect where it is significantly lower (about -28 dB), thus evidencing important variations in the seafloor texture from coarse sand in the continental shelf to muddy sand in the canyon rim. The preferential deposition of fine sediments in this area would explain the null density of rhodoliths (Fig. 2), generating another important area observed is to the south, at greater depth, with an important transformation of relieve feature and sediment. The ripples and rhodoliths gradually disappeared and the sediment changed from coarse sand and gravel to finer sediment. Fishing activity alone cannot explain this impressive transformation because as already mentioned, in the set of degraded ripples the applied fishing effort was much higher. These changes in sediments and rhodoliths are related to the geomorphology of the study area, which is located to the south of a large morphological step that extends along the middle shelf to the canyon rim where the fine sediments (muddy sands) are deposited, as evidenced by backscatter data (Fig. 1d) and sediment information (ITGE, 1989; Díaz and Maldonado, 1990).

However, not only natural conditions are related to the presence of Maërl bed. It was observed that fishing activity generates huge negative effects causing important degradation of these sea bottoms. In the studied area a restructuration of the characteristics of relief affecting the most representative assemblage of the Maërl habitat was reported (Fig. 4): the megaripple assemblages gradually changed to an assemblage of degraded ripples with a consequent important reduction in the abundance of rhodoliths and the associated biodiversity. Further, when fishing activity showed very high levels of fishing effort, there was a transition of degradation of the sediment from gravel and sands to muddy sand (Garcia-de-Vinuesa et al., 2018; Tauran et al., 2020).

Notably, the assemblage of degraded ripples was able to be detected thanks to the 3D model elaboration (Figs. 7a, b). The observation of the video did not allow for clear identification of the seabeds with smooth degraded ripples, because on the screen it looked like a featureless and uniform bottom on. The same approach of recreated 3D representations of video transects has been developed on marine vertical structures (Robert et al., 2017; Fabri et al., 2019).

Fishing effort is an important effect to consider in relation to changes in habitat at environmental status level. The fragmentation images along the transect show evidence of a significant reduction in the ecological integrity of the calcareous red algae habitat where fishing activity takes place. It is evident that the transect section within the permanent trawl closure zone has the best level of integrity with higher and well-developed megaripples and higher abundance of rhodoliths (Demestre et al., 2008; Barberá et al., 2017). The same can be said at the level of integrity for one of the gorgonian zones that lies on a transect within the closed area (Fig. 4c). However, there is a second gorgonian zone in the middle of the fishing ground. The permanence in this area can only be explained by the presence of large rocky outcrops (beach rocks). The two areas of gorgonians (*Paramuricea clavata*) observed in the video images are associated with local rocky outcrops surrounded by coarse sediments (Fig. 2). These rocky outcrops correspond to former cemented beaches extending along the mid-shelf to the canyon rim at 35–50 m water depth (Lastras et al., 2011; Durán et al., 2013) or scattered rocky outcrops at 70 m water depth, within the canyon rim, thereby providing the favourable substrate for these collarigenous rocky outcrops assemblage.

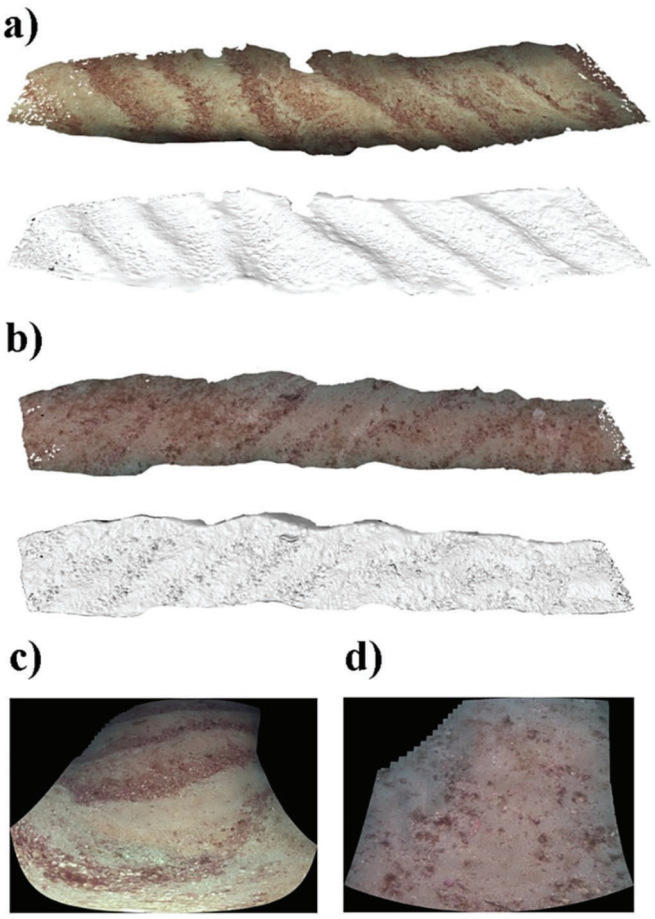


Fig. 7. 3D images of the mosaic and hillshade digital elevation model: a) megaripples, b) degraded ripples and photomosaic of c) megaripples d) degraded ripples.

Despite the advantages of using a non-intrusive methodology, like the one explored in this paper, there is some lack of precisions in analysing observations of the seabed by video (Collie et al., 2000). At species, and even taxa, level only those bigger than 2–3 cm can be well identified, which are basically organisms bigger than the size of the epifauna. The results of the Shannon index evidence this lack showing a higher number of species on muddy sediment than on medium and coarse sand, and even more species in assemblages without rhodoliths than in those with a medium-low or high abundance of rhodoliths (Fig. 5). The Maërl itself masks and hides the organisms that inhabit it, and because the muddy bottom is clearer and homogenous, more organisms can be seen on top of the sediment.

Fragmentation-connectivity is another right indicator allowing to estimate the level of the Good Environmental Status (Hiddink et al., 2006). Habitat fragmentation inevitably leads to discontinuities in a seabed that initially maintained a certain stable continuity. Habitat fragmentation can occur as a result of a natural phenomenon or an anthropogenic activity like trawling. Degraded ripples areas appear along the analysed transect and are always related to the megarripples showing the existence of a transition both in the relief and in the abundance of rhodoliths. The abundance of species or taxa can also be considered as a valid information to know the condition of biodiversity along the transect. This comprehensive information indicates that the habitat has undergone fragmentation forming assemblages with some patches of change but with structural continuity throughout the habitat, which is evidence of resilience. In other words, the condition of the environment has remained good.

It would obviously seem, that the ecological integrity of the Maërl bed has completely disappeared. However, it is important to bear in mind that, despite the important differences in the integrity characteristics among the four observed assemblage (megaripples, degraded ripples, coralligenous rocky outcrops and featureless muddy areas) we must consider that good environment status or good integrity does not always corresponds to a (practically)-pristine status. Good ecological situation can be found in communities, habitats and ecosystems where, despite the interaction of existing different impacts, there are situations of equilibrium that offer ecological sustainability exists (Rice et al., 2012; Thrush et al., 2012).

6. Conclusions

In the present study we propose an approach to describe and characterise the vulnerable calcareous red algae assemblages in order to analyse their ecological integrity. This approach aims to reconstruct the information from the video transect to produce a habitat mapping using the information gathered from a non-intrusive sampling methods that avoids the use of damaging methods. From the analysis of the information derived from bathymetry, backscatter and video images, we were able to identify and characterise four assemblages: megaripples, degraded ripples, coralligenous rocky outcrops and featureless muddy areas. Different reliefs and bottom types, and the abundance of rhodoliths and species diversity were estimated in each assemblage. The results evidence an important reduction of the good environment status in the assemblages outside the closed fishing area. It is imperative that the entire Maërl habitat be enclosed within the permanently closed fishing area because it is the last opportunity to maintain the ecological integrity at the levels of sustainability and equilibrium throughout the Maërl

bed and the coralligenous rocky outcrops of this bottom and to keep the different assemblages in good environment conditions.

CRediT authorship contribution statement

Montserrat Demestre: Conceptualization, Methodology, Visualization, Data curation, Formal analysis, Writing – original draft, Writing – review & editing, Investigation, Funding acquisition. **Sara Soto:** Conceptualization, Methodology, Visualization, Formal analysis, Writing – original draft, Writing – review & editing. **Ruth Durán:** Conceptualization, Methodology, Visualization, Formal analysis, Writing – original draft, Writing – review & editing. **José Antonio García del Arco:** Conceptualization, Methodology, Visualization, Formal analysis, Writing – original draft, Writing – review & editing. **Andrea Cabrito:** Methodology, Visualization, Formal analysis, Writing – original draft, Writing – review & editing. **Laia Illa-Lopez:** Methodology, Visualization, Formal analysis, Writing – original draft, Writing – review & editing. **Francesc Maynou:** Methodology, Visualization, Formal analysis, Writing – original draft, Writing – review & editing. **Pilar Sánchez:** Methodology, Visualization, Writing – original draft. **Alfredo García-de-Vinuesa:** Methodology, Visualization, Writing – original draft. **Mickail Emelianov:** Methodology, Visualization, Writing – original draft.

Declaration of competing interest

On behalf of all authors, the corresponding author states that there is no conflict of interest.

Data availability

Data will be made available on request.

Acknowledgements

This research work was developed on the framework of the I+D+I Project CRIMA (RTI2018-095770-B100) funded by MCIU / AEI / FEDER, EU. ABRIC (Ref. RTI2018-096434-B-I00) project and the Grant 2021 SGR 663 of the Generalitat of Catalunya have also contributed with the study. The authors would like to thank J. Guillén from the Institute of Marine Science for his comments that improve this manuscript and the Secretaría General de Pesca (SGP) for the 2004 Espace Project dataset. We are grateful to Dr. Jordi Rull (Facultat de Farmàcia i Ciències de l'Alimentació - UB) and José Manuel Fortuño (ICM-CSIC) for taxonomic expertise on coralligenous red algae. Thanks also to José Guzman, a trawler fisherman from Blanes, for his invaluable help in sharing with us his vast knowledge of the benthic seabed. We also thank the captain and crew of the R/V Sarmiento de Gamboa and the pilots of the ROV LIROPUS for their efficient cooperation at sea during the CRIMA cruise. This work is contributing to the ICM's 'Center of Excellence' Severo Ochoa (CEX2019-000928-S).

References

Ballesteros, E., 2006. Mediterranean coralligenous assemblages: a synthesis of present knowledge. Oceanogr. Mar. Biol. 44, 123–195.

Ballesteros, E., Mariani, S., Cefali, M.E., Terrades, M., Chappuis, E., 2014. Manual Dels hàbitats Litorals a Catalunya. Generalitat de Catalunya, Departament de Territori i Sostenibilitat, Barcelona, p. 251.

Barberá, C., Bordehore, C., Borg, J.A., Glémarec, M., Grall, J., Hall-Spencer, J.M., et al., 2003. Conservation and management of Northeast Atlantic and Mediterranean maerl beds. Aquat. Conserv. Mar. Freshwat. Ecosyst. 13, 65–76. https://doi.org/10.1002/aqc.569.

Barberá, C., Moranta, J., Ordines, F., Ramón, M., de Mesa, A., Díaz-Valdés, M., Grau, A. M., Massutí, E., 2012. Biodiversity and habitat mapping of Menorca Chanel (western Mediterranean): implications for conservation. Biodivers. Conserv. 21, 701–728. https://doi.org/10.1007/s10531-011-0210.

Barberá, C., Mallol, S., Vergés, A., Cabanellas-Reboredo, M., Díaz, D., Goñi, R., 2017. Maerl beds inside and outside a 25-year-old no-take area. Mar. Ecol. Prog. Ser. 572, 77–90. https://doi.org/10.3354/meps12110.

Beaman, R.J., Daniell, J.J., Harris, P.T., 2005. Geology–benthos relationships on a temperate rocky bank, eastern Bass Strait. Australia. Mar. Freshw. Res. 56, 943–958. https://doi.org/10.1071/MF04306.

Beisiegel, K., Darr, A., Gogina, M., Zettler, M.L., 2017. Benefits and shortcomings of non-destructive benthic imagery for monitoring hard-bottom habitats. Mar. Pollut. Bull. 121, 5–15. https://doi.org/10.1016/j.marpolbul.2017.04.009.

Bicknell, A.W., Godley, B.J., Sheehan, E.V., Votier, S.C., Witt, M.J., 2016. Camera technology for monitoring marine biodiversity and human impact. Front. Ecol. Environ. 14, 424–432. https://doi.org/10.1002/fee.1322.

Bordehore, C., Ramos-Esplá, A.A., Riosmena-Rodríguez, R., 2003. Comparative study of two maerl beds with different otter trawling history, Southeast Iberian Peninsula. Aquat. Conserv. Mar. Freswater Ecosyst. 13, 43–54. https://doi.org/10.1002/aqc.567.

Boudouresque, C., Bernard, G., Bonhomme, P., Tunesi, L., 2012. Protection and Conservation of *Posidonia oceanica* Meadows. Ramoge and RAC/SPA publishers, Tunis.

Chaudhary, C., Richardson, A.J., Schoeman, D.S., Costello, M.J., 2021. Global warming is causing a more pronounced dip in marine species richness around the equator. Proc. Natl. Acad. Sci. U. S. A. 118, 1–6. https://doi.org/10.1073/pnas.2015094118.

Clarke, K.R., Warwick, R.M., 1994. Changes in Marine Communities: An Approach to Statistical Analysis and Interpretation, second ed. Primer-E, Plymouth.

Collie, J.S., Escanero, G.A., Valentine, P.C., 2000. Photographic evaluation of the impacts of bottom fishing on benthic epifauna, ICES. J. Mar. Sci. 57, 987–1001. https://doi.org/10.1006/jmsc.2000.0584.

Cresswell, A.K., Ryan, N.M., Heyward, A.J., Smith, A.N.H., Colquhoun, J., Case, M., Birt, M.J., Chinkin, M., Wyatt, M., Radford, B., Costello, P., Gilmour, J.P., 2021. A quantitative comparison of towed-camera and diver-camera transects for monitoring coral reefs. PeerJ 9, e11090. https://doi.org/10.7717/peerj.11090.

Da Silva, R.P., Kawai, G.S.D., de Andrade, F.R.D., Bezzon, V.D.N., Ferraz, H.G., 2021. Characterisation and traceability of talcium tarbonate from the seaweed *Lithothamnium*. Solids 2, 192–211. https://doi.org/10.3390/solids2020013.

de Juan, S., Demestre, M., 2012. A trawl disturbance indicator to quantify large scale fishing impact on benthic ecosystems. Ecol. Indic. 18, 183–190. https://doi.org/10.1016/j.ecolind.2011.11.020.

de Juan, S., Demestre, M., Sanchez, P., 2011. Exploring the degree of trawling disturbance by the analysis of benthic communities ranging from a heavily exploited fishing ground to an undisturbed area in the NW Mediterranean. Sci. Mar. 75, 507–516.

de Juan, S., Hinz, H., Sartor, P., Vitale, S., Bentes, L., Bellido, J.M., Musumeci, C., Massi, D., Gancitano, V., Demestre, M., 2020. Vulnerability of demersal fish assemblages to trawling activities: a traits-based index. Front. Mar. Sci. 7, 44. https://doi.org/10.3389/fmars.2020.00044.

Demestre, M., Sbrana, M., Álvarez, F., Sánchez, P., 1997. Analysis of the interaccion of fishing gear in Mullus barbatus fisheries in the Western Mediterranean. J. Appl. Ichthyol. 13, 49–56.

Demestre, M., Sánchez, P., Abelló, P., 2000. Demersal fish assemblages of the continental shelf and upper slope of the Catalan coast, NW Mediterranean. J. Mar. Biol. Assoc. U. K. 80, 981–988.

Demestre, M., de Juan, S., Sartor, P., Ligas, A., 2008. A. Seasonal closures as a measure of trawling effort control in two Mediterranean trawling grounds: effects on epibenthic communities. Mar. Pollut. Bull. 56, 1765–1773. https://doi.org/10.1016/j.marpolbul.2008.06.004.

Demestre, M., Muntadas, A., de Juan, S., Mitilineou, C., Sartor, P., Mas, J., Kavadas, S., Martín, J., 2015. The need for fine-scale assessment of trawl fishing effort to inform on an ecosystem approach to fisheries: exploring three data sources in Mediterranean trawling grounds. Mar. Policy 62, 134–143. https://doi.org/10.1016/j.marpol.2015.09.012.

Demestre, M., Muntadas, A., Duran, R., García-de-Vinuesa, A., Sanchez, P., Mas, J., Franco, I., Muñoz, A., Guillen, J., 2017. Characterization of benthic communities in a subaqueous dune field on the continental shelf (Mar Menor, western Mediterranean). In: Guillén, J., Acosta, J., Chiocci, F.L., Palanques, A. (Eds.), Atlas of Bedforms the Western Mediterranean. Springer, pp. 207–214. https://doi.org/10.1007/978-3-319-33940-5_32.

Díaz, J.I., Maldonado, A., 1990. Transgressive sand bodies on the Maresme continental shelf, western Mediterranean Sea. Mar. Geol. 91, 53–72. https://doi.org/10.1016/0025-3227(90)90132-4.

Duarte, C.M., Losada, I.J., Hendriks, I.E., Mazarrasa, I., Marbà, N., 2013. The role of coastal plant communities for climate change mitigation and adaptation. Nat. Clim. Chang. 3, 961–968. https://doi.org/10.1038/nclimate1970.

Durán, R., Canals, M., Lastras, G., Micallef, A., Amblas, D., Pedrosa-Pàmies, R., Sanz, J.L., 2013. Sediment dynamics and post-glacial evolution of the continental shelf around the Blanes submarine canyon head (NW Mediterranean). Prog. Oceanogr. 118, 28–46. https://doi.org/10.1016/j.pocean.2013.07.031.

Durán, R., Canals, M., Sanz, J.L., Lastras, G., Amblas, D., Micallef, A., 2014. Morphology and sediment dynamics of the northern Catalan continental shelf, northwestern Mediterranean Sea. Geomorgology 204, 1–20. https://doi.org/10.1016/j.geomorph.2012.10.004.

Durán, R., Guillén, J., Muñoz, A., 2017. Sorted bedforms beveloped on sandy deposits derived from small ephemeral streams (Catalan Continental Shelf). In: Guillén, J., Acosta, J., Chiocci, F., Palanques, A. (Eds.), Atlas of Bedforms in the Western Mediterranean. Springer, pp. 127–133. https://doi.org/10.1007/978-3-319-33940-5_21.

Fabri, M.C., Vinha, B., Allais, A.G., Bouhier, M.E., Dugornay, O., Gaillot, A., Arnaubec, A., 2019. Evaluating the ecological status of cold-water coral habitats using non-invasive methods: an example from Cassidaigne canyon, northwestern Mediterranean Sea. Prog. Oceanogr. 178, 102172 https://doi.org/10.1016/j.pocean.2019.102172.

Fragkopoulou, E., Serrão, E.A., Horta, P.A., Koerich, G., Assis, J., 2021. Bottom trawling threatens future climate refugia of Rhodoliths globally. Front. Mar. Sci. 7, 594537 https://doi.org/10.3389/fmars.2020.594537.

García del Arco, J.A., Gorelli, G., Carretón, M., Martínez Posse, L., Company, J.B., 2015. Uso de software libre para el estudio del esfuerzo pesquero en la costa de Cataluña. IX Jornadas de SIG Libre, Girona, Spain. http://hdl.handle.net/10256/10369.

García del Arco, J.A., Company, J.B., Aguzzi, J., Gorelli, G., 2016. Integrating data from vessel monitoring system and fish landings in Mediterranean small fleets, using a PostgreSQL database with PostGIS extension. In: 7th International Workshop on Marine Technology, MARTECH, 2016. Vilanova i la Geltrú, Spain. http://hdl.handle.net/2117/99935.

Garcia-de-Vinuesa, A., 2021. Evaluación de la vulnerabilidad y del estado de conservación de ecosistemas marinos bentónicos especialmente productivos del Mediterráneo frente al impacto de la pesca de arrastre, para impulsar su correcta gestión. Ph.D. thesis,. Univ, Barcelona.

Garcia-de-Vinuesa, A., Sola, I., Quattrocchi, F., Maynou, F., Demestre, M., 2018. Linking trawl fleet dynamics and the spatial distribution of exploited species can help to avoid unwanted catches: the case of the NW Mediterranean fishing grounds. Sci. Mar. 82, S1. https://doi.org/10.3989/scimar.04755.17A.

García-de-Vinuesa, A., Demestre, M., Lloret, J., 2022. Fatty acids as trophic markers and indicators of the quality of benthic habitats: the example of maerl and crinoid beds in the northwestern Mediteranean. J. Sea Res. 187, 102254 https://doi.org/10.1016/j.seares.2022.102254.

Gómez-Gras, D., Linares, C., Dornelas, M., Madin, J.S., Brambilla, V., Ledoux, J.-B., López-Sendino, P., Bensoussan, N., Garrabou, J., 2021. Climate change transforms the functional identity of Mediterranean coralligenous assemblages. Ecol. Lett. 24, 1038–1051. https://doi.org/10.1111/ele.13718.

Hiddink, J.G., Jennings, S.R., Kaiser, M.J., 2006. Indicators of the ecological impact of bottom-trawl disturbance on seabed communities. Ecosystems 9, 1990–1999. https://doi.org/10.1007/s10021-005-0164-9.

Holmes, K.W., Van Niel, K.P., Radford, B., Kendrick, G.A., Grove, S.L., 2008. Modelling distribution of marine benthos from hydroacoustics and underwater video. Cont. Shelf Res. 28, 1800–1810. https://doi.org/10.1016/j.csr.2008.04.016.

Ingrassia, M., Pierdomenico, M., Casalbore, D., Falese, F.G., Chiocci, F.L., 2023. A review of Rhodolith/Maerl beds of the Italian seas. Diversity 15, 859. https://doi.org/10.3390/d15070859.

ITGE, 1989. Mapa Geológico de la Plataforma Continental Española y Zonas Adyacentes 1:200,000. Instituto Tecnológico GeoMinero de España, Madrid, Mem. Expl. (Barcelona), Vol. 35/42E:117 pp.

Lastras, G., Canals, M., Amblas, D., Lavoie, C., Church, I., De Mol, B., Duran, R., Calafat, A.M., Hughes-Clarke, J.E., Smith, C.J., Heussner, S., 2011. Understanding sediment dynamics of two large submarine valleys from seafloor data: Blanes and La Fonera canyons, northwestern Mediterranean Sea. Mar. Geol. 280, 20–39. https://doi.org/10.1016/j.margeo.2010.11.005.

Lee, S., Wolberg, G., Shin, S.Y., 1997. Scattered data interpolation with multilevel B-splines. IEEE Trans. Vis. Comput. Graph. 3, 228–244. https://doi.org/10.1109/2945.620490.

Liquete, C., Canals, M., Ludwig, W., Arnau, P., 2009. Sediment discharge of the rivers of Catalonia, NE Spain, and the influence of human impacts. J. Hydrol. 366, 76–88. https://doi.org/10.1016/j.jhydrol.2008.12.013.

Lloret, J., 2015. Ecosistemas marinos y salud humana riesgos y beneficios procedentes del mar. Med. Econ. 27, 179–197.

Long, S., Sparrow-Scinocca, B., Blicher, M.E., Arboe, N.H., Fuhrmann, M., Kemp, K.M., Nygaard, R., Zinglersen, K., Yesson, C., 2020. Identification of a soft coral garden candidate vulnerable marine ecosystem (VME) Using Video Imagery, Davis Strait. West Greenland. Front. Mar. Sci. 7, 460. https://doi.org/10.3389/fmars.2020.00460.

López-Garrido, P.H., Barry, J.P., González-Gordillo, J.I., Escobar-Briones, E., 2020. ROV's video recordings as a tool to estimate variation in megabenthic epifauna diversity and community composition in the Guaymas Basin. Front. Mar. Sci. 7, 154. https://doi.org/10.3389/fmars.2020.00154.

Martin, C.S., Giannoulaki, M., De Leo, F., Scardi, M., Salomidi, M., Knittweis, Pace, M.L., et al., 2014. Coralligenous and maërl habitats: predictive modelling to identify their spatial distribution across the Mediterranean Sea. Sci. Rep. 4, 5073. https://doi.org/10.1038/srep05073.

Millar, K.R., Gagnon, P., 2018. Mechanisms of stability of rhodolith beds: sedimentological aspects. Mar. Ecol. Prog. Ser. 594, 65–83. https://www.jstor.org/stable/26502999.

Muntadas, A., Demestre, M., de Juan, S., Frid, C.L.J., 2014. Trawling disturbance on benthic ecosystems and consequences on commercial species: a northwestern Mediterranean case study. Sci. Mar. 78S1, 53–65. https://doi.org/10.3989/scimar.04024.19A.

Oksanen, J., Simpson, G., Blanchet, F., Kindt, R., Legendre, P., Minchin, P., et al., 2022. _vegan: community ecology package_R package version 2.6-4. https://CRAN.R-project.org/package=vegan.

Peña, V., Bárbara, I., 2004. Diferenciación morfológica y anatómica entre *Lithothamnion coralloides* y *Phymatolithon calcareum* (corallinales, Rhodophyta) en dos bancos de maërl de la Ría de Arousa (N.O. Península Ibérica). An. Biol. 26, 21–27.

PostGis Project Steering Committee, 2023. PostGIS, spatial and geographic objects for postgreSQL. URL.PostGis: Project Steering Committee, 2018. Web Site. https://postgis.net/.

Price, D.M., Robert, K., Callaway, A., Lo Iacono, C., Hall, R.A., Huvenne, V.A.I., 2019. Using 3D photogrammetry from ROV video to quantify cold-water coral reef structural complexity and investigate its influence on biodiversity and community assemblage. Coral Reefs 38, 1007–1021. https://doi.org/10.1007/s00338-019-01827-3.

QGIS Development Team, 2021. QGIS Geographic Information System. Open Source Geospatial Foundation Project. https://qgis.org.QGIS: Web Site: https://www.qgis.org/es/site/.

R Core Team, 2022. R: A Language and Environment for Statistical Computing. R Foundation for Statistical Computing, Vienna, Austria. URL. https://www.R-project.org/.

Rendina, F., Buonocore, E., Cocozza di Montanara, A., Russo, G.F., 2022. The scientific research on rhodolith beds: a review through bibliometric network analysis. Eco. Inform. 70, 101738 https://doi.org/10.1016/j.ecoinf.2022.101738.

Rice, J., Arvanitidis, C., Borja, A., Frid, C., Hiddink, J.G., Krause, J., et al., 2012. Indicators for sea-floor integrity under the European Marine Strategy Framework Directive. Ecol. Indic. 12, 174–184. https://doi.org/10.1016/j.ecolind.2011.03.021.

Rhodolith/Maërl beds: A global perspective. In: Riosmena-Rodríguez, R., Nelson, W., Aguirre, J. (Eds.), 2017. Coastal Research Library 15. Springer International Publishing, Switzerland. https://doi.org/10.1007/978-3-319-29315-8.

Robert, K., Huvenne, V.A.I., Georgiopoulou, A., Jones, D.O.B., Marsh, L., Carter, G.D.O., Chaumillon, L., 2017. New approaches to high-resolution mapping of marine vertical structures. Sci. Rep. 7, 9005. https://doi.org/10.1038/s41598-017-09382-z.

Rovira, A., Batalla, R.J., Sala, M., 2005. Fluvial sediment budget of a Mediterranean river: the lower Tordera (Catalan Coastal Ranges, NE Spain). Catena 60, 19–42. https://doi.org/10.1016/j.catena.2004.11.001.

Russo, T., Parisi, A., Cataudella, S., 2011. New insights in interpolating fishing tracks from VMS data for different métiers. Fish. Res. 108, 184–194. https://doi.org/10.1016/fishres.2010.12.020.

Sánchez, P., Demestre, M., Martín, P., 2004. Characterization of the discards generated by bottom trawling in the northwestern Mediterranean. Fish. Res. 67, 71–80. https://doi.org/10.1016/j.fishres.2003.08.004.

Steller, D.L., Riosmena-Rodríguez, R., Foster, M.S., Roberts, C.A., 2003. Rhodolith bed diversity in the Gulf of California: the importance of rhodolith structure and consequences of disturbance. Aquat. Conserv. Mar. Freshwat. Ecosyst. 13, S5–S20. https://doi.org/10.1002/aqc.564.

Tauran, A., Dubreuil, J., Guyonnet, B., Grall, J., 2020. Impact of fishing gears and fishing intensities on maerl beds: an experimental approach. J. Exp. Mar. Biol. Ecol. 533, 51472. https://doi.org/10.1016/j.jembe.2020.151472.

Thrush, S.F., Hewitt, J.E., Lohrer, A.M., 2012. Interaction networks in coastal soft-sediments highlight the potential for change in ecological resilience. Ecol. Appl. 22, 1213–1223. https://doi.org/10.1890/11-1403.1.

Toscano, F., Vigliotti, M., Simone, L., 2006. Variety of coralline algal deposits (rhodalgal facies) from the Bays of Naples and Pozzuoli (northern Tyrrhenian Sea, Italy). In: Pedley, H.M., Carannante, G. (Eds.), Cool-Water Carbonates: Depositional Systems and Paleoenvironmental Controls, Geological Society, London, Special Publications, 225, pp. 85–94. https://doi.org/10.1144/GSL.SP.2006.255.01.07.

Tuya, F., Schubert, N., Aguirre, J., Basso, D., Bastos, E.O., Berchez, F., et al., 2023. Levelling-up rhodolith-bed science to address global-scale conservation challenges, 2023. Sci. Total Environ. 892, 164818 https://doi.org/10.1016/j.scitotenv.2023.164818.

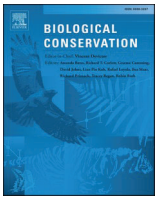
Biological Conservation 289 (2024) 110394



Contents lists available at ScienceDirect

Biological Conservation

journal homepage: www.elsevier.com/locate/biocon



Review



Effects of climate change on marine coastal ecosystems – A review to guide research and management

Ewan Trégarot [a,*], Juan Pablo D'Olivo [b], Andrea Zita Botelho [c,d], Andrea Cabrito [e], Gabriel O. Cardoso [b], Gema Casal [f], Cindy C. Cornet [a], Simon M. Cragg [g], A. Karima Degia [h], Stein Fredriksen [i], Elisa Furlan [j,k], Georg Heiss [b], Diego K. Kersting [l], Jean-Philippe Maréchal [m], Erik Meesters [n], Bethan C. O'Leary [o,p], Géraldine Pérez [q], Cristina Seijo-Núñez [r], Rémy Simide [q], Matthijs van der Geest [n], Silvia de Juan [s]

[a] Centre for Blue Governance, Portsmouth Business School, University of Portsmouth, Portsmouth PO1 3DE, United Kingdom
[b] Freie Universität Berlin, Dept. of Earth Sciences, Malteserstraße 74 100, D-12249 Berlin, Germany
[c] Faculty of Sciences and Technology, University of the Azores, Ponta Delgada, Portugal
[d] CIBIO, InBio Associate Laboratory, Research Centre in Biodiversity and Genetic Resources, InBio Associate Laboratory, Ponta Delgada, Portugal
[e] Institut de Ciències del Mar, Passeig marítim de la Barceloneta 37, 08003 Barcelona, Spain
[f] Gema Casal National Centre for Geocomputation, Maynooth University, 2nd Floor Iontas Building, Maynooth, Co. Kildare, Ireland
[g] Institute of Marine Sciences and Centre for Enzyme Innovation, University of Portsmouth, Portsmouth PO4 9LY, United Kingdom
[h] Centre for Resource Management and Environmental Studies, The University of the West Indies, Cave Hill Campus, St Michael BB11000, Barbados
[i] University of Oslo, Department of Biosciences, Blindernveien, 310371 Oslo, Norway
[j] Centro Euro-Mediterraneo sui Cambiamenti Climatici and Università Ca' Foscari Venezia, CMCC@Ca'Foscari–Edificio Porta dell'Innovazione, 2nd floor, Via della Libertà, 12, 30175 Venice, Italy
[k] Department of Environmental Sciences, Informatics and Statistics, University Ca' Foscari Venice, I-30170 Venice, Italy
[l] Instituto de Acuicultura de Torre de la Sal (IATS-CSIC), Ribera de Cabanes, 12595 Castelló, Spain
[m] Nova Blue Environment, 97233 Schoelcher, Martinique
[n] Wageningen Marine Research, Wageningen University & Research, P.O. Box 57, 1780 AB Den Helder, the Netherlands
[o] Department of Ecology & Conservation, Faculty of Environment, Science and Economy, University of Exeter, Penryn Campus, Penryn TR10 9FE, United Kingdom
[p] Department of Environment and Geography, University of York, York YO10 5NG, United Kingdom
[q] Institut océanographique Paul Ricard, Île des Embiez, 83140 Six-Fours-les-Plages, France
[r] cE3c-Centre for Ecology, Evolution and Environmental Changes, Azorean Biodiversity Group, CHANGE – Global Change and Sustainability Institute, Faculty of Sciences and Technology, University of the Azores, 9500-321 Ponta Delgada, Portugal
[s] The Mediterranean Institute for Advanced Studies, Miquel Marques 21, 07190, Balearic Islands, Spain

ARTICLE INFO

Keywords:
Marine and coastal ecosystems
Climate change
Local stressors
Ecological thresholds
Conservation

ABSTRACT

There is growing concern over climate models that project significant changes in the oceans, with consequences on marine biodiversity and human well-being. However, marine and coastal ecosystems respond differently to climate change-related stressors depending on the ecosystem, species composition and interactions, geomorphologic settings, and spatial distribution, but also on the presence of local stressors interacting cumulatively with climate change-related pressures. Our paper provides a comprehensive review of the current literature about the effects of climate-related pressures on marine and coastal ecosystems and how local stressors affect their resilience. Our work focuses on key marine and coastal ecosystems from three ecoregions: the Caribbean Sea (coral reefs, mangrove forests, seagrass beds), the Mediterranean Sea (the coral *Cladocora caespitosa*, maërl beds and seagrass beds) and the North-East Atlantic, which include kelp forests, maërl beds, salt marshes and seagrass beds. This review highlights the need for a more comprehensive, multi-species, and multi-stressors approach to predict better changes at the ecosystem and seascape levels of marine and coastal ecosystems. Nevertheless, there is enough evidence to argue that addressing locally key manageable stressors common to multiple ecosystems, such as nutrient enrichment, coastal development, hydrologic disturbances, anchoring or

* Corresponding author.
E-mail address: ewan.tregarot@port.ac.uk (E. Trégarot).

https://doi.org/10.1016/j.biocon.2023.110394
Received 6 May 2023; Received in revised form 19 October 2023; Accepted 26 November 2023
Available online 21 December 2023
0006-3207/© 2023 The Author(s). Published by Elsevier Ltd. This is an open access article under the CC BY-NC license (http://creativecommons.org/licenses/by-nc/4.0/).

sedimentation, will reduce the identified adverse effects of climate change. This knowledge is critical for practical conservation actions and coastal and marine spatial management at the ecoregion scale and beyond.

1. Introduction

Despite the implementation of the Paris Agreement, climate models project significant changes in the state of the oceans over the next century with consequences on the entire Earth system, including marine biodiversity and human well-being (Bindoff et al., 2019; IPCC, 2022). Globally, coral reefs, kelp and mangrove forests, salt marshes, seagrass beds and other bio-engineers rank among the most vulnerable marine and coastal ecosystems (hereafter MCE) to climate change (Duarte et al., 2013; Roberts et al., 2017; Spalding et al., 2014). Apart from global stressors, local anthropogenic stressors are also known to severely impact MCEs and can affect the safe operating space, or tolerance, of MCEs to the effects of climate change (Carilli et al., 2009; Scheffer et al., 2015). As a consequence, the combined effects of local anthropogenic stressors make it difficult to define the magnitude of these climate change-related impacts (Bindoff et al., 2019). Rising temperatures and extreme weather events have already affected marine environments globally (Wernberg et al., 2013; Halpern et al., 2015; Poloczanska et al., 2016; Pinsky et al., 2019). While climate change (hereafter CC) cannot be locally managed or contained, local stressors can be (Elliott et al., 2015). Besides, local actions to support healthy natural environments can contribute to CC mitigation and adaptation (Roberts et al., 2017). Therefore, without devaluing the urgency to drastically reduce greenhouse gas emissions into the atmosphere, it is crucial to understand which local stressors (hereafter LS) need to be managed to increase the resilience of MCEs to CC, where resilience is defined as the ability of an ecosystem or species to resist and recover from a disturbance (Holling, 1973). Nevertheless, few studies consider the interactive effects of CC and LS or whether the outcomes of such interactions are species- or ecoregion-specific (Gissi et al., 2021; Furlan et al., 2019).

To address this knowledge gap, this paper aims to provide a comprehensive review of the current literature about the effects of climate-related pressures on MCEs and how local anthropogenic stressors affect their resilience. Our review has been done within the frame of the European Commission-funded project MaCoBioS (macobios.eu). Therefore, it focuses on six key MCEs that are predominant in Europe and its Overseas Territories, covering three ecoregions: North-East Atlantic kelp forests, salt marshes and seagrass beds; Mediterranean coral *Cladocora caespitosa*, maërl and seagrass beds; and Caribbean coral reefs, mangrove forests and seagrass beds. While the conservation interest of seagrasses, mangroves and coral reefs is unquestionable, the inclusion of maërl beds and the single species *C. caespitosa* is not less important. Similar to tropical corals, *C. caespitosa* primarily thrives in shallow habitats and shares the main traits of tropical reef-building corals (Kružić and Benković, 2008; Kersting and Linares, 2012). Moreover, it is one of the best studied bioindicators of long-term climate change effects (Kersting et al., 2013; Kersting and Linares, 2019). For those reasons, this species was deemed more appropriate than other species from the Mediterranean coralligenous assemblages. The ecology of North-East Atlantic and Mediterranean maërl beds has received little attention in contrast to other MCEs (Barbera et al., 2003), but their structural functionality is analogous to kelp forests or even coral reefs, through the complex habitats they provide, supporting a very rich biodiversity. Yet, gathering and consolidating existing knowledge, as well as addressing critical gaps, is paramount for their preservation (Tuya et al., 2023).

These subtidal and intertidal MCEs are among the most productive and valuable ecosystems on Earth, providing habitat for a wide range of commercial and non-commercial species, food and raw materials, coastal protection from storms and erosion, and cultural services, such as tourism and recreative activities (Liquete et al., 2013). Moreover, some of these MCEs are key contributors to CC mitigation due to their high carbon storage (e.g., seagrasses, mangroves, salt marshes) (Duarte et al., 2013). Nevertheless, these MCEs remain highly vulnerable to the effects of CC and LS (Simeoni et al., 2023). Therefore, studies from all three ecoregions in Europe (Mediterranean, North-East Atlantic), and the Caribbean, were included in this review, to cover a wide range of environmental contexts representative of where strong human pressures and vulnerability to CC drivers combine in threatening MCEs.

The specific objectives of the paper are threefold: to identify the state of knowledge regarding (i) the impact of different CC stressors on key MCEs and (ii) the safe operating space limits of these MCEs, and (iii) to identify key LS that can be managed to reduce the identified adverse effects of CC per MCE framed within its local and regional socio-ecological context. Such knowledge is critical for practical conservation actions and coastal and marine spatial management at the ecoregion scale and beyond.

2. Literature review methods

A literature review on the Scopus database was conducted, considering any research papers published until December 2021. Search strings for each MCE were constructed in the following form: climate change driver (e.g., climate change, global change, warming, heat wave, acidification) AND local stressor (e.g., impact, disturbance, pressure) AND ecosystem limit (e.g., threshold, tipping point, recovery, loss, shift) AND ecosystem type (e.g., seagrass beds, salt marshes, kelp forests, maërl beds, coral reefs, or mangroves) AND region (North-East Atlantic, Caribbean, Mediterranean). Full search strings are included in the Supplementary material (SM-1). For seagrasses, the literature review focused on the species considered representative of the three ecoregions: *Zostera marina* in the North-East Atlantic, *Posidonia oceanica* in the Mediterranean and *Thalassia testudinum* in the Caribbean. Although the review focused on studies from those three ecoregions, we also included other ecoregions considered relevant, such as the Gulf of Mexico (associated with the Caribbean) or the Arctic (related to the North-East Atlantic). Global studies were considered if they included our study ecoregions. However, we will refer only to the three targeted ecoregions to simplify the reading. Only publications in English were included. In total, 2576 articles were returned by these searches.

Articles were screened according to the following eligibility criteria, (i) studies conducted on the focal species or MCE within a defined geographical area (see above) or results from laboratory and mesocosm experiments, (ii) studies focusing on the effects of CC with or without LS on the selected MCEs. Articles were first screened based on title and abstract, resulting in 705 articles. The full texts of these remaining articles were screened, and 295 articles were retained for this work: 108 focused on coral reefs in the Caribbean; 17 on the Mediterranean coral *Cladocora caespitosa*; 34 on kelp forests in the North-East Atlantic; 13 on maërl beds in North-East Atlantic and the Mediterranean; 50 on mangrove forests in the Caribbean; 25 on salt marshes in the North-East Atlantic and the Mediterranean; 48 on seagrasses in the North-East Atlantic ($n = 14$), Mediterranean ($n = 25$), and the Caribbean ($n = 9$).

When an article included more than one response variable for the ecosystem of interest, each response was included as a separate entry in the results table and referred to as studies hereafter. Therefore, the total number of studies analysed exceeds the number of articles retained. Meta-data, i.e., information describing the study, was extracted from the 295 articles resulting in 946 studies analysed (the complete list of articles from which data were extracted is included in Supplementary material SM-2). Data was compiled in an output table built on the key questions underpinning this review paper: the nature of the study (e.g.,

experiments in fieldwork or laboratory, temporal series, models), the response variables assessed (i.e., the ecological variable measured in the study), the CC drivers and LS, and identification of operational limits or ecosystem tipping points.

Response variables are measurable features of an organism, individual, population, habitat or ecosystem responding to environmental change. A total of 581 response variables were identified and iteratively coded into eight response variable categories to facilitate data analysis: (i) density/abundance (includes survival or mortality), (ii) distribution, (iii) growth, (iv) habitat structure, (v) metabolism, (vi) photosynthesis/respiration, (vii) reproduction, (viii) other (e.g., "sediment accretion rate", "grazing", or variables related to "paleo-ecology").

The CC drivers of ecosystem change were catalogued as (i) warming, including heatwaves, (ii) extreme weather events, with specific emphasis on storms and hurricanes, (iii) atmospheric CO_2 concentration, (iv) ocean acidification, (v) sea level rise, (vi) salinity (hypo- or hypersalinity), (vii) cooling, reflected by the duration and severity of freezing events, (viii) rainfall regimes, and (ix) inundation. To summarise the general effect of CC drivers on MCEs from multiple studies, we considered the overall effect of a CC stressor to be positive, negative, neutral or unclear when >50 % of the responses were positive, negative, neutral or unclear, respectively (e.g., 60 % negatives and 40 % positives = negative overall effect). An 'unclear' overall effect was assigned when it was uncertain whether the response of a variable was negative, positive or neutral to the ecosystem, population, or individual, and not explicitly specified in the reviewed articles. We visually nuanced the effects between fully (100 %) and mostly [51 %–99 %] positive, negative, neutral or unclear with two shades of colour in the figures. The overall effect was considered 'mixed' if there was an equal number of responses between positive, negative, neutral, unclear, or none of the responses reached a 51 % threshold (e.g., 50 % positive and 50 % negative, or 20 % negative, 40 % neutral, 40 % positive). Details about the exact number of studies per type of effect are summarised in Supplementary materials (SM-3, Figs. S1, S3 and S5).

The LS were classified into 12 categories (Table 1). When interactive effects between CC drivers and LS were tested, the outcome was recorded (i.e., significant interaction or no interaction) as well as the nature of the interaction, if any (i.e., additive, synergistic, antagonistic) and the overall effect (negative, positive, neutral, mixed, unclear) of tested interactions on the MCE. The cumulative overall effect from CC drivers combined with LS was determined following the rules previously described. Details about the exact number of studies per type of effect are summarised in Supplementary materials (SM-3, Tables S2, S4 and S6).

The output table included descriptions of any tipping points or response data that can aid in identifying the safe operating space of the MCE, when such data were reported. Tipping points are understood as the point where following a perturbation, a self-propagated change can eventually cause a system to shift to a qualitatively different state. Safe operating space is understood as the range of environmental conditions that lies between tipping points for which the functioning of the ecosystem remains stable (Scheffer et al., 2015).

3. Results

3.1. Caribbean

3.1.1. Coral reefs

Among all 108 articles, studies of CC effects on Caribbean corals are heavily slanted towards warming (85 % of the studies) (Fig. 1).

Marine heat waves are a primary concern of warming studies (75 %) as they have triggered bleaching events responsible for massive coral mortality worldwide (Eakin et al., 2010; Eakin et al., 2022). Repeated exposure to elevated temperatures can cause general net tissue loss (Neal et al., 2017) and switching to thermal-tolerant symbionts can decrease calcification rates (Ortiz et al., 2013). Sexual reproduction is

Table 1
Proportion of studies per local stressor. N is the number of studies considering both climate change and local stressors.

Ecoregions	Ecosystem	Coastal development	Hydrologic disturbance	Disease	Fishing	Grazing	Invasive species	Nutrient enrichment	Pollution	Recreational activities	Sedimentation	Turbidity	Sulfide stress
Caribbean	Coral reefs N = 77	6 %	–	9 %	13 %	17 %	1 %	11 %	4 %	1 %	6 %	–	–
	Mangrove forests N = 39	2 %	3 %	–	–	–	–	8 %	3 %	–	1 %	–	1 %
	Seagrass beds N = 15	–	–	–	–	–	9 %	–	9 %	9 %	–	–	57 %
Mediterranean	Corals N = 2	–	–	–	–	–	6 %	6 %	–	–	–	–	–
	Maërl beds N = 2	–	–	–	8 %	–	8 %	–	–	–	–	–	–
	Seagrass beds N = 24	4 %	–	–	1 %	–	–	12 %	1 %	1 %	–	–	1 %
North-East Atlantic	Kelp forests N = 48	–	–	–	1 %	8 %	0 %	3 %	–	–	3 %	1 %	–
	Maërl beds N = 6	–	–	–	15 %	8 %	8 %	8 %	–	–	8 %	–	–
	Salt marshes N = 20	5 %	–	–	–	–	1 %	5 %	4 %	–	1 %	–	–
	Seagrass beds N = 65	–	–	–	–	–	–	41 %	–	–	–	–	7 %

Marine & Coastal Ecosystems Caribbean	RESPONSE VARIABLE CATEGORIES	CLIMATE CHANGE								
		Warming / heat waves	Extreme weather events	Atmospheric CO_2 concentration	Ocean acidification	Sea level rise	Salinity (hyper)	Cooling	Rainfall regimes (reduced)	Inundation
 CORAL REEFS	Density/Abundance	20%	25%		4%					
	Distribution									
	Growth	10%	8%		32%	20%				
	Habitat structure	21%	42%		18%	80%				
	Metabolism	6%			7%					
	Photosynthesis/Respiration	9%			18%					
	Reproduction	14%	8%		14%					
	Other	19%	17%		7%					
	Total number of studies	**78**	**12**		**28**	**5**				
 MANGROVE FORESTS	Density/Abundance	7%	17%			8%	16%	63%	21%	
	Distribution	10%				23%			7%	
	Growth	46%	22%	100%		54%	50%	5%	36%	67%
	Habitat structure	2%	22%					16%	36%	
	Metabolism	5%				15%	8%			
	Photosynthesis/Respiration	29%	28%				26%	16%		33%
	Reproduction		11%							
	Other									
	Total number of studies	**42**	**18**	**15**		**13**	**39**	**19**	**14**	**9**
 SEAGRASS BEDS *Thalassia testudinum*	Density/Abundance	20%	33%				20%			
	Distribution	20%	67%			100%				
	Growth	20%					20%			
	Habitat structure									
	Metabolism	20%					20%			
	Photosynthesis/Respiration	20%					40%			
	Reproduction									
	Other									
	Total number of studies	**5**	**3**			**1**	**10**			

Response Legend Fully / Mostly Negative; Fully / Mostly Positive; Fully / Mostly Neutral; Fully / Mostly Unclear; Mixed; Not tested

Fig. 1. Summary of studies per climate change drivers and general effects on broad response variable categories in marine and coastal ecosystems of the Caribbean, including the Gulf of Mexico. Percentage values represent the proportion of studies per response variable from the total number of studies per CC driver, indicated in bold for each ecosystem.

critical for resilience, but many studies demonstrated negative effects of thermal stress on coral reproduction, including decreases in larvae survivorship and settlement, inhibition of fertilisation, increased post-settlement mortality and loss of genotypic diversity (LaJeunesse et al., 2009; Randall and Szmant, 2009; Baums et al., 2013; Ross et al., 2013; Davies et al., 2016; Ross et al., 2017); however, inter-species variability is observed (Ross et al., 2013; Randall and Szmant, 2009). In many cases, when temperatures are 1–1.5 °C above the maximum monthly sea surface temperature, increased mortality (Langdon et al., 2018), reduced larvae survivorship (LaJeunesse et al., 2009) and slower healing time (Kaufman et al., 2021) were observed. However, not only the magnitude but also the duration of thermal anomalies is crucial. For example, the number of days at >30.5 °C was the most significant metric characterising bleaching years (Manzello et al., 2007a), although threshold values can be affected by physical or biological factors such as depth or symbiont type (Smith et al., 2016; Buddemeier et al., 2011).

Ocean acidification was the second most studied CC driver (25 % of studies) affecting Caribbean coral reefs. Growth assessments accounted for 43 % of studies and examined the formation or dissolution of coral skeletons, or reef framework, in the face of changes in carbonate parameters, such as aragonite saturation state and dissolved inorganic carbon. Overall, results showed negative effects on coral calcification (Mumby et al., 2013; Camp et al., 2016; Langdon et al., 2018; Martinez et al., 2019), reproduction (Albright et al., 2010; Albright and Langdon, 2011; Davies et al., 2016), and photosynthesis (Bedwell-Ivers et al., 2017; Martinez et al., 2019), but in many cases exhibited neutral (Towle et al., 2015; Bedwell-Ivers et al., 2017; Langdon et al., 2018) or unclear (Kennedy et al., 2013) responses. Akin to thermal stress, some species may be more sensitive to ocean acidification (Langdon et al., 2018; Bedwell-Ivers et al., 2017; Martinez et al., 2019).

Warming and acidification are predicted to interact with each other (Kennedy et al., 2013; Freeman et al., 2013; Buddemeier et al., 2008; Davies et al., 2016). Modelled data suggests that a warming of 2.6 °C reduces cover by 15 %, but when saturation state is considered at CO_2 values for 2100 (710 ppmv), declines in cover reach 41 %–60 % (Buddemeier et al., 2008).

Sea level rise comprised 4 % of studies focused on the ability of coral reefs to protect our coasts. However, with increased sea level, wave energy dissipation is reduced, resulting in enhanced reef erosion (catalogued here as part of growth), compromising reef accretion, and affecting habitat structure (Blanchon et al., 2017; Yates et al., 2017; Wegner and Ellis, 2017; de Bakker et al., 2019).

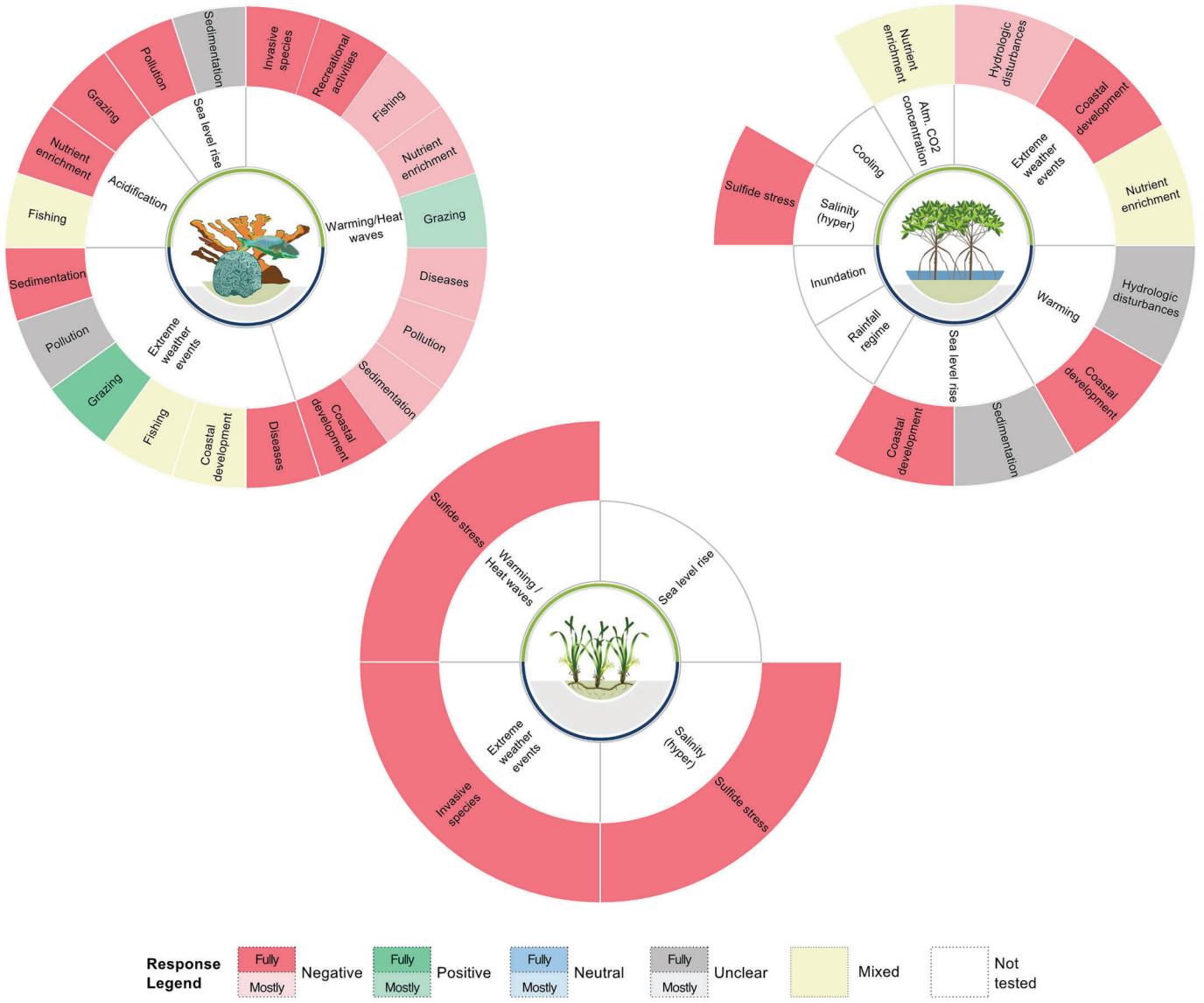


Fig. 2. Cumulative overall effects of local stressors combined with climate change drivers for marine and coastal ecosystems in the Caribbean. Top left: coral reefs; top right: mangrove forests; bottom: seagrass beds (i.e. *Thalassia testudinum*).

Extreme weather events (13 % of studies) are generally negative for corals as they cause physical destruction, resulting in coral cover decline and affecting the number of juveniles and small-size corals (Steneck et al., 2019; Crabbe, 2011). In particular cases, these events can increase asexual reproduction (Foster et al., 2013). The interaction of hurricanes with other climate drivers is complex. In fact, hurricanes can induce local cooling, mitigating the effects of marine heat waves and reducing the recovery time after bleaching (Manzello et al., 2007b).

Studies on the interactive effects of CC and LS have intensely focused on warming, terrestrial run-off (pollution, nutrients, and sediments) and grazing (Table 1, Fig. 2). Higher nutrient concentration, resulting from coastal run-off, acts in synergy with increased temperatures to favour shifts to algal-dominated communities (DeBose et al., 2013) and promote pathological affections (Castañeda-Chávez et al., 2018). The effect of nutrients and thermal stress varied between species and showed mixed effects, such as increased larval settlement and mortality (Serrano et al., 2018).

3.1.2. Mangrove forests

Out of 50 articles, associated studies reported the effects of warming (24 %) and cooling (11 %), hypersalinity (22 %), extreme weather events (10 %), sea level rise (7 %), rainfall regime (8 %), atmospheric CO_2 concentration and inundation (5 %) on mangrove forests (Fig. 1).

Warming and atmospheric CO_2 concentration were the only investigated drivers that had a positive effect on the growth rate of a mangrove *Avicennia germinans* (McKee and Rooth, 2008; Chapman et al., 2021; Akaji et al., 2019), although the overall effect remains mixed, unlike the overall effect of warming on metabolism classified as positive (Akaji et al., 2019). The effects of cooling, however, negatively impact all aspects of mangrove forests, such as habitat structure, metabolism, and photosynthesis, with a mixed overall effect on density/abundance (Cavanaugh et al., 2015; Osland et al., 2017; Krauss et al., 2008). Rooting gets inhibited below 15 °C and above 37 °C for *A. germinans* and *Rhizophora mangle* (Krauss et al., 2008). Photosynthesis will cease if leaf temperature climbs to 38–40 °C (McKee et al., 2012), and photoinactivation generally occurs below −6.1 °C, −5.3 °C, and −3.7 °C for *A. germinans*, *R. mangle* and *Laguncularia racemosa*, respectively (Cavanaugh et al., 2015).

Sea level rise affects mangrove distribution, causing shoreline retreat and mangrove forest degradation (Cohen et al., 2021). However, understanding the ability of mangrove forests to cope with sea level rise is difficult given the multiple factors in the equation (e.g., rooting expansion, sediment accretion, subsidence, sea level rise). Half of the studies on sea level rise focused on sediment accretion rate or vertical growth. Increased sediment inputs may promote forest expansion in some cases (Cohen et al., 2021), but the interaction of sedimentation with sea level rise remains complex and unclear (Xie et al., 2020). Two studies (McKee, 2011; Koch et al., 2015) attempted to assess thresholds in the rate of sea level rise, and these were site-specific. Koch et al. (2015) estimated that above 3 mm year^{-1} of sea level rise, mangrove forests would be lost in the Everglades with varying degrees of tolerance according to the type of mangroves (fringe, dwarf, scrub).

Reduced rainfall generally tends to lessen the growth rate of *Avicennia marina*, *R. mangle* and *L. racemosa* (Bompy et al., 2014). Mangrove forests have adapted to survive in a saline environment with species-specific tolerances. However, drought episodes can lead to hypersaline conditions, which increase *R. mangle* propagule mortality. Krauss et al. (2008) state that salinity ranging between 0 and 57 PSU is optimal for rooting success. Under hypersaline conditions of 60 PSU and above, Devaney et al. (2021) observed a 100 % mortality of propagules for *R. mangle*. The global-scale threshold of mean annual precipitation is 0.78 m, below which mangrove forests abundance strongly decreases (Osland et al., 2017; Gabler et al., 2017).

Extreme weather events can profoundly affect habitat structure, often increasing the number of dead and decaying trees (Walcker et al., 2019), reducing growth rate, and causing a lower leaf area index in *R. mangle* and *A. germinans* (Feller et al., 2015). Studies show that *R. mangle* is much more sensitive than *A. germinans* with any damage to its tree structure, except for small branch breaks, associated with over 60 % mortality. Conversely, only significant damage, such as toppling or trunk break below breast height, caused mortality of *A. germinans* stems to rise by over 10 %. Imbert (2018) found that basal area loss increased significantly above 110–150 km h^{-1} for basin mangroves and above 178–209 km h^{-1} for fringe and scrub mangroves in east Caribbean mangrove forests.

Few articles examined the interactions between CC drivers and LS (Table 1, Fig. 2). Coastal development (2 % of mangrove studies), often combined with hydrologic disturbances (2 %) and nutrient enrichment (10 %), were the main threats reported as reducing mangrove forest resilience to the effects of CC. Nutrient inputs can increase the growth of scrub mangrove trees. Still, that benefit is offset by a decrease in their resilience to hurricane damage, potentially destabilising the system (Feller et al., 2015; Walcker et al., 2019). If undisturbed by LS, the reduced density of *R. mangle* trees following hurricanes can increase average diameter at breast height and aboveground biomass (Gulf of Mexico, Griffiths and Mitsch, 2021). Hayden and Granek (2015) showed that sediment elevation increased at intact mangrove plots but decreased at cleared mangrove plots. Attempts to increase sedimentation (for instance, from beach nourishment) were found to benefit mangrove forests temporarily (Cohen et al., 2021). Hughes et al. (2018) studied the response of *A. germinans* to oiling and found a greater reduction in survival when *A. germinans* grew alone (21 % reduction) rather than with *S. alterniflora* (12 % reduction) throughout the experiment. No threshold was reported relative to LS interacting with CC drivers.

3.1.3. Seagrass beds – Thalassia testudinum

Research efforts on the effect of CC on *T. testudinum* (9 articles) have mainly focused on hypersalinity (44 % of the studies) but also warming (22 %), extreme weather events (22 %) and sea level rise (11 %; Fig. 1).

Hypersalinity had a negative effect on plant growth rate (Koch et al., 2007c; Koch et al., 2007b), density/abundance (Koch et al., 2007c; Koch et al., 2007b) and photosynthesis (Koch et al., 2007c; Koch et al., 2007b; Howarth and Durako, 2013; Johnson et al., 2018; Fig. 1). *T. testudinum* was highly tolerant to hypersaline conditions up to a 60 PSU threshold level when salinity was slowly increased (1 PSU day^{-1}). However, pulsed salinity treatments, without a slow osmotic adjustment period, reduced threshold levels of salinity by 20 PSU to approximately 45 PSU (Koch et al., 2007c). Hypersalinity at 65 PSU seems to affect the oxidizing capacity of *T. testudinum* and places subtle demands on the positive oxygen balance in the ecosystem (Koch et al., 2007b).

Warming affects the spatial distribution of seagrass, specifically from long-term and acute heat stress (Carlson et al., 2018). Experimentally increased temperature reduced growth rate and photosynthesis efficiency (Koch et al., 2007a), although it did not affect biomass (Koch et al., 2007a). While plants survived 38 days of temperature treatments, there was a clear thermal threshold above 33 °C where *T. testudinum* growth declined, and leaf quantum efficiencies (F_v/F_m) fell below the lower "stress" threshold of 0.7 (Koch et al., 2007a).

Extreme weather events reduced cover, especially in exposed meadows (Hernández-Delgado et al., 2020; James et al., 2021). Most of the documented impacts of hurricanes were associated with sediment bedload (horizontal transport) and displacement of coral rubble, which resulted in plant burial and suffocation of *T. testudinum* (Hernández-Delgado et al., 2020; James et al., 2021).

Sea level rise had a negative impact on spatial distribution, with a predicted decline in cover of 20 % for every metre of sea level rise along the Florida Gulf Coast (McHenry et al., 2021). However, the exact impact of sea level rise on the distribution and total cover of a *T. testudinum* population seemed to depend heavily on the local context (e.g., the possibility of moving shoreward).

Very few articles looked at interactions between CC drivers and LS

(Fig. 2); however, Hernández-Delgado et al. (2020) found that a shift in vegetation cover triggered by hurricanes favours the invasion of invasive seagrass (i.e., *Halophila stipulacea*) over *T. testudinum* (Fig. 2). In addition, an increased oxygen demand and high sulfate reduction rates in sediments were suggested to explain the frequent die-off events in Florida Bay, particularly after periods of high temperature and salinity (Koch et al., 2007b). As such, it was hypothesized that the interaction between hypersalinity and sulfide toxicity in *T. testudinum* is their synergistic effect on the critical oxygen balance of the plant (Koch et al., 2007b; Johnson et al., 2018). The oxygen threshold for sulfide intrusion in *T. testudinum* was found to be 1.3 (at 35 PSU) to 1.5 kPa O_2 (at 65 PSU) in the meristem or 7–8 % of overlying water saturation with no significant difference in the salinity treatments (Johnson et al., 2018). Results also indicated that high temperatures (>33 °C), high salinity (>45 PSU) and organic loading-induced porewater sulfide stressors have the potential to disrupt carbon metabolism in *T. testudinum* (Koch et al., 2007a; Koch et al., 2007b).

3.2. Mediterranean

3.2.1. Coral – Cladocora caespitosa

In total 13 articles were analysed, of which warming is the most studied CC driver in *Cladocora caespitosa* coral beds and micro-reefs (88 %) (Fig. 3). Summer heatwaves have been impacting this coral since the beginning of the 2000s, triggering widespread and recurrent mass mortality events (Kersting et al., 2013; Garrabou et al., 2009). Although there are differences among regions, seawater temperature maintained over the 26 °C–28 °C threshold range has been reported to trigger warming-induced necrosis in this coral.

Experimental studies assessing the impact of acidification (12 % of the studies) show contrasting results. On one side, pH values projected for the end of the century caused a reduction of ~30 % in *C. caespitosa* calcification rates (Movilla et al., 2012). On the other side, Rodolfo-Metalpa et al. (2009) found that a similar decrease in pH, alone or in combination with warming, had no significant effect on photosynthesis and calcification.

Two studies (12 %) have shown interactive effects of CC and LS on *C. caespitosa* (Table 1, Fig. 4). Invasive algae could interact synergistically with warming, increasing mortality in this species (Kersting et al.,

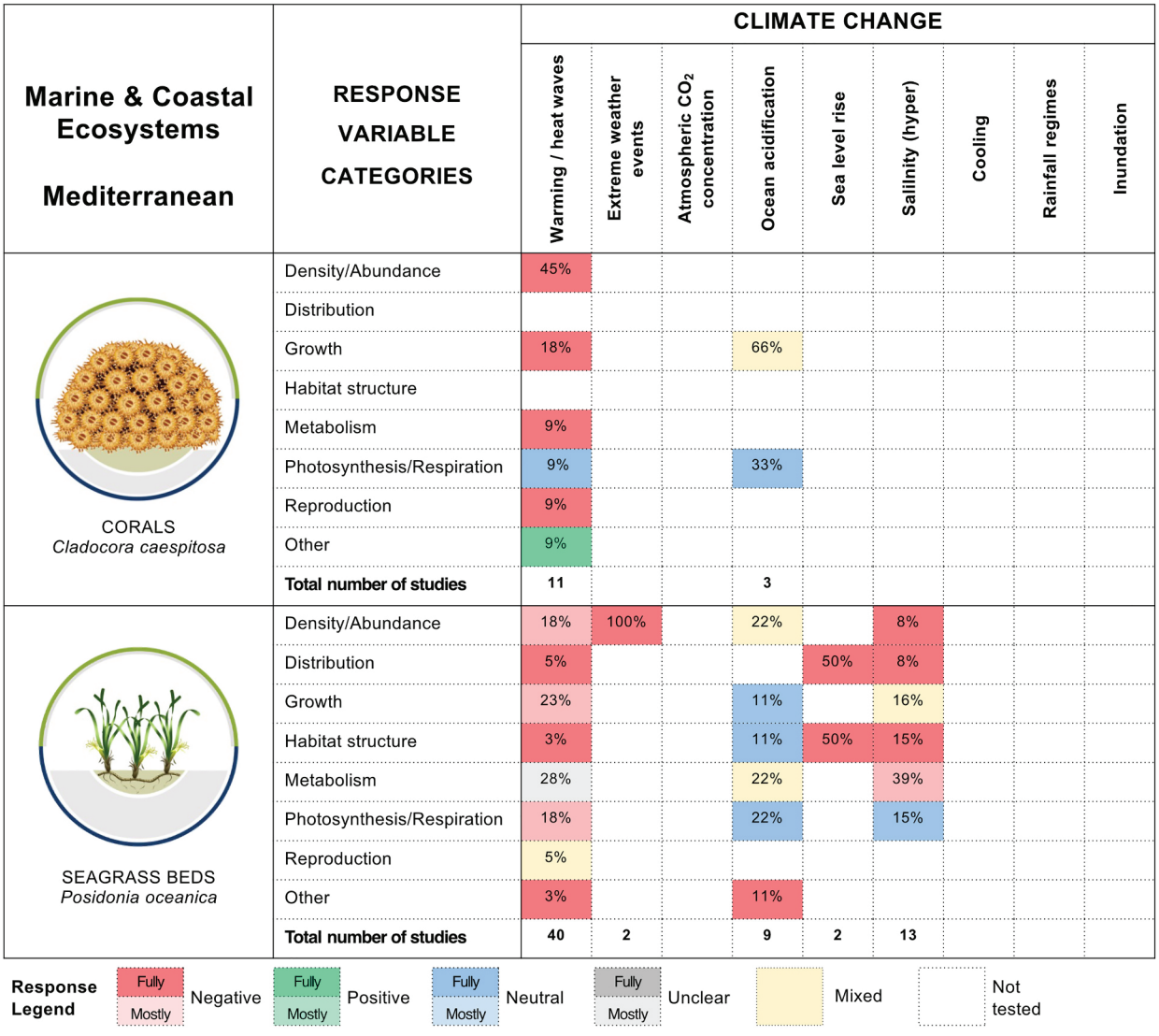


Fig. 3. Summary of studies per climate change drivers and general effects on broad response variable categories in marine and coastal ecosystems of the Mediterranean. Percentage values represent the proportion of studies per response variable from the total number of studies per CC driver, indicated in bold for each ecosystem. Mediterranean outputs on maërl beds and salt marshes are included in Fig. 5.

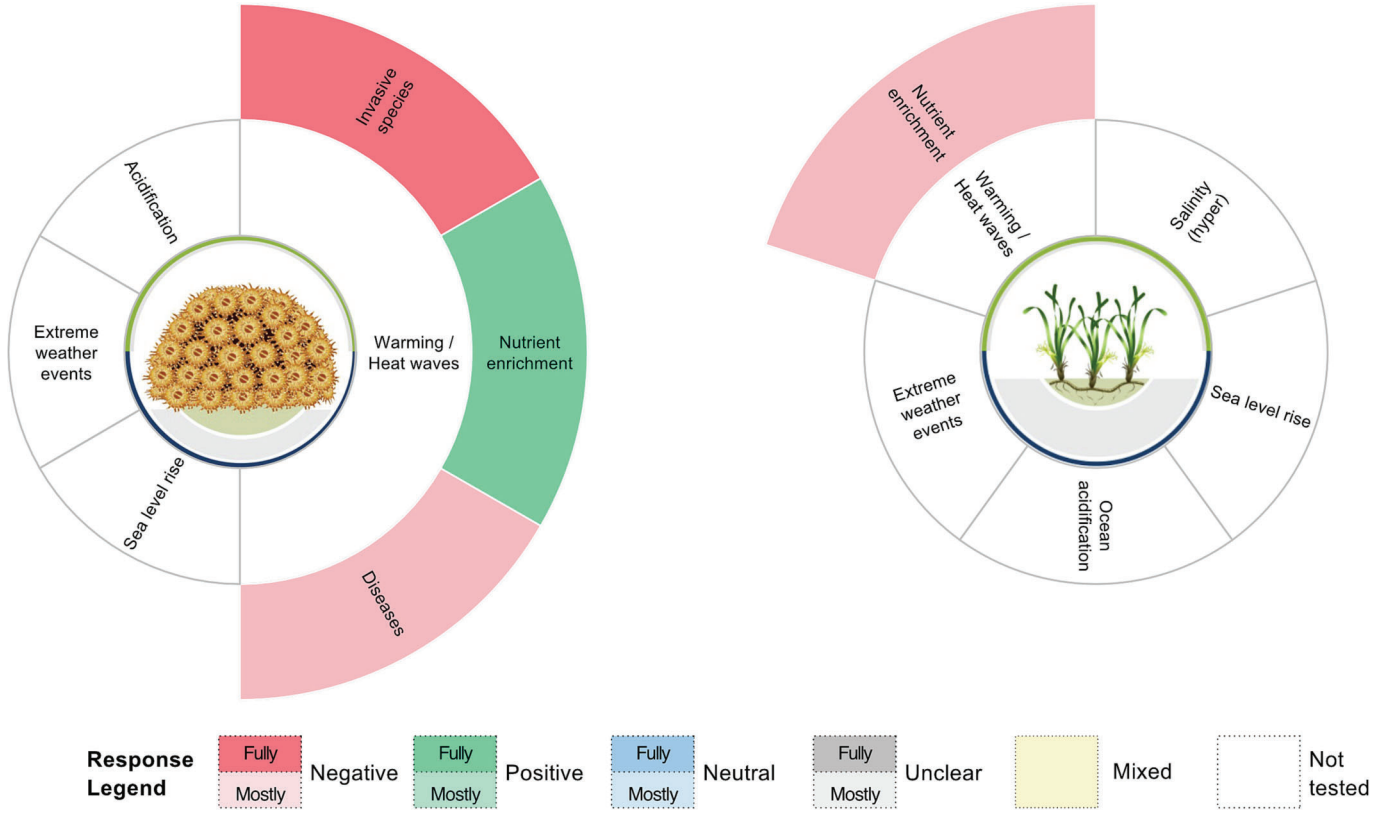


Fig. 4. Cumulative overall effects of local stressors combined with climate change drivers for marine and coastal ecosystems in the Mediterranean. Left: Coral (i.e. *Cladocora caespitosa*); right: Seagrass beds (i.e., *Posidonia oceanica*).

2015), and local nutrient enrichment could reduce the adverse effects of summer heatwaves on the corals (Hadjioannou et al., 2019).

Cladocora caespitosa shows highly parsimonious population dynamics (slow growth and low recruitment rates), which makes it highly vulnerable to catastrophic disturbances such as warming-related mortality events (Kersting et al., 2014b). However, recoveries from CC disturbances have also been reported for this species, showing a survival strategy that allows it to withstand and partially recover from thermal stress (Kersting and Linares, 2019).

3.2.2. *Maërl beds*

Only two articles focused on Mediterranean maërl beds, with acidification (50 %) and warming (50 %) as primary concerns. There is no empirical information on the effects of warming on maërl beds; however, it is expected to affect their extension due to their fragmented distribution ranges and poor dispersal capacity (Kružić, 2014).

Regarding acidification, field-based studies in the Mediterranean have identified the presence of maërl only a few metres away from hydrothermal vents, at a pH between 7.7 and 8.2; however, maërl was absent at pH below 7 (Linares et al., 2015). Experiments have observed that below optimal pH conditions 8.16–8.21, the maërl-forming species increase calcification rates to compensate for the adverse effects of the acidified environment until reaching a pH threshold at 7.7–7.9 (Kružić, 2014).

In terms of LS, trawling activities in the deep areas cause massive mortality of maërl by crushing and burying the rhodoliths (de Juan et al., 2013). Increased near-bottom turbidity caused by trawling also affects maërl beds due to light attenuation, identified in the global modelling study by Fragkopoulou et al. (2021).

In the shallower areas with higher light irradiance, maërl beds would be more affected by invasive algae species. At least three species are known to threaten these habitats in the Mediterranean: *Womersleyella setacea*, *Caulerpa racemosa* v. *cylindracea* and *Caulerpa taxifolia*. By covering the basal stratum, invasive algal species decrease rhodolith survival (Kružić, 2014).

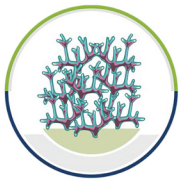
3.2.3. *Seagrass beds – Posidonia oceanica*

The effects of CC drivers were principally negative on *P. oceanica* (25 articles), except for ocean acidification (8 % of the studies), which generally has a neutral impact (Fig. 3), probably due to the pH buffering capacity of Posidonia (Cox et al., 2016).

Warming (68 % of studies) was reported to have a negative impact due to enhanced mortality (Marbà and Duarte, 2009; Guerrero-Meseguer et al., 2017; Hernán et al., 2017; Pazzaglia et al., 2020), reduced growth rate (Olsen et al., 2012; Guerrero-Meseguer et al., 2017; Ruiz et al., 2018; Marín-Guirao et al., 2018; Traboni et al., 2018; Marín-Guirao et al., 2019; Ruocco et al., 2019), reduced distribution (Chefaoui et al., 2018; Papaki et al., 2020), and increased grazing rate (Hernán et al., 2017). Temperature above 27 °C has been found to limit the growth of *P. oceanica* (Guerrero-Meseguer et al., 2017; Ruiz et al., 2018). If the water temperature increases by 15 %, more than half of *P. oceanica* meadows may be replaced by *Cymodocea nodosa* (Papaki et al., 2020). The negative effect of warming was also observed at the physiological level by modifying the carbon balance (Hernán et al., 2017; Marín-Guirao et al., 2018) and photosynthesis/respiration rates (Marín-Guirao et al., 2016; Guerrero-Meseguer et al., 2017; Marín-Guirao et al., 2018; Ruocco et al., 2019; Nguyen et al., 2021). Nevertheless, the physiological resistance to warming seems to vary with depth, latitudinal range, and level of eutrophication. Plants in deeper areas experience higher heat-induced photosynthetic injury and impaired carbon balance (Marín-Guirao et al., 2016; Marín-Guirao et al., 2017a; Tutar et al., 2017); plants in more eutrophic waters show reduced physiological resistance to warming (see Fig. 4, Pazzaglia et al., 2020); and populations adapted to colder waters accumulated significantly more fatty acids following heat stress than the ones adapted to warmer waters (Beca-Carretero et al., 2018; Marín-Guirao et al., 2019). However, most

studies that investigated the effect of warming on metabolism in *P. oceanica* could not determine whether the response was negative, positive or neutral at the ecosystem, population or individual level. As such, the overall effect of warming on metabolism in *P. oceanica* was considered unclear.

Hypersalinity (16 %) has a negative impact on habitat structure (Ruiz et al., 2009; Marín-Guirao et al., 2017b) and distribution (Houngnandan et al., 2019), while no effect was found on photosynthesis or respiration (Marín-Guirao et al., 2013; Marín-Guirao et al., 2017b). Hypersalinity also has negative effects on metabolism: a

Marine & Coastal Ecosystems – North-East Atlantic	RESPONSE VARIABLE CATEGORIES	CLIMATE CHANGE								
		Warming / heat waves	Extreme weather events	Atmospheric CO_2 concentration	Ocean acidification	Sea level rise	Salinity (hypo)	Cooling	Rainfall regimes (reduced)	Inundation
 KELP FORESTS	Density/Abundance	9%								
	Distribution	23%					58%			
	Growth	20%					8%			
	Habitat structure	2%	100%							
	Metabolism	16%								
	Photosynthesis/Respiration	17%					17%			
	Reproduction	13%					17%			
	Other									
	Total number of studies	**179**	**1**				**12**			
 MAËRL BEDS	Density/Abundance									
	Distribution	33%			9%					
	Growth	33%			36%					
	Habitat structure									
	Metabolism	33%			27%					
	Photosynthesis/Respiration				27%					
	Reproduction									
	Other									
	Total number of studies	**4**			**13**					
 SALT MARSHES	Density/Abundance	3%		7%		7%			6%	
	Distribution									
	Growth	16%		21%		12%				
	Habitat structure	32%		14%		52%			69%	
	Metabolism					5%			19%	
	Photosynthesis/Respiration	41%		29%		15%			6%	
	Reproduction	8%		21%		8%				
	Other		100%	7%		2%				
	Total number of studies	**37**	**1**	**14**		**60**			**16**	
 SEAGRASS BEDS *Zostera marina*	Density/Abundance	18%					15%			
	Distribution	3%	100%				8%			
	Growth	15%					15%			
	Habitat structure	9%					15%			
	Metabolism	42%					38%			
	Photosynthesis/Respiration	12%					8%			
	Reproduction									
	Other									
	Total number of studies	**33**	**1**				**13**			

Response Legend: Fully / Mostly Negative; Fully / Mostly Positive; Fully / Mostly Neutral; Fully / Mostly Unclear; Mixed; Not tested

Fig. 5. Summary of studies per CC drivers and general effects on broad response variable categories in marine and coastal ecosystems of the North-East Atlantic. For maërl beds, articles from the Mediterranean (2) and North Atlantic (9) are merged due to the low number of articles. For salt marshes, the four articles (39 studies) covering the Mediterranean were also included, considering they studied genus and/or species found in the North-East Atlantic and were thus deemed relevant for our analysis. Percentage values represent the proportion of studies per response variable from the total number of studies per CC driver, indicated in bold for each ecosystem.

negative effect on rhizome non-structural carbohydrate content (Ruiz et al., 2009) and leaf pigment content (Marín-Guirao et al., 2013), and a positive effect on necrotic leaf area (Ruiz et al., 2009). However, some studies reported no effect on non-photochemical quenching (NPQ) and level of xanthophyll de-epoxidation (Marín-Guirao et al., 2013) or mixed effects on metabolism (Marín-Guirao et al., 2017b). The impact of hypersalinity is not considered to be driven by CC but instead was attributed to LS, such as hypersaline effluents from desalinisation plants or coastal lagoons (Ruiz et al., 2009; Marín-Guirao et al., 2017b). Salinity tolerance was identified to be 38 PSU, which is close to the mean salinity in the Mediterranean Sea (Ruiz et al., 2009). However, *P. oceanica* meadows experiencing long-term salinity fluctuation show adaptive capacity by reducing shoot size (Marín-Guirao et al., 2017b).

Increased sedimentation due to extreme weather events (4 %) can be detrimental to *P. oceanica*, for which 4–5 cm of sedimentation starts to induce shoot mortality with near-complete mortality at a burial level of 8–9 cm (Gera et al., 2014).

Sea level rise (4 %) was suggested to have a negative impact on distribution and habitat structure. This negative effect was attributed to an attenuation of the amount of light at the seabed, reducing photosynthetic activity in *P. oceanica*, which eventually can cause mortality, especially in meadows at the lower limit (Pergent et al., 2015).

Only one study by Pazzaglia et al. (2020) tested for interactive effects between CC stressors and LS on various response variables in *P. oceanica* plants collected from populations from two environments with different nutrient load history (i.e., growing under chronic cultural eutrophication or growing in oligotrophic pristine waters). Plants experiencing chronic cultural eutrophication were more sensitive to further exposure to multiple stressors than plants growing in oligotrophic habitats and appeared to be weaker during the treatments, showing the highest mortality rate, especially under increased temperature (Pazzaglia et al., 2020).

3.3. North-East Atlantic

3.3.1. Kelp forests

All reviewed articles (34 articles) had warming as their main CC driver, from which 35 % of the studies had heatwaves, 15 % had salinity, and 6 % had storms (Fig. 5). Most studies corresponded to laboratory or modelling experiments where a response variable changed depending on a limited number of established conditions (often one or two variables).

Temperature threshold values that differ between sporophyte and gametophyte have been defined for several kelp species. For example, in *Laminaria digitata* and *Laminaria hyperborea*, the sporophyte dies at temperatures higher than 23 °C (Derrien-Courtel et al., 2013; Liesner et al., 2020) while the gametophytes of both species show different thermal behaviour. Gametophytes of *L. digitata* can tolerate temperatures around 25 °C (Martins et al., 2020), while gametophytes of *L. hyperborea* have a maximum temperature of 18 °C for growth and reproduction (Derrien-Courtel et al., 2013). *Laminaria ochroleuca*, with southern distribution limits, presents a higher tolerance to temperature with threshold values of 25 °C for gametophyte and sporophyte (Derrien-Courtel et al., 2013). The warming temperature may change the distribution of some species, as seen along the Cantabrian coast of Spain (Díez et al., 2012). Here two species, *Saccorhiza polyschides* and *L. ochroleuca* were lost entirely from 1991 to 2008, whereas Araújo et al. (2016) showed that the same two species had an unchanged presence on the Galician coast of Spain and in north Portugal. Warming may also alter the species' dominance, where the warm-water species *L. ochroleuca* takes over the cold-water species *L. hyperborea* (Teagle et al., 2018). Thermal stress might trigger a shift from a kelp forest to a turf community (Filbee-Dexter et al., 2016; Filbee-Dexter and Wernberg, 2018; Feehan et al., 2019), and as turf communities trap sediments, such a shift prevents kelp from re-establishing (Feehan et al., 2019). There are additional suggested drivers for this change, like eutrophication leading to epiphytism, pollution and storms (Filbee-Dexter and Wernberg, 2018). Warming and radiation, as well as their interaction, can alter the physiological processes of kelp, such as photosynthesis (Fredersdorf et al., 2009; Pereira et al., 2015; Hargrave et al., 2017) or metabolism (Müller et al., 2012; Olischläger and Wiencke, 2013). In Arctic regions, ice-thickness, which is tightly linked to warming, was also found to influence the distribution of kelp due to its influence in the light regimes (Assis et al., 2018; Assis et al., 2016).

Regarding the effects of salinity, sporophytes of *Alaria esculenta* showed minor effects of decreased salinity, while zoospores were more sensitive (Fredersdorf et al., 2009). Only a few studies reported threshold values for salinity. For example, Fredersdorf et al. (2009) found that a salinity below 5 PSU affects the photosynthesis of *A. esculenta*. In comparison, Assis et al. (2018) observed that salinity values lower than 7.9 PSU trigger bleaching and stop the growth in *L. hyperborea*. According to Franco et al. (2018), the golden kelp (*L. ochroleuca*) will not enter the Baltic Sea (PSU $<$ 15), even if the temperature changes.

Extreme weather events have also been considered through models or experiments that simulate the storm effects, but no studies looked at the state of kelp populations before and after real storms. These modelled experiments report negative effects, including a severe reduction in invertebrate and fish populations after mechanical stress, like the physical removal of kelp (Norderhaug et al., 2020).

Most studies considering the interaction of CC and LS focused on *Saccharina latissima*. The LS were physical stress such as grazing (8 %), followed by nutrient enrichment and eutrophication (3 %) and sedimentation (3 %) (Table 1, Fig. 6). Grazing has been found to negatively affect kelp populations in most cases (O'Brien and Scheibling, 2018), except for grazing on turf communities. Under certain conditions, grazing may have positive effects that counteract the negative effects of sedimentation. For example, after laboratory experiments, Zacher et al. (2016) reported that with 1 g of sediment cover, sporophytes of *S. latissima* only developed when grazers were present (sediment removal). Nutrient enrichment, including eutrophication, generally negatively affects kelp populations; however, the magnitude of these effects is species-specific. While Moy and Christie (2012) reported eutrophication to have a negative effect on the abundance of *S. latissima*, Martins et al. (2017) did not find any significant effect of nutrient enrichment or its interaction with temperature on the life stage transitions of *Laminaria digitata*. The physical stress included a variety of factors that can produce different effects on kelp populations. The ones resulting from fishing activities (i.e. kelp trawling), which are analogous to the effects of extreme weather events, negatively affected kelp and its associated populations. For example, Norderhaug et al. (2020) conducted experiments of kelp trawling on *L. hyperborea* populations and reported a reduction of 67 % in epiphytes and 87 % in invertebrate populations.

3.3.2. Maërl beds

The review identified nine articles on North-East Atlantic maërl beds and two global articles on warming (Cornwall et al., 2019) and trawling effects on maërl (Fragkopoulou et al., 2021) for a total of 22 studies.

Ocean acidification (82 % of the studies) generally alters the metabolism of maërl-forming species (e.g., Burdett et al., 2012; Sordo et al., 2018) and reduces their calcification rates (e.g., Donald et al., 2017; Legrand et al., 2017; Burdett et al., 2018) although it remains a mixed result due to neutral and unclear effects (Fig. 5). Similar to Mediterranean studies, Donald et al. (2017) suggests that for *Neogoniolithon* sp., the optimal pH is 8, and the limit is 7.5. Ocean acidification might also negatively affect grazers (e.g., gastropods, sea urchins) and thus decreasing their control on epiphytes growth over maërl beds, which has negative consequences on rhodolith photosynthesis (Legrand et al., 2017).

Warming is causing negative effects on the calcification (referred to as growth in Fig. 5) of maërl-forming species (e.g., Cornwall et al.,



Fig. 6. Cumulative overall effects of local stressors combined with climate change drivers for marine and coastal ecosystems in the North-East Atlantic. Top left: kelp forests; top right: maërl beds; bottom left: seagrass beds (i.e., *Zostera marina*); bottom right: salt marshes.

2019). Higher latitudes are expected to be the refuge for maërl beds in the North-East Atlantic due to the lower temperatures (Simon-Nutbrown et al., 2020). However, while one study by Cornwall et al. (2019) observed that a 5.23 °C increase above baseline temperature decreases calcification, there is limited knowledge of the temperature tolerance for maërl-forming species. One species (*Lithothamnium coralloides*) is reported to have a higher affinity for low temperatures (Qui-Minet et al., 2019); however, for temperature, pH, or light availability, the limiting thresholds would probably differ between rhodolith species (Fragkopoulou et al., 2021), with species-specific responses.

A combined effect of warming and ocean acidification implies that under all RCPs, a significant decrease in suitable habitat for maërl beds is predicted, with at least a 38 % decline by 2050, down to 83,7 % in 2100 under RCP 8.5 (Simon-Nutbrown et al., 2020).

Other interactions with LS involve fishing activities, invasive species and sedimentation (Fig. 6). On top of the direct physical impact of bottom trawling, increased near-bottom turbidity caused by trawling affects maërl beds distributed nearby fishing areas due to light attenuation, which causes additional losses of rhodoliths (Fragkopoulou et al., 2021). Few studies provide empirical evidence on the effects of increased sediment input on maërl survival. In the case of *Lithothamnion* sp. in the Bay of Brest (Brittany), the death of the rhodoliths occurs after 41 days of being buried by sediment (Ehrhold et al., 2021).

3.3.3. *Salt marshes*

While there is extensive literature on the effects of CC stressors on salt marshes, only 25 relevant articles were found for the European area, with 128 studies extracted. Four articles focus on the Mediterranean,

with genus and/or species also found in the North-East Atlantic and therefore deemed relevant for our analysis here. Sea level rise (47 % of the studies) and warming (29 %) were the main CC drivers affecting salt marshes. However, the effects of rainfall regime (13 %), atmospheric CO_2 concentration (11 %) and extreme weather events (1 %) were also studied to a lesser extent (Fig. 5). It is worth noticing that the effects of these stressors were highly mixed due to the different species' responses in these often highly diverse environmental settings.

The effects of increased temperature on salt marshes were mixed, with some studies reporting a decrease in salt marshes' extent area and the growth of some species (Duarte et al., 2021; Mateos-Naranjo et al., 2021), while other studies reported increase in extent areas, growth (Duarte et al., 2021; Bitoun et al., 2018; Gray and Mogg, 2001), and biomass, therefore contributing to carbon sequestration (Couto et al., 2014; Gray and Mogg, 2001; Strain et al., 2017). Interestingly, increased temperatures also led to opposite responses in the photosynthetic efficiency of the plants depending on species studied in the same region (Duarte et al., 2016; Carreiras et al., 2020; Duarte et al., 2021), but also for the same species (*Halimione portulacoides*) studied twice in the same region (Carreiras et al., 2020; Duarte et al., 2021).

Increased salinity associated with sea-level rise would lead to a community shift from species with stiff stems to species with more flexible stems, characteristics of pioneer/low marsh communities (Zhu et al., 2020b). Boorman (1992) further found that increasing sea level rise, combined to some extent with coastal development, would lead to a progressive loss of marsh zones with only pioneer/low marsh communities remaining at the highest level of sea level rise. Whether in the North-East Atlantic or the Mediterranean, studies found that sea level rise would overall negatively affect salt marshes' extent area (Boorman, 1992; Duarte et al., 2021) and biomass (Strain et al., 2017; González-Orenga et al., 2020; Brown et al., 2006; Wong et al., 2015; Reents et al., 2021), but also their growth (Duarte et al., 2021), survival and abundance (Castillo et al., 2000; Duarte et al., 2021; Brown et al., 2006), and reproduction (Szymansky et al., 2021; Zhu et al., 2020a; Mesa-Marín et al., 2019).

Only five articles have identified thresholds or tipping points for salt marshes, all related to sea level rise. Some studies in the Mediterranean looked at the effect of the inundation period related to the mean sea level, for which a 37.5 % period (and above) relating to a decrease of 5 cm below the current mean sea level could lead to a die-off of *Spartina veneta* (Strain et al., 2017). *Spartina* spp. showed a higher tolerance with a threshold at 73 % of the inundation period corresponding to a 10 cm rise above the current mean sea level (Strain et al., 2017). Other studies in the North-East Atlantic looked at the sea level rise threshold itself, varying from 0.5 m to 1.5 m, with successive mortality from high to low marshes plants (Boorman, 1992; Castillo et al., 2000). Furthermore, besides the increase in inundation period, the wave-imposed sheer water stress on the tidal flat associated with sea level rise could significantly affect the reproduction of *Spartina anglica*, with <10 % of seed retention from a threshold of 0.022 Pa and above (Zhu et al., 2020a). Finally, sea level rise could also significantly affect the reproduction of *Salicornia ramosissima* through the associated increased salinity, considering no germination was observed above a 1030 mM NaCl threshold under laboratory conditions (Mesa-Marín et al., 2019).

Nine articles looked at LS, which were coastal development, dredging, grazing, invasive species, nutrient enrichment, pollution, and sedimentation, but only two of them looked at the interactions between CC drivers and LS, and both focused on heavy metal pollution (Table 1, Fig. 6). Indeed, in the Tagus estuary, Portugal, *Spartina patens* and *Halimione portulacoides* from heavy metal contaminated areas seemed more resilient and tolerant to salt stress resulting from sea level rise and more resistant to heat stress, respectively, than the same species from pristine areas. However, the underlying mechanisms remain unclear (Carreiras et al., 2020; Carreiras et al., 2021). Finally, while the interaction is not formally tested, coastal development would hamper salt marshes' ability to cope with sea level rise by preventing their landward migration even where their accretion rate would be sufficient to keep up with sea level rise (Boorman, 1992), a phenomenon better known as "coastal squeeze" (e.g., Doody, 2013).

3.3.4. Seagrass beds – Zostera marina

Out of the 14 articles, the major CC stressor studied for *Z. marina* is warming (72 % of the studies), which has a negative effect on density and abundance (Holmer and Bondgaard, 2001; Ehlers et al., 2008; Bergmann et al., 2010; Salo and Pedersen, 2014; Franssen et al., 2014; Moreno-Marín et al., 2018), rates of photosynthesis (Holmer and Bondgaard, 2001; Winters et al., 2011; Mota et al., 2018), habitat structure (Holmer and Bondgaard, 2001; Ehlers et al., 2008; Salo and Pedersen, 2014), distributional range (Torn et al., 2020), and growth (Holmer and Bondgaard, 2001; Salo and Pedersen, 2014; Moreno-Marín et al., 2018), although some studies found no effect of warming on growth (Bergmann et al., 2010; Salo and Pedersen, 2014). Looking at the metabolism, warming was reported to decrease the non-structural carbohydrate reserves in roots (Holmer and Bondgaard, 2001) and leaves (Moreno-Marín et al., 2018), increased heat-shock-protein up-regulation which indicated molecular stress (Franssen et al., 2011; Franssen et al., 2014; Jueterbock et al., 2016), and increased toxic sulfide intrusion (Pedersen et al., 2004). In contrast, warming was reported to reduce the abundance of the pathogen *Labyrinthula zosterae* in *Z. marina* tissues (i.e. wasting disease; Brakel et al., 2019). Overall, a temperature above 25 °C had a negative impact on *Z. marina*'s survival (Moreno-Marín et al., 2018).

Hyposalinity was reported to have a negative effect on the distributional range (Torn et al., 2020), density and abundance, growth, habitat structure and metabolism (Salo and Pedersen, 2014; Villazán et al., 2015), necrotic lesion coverage due to infection with *L. zosterae* (i.e., wasting disease; Brakel et al., 2019) and carbon balance through increased respiration rates (Villazán et al., 2015). Below 12.5 PSU, the growth of *Z. marina* decreases, and mortality increases (Villazán et al., 2015).

Only three articles investigated the effects of CC-drivers combined with LS on *Z. marina* performance (Fig. 6). Experimental work by Villazán et al. (2015) showed that increased ammonium availability, which is considered a LS (nutrient enrichment), amplified the adverse effect of low salinity on growth-related variables and survival. In addition, Moreno-Marín et al. (2018) showed that individual exposure to either heat or shade had a negative effect on *Z. marina* performance, which, to some extent, was also the case for the effect of high nitrogen availability. While the combined effects of these stressors were additive, a synergistic effect on mortality was found for *Z. marina* plants exposed to all three stressors simultaneously (Moreno-Marín et al., 2018). Finally, Brakel et al. (2019) found that light conditions had no interactive effects with elevated temperatures on the physiological resistance of *Z. marina* to infection by the pathogen *L. zosterae*, nor on a cluster of *Z. marina* fitness variables (i.e., leaf growth rate, shoot survival, leaf sucrose content). They also found that light conditions did not alter the negative effect of reduced salinity on necrotic lesion coverage (%) 2 days after inoculation with *L. zosterae*. Interestingly, Brakel et al. (2019) did find a negative synergistic interaction between high temperatures and low salinity on the abundance of the pathogen *L. zosterae* within leaf tissue, preventing wasting disease symptoms.

4. Discussion

4.1. Drivers of change of marine coastal ecosystems in the Caribbean ecoregion

The Caribbean coastal and marine ecosystems are threatened by sea level rise, warming, stronger hurricanes, and drier conditions, with coral reefs, mangroves, and seagrass particularly vulnerable (Beckford and Rhiney, 2016; Rull, 2022).

Sea level rise and ocean acidification are mostly a concern for

mangrove forests and coral reefs, respectively. The pace at which mangroves can cope with sea level rise is highly dependent on the geomorphology and the net balance between sedimentation and erosion. As such, understanding the mechanisms that determine sediment accretion rate is crucial to assessing the adaptive capacity of mangrove forests to sea level rise. Even though the impacts of ocean acidification on coral calcification rates are mostly negative and species dependent, they remain, in many cases, not severe. The severity of marine heat waves is, however, of primary concern for coral reefs as these events can decimate coral populations through bleaching and associated mortality, leading to communities dominated by thermal-resistant species (Smith et al., 2013) or dominated by algae (McCook et al., 2001) if the reef is under the influence of local stressors such as increased nutrient inputs, which further favour algae dominance over corals (Lapointe, 1997). The combination of warming and nutrient enrichment also favours the prevalence of coral diseases (Randall and van Woesik, 2015; Randazzo-Eisemann et al., 2022). Based on models trained with environmental data from the Caribbean/Atlantic, global coral reef loss by 2100 is predicted to be 83 % for Representative Concentration Pathway (RCP) RCP4.5 and 88 % for RCP8.5 (Freeman et al., 2013). Tropical seagrass beds dominated by native *T. testudinum* might suffer from rapid, large-scale die-off events from the combination of high temperatures, high salinity and the interactive stressor sulfide (Koch et al., 2007a; Koch et al., 2007b; Johnson et al., 2018). Mangrove forests are also highly vulnerable hypersaline conditions due to drought episodes resulting from warming and longer dry seasons.

In the context of coral mortality and acidification, calcification rates decrease, vertical growth cannot keep up with sea level rise, and the reef is flattening from bioerosion and continues its shift to weedy species. With a flattened reef, the services provided by the reef are strongly affected, and the risk of coastal hazards from the combination of sea level rise and extreme weather events is a concern for coastal communities, including associated ecosystems. The increase in their intensity and frequency threatens all MCEs, especially if the recovery period between two successive events is not sufficient. In this case, opportunistic (invasive) or more resilient species might dominate during recovery (Snedaker et al., 1992). If coral reefs' ability to attenuate wave energy decreases, seagrass and mangrove forests could attenuate the remaining waves' energy and still protect the coast during extreme weather events, but higher hydrodynamics on the long term is not ideal for the settlement of mangrove trees. Short-term and long-term CC impacts, therefore, depend heavily on the local context of MCEs (e.g., exposure, presence of invasive species, and local stressors). Since the invasive seagrass species *Halophila stipulacea* has spread across most of the Eastern Caribbean islands (Winters et al., 2020), extreme weather events might facilitate the shift from native to invasive vegetation. The combined effects could have significant consequences on seagrass ecosystem resilience and on the ability of the native seagrass species *T. testudinum* to persist and adapt to projected climate change impacts (Hernández-Delgado et al., 2020).

4.1.1. Management recommendations for the Caribbean ecoregion

4.1.1.1. Towards a watershed approach to coastal ecosystems conservation. Due to tropical coastal ecosystems' intrinsic complexity and spatial variability, management cannot be designed using a "one size fits all" approach. Instead, local dynamics and stressors must be carefully considered (Blackwood et al., 2018). Reducing land-based local stressors from the catchment areas will increase MCEs resilience to CC (e.g., reduced nutrient input increased resilience to hurricanes in mangrove forests, see Walcker et al., 2019) and, in turn, contribute to mitigating its effects through the regulating services they provide (e.g., climate regulation and coastal protection). Therefore, a watershed approach to coastal ecosystem conservation is fundamental to reducing the impact of LS and allowing these ecosystems to adapt naturally to climate change. Moreover, extreme weather events generally accentuate the negative effects of human alterations on the coastal environment and adjacent catchment areas, which increase sedimentation, turbidity and inputs of land-based nutrients and pollutants from terrestrial run-offs, translating into negative effects on coral reef benthic communities (Przeslawski et al., 2008; Otaño-Cruz et al., 2019) and associated ecosystems. For example, land clearing (if not directly mangrove forests) tends to increase turbidity and sedimentation, while agriculture (e.g., sugar cane) and poor water treatment facilities will strongly increase nutrient load in the coastal environment. These will strongly affect community structure on coral reefs, with the overgrowth of macroalgae (Pandolfi and Jackson, 2006) and survival of seagrass beds through eutrophication and light-limitation-induced sulfide stress (Johnson et al., 2018). Limiting land clearing and soil artificialisation, increasing wastewater treatment capacity, and reducing the use of fertilisers are just a few directions that could benefit MCEs greatly and sustain the service they provide to coastal communities.

4.1.1.2. Consider the connectivity between MCEs. The interconnectivity of coral reefs, seagrass beds and mangrove forests implies that managing a local stressor specifically for coral reefs will indirectly benefit mangrove forests and seagrass beds, and vice versa. For instance, managing fisheries, mainly to protect herbivorous species, can reduce reef degradation associated with warming and extreme events (Mumby et al., 2014; Edwards et al., 2011) by preventing macroalgal growth and promoting the recovery in coral cover and density (Bozec et al., 2016; Steneck et al., 2019). Healthy reefs provide sheltered conditions for seagrass and mangrove to develop, providing additional coastal protection against extreme weather events and sea level rise. Managing mangroves and seagrass beds can benefit fish populations as they provide shelter and food for juveniles and adults. It will also significantly improve the water quality by absorbing excess nutrients and trapping sediment, all having cascading benefits on coral reefs (Barbier et al., 2011; Lamb et al., 2017). Mangroves can also act as light refuges and mediate coral bleaching and survival during marine heat waves (Stewart et al., 2021), just like upwelling areas in the Caribbean that have a particular conservation value because of lower rates of thermal warming (Chollett and Mumby, 2013).

4.1.1.3. Promote community-based ecological restoration actions. Working with nature to consider MCEs ecology and biology to restore degraded MCEs by mimicking natural processes is necessary. For instance, any climate change driver or hydrologic disturbances that might lead to hypersaline conditions will significantly affect mangrove forests' structure, distribution, and productivity (Yoshikai et al., 2022). These changing conditions might alter the structure of the mangrove forests, going from tall mangrove forests to shrub mangroves and dead mudflat zones. del Mar Delgado-Serrano et al. (2017) provide a portfolio of successful cases of community-based management of environmental challenges in Latin America and the Caribbean. More recently, an excellent example of community-based ecological mangrove restoration can be found in Bonaire, in the Caribbean, aiming at maintaining and restoring the channels to restore water flow between the front and back of the mangroves in order to prevent the harmful effects of hypersalinity (van Zee, 2022). If successful, this initiative will give a chance to mangrove trees to thrive and be more resilient to CC.

4.2. Drivers of change of MCEs in the Mediterranean ecoregion

The Mediterranean is a climate change hotspot, and the sea surface temperature increase rate is 3 to 4 times higher than in the global ocean (Juza and Tintoré, 2021). Since the beginning of the 2000s, the Mediterranean Sea has been impacted by recurrent marine heat waves (Garrabou et al., 2009; Kersting et al., 2013; Marbà et al., 2015), whose intensity has significantly increased during the last years threatening

ecosystems' condition and functioning (Garrabou et al., 2022). Against this background, most of the studies on the impact of warming on Mediterranean benthic organisms started after the widespread mass mortality event of 2003 in the North-West Mediterranean Sea (Garrabou et al., 2009; Kersting et al., 2013).

Mediterranean shallow zooxanthellate corals (*C. caespitosa*) are among the benthic organisms most impacted by warming (Garrabou et al., 2009; Kersting et al., 2013), and future predictions will most likely increase the already worrying mortalities. Nevertheless, despite their vulnerability to increased temperatures, it has been found that these corals own specific mechanisms that could improve their long-term resilience to warming, like the long-term recovery processes described in warming-impacted *C. caespitosa* populations (Kersting and Linares, 2019). Likewise, in seagrass beds, a warming-induced flowering has been observed in *Posidonia oceanica*, which could be an adaptative strategy to increase the diversity of genetic and phenotypic responses to warming, escaping stressful temperature conditions, and potentially populating new areas (Ruiz et al., 2018; Marín-Guirao et al., 2019). However, *P. oceanica*-dominated seagrass beds could be replaced by *Cymodocea nodosa*-dominated seagrass beds if the water temperature increases significantly (Papaki et al., 2020). On the other hand, the deeper extension of maërl beds in the Mediterranean will most likely have a refuge function due to moderate increases in temperature and acidification at these depths, as long as they remain trawling-free (Fragkopoulou et al., 2021). In the shallower areas though, the higher irradiance might drive the proliferation of filamentous algae that overgrow on maërl beds when temperatures and nutrients load increase. Over 1000 non-indigenous species have been reported in the Mediterranean Sea (Zenetos et al., 2010, 2012), many originating from the Red Sea or the Atlantic, finding suitable environmental conditions as the Mediterranean Sea is getting warmer (Öztürk, 2021); invasive algae threaten key coastal ecosystems such as seagrass meadows (Klein and Verlaque, 2008) or coral beds (Kersting et al., 2014a).

Other significant effects include acidification, which is expected to drop by 0.4 unit by 2100, while the sea level is expected to rise between 0.43 and 2.5 m by 2100, depending on scenarios and projections (MedECC, 2020). Ocean acidification threatens mostly calcifying organisms such as the coral *C. caespitosa* and maërl. The fragmentation of the rhodoliths by the physical impact of trawling would probably accelerate de-calcification processes. The liberation of the carbon pools into CO_2 would further increase ocean acidification and atmospheric CO_2 emissions. Sea level rise will increase the risk of coastal flooding and storm surges and will likely affect the deep seagrass meadows at their lower limit. Mediterranean salt marshes might also suffer from sea level rise due to a combination of increased inundation period and salinity (Strain et al., 2017; González-Orenga et al., 2020).

In the Mediterranean, human-induced pressures such as coastal development, pollution, anchoring, fishing, and invasive species reduce the resilience of seagrass meadows, corals and maërl beds to CC drivers, increasing the risk of collapse by reaching a tipping point. Given that the reach of tipping points has already been evidenced after the recurrent heatwaves in summer over the past decade that caused impaired physiological and physical damage to *P. oceanica* meadows (Guerrero-Meseguer et al., 2017; Ruiz et al., 2018; Hernán et al., 2017) and mass mortality events since the beginning of the 2000s for the coral *C. caespitosa* (Kersting et al., 2013), environmental management actions must be reinforced.

4.2.1. Management recommendations for the Mediterranean ecoregion

4.2.1.1. Promote transnational actions. In the Mediterranean region, key management actions include regulating fishing activities over vulnerable habitats, a single action that is challenged by the large proportion of international waters in a region shared by many European and non-European countries (de Juan et al., 2012). The European Union has implemented such regulations, prohibiting trawl fishing over Mediterranean coralligenous and maërl bottoms as specified in EC Regulation 1997/2006. In 2008, a Mediterranean-wide Action Plan for the Conservation of the Coralligenous and Other Calcareous Bio-concretions in the Mediterranean Sea was adopted under UN Environment/MAP. Furthermore, two common maërl-forming Mediterranean species, *Lithothamnion corallioides* and *Phymatolithon calcareum*, are covered by Annex V of the Habitats Directive. However, effective protection of maërl beds is hampered by limited published information on their actual presence, which challenges the implementation of protective measures.

Slowing the transit of non-indigenous species to the Mediterranean Sea through regional cooperation is another critical management action which should be prioritised and thoroughly investigated. Prevention, surveillance, citizen awareness raising, and control strategies should all be increased to prevent the introduction of alien species, detect their presence early and implement the right control measure. Furthermore, effectively protecting key species and habitats (Öztürk, 2021) makes them more resistant to invaders (i.e., biotic resistance hypothesis - Elton, 1958; Levine and D'Antonio, 1999).

An essential regional-level strategy involves the efficient implementation of marine protected areas networks that simultaneously monitor the impact of various management measures such as the reduction of destructive bottom-contact fishing nets, the implementation of invasive species monitoring program, and the stringent protection of highly sensitive species such as coral and *Cladocora*. However, implementing effective marine protected areas requires consensus or compromises among users (Costa et al., 2022) and nations, a challenge in the Mediterranean basin with multiple nations and policy frameworks (de Juan et al., 2012). But this is an important goal to achieve in the region as the connectivity between MCEs means they all benefit from each other.

4.2.1.2. Consider cumulative pressures. Henceforth, forthcoming protection measures and restoration programs must adopt a large-scale approach, exemplified by well-connected MPA networks, to effectively address the cumulative risks stemming from climate change-related and local stressors, which operate across various scales. The Mediterranean Sea is one of the basins where high coastal development and sea-based economies collide with ecological peculiarities requiring a careful conservation and management, so that a cumulative impact assessment can be particularly useful and recommendable. Between 60 and 99 % of the territorial waters of EU member states are subject to high cumulative impacts (Micheli et al., 2013). The paucity of quantified cumulative pressures and impacts assessment stresses the need for more incisive efforts to collect empirical evidence on ecosystem-specific responses to human pressure (Bevilacqua et al., 2018). As demonstrated by Pazzaglia et al. (2020), different nutrient loads impact *P. oceanica* physiological performance and morphological traits, highlighting the influence of local pressures in eliciting diverse adaptive strategies in response to global environmental changes, such as marine heatwaves that affect regional scales. With the predicted sea surface temperature increase, it has been suggested that *P. oceanica* would lose its functionality by reducing 90 % of its shoot density globally by 2049 (Jordà et al., 2012). While we need to be prepared for the loss of ecosystem services provided by *P. oceanica* meadows, we should also anticipate the loss of functionality of associated habitats due to collateral damages from the loss of *P. oceanica* meadows. This seascape approach extends its benefits to multiple key ecosystems. For instance, when conservation measures are implemented at the seascape level, seagrasses enhance water quality by efficiently filtering out pollution, pathogens, and nutrients, as demonstrated by Lamb et al. (2017). This, in turn, contributes to the well-being of associated habitats, including maërl beds and coralligenous habitats featuring *C. caespitosa*.

4.3. Drivers of change of marine coastal ecosystems in the North-East Atlantic ecoregion

In Northern Europe, temperatures will rise at a rate exceeding global mean temperature changes. The frequency and intensity of hot extremes, including marine heatwaves, are projected to continue increasing regardless of the greenhouse gas emissions scenario used. Extreme sea level rise events will become more frequent and more intense, leading to more coastal flooding, and severe windstorms are projected to increase at global warming of 2 °C and above (IPCC, 2022). Finally, pluvial flooding, attributed to human influence, is projected to increase further.

As seawater temperatures increase, scientists expect to see poleward expansions and contractions at lower latitudes of suitable habitats for kelp forests and maërl beds, with adverse effects on the associated biodiversity. For instance, assemblages associated with the cold-water species *Laminaria hyperborea* were on average > 12 times more diverse and supported >3600 times more biomass than the warm-water species *L. ochroleuca* because the latter has a stipe devoid of epibionts (Teagle et al., 2018). However, increased temperature could also have a positive effect on kelp forests. In northern Norway, increasing temperature along the coast allowed the southern population of crabs to move northwards, controlling sea urchins' grazing pressure on the kelp (Christie et al., 2019). Fagerli et al. (2013) found that increased temperature could reduce the sea urchins' fecundity, meaning less offspring, which benefits kelp forests. However, warming is also a driver for invasive species that could particularly influence the warmer shallow areas, generating competition for resources or a niche (Brodie et al., 2014). If ocean acidification and warming were to affect grazers' physiology (e.g., sea urchins), their control over epiphytes would decrease, resulting in negative consequences for maërl beds and potentially for kelp forests too.

The increased frequency and intensity of rainfall events result in many secondary effects such as increased pluvial flooding, terrestrial run-off transporting terrigenous material (e.g., humus substances, sediment), and freshwater discharge lowering the salinity and increasing nutrient inputs into the sea. Underwater light limitation due to freshwater discharge-related sediment and nutrient input will lead to a shallower growth maximum with a concurrent reduction in biodiversity for kelp, maërl, and seagrasses. Lower salinity and warming are also likely to reduce *Zostera marina* growth, density, and subsequently, their productivity and habitat complexity (Holmer and Bondgaard, 2001; Ehlers et al., 2008; Salo and Pedersen, 2014), the latter being essential for associated species. Given the predicted salinity decrease and warming of the Baltic Sea, these results supported the idea that isolates of wasting disease pathogen *Labyrinthula zosterae* do not represent an immediate risk for *Z. marina* beds in the Baltic Sea.

Finally, sea level rise would mostly affect salt marshes, although with some variability depending on species and regions. Indeed, in some cases, salt marshes are currently able to keep up with sea level rise considering high enough accretion rates (Ladd et al., 2019), but in other cases, the extent area of the ecosystem has already started declining or is projected to decline in the future (Duarte et al., 2021; Richards et al., 2008; Carrasco et al., 2021). For instance, the native *Spartina* spp. shows a higher tolerance to inundation related to sea level rise. However, a shift from this perennial plant to the annual succulent *Salicornia veneta* has already been observed under the combined effect of heat waves and drought, increasing the long-term vulnerability of the ecosystem in the face of sea level rise (Strain et al., 2017). Furthermore, there is also quite a variability depending on the model used to predict future sea level rise scenarios. For example, physical models such as general atmosphere-ocean circulation models reported increments of 0.28–0.98 m in 2100, with respect to the levels in 1986–2005 (Church et al., 2013), while semi-empirical models report predictions by 2100 of 0.5–1.4 m, with respect to 1990 levels (Vermeer and Rahmstorf, 2009) or 0.57–1.1 m by 2100 considering the levels in 1980–2000 (Jevrejeva et al., 2012). More recent studies that considered ice-sheet contributions have estimated that the global mean sea level could exceed 2 m by 2100 with respect to the levels in 2000 (DeConto and Pollard, 2016). Predicting how salt marshes and other MCEs in the North-East Atlantic are going to be affected by sea level rise, therefore, remains a significant challenge.

4.3.1. Management recommendations in North-East Atlantic

4.3.1.1. Improve water quality by reducing nutrient and sediment load. Nutrient enrichment from run-off can cause the opportunistic algae to overgrow the kelps, maërl and seagrasses, limiting light and CO_2 availability for healthy growth. Increased ammonium loading due to freshwater discharge will amplify the adverse effect of low salinity on growth-related variables and survival in *Z. marina*, putting estuarine seagrass beds particularly at risk (Villazán et al., 2015). Overall, MCEs in North-East Atlantic are all vulnerable to terrestrial run-off, sedimentation, and nutrient loading from agriculture, aquaculture, and coastal development. All those local stressors that strongly affect the water quality should be the primary focus of coastal management, knowing that some MCEs contribute to increased water quality, like seagrass beds, salt marshes or kelp forests. Still, reducing nutrient releases through better treatment of sewage and lowering fertiliser use could counteract the excessive growth of epiphytes over vegetated coastal habitats.

4.3.1.2. Allow recovery by reducing coastal and marine resources exploitation. Overfishing may lead to the same result as nutrient enrichment, creating a cascade effect. Removing large predatory fishes will increase the number of smaller fishes that eat the grazers (e.g., snails and small crustaceans). With fewer grazers, the epiphytes can flourish. In combination with other local factors, the replacement of kelp forests by turf communities (Filbee-Dexter and Wernberg, 2018; Nepper-Davidsen et al., 2019; Moy and Christie, 2012) would have a severe impact on the ability of kelp to re-establish because of a thick sediment layer on the bottom trapped by turf communities, preventing kelp spores from finding a hard bottom substrate where they can germinate. Pessarrodona et al. (2021) showed that the shift from kelp communities to ground-covering turf assemblages resulted in global miniaturisation and homogenisation of underwater habitat structures. Therefore, sustainable management of coastal fisheries (artisanal and recreational) is a priority too. Local removal actions of sea urchins could help kelp forest ecosystems by releasing the grazing pressure and avoiding shifting into large, denuded areas. In the last decades, harvesting wild kelp populations at sea has increased in northern Europe, where kelp is used as human food, a source of alginate for many applications, fertiliser for agriculture, and biofuel production (Peteiro et al., 2016). The implementation of long-term conservation measures is necessary for sustainable exploitation and the protection of the resource.

4.3.1.3. Promote a better management of coastal urbanisation. Given sea level rise predictions, salt marshes' integrity could be at stake. Ensuring salt marshes have enough space to shift inland as sea level rises and restoring sediment inputs would maintain their presence and the services they provide to coastal communities, particularly controlling coastal erosion and protecting our coastline against flooding and storm surge events. Policy towards coastal management should continue moving away from land claims for economic growth in favour of salt marsh conservation to maintain the seascape's integrity and sustain ecosystem services (Foster et al., 2013; Ladd et al., 2021).

4.4. Knowledge gaps and future recommendations for assessing safe operating space and thresholds

Limitations that inevitably come with an extensive literature review also mean that many valuable articles, or grey literature, could have

been missed in English or other languages. Additionally, as this review focused on the effects of climate change with or without local stressors and conditioned by a list of keywords relative to thresholds or safe operating spaces, many valuable studies were omitted, including the ones looking solely at the impact of local stressors. Despite those limitations, the effects of climate change drivers are relatively well-defined in the scientific literature, although their interaction and the frequency of consequent events (e.g., extreme weather, heat waves) remain poorly studied. However, important knowledge gaps remain, mostly about their interaction with local stressors, many of which, such as recreational activities (anchoring, recreational fishing) in the Mediterranean Sea, holopelagic Sargassum rafts in the Caribbean (Banaszak, 2021), aquaculture in North-East Atlantic (Haugland et al., 2021) along with global pressures such as pollution, marine litter, over-sedimentation, bottom trawling, and hydrologic disturbances that are known to impact MCEs and therefore, affect their resilience to climate change drivers (Boudouresque et al., 2009; Orth et al., 2006; Fragkopoulou et al., 2021; Lincoln et al., 2022).

Information on thresholds and safe operating space were retrieved from the literature for most ecosystems for at least one CC-related pressure. However, the current state of knowledge also highlights the difficulty of precisely determining thresholds and safe operating spaces, but see Papaki et al. (2020), who used current seagrass distribution in the Mediterranean with environmental conditions to identify safe operating spaces. Experiment size, costs, and project time constraints often limit experimental settings to test two or three temperature targets based on IPCC-predicted future scenarios. Therefore, it is difficult to establish when a threshold for an environmental factor is exactly crossed (de Juan et al., 2018). Furthermore, the complex interactions with other climate change drivers and local stressors make thresholds not fixed values, and we were not able to assess the effect of local stressors on those CC thresholds or safe operating space from this literature review.

Another limitation when investigating threshold values for CC drivers and local stressors is that these have only been experimentally tested for a limited number of coral or salt marsh species, for instance, and responses can vary significantly between species. For example, corals' control of pH and calcification response are species-specific and have only been tested for very few species. Knowing the thresholds and optimal values for a few species limits our capacity to translate physiological responses to population and community as coral reefs are diverse ecosystems. Some species interaction studies conclude that the response of the maërl bed community to climate change will be strongly conditioned by changes in species interactions (Legrand et al., 2017).

Local biophysical factors may affect acclimatisation potential further hampering the establishment of species-specific threshold values for MCEs. For instance, in the temperate North-East Atlantic, the seagrass *Z. marina* is distributed along an extensive thermal range from low to high latitudes. Their populations respond differently to heat stress, with the southern population recovering faster from heat stress than the northern population (Winters et al., 2011; Jueterbock et al., 2016), which also has been shown for *P. oceanica* populations studied along a latitudinal gradient in the Mediterranean Sea's (Beca-Carretero et al., 2018).

In addition, benefits arising from the connectivity between MCEs could increase the adaptive capacity of MCEs to cumulative pressures. For example, mangroves can reduce bleaching susceptibility by providing light refugia to corals (Stewart et al., 2021), while coral reefs protect mangrove communities (Wegner and Ellis, 2017) and seagrass beds against waves and storms. These mutual synergies increase the resilience and services of individual MCEs to different stressors. They should, thus, be further explored, particularly in relation to the combined effects of climate change and local stressors.

5. Conclusion

As illustrated in this review, environmental conditions in the different ecoregions are changing with time, and climate change and local stressors can considerably affect the physiology of foundation species, populations, and communities. The potential impacts that could arise from co-occurring climate change and local stressors have started to be defined and quantified, but many have not been tested yet, or the effects remain unclear. Given species-specific nonlinear responses and thresholds, we can still anticipate future climate impacts from the reviewed ecological studies. Some authors have even been able to simulate IPCC scenarios on MCEs, using the upper tolerance limit for several species to predict future distribution if the temperature is increasing (Assis et al., 2016; Assis et al., 2018; Fernández-Martínez et al., 2019). This review highlights the need for a more comprehensive, multi-species, multi-ecosystems, and multi-stressors approach to predict better changes at the ecosystem and seascape levels of MCEs. Research needs broad-spanned long-term monitoring of the ecological condition and extent of MCEs, using field-based surveys coupled, if relevant, with remote sensing applications. These prolonged monitoring programs and observational networks are necessary for detecting and attributing ecological changes in response to climate change and other human pressures. Furthermore, research should continue with laboratory and field process studies, manipulative experiments, and modelling from small-scale process simulations to large-scale coupled biophysical models. Developing ambitious management techniques such as nature-based solutions to maintain, enhance or recover the ecological condition of MCEs is thus an urgent need to build more resilient ecosystems to face climate change threats. While it is difficult to predict future changes, improving ecological forecasting capabilities to support climate adaptation strategies and policy decisions is key for effectively implementing nature-based solutions.

Supplementary data to this article can be found online at https://doi.org/10.1016/j.biocon.2023.110394.

CRediT authorship contribution statement

Ewan Trégarot (conceptualization, data curation, formal analysis, funding acquisition, methodology, supervision, visualisation, writing original draft, review & editing)
Juan Pablo D'Olivo (conceptualization, data curation, supervision, formal analysis, writing original draft, review & editing)
Andrea Zita Botelho (data curation, formal analysis)
Andrea Cabrito (data curation, formal analysis, visualisation, review & editing)
Gabriel O. Cardoso (formal analysis, review & editing)
Gema Casal (data curation, formal analysis, writing original draft, review & editing)
Cindy C. Cornet (conceptualization, funding acquisition, project administration, data curation, supervision, formal analysis, writing original draft, review & editing)
Simon M. Cragg (data curation, formal analysis, review & editing)
Anna Karima Degia (formal analysis)
Stein Fredriksen (data curation, supervision, formal analysis; writing original draft, review & editing)
Elisa Furlan (data curation, review & editing)
Georg Heiss (data curation, supervision, writing original draft)
Diego K. Kersting (conceptualization, data curation, supervision, formal analysis, writing original draft, review & editing)
Jean-Philippe Maréchal (data curation)
Erik Meesters (data curation)
Bethan C. O'Leary (conceptualization, data curation, writing original draft, review & editing)
Géraldine Pérez (data curation, formal analysis, writing original draft)
Cristina Seijo-Núñez (conceptualization, methodology, data curation)
Rémy Simide (conceptualization, data curation, formal analysis, writing original draft)

Matthijs van der Geest (conceptualization, methodology, data curation, supervision, formal analysis, writing original draft, review & editing)
Silvia de Juan (conceptualization, methodology, data curation, supervision, writing original draft, review & editing).

Declaration of competing interest

The authors declare that they have no known competing financial interests or personal relationships that could have appeared to influence the work reported in this paper.

Data availability

Data will be made available on request.

Acknowledgement

The study received funding from the European Union's Horizon 2020 Research and Innovation Programme under Grant Agreement no. 869710 (EU-MaCoBioS - https://macobios.eu/). We would like to thank Thierry Caroff for the design of marine and coastal ecosystems' icons. The authors are also thankful to the anonymous reviewers for their careful reading of the manuscript and their many insightful comments and suggestions.

References

Akaji, Y., Inoue, T., Tomimatsu, H., Kawanishi, A., 2019. Photosynthesis, respiration, and growth patterns of Rhizophora stylosa seedlings in relation to growth temperature. Trees 33, 1041–1049.
Albright, R., Langdon, C., 2011. Ocean acidification impacts multiple early life history processes of the Caribbean coral *Porites astreoides*. Glob. Chang. Biol. 17, 2478–2487. https://doi.org/10.1111/j.1365-2486.2011.02404.x.
Albright, R., Mason, B., Miller, M., Langdon, C., 2010. Ocean acidification compromises recruitment success of the threatened Caribbean coral *Acropora palmata*. Proc. Natl. Acad. Sci. U. S. A. 107, 20400–20404. https://doi.org/10.1073/pnas.1007273107.
Araújo, R.M., Assis, J., Aguillar, R., Airoldi, L., Bárbara, I., Bartsch, I., Bekkby, T., Christie, H., Davoult, D., Derrien-Courtel, S., Fernandez, C., Fredriksen, S., Gevaert, F., Gundersen, H., Le Gal, A., Lévêque, L., Mieszkowska, N., Norderhaug, K. M., Oliveira, P., Puente, A., Rico, J.M., Rinde, E., Schubert, H., Strain, E.M., Valero, M., Viard, F., Sousa-Pinto, I., 2016. Status, trends and drivers of kelp forests in Europe: an expert assessment. Biodivers. Conserv. 25, 1319–1348. https://doi.org/10.1007/s10531-016-1141-7.
Assis, J., Lucas, A.V., Barbara, I., Serrao, E.A., 2016. Future climate change is predicted to shift long-term persistence zones in the cold-temperate kelp *Laminaria hyperborea*. Mar. Environ. Res. 113, 174–182. https://doi.org/10.1016/j.marenvres.2015.11.005.
Assis, J., Araujo, M.B., Serrao, E.A., 2018. Projected climate changes threaten ancient refugia of kelp forests in the North Atlantic. Glob. Chang. Biol. 24, e55–e66. https://doi.org/10.1111/gcb.13818.
de Bakker, D.M., van Duyl, F.C., Perry, C.T., Meesters, E.H., 2019. Extreme spatial heterogeneity in carbonate accretion potential on a Caribbean fringing reef linked to local human disturbance gradients. Glob. Chang. Biol. 25, 4092–4104. https://doi.org/10.1111/gcb.14800.
Banaszak, A.T., 2021. Contamination of coral reefs in the Mexican Caribbean. Anthropogenic Pollut. Aquat. Ecosyst. 113–129.
Barbera, C., Bordehore, C., Borg, J.A., Glémarec, M., Grall, J., Hall-Spencer, J.M., De La Huz, C.H., Lanfranco, E., Lastra, M., Moore, P.G., Mora, J., 2003. Conservation and management of northeast Atlantic and Mediterranean maerl beds. Aquat. Conserv. Mar. Freshwat. Ecosyst. 13, S65–S76.
Barbier, E.B., Hacker, S.D., Kennedy, C., Koch, E.W., Stier, A.C., Silliman, B.R., 2011. The value of estuarine and coastal ecosystem services. Ecol. Monogr. 81, 169–193. https://doi.org/10.1890/10-1510.1.
Baums, I.B., Devlin-Durante, M.K., Polato, N.R., Xu, D., Giri, S., Altman, N.S., Ruiz, D., Parkinson, J.E., Boulay, J.N., 2013. Genotypic variation influences reproductive success and thermal stress tolerance in the reef building coral, *Acropora palmata*. Coral Reefs 32, 703–717. https://doi.org/10.1007/s00338-013-1012-6.
Beca-Carretero, P., Guiheneuf, F., Marín-Guirao, L., Bernardeau-Esteller, J., Garcia-Munoz, R., Stengel, D.B., Ruiz, J.M., 2018. Effects of an experimental heat wave on fatty acid composition in two Mediterranean seagrass species. Mar. Pollut. Bull. 134, 27–37. https://doi.org/10.1016/j.marpolbul.2017.12.057.
Beckford, C.L., Rhiney, K., 2016. Geographies of globalization, climate change and food and agriculture in the Caribbean. In: Beckford, C.L., Rhiney, K. (Eds.), Globalization, Agriculture and Food in the Caribbean: Climate Change, Gender and Geography. Palgrave Macmillan UK, London, pp. 3–22. https://doi.org/10.1057/978-1-137-53837-6_1.
Bedwell-Ivers, H.E., Koch, M.S., Peach, K.E., Joles, L., Dutra, E., Manfrino, C., Woodson, B., 2017. The role of *in hospite* zooxanthellae photophysiology and reef chemistry on elevated pCO_2 effects in two branching Caribbean corals: *Acropora cervicornis* and *Porites divaricata*. ICES J. Mar. Sci. 74, 1103–1112. https://doi.org/10.1093/icesjms/fsw026.
Bergmann, N., Winters, G., Rauch, G., Eizaguirre, C., Gu, J., Nelle, P., Fricke, B., Reusch, T.B., 2010. Population-specificity of heat stress gene induction in northern and southern eelgrass *Zostera marina* populations under simulated global warming. Mol. Ecol. 19, 2870–2883. https://doi.org/10.1111/j.1365-294X.2010.04731.x.
Bevilacqua, S., Guarnieri, G., Farella, G., Terlizzi, A., Fraschetti, S., 2018. A regional assessment of cumulative impact mapping on Mediterranean coralligenous outcrops. Sci. Rep. 8, 1757. https://doi.org/10.1038/s41598-018-20297-1.
Bindoff, N.L., Cheung, W.W., Kairo, J.G., Arístegui, J., Guinder, V.A., Hallberg, R., Hilmi, N., Jiao, N., Karim, M.S., Levin, L., 2019. Changing Ocean, Marine Ecosystems, and Dependent Communities.
Bitoun, R.E., Collin, A., James, D., Pioch, S., 2018. Modelling saltmarsh spatial evolution at high resolution from 1948 to 2100 (Beaussais's Bay, France). J. Coast. Res. 85 (10085), 676–680.
Blackwood, J.C., Okasaki, C., Archer, A., Matt, E.W., Sherman, E., Montovan, K., 2018. Modeling alternative stable states in Caribbean coral reefs. Nat. Resour. Model. 31 (1), e12157.
Blanchon, P., Richards, S., Bernal, J.P., Cerdeira-Estrada, S., Ibarra, M.S., Corona-Martínez, L., Martell-Dubois, R., 2017. Retrograde accretion of a Caribbean fringing reef controlled by hurricanes and sea-level rise. Front. Earth Sci. 5 https://doi.org/10.3389/feart.2017.00078.
Bompy, F., Lequeue, G., Imbert, D., Dulormne, M., 2014. Increasing fluctuations of soil salinity affect seedling growth performances and physiology in three Neotropical mangrove species. Plant Soil 380, 399–413. https://doi.org/10.1007/s11104-014-2100-2.
Boorman, L., 1992. The environmental consequences of climatic change on British salt marsh vegetation. Wetl. Ecol. Manag. 2 https://doi.org/10.1007/BF00178130.
Boudouresque, C.F., Bernard, G., Pergent, G., Shili, A., Verlaque, M., 2009. Regression of Mediterranean seagrasses caused by natural processes and anthropogenic disturbances and stress: a critical review. Bot. Mar. 52, 395–418. https://doi.org/10.1515/bot.2009.057.
Bozec, Y.M., O'Farrell, S., Bruggemann, J.H., Luckhurst, B.E., Mumby, P.J., 2016. Tradeoffs between fisheries harvest and the resilience of coral reefs. Proc. Natl. Acad. Sci. U. S. A. 113, 4536–4541. https://doi.org/10.1073/pnas.1601529113.
Brakel, J., Jakobsson-Thor, S., Bockelmann, A.-C., Reusch, T.B.H., 2019. Modulation of the eelgrass – *Labyrinthula zosterae* interaction under predicted ocean warming, salinity change and light limitation. Front. Mar. Sci. 6 https://doi.org/10.3389/fmars.2019.00268.
Brodie, J., Williamson, C.J., Smale, D.A., Kamenos, N.A., Mieszkowska, N., Santos, R., Cunliffe, M., Steinke, M., Yesson, C., Anderson, K.M., Asnaghi, V., Brownlee, C., Burdett, H.L., Burrows, M.T., Collins, S., Donohue, P.J.C., Harvey, B., Foggo, A., Noisette, F., Nunes, J., Ragazzola, F., Raven, J.A., Schmidt, D.N., Suggett, D., Teichberg, M., Hall-Spencer, J.M., 2014. The future of the northeast Atlantic benthic flora in a high CO_2 world. Ecol. Evol. 4, 2787–2798. https://doi.org/10.1002/ece3.1105.
Brown, C.E., Pezeshki, S.R., DeLaune, R.D., 2006. The effects of salinity and soil drying on nutrient uptake and growth of Spartina alterniflora in a simulated tidal system. Environ. Exp. Bot. 58 (1–3), 140–148.
Buddemeier, R.W., Jokiel, P.L., Zimmerman, K.M., Lane, D.R., Carey, J.M., Bohling, G.C., Martinich, J.A., 2008. A modeling tool to evaluate regional coral reef responses to changes in climate and ocean chemistry. Limnol. Oceanogr. Methods 6, 395–411. https://doi.org/10.4319/lom.2008.6.395.
Buddemeier, R.W., Lane, D.R., Martinich, J.A., 2011. Modeling regional coral reef responses to global warming and changes in ocean chemistry: Caribbean case study. Clim. Chang. 109, 375–397. https://doi.org/10.1007/s10584-011-0022-z.
Burdett, H.L., Aloisio, E., Calosi, P., Findlay, H.S., Widdicombe, S., Hatton, A.D., Kamenos, N.A., 2012. The effect of chronic and acute low pH on the intracellular DMSP production and epithelial cell morphology of red coralline algae. Mar. Biol. Res. 8, 756–763. https://doi.org/10.1080/17451000.2012.676189.
Burdett, H.L., Perna, G., McKay, L., Broomhead, G., Kamenos, N.A., 2018. Community-level sensitivity of a calcifying ecosystem to acute in situ CO_2 enrichment. Mar. Ecol. Prog. Ser. 587, 73–80. https://doi.org/10.3354/meps12421.
Camp, E.F., Smith, D.J., Evenhuis, C., Enochs, I., Manzello, D., Woodcock, S., Suggett, D. J., 2016. Acclimatization to high-variance habitats does not enhance physiological tolerance of two key Caribbean corals to future temperature and pH. Proc. Biol. Sci. 283 https://doi.org/10.1098/rspb.2016.0442.
Carilli, J.E., Norris, R.D., Black, B.A., Walsh, S.M., McField, M., 2009. Local stressors reduce coral resilience to bleaching. PLoS One 4. https://doi.org/10.1371/journal.pone.0006324.
Carlson, D.F., Yarbro, L.A., Scolaro, S., Poniatowski, M., McGee-Absten, V., Carlson, P.R., 2018. Sea surface temperatures and seagrass mortality in Florida Bay: spatial and temporal patterns discerned from MODIS and AVHRR data. Remote Sens. Environ. 208, 171–188. https://doi.org/10.1016/j.rse.2018.02.014.
Carrasco, A.R., Kombiadou, K., Amado, M., Matias, A., 2021. Past and future marsh adaptation: lessons learned from the Ria Formosa lagoon. Sci. Total Environ. 790, 148082 https://doi.org/10.1016/j.scitotenv.2021.148082.
Carreiras, J., Alberto Pérez-Romero, J., Mateos-Naranjo, E., Redondo-Gómez, S., Rita Matos, A., Caçador, I., Duarte, B., 2020. The effect of heavy metal contamination pre-conditioning in the heat stress tolerance of native and invasive Mediterranean halophytes. Ecol. Indic. 111 https://doi.org/10.1016/j.ecolind.2019.106045.
Carreiras, J., Perez-Romero, J.A., Mateos-Naranjo, E., Redondo-Gomez, S., Matos, A.R., Cacador, I., Duarte, B., 2021. Heavy metal pre-conditioning history modulates

Spartina patens physiological tolerance along a salinity gradient. Plants 10. https://doi.org/10.3390/plants10102072.
Castañeda-Chávez, M.d.R., Lango-Reynoso, F., García-Fuentes, J.L., Reyes-Aguilar, Á.R., 2018. Bacteria that affects coral health with an emphasis on the Gulf of Mexico and the Caribbean Sea. Lat. Am. J. Aquat. Res. 46, 880–889. https://doi.org/10.3856/vol46-issue5-fulltext-2.
Castillo, J.M., Fernández-Baco, L., Castellanos, E.M., Luque, C.J., Figueroa, M.E., Davy, A.J., 2000. Lower limits of *Spartina densiflora* and *S. maritima* in a Mediterranean salt marsh determined by different ecophysiological tolerances. J. Ecol. 88, 801–812. https://doi.org/10.1046/j.1365-2745.2000.00492.x.
Cavanaugh, K.C., Parker, J.D., Cook-Patton, S.C., Feller, I.C., Williams, A.P., Kellner, J.R., 2015. Integrating physiological threshold experiments with climate modeling to project mangrove species' range expansion. Glob. Chang. Biol. 21, 1928–1938. https://doi.org/10.1111/gcb.12843.
Chapman, S.K., Feller, I.C., Canas, G., Hayes, M.A., Dix, N., Hester, M., Morris, J., Langley, J.A., 2021. Mangrove growth response to experimental warming is greatest near the range limit in northeast Florida. Ecology 102 (6), e03320.
Chefaoui, R.M., Duarte, C.M., Serrao, E.A., 2018. Dramatic loss of seagrass habitat under projected climate change in the Mediterranean Sea. Glob. Chang. Biol. 24, 4919–4928. https://doi.org/10.1111/gcb.14401.
Chollett, I., Mumby, P.J., 2013. Reefs of last resort: locating and assessing thermal refugia in the wider Caribbean. Biol. Conserv. 167, 179–186. https://doi.org/10.1016/j.biocon.2013.08.010.
Christie, H.C., Gundersen, H., Rinde, E., Filbee-Dexter, K., Norderhaug, K.M., Pedersen, T., Bekkby, T., Gitmark, J.K., Fagerli, C.W., 2019. Can multitrophic interactions and ocean warming influence large-scale kelp recovery? Ecol. Evol. https://doi.org/10.1002/ece3.4963.
Church, J.A., Clark, P.U., Cazenave, A., Gregory, J.M., Jevrejeva, S., Levermann, A., Merrifield, M.A., Milne, G.A., Nerem, R.S., Nunn, P.D., Payne, A.J., 2013. Sea Level Change. PM Cambridge University Press.
Cohen, M.C.L., de Souza, A.V., Liu, K.-B., Rodrigues, E., Yao, Q., Pessenda, L.C.R., Rossetti, D., Ryu, J., Dietz, M., 2021. Effects of beach nourishment project on coastal geomorphology and mangrove dynamics in Southern Louisiana, USA. Remote Sens. 13 https://doi.org/10.3390/rs13142688.
Cornwall, C.E., Diaz-Pulido, G., Comeau, S., 2019. Impacts of ocean warming on coralline algal calcification: meta-analysis, knowledge gaps, and key recommendations for future research. Front. Mar. Sci. 6 https://doi.org/10.3389/fmars.2019.00186.
Costa, H., Guimarães, M.H., Rangel, M., Ressurreicão, A., Monteiro, P., Oliveira, F., Bentes, L., Sales Henriques, N., Sousa, I., Alexandre, S., Pontes, J., 2022. Co-design of a marine protected area zoning and the lessons learned from it. Front. Mar. Sci. 9.
Couto Martins, I., Duarte, B., Caçador, I., Marques, J.C., T., 2014. Modelling the effects of global temperature increase on the growth of salt marsh plants. Appl. Ecol. Environ. Res. 12, 753–764. https://doi.org/10.15666/aeer/1203_753764.
Cox, T.E., Gazeau, F., Alliouane, S., Hendriks, I.E., Mahacek, P., Le Fur, A., Gattuso, J.-P., 2016. Effects of in situ CO_2 enrichment on structural characteristics, photosynthesis, and growth of the Mediterranean seagrass *Posidonia oceanica*. Biogeosciences 13, 2179–2194. https://doi.org/10.5194/bg-13-2179-2016.
Crabbe, M.J.C., 2011. Coral resilience on the reefs of Jamaica. Underw. Technol. 30, 65–70. https://doi.org/10.3723/ut.30.065.
Davies, S.W., Marchetti, A., Ries, J.B., Castillo, K.D., 2016. Thermal and pCO_2 stress elicit divergent transcriptomic responses in a resilient coral. Front. Mar. Sci. 3 https://doi.org/10.3389/fmars.2016.00112.
DeBose, J.L., Nuttall, M.F., Hickerson, E.L., Schmahl, G.P., 2013. A high-latitude coral community with an uncertain future: Stetson Bank, northwestern Gulf of Mexico. Coral Reefs 32, 255–267. https://doi.org/10.1007/s00338-012-0971-3.
DeConto, R.M., Pollard, D., 2016. Contribution of Antarctica to past and future sea-level rise. Nature 531, 591–597. https://doi.org/10.1038/nature17145.
Derrien-Courtel, S., Le Gal, A., Grall, J., 2013. Regional-scale analysis of subtidal rocky shore community. Helgol. Mar. Res. 67 (4), 697–712.
Devaney, J.L., Pullen, J., Feller, I.C., Parker, J.D., 2021. Low humidity and hypersalinity reduce cold tolerance in mangroves. Estuar. Coast. Shelf Sci. 248 https://doi.org/10.1016/j.ecss.2020.107015.
Díez, I., Muguerza, N., Santolaria, A., Ganzedo, U., Gorostiaga, J.M., 2012. Seaweed assemblage changes in the eastern Cantabrian Sea and their potential relationship to climate change. Estuar. Coast. Shelf Sci. 99, 108–120. https://doi.org/10.1016/j.ecss.2011.12.027.
Donald, H.K., Ries, J.B., Stewart, J.A., Fowell, S.E., Foster, G.L., 2017. Boron isotope sensitivity to seawater pH change in a species of *Neogoniolithon* coralline red alga. Geochim. Cosmochim. Acta 217, 240–253. https://doi.org/10.1016/j.gca.2017.08.021.
Doody, J.P., 2013. Coastal squeeze and managed realignment in southeast England, does it tell us anything about the future? Ocean Coast. Manag. 79, 34–41. https://doi.org/10.1016/j.ocecoaman.2012.05.008.
Duarte, C.M., Losada, I.J., Hendriks, I.E., Mazarrasa, I., Marbà, N., 2013. The role of coastal plant communities for climate change mitigation and adaptation. Nat. Clim. Chang. 3, 961–968. https://doi.org/10.1038/nclimate1970.
Duarte, B., Marques, J.C., Caçador, I., 2016. Ecophysiological response of native and invasive Spartina species to extreme temperature events in Mediterranean marshes. Biol. Invasions 18, 2189–2205. https://doi.org/10.1007/s10530-015-0958-4.
Duarte, B., Carreiras, J., Caçador, I., 2021. Climate change impacts on salt marsh blue carbon, nitrogen and phosphorous stocks and ecosystem services. Appl. Sci. 11 https://doi.org/10.3390/app11041969.
Eakin, C.M., Morgan, J.A., Heron, S.F., Smith, T.B., Liu, G., Alvarez-Filip, L., Baca, B., Bartels, E., Bastidas, C., Bouchon, C., Brandt, M., Bruckner, A.W., Bunkley-Williams, L., Cameron, A., Causey, B.D., Chiappone, M., Christensen, T.R.L., Crabbe, M.J.C., Day, O., de la Guardia, E., Díaz-Pulido, G., DiResta, D., Gil-Agudelo, D.L., Gilliam, D.S., Ginsburg, R.N., Gore, S., Guzmán, H.M., Hendee, J.C., Hernández-Delgado, E.A., Husain, E., Jeffrey, C.F.G., Jones, R.J., Jordán-Dahlgren, E., Kaufman, L.S., Kline, D.I., Kramer, P.A., Lang, J.C., Lirman, D., Mallela, J., Manfrino, C., Maréchal, J.-P., Marks, K., Mihaly, J., Miller, W.J., Mueller, E.M., Muller, E.M., Orozco Toro, C.A., Oxenford, H.A., Ponce-Taylor, D., Quinn, N., Ritchie, K.B., Rodríguez, S., Ramírez, A.R., Romano, S., Samhouri, J.F., Sánchez, J.A., Schmahl, G.P., Shank, B.V., Skirving, W.J., Steiner, S.C.C., Villamizar, E., Walsh, S.M., Walter, C., Weil, E., Williams, E.H., Roberson, K.W., Yusuf, Y., 2010. Caribbean corals in crisis: record thermal stress, bleaching, and mortality in 2005. PLoS One 5, e13969. https://doi.org/10.1371/journal.pone.0013969.
Eakin, C.M., Devotta, D., Heron, S., Connolly, S., Liu, G., Geiger, E., Cour, J.D.L., Gomez, A., Skirving, W., Baird, A., Cantin, N., Couch, C., Donner, S., Gilmour, J., Gonzalez-Rivero, M., Gudka, M., Harrison, H., Hodgson, G., Hoegh-Guldberg, O., Hoey, A., Hoogenboom, M., Hughes, T., Johnson, M., Kerry, J., Mihaly, J., Muñiz-Castillo, A., Obura, D., Pratchett, M., Rivera-Sosa, A., Ross, C., Stein, J., Thompson, A., Torda, G., Viehman, T.S., Walter, C., Wilson, S., Marsh, B., Spady, B., Dyer, N., Adam, T., Alidoostsalimi, M., Alidoostsalimi, P., Alvarez-Filip, L., Álvarez-Noriega, M., Bahr, K., Barnes, P., Sandoval, J.B., Baum, J., Bauman, A., Beger, M., Berry, K., Bessell-Browne, P., Bigot, L., Bonito, V., Brodnicke, O., Burdick, D., Burkepile, D., Burt, A., Burt, J., Butler, I., Caldwell, J., Chancerelle, Y., Chen, C.A., Cherh, K.-L., Childress, M., Coken, D., Coward, G., Crabbe, M.J., Dallison, T., Dalton, S., DeCarlo, T., Drury, C., Drysdale, I., Edwards, C., Eggertsen, L., Elma, E., Ennis, R., Evans, R., Eyal, G., Fenner, D., Figueroa-Zavala, B., Fisch, J., Fox, M., Gadoutsis, E., Gilbert, A., Halford, A., Heintz, T., Hewlett, J., Hobbs, J.-P.A., Hoot, W., Houk, P., Johnston, L., Johnston, M., Kayanne, H., Kennedy, E., Kikuchi, R., Kloiber, U., Koike, H., Kramer, L., Kuo, C.-Y., Lang, J., Leadbeater, A., Leão, Z., Lee, J., Lewis, C., Lirman, D., Longo, G., MacDonald, C., Mangubhai, S., Silva, I.d., Mason-Parker, C., McDonough, V., McField, M., Mello, T., Agathe, C.M., Moldzio, S., Monroe, A., Montefalcone, M., Moses, K., Mostafavi, P.G., Moura, R., Munasinghe, C., Nakamura, T., Nicet, J.-B., Nuttall, M., Oliveira, M., Oxenford, H., Pandolfi, J., Patankar, V., Perez, D., Perera, N., Prabuning, D., Precht, W., Raj, K.D., Reimer, J., Richardson, L., Rotjan, R., Ryan, N., Salm, R., Sandin, S., Schopmeyer, S., Shokri, M., Smith, J., Smith, K., Smith, S.R., Smith, T., Sommer, B., Soto, M., Sykes, H., Tagarino, K., Teoh, M., Thai, M., Toh, T., Tredinnick, A., Tso, A., Tyley, H., Ussi, A., Vaterlaus, C., Vermeij, M., Vo, S.T., Voolstra, C., Wee, H.B., Weiler, B., Yahya, S., Yeemin, T., Ziegler, M., Kimura, T., Manzello, D., 2022. The 2014-17 Global Coral Bleaching Event: The Most Severe and Widespread Coral Reef Destruction. https://doi.org/10.21203/rs.3.rs-1555992/v1 (PREPRINT (Version 1) available at Research Square).
Edwards, H.J., Elliott, I.A., Eakin, C.M., Irikawa, A., Madin, J.S., McField, M., Morgan, J. A., Van Woesik, R., Mumby, P.J., 2011. How much time can herbivore protection buy for coral reefs under realistic regimes of hurricanes and coral bleaching? Glob. Chang. Biol. 17, 2033–2048. https://doi.org/10.1111/j.1365-2486.2010.02366.x.
Ehlers, A., Worm, B., Reusch, T.B.H., 2008. Importance of genetic diversity in eelgrass *Zostera marina* for its resilience to global warming. Mar. Ecol. Prog. Ser. 355, 1–7. https://doi.org/10.3354/meps07369.
Ehrhold, A., Jouet, G., Le Roy, P., Jorry, S.J., Grall, J., Reixach, T., Lambert, C., Gregoire, G., Goslin, J., Roubi, A., Penaud, A., Vidal, M., Siano, R., 2021. Fossil maerl beds as coastal indicators of late Holocene palaeo-environmental evolution in the Bay of Brest (Western France). Palaeogeogr. Palaeoclimatol. Palaeoecol. 577 https://doi.org/10.1016/j.palaeo.2021.110525.
Elliott, M., Borja, Á., McQuatters-Gollop, A., Mazik, K., Birchenough, S., Andersen, J.H., Painting, S., Peck, M., 2015. Force majeure: will climate change affect our ability to attain Good Environmental Status for marine biodiversity? Mar. Pollut. Bull. 95, 7–27. https://doi.org/10.1016/j.marpolbul.2015.03.015.
Elton, C.S., 1958. The Ecology of Invasions by Animals and Plants. Methuen, London.
Fagerli, C.W., Norderhaug, K.M., Christie, H.C., 2013. Lack of sea urchin settlement may explain kelp forest recovery in overgrazed areas in Norway. Mar. Ecol. Prog. Ser. 488, 119–132. https://doi.org/10.3354/meps10413.
Feehan, C.J., Grace, S.P., Narvaez, C.A., 2019. Ecological feedbacks stabilize a turf-dominated ecosystem at the southern extent of kelp forests in the Northwest Atlantic. Sci. Rep. 9, 7078. https://doi.org/10.1038/s41598-019-43536-5.
Feller, I.C., Dangremond, E.M., Devlin, D.J., Lovelock, C.E., Proffitt, C.E., Rodriguez, W., 2015. Nutrient enrichment intensifies hurricane impact in scrub mangrove ecosystems in the Indian River Lagoon, Florida, USA. Ecology 96, 2960–2972. https://doi.org/10.1890/14-1853.1.
Fernández-Martínez, M., Sardans, J., Chevallier, F., Ciais, P., Obersteiner, M., Vicca, S., Canadell, J.G., Bastos, A., Friedlingstein, P., Sitch, S., Piao, S.L., 2019. Global trends in carbon sinks and their relationships with CO2 and temperature. Nat. Clim. Chang. 9 (1), 73–79.
Filbee-Dexter, K., Wernberg, T., 2018. Rise of turfs: a new battlefront for globally declining kelp forests. BioScience 68, 64–76. https://doi.org/10.1093/biosci/bix147.
Filbee-Dexter, K., Feehan, C.J., Scheibling, R.E., 2016. Large-scale degradation of a kelp ecosystem in an ocean warming hotspot. Mar. Ecol. Prog. Ser. 543, 141–152. https://doi.org/10.3354/meps11554.
Foster, N.L., Baums, I.B., Sanchez, J.A., Paris, C.B., Chollett, I., Agudelo, C.L., Vermeij, M. J., Mumby, P.J., 2013. Hurricane-driven patterns of clonality in an ecosystem engineer: the Caribbean coral *Montastraea annularis*. PLoS One 8, e53283. https://doi.org/10.1371/journal.pone.0053283.
Fragkopoulou, E., Serrão, E.A., Horta, P.A., Koerich, G., Assis, J., 2021. Bottom trawling threatens future climate refugia of rhodoliths globally. Front. Mar. Sci. 7 https://doi.org/10.3389/fmars.2020.594537.

Franco, J.N., Tuya, F., Bertocci, I., Rodríguez, L., Martínez, B., Sousa-Pinto, I., Arenas, F., Van Alstyne, K., 2018. The 'golden kelp' *Laminaria ochroleuca* under global change: integrating multiple eco-physiological responses with species distribution models. J. Ecol. 106, 47–58. https://doi.org/10.1111/1365-2745.12810.

Franssen, S.U., Gu, J., Bergmann, N., Winters, G., Klostermeier, U.C., Rosenstiel, P., Bornberg-Bauer, E., Reusch, T.B., 2011. Transcriptomic resilience to global warming in the seagrass *Zostera marina*, a marine foundation species. Proc. Natl. Acad. Sci. U. S. A. 108, 19276–19281. https://doi.org/10.1073/pnas.1107680108.

Franssen, S.U., Gu, J., Winters, G., Huylmans, A.K., Wienpahl, I., Sparwel, M., Coyer, J. A., Olsen, J.L., Reusch, T.B., Bornberg-Bauer, E., 2014. Genome-wide transcriptomic responses of the seagrasses *Zostera marina* and *Nanozostera noltii* under a simulated heatwave confirm functional types. Mar. Genomics 15, 65–73. https://doi.org/10.1016/j.margen.2014.03.004.

Fredersdorf, J., Muller, R., Becker, S., Wiencke, C., Bischof, K., 2009. Interactive effects of radiation, temperature and salinity on different life history stages of the Arctic kelp *Alaria esculenta* (Phaeophyceae). Oecologia 160, 483–492. https://doi.org/10.1007/s00442-009-1326-9.

Freeman, L.A., Kleypas, J.A., Miller, A.J., 2013. Coral reef habitat response to climate change scenarios. PLoS One 8, e82404. https://doi.org/10.1371/journal.pone.0082404.

Furlan, E., Torresan, S., Critto, A., Lovato, T., Solidoro, C., Lazzari, P., Marcomini, A., 2019. Cumulative Impact Index for the Adriatic Sea: accounting for interactions among climate and anthropogenic pressures. Sci. Total Environ. 670, 379–397. https://doi.org/10.1016/j.scitotenv.2019.03.021.

Gabler, C.A., Osland, M.J., Grace, J.B., Stagg, C.L., Day, R.H., Hartley, S.B., Enwright, N. M., From, A.S., McCoy, M.L., McLeod, J.L., 2017. Macroclimatic change expected to transform coastal wetland ecosystems this century. Nat. Clim. Chang. 7, 142–147. https://doi.org/10.1038/nclimate3203.

Garrabou, J., Coma, R., Bensoussan, N., Bally, M., Chevaldonné, P., Cigliano, M., Diaz, D., Harmelin, J.G., Gambi, M.C., Kersting, D.K., Ledoux, J.B., Lejeusne, C., Linares, C., Marschal, C., Pérez, T., Ribes, M., Romano, J.C., Serrano, E., Teixido, N., Torrents, O., Zabala, M., Zuberer, F., Cerrano, C., 2009. Mass mortality in Northwestern Mediterranean rocky benthic communities: effects of the 2003 heat wave. Glob. Chang. Biol. 15, 1090–1103. https://doi.org/10.1111/j.1365-2486.2008.01823.x.

Garrabou, J., Gómez-Gras, D., Medrano, A., Cerrano, C., Ponti, M., Schlegel, R., Bensoussan, N., Turicchia, E., Sini, M., Gerovasileiou, V., Teixido, N., Mirasole, A., Tamburello, L., Cebrian, E., Rilov, G., Ledoux, J.B., Souissi, J.B., Khamassi, F., Ghanem, R., Benabdi, M., Grimes, S., Ocaña, O., Bazairi, H., Hereu, B., Linares, C., Kersting, D.K., Rovira, G., Ortega, J., Casals, D., Pagès-Escolà, M., Margarit, N., Capdevila, P., Verdura, J., Ramos, A., Izquierdo, A., Barbera, C., Rubio-Portillo, E., Anton, I., López-Sendino, P., Díaz, D., Vázquez-Luis, M., Duarte, C., Marbà, N., Aspillaga, E., Espinosa, F., Grech, D., Guala, I., Azzurro, E., Farina, S., Cristina Gambi, M., Chimienti, G., Montefalcone, M., Azzola, A., Mantas, T.P., Fraschetti, S., Ceccherelli, G., Kipson, S., Bakran-Petricioli, T., Petricioli, D., Jimenez, C., Katsanevakis, S., Kizilkaya, I.T., Kizilkaya, Z., Sartoretto, S., Elodie, R., Ruitton, S., Comeau, S., Gattuso, J.P., Harmelin, J.G., 2022. Marine heatwaves drive recurrent mass mortalities in the Mediterranean Sea. Glob. Chang. Biol. 28, 5708–5725. https://doi.org/10.1111/gcb.16301.

Gera, A., Pagès, J.F., Arthur, R., Farina, S., Roca, G., Romero, J., Alcoverro, T., 2014. The effect of a centenary storm on the long-lived seagrass *Posidonia oceanica*. Limnol. Oceanogr. 59, 1910–1918. https://doi.org/10.4319/lo.2014.59.6.1910.

Gissi, E., Manea, E., Mazaris, A.D., Fraschetti, S., Almpanidou, V., Bevilacqua, S., Coll, M., Guarnieri, G., Lloret-Lloret, E., Pascual, M., Petza, D., Rilov, G., Schonwald, M., Stelzenmüller, V., Katsanevakis, S., 2021. A review of the combined effects of climate change and other local human stressors on the marine environment. Sci. Total Environ. 755, 142564 https://doi.org/10.1016/j.scitotenv.2020.142564.

González-Orenga, S., Trif, C., Donat-Torres, M.P., Llinares, J.V., Collado, F., Ferrer-Gallego, P.P., Laguna, E., Boscaiu, M., Vicente, O., 2020. Responses to increased salinity and severe drought in the eastern Iberian endemic species *Thalictrum maritimum* (Ranunculaceae), threatened by climate change. Plants 9. https://doi.org/10.3390/plants9101251.

Gray, A.J., Mogg, R.J., 2001. Climate impacts on pioneer saltmarsh plants. Clim. Res. 18 (1–2), 105–112.

Griffiths, L.N., Mitsch, W.J., 2021. Estimating the effects of a hurricane on carbon storage in mangrove wetlands in Southwest Florida. Plants 10. https://doi.org/10.3390/plants10081749.

Guerrero-Meseguer, L., Marin, A., Sanz-Lazaro, C., 2017. Future heat waves due to climate change threaten the survival of *Posidonia oceanica* seedlings. Environ. Pollut. 230, 40–45. https://doi.org/10.1016/j.envpol.2017.06.039.

Hadjioannou, L., Jimenez, C., Rottier, C., Sfenthourakis, S., Ferrier-Pagès, C., 2019. Response of the temperate scleractinian coral *Cladocora caespitosa* to high temperature and long-term nutrient enrichment. Sci. Rep. 9, 1–11. https://doi.org/10.1038/s41598-019-50716-w.

Halpern, B.S., Frazier, M., Potapenko, J., Casey, K.S., Koenig, K., Longo, C., Lowndes, J. S., Rockwood, R.C., Selig, E.R., Selkoe, K.A., Walbridge, S., 2015. Spatial and temporal changes in cumulative human impacts on the world's ocean. Nat. Commun. 6, 7615. https://doi.org/10.1038/ncomms8615.

Hargrave, M.S., Foggo, A., Pessarrodona, A., Smale, D.A., 2017. The effects of warming on the ecophysiology of two co-existing kelp species with contrasting distributions. Oecologia 183, 531–543. https://doi.org/10.1007/s00442-016-3776-1.

Haugland, B.T., Armitage, C.S., Kutti, T., Husa, V., Skogen, M.D., Bekkby, T., Carvajalino-Fernández, M.A., Bannister, R.J., White, C.A., Norderhaug, K.M., Fredriksen, S., 2021. Large-scale salmon farming in Norway impacts the epiphytic community of Laminaria hyperborea. Aquac. Environ. Interact. 13, 81–100.

Hayden, H.L., Granek, E.F., 2015. Coastal sediment elevation change following anthropogenic mangrove clearing. Estuar. Coast. Shelf Sci. 165, 70–74. https://doi.org/10.1016/j.ecss.2015.09.004.

Hernán, G., Ortega, M.J., Gándara, A.M., Castejón, I., Terrados, J., Tomas, F., 2017. Future warmer seas: increased stress and susceptibility to grazing in seedlings of a marine habitat-forming species. Glob. Chang. Biol. 23, 4530–4543. https://doi.org/10.1111/gcb.13768.

Hernández-Delgado, E.A., Toledo-Hernández, C., Ruíz-Díaz, C.P., Gómez-Andújar, N., Medina-Muñiz, J.L., Canals-Silander, M.F., Suleimán-Ramos, S.E., 2020. Hurricane impacts and the resilience of the invasive sea vine, *Halophila stipulacea*: a case study from Puerto Rico. Estuar. Coasts 43, 1263–1283. https://doi.org/10.1007/s12237-019-00673-4.

Holling, C.S., 1973. Resilience and stability of ecological systems. Annu. Rev. Ecol. Syst. 4, 1–23. https://doi.org/10.1146/annurev.es.04.110173.000245.

Holmer, M., Bondgaard, E.J., 2001. Photosynthetic and growth response of eelgrass to low oxygen and high sulfide concentrations during hypoxic events. Aquat. Bot. 70, 29–38. https://doi.org/10.1016/S0304-3770(00)00142-X.

Houngnandan, F., Deter, J., Kefi, S., 2019. How anthropogenic pressures and environmental variables influence the spatial configuration of the seagrass *Posidonia oceanica* in France?. In: OCEANS 2019 - Marseille, pp. 1–7. https://doi.org/10.1109/OCEANSE.2019.8867163.

Howarth, J.F., Durako, M.J., 2013. Variation in pigment content of *Thalassia testudinum* seedlings in response to changes in salinity and light. Bot. Mar. 56, 261–273. https://doi.org/10.1515/bot-2012-0226.

Hughes, A.R., Cebrian, J., Heck, K., Goff, J., Hanley, T.C., Scheffel, W., Zerebecki, R.A., 2018. Effects of oil exposure, plant species composition, and plant genotypic diversity on salt marsh and mangrove assemblages. Ecosphere 9. https://doi.org/10.1002/ecs2.2207.

Imbert, D., 2018. Hurricane disturbance and forest dynamics in east Caribbean mangroves. Ecosphere 9. https://doi.org/10.1002/ecs2.2231.

IPCC, 2022. In: Pörtner, H.-O., Roberts, D.C., Tignor, M., Poloczanska, E.S., Mintenbeck, K., Alegría, A., Craig, M., Langsdorf, S., Löschke, S., Möller, V., Okem, A., Rama, B. (Eds.), Climate Change 2022: Impacts, Adaptation, and Vulnerability. Contribution of Working Group II to the Sixth Assessment Report of the Intergovernmental Panel on Climate Change. Cambridge University Press, Cambridge, UK and New York, NY, USA. https://doi.org/10.1017/9781009325844 (3056 pp.).

James, R.K., Lynch, A., Herman, P.M.J., van Katwijk, M.M., van Tussenbroek, B.I., Dijkstra, H.A., van Westen, R.M., van der Boog, C.G., Klees, R., Pietrzak, J.D., Slobbe, C., Bouma, T.J., 2021. Tropical biogeomorphic seagrass landscapes for coastal protection: persistence and wave attenuation during major storms events. Ecosystems 24, 301–318. https://doi.org/10.1007/s10021-020-00519-2.

Jevrejeva, S., Moore, J.C., Grinsted, A., 2012. Sea level projections to AD2500 with a new generation of climate change scenarios. Glob. Planet. Chang. 80-81, 14–20. https://doi.org/10.1016/j.gloplacha.2011.09.006.

Johnson, C.R., Koch, M.S., Pedersen, O., Madden, C.J., 2018. Hypersalinity as a trigger of seagrass (*Thalassia testudinum*) die-off events in Florida Bay: evidence based on shoot meristem O_2 and H_2S dynamics. J. Exp. Mar. Biol. Ecol. 504, 47–52. https://doi.org/10.1016/j.jembe.2018.03.007.

Jordà, G., Marbà, N., Duarte, C.M., 2012. Mediterranean seagrass vulnerable to regional climate warming. Nat. Clim. Chang. 2, 821–824. https://doi.org/10.1038/nclimate1533.

de Juan, S., Moranta, J., Hinz, H., Barberá, C., Ojeda-Martinez, C., Oro, D., Ordines, F., Ólafsson, E., Demestre, M., Massutí, E., Lleonart, J., 2012. A regional network of sustainable managed areas as the way forward for the implementation of an ecosystem-based fisheries management in the Mediterranean. Ocean Coast. Manag. 65, 51–58. https://doi.org/10.1016/j.ocecoaman.2012.04.024.

de Juan, S., Iacono, C.L., Demestre, M., 2013. Benthic habitat characterisation of soft-bottom continental shelves: integration of acoustic surveys, benthic samples and trawling disturbance intensity. Estuar. Coast. Shelf Sci. 117, 199–209.

de Juan, S., Hewitt, J., Subida, M.D., Thrush, S., 2018. Translating Ecological Integrity terms into operational language to inform societies. J. Environ. Manag. 228, 319–327. https://doi.org/10.1016/j.jenvman.2018.09.034.

Jueterbock, A., Franssen, S.U., Bergmann, N., Gu, J., Coyer, J.A., Reusch, T.B., Bornberg-Bauer, E., Olsen, J.L., 2016. Phylogeographic differentiation versus transcriptomic adaptation to warm temperatures in *Zostera marina*, a globally important seagrass. Mol. Ecol. 25, 5396–5411. https://doi.org/10.1111/mec.13829.

Juza, M., Tintoré, J., 2021. Multivariate sub-regional ocean indicators in the Mediterranean Sea: from event detection to climate change estimations. Front. Mar. Sci. 8 https://doi.org/10.3389/fmars.2021.610589.

Kaufman, M.L., Watkins, E., van Hooidonk, R., Baker, A.C., Lirman, D., 2021. Thermal history influences lesion recovery of the threatened Caribbean staghorn coral *Acropora cervicornis* under heat stress. Coral Reefs 40, 289–293. https://doi.org/10.1007/s00338-020-02025-2.

Kennedy, E.V., Perry, C.T., Halloran, P.R., Iglesias-Prieto, R., Schonberg, C.H., Wisshak, M., Form, A.U., Carricart-Ganivet, J.P., Fine, M., Eakin, C.M., Mumby, P.J., 2013. Avoiding coral reef functional collapse requires local and global action. Curr. Biol. 23, 912–918. https://doi.org/10.1016/j.cub.2013.04.020.

Kersting, D.K., Linares, C., 2012. Cladocora caespitosa bioconstructions in the Columbretes Islands Marine Reserve (Spain, NW Mediterranean): distribution, size structure and growth. Mar. Ecol. 33, 427–436. https://doi.org/10.1111/j.1439-0485.2011.00508.x.

Kersting, D.K., Linares, C., 2019. Living evidence of a fossil survival strategy raises hope for warming-affected corals. Sci. Adv. 5, eaax2950 https://doi.org/10.1126/sciadv.aax2950.

Kersting, D.K., Bensoussan, N., Linares, C., 2013. Long-term responses of the endemic reef-builder *Cladocora caespitosa* to Mediterranean warming. PLoS One 8, e70820. https://doi.org/10.1371/journal.pone.0070820.
Kersting, D.K., Ballesteros, E., De Caralt, S., Linares, C., 2014a. Invasive macrophytes in a marine reserve (Columbretes Islands, NW Mediterranean): spread dynamics and interactions with the endemic scleractinian coral Cladocora caespitosa. Biol. Invasions 16, 1599–1610.
Kersting, D.K., Teixidó, N., Linares, C., 2014b. Recruitment and mortality of the temperate coral *Cladocora caespitosa*: implications for the recovery of endangered populations. Coral Reefs 33, 403–407. https://doi.org/10.1007/s00338-014-1144-3.
Kersting, D.K., Cebrian, E., Casado, C., Teixidó, N., Garrabou, J., Linares, C., 2015. Experimental evidence of the synergistic effects of warming and invasive algae on a temperate reef-builder coral. Sci. Rep. 5, 18635 https://doi.org/10.1038/srep18635.
Klein, J., Verlaque, M., 2008. The Caulerpa racemosa invasion: a critical review. Mar. Pollut. Bull. 56 (2), 205–225.
Koch, M.S., Schopmeyer, S., Kyhn-Hansen, C., Madden, C.J., 2007a. Synergistic effects of high temperature and sulfide on tropical seagrass. J. Exp. Mar. Biol. Ecol. 341, 91–101. https://doi.org/10.1016/j.jembe.2006.10.004.
Koch, M.S., Schopmeyer, S.A., Holmer, M., Madden, C.J., Kyhn-Hansen, C., 2007b. *Thalassia testudinum* response to the interactive stressors hypersalinity, sulfide and hypoxia. Aquat. Bot. 87, 104–110. https://doi.org/10.1016/j.aquabot.2007.03.004.
Koch, M.S., Schopmeyer, S.A., Kyhn-Hansen, C., Madden, C.J., Peters, J.S., 2007c. Tropical seagrass species tolerance to hypersalinity stress. Aquat. Bot. 86, 14–24. https://doi.org/10.1016/j.aquabot.2006.08.003.
Koch, M.S., Coronado, C., Miller, M.W., Rudnick, D.T., Stabenau, E., Halley, R.B., Sklar, F.H., 2015. Climate change projected effects on coastal foundation communities of the Greater Everglades using a 2060 scenario: need for a new management paradigm. Environ. Manag. 55, 857–875. https://doi.org/10.1007/s00267-014-0375-y.
Krauss, K.W., Lovelock, C.E., McKee, K.L., López-Hoffman, L., Ewe, S.M.L., Sousa, W.P., 2008. Environmental drivers in mangrove establishment and early development: a review. Aquat. Bot. 89, 105–127. https://doi.org/10.1016/j.aquabot.2007.12.014.
Kružić, P., 2014. Bioconstructions in the Mediterranean: present and future. In: Goffredo, S., Dubinsky, Z. (Eds.), The Mediterranean Sea: Its History and Present Challenges. Springer Netherlands, Dordrecht, pp. 435–447. https://doi.org/10.1007/978-94-007-6704-1_25.
Kružić, P., Benković, L., 2008. Bioconstructional features of the coral Cladocora caespitosa (Anthozoa, Scleractinia) in the Adriatic Sea (Croatia). Mar. Ecol. 29, 125–139. https://doi.org/10.1111/j.1439-0485.2008.00220.x.
Ladd, C.J.T., Duggan-Edwards, M.F., Bouma, T.J., Pagès, J.F., Skov, M.W., 2019. Sediment supply explains long-term and large-scale patterns in salt marsh lateral expansion and erosion. Geophys. Res. Lett. 46, 11178–11187. https://doi.org/10.1029/2019GL083315.
Ladd, C.J.T., Duggan-Edwards, M.F., Pagès, J.F., Skov, M.W., 2021. Saltmarsh resilience to periodic shifts in tidal channels. Front. Mar. Sci. 8 https://doi.org/10.3389/fmars.2021.757715.
LaJeunesse, T.C., Smith, R.T., Finney, J., Oxenford, H., 2009. Outbreak and persistence of opportunistic symbiotic dinoflagellates during the 2005 Caribbean mass coral 'bleaching' event. Proc. Biol. Sci. 276, 4139–4148. https://doi.org/10.1098/rspb.2009.1405.
Lamb, J.B., van de Water, J.A.J.M., Bourne, D.G., Altier, C., Hein, M.Y., Fiorenza, E.A., Abu, N., Jompa, J., Harvell, C.D., 2017. Seagrass ecosystems reduce exposure to bacterial pathogens of humans, fishes, and invertebrates. Science 355, 731–733. https://doi.org/10.1126/science.aal1956.
Langdon, C., Albright, R., Baker, A.C., Jones, P., 2018. Two threatened Caribbean coral species have contrasting responses to combined temperature and acidification stress. Limnol. Oceanogr. 63, 2450–2464. https://doi.org/10.1002/lno.10952.
Lapointe, B.E., 1997. Nutrient thresholds for bottom-up control of macroalgal blooms on coral reefs in Jamaica and southeast Florida: the ecology and oceanography of harmful algal blooms. Limnol. Oceanogr. 42, 1119–1131. https://doi.org/10.4319/lo.1997.42.5_part_2.1119.
Legrand, E., Riera, P., Lutier, M., Coudret, J., Grall, J., Martin, S., 2017. Species interactions can shift the response of a maerl bed community to ocean acidification and warming. Biogeosciences 14, 5359–5376. https://doi.org/10.5194/bg-14-5359-2017.
Levine, J.M., D'Antonio, C.M., 1999. Elton revisited: a review of evidence linking diversity and invasibility. Oikos 87, 15–26. https://doi.org/10.2307/3546992.
Liesner, D., Fouqueau, L., Valero, M., Roleda, M.Y., Pearson, G.A., Bischof, K., Valentin, K., Bartsch, I., 2020. Heat stress responses and population genetics of the kelp Laminaria digitata (Phaeophyceae) across latitudes reveal differentiation among North Atlantic populations. Ecol. Evol. 10 (17), 9144–9177.
Linares, C., Vidal, M., Canals, M., Kersting, D.K., Amblas, D., Aspillaga, E., Cebrian, E., Delgado-Huertas, A., Diaz, D., Garrabou, J., Hereu, B., Navarro, L., Teixido, N., Ballesteros, E., 2015. Persistent natural acidification drives major distribution shifts in marine benthic ecosystems. Proc. Biol. Sci. 282, 20150587 https://doi.org/10.1098/rspb.2015.0587.
Lincoln, S., Andrews, B., Birchenough, S.N., Chowdhury, P., Engelhard, G.H., Harrod, O., Pinnegar, J.K., Townhill, B.L., 2022. Marine litter and climate change: inextricably connected threats to the world's oceans. Sci. Total Environ. 837, 155709.
Liquete, C., Piroddi, C., Drakou, E.G., Gurney, L., Katsanevakis, S., Charef, A., Egoh, B., 2013. Current status and future prospects for the assessment of marine and coastal ecosystem services: a systematic review. PLoS One 8, e67737. https://doi.org/10.1371/journal.pone.0067737.
Manzello, D.P., Berkelmans, R., Hendee, J.C., 2007a. Coral bleaching indices and thresholds for the Florida Reef Tract, Bahamas, and St. Croix, US Virgin Islands. Mar. Pollut. Bull. 54, 1923–1931. https://doi.org/10.1016/j.marpolbul.2007.08.009.
Manzello, D.P., Brandt, M., Smith, T.B., Lirman, D., Hendee, J.C., Nemeth, R.S., 2007b. Hurricanes benefit bleached corals. Proc. Natl. Acad. Sci. U. S. A. 104, 12035–12039. https://doi.org/10.1073/pnas.0701194104.
del Mar Delgado-Serrano, M., Mistry, J., Matzdorf, B., Leclerc, G., 2017. Community-based management of environmental challenges in Latin America and the Caribbean. Ecol. Soc. 22 https://doi.org/10.5751/ES-08924-220104.
Marbà, N., Duarte, C.M., 2009. Mediterranean warming triggers seagrass (*Posidonia oceanica*) shoot mortality. Glob. Chang. Biol. 16, 2366–2375. https://doi.org/10.1111/j.1365-2486.2009.02130.x.
Marbà, N., Jordà, G., Agustí, S., Girard, C., Duarte, C.M., 2015. Footprints of climate change on Mediterranean Sea biota. Front. Mar. Sci. 2, 1–11. https://doi.org/10.3389/fmars.2015.00056.
Marín-Guirao, L., Ruiz, J.M., Sandoval-Gil, J.M., Bernardeau-Esteller, J., Stinco, C.M., Meléndez-Martínez, A., 2013. Xanthophyll cycle-related photoprotective mechanism in the Mediterranean seagrasses *Posidonia oceanica* and *Cymodocea nodosa* under normal and stressful hypersaline conditions. Aquat. Bot. 109, 14–24. https://doi.org/10.1016/j.aquabot.2013.03.006.
Marín-Guirao, L., Ruiz, J.M., Dattolo, E., Garcia-Munoz, R., Procaccini, G., 2016. Physiological and molecular evidence of differential short-term heat tolerance in Mediterranean seagrasses. Sci. Rep. 6, 28615 https://doi.org/10.1038/srep28615.
Marín-Guirao, L., Entrambasaguas, L., Dattolo, E., Ruiz, J.M., Procaccini, G., 2017a. Molecular mechanisms behind the physiological resistance to intense transient warming in an iconic marine plant. Front. Plant Sci. 8, 1142. https://doi.org/10.3389/fpls.2017.01142.
Marín-Guirao, L., Sandoval-Gil, J.M., García-Muñoz, R., Ruiz, J.M., 2017b. The stenohaline seagrass *Posidonia oceanica* can persist in natural environments under fluctuating hypersaline conditions. Estuar. Coasts 40, 1688–1704. https://doi.org/10.1007/s12237-017-0242-1.
Marín-Guirao, L., Bernardeau-Esteller, J., Garcia-Munoz, R., Ramos, A., Ontoria, Y., Romero, J., Perez, M., Ruiz, J.M., Procaccini, G., 2018. Carbon economy of Mediterranean seagrasses in response to thermal stress. Mar. Pollut. Bull. 135, 617–629. https://doi.org/10.1016/j.marpolbul.2018.07.050.
Marín-Guirao, L., Entrambasaguas, L., Ruiz, J.M., Procaccini, G., 2019. Heat-stress induced flowering can be a potential adaptive response to ocean warming for the iconic seagrass Posidonia oceanica. Mol. Ecol. 28 (10), 2486–2501.
Martinez, A., Crook, E.D., Barshis, D.J., Potts, D.C., Rebolledo-Vieyra, M., Hernandez, L., Paytan, A., 2019. Species-specific calcification response of Caribbean corals after 2-year transplantation to a low aragonite saturation submarine spring. Proc. Biol. Sci. 286, 20190572 https://doi.org/10.1098/rspb.2019.0572.
Martins, N., Tanttu, H., Pearson, G.A., Serrão, E.A., Bartsch, I., 2017. Interactions of daylength, temperature and nutrients affect thresholds for life stage transitions in the kelp *Laminaria digitata* (Phaeophyceae). Bot. Mar. 60 https://doi.org/10.1515/bot-2016-0094.
Martins, N., Pearson, G.A., Bernard, J., Serrao, E.A., Bartsch, I., 2020. Thermal traits for reproduction and recruitment differ between Arctic and Atlantic kelp Laminaria digitata. PLoS One 15 (6), e0235388.
Mateos-Naranjo, E., López-Jurado, J., Mesa-Marín, J., Luque, C.J., Castellanos, E.M., Pérez-Romero, J.A., Redondo-Gómez, S., 2021. Understanding the impact of a complex environmental matrix associated with climate change on the European marshes engineer species Spartina martima. Environ. Exp. Bot. 182, 104304.
McCook, L., Jompa, J., Diaz-Pulido, G., 2001. Competition between corals and algae on coral reefs: a review of evidence and mechanisms. Coral Reefs 19, 400–417.
McHenry, J., Rassweiler, A., Hernan, G., Uejio, C.K., Pau, S., Dubel, A.K., Lester, S.E., Grech, A., 2021. Modelling the biodiversity enhancement value of seagrass beds. Divers. Distrib. 27, 2036–2049. https://doi.org/10.1111/ddi.13379.
McKee, K.L., 2011. Biophysical controls on accretion and elevation change in Caribbean mangrove ecosystems. Estuar. Coast. Shelf Sci. 91 (4), 475–483.
McKee, K.L., Rooth, J.E., 2008. Where temperate meets tropical: multi-factorial effects of elevated CO2, nitrogen enrichment, and competition on a mangrove-salt marsh community. Glob. Chang. Biol. 14 (5), 971–984.
McKee, K., Rogers, K., Saintilan, N., 2012. Response of salt marsh and mangrove wetlands to changes in atmospheric CO2, climate, and sea level. In: Global Change and the Function and Distribution of Wetlands. Springer Netherlands, Dordrecht, pp. 63–96.
MedECC, 2020. Climate and environmental change in the Mediterranean Basin – current situation and risks for the future. In: Cramer, W., Guiot, J., Marini, K. (Eds.), First Mediterranean Assessment Report. Union for the Mediterranean, Plan Bleu, UNEP/MAP, Marseille, France, pp. 1–632. https://doi.org/10.5281/zenodo.4768833.
Mesa-Marín, J., Pérez-Romero, J.A., Mateos-Naranjo, E., Bernabeu-Meana, M., Pajuelo, E., Rodríguez-Llorente, I.D., Redondo-Gómez, S., 2019. Effect of plant growth-promoting Rhizobacteria on Salicornia ramosissima seed germination under salinity, CO2 and temperature stress. Agronomy 9 (10), 655.
Micheli, F., Halpern, B.S., Walbridge, S., Ciriaco, S., Ferretti, F., Fraschetti, S., Lewison, R., Nykjaer, L., Rosenberg, A.A., 2013. Cumulative human impacts on Mediterranean and Black Sea marine ecosystems: assessing current pressures and opportunities. PLoS One 8, e79889. https://doi.org/10.1371/journal.pone.0079889.
Moreno-Marín, F., Brun, F.G., Pedersen, M.F., 2018. Additive response to multiple environmental stressors in the seagrass *Zostera marina* L. Limnol. Oceanogr. 63, 1528–1544. https://doi.org/10.1002/lno.10789.
Mota, C.F., Engelen, A.H., Serrao, E.A., Coelho, M.A.G., Marba, N., Krause-Jensen, D., Pearson, G.A., 2018. Differentiation in fitness-related traits in response to elevated temperatures between leading and trailing edge populations of marine macrophytes. PLoS One 13, e0203666. https://doi.org/10.1371/journal.pone.0203666.
Movilla, J., Calvo, E., Pelejero, C., Coma, R., Serrano, E., Fernández-Vallejo, P., Ribes, M., 2012. Calcification reduction and recovery in native and non-native Mediterranean

corals in response to ocean acidification. J. Exp. Mar. Biol. Ecol. 438, 144–153. https://doi.org/10.1016/j.jembe.2012.09.014.
Moy, F.E., Christie, H., 2012. Large-scale shift from sugar kelp (*Saccharina latissima*) to ephemeral algae along the south and west coast of Norway. Mar. Biol. Res. 8, 309–321. https://doi.org/10.1080/17451000.2011.637561.
Müller, R., Desel, C., Steinhoff, F.S., Wiencke, C., Bischof, K., 2012. UV-radiation and elevated temperatures induce formation of reactive oxygen species in gametophytes of cold-temperate/Arctic kelps (Laminariales, Phaeophyceae). Phycol. Res. 60, 27–36. https://doi.org/10.1111/j.1440-1835.2011.00630.x.
Mumby, P.J., Steneck, R.S., Hastings, A., 2013. Evidence for and against the existence of alternate attractors on coral reefs. Oikos 122, 481–491. https://doi.org/10.1111/j.1600-0706.2012.00262.x.
Mumby, P.J., Wolff, N.H., Bozec, Y.-M., Chollett, I., Halloran, P., 2014. Operationalizing the resilience of coral reefs in an era of climate change. Conserv. Lett. 7, 176–187. https://doi.org/10.1111/conl.12047.
Neal, B.P., Khen, A., Treibitz, T., Beijbom, O., O'Connor, G., Coffroth, M.A., Knowlton, N., Kriegman, D., Mitchell, B.G., Kline, D.I., 2017. Caribbean massive corals not recovering from repeated thermal stress events during 2005-2013. Ecol. Evol. 7, 1339–1353. https://doi.org/10.1002/ece3.2706.
Nepper-Davidsen, J., Andersen, D.T., Pedersen, M.F., 2019. Exposure to simulated heatwave scenarios causes long-term reductions in performance in *Saccharina latissima*. Mar. Ecol. Prog. Ser. 630, 25–39. https://doi.org/10.3354/meps13133.
Nguyen, H.M., Bulleri, F., Marín-Guirao, L., Pernice, M., Procaccini, G., 2021. Photo-physiology and morphology reveal divergent warming responses in northern and southern hemisphere seagrasses. Mar. Biol. 168 https://doi.org/10.1007/s00227-021-03940-w.
Norderhaug, K.M., Filbee-Dexter, K., Freitas, C., Birkely, S.R., Christensen, L., Mellerud, I., Thormar, J., van Son, T., Moy, F., Vázquez Alonso, M., Steen, H., 2020. Ecosystem-level effects of large-scale disturbance in kelp forests. Mar. Ecol. Prog. Ser. 656, 163–180. https://doi.org/10.3354/meps13426.
O'Brien, J.M., Scheibling, R.E., 2018. Low recruitment, high tissue loss, and juvenile mortality limit recovery of kelp following large-scale defoliation. Mar. Biol. 165 https://doi.org/10.1007/s00227-018-3423-y.
Olischläger, M., Wiencke, C., 2013. Seasonal fertility and combined effects of temperature and UV-radiation on *Alaria esculenta* and *Laminaria digitata* (Phaeophyceae) from Spitsbergen. Polar Biol. 36, 1019–1029. https://doi.org/10.1007/s00300-013-1325-5.
Olsen, Y.S., Sánchez-Camacho, M., Marbà, N., Duarte, C.M., 2012. Mediterranean seagrass growth and demography responses to experimental warming. Estuar. Coasts 35, 1205–1213. https://doi.org/10.1007/s12237-012-9521-z.
Orth, R.J., Carruthers, T.J.B., Dennison, W.C., Duarte, C.M., Fourqurean, J.W., Heck, K. L., Hughes, A.R., Kendrick, G.A., Kenworthy, W.J., Olyarnik, S., Short, F.T., Waycott, M., Williams, S.L., 2006. A global crisis for seagrass ecosystems. BioScience 56, 987–996. https://doi.org/10.1641/0006-3568(2006)56[987:AGCFSE]2.0.CO;2.
Ortiz, J.C., Gonzalez-Rivero, M., Mumby, P.J., 2013. Can a thermally tolerant symbiont improve the future of Caribbean coral reefs? Glob. Chang. Biol. 19, 273–281. https://doi.org/10.1111/gcb.12027.
Osland, M.J., Feher, L.C., Griffith, K.T., Cavanaugh, K.C., Enwright, N.M., Day, R.H., Stagg, C.L., Krauss, K.W., Howard, R.J., Grace, J.B., Rogers, K., 2017. Climatic controls on the global distribution, abundance, and species richness of mangrove forests. Ecol. Monogr. 87, 341–359. https://doi.org/10.1002/ecm.1248.
Otaño-Cruz, A., Montañez-Acuña, A.A., García-Rodríguez, N.M., Díaz-Morales, D.M., Benson, E., Cuevas, E., Ortiz-Zayas, J., Hernández-Delgado, E.A., 2019. Caribbean near-shore coral reef benthic community response to changes on sedimentation dynamics and environmental conditions. Front. Mar. Sci. 6 https://doi.org/10.3389/fmars.2019.00551.
Öztürk, B., 2021. Non-indigenous Species in the Mediterranean and the Black Sea. Food and Agriculture Organization of the United Nations, Rome.
Pandolfi, J.M., Jackson, J.B., 2006. Ecological persistence interrupted in Caribbean coral reefs. Ecol. Lett. 9, 818–826. https://doi.org/10.1111/j.1461-0248.2006.00933.x.
Papaki, D., Kokkos, N., Sylaios, G., 2020. A fuzzy inference system for seagrass distribution modeling in the Mediterranean sea: a first approach. Water 12. https://doi.org/10.3390/w12102949.
Pazzaglia, J., Santillán-Sarmiento, A., Helber, S.B., Ruocco, M., Terlizzi, A., Marín-Guirao, L., Procaccini, G., 2020. Does warming enhance the effects of eutrophication in the seagrass Posidonia oceanica? Front. Mar. Sci. 7, 564805.
Pedersen, O., Binzer, T., Borum, J., 2004. Sulphide intrusion in eelgrass (*Zostera marina* L.). Plant Cell Environ. 27, 595–602. https://doi.org/10.1111/j.1365-3040.2004.01173.x.
Pereira, T.R., Engelen, A.H., Pearson, G.A., Valero, M., Serrão, E.A., 2015. Response of kelps from different latitudes to consecutive heat shock. J. Exp. Mar. Biol. Ecol. 463, 57–62. https://doi.org/10.1016/j.jembe.2014.10.022.
Pergent, G., Pergent-Martini, C., Bein, A., Dedeken, M., Oberti, P., Orsini, A., Santucci, J. F., Short, F., 2015. Dynamic of *Posidonia oceanica* seagrass meadows in the northwestern Mediterranean: could climate change be to blame? C. R. Biol. 338, 484–493. https://doi.org/10.1016/j.crvi.2015.04.011.
Pessarrodona, A., Filbee-Dexter, K., Alcoverro, T., Boada, J., Feehan, C.J., Fredriksen, S., Grace, S.P., Nakamura, Y., Narvaez, C.A., Norderhaug, K.M., Wernberg, T., 2021. Homogenization and miniaturization of habitat structure in temperate marine forests. Glob. Chang. Biol. 27, 5262–5275. https://doi.org/10.1111/gcb.15759.
Peteiro, C., Sánchez, N., Martínez, B., 2016. Mariculture of the Asian kelp *Undaria pinnatifida* and the native kelp *Saccharina latissima* along the Atlantic coast of Southern Europe: an overview. Algal Res. 15, 9–23. https://doi.org/10.1016/j.algal.2016.01.012.
Pinsky, M.L., Eikeset, A.M., McCauley, D.J., Payne, J.L., Sunday, J.M., 2019. Greater vulnerability to warming of marine versus terrestrial ectotherms. Nature 569, 108–111. https://doi.org/10.1038/s41586-019-1132-4.
Poloczanska, E.S., Burrows, M.T., Brown, C.J., Molinos, J.G., Halpern, B.S., Hoegh-Guldberg, O., Kappel, C.V., Moore, P.J., Richardson, A.J., Schoeman, D.S., Sydeman, W.J., 2016. Responses of marine organisms to climate change across oceans. Front. Mar. Sci. 3 https://doi.org/10.3389/fmars.2016.00062.
Przeslawski, R., Ahyong, S., Byrne, M., Wörheide, G., Hutchings, P.A.T., 2008. Beyond corals and fish: the effects of climate change on noncoral benthic invertebrates of tropical reefs. Glob. Chang. Biol. 14, 2773–2795. https://doi.org/10.1111/j.1365-2486.2008.01693.x.
Qui-Minet, Z.N., Coudret, J., Davoult, D., Grall, J., Mendez-Sandin, M., Cariou, T., Martin, S., 2019. Combined effects of global climate change and nutrient enrichment on the physiology of three temperate maerl species. Ecol. Evol. 9, 13787–13807.
Randall, C.J., Szmant, A.M., 2009. Elevated temperature reduces survivorship and settlement of the larvae of the Caribbean scleractinian coral, *Favia fragum* (Esper). Coral Reefs 28, 537–545. https://doi.org/10.1007/s00338-009-0482-z.
Randall, C.J., van Woesik, R., 2015. Contemporary white-band disease in Caribbean corals driven by climate change. Nat. Clim. Chang. 5, 375–379. https://doi.org/10.1038/nclimate2530.
Randazzo-Eisemann, Á., Garza-Pérez, J.R., Figueroa-Zavala, B., 2022. The role of coral diseases in the flattening of a Caribbean Coral Reef over 23 years. Mar. Pollut. Bull. 181, 113855.
Reents, S., Mueller, P., Tang, H., Jensen, K., Nolte, S., 2021. Plant genotype determines biomass response to flooding frequency in tidal wetlands. Biogeosciences 18 (2), 403–411.
Richards, J.A., Mokrech, M., Berry, P.M., Nicholls, R.J., 2008. Regional assessment of climate change impacts on coastal and fluvial ecosystems and the scope for adaptation. Clim. Chang. 90, 141–167. https://doi.org/10.1007/s10584-008-9451-8.
Roberts, C.M., O'Leary, B.C., McCauley, D.J., Cury, P.M., Duarte, C.M., Lubchenco, J., Pauly, D., Sáenz-Arroyo, A., Sumaila, U.R., Wilson, R.W., Worm, B., Castilla, J.C., 2017. Marine reserves can mitigate and promote adaptation to climate change. Proc. Natl. Acad. Sci. U. S. A. 114, 6167–6175. https://doi.org/10.1073/pnas.1701262114.
Rodolfo-Metalpa, R., Martin, S., Ferrier-Pagès, C., Gattuso, J.-P., 2009. Response of the temperate coral *Cladocora caespitosa* to mid-and long-term exposure to pCO_2 and temperature levels projected in 2100. Biogeosci. Discuss. 6 https://doi.org/10.5194/bg-7-289-2010.
Ross, C., Ritson-Williams, R., Olsen, K., Paul, V.J., 2013. Short-term and latent post-settlement effects associated with elevated temperature and oxidative stress on larvae from the coral *Porites astreoides*. Coral Reefs 32, 71–79. https://doi.org/10.1007/s00338-012-0956-2.
Ross, C., Fogarty, N.D., Ritson-Williams, R., Paul, V.J., 2017. Interspecific variation in coral settlement and fertilization success in response to hydrogen peroxide exposure. Biol. Bull. 233, 206–218. https://doi.org/10.1086/696215.
Ruiz, J.M., Marín-Guirao, L., Sandoval-Gil, J.M., 2009. Responses of the Mediterranean seagrass *Posidonia oceanica* to in situ simulated salinity increase. Bot. Mar. 52, 459–470. https://doi.org/10.1515/bot.2009.051.
Ruiz, J.M., Marin-Guirao, L., Garcia-Munoz, R., Ramos-Segura, A., Bernardeau-Esteller, J., Perez, M., Sanmarti, N., Ontoria, Y., Romero, J., Arthur, R., Alcoverro, T., Procaccini, G., 2018. Experimental evidence of warming-induced flowering in the Mediterranean seagrass *Posidonia oceanica*. Mar. Pollut. Bull. 134, 49–54. https://doi.org/10.1016/j.marpolbul.2017.10.037.
Rull, V., 2022. Responses of Caribbean mangroves to quaternary climatic, eustatic, and anthropogenic drivers of ecological change: a review. Plants 11, 3502. https://doi.org/10.3390/plants11243502.
Ruocco, M., De Luca, P., Marín-Guirao, L., Procaccini, G., 2019. Differential leaf age-dependent thermal plasticity in the keystone seagrass Posidonia oceanica. Front. Plant Sci. 10, 1556.
Salo, T., Pedersen, M.F., 2014. Synergistic effects of altered salinity and temperature on estuarine eelgrass (*Zostera marina*) seedlings and clonal shoots. J. Exp. Mar. Biol. Ecol. 457, 143–150. https://doi.org/10.1016/j.jembe.2014.04.008.
Scheffer, M., Barrett, S., Carpenter, S.R., Folke, C., Green, A.J., Holmgren, M., Hughes, T. P., Kosten, S., Leemput, I.A.v.d., Nepstad, D.C., Nes, E.H.v., Peeters, E., Walker, B., 2015. Creating a safe operating space for iconic ecosystems. Science 347, 1317–1319. https://doi.org/10.1126/science.aaa3769.
Serrano, X.M., Miller, M.W., Hendee, J.C., Jensen, B.A., Gapayao, J.Z., Pasparakis, C., Grosell, M., Baker, A.C., 2018. Effects of thermal stress and nitrate enrichment on the larval performance of two Caribbean reef corals. Coral Reefs 37, 173–182. https://doi.org/10.1007/s00338-017-1645-y.
Simeoni, C., Furlan, E., Pham, H.V., Critto, A., de Juan, S., Trégarot, E., Cornet, C.C., Meesters, E., Fonseca, C., Botelho, A.Z., Krause, T., N'Guetta, A., Cordova, F.E., Failler, P., Marcomini, A., 2023. Evaluating the combined effect of climate and anthropogenic stressors on marine coastal ecosystems: insights from a systematic review of cumulative impact assessment approaches. Sci. Total Environ. 861, 160687 https://doi.org/10.1016/j.scitotenv.2022.160687.
Simon-Nutbrown, C., Hollingsworth, P.M., Fernandes, T.F., Kamphausen, L., Baxter, J. M., Burdett, H.L., 2020. Species distribution modeling predicts significant declines in coralline algae populations under projected climate change with implications for conservation policy. Front. Mar. Sci. 7, 575825.
Smith, T.B., Brandt, M.E., Calnan, J.M., Nemeth, R.S., Blondeau, J., Kadison, E., Taylor, M., Rothenberger, P., 2013. Convergent mortality responses of Caribbean coral species to seawater warming. Ecosphere 4. https://doi.org/10.1890/es13-00107.1.

Smith, T.B., Gyory, J., Brandt, M.E., Miller, W.J., Jossart, J., Nemeth, R.S., 2016. Caribbean mesophotic coral ecosystems are unlikely climate change refugia. Glob. Chang. Biol. 22, 2756–2765. https://doi.org/10.1111/gcb.13175.

Snedaker, S.C., Brown, M.S., Lahmann, E.J., Rafael, J.A., 1992. Recovery of a mixed-species mangrove forest in South Florida following canopy removal. J. Coast. Res. 8, 919–925.

Sordo, L., Santos, R., Barrote, I., Silva, J., 2018. High CO_2 decreases the long-term resilience of the free-living coralline algae *Phymatolithon lusitanicum*. Ecol. Evol. 8, 4781–4792. https://doi.org/10.1002/ece3.4020.

Spalding, M.D., Ruffo, S., Lacambra, C., Meliane, I., Hale, L.Z., Shepard, C.C., Beck, M. W., 2014. The role of ecosystems in coastal protection: adapting to climate change and coastal hazards. Ocean Coast. Manag. 90, 50–57. https://doi.org/10.1016/j.ocecoaman.2013.09.007.

Steneck, R.S., Arnold, S.N., Boenish, R., de León, R., Mumby, P.J., Rasher, D.B., Wilson, M.W., 2019. Managing recovery resilience in coral reefs against climate-induced bleaching and hurricanes: a 15 year case study from Bonaire, Dutch Caribbean. Front. Mar. Sci. 6 https://doi.org/10.3389/fmars.2019.00265.

Stewart, H.A., Kline, D.I., Chapman, L.J., Altieri, A.H., 2021. Caribbean mangrove forests act as coral refugia by reducing light stress and increasing coral richness. Ecosphere 12, e03413. https://doi.org/10.1002/ecs2.3413.

Strain, E.M.A., van Belzen, J., Comandini, P., Wong, J., Bouma, T.J., Airoldi, L., Hughes, A.R., 2017. The role of changing climate in driving the shift from perennial grasses to annual succulents in a Mediterranean saltmarsh. J. Ecol. 105, 1374–1385. https://doi.org/10.1111/1365-2745.12799.

Szymansky, C.M., Muscolo, A., Yeo, M., Colville, L., Clatworthy, I., Salge, T., Seal, C.E., 2021. Elemental localisation and a reduced glutathione redox state protect seeds of the halophyte Suaeda maritima from salinity during over-wintering and germination. Environ. Exp. Bot. 190, 104569.

Teagle, H., Smale, D.A., Schoeman, D., 2018. Climate-driven substitution of habitat-forming species leads to reduced biodiversity within a temperate marine community. Divers. Distrib. 24, 1367–1380. https://doi.org/10.1111/ddi.12775.

Torn, K., Peterson, A., Herkül, K., 2020. Predicting the impact of climate change on the distribution of the key habitat-forming species in the NE Baltic Sea. J. Coast. Res. 95 https://doi.org/10.2112/si95-035.1.

Towle, E.K., Enochs, I.C., Langdon, C., 2015. Threatened Caribbean coral is able to mitigate the adverse effects of ocean acidification on calcification by increasing feeding rate. PLoS One 10, e0123394. https://doi.org/10.1371/journal.pone.0123394.

Traboni, C., Mammola, S.D., Ruocco, M., Ontoria, Y., Ruiz, J.M., Procaccini, G., Marin-Guirao, L., 2018. Investigating cellular stress response to heat stress in the seagrass *Posidonia oceanica* in a global change scenario. Mar. Environ. Res. 141, 12–23. https://doi.org/10.1016/j.marenvres.2018.07.007.

Tutar, O., Marin-Guirao, L., Ruiz, J.M., Procaccini, G., 2017. Antioxidant response to heat stress in seagrasses. A gene expression study. Mar. Environ. Res. 132, 94–102. https://doi.org/10.1016/j.marenvres.2017.10.011.

Tuya, F., Schubert, N., Aguirre, J., Basso, D., Bastos, E.O., Berchez, F., Bernardino, A.F., Bosch, N.E., Burdett, H.L., Espino, F., Fernández-Gárcia, C., 2023. Levelling-up rhodolith-bed science to address global-scale conservation challenges. Sci. Total Environ., 164818 https://doi.org/10.1016/j.scitotenv.2023.164818.

Vermeer, M., Rahmstorf, S., 2009. Global sea level linked to global temperature. Proc. Natl. Acad. Sci. U. S. A. 106, 21527–21532. https://doi.org/10.1073/pnas.0907765106.

Villazán, B., Salo, T., Brun, F.G., Vergara, J.J., Pedersen, M.F., 2015. High ammonium availability amplifies the adverse effect of low salinity on eelgrass *Zostera marina*. Mar. Ecol. Prog. Ser. 536, 149–162. https://doi.org/10.3354/meps11435.

Walcker, R., Laplanche, C., Herteman, M., Lambs, L., Fromard, F., 2019. Damages caused by hurricane Irma in the human-degraded mangroves of Saint Martin (Caribbean). Sci. Rep. 9, 18971 https://doi.org/10.1038/s41598-019-55393-3.

Wegner, C.E., Ellis, J.T., 2017. The influence of sea-level rise on wave-energy dissipation and wave-driven currents at Buck Island Reef National Monument. J. Coast. Res. 331, 56–66. https://doi.org/10.2112/JCOASTRES-D-15-00052.1.

Wernberg, T., Smale, D.A., Tuya, F., Thomsen, M.S., Langlois, T.J., De Bettignies, T., Bennett, S., Rousseaux, C.S., 2013. An extreme climatic event alters marine ecosystem structure in a global biodiversity hotspot. Nat. Clim. Chang. 3, 78–82. https://doi.org/10.1038/nclimate1627.

Winters, G., Nelle, P., Fricke, B., Rauch, G., Reusch, T.B.H., 2011. Effects of a simulated heat wave on photophysiology and gene expression of high- and low-latitude populations of *Zostera marina*. Mar. Ecol. Prog. Ser. 435, 83–95. https://doi.org/10.3354/meps09213.

Winters, G., Beer, S., Willette, D.A., Viana, I.G., Chiquillo, K.L., Beca-Carretero, P., Villamayor, B., Azcárate-García, T., Shem-Tov, R., Mwabvu, B., Migliore, L., Rotini, A., Oscar, M.A., Belmaker, J., Gamliel, I., Alexandre, A., Engelen, A.H., Procaccini, G., Rilov, G., 2020. The tropical seagrass *Halophila stipulacea*: reviewing what we know from its native and invasive habitats, alongside identifying knowledge gaps. Front. Mar. Sci. 7 https://doi.org/10.3389/fmars.2020.00300.

Wong, J.X., Van Colen, C., Airoldi, L., 2015. Nutrient levels modify saltmarsh responses to increased inundation in different soil types. Mar. Environ. Res. 104, 37–46.

Xie, D., Schwarz, C., Brückner, M.Z.M., Kleinhans, M.G., Urrego, D.H., Zhou, Z., van Maanen, B., 2020. Mangrove diversity loss under sea-level rise triggered by bio-morphodynamic feedbacks and anthropogenic pressures. Environ. Res. Lett. 15 https://doi.org/10.1088/1748-9326/abc122.

Yates, K.K., Zawada, D.G., Smiley, N.A., Tiling-Range, G., 2017. Divergence of seafloor elevation and sea level rise in coral reef ecosystems. Biogeosciences 14, 1739–1772. https://doi.org/10.5194/bg-14-1739-2017.

Yoshikai, M., Nakamura, T., Suwa, R., Sharma, S., Rollon, R., Yasuoka, J., Egawa, R., Nadaoka, K., 2022. Predicting mangrove forest dynamics across a soil salinity gradient using an individual-based vegetation model linked with plant hydraulics. Biogeosciences 19, 1813–1832. https://doi.org/10.5194/bg-19-1813-2022.

Zacher, K., Bernard, M., Bartsch, I., Wiencke, C., 2016. Survival of early life history stages of Arctic kelps (Kongsfjorden, Svalbard) under multifactorial global change scenarios. Polar Biol. 39, 2009–2020. https://doi.org/10.1007/s00300-016-1906-1.

van Zee, R., 2022. The Role of Creeks for Tidal Exchange in the Mangrove Forest of Lac Bay, Bonaire. University of Twente (Master's thesis).

Zenetos, A., Gofas, S., Verlaque, M., Cinar, M.E., Garcia Raso, J.E., Bianchi, C.N., Morri, C., Azzurro, E., Bilecenoglu, M., Froglia, C., Siokou, I., Violanti, D., Sfriso, A., San Martin, G., Giangrande, A., Katagan, T., Ballesteros, E., Ramos-Espla, A.A., Mastrototaro, F., Ocana, O., Zingone, A., Gambi, M.C., Streftaris, N., 2010. Alien species in the Mediterranean Sea by 2010. A contribution to the application of European Union's Marine Strategy Framework Directive (MSFD). Part I. Spatial distribution. Mediterr. Mar. Sci. 11, 381–493. https://doi.org/10.12681/mms.87.

Zenetos, A., Gofas, S., Morri, C., Rosso, A., Violanti, D., Garcia Raso, J.E., Cinar, M.E., Almogi-Labin, A., Ates, A.S., Azzurro, E., Ballesteros, E., Bianchi, C.N., Bilecenoglu, M., Gambi, M.C., Giangrande, A., Gravili, C., Hyams-Kaphzan, O., Karachle, P.K., Katsanevakis, S., Lipej, L., Mastrototaro, F., Mineur, F., Pancucci-Papadopoulou, M.A., Ramos Espla, A., Salas, C., San Martin, G., Sfriso, A., Streftaris, N., Verlaque, M., 2012. Alien species in the Mediterranean Sea by 2012. A contribution to the application of European Union's Marine Strategy Framework Directive (MSFD). Part 2. Introduction trends and pathways. Mediterr. Mar. Sci. 13, 328–352. https://doi.org/10.12681/mms.327.

Zhu, Z., Belzen, J., Zhu, Q., Koppel, J., Bouma, T.J., 2020a. Vegetation recovery on neighboring tidal flats forms an Achilles' heel of saltmarsh resilience to sea level rise. Limnol. Oceanogr. 65, 51–62. https://doi.org/10.1002/lno.11249.

Zhu, Z., Yang, Z., Bouma, T.J., 2020b. Biomechanical properties of marsh vegetation in space and time: effects of salinity, inundation and seasonality. Ann. Bot. 125, 277–290. https://doi.org/10.1093/aob/mcz063.

Check for updates

Aquatic Conservation: Marine and Freshwater Ecosystems

WILEY

PERSPECTIVE OPEN ACCESS

A Common Terminology to Unify Research and Conservation of Coralline Algae and the Habitats They Create

Victor L. Jardim[1] | Jacques Grall[1,2] | M. Beatriz Barros-Barreto[3] | Anaëlle Bizien[2] | Thomas Benoit[4] | Juan C. Braga[5] | Juliet Brodie[6] | Thomas Burel[1] | Andrea Cabrito[7] | Guillermo Diaz-Pulido[8] | Patrick Gagnon[9] | Jason M. Hall-Spencer[10,11] | Mathieu Helias[12,13] | Paulo Antunes Horta[14] | Siddhi Joshi[15] | Nick A. Kamenos[15,16] | Regina Kolzenburg[15] | Erik C. Krieger[17,18] | Erwann Legrand[19] | Tessa M. Page[20] | Viviana Peña[21] | Federica Ragazzola[22,23] | Lina M. Rasmusson[24] | Francesco Rendina[25] | Nadine Schubert[26] | João Silva[26] | Frederico T. S. Tâmega[27] | Adeline Tauran[28] | Heidi L. Burdett[15,16]

[1]Université de Brest, CNRS, IRD, Ifremer, LEMAR, IUEM, Plouzané, France | [2]UAR 3113, Observatoire Marin, Université de Brest, Plouzané, France | [3]Department of Botany, Federal University of Rio de Janeiro, Rio de Janeiro, Brazil | [4]Ifremer, Centre de Bretagne, DYNECO, Laboratory of Coastal Benthic Ecology, Plouzané, France | [5]Departamento de Estratigrafía y Paleontología, Universidad de Granada, Granada, Spain | [6]Natural History Museum, Research, London, UK | [7]Institut de Ciències del Mar (ICM), CSIC, Barcelona, Spain | [8]School of Environment and Science, Coastal & Marine Research Centre, Griffith University, Nathan, Queensland, Australia | [9]Department of Ocean Sciences, Ocean Sciences Centre, Memorial University of Newfoundland, St. John's, Newfoundland and Labrador, Canada | [10]School of Biological and Marine Sciences, University of Plymouth, Plymouth, UK | [11]Shimoda Marine Research Center, University of Tsukuba, Shimoda, Japan | [12]Conservatoire National des Arts et Métiers, INTECHMER, Cherbourg-en-Cotentin, France | [13]Normandie Université, UNICAEN, Laboratoire des Sciences Appliquées de Cherbourg, Cherbourg-en-Cotentin, France | [14]Departamento de Botânica, Universidade Federal de Santa Catarina, Florianópolis, Brazil | [15]Umeå Marine Sciences Centre, Umeå University, Umeå, Sweden | [16]Department of Ecology & Environmental Science, Umeå University, Umeå, Sweden | [17]Red Sea Research Center, King Abdullah University of Science and Technology, Thuwal, Saudi Arabia | [18]School of Biological Sciences, Victoria University of Wellington, Wellington, New Zealand | [19]Institute of Marine Research, Bergen, Norway | [20]School of Ocean and Earth Science, University of Southampton, National Oceanography Centre Southampton, Southampton, UK | [21]Facultad de Ciencias, BIOCOST Research Group, A Coruña, Spain | [22]Genoa Marine Center, Stazione Zoologica Anton Dohrn, Villa del Principe, Genoa, Italy | [23]National Biodiversity Future Center (NBFC), Palermo, Italy | [24]Department of Biological and Environmental Sciences, University of Gothenburg, Gothenburg, Sweden | [25]Department of Science and Technology, Laboratory of Marine Ecology, Centro Direzionale, University of Naples Parthenope, Naples, Italy | [26]Centre of Marine Sciences (CCMAR/CIMAR LA), Campus de Gambelas, Universidade do Algarve, Faro, Portugal | [27]Departamento de Biotecnologia Marinha, Instituto de Estudos do Mar Almirante Paulo Moreira (IEAPM), Arraial do Cabo, Brazil | [28]Université de Bordeaux, CNRS, Bordeaux INP, EPOC, UMR 5805, Station Marine d'Arcachon, Pessac, France

Correspondence: Victor L. Jardim (victor.leitejardim@univ-brest.fr)

Received: 11 June 2024 | **Revised:** 4 March 2025 | **Accepted:** 7 March 2025

Funding: This work was supported by Wiley.

Keywords: algal ridges | carbonate crust | CCA | coral–algal reefs | coralligenous | coralline algae | linguistic uncertainty | maerl | rhodolith | typology

ABSTRACT

Linguistic uncertainty is a prime source of uncertainty pervading ecology and conservation. Coralline algae are a widespread and diverse group of calcifying red macroalgae that underpin coastal ecosystem function and service provision. Recent increasing interest in coralline algae in the scientific literature has revealed a diverse but confusing terminology at organism to habitat scales. Coralline algal research and conservation are international and multidisciplinary, so there are geographic and disciplinary imbalances in research and conservation efforts. To reach consensus and reduce uncertainty, we propose a unified terminology. We review trends in cultural and scientific use of coralline algal terms and propose a system based on six morphologies: (1) attached, (2) free-living geniculate, (3) encrusting and free-living nongeniculate coralline algae, the latter either being (4)

This is an open access article under the terms of the Creative Commons Attribution License, which permits use, distribution and reproduction in any medium, provided the original work is properly cited.

© 2025 The Author(s). *Aquatic Conservation: Marine and Freshwater Ecosystems* published by John Wiley & Sons Ltd.

nucleated or (5) non-nucleated thalli or (6) fragments. We take inspiration from other coastal systems that have achieved consensus through umbrella terms, such as 'coral' and 'kelp', to accelerate global progress in coralline algal research and conservation. We characterise 14 coralline algae–dominated habitat global types, falling within seven functional groups, four biomes and four realms: (1) freshwater coralline streams; (2) coralline tide pools; (3) intertidal coralline rims and (4) turf; (5) coralline sea caves; (6) coral–algal reefs; (7) algal ridges; (8) coralligenous reefs; subtidal (9) carbonate crusts, (10) coralline barrens and (11) turf; and (12) articulith, (13) maerl and (14) rhodolith beds, which fall into the coralline algal bed functional group. We hope this unified terminology promotes data comparison, enables cross-boundary and cross-sector sharing of best practices, develops capacity for meta-analyses and improves conservation strategies.

1 | Introduction

A subject with strong cultural, scientific and/or socio-economic connections is usually associated with a high diversity of terms to describe it, because language and human cognition and perception are deeply intertwined (Drew 2005; Klemfuss et al. 2012; Thierry 2016). Similarly, the stronger the connections of a people to a species or group of species, the higher the number of words to describe them (Drew 2005). This pattern can also be seen in scientific language. However, while a diverse terminology can enable specific descriptions, it can also hinder broader scientific understanding of the subject. This is due to increasing uncertainty (Kéfi et al. 2019; Kovalenko et al. 2012), where there is a lack of a unique and complete understanding of a subject. Uncertainty can arise from contrasting multiple knowledge—distinct but equally valid views (Brugnach et al. 2008). Linguistic uncertainty has been identified as one of the main classes of uncertainty that impairs ecological knowledge and effective conservation strategies (Regan et al. 2002; Kujala et al. 2013).

Coralline algae are a highly diversified, globally distributed group of red calcifying macroalgae (Corallinophycidae, Rhodophyta) that thrive in marine and locally in freshwater environments under a wide range of conditions (Johansen 1981; Žuljević et al. 2016). Following pioneering taxonomy-driven work at the end of the 19th century (Foslie 1894; Woelkerling et al. 2005; Woelkerling 2008), coralline algae have received increasing attention in the scientific literature (Figure 1). This interest came from the recognition of their global importance for coastal ecosystem function, service provision and biogeochemical cycling, their sensitivity to projected environmental change and their value in palaeoecological records (McCoy and Kamenos 2015). Similarly, given the biological resources provided by the habitats these coralline algae create, there is increasing concern related to their exploitation (Grall and Hall-Spencer 2003; Riosmena-Rodríguez 2017; Berchez 2022; Mógor et al. 2021; Ramos et al. 2023). Such recognition is driving conservation efforts, with coralline algae being increasingly included in marine management frameworks around the world (European Commission et al. 2016; Keith, Fragkopolou, et al. 2022; Brodie et al. 2023; Axelsson 2023).

As a consequence of increasing recognition and the unmatched morphological diversity of the group, the terminology used for coralline algae and the habitats they form has also become diverse, sometimes leading to linguistic uncertainty (McCoy and Kamenos 2015). The European Red List of Habitats (European Commission et al. 2016) exemplifies this linguistic uncertainty in coralline algal science and conservation. This document alone has 11 names for coralline algal habitats and includes numerous others in which coralline algae are notable components (Figure 2; Table S1). Among the terms used, some are polysemic (have multiple meanings) and context dependent, while some are synonymous. This linguistic uncertainty has the potential to lead to misunderstandings among researchers, decision-makers and other stakeholders, transcending into policy-making (Norton 1998; Milner-Gulland and Shea 2017) and public engagement (Vigliano Relva and Jung 2021).

Coralline algal research and conservation are inherently international and disciplinarily diverse due to the worldwide distribution and the diversity of the algal group. This leads to local and regional scale variations in priorities: Coralline algal research disciplines are not evenly developed worldwide (Rendina et al. 2022) and conservation efforts depend on local pressures and stakeholders (Keith, Ferrer-Paris, et al. 2022). Here, we highlight the importance of unification and community consensus as a tool for contextualisation, to ensure readers understand the meaning of a term (Crump et al. 1999). We review how coralline algal terminology has evolved since the 18th century at organism and habitat levels, identifying long-term trends in cultural and scientific usages of these terms and proposing a unified typology for coralline algal habitats, providing authors with terms that can make communication about these algae more efficient. We hope this will help advance coralline algal research and conservation by (1) facilitating observational and experimental data comparisons; (2) enabling cross-boundary and cross-sector sharing of technique developments, best practices and conservation strategies; and (3) improving meta-analyses, as synonyms can be missed in published literature leading to skewed results (Hodges 2008; Stroud et al. 2015; Cira et al. 2019).

2 | Facilitating Progress in Coralline Algal Research and Conservation Worldwide

A unified terminology for coralline algal habitats may foster better international research collaboration, accelerating the advancement of coralline algal research frontiers and base conservation strategies on a more coherent foundation. In other coastal systems, this has been achieved—'coral', 'kelp', 'seagrass' and 'mangrove' are umbrella terms for 10s–1000s of species with high intravariability, and all have similarly simple habitat terms. The cohesive terminology and grouping of such diverse habitats has facilitated their international recognition within research,

10990755, 2025, 3, Downloaded from https://onlinelibrary.wiley.com/doi/10.1002/aqc.70121 by Csic Organización Central Om (Oficialia Mayor) (Urici), Wiley Online Library on [25/03/2025]. See the Terms and Conditions (https://onlinelibrary.wiley.com/terms-and-conditions) on Wiley Online Library for rules of use; OA articles are governed by the applicable Creative Commons License

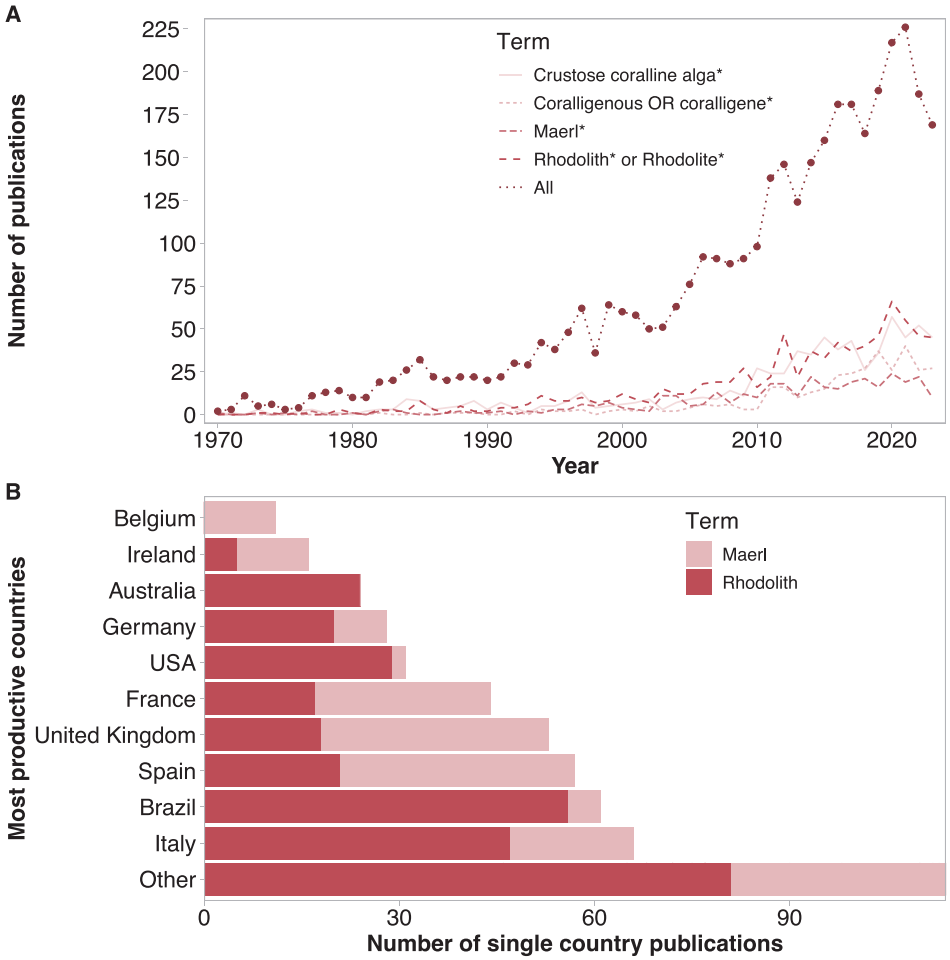


FIGURE 1 | Scopus search for publications containing coralline algal terms in the title, abstract or keywords from 1970 to 2023. (A) Search terms: 'coralline alga*' OR 'coralline red alga*' OR 'coralligene*' OR 'coralligenous' OR 'maerl*' OR 'rhodolite*' OR 'rhodolith*'. Total number of publications = 3713. Total and individual term trends are shown—note that one publication may contain more than one term. (B) Number of single-country publications containing the terms (maerl*) or rhodolith ('rhodolith*' OR 'rhodolite*'), showing the 10 most productive countries to illustrate regional and global trends, created with the 'bibliometrix' R package (Aria and Cuccurullo 2017; R Core Team 2024).

conservation and more widely, with numerous examples of global datasets and assessments (Hamilton and Casey 2016; Krumhansl et al. 2016; McKenzie et al. 2020; Sully et al. 2019; van Katwijk et al. 2016; van Woesik and Kratochwill 2022). Recognition for the importance of coralline algal research lags far behind—we believe due in part to the disparate terminology used at organism to habitat levels. Similarly, global datasets for coralline algae and the habitats they form are lacking, despite increasing academic attention (Figure 1).

Ecosystem conservation and management is typically implemented through local action, which may lead to both epistemic and linguistic uncertainty when aggregated at larger scales (Box 1; Keith, Ferrer-Paris, et al. 2022). However, international and interdisciplinary studies, which depend on a coordinated scientific community, enable cross-comparisons between baseline knowledge, ecological status and conservation efforts and help share successful policies and protect coralline algal habitats globally (Wilson et al. 2004; Brodie 2009; Tuya et al. 2023). Scaling-up local ecological data helps global conservation (Agardy 2005; Edgar et al. 2016, 2014; Rowland et al. 2020) and is needed for coralline algal conservation as at present, this is a data-deficient topic (Ferrigno et al. 2023; McCoy and Kamenos 2015; van der Heijden and Kamenos 2015; Rendina et al. 2022; Ferrigno et al. 2023). Addressing linguistic uncertainty will help resolve this and better set conservation objectives (Milner-Gulland and Shea 2017).

An increasing number of studies proposing unified terminologies to resolve language uncertainty in ecology often resort to trait-based and functional approaches (Bellwood et al. 2024; Ellison 2019; Keith, Ferrer-Paris, et al. 2022; Streit and Bellwood 2023). Here, we review the terms used for coralline algae and propose a unified typology at first the organism and then the habitat level. We then define coralline algae–dominated habitats based on the International Union for Conservation of Nature (IUCN) Global Ecosystem Typology (GET) (Keith, Ferrer-Paris, et al. 2022).

3 | The Emergence of a Diverse Terminology

All orders within the Corallinophycidae (Phylum: Rhodophyta), except the Rhodogorgonales, fall under the umbrella term 'coralline algae'—almost all of which have- extensive calcification in the cell walls (Jeong et al. 2021). The Rhodogorgonales have a very different calcification process and a gorgonian-like filamentous morphology (Fredericq and Norris 1995). The

10990755, 2025, 3, Downloaded from https://onlinelibrary.wiley.com/doi/10.1002/aqc.70121 by Csic Organización Central Om (Oficialia Mayor) (Urici), Wiley Online Library on [25/03/2025]. See the Terms and Conditions (https://onlinelibrary.wiley.com/terms-and-conditions) on Wiley Online Library for rules of use; OA articles are governed by the applicable Creative Commons License

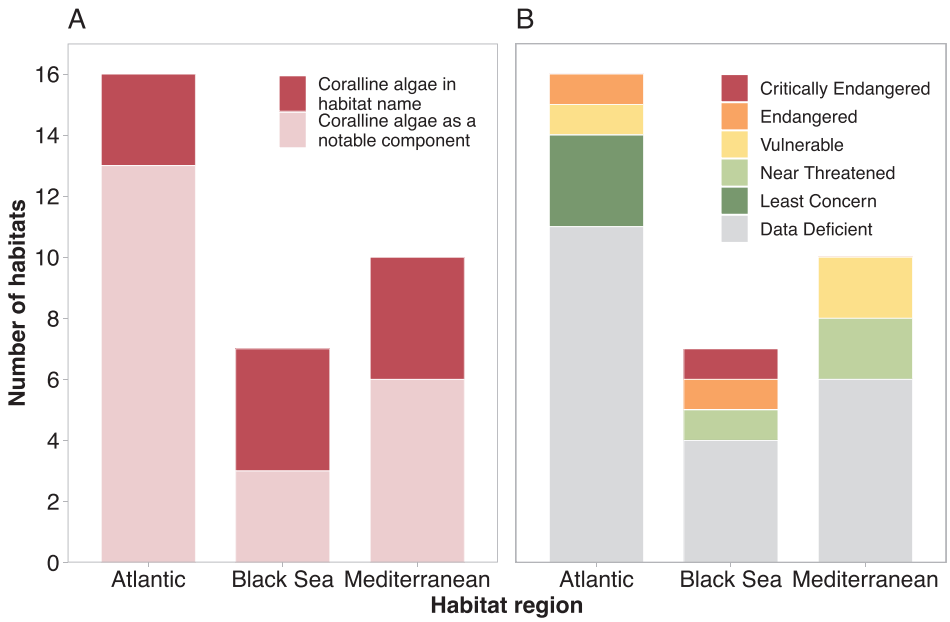


FIGURE 2 | Coralline algae in the European Red List of Habitats (European Commission et al. 2016). (A) The number of habitats where coralline algae are in the habitat name ($n = 11$) or are listed as a notable component in the habitat description ($n = 22$) and (B) the current conservation status of coralline algal-associated habitats across the Mediterranean, Black Sea and Atlantic regions. Further information on each habitat is provided in Table S1.

coralline algae are divided into two groups based on morphology (Figure 3): geniculate (erect fronds with uncalcified segments known as genicula) and nongeniculate (thalli lacking uncalcified segments). However, this morphological division is not reflected in their phylogeny. The order Corallinales has both geniculate and nongeniculate taxa, sometimes in a single genus, assuming evolutionary reversals of some taxa to the ancestral, nongeniculate state (Hind et al. 2018). Nongeniculate coralline algae can have a free-living or encrusting morphology, the latter being flat or with branch-like protuberances (Irvine and Chamberlain 1994). Some species are exclusively encrusting, while others can be found both free-living or encrusting (Hernandez-Kantun et al. 2016).

Besides the presence of genicula, coralline algae present great morphological and functional diversity. They greatly vary in size, thickness and shape, varying from (small) to (large). The group also presents several life strategies: parasitic, semiendophytic, epilithic, epiphytic, epizoic or live as epibionts on man-made surfaces such as glass, plastic and metal (Adey and Sperapani 1971; Adey and Macintyre 1973; Harvey et al. 2005; Dean et al. 2015; McCoy and Kamenos 2015). This diversity is thought to be at least partially due to the presence of secondary pits and vegetative cell fusions that allow the translocation of photosynthates to living cells beneath photosynthetic tissues, allowing lateral growth (Steneck 1983, 1986). The morphological and functional diversity of the group has contributed to the proliferation of terms used to describe coralline algae.

3.1 | Free-Living Nongeniculate Coralline Algae

Free-living, nodule forming, nongeniculate coralline algae have been documented since the mid-18th century (e.g., Linnaeus 1758; Ellis and Solander 1786), although they were thought to be animals that looked like plants (zoophytes) until Philippi (1837) identified them as photosynthetic organisms. Initially classified as *Millepora* hydrocorals (Ellis and Solander 1786; Pallas 1766) and later as *Nullipora* zoophytes (Lamarck 1801), they were then identified as coralline algae of the genera *Lithothamnion* Heydrich and *Lithophyllum* Philippi, in the mid-late 1800s (Wiegmann 1837; Chauvin 1842; Foslie 1894). Since then, multiple terms have arisen from both traditional and scientific ecological knowledge, with varying consensus over their interchangeability such as coatings, nodules, maerl, rhodoliths, rhodolites or rhodoids; there are at least 12 terms used in the academic literature for free-living coralline algae (Riosmena-Rodríguez 2017).

For example, in the early 20th century the Breton word maerl (*maërl*, in French) started gaining popularity in the scientific community (Lemoine 1910), although it had been used for centuries by Celtic and French people in reference to the coralline algae exploited for soil treatment—as a variant of 'marne' the word for calcareous rocks (Augris and Berthou 1990). The terms 'maerl' and 'maerl beds' have been historically used for unattached coralline algal habitats created by *L. corallioides* (P.Crouan & H.Crouan) P. Crouan & H. Crouan, *Boreolithothamnion glaciale* (Kjellman) P.W.Gabrielson, Maneveldt, Hughey & V. Peña (previously *Lithothamnion glaciale*) and *P. calcareum* (Pallas) W.H.Adey & D.L.McKibbin ex Woelkering & L.M.Irvine in the Northeast (NE) Atlantic and subarctic seas (Cabioch 1969; Adey and Macintyre 1973; Barbera et al. 2003; Wilson et al. 2004; Hinojosa-Arango et al. 2009; Peña et al. 2014; Jenkins et al. 2021). These species often lack a nucleus, the main reason why many now consider only such forms as maerl (sensu stricto). At least 13 different maerl-forming species have been identified in the NE Atlantic with many different growth forms (Peña et al. 2013, 2021; Pardo et al. 2014; Qui-Minet et al. 2021; Helias and Burel 2023). The term maerl sensu lato has sometimes been

10990755, 2025, 3, Downloaded from https://onlinelibrary.wiley.com/doi/10.1002/aqc.70121 by Csic Organización Central Om (Oficialia Mayor) (Urici), Wiley Online Library on [25/03/2025]. See the Terms and Conditions (https://onlinelibrary.wiley.com/terms-and-conditions) on Wiley Online Library for rules of use; OA articles are governed by the applicable Creative Commons License

Box 1. Rhodolith/maerl beds: a tale of detrimental linguistic uncertainty in conservation efforts and how human connection may improve it

An example of linguistic uncertainty affecting conservation is a lack of cohesion on free-living non-geniculate coralline algae terminology. The European Red List of Habitats (Table S1) uses the term 'maerl beds' for the Atlantic but "rhodolith beds" for the Mediterranean, although both are defined as "*sedimentary bottoms characterised by any morphology and species of unattached non-geniculate calcareous red algae*" (European Commission et al., 2016). Curiously, *Lithothamnion corallioides* and *Phymatolithon calcareum*, typically associated with the term 'maerl' in the Atlantic, are explicitly listed in the European Red List as the main species found in "Mediterranean rhodolith beds". The latest OSPAR commission Benthic Habitats report recognises maerl beds as threatened and/or in decline, but does not consider rhodolith beds (OSPAR, 2023).

While maerl beds in the Atlantic are recognised as Endangered or Vulnerable, Mediterranean rhodolith beds are considered 'data deficient' on the European Red List of Habitats (European Commission et al., 2016), despite extensive research conducted on Mediterranean coralline algal beds (Jacquotte, 1962; Pérès and Picard, 1964; Basso, 1998; Barbera et al., 2003; Bordehore et al., 2003; Ordines and Massutí, 2009; Sciberras et al., 2009; Sanz-Lázaro et al., 2011; Barberá et al., 2012; Micallef et al., 2012; Savini et al., 2012; Martin et al., 2014). Therefore, linguistic uncertainty is probably partly responsible for the 'data deficient' status. Indeed, Mediterranean coralline algal beds may be facing even more extreme conditions than those in the Atlantic zone and may deserve a higher conservative status (Rindi et al., 2019).

Besides baseline scientific knowledge, the deep historical roots and cultural connections humans have with the ocean cannot be overstated and might be reflected on the different levels of protection given to coralline algal beds worldwide (Poe et al., 2013; Bennett, 2019). For instance, the term 'maerl' has an important historical and cultural heritage value in many places in the North Atlantic, especially in Brittany, France. A local festival called '*La fête du maërl*' takes place every four years in Plougastel-Daoulas in the Bay of Brest, attracting more than 5000 people with art exhibits, traditional dancing and historical re-enactments to remember those who extracted coralline algae for a living, and to raise awareness of the ecological and socioeconomic importance of these habitats (Friant and Marie, 2010; Péron and Marie, 2010; Noisette, 2013).

used to include nucleated growth forms of unattached coralline algae and the habitats they form in the Mediterranean (Barberá et al. 2017) and NE Atlantic (Axelsson 2023).

In the second half of the 20th century, the terms rhodolith and rhodolith beds were first introduced to describe 'unattached aggregations of calcareous red algae' (Barnes et al. 1970, 1971). This broad definition could, therefore, include free-living thalli of noncoralline calcifying red algae such as Peyssonneliaceae (subcl. Rhodymeniophycidae) species (Buchbinder and Halley 1985). However, these other calcifying red algae are usually associated with corallines and are seldom the dominant nodule-forming component, with exceptions in transition zones (Ballesteros 1994; Basso 2012; Bianchi and Morri 2025; V. A. Bracchi, Bazziacalupo, et al. 2022; Deinhart et al. 2022). The terms rhodolite and rhodoid were also proposed at the time (Bosellini and Ginsburg 1971; Peryt 1983), but because these had previously been used to describe a variety of red garnets and other coated grains, they were discarded for coralline algal nodules (Adey and Macintyre 1973; Ginsburg and Bosellini 1973). Since then, rhodolith has become the most widely used term for free-living nongeniculate coralline algae (Rendina et al. 2022) except in Europe, where maerl is more commonly used (Figure 1B). Although the first definitions of rhodolith sensu lato did not distinguish among nucleated and non-nucleated nodular calcifying red algal growths, Steneck (1986) only consider those that grow around a nucleus as rhodoliths sensu stricto. Nucleated nodules can also be further classified based on the relative contribution of the coralline algal component to the whole nodule structure into coatings (< 50%) or rhodoliths

10990755, 2025, 3, Downloaded from https://onlinelibrary.wiley.com/doi/10.1002/aqc.70121 by Csic Organización Central Om (Oficialia Mayor) (Urici), Wiley Online Library on [25/03/2025]. See the Terms and Conditions (https://onlinelibrary.wiley.com/terms-and-conditions) on Wiley Online Library for rules of use; OA articles are governed by the applicable Creative Commons License

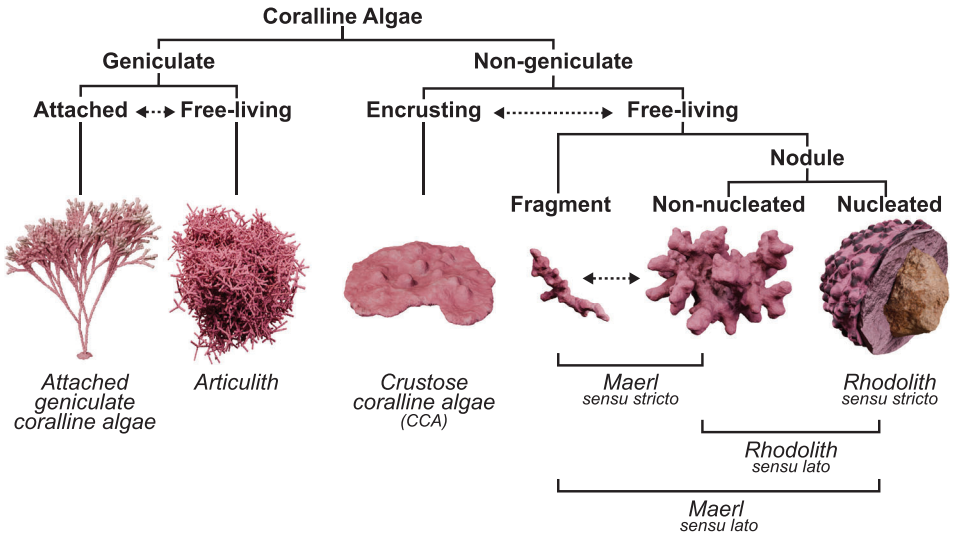


FIGURE 3 | Proposed morphological organismal typology for coralline algae. Note that rhodolith and maerl both have historically been given both strict and broad definitions. Rhodolith sensu stricto only includes nucleated nodules, while maerl sensu stricto includes only non-nucleated forms. While rhodolith sensu lato includes only nodular forms, maerl sensu lato also includes nonnodular fragments. Here, we present historical uses so that authors can be specific about which morphotypes are referred to when using any of the terms. The represented morphologies are examples of the variety in growth forms. Arrows represent reproductive strategies that enable shifts between different types: Attached algae can grow into free-living forms, while free-living reproductive forms can produce spores that will grow into attached forms.

(> 50%) (Steneck 1983; Basso 1998). The nucleus can be of biotic or abiotic origin, and nucleated rhodoliths can be composed of one or several thalli, often with multiple species on individual nodules (Riosmena-Rodríguez 2017). There is growing use of rhodoliths sensu lato as a general term for coralline algal nodules, particularly those with nuclei, while maerl sensu stricto remains the term commonly used for non-nucleated free-living nongeniculate coralline algae (Foster 2001; Arnold et al. 2021; Bélanger and Gagnon 2023).

Subclassifications have been created to reflect the morphological diversity of free-living nongeniculate coralline algae and introduce a rich terminology that can be source of linguistic uncertainty. For instance, both Bosence (1983) and Basso (1998) proposed the term 'boxwork' for different types of nodules. Bosence (1983) distinguished them in three classes: branching, columnar and laminar, with the latter being divided into concentric and nonconcentric nodules (boxwork). Basso (1998) proposed three classes: boxwork rhodoliths (large, multispecific, laminar to columnar nucleated nodules with multiple voids), *prâlines* (small, monospecific, laminar, branching or columnar nucleated nodules) and unattached branches (small, monospecific, unattached non-nucleated branches). Although useful to describe specific morphologies, when using subclassifications, authors should be explicit about their meanings to avoid confusion.

3.2 | Encrusting Nongeniculate Coralline Algae

Much like free-living forms of nongeniculate coralline algae, descriptions of encrusting forms date back to the 1700s. Pérès and Picard (1964) provide a wealth of information on the variety of habitats these algae can form and an evocative variety of French terms used to describe these habitats. The term crustose coralline algae became popular at the end of the 20th century, when it was initially used as a synonym for nongeniculate coralline algae (Adey and Macintyre 1973; Bosence 1983; Steneck 1986). Nowadays, crustose coralline algae usually refers to encrusting (sessile) nongeniculate corallines only (McCoy and Kamenos 2015), although free-living forms are sometimes also referred to as crustose coralline algae (Amado-Filho et al. 2012; Pereira-Filho et al. 2012; V. Bracchi, Caronni, et al. 2022; Rebelo et al. 2022). This ambiguity is understandable since many encrusting species may grow on mobile substrata (biogenic, lithic or man-made) to create nucleated free-living specimens (Foster 2001). The term 'crustose' can also be misleading as many nongeniculate species have calcified upright branches (Woelkerling et al. 2005). Additionally, many geniculate species can be confused with encrusting nongeniculate species in early development stages, as they present a nongeniculate basal crust preceding the formation of upright geniculate fronds (Irvine and Chamberlain 1994).

Much of the diversity of terms regarding encrusting nongeniculate coralline algae stems from the wide variety of habitats that they form. These include coralline algal rims, buttresses, platforms, cornices and *trottoirs*, coralline algal-dominated tide pools and sea caves, coral–algal reefs, coralline algal carbonate crusts (or cor-stromes) and coralligenous reefs, the latter also being known as coralligenous assemblages, formations, concretions, coralligène or simply coralligenous (Marion 1883). The similarities and differences among these habitats are discussed below, in the habitat typology section.

3.3 | Geniculate Coralline Algae

Geniculate coralline algae were first described as zoophytes in the 18th century (Linnaeus 1758). The name comes from their genicula, an uncalcified, joint-like cell structure, separating two intergenicula, the calcified segments of the upright

10990755, 2025, 3, Downloaded from https://onlinelibrary.wiley.com/doi/10.1002/aqc.70121 by Csic Organización Central Om (Oficialia Mayor) (Urici), Wiley Online Library on [25/03/2025]. See the Terms and Conditions (https://onlinelibrary.wiley.com/terms-and-conditions) on Wiley Online Library for rules of use; OA articles are governed by the applicable Creative Commons License

fronds usually developed from a nongeniculate basal disc. The term genicula was initially employed for *Equisetum* plants (Blackstone 1746), then for Cnidarians by Linnaeus (1758) and Ellis and Solander (1786), and was subsequently applied to corallines (Harvey 1847).

The Corallinales is the only order of coralline algae with geniculate species (Walker et al. 2009). The presence of genicula was long considered the most important character for taxonomic distinction (Johansen 1981). However, the presence of genicula is a derived character that has arisen in the descendants of nongeniculate coralline algae multiple times (Aguirre et al. 2010; Peña et al. 2020). Hind et al. (2018) also suggest that evolutionary reversals have occurred within the subfamily Corallinoideae, twice within the geniculate genus *Bossiella* P.C. Silva.

The genicula development pattern differs from one genus to another, either through the development of uncalcified cells (apical growth for the Metagoniolithoideae or subapical growth for the genus *Lithothrix* Gray) and/or by decalcification (important in Lithophylloideae) (McCoy et al. 2023). The genicula grant these algae some degree of physical flexibility and were initially called *articulis* by Linnaeus—hence the popularity of the alternative term 'articulated coralline algae' (Johansen 1981).

Geniculate taxa are usually epilithic and typically occur in the intertidal and subtidal zones from polar to tropical environments (Stewart 1982; Kelaher et al. 2001), although species can also be epiphytic or epizoic. They are often strongly attached by crustose or stoloniferous holdfasts, which can be extensive and sometimes confused for an encrusting nongeniculate coralline algae base (Brodie et al. 2013). Some geniculate corallines can be free-living and create extensive habitats similar to free-living nongeniculate coralline algae beds—these understudied growth forms have been recently named 'articuliths' (Tâmega et al. 2017, 2021).

3.4 | Creating International Cohesion Through a Unified Typology

As coralline algal science and interest from conservation and policy sectors have grown, the diversity of terms used to describe these algae and their associated habitats has also increased. Although a diversity of terms enables specificity in organismal/habitat descriptions, the definition of terms and the extent of 'interchangeability' between terms is not internationally consistent, creating uncertainty. Adoption of specific terms (and rejection or delineation of others), namely, in policy documents, creates uncertainty and places coralline algal habitats at greater risk of inadequate protection measures.

4 | Proposed Organismal Typology

Some terms, such as crustose coralline algae and nongeniculate coralline algae, have been used interchangeably when they designate organisms with different life histories and ecological functions. On the other hand, organisms with similar traits and functions have been named differently on cultural and morphological bases, as in the case of the free-living nongeniculate coralline algae. Informed by both terminology history and morphological differentiation (discussed above), we propose a unified organismal typology (Box 2 and Figure 3).

In this typology, coralline algae are initially distinguished by their structural morphology, leading to the categorisation of geniculate and nongeniculate forms. The mode of attachment is then used to further differentiate these forms. This includes attached and free-living geniculate forms, as well as encrusting (sessile) and free-living nongeniculate forms. Free-living nongeniculate types can be nodules or fragments—the latter having only one long axis (Figure 3). Encrusting nongeniculate forms may have branches which, when detached, can become free-living fragments or non-nucleated nodules—referred to as 'maerl' in the strictest sense. The broader term 'maerl' can encompass all free-living forms, including nucleated and non-nucleated nodules and fragments. Conversely, the term 'rhodolith' in its broadest sense and following the original definition by Barnes et al. (1971) may include noncoralline calcifying red algae and encompasses all free-living nodules, while in its strictest sense, it specifically refers only to nucleated nodules of free-living nongeniculate coralline algae. Importantly, we do not prescribe authors necessarily use the terms sensu lato and sensu stricto when referring to maerl or rhodoliths, but instead, advocate authors are explicit about which type of coralline algae is being referred to (nucleated nodules, non-nucleated nodules or fragments) whenever they use one term or the other—as many definitions exist.

5 | Proposed Habitat Typology

International cohesion among coralline terminology might be even more important at the habitat level for conservation and management. When different terms are employed to habitats with similar ecological traits and functions, dissimilar protection levels might be applied (Kujala et al. 2013). In this sense, a functional approach could be an effective alternative basis for a unified terminology (Hattam et al. 2021; Streit and Bellwood 2023). Many coralline algal species can be considered multi-influence engineers, as they can affect several biotic and abiotic processes and resultant ecosystem functions (Byers 2022). Therefore, we propose a unified morphofunctional habitat typology in which we describe and group coralline algae–dominated habitats following the IUCN's GET (global-ecosystems.org). The GET units are based on (1) ecosystem functions and ecological processes, (2) their characteristic biota, (3) conceptual consistency throughout the whole biosphere, (4) a scalable structure, (5) spatially explicit units and (6) descriptive parsimony (Keith, Ferrer-Paris, et al. 2022).

5.1 | IUCN's Global Typology

The GET has three upper hierarchical levels (Figure 4): 11 realms (Level 1), including atmospheric (which is taken into account but has no lower hierarchical units), freshwater, marine, terrestrial, subterranean and six transitional realms not relevant here; 25 functional biomes (Level 2); and 110 functional groups (Level 3). Biomes are components of a realm with similar ecosystem structure and one or a few common major ecological drivers

10990755, 2025, 3, Downloaded from https://onlinelibrary.wiley.com/doi/10.1002/aqc.70121 by Csic Organización Central Om (Oficialia Mayor) (Urici), Wiley Online Library on [25/03/2025]. See the Terms and Conditions (https://onlinelibrary.wiley.com/terms-and-conditions) on Wiley Online Library for rules of use; OA articles are governed by the applicable Creative Commons License

Box 2. Coralline algae organismal typology and definition key

Coralline algae 1
- Geniculate 2
  - Attached 3
  - Free-living 4
- Non-geniculate 5
  - Encrusting 6
  - Free-living 7
    - Fragment[a,b] 8
    - Nodule 9
      - Nucleated[c,d] 10
      - Non-nucleated[a,b,d] 11

1. Calcifying benthic red algae within the Corallinophycidae (exc. Rhodogorgonales, Rhodophyta)
2. Corallinales species with calcified frond segments separated by genicula (uncalcified cells)
3. Geniculate coralline algae attached to substrata by crustose or stoloniferous holdfasts
4. Geniculate coralline algae living unattached in nodular forms known as articuliths
5. Fully calcified coralline algae lacking genicula
6. Non-geniculate coralline algae attached to substrata, also known as Crustose Coralline Algae
7. Non-geniculate coralline algae living unattached as fragments or nodules
8. Fragments of branching encrusting and free-living non-geniculate coralline algae
9. Nodular growths of free-living non-geniculate coralline algae
10. Free-living non-geniculate coralline algae growing as nodules over a biogenic or abiotic nucleus.
11. Free-living non-geniculate coralline algae growing in nodular forms from unattached fragments

a. Maerl *sensu stricto*. Includes non-nucleated nodules of free-living non-geniculate coralline algae and fragments of branching non-geniculate coralline algae
b. Maerl *sensu lato*. Includes all free-living non-geniculate coralline algae.
c. Rhodolith *sensu stricto*. Includes nucleated nodules of free-living non-geniculate coralline algae.
d. Rhodolith *sensu lato*. Includes all nodules of non-geniculate coralline algae and other non-coralline calcareous red algae of the presence of nuclei.

and functions. Functional groups are similar systems within a biome that share common ecological drivers and present similar biotic traits. Functional groups can be further divided into three bottom hierarchical levels: regional subgroups (Level 4), global types (Level 5) and subglobal types (Level 6). Level 4 units are based on ecoregions and are not applied here because many regions are data deficient for coralline algae (European Commission et al. 2016; Rendina et al. 2022; Brodie et al. 2023). Lower Levels 5 and 6 are independent of Level 4 and have a bottom-up hierarchy. Global types (Level 5) are defined by the aggregation of subglobal types (Level 6, regional expressions of functional groups) based on compositional resemblance. Global types grouped into the same functional group share similar ecological processes, drivers and services but present different biotic composition.

Level 6 units are regional expressions of functional groups that are explicitly linked to local knowledge and are aggregated based on subglobal classifications. Aggregation of subglobal units to broader global units (Level 5) is based on compositional

10990755, 2025, 3, Downloaded from https://onlinelibrary.wiley.com/doi/10.1002/aqc.70121 by Csic Organización Central Om (Oficialia Mayor) (Urici), Wiley Online Library on [25/03/2025]. See the Terms and Conditions (https://onlinelibrary.wiley.com/terms-and-conditions) on Wiley Online Library for rules of use; OA articles are governed by the applicable Creative Commons License

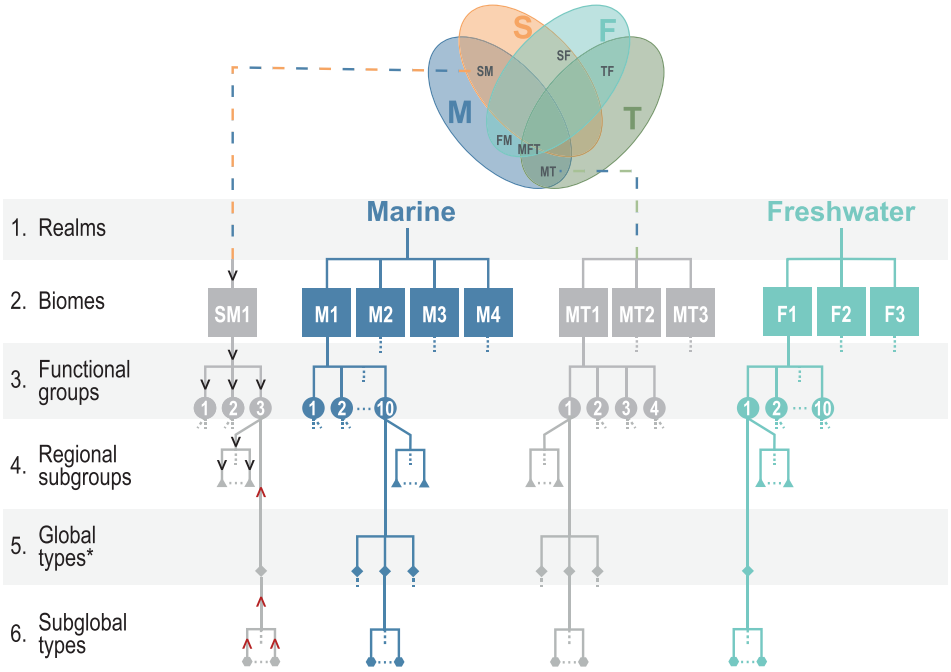


FIGURE 4 | Simplified IUCN's Global Ecosystem Typology (GET) showing only the realms containing coralline algal habitats. There are three upper hierarchical levels: 1—realms, 2—biomes and 3—functional groups. Level 3 levels can be further divided into 4—regional subgroups, 5—global types and 6—subglobal types. Four core realms represent major components of the biosphere: terrestrial, freshwater, marine and subterranean (the atmospheric realm is also taken into account but has no lower level units). Six additional transitional realms are defined as combinations of the four core realms. Core realms are coloured, while transitional realms are grey. Whenever a unit presents more than four lower levels, dashed lines are used to represent them. Lower levels of a single unit at each upper level are shown to simplify the diagram. Arrows indicate top-down (black) and bottom-up (red) structures. F = freshwater; M = marine; S = subterranean; T = terrestrial. Adapted from Keith, Ferrer-Paris, et al. (2022). Unit names are shown in Figure 5.

resemblance and is necessary to address uncertainty from contrasting multiple knowledge (Brugnach et al. 2008; Keith, Ferrer-Paris, et al. 2022). Therefore, under the post-2020 Global Biodiversity Framework, the IUCN's Red List Index of Ecosystems (RLIE) is used to inform the IUCN's Red List of Ecosystems and takes GET into account (Bland et al. 2019; Nicholson et al. 2021). The RLIE summarises the risk status and trends of ecosystems and can be reported at national or global levels and disaggregated by ecosystem type, using the GET (Rowland et al. 2020).

We characterise a nonexhaustive list of 10 coralline algae–dominated global types, falling within seven IUCN functional groups, four biomes and four realms (Figure 5). The global types we propose are based on subglobal habitats (GET Level 6) and grouped based on the main coralline algae morphologies (cf. Box 2 and Figure 3) and their compositional and functional resemblances.

5.2 | The Freshwater Realm (F)

In the freshwater realm (F), classified under the rivers and streams biome (F1) and the permanent upland streams functional group (F1.1), a unique encrusting nongeniculate coralline algae habitat has been documented in the Cetina river karst watershed in Croatia (Žuljević et al. 2016; Koletić et al. 2020). It is formed by *Pneophyllum cetinaensis*, the only known freshwater member of the Corallinales, colonising every hard substratum available as well as roots and mollusc shells (Žuljević et al. 2016; Necchi and Vis 2021). No studies have yet investigated the role of this coralline algae freshwater habitat on shaping associated assemblages. Unfortunately, this habitat is under strong human pressures, as the river crosses two cities and has several hydroelectric power plants, dams and artificial lakes along its course (Žuljević et al. 2016).

5.3 | The Marine–Terrestrial Transitional Realm (MT)

In the marine–terrestrial transitional realm (MT), three coralline global types are identified, all included in the shorelines biome and rocky shorelines functional group (MT1.1). Geniculate coralline algae can be a dominant part of rocky shoreline habitats. They are autogenic ecosystem engineers, forming turf that provides shelter to well-developed macrofaunal and macroalgal communities (Stewart 1982; Grahame and Hanna 1989; Kelaher et al. 2001; Nelson 2009). However, they are increasingly at threat from rising seawater water temperature, marine heatwaves and ocean acidification (Brodie et al. 2014; Williamson et al. 2014; Rendina et al. 2019; Kolzenburg et al. 2021).

Encrusting nongeniculate coralline algae may also be the main habitat-forming species in rocky shorelines, forming coralline algae–coated tide pools or intertidal encrusting coralline algae rims depending on their position in the shoreline and spatial organisation. Tide pools dominated by encrusting nongeniculate coralline algae can be found up to the upper intertidal zone,

10990755, 2025, 3, Downloaded from https://onlinelibrary.wiley.com/doi/10.1002/aqc.70121 by Csic Organización Central Om (Oficialia Mayor) (Urici), Wiley Online Library on [25/03/2025]. See the Terms and Conditions (https://onlinelibrary.wiley.com/terms-and-conditions) on Wiley Online Library for rules of use; OA articles are governed by the applicable Creative Commons License

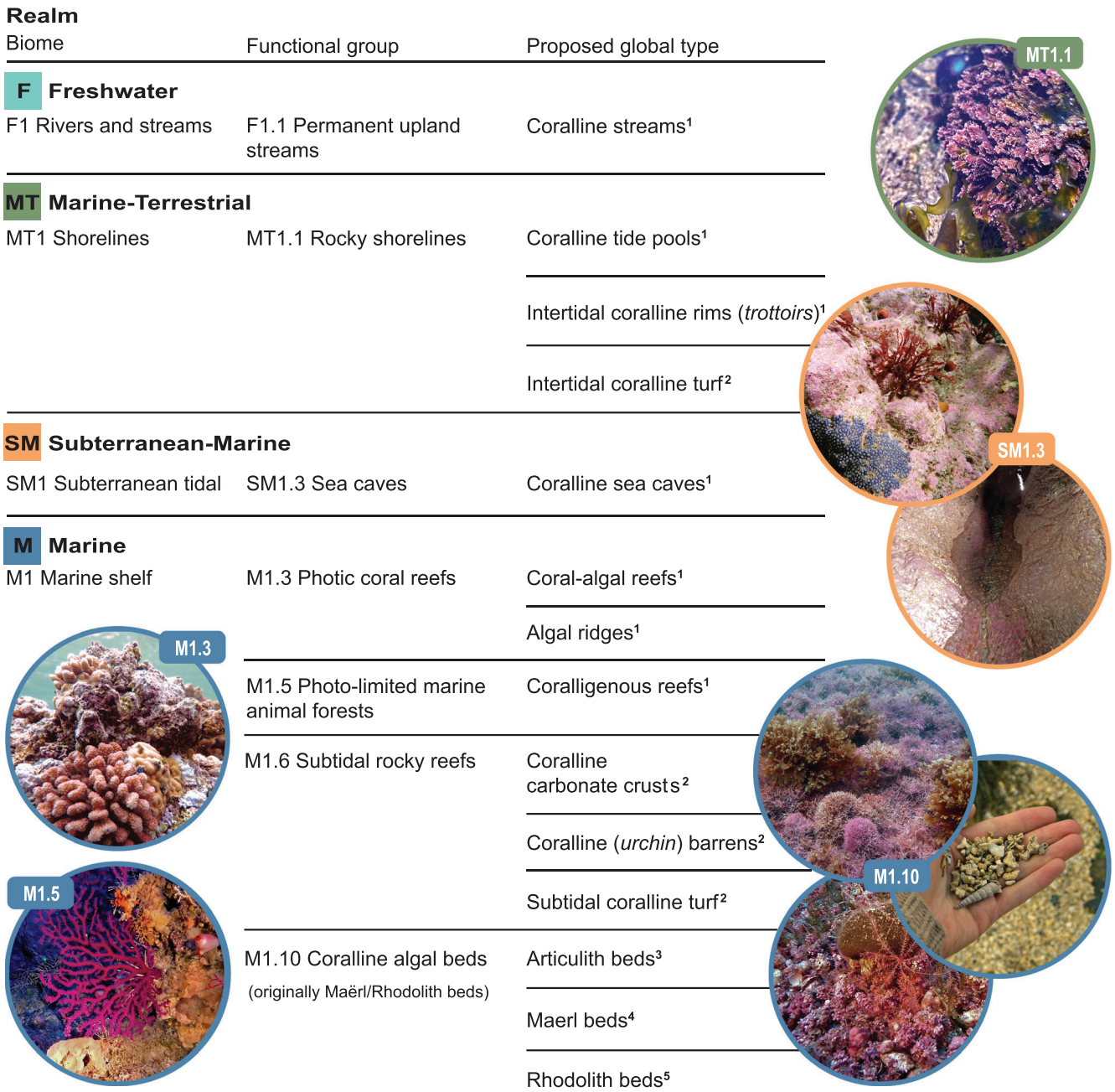


FIGURE 5 | Coralline algae–associated habitat nomenclature and typology, following the IUCN's Global Ecosystem Typology. New global types are proposed here, based on functional and compositional resemblances among subglobal types. Recommended habitat names are proposed as global types for consistency within the coralline algae community. Superscript numbers represent the dominant morphotypes of habitat-forming coralline algae, as described in Figure 3: 1 = encrusting nongeniculate coralline algae; 2 = attached geniculate coralline algae; 3 = free-living geniculate coralline algae nodules; 4 = free-living nongeniculate coralline algae nodules and fragments; 5 = free-living calcifying coralline algae nodules (including noncoralline species). Exemplary habitat photographs: MT1.1 = intertidal coralline turf, Brittany, France (credit: Victor L. Jardim); SM1.3 = coralline algae sea cave, Brittany France (credit: Jacques Grall); M1.3 = coral–algal reef, Great Barrier Reef, Australia (credit: Tessa Page); M1.5 = coralligenous reef, Sorrento, Italy (credit: Francesco Rendina); M1.10 (from top to bottom) = articulith bed, Rio de Janeiro, Brazil (credit: Frederico Tamega), Carraroe maerl beach composed mostly of nongeniculate coralline algae fragments, County Galway, Ireland (credit: Siddhi Joshi) and rhodolith bed Capri, Italy (credit: Francesco Rendina).

making them environmentally variable habitats characterised by distinct seasonal and diurnal cycles (Legrand et al. 2018) and intense biotic pressures, such as grazing (Steneck et al. 1991; Wai and Williams 2006). Coralline algae–dominated tide pools are usually dominated by a few species of encrusting nongeniculate coralline species (Wai and Williams 2006; Dorey et al. 2023). Although tide pools usually present low diversity of associated organisms when compared to subtidal communities, they are more diverse than the surrounding emergent rock habitats (Firth et al. 2014).

Intertidal encrusting nongeniculate coralline algae rims are formed through the coalescence of numerous coralline algae thalli on vertical or subvertical rocky surfaces (Verlaque 2010).

10990755, 2025, 3, Downloaded from https://onlinelibrary.wiley.com/doi/10.1002/aqc.70121 by Csic Organización Central Om (Oficialia Mayor) (Urici), Wiley Online Library on [25/03/2025]. See the Terms and Conditions (https://onlinelibrary.wiley.com/terms-and-conditions) on Wiley Online Library for rules of use; OA articles are governed by the applicable Creative Commons License

Coralline algae rims usually present a porous upper layer of living coralline algae over dead algae, an intermediate hardened multilayered sedimentary matrix with filled-up interstices and a highly colonised lower eroded matrix of dead crustose coralline algae (Pezzolesi et al. 2017). These habitats, also known as *trottoirs* in the Mediterranean, are understudied and face numerous threats, namely, sea-level rise, human mechanical impact and pollution, which grants them Vulnerable status on the European Red List of Habitats (European Commission et al. 2016; Blanfuné et al. 2023).

5.4 | The Subterranean-Marine Transitional Real (SM)

In the subterranean-marine transitional real (SM), sea caves (SM1.3) are special refuge habitats acting as biodiversity reservoirs (Bussotti et al. 2006; Gerovasileiou and Bianchi 2021). They are formed in a variety of rock types and can include biogenic habitats dominated by encrusting nongeniculate coralline algae (Adey and Vassar 1975; Gerovasileiou and Bianchi 2021). Sea caves have strong biotic zonation due to gradients in light and hydrography, with low-light communities dominated by coralline algae in cave entrances (Guido et al. 2019; Gerovasileiou and Bianchi 2021). Although highly diverse, sea caves are considered low resilient habitats and face many threats, including invasive species, global change and local human impacts (Tillin 2015; Gerovasileiou and Bianchi 2021).

5.5 | The Marine Realm (M)

In the marine realm (M), we identify six global habitat types in which coralline algae are the main biogenic component, all of them in the marine shelf (M1) biome. In photic coral reefs (M1.3), encrusting nongeniculate coralline algae dominate forming coral–algal reefs. Tropical coral–algal reefs (also known as algal reefs) form thick, mostly calcified frameworks of coralline algal crusts, corals, foraminifera, vermetids, serpulids and boring organisms (Littler 1973; Adey 1978, 1998). Encrusting nongeniculate coralline algae can characterise both inshore and fringing reefs, as well as mid and outer-shelf reefs, and thick coralline algal crusts are often more abundant in outer-shelf reefs (Dean et al. 2015). In the tropics, encrusting nongeniculate coralline algae often dominate the windward most exposed crests of reefs, sometimes accounting for up to 90% of the composition of reef crests, creating algal ridges (Adey and McKibbin 1970; Adey 1998). Coralline algae can contribute more than corals to coral reef carbonate production in some reefs (Cornwall et al. 2023). The Taoyuan Algal Reef (Taiwan) is the largest known subtropical intertidal algal reef; it spans over 27 km on a tidal flat and is approximately 4 m thick (Liou et al. 2017; Zhan et al. 2022). It is thought to harbour high coralline algal endemism and overall diversity but is threatened by coastal development and industrial waste run-off (Kuo et al. 2020; Heard et al. 2021; Chen et al. 2022; Zhan et al. 2022). All tropical coral reefs assessed on the IUCN's Red List of Habitats are either endangered or critically endangered (Bland et al. 2019, 2017). Their conservation status is primarily based on increased frequency and severity of warming-induced coral bleaching events (Hughes et al. 2017; Sully et al. 2019; Andrello et al. 2022). The impacts of warming on tropical coralline algae per se are varied, but overall, encrusting nongeniculate coralline algae seem less sensitive to warming stress than scleractinian corals (Cornwall et al. 2022). However, the impacts of global change and human activities on coralline algae need to be better understood and integrated when discussing the vulnerability of coralline algal habitats (Kuffner et al. 2008; Diaz-Pulido et al. 2012; Webster et al. 2013; Cornwall et al. 2017; Heard et al. 2021; Kluibenschedl et al. 2023).

Coralline algae are the deepest known macroalgae and have been found at 268-m depth (Littler et al. 1985), with encrusting nongeniculate coralline algae often being the dominant component of photo-limited marine animal forests (M1.5), forming coralligenous reefs. Coralligenous reefs (also known as coralligenous assemblages, formations, concretions or simply coralligenous) are typical mesophotic habitats of the Mediterranean Sea (Ballesteros 2006). They are among some of the best studied coralline algal habitats (Ferrigno et al. 2023) and were first described by Marion (1883). The term comes from the French word *coralligène*, which means 'coral maker', and is used to describe coralline algae dominated hard bottom communities (Basso et al. 2022). Coralligenous reefs are usually characterised by several layers of encrusting nongeniculate coralline algae (from a few centimetres to several metres thickness) over several kilometres on either rocky walls in the intertidal or subhorizontal sedimentary or rocky substrata in the subtidal, occurring at depths of over 150 m (Bosence 1983; Basso et al. 2022).

Subtidal rocky reefs (M1.6) are often dominated by coralline algae in the photic zone. In Subarctic and Arctic regions, encrusting nongeniculate coralline algae coat most subtidal rocky surfaces and can form thick carbonate crusts (or cor-stromes) that can be as thick as 0.5 m. Coralline algal carbonate crusts occur both in the Atlantic and Pacific ocean basins and may be composed of different taxa, although *Clathromorphum* Foslie and *Boreolithothamnion* species are the most abundant (Adey et al. 2013). In the Arctic, these carbonate crusts may be extremely long-lived, with *Clathromorphum* specimens aged up to 1200 years BP (Adey et al. 2015). This, in combination with their capacity to incorporate certain elements and isotopes in their band-like growth structures, can be useful for biogeochemical analyses and paleoclimate reconstructions (Adey et al. 2013; Halfar et al. 2013; Gould et al. 2022). Carbonate crusts are highly diverse habitats, harbouring macrobenthic communities as diverse as those found in surrounding habitats dominated by canopy macroalgae (Chenelot et al. 2011).

Similarly, encrusting nongeniculate coralline algae are the main biogenic components of subtidal rocky reef habitats usually known as 'urchin barrens'. These often-extensive habitats are distributed worldwide and emerge from a stable-state shift from structurally complex, macroalgae-dominated seascapes (such as kelp forests) to expanses of coralline-encrusted rock due to intense sea urchin grazing (Filbee-Dexter and Scheibling 2014). Even after the drivers of sea urchin outbreaks subside, these barrens often persist, sometimes maintained by other grazers such as limpets (Melis et al. 2019; Piazzi et al. 2016). While often associated with a loss of key ecosystem functions (Eger et al. 2024), coralline barrens are not devoid of life. They support diverse assemblages of benthic mega-invertebrates and can present

10990755, 2025, 3, Downloaded from https://onlinelibrary.wiley.com/doi/10.1002/aqc.70121 by Csic Organización Central Om (Oficialia Mayor) (Urici), Wiley Online Library on [25/03/2025]. See the Terms and Conditions (https://onlinelibrary.wiley.com/terms-and-conditions) on Wiley Online Library for rules of use; OA articles are governed by the applicable Creative Commons License

structurally complex nongeniculate coralline species that provide habitat for a variety of organisms (Agnetta et al. 2024; Ramos et al. 2025).

Geniculate coralline algae are also major colonisers of rocky shores, forming coralline turfs. This habitat can be found worldwide across diverse environments, ranging from polar to tropical regions (Nelson 2009). Geniculate coralline algal turf habitats are characterised by the dense aggregation of geniculate fronds, forming cohesive mats that can reach heights of up to 15 cm (Connell et al. 2014). Their thalli, composed of stiff branches, provide a substratum for the attachment of numerous epiphytes (Soltan et al. 2001) while their three-dimensional structure fosters a high diversity of organisms, particularly small invertebrates (Kelaher and Castilla 2005; Berthelsen et al. 2014; Marchini et al. 2019; Ragazzola et al. 2021).

Finally, the IUCN GET recognises 'Rhodolith/Maerl beds' (M1.10) (Keith, Fragkopolou, et al. 2022). These coralline algal beds are aggregations of alive and dead free-living nongeniculate coralline algae that cover extensive benthic areas (Riosmena-Rodríguez 2017) and are common in fossil deposits (Aguirre et al. 2017). They are distributed worldwide and have a wide-depth range from intertidal to mesophotic zones (Davies et al. 2004; Wilson and Blake 2011; Pereira-Filho et al. 2012; Basso et al. 2016; Veras et al. 2020; Pierri et al. 2024). Here, we propose that FEG M1.10 is renamed as coralline algal beds—also including articulith beds (formed by geniculate coralline algal nodules) and removing linguistic uncertainty related to different morphotypes and locations. In the global typology, GET M1.10 is defined as benthic carbonate systems dominated by free-living, slow-growing, long-lived coralline algae covering 30%–100% of the seafloor within the beds, providing autochthonous energy to the system. In the GET definition, only nongeniculate coralline algae are included; however, the ecosystem properties, resources, ambient environmental conditions, disturbance regimes and biotic interactions used to define them could also be applied to free-living geniculate coralline algae (Keith, Fragkopolou, et al. 2022). For instance, rhodolith and maerl beds are grouped on the basis of moderate productivity (Martin et al. 2005; Riosmena-Rodríguez 2017; Qui-Minet et al. 2022), high associated biodiversity (Peña et al. 2014; Boyé et al. 2019; Helias and Burel 2023) and high structural complexity (Jardim et al. 2022; Bélanger and Gagnon 2023; Cabrito et al. 2024). Although understudied and possibly rare, articulith beds probably share most of these characteristics, are formed through similar processes and face similar pressures (Tâmega et al. 2017, 2021). Little is known, however, about the durability of the structure of articuliths, which may not be as long-lasting as the thalli formed by nongeniculate corallines—although closely packed thalli can protect geniculate corallines from breakage, a feature that may be enhanced in articuliths (Martone and Denny 2008a, 2008b).

6 | Conclusion

Inconsistent definitions can lead to ecological uncertainty and variable conservation policies for habitats with similar traits, functions and services and facing similar anthropic pressures. We have suggested a consistent set of terms to describe coralline algae and coralline algal habitats to help put them into a global context to support local actions and decision-making (Keith, Ferrer-Paris, et al. 2022). We highlight the importance of clarifying uncertain terms and simplifying dichotomies through contextualisation when using polysemic or synonymous terms. We resolve, in an integrative and adaptive way, a long-lasting debate on the use of the terms 'maerl' and 'rhodolith' through the umbrella term 'coralline algal beds' and explicit definitions that allow established terms in local and global scientific and management frameworks to coexist without creating uncertainty. Language is adaptative and ever-changing, and while a diverse coralline algal terminology reflects the widespread distribution and growing scientific and conservation relevance of the group, authors must have a contextualisation tool to simplify and clarify the terms they use. In this context, we urge the scientific community to adopt a more cohesive terminology for coralline algae, to improve scientific progression and international collaborations and to facilitate conservation, public understanding and stakeholder engagement.

Acknowledgements

We thank Elsevier and Aquatic Conservation: Freshwater and Marine Ecosystems for sponsoring the 7th International Coralline Algae Meeting, in which the terminology of coralline algae was discussed. We also thank Dr Guilherme H. Pereira-Filho and Dr Ricardo Bahia for their insights and feedback on the final manuscript.

Conflicts of Interest

The authors declare no conflicts of interest.

Data Availability Statement

Data sharing is not applicable to this article as no new data were created or analysed in this study.

References

Adey, W. H. 1978. "Algal Ridges of the Caribbean Sea and West Indies." *Phycologia* 17: 361–367. https://doi.org/10.2216/i0031-8884-17-4-361.1.

Adey, W. H. 1998. "Coral Reefs: Algal Structured and Mediated Ecosystems in Shallow, Turbulent, Alkaline Waters." *Journal of Phycology* 34: 393–406.

Adey, W. H., J. Halfar, and B. Williams. 2013. "The Coralline Genus *Clathromorphum* Foslie emend. Adey: Biological, Physiological, and Ecological Factors Controlling Carbonate Production in an Arctic-Subarctic Climate Archive." *Smithsonian Contributions to the Marine Sciences* 40: 1–41. https://doi.org/10.5479/si.1943667X.40.1.

Adey, W. H., J. J. Hernandez-Kantun, G. Johnson, and P. W. Gabrielson. 2015. "DNA Sequencing, Anatomy, and Calcification Patterns Support a Monophyletic, Subarctic, Carbonate Reef-Forming Clathromorphum (Hapalidiaceae, Corallinales, Rhodophyta)." *Journal of Phycology* 51: 189–203. https://doi.org/10.1111/jpy.12266.

Adey, W. H., and I. G. Macintyre. 1973. "Crustose Coralline Algae: A Re-Evaluation in the Geological Sciences." *GSA Bulletin* 84: 883–904. https://doi.org/10.1130/0016–7606(1973)84<883:CCAARI>2.0.CO;2.

Adey, W. H., and D. L. McKibbin. 1970. "Studies on the Maerl Species *Phymatolithon calcareum* (Pallas) nov. comb. and *Lithothamnium corralloides* Crouan in the Ria de Vigo." *Botanica Marina* 13: 100–106. https://doi.org/10.1515/botm.1970.13.2.100.

Adey, W. H., and C. P. Sperapani. 1971. "The Biology of *Kvaleya epilaeve*, a New Parasitic Genus and Species of Corallinaceae." *Phycologia* 10: 29–42. https://doi.org/10.2216/i0031-8884-10-1-29.1.

10990755, 2025, 3, Downloaded from https://onlinelibrary.wiley.com/doi/10.1002/aqc.70121 by Csic Organización Central Om (Oficialia Mayor) (Urici), Wiley Online Library on [25/03/2025]. See the Terms and Conditions (https://onlinelibrary.wiley.com/terms-and-conditions) on Wiley Online Library for rules of use; OA articles are governed by the applicable Creative Commons License

Adey, W. H., and J. M. Vassar. 1975. "Colonization, Succession and Growth Rates of Tropical Crustose Coralline Algae (Rhodophyta, Cryptonemiales)." *Phycologia* 14: 55–69. https://doi.org/10.2216/i0031-8884-14-2-55.1.

Agardy, T. 2005. "Global Marine Conservation Policy Versus Site-Level Implementation: The Mismatch of Scale and Its Implications." *Marine Ecology Progress Series* 300: 242–248.

Agnetta, D., C. Bonaviri, F. Badalamenti, F. Di Trapani, and P. Gianguzza. 2024. "Coralline Barrens and Benthic Mega-Invertebrates: An Intimate Connection." *Marine Environmental Research* 199: 106579. https://doi.org/10.1016/j.marenvres.2024.106579.

Aguirre, J., J. C. Braga, and D. Bassi. 2017. "Rhodoliths and Rhodolith Beds in the Rock Record." In *Rhodolith/Maërl Beds: A Global Perspective, Coastal Research Library*, edited by R. Riosmena-Rodríguez, W. Nelson, and J. Aguirre, 105–138. Springer International Publishing. https://doi.org/10.1007/978-3-319-29315-8_5.

Aguirre, J., F. Perfectti, and J. C. Braga. 2010. "Integrating Phylogeny, Molecular Clocks, and the Fossil Record in the Evolution of Coralline Algae (Corallinales and Sporolithales, Rhodophyta)." *Paleobiology* 36: 519–533. https://doi.org/10.1666/09041.1.

Amado-Filho, G. M., G. H. Pereira-Filho, R. G. Bahia, D. P. Abrantes, P. C. Veras, and Z. Matheus. 2012. "Occurrence and Distribution of Rhodolith Beds on the Fernando de Noronha Archipelago of Brazil." *Aquatic Botany* 101: 41–45. https://doi.org/10.1016/j.aquabot.2012.03.016.

Andrello, M., E. S. Darling, A. Wenger, A. F. Suárez-Castro, S. Gelfand, and G. N. Ahmadia. 2022. "A Global Map of Human Pressures on Tropical Coral Reefs." *Conservation Letters* 15: e12858. https://doi.org/10.1111/conl.12858.

Aria, M., and C. Cuccurullo. 2017. "Bibliometrix: An R-Tool for Comprehensive Science Mapping Analysis." *Journal of Informetrics* 11: 959–975. https://doi.org/10.1016/j.joi.2017.08.007.

Arnold, C., D. Bélanger, and P. Gagnon. 2021. "Growth Resilience of Subarctic Rhodoliths (*Lithothamnion glaciale*, Rhodophyta) to Chronic Low Sea Temperature and Irradiance." *Journal of Phycology* 58: 251–266. https://doi.org/10.1111/jpy.13231.

Augris, C., and P. Berthou. 1990. "Les Gisements de Maërl en Bretagne (Report)."

Axelsson, M. B. 2023. *A Categorisation System for Maerl Bed Habitats in England, NERR123*. Natural England.

Ballesteros, E. 1994. "The Deep-Water Peyssonnelia Beds From the Balearic Islands (Western Mediterranean)." *Marine Ecology* 15: 233–253. https://doi.org/10.1111/j.1439-0485.1994.tb00055.x.

Ballesteros, E. 2006. "Mediterranean Coralligenous Assemblages: A Synthesis of Present Knowledge." *Oceanography and Marine Biology: An Annual Review* 48: 123–195.

Barbera, C., C. Bordehore, J. A. Borg, et al. 2003. "Conservation and Management of Northeast Atlantic and Mediterranean Maerl Beds." *Aquatic Conservation: Marine and Freshwater Ecosystems* 13: S65–S76. https://doi.org/10.1002/aqc.569.

Barberá, C., S. Mallol, A. Vergés, M. Cabanellas-Reboredo, D. Díaz, and R. Goñi. 2017. "Maerl Beds Inside and Outside a 25-Year-Old No-Take Area." *Marine Ecology Progress Series* 572: 77–90. https://doi.org/10.3354/meps12110.

Barberá, C., J. Moranta, F. Ordines, et al. 2012. "Biodiversity and Habitat Mapping of Menorca Channel (Western Mediterranean): Implications for Conservation." *Biodiversity and Conservation* 21: 701–728. https://doi.org/10.1007/s10531-011-0210-1.

Barnes, J., D. J. Bellamy, D. J. Jones, et al. 1971. "Morphology and Ecology of the Reef Front of Aldabra." *Symposia of the Zoological Society of London* 28: 87–114.

Barnes, J., D. J. Bellamy, D. J. Jones, B. A. Whitton, E. Drew, and J. Lythgoe. 1970. "Sublittoral Reef Phenomena of Aldabra." *Nature* 225: 268–269. https://doi.org/10.1038/225268a0.

Basso, D. 1998. "Deep Rhodolith Distribution in the Pontian Islands, Italy: A Model for the Paleoecology of a Temperate Sea." *Palaeogeography Palaeoclimatology Palaeoecology* 137: 173–187. https://doi.org/10.1016/S0031-0182(97)00099-0.

Basso, D. 2012. "Carbonate Production by Calcareous Red Algae and Global Change." *Geodiversitas* 34: 13–33. https://doi.org/10.5252/g2012n1a2.

Basso, D., L. Babbini, S. Kaleb, V. A. Bracchi, and A. Falace. 2016. *Monitoring Deep Mediterranean Rhodolith Beds, Aquatic Conservation: Marine and Freshwater Ecosystems*. John Wiley and Sons Ltd. https://doi.org/10.1002/aqc.2586.

Basso, D., V. A. Bracchi, P. Bazzicalupo, M. Martini, F. Maspero, and G. Bavestrello. 2022. "Living Coralligenous as Geo-Historical Structure Built by Coralline Algae." *Frontiers in Earth Science* 10: 961632.

Bélanger, D., and P. Gagnon. 2023. "Spatiotemporal Variability in Subarctic *Lithothamnion glaciale* Rhodolith Bed Structural Complexity and Macrofaunal Diversity." *Diversity* 15: 774. https://doi.org/10.3390/d15060774.

Bellwood, D., S. Brandl, M. McWilliam, R. Streit, H. Yan, and S. Tebbett. 2024. "Studying Functions on Coral Reefs: Past Perspectives, Current Conundrums, and Future Potential." *Coral Reefs* 43: 281–297. https://doi.org/10.1007/s00338-024-02474-z.

Bennett, N. J. 2019. "Marine Social Science for the Peopled Seas." *Coastal Management* 47: 244–252. https://doi.org/10.1080/08920753.2019.1564958.

Berchez, F. 2022. "Brazil: Heed Price of Marine Mining for an Alternative Fertilizer." *Nature* 607: 239. https://doi.org/10.1038/d41586-022-01890-x.

Berthelsen, A., J. Hewitt, and R. Taylor. 2014. "Coralline Turf-Associated Fauna Are Affected More by Spatial Variability Than by Host Species Identity." *Marine Biodiversity* 45: 689–699. https://doi.org/10.1007/s12526-014-0270-z.

Bianchi, C. N., and C. Morri. 2025. "Different Rhodolith Assemblages Host Distinct Associated Species but Similar Ecological Groups: A Case Study in NW Mediterranean Sea." *Aquatic Botany* 196: 103826. https://doi.org/10.1016/j.aquabot.2024.103826.

Blackstone, J. 1746. *Specimen Botanicum quo Plantarum Plurium Rariorum Angliae Indigenarum Loci Natales Illustrantur*. Typis Gulielmi Faden. https://doi.org/10.5962/bhl.title.106704.

Bland, L. M., E. Nicholson, R. M. Miller, et al. 2019. "Impacts of the IUCN Red List of Ecosystems on Conservation Policy and Practice." *Conservation Letters* 12: e12666. https://doi.org/10.1111/conl.12666.

Bland, L. M., T. J. Regan, M. N. Dinh, et al. 2017. "Using Multiple Lines of Evidence to Assess the Risk of Ecosystem Collapse." *Proceedings of the Royal Society B: Biological Sciences* 284: 20170660. https://doi.org/10.1098/rspb.2017.0660.

Blanfuné, A., C.-F. Boudouresque, M. Verlaque, A. Minne, F. Noisette, and T. Thibaut. 2023. "Impact of Sea Level Rise on the Mediterranean *Lithophyllum byssoides* Rims." *Scientific Reports* 13: 10577. https://doi.org/10.1038/s41598-023-37110-3.

Bordehore, C., A. A. Ramos-Esplá, and R. Riosmena-Rodríguez. 2003. "Comparative Study of Two Maerl Beds With Different Otter Trawling History, Southeast Iberian Peninsula." *Aquatic Conservation: Marine and Freshwater Ecosystems* 13: S43–S54. https://doi.org/10.1002/aqc.567.

Bosellini, A., and R. N. Ginsburg. 1971. "Form and Internal Structure of Recent Algal Nodules (Rhodolites) From Bermuda." *Journal of Geology* 79: 669–682.

10990755, 2025, 3, Downloaded from https://onlinelibrary.wiley.com/doi/10.1002/aqc.70121 by Csic Organización Central Om (Oficialia Mayor) (Urici), Wiley Online Library on [25/03/2025]. See the Terms and Conditions (https://onlinelibrary.wiley.com/terms-and-conditions) on Wiley Online Library for rules of use; OA articles are governed by the applicable Creative Commons License

Bosence, D. W. J. 1983. "Coralline Algal Reef Frameworks." *Journal of the Geological Society* 140: 365–376. https://doi.org/10.1144/gsjgs.140.3.0365.

Boyé, A., É. Thiébaut, J. Grall, et al. 2019. "Trait-Based Approach to Monitoring Marine Benthic Data Along 500 km of Coastline." *Diversity and Distributions* 25: 1879–1896. https://doi.org/10.1111/ddi.12987.

Bracchi, V., S. Caronni, A. Meroni, et al. 2022. "Morphostructural Characterization of the Heterogeneous Rhodolith Bed at the Marine Protected Area "Capo Carbonara" (Italy) and Hydrodynamics." *Diversity* 14: 51. https://doi.org/10.3390/d14010051.

Bracchi, V. A., P. Bazzicalupo, L. Fallati, et al. 2022. "The Main Builders of Mediterranean Coralligenous: 2D and 3D Quantitative Approaches for Its Identification." *Frontiers in Earth Science* 10: 910522.

Brodie, J., R. H. Walker, C. Williamson, and L. M. Irvine. 2013. "Epitypification and Redescription of *Corallina officinalis* L., the Type of the Genus, and *C. elongata* Ellis *et* Solander (Corallinales, Rhodophyta)." *Cryptogamie Algologie* 34: 49–56.

Brodie, J., J. Wilbraham, C. Maggs, et al. 2023. "Red List for British Seaweeds: Evaluating the IUCN Methodology for Non-Standard Marine Organisms." *Biodiversity and Conservation* 32: 1–19. https://doi.org/10.1007/s10531-023-02649-0.

Brodie, J., C. J. Williamson, D. A. Smale, et al. 2014. "The Future of the Northeast Atlantic Benthic Flora in a High CO_2 World." *Ecology and Evolution* 4: 2787–2798. https://doi.org/10.1002/ece3.1105.

Brodie, J. F. 2009. "Is Research Effort Allocated Efficiently for Conservation? Felidae as a Global Case Study." *Biodiversity and Conservation* 18: 2927–2939. https://doi.org/10.1007/s10531-009-9617-3.

Brugnach, M., A. Dewulf, C. Pahl-Wostl, and T. Taillieu. 2008. "Toward a Relational Concept of Uncertainty: About Knowing Too Little, Knowing Too Differently, and Accepting Not to Know." *Ecology and Society* 13: 30. https://doi.org/10.5751/ES-02616-130230.

Buchbinder, B., and R. B. Halley. 1985. "Occurrence and Preservation of Eocene Squamariacean and Coralline Rhodoliths: Eua, Tonga." In *Paleoalgology*, edited by D. F. Toomey and M. H. Nitecki, 248–256. Springer. https://doi.org/10.1007/978-3-642-70355-3_19.

Bussotti, S., A. Terlizzi, S. Fraschetti, G. Belmonte, and F. Boero. 2006. "Spatial and Temporal Variability of Sessile Benthos in Shallow Mediterranean Marine Caves." *Marine Ecology Progress Series* 325: 109–119. https://doi.org/10.3354/meps325109.

Byers, J. E. 2022. "Using Ecosystem Engineers to Enhance Multiple Ecosystem Processes." *Functional Ecology* 38: 22–36. https://doi.org/10.1111/1365-2435.14130.

Cabioch, J. 1969. "Les Fonds de Maërl de la Baie de Morlaix et Leur Peuplement Végétal." *Cahiers de Biologie Marine* 10: 139–161.

Cabrito, A., S. de Juan, H. Hinz, and F. Maynou. 2024. "Morphological Insights Into the Three-Dimensional Complexity of Rhodolith Beds." *Marine Biology* 171: 127. https://doi.org/10.1007/s00227-024-04437-y.

Chauvin, J. F. 1842. *Recherches sur l'Organisation, la Fructification et la Classification de Plusieurs Genres d'Algues: Avec la Description de Quelques Espèces Inédites on peu Connues: Essai d'une Répartition des Polypiers Calcifères de Lamouroux Dans la Classe des Algues*. Éditeur non Identifié.

Chen, M.-H., Y.-Y. Huang, B.-Y. Huang, et al. 2022. "Historical Connectivity and Demography of the Ferocious Reef Crab, *Eriphia ferox* (Crustacea; Eriphiidae), Demonstrate That Taoyuan Algal Reef Is an Essential Population Source Along the East Taiwan Strait." *Frontiers in Marine Science* 8: 799989. https://doi.org/10.3389/fmars.2021.799989.

Chenelot, H., S. C. Jewett, and M. K. Hoberg. 2011. "Macrobenthos of the Nearshore Aleutian Archipelago, With Emphasis on Invertebrates Associated With *Clathromorphum nereostratum* (Rhodophyta, Corallinaceae)." *Marine Biodiversity* 41: 413–424. https://doi.org/10.1007/s12526-010-0071-y.

Cira, T. M., K. Quick, and R. C. Venette. 2019. "Watch Your Language: Consequences of Linguistic Uncertainty for Insect Management." *American Entomologist* 65: 258–267. https://doi.org/10.1093/ae/tmz068.

Connell, S. D., M. S. Foster, and L. Airoldi. 2014. "What Are Algal Turfs? Towards a Better Description of Turfs." *Marine Ecology Progress Series* 495: 299–307. https://doi.org/10.3354/meps10513.

Cornwall, C., J. Carlot, O. Branson, et al. 2023. "Crustose Coralline Algae Can Contribute More Than Corals to Coral Reef Carbonate Production." *Communications Earth & Environment* 4: 105. https://doi.org/10.1038/s43247-023-00766-w.

Cornwall, C. E., S. Comeau, and M. T. McCulloch. 2017. "Coralline Algae Elevate pH at the Site of Calcification Under Ocean Acidification." *Global Change Biology* 23: 4245–4256. https://doi.org/10.1111/gcb.13673.

Cornwall, C. E., B. P. Harvey, S. Comeau, et al. 2022. "Understanding Coralline Algal Responses to Ocean Acidification: Meta-Analysis and Synthesis." *Global Change Biology* 28: 362–374. https://doi.org/10.1111/gcb.15899.

Crump, N. S., E. J. Cother, and G. J. Ash. 1999. "Clarifying the Nomenclature in Microbial Weed Control." *Biocontrol Science and Technology* 9: 89–97. https://doi.org/10.1080/09583159929947.

Davies, P. J., J. C. Braga, M. Lund, and J. M. Webster. 2004. "Holocene Deep Water Algal Buildups on the Eastern Australian Shelf." *PALAIOS* 19: 598–609.

Dean, A., R. Steneck, D. Tager, and J. Pandolfi. 2015. "Distribution, Abundance and Diversity of Crustose Coralline Algae on the Great Barrier Reef." *Coral Reefs* 34: 581–594. https://doi.org/10.1007/s00338-015-1263-5.

Deinhart, M., M. S. Mills, and T. Schils. 2022. "Community Assessment of Crustose Calcifying Red Algae as Coral Recruitment Substrates." *PLoS ONE* 17: e0271438. https://doi.org/10.1371/journal.pone.0271438.

Diaz-Pulido, G., K. R. N. Anthony, D. I. Kline, S. Dove, and O. Hoegh-Guldberg. 2012. "Interactions Between Ocean Acidification and Warming on the Mortality and Dissolution of Coralline Algae." *Journal of Phycology* 48: 32–39. https://doi.org/10.1111/j.1529-8817.2011.01084.x.

Dorey, N., S. Martin, and L. Kwiatkowski. 2023. "Ocean Acidification Enhances Primary Productivity and Nocturnal Carbonate Dissolution in Intertidal Rock Pools." *Biogeosciences* 20: 4289–4306. https://doi.org/10.5194/bg-20-4289-2023.

Drew, J. A. 2005. "Use of Traditional Ecological Knowledge in Marine Conservation." *Conservation Biology* 19: 1286–1293. https://doi.org/10.1111/j.1523-1739.2005.00158.x.

Edgar, G. J., A. E. Bates, T. J. Bird, et al. 2016. "New Approaches to Marine Conservation Through the Scaling Up of Ecological Data." *Annual Review of Marine Science* 8: 435–461. https://doi.org/10.1146/annurev-marine-122414-033921.

Edgar, G. J., R. D. Stuart-Smith, T. J. Willis, et al. 2014. "Global Conservation Outcomes Depend on Marine Protected Areas With Five Key Features." *Nature* 506: 216–220. https://doi.org/10.1038/nature13022.

Eger, A. M., C. O. Blain, A. L. Brown, S. S. W. Chan, K. I. Miller, and A. Vergés. 2024. "Kelp Forests Versus Urchin Barrens: A Comparison of Ecosystem Functions and Services Provided by Two Alternative Stable Marine Habitats." *Proceedings of the Royal Society B: Biological Sciences* 291: 20241539. https://doi.org/10.1098/rspb.2024.1539.

Ellis, J., and D. C. Solander. 1786. *The Natural History of Many Curious and Uncommon Zoophytes: Collected From Various Parts of the Globe*. B. White and Son.

Ellison, A. M. 2019. "Foundation Species, Non-Trophic Interactions, and the Value of Being Common." *iScience* 13: 254–268. https://doi.org/10.1016/j.isci.2019.02.020.

10990755, 2025, 3, Downloaded from https://onlinelibrary.wiley.com/doi/10.1002/aqc.70121 by Csic Organización Central Om (Oficialia Mayor) (Urici), Wiley Online Library on [25/03/2025]. See the Terms and Conditions (https://onlinelibrary.wiley.com/terms-and-conditions) on Wiley Online Library for rules of use; OA articles are governed by the applicable Creative Commons License

European Commission, Directorate-General for Environment, J. R. Rodwell, et al. 2016. *European Red List of Habitats. Part 1, Marine Habitats*. Publications Office of the European Union. https://doi.org/10.2779/032638.

Ferrigno, F., F. Rendina, R. Sandulli, and G. Russo. 2023. "Coralligenous Assemblages: Research Status and Trends of a Key Mediterranean Biodiversity Hotspot Through Bibliometric Analysis." *Ecological Questions* 35: 1–32. https://doi.org/10.12775/EQ.2024.002.

Filbee-Dexter, K., and R. E. Scheibling. 2014. "Sea Urchin Barrens as Alternative Stable States of Collapsed Kelp Ecosystems." *Marine Ecology Progress Series* 495: 1–25. https://doi.org/10.3354/meps10573.

Firth, L. B., M. Schofield, F. J. White, M. W. Skov, and S. J. Hawkins. 2014. "Biodiversity in Intertidal Rock Pools: Informing Engineering Criteria for Artificial Habitat Enhancement in the Built Environment." *Marine Environmental Research: Special Issue: Managing Biodiversity in a Changing Ocean* 102: 122–130. https://doi.org/10.1016/j.marenvres.2014.03.016.

Foslie, M. 1894. *The Norwegian Forms of Lithothamnion*. Royal Norwegian Society of Sciences and Letters.

Foster, M. S. 2001. "Rhodoliths: Between Rocks and Soft Places." *Journal of Phycology* 37: 659–667. https://doi.org/10.1046/j.1529-8817.2001.00195.x.

Fredericq, S., and J. Norris. 1995. "A New Order (Rhodogorgonales) and Family (Rhodogorgonaceae) of Red Algae Composed of Two Tropical Calciferous Genera, *Renouxia* gen. nov. and *Rhodogorgon*." *Cryptogamic Botany* 5: 316–331.

Friant, G., and G. Marie. 2010. "Diagnostic sur le Patrimoine Maritime Culturel Immatériel des Communes Littorales du Parc Naturel Marin d'Iroise."

Gerovasileiou, V., and C. Bianchi. 2021. "Mediterranean Marine Caves: A Synthesis of Current Knowledge." *Oceanography and Marine Biology* 59: 1–88.

Ginsburg, R. N., and A. Bosellini. 1973. "Form and Internal Structure of Recent Algal Nodules (Rhodolites) From Bermuda: A Reply." *Journal of Geology* 81: 239. https://doi.org/10.1086/627843.

Gould, J., J. Halfar, W. H. Adey, and J. B. Ries. 2022. "Growth as a Function of Sea Ice Cover, Light and Temperature in the Arctic/Subarctic Coralline *C. compactum*: A Year-Long In Situ Experiment in the High Arctic." *Frontiers in Marine Science* 9: 900033.

Grahame, J., and F. S. Hanna. 1989. "Factors Affecting the Distribution of the Epiphytic Fauna of *Corallina officinalls* (L.) on an Exposed Rocky Shore." *Ophelia* 30: 113–129. https://doi.org/10.1080/00785326.1989.10430839.

Grall, J., and J. M. Hall-Spencer. 2003. "Problems Facing Maerl Conservation in Brittany." *Aquatic Conservation: Marine and Freshwater Ecosystems* 13: S55–S64. https://doi.org/10.1002/aqc.568.

Guido, A., V. Gerovasileiou, F. Russo, et al. 2019. "Composition and Biostratinomy of Sponge-Rich Biogenic Crusts in Submarine Caves (Aegean Sea, Eastern Mediterranean)." *Palaeogeography Palaeoclimatology Palaeoecology* 534: 109338. https://doi.org/10.1016/j.palaeo.2019.109338.

Halfar, J., W. H. Adey, A. Kronz, S. Hetzinger, E. Edinger, and W. W. Fitzhugh. 2013. "Arctic Sea-Ice Decline Archived by Multicentury Annual-Resolution Record From Crustose Coralline Algal Proxy." *Proceedings of the National Academy of Sciences* 110: 19737–19741. https://doi.org/10.1073/pnas.1313775110.

Hamilton, S. E., and D. Casey. 2016. "Creation of a High Spatio-Temporal Resolution Global Database of Continuous Mangrove Forest Cover for the 21st Century (CGMFC-21)." *Global Ecology and Biogeography* 25: 729–738. https://doi.org/10.1111/geb.12449.

Harvey, A., W. Woelkerling, T. Farr, K. Neill, and W. Nelson. 2005. *Coralline Algae of Central New Zealand an Identification Guide to Common "Crustose" Species*. 57th ed. NIWA.

Harvey, W. H. 1847. *Nereis australis, or Algae of the Southern Ocean: Being Figures and Descriptions of Marine Plants, Collected on the Shores of the Cape of Good Hope, the Extra-Tropical Australian Colonies, Tasmania, New Zealand, and the Antarctic Regions*. Herbarium of the Dublin University.

Hattam, C., S. Broszeit, O. Langmead, et al. 2021. "A Matrix Approach to Tropical Marine Ecosystem Service Assessments in South East Asia." *Ecosystem Services* 51: 101346. https://doi.org/10.1016/j.ecoser.2021.101346.

Heard, J., W.-C. Tung, Y.-D. Pei, et al. 2021. "Coastal Development Threatens Datan Area Supporting Greatest Fish Diversity at Taoyuan Algal Reef, Northwestern Taiwan." *Aquatic Conservation: Marine and Freshwater Ecosystems* 31: 590–604. https://doi.org/10.1002/aqc.3477.

Helias, M., and T. Burel. 2023. *Maerl-Associated Macroalgae in the Bay of Brest (Brittany, France)*. Vol. 53, 14. Marine Biodiversity. https://doi.org/10.1007/s12526-022-01322-z.

Hernandez-Kantun, J. J., J. M. Hall-Spencer, J. Grall, et al. 2016. "North Atlantic Rhodolith Beds." *Rhodolith/Maërl Beds: A Global Perspective*: 265–279. https://doi.org/10.1007/978-3-319-29315-8_10.

Hind, K. R., P. W. Gabrielson, C. Jensen, and P. T. Martone. 2018. "Evolutionary Reversals in Bossiella (Corallinales, Rhodophyta): First Report of a Coralline Genus With Both Geniculate and Nongeniculate Species." *Journal of Phycology* 54: 788–798. https://doi.org/10.1111/jpy.12788.

Hinojosa-Arango, G., C. A. Maggs, and M. P. Johnson. 2009. "Like a Rolling Stone: The Mobility of Maerl (Corallinaceae) and the Neutrality of the Associated Assemblages." *Ecology* 90: 517–528. https://doi.org/10.1890/07-2110.1.

Hodges, K. E. 2008. "Defining the Problem: Terminology and Progress in Ecology." *Frontiers in Ecology and the Environment* 6: 35–42. https://doi.org/10.1890/060108.

Hughes, T. P., J. T. Kerry, M. Álvarez-Noriega, et al. 2017. "Global Warming and Recurrent Mass Bleaching of Corals." *Nature* 543: 373–377. https://doi.org/10.1038/nature21707.

Irvine, L. M., and Y. M. Chamberlain. 1994. *Seaweeds of the British Isles, Volume 1 Rhodophyta, Part 2B. Corallinales, Hildenbrandiales*. Natural History Museum.

Jacquotte, R. 1962. "Etude des Fonds de Maërl de Méditerranée." *Recueils des Travaux de la Station Marine d'Endoume* 26: 141–216.

Jardim, V. L., O. Gauthier, C. Toumi, and J. Grall. 2022. "Quantifying Maerl (Rhodolith) Habitat Complexity Along an Environmental Gradient at Regional Scale in the Northeast Atlantic." *Marine Environmental Research* 181: 105768. https://doi.org/10.1016/j.marenvres.2022.105768.

Jenkins, T., M.-L. Guillemin, C. Simon Nutbrown, H. Burdett, J. Stevens, and V. Peña. 2021. "Whole Genome Genotyping Reveals Discrete Genetic Diversity in North-East Atlantic Maerl Beds." *Evolutionary Applications* 14: 1558–1571. https://doi.org/10.1111/eva.13219.

Jeong, S. Y., W. A. Nelson, J. E. Sutherland, et al. 2021. "Corallinapetrales and Corallinapetraceae: A New Order and Family of Coralline Red Algae Including *Corallinapetra gabrielii* comb. nov." *Journal of Phycology* 57: 849–862. https://doi.org/10.1111/jpy.13115.

Johansen, H. W. 1981. *Coralline Algae: A First Synthesis*. CRC Press.

Kéfi, S., V. Domínguez-García, I. Donohue, C. Fontaine, E. Thébault, and V. Dakos. 2019. "Advancing Our Understanding of Ecological

10990755, 2025, 3, Downloaded from https://onlinelibrary.wiley.com/doi/10.1002/aqc.70121 by Csic Organización Central Om (Oficialia Mayor) (Urici), Wiley Online Library on [25/03/2025]. See the Terms and Conditions (https://onlinelibrary.wiley.com/terms-and-conditions) on Wiley Online Library for rules of use; OA articles are governed by the applicable Creative Commons License

Stability." *Ecology Letters* 22: 1349–1356. https://doi.org/10.1111/ele.13340.

Keith, D. A., J. R. Ferrer-Paris, E. Nicholson, et al. 2022. "A Function-Based Typology for Earth's Ecosystems." *Nature* 610: 513–518. https://doi.org/10.1038/s41586-022-05318-4.

Keith, D. A., E. Fragkopolou, J. Assis, and N. Schubert. 2022. "M1.10 Rhodolith/Maërl Beds." In *A Function-Based Typology for Earth's Ecosystems—Appendix S4. The IUCN Global Ecosystem Typology v2.1: Descriptive Profiles for Biomes and Ecosystem Functional Groups*. Nature.

Kelaher, B. P., and J. C. Castilla. 2005. "Habitat Characteristics Influence Macrofaunal Communities in Coralline Turf More Than Mesoscale Coastal Upwelling on the Coast of Northern Chile." *Estuarine, Coastal and Shelf Science* 63: 155–165. https://doi.org/10.1016/j.ecss.2004.10.017.

Kelaher, B. P., M. G. Chapman, and A. J. Underwood. 2001. "Spatial Patterns of Diverse Macrofaunal Assemblages in Coralline Turf and Their Associations With Environmental Variables." *Journal of the Marine Biological Association of the United Kingdom* 81: 917–930. https://doi.org/10.1017/S0025315401004842.

Klemfuss, N., B. Prinzmetal, and R. Ivry. 2012. "How Does Language Change Perception: A Cautionary Note." *Frontiers in Psychology* 3: 78.

Kluibenschedl, A., C. Cornwall, W. Nelson, M. Lamare, D. Pritchard, and C. Hepburn. 2023. "Interactive Effects of Ocean Acidification and Water Flow on Growth and Recruitment of Early Successional Coralline Algal Communities." *Phycologia* 62: 637–647. https://doi.org/10.1080/00318884.2023.2272776.

Koletić, N., A. Alegro, A. Rimac, N. Vuković, and V. Šegota. 2020. "Catalogue of Croatian Freshwater Rhodophytes." *Phytotaxa* 434: 151–169. https://doi.org/10.11646/phytotaxa.434.2.2.

Kolzenburg, R., F. D'Amore, S. McCoy, and F. Ragazzola. 2021. "Marginal Populations Show Physiological Adaptations and Resilience to Future Climatic Changes Across a North Atlantic Distribution." *Environmental and Experimental Botany* 188: 104522. https://doi.org/10.1016/j.envexpbot.2021.104522.

Kovalenko, K. E., S. M. Thomaz, and D. M. Warfe. 2012. "Habitat Complexity: Approaches and Future Directions." *Hydrobiologia* 685: 1–17. https://doi.org/10.1007/s10750-011-0974-z.

Krumhansl, K. A., D. K. Okamoto, A. Rassweiler, et al. 2016. "Global Patterns of Kelp Forest Change Over the Past Half-Century." *Proceedings of the National Academy of Sciences* 113: 13785–13790. https://doi.org/10.1073/pnas.1606102113.

Kuffner, I. B., A. J. Andersson, P. L. Jokiel, K. S. Rodgers, and F. T. Mackenzie. 2008. "Decreased Abundance of Crustose Coralline Algae due to Ocean Acidification." *Nature Geoscience* 1: 114–117. https://doi.org/10.1038/ngeo100.

Kujala, H., M. A. Burgman, and A. Moilanen. 2013. "Treatment of Uncertainty in Conservation Under Climate Change." *Conservation Letters* 6: 73–85. https://doi.org/10.1111/j.1755-263X.2012.00299.x.

Kuo, C.-Y., S. Keshavmurthy, A. Chung, et al. 2020. "Demographic Census Confirms a Stable Population of the Critically-Endangered Caryophyllid Coral *Polycyathus chaishanensis* (Scleractinia; Caryophyllidae) in the Datan Algal Reef, Taiwan." *Scientific Reports* 10: 10585. https://doi.org/10.1038/s41598-020-67653-8.

Lamarck, J. B. P. A. D. 1801. *Système des Animaux Sans Vertèbres, ou, Tableau Général des Classes, des Ordres et des Genres de ces Animaux : Présentant Leurs Caractères Essentiels et Leur Distribution, d'Après la Considération de Leurs Rapports Naturels et de Leur Organisation, et Suivant l'Arrangement Établi Dans les Galeries du Muséum d'Hist. Naturelle, Parmi Leurs Dépouilles Conservées : Précédé du Discours d'Ouverture du Cours de Zoologie, Donné Dans le Muséum National d'Histoire Naturelle l'An 8 de la République*. Muséum National d'Histoire Naturelle. https://doi.org/10.5962/bhl.title.116650.

Legrand, E., P. Riera, O. Bohner, et al. 2018. "Impact of Ocean Acidification and Warming on the Productivity of a Rock Pool Community." *Marine Environmental Research* 136: 78–88. https://doi.org/10.1016/j.marenvres.2018.02.010.

Lemoine, P. 1910. "Essai de classification des Mélobésiées basée sur la structure anatomique." *Bulletin de la Société Botanique de France* 57, no. 5: 323–331.

Linnaeus, C. 1758. *Systema Naturae per Regna Tria Naturae: Secundum Classes, Ordines, Genera, Species, cum Characteribus, Differentiis, Synonymis, Locis*. Holmiae, Impensis Direct. Laurentii Salvii. https://doi.org/10.5962/bhl.title.542.

Liou, C.-Y., S.-Y. Yang, and C. A. Chen. 2017. "Unprecedented Calcareous Algal Reefs in Northern Taiwan Merit High Conservation Priority." *Coral Reefs* 36: 1253. https://doi.org/10.1007/s00338-017-1619-0.

Littler, M. M. 1973. "The Population and Community Structure of Hawaiian Fringing-Reef Crustose Corallinaceae (Rhodophyta, Cryptonemiales)." *Journal of Experimental Marine Biology and Ecology* 11: 103–120. https://doi.org/10.1016/0022-0981(73)90050-6.

Littler, M. M., D. S. Littler, S. M. Blair, and J. N. Norris. 1985. "Deepest Known Plant Life Discovered on an Uncharted Seamount." *Science* 227: 57–59. https://doi.org/10.1126/science.227.4682.57.

Marchini, A., F. Ragazzola, C. Vasapollo, et al. 2019. "Intertidal Mediterranean Coralline Algae Habitat Is Expecting a Shift Toward a Reduced Growth and a Simplified Associated Fauna Under Climate Change." *Frontiers in Marine Science* 6: 106. https://doi.org/10.3389/fmars.2019.00106.

Marion, A. F. 1883. *Esquisse d'Une Topographie Zoologique du Golfe de Marseille*. Cayer et cie.

Martin, C. S., M. Giannoulaki, F. De Leo, et al. 2014. "Coralligenous and Maërl Habitats: Predictive Modelling to Identify Their Spatial Distributions Across the Mediterranean Sea." *Scientific Reports* 4: 5073. https://doi.org/10.1038/srep05073.

Martin, S., J. Clavier, J.-M. Guarini, et al. 2005. "Comparison of *Zostera marina* and Maerl Community Metabolism." *Aquatic Botany* 83: 161–174. https://doi.org/10.1016/j.aquabot.2005.06.002.

Martone, P. T., and M. W. Denny. 2008a. "To Break a Coralline: Mechanical Constraints on the Size and Survival of a Wave-Swept Seaweed." *Journal of Experimental Biology* 211: 3433–3441. https://doi.org/10.1242/jeb.020495.

Martone, P. T., and M. W. Denny. 2008b. "To Bend a Coralline: Effect of Joint Morphology on Flexibility and Stress Amplification in an Articulated Calcified Seaweed." *Journal of Experimental Biology* 211: 3421–3432. https://doi.org/10.1242/jeb.020479.

McCoy, S., and N. Kamenos. 2015. "Coralline Algae (Rhodophyta) in a Changing World: Integrating Ecological, Physiological, and Geochemical Responses to Global Change." *Journal of Phycology* 51: 6–24. https://doi.org/10.1111/jpy.12262.

McCoy, S., C. M. Pueschel, C. E. Cornwall, et al. 2023. "Calcification in the Coralline Red Algae: A Synthesis." *Phycologia* 62: 648–666. https://doi.org/10.1080/00318884.2023.2285673.

McKenzie, L. J., L. M. Nordlund, B. L. Jones, L. C. Cullen-Unsworth, C. Roelfsema, and R. K. F. Unsworth. 2020. "The Global Distribution of Seagrass Meadows." *Environmental Research Letters* 15: 074041. https://doi.org/10.1088/1748–9326/ab7d06.

Melis, R., G. Ceccherelli, L. Piazzi, and M. Rustici. 2019. "Macroalgal Forests and Sea Urchin Barrens: Structural Complexity Loss, Fisheries Exploitation and Catastrophic Regime Shifts." *Ecological Complexity* 37: 32–37. https://doi.org/10.1016/j.ecocom.2018.12.005.

Micallef, A., T. P. Le Bas, V. A. I. Huvenne, P. Blondel, V. Hühnerbach, and A. Deidun. 2012. "A Multi-Method Approach for Benthic Habitat Mapping of Shallow Coastal Areas With High-Resolution Multibeam

10990755, 2025, 3, Downloaded from https://onlinelibrary.wiley.com/doi/10.1002/aqc.70121 by Csic Organización Central Om (Oficialia Mayor) (Urici), Wiley Online Library on [25/03/2025]. See the Terms and Conditions (https://onlinelibrary.wiley.com/terms-and-conditions) on Wiley Online Library for rules of use; OA articles are governed by the applicable Creative Commons License

Data." *Continental Shelf Research* 39–40: 14–26. https://doi.org/10.1016/j.csr.2012.03.008.

Milner-Gulland, E. J., and K. Shea. 2017. "Embracing Uncertainty in Applied Ecology." *Journal of Applied Ecology* 54: 2063–2068. https://doi.org/10.1111/1365-2664.12887.

Mógor, Á., J. Amatussi, G. Mogor, and L. Gemin. 2021. "Biostimulant Action of *Lithothamnium* sp. Promoting Growth, Yield, and Biochemical and Chemical Changes on Onion." *Journal of Applied Phycology* 33: 1905–1913. https://doi.org/10.1007/s10811-021-02394-3.

Necchi, O., Jr., and M. L. Vis. 2021. "Subphylum Eurhodophytina, Classes Bangiophyceae and Florideophyceae, Subclasses Corallinophycidae, Hildenbrandiophycidae, and Rhodymeniophycidae." In *Freshwater Red Algae: Phylogeny, Taxonomy and Biogeography*, edited by M. L. Vis and O. Necchi Jr., 57–94. Springer International Publishing. https://doi.org/10.1007/978-3-030-83970-3_3.

Nelson, W. A. 2009. "Calcified Macroalgae—Critical to Coastal Ecosystems and Vulnerable to Change: A Review." *Marine and Freshwater Research* 60: 787–801. https://doi.org/10.1071/MF08335.

Nicholson, E., K. E. Watermeyer, J. A. Rowland, et al. 2021. "Scientific Foundations for an Ecosystem Goal, Milestones and Indicators for the Post-2020 Global Biodiversity Framework." *Nature Ecology & Evolution* 5: 1338–1349. https://doi.org/10.1038/s41559-021-01538-5.

Noisette, F. 2013. *Impacts de l'Acidification des Océans sur les Organismes Benthiques Calcifiants des Milieux Côtiers Tempérés*. PhD Thesis. Université Pierre et Marie Curie—Paris VI.

Norton, B. G. 1998. "Improving Ecological Communication: The Role of Ecologists in Environmental Policy Formation." *Ecological Applications* 8: 350–364. https://doi.org/10.1890/1051-0761(1998)008[0350:IECTRO]2.0.CO;2.

Ordines, F., and E. Massutí. 2009. "Relationships Between Macro-Epibenthic Communities and Fish on the Shelf Grounds of the Western Mediterranean." *Aquatic Conservation: Marine and Freshwater Ecosystems* 19: 370–383. https://doi.org/10.1002/aqc.969.

OSPAR. 2023. "Benthic Habitats Thematic Assessment." In *OSPAR, 2023: Quality Status Report 2023*. OSPAR Commission.

Pallas, P. S. 1766. *Elenchus Zoophytorum Sistens Generum Adumbrationes Generaliores et Specierum Cognitarum Succintas Descriptiones, cum Selectis Auctorum Synonymis*. Apud Petrum van Cleef.

Pardo, C., L. Lopez, V. Peña, et al. 2014. "A Multilocus Species Delimitation Reveals a Striking Number of Species of Coralline Algae Forming Maerl in the OSPAR Maritime Area." *PLoS ONE* 9: e104073. https://doi.org/10.1371/journal.pone.0104073.

Peña, V., I. Bárbara, J. Grall, C. A. Maggs, and J. M. Hall-Spencer. 2014. "The Diversity of Seaweeds on Maerl in the NE Atlantic." *Marine Biodiversity* 44: 533–551. https://doi.org/10.1007/s12526-014-0214-7.

Peña, V., R. Barreiro, J. Hall-Spencer, and J. Grall. 2013. "*Lithophyllum* spp. Form Unusual Maerl Beds in the North East Atlantic: The Case Study of *L. fasciculatum* (Lamarck) Foslie, 1898, in Brittany." *An aod—Les Cahiers Naturalistes de l'Observatoire Marin* II, no. 2: 11–21.

Peña, V., D. Bélanger, P. Gagnon, et al. 2021. "Lithothamnion (Hapalidiales, Rhodophyta) in the Changing Arctic and Subarctic: DNA Sequencing of Type and Recent Specimens Provides a Systematics Foundation*." *European Journal of Phycology* 56: 468–493. https://doi.org/10.1080/09670262.2021.1880643.

Peña, V., C. Vieira, J. C. Braga, et al. 2020. "Radiation of the Coralline Red Algae (Corallinophycidae, Rhodophyta) Crown Group as Inferred From a Multilocus Time-Calibrated Phylogeny." *Molecular Phylogenetics and Evolution* 150: 106845. https://doi.org/10.1016/j.ympev.2020.106845.

Pereira-Filho, G. H., G. M. Amado-Filho, R. L. De Moura, et al. 2012. "Extensive Rhodolith Beds Cover the Summits of Southwestern Atlantic Ocean Seamounts." *Journal of Coastal Research* 28: 261–269. https://doi.org/10.2112/11T-00007.1.

Pérès, J.-M., and J. Picard. 1964. *Nouveau Manuel de Bionomie Benthique de la mer Méditerranée*. Station Marine d'Endoume.

Péron, F., and G. Marie. 2010. *Atlas du Patrimoine Maritime du Finistère*. Le Télégramme.

Peryt, T. M. 1983. "Classification of Coated Grains." In *Coated Grains*, edited by T. M. Peryt, 3–6. Springer. https://doi.org/10.1007/978-3-642-68869-0_1.

Pezzolesi, L., A. Falace, S. Kaleb, J. Hernandez-Kantun, C. Cerrano, and F. Rindi. 2017. "Genetic and Morphological Variation in an Ecosystem Engineer, *Lithophyllum byssoides* (Corallinales, Rhodophyta)." *Journal of Phycology* 53: 146–160. https://doi.org/10.1111/jpy.12488.

Philippi, R. A. 1837. "Beweis, Dass die Nulliporen Pflanzen Sind." *Archiv für Naturgeschichte* 3: 387–393. pl. 9, figs 2–6.

Piazzi, L., F. Bulleri, and G. Ceccherelli. 2016. "Limpets Compensate Sea Urchin Decline and Enhance the Stability of Rocky Subtidal Barrens." *Marine Environmental Research* 115: 49–55. https://doi.org/10.1016/j.marenvres.2016.01.009.

Pierri, C., C. Longo, A. Falace, et al. 2024. "Invertebrate Diversity Associated With a Shallow Rhodolith Bed in the Mediterranean Sea (Mar Piccolo of Taranto, South-East Italy)." *Aquatic Conservation: Marine and Freshwater Ecosystems* 34: e4054. https://doi.org/10.1002/aqc.4054.

Poe, M., K. Norman, and P. Levin. 2013. "Cultural Dimensions of Socioecological Systems: Key Connections and Guiding Principles for Conservation in Coastal Environments." *Conservation Letters* 7: 166–175. https://doi.org/10.1111/conl.12068.

Qui-Minet, Z. N., D. Davoult, J. Grall, et al. 2021. "Physiology of Maerl Algae: Comparison of Inter- and Intraspecies Variations." *Journal of Phycology* 57: 831–848. https://doi.org/10.1111/jpy.13119.

Qui-Minet, Z. N., D. Davoult, J. Grall, and S. Martin. 2022. "The Relative Contribution of Fleshy Epiphytic Macroalgae to the Production of Temperate Maerl (Rhodolith) Beds." *Marine Ecology Progress Series* 693: 69–82. https://doi.org/10.3354/meps14089.

R Core Team. 2024. *R: A Language and Environment for Statistical Computing*. R Foundation for Statistical Computing.

Ragazzola, F., A. Marchini, M. Adani, et al. 2021. "An Intertidal Life: Combined Effects of Acidification and Winter Heatwaves on a Coralline Alga *(Ellisolandia elongata)* and Its Associated Invertebrate Community." *Marine Environmental Research* 169: 105342. https://doi.org/10.1016/j.marenvres.2021.105342.

Ramos, D. A. E., J. Del Río, J. Peñas, and J. C. Braga. 2025. "An Unusual Protuberant *Lithophyllum* sp. From Southern Spain Increases Structural Complexity in Urchin Barrens." *Aquatic Conservation: Marine and Freshwater Ecosystems* 35: e70090. https://doi.org/10.1002/aqc.70090.

Ramos, E. P., T. R. Ferreira, D. B. de Aguiar, F. L. Alves, and S. Dousseau-Arantes. 2023. "*Lithothamnion* sp. as Biostimulant in Plant Cultivation." *Pesquisa Agropecuária Tropical* 53: e76273. https://doi.org/10.1590/1983-40632023v5376273.

Rebelo, A. C., S. Teichert, V. Bracchi, M. Rasser, and D. Basso. 2022. "Editorial: Crustose Coralline Red Algae Frameworks and Rhodoliths: Past and Present." *Frontiers in Earth Science* 10: 1090091. https://doi.org/10.3389/feart.2022.1090091.

Regan, H. M., M. Colyvan, and M. A. Burgman. 2002. "A Taxonomy and Treatment of Uncertainty for Ecology and Conservation Biology." *Ecological Applications* 12: 618–628. https://doi.org/10.1890/1051-0761(2002)012[0618:ATATOU]2.0.CO;2.

Rendina, F., P. J. Bouchet, L. Appolloni, et al. 2019. "Physiological Response of the Coralline Alga *Corallina officinalis* L. to Both Predicted Long-Term Increases in Temperature and Short-Term Heatwave

10990755, 2025, 3, Downloaded from https://onlinelibrary.wiley.com/doi/10.1002/aqc.70121 by Csic Organización Central Om (Oficialia Mayor) (Urici), Wiley Online Library on [25/03/2025]. See the Terms and Conditions (https://onlinelibrary.wiley.com/terms-and-conditions) on Wiley Online Library for rules of use; OA articles are governed by the applicable Creative Commons License

Events." *Marine Environmental Research* 150: 104764. https://doi.org/10.1016/j.marenvres.2019.104764.

Rendina, F., E. Buonocore, A. C. di Montanara, and G. F. Russo. 2022. "The Scientific Research on Rhodolith Beds: A Review Through Bibliometric Network Analysis." *Ecological Informatics* 70: 101738. https://doi.org/10.1016/j.ecoinf.2022.101738.

Rindi, F., J. C. Braga, S. Martin, et al. 2019. "Coralline Algae in a Changing Mediterranean Sea: How Can We Predict Their Future, if We Do Not Know Their Present?" *Frontiers in Marine Science* 6: 723. https://doi.org/10.3389/fmars.2019.00723.

Riosmena-Rodríguez, R. 2017. "Natural History of Rhodolith/Maërl Beds: Their Role in Near-Shore Biodiversity and Management." In *Rhodolith/Maërl Beds: A Global Perspective, Coastal Research Library*, edited by R. Riosmena-Rodríguez, W. Nelson, and J. Aguirre, 3–26. Springer International Publishing. https://doi.org/10.1007/978-3-319-29315-8_1.

Rowland, J. A., L. M. Bland, D. A. Keith, et al. 2020. "Ecosystem Indices to Support Global Biodiversity Conservation." *Conservation Letters* 13: e12680. https://doi.org/10.1111/conl.12680.

Sanz-Lázaro, C., M. D. Belando, L. Marín-Guirao, F. Navarrete-Mier, and A. Marín. 2011. "Relationship Between Sedimentation Rates and Benthic Impact on Maërl Beds Derived From Fish Farming in the Mediterranean." *Marine Environmental Research* 71: 22–30. https://doi.org/10.1016/j.marenvres.2010.09.005.

Savini, A., D. Basso, V. A. Bracchi, C. Corselli, and M. Pennetta. 2012. "Maerl-Bed Mapping and Carbonate Quantification on Submerged Terraces Offshore the Cilento Peninsula (Tyrrhenian Sea, Italy)." *Geodiversitas* 34: 77–98. https://doi.org/10.5252/g2012n1a5.

Sciberras, M., M. Rizzo, J. R. Mifsud, et al. 2009. "Habitat Structure and Biological Characteristics of a Maerl Bed Off the Northeastern Coast of the Maltese Islands (Central Mediterranean)." *Marine Biodiversity* 39: 251–264. https://doi.org/10.1007/s12526-009-0017-4.

Soltan, D., M. Verlaque, C. François Boudouresque, and P. Francour. 2001. "Changes in Macroalgal Communities in the Vicinity of a Mediterranean Sewage Outfall After the Setting Up of a Treatment Plant." *Marine Pollution Bulletin* 42: 59–70. https://doi.org/10.1016/S0025-326X(00)00116-8.

Steneck, R., S. Hacker, and M. Dethier. 1991. "Mechanisms of Competitive Dominance Between Crustose Coralline Algae: An Herbivore-Mediated Competitive Reversal." *Ecology* 72: 938–950. https://doi.org/10.2307/1940595.

Steneck, R. S. 1983. "Escalating Herbivory and Resulting Adaptive Trends in Calcareous Algal Crusts." *Paleobiology* 9: 44–61. https://doi.org/10.1017/S0094837300007375.

Steneck, R. S. 1986. "The Ecology of Coralline Algal Crusts: Convergent Patterns and Adaptative Strategies." *Annual Review of Ecology and Systematics* 17: 273–303. https://doi.org/10.1146/annurev.es.17.110186.001421.

Stewart, J. G. 1982. "Anchor Species and Epiphytes in Intertidal Algal Turf." *Pacific Science* 36, no. 1: 45–59.

Streit, R. P., and D. R. Bellwood. 2023. "To Harness Traits for Ecology, Let's Abandon 'Functionality'." *Trends in Ecology & Evolution* 38: 402–411. https://doi.org/10.1016/j.tree.2022.11.009.

Stroud, J. T., M. R. Bush, M. C. Ladd, R. J. Nowicki, A. A. Shantz, and J. Sweatman. 2015. "Is a Community Still a Community? Reviewing Definitions of Key Terms in Community Ecology." *Ecology and Evolution* 5: 4757–4765. https://doi.org/10.1002/ece3.1651.

Sully, S., D. E. Burkepile, M. K. Donovan, G. Hodgson, and R. van Woesik. 2019. "A Global Analysis of Coral Bleaching Over the Past Two Decades." *Nature Communications* 10: 1264. https://doi.org/10.1038/s41467-019-09238-2.

Tâmega, F. T., G. H. H. Perna, P. Spotorno-Oliveira, R. Riosmena-Rodríguez, and J. E. de Gonçalves. 2017. "A Unique Free-Living Geniculate Coralline Algal Bed Formation." *Marine Biodiversity* 47: 373–374. https://doi.org/10.1007/s12526-016-0487-0.

Tâmega, F. T., B. N. Torrano-Silva, M. C. Oliveira, et al. 2021. "Identification of 'Articuliths' in a Unique Algal Bed Formation From Brazil and Description of *Jania cabista* sp. nov. (Corallinales, Rhodophyta)." *Phycologia* 60: 283–302. https://doi.org/10.1080/00318884.2021.1916279.

Thierry, G. 2016. "Neurolinguistic Relativity: How Language Flexes Human Perception and Cognition." *Language Learning* 66: 690–713. https://doi.org/10.1111/lang.12186.

Tillin, H. 2015. "Foliose Seaweeds and Coralline Crusts in Surge Gully Entrances." In *Marine Life Information Network: Biology and Sensitivity Key Information Reviews [Online]*, edited by H. Tyler-Walters and K. Hiscock. Marine Biological Association of the United Kingdom.

Tuya, F., N. Schubert, J. Aguirre, et al. 2023. "Levelling-Up Rhodolith-Bed Science to Address Global-Scale Conservation Challenges." *Science of the Total Environment* 892: 164818. https://doi.org/10.1016/j.scitotenv.2023.164818.

van der Heijden, L. H., and N. A. Kamenos. 2015. "Reviews and Syntheses: Calculating the Global Contribution of Coralline Algae to Total Carbon Burial." *Biogeosciences* 12: 6429–6441. https://doi.org/10.5194/bg-12-6429-2015.

van Katwijk, M. M., A. Thorhaug, N. Marbà, et al. 2016. "Global Analysis of Seagrass Restoration: The Importance of Large-Scale Planting." *Journal of Applied Ecology* 53: 567–578. https://doi.org/10.1111/1365-2664.12562.

van Woesik, R., and C. Kratochwill. 2022. "A Global Coral-Bleaching Database, 1980–2020." *Scientific Data* 9: 20. https://doi.org/10.1038/s41597-022-01121-y.

Veras, P., I. Pierozzi-Jr, J. B. Lino, et al. 2020. "Drivers of Biodiversity Associated With Rhodolith Beds From Euphotic and Mesophotic Zones: Insights for Management and Conservation." *Perspectives in Ecology and Conservation* 18: 37–43. https://doi.org/10.1016/j.pecon.2019.12.003.

Verlaque, M. 2010. "Field Methods to Analyse the Condition of Mediterranean *Lithophyllum byssoides* (Lamarck) Foslie Rims." *Scientific Reports of Port-Cros National Park* 24: 185–196.

Vigliano Relva, J., and J. Jung. 2021. "Through the Eyes of Another: Using a Narrative Lens to Navigate Complex Social-Ecological Systems and to Embrace Multiple Ways of Knowing." *Frontiers in Marine Science* 8: 678796.

Wai, T.-C., and G. A. Williams. 2006. "Effect of Grazing on Coralline Algae in Seasonal, Tropical, Low-Shore Rock Pools: Spatio-Temporal Variation in Settlement and Persistence." *Marine Ecology Progress Series* 326: 99–113. https://doi.org/10.3354/meps326099.

Walker, R., J. Brodie, S. Russell, L. Irvine, and S. Orfanidis. 2009. "Biodiversity of Coralline Algae in the Northeastern Atlantic Including *Corallina caespitosa* sp. nov. (Corallinoideae, Rhodophyta)." *Journal of Phycology* 45: 287–297. https://doi.org/10.1111/j.1529-8817.2008.00637.x.

Webster, N. S., S. Uthicke, E. S. Botté, F. Flores, and A. P. Negri. 2013. "Ocean Acidification Reduces Induction of Coral Settlement by Crustose Coralline Algae." *Global Change Biology* 19: 303–315. https://doi.org/10.1111/gcb.12008.

Wiegmann, F. A. 1837. *Archiv für Naturgeschichte*. 3rd ed. Nicolai'schen Buchhandlung.

Williamson, C. J., J. Najorka, R. Perkins, M. L. Yallop, and J. Brodie. 2014. "Skeletal Mineralogy of Geniculate Corallines: Providing Context for Climate Change and Ocean Acidification Research." *Marine Ecology Progress Series* 513: 71–84. https://doi.org/10.3354/meps10929.

10990755, 2025, 3, Downloaded from https://onlinelibrary.wiley.com/doi/10.1002/aqc.70121 by Csic Organización Central Om (Oficialia Mayor) (Urici), Wiley Online Library on [25/03/2025]. See the Terms and Conditions (https://onlinelibrary.wiley.com/terms-and-conditions) on Wiley Online Library for rules of use; OA articles are governed by the applicable Creative Commons License

Wilson, B., and S. Blake. 2011. "Notes on the Origins and Biogeomorphology of Montgomery Reef, Kimberley, Western Australia." *Journal of the Royal Society of Western Australia* 94: 107–119.

Wilson, S., C. Blake, J. A. Berges, and C. A. Maggs. 2004. "Environmental Tolerances of Free-Living Coralline Algae (Maerl): Implications for European Marine Conservation." *Biological Conservation* 120: 279–289. https://doi.org/10.1016/j.biocon.2004.03.001.

Woelkerling, W. J. 2008. *The Coralline Red Algal Herbarium of Mikael Foslie and Its Impact on Scientific Research*. Vol. 16. Gunneria 79.

Woelkerling, W. J., G. Gustavsen, H. Myklebost, T. Prestø, and S. Såstad. 2005. *The Coralline Red Algal Herbarium of Mikael Foslie: Revised Catalogue With Analyses*. Gunneria 77.

Zhan, S. H., L. Chen, C.-P. Liao, et al. 2022. "Geographic Distance, Sedimentation, and Substrate Shape Cryptic Crustose Coralline Algal Assemblages in the World's Largest Subtropical Intertidal Algal Reef." *Molecular Ecology* 31: 3056–3071. https://doi.org/10.1111/mec.16455.

Žuljević, A., S. Kaleb, V. Peña, et al. 2016. "First Freshwater Coralline Alga and the Role of Local Features in a Major Biome Transition." *Scientific Reports* 6: 19642. https://doi.org/10.1038/srep19642.

Supporting Information

Additional supporting information can be found online in the Supporting Information section.

10990755, 2025, 3, Downloaded from https://onlinelibrary.wiley.com/doi/10.1002/aqc.70121 by Csic Organización Central Om (Oficialia Mayor) (Urici), Wiley Online Library on [25/03/2025]. See the Terms and Conditions (https://onlinelibrary.wiley.com/terms-and-conditions) on Wiley Online Library for rules of use; OA articles are governed by the applicable Creative Commons License

“ …Sigue nadando…”

Dory.

